Authors are requested to submit three copies of manuscripts and illustrations to the Editorial Department, Institute of Radio Engineers, 1 East 79 St., New York 21, N. Y.

PROCEEDINGS OF THE IRE®

Published Monthly by
The Institute of Radio Engineers, Inc.

VOLUME 45 — *June, 1957* — NUMBER 6

CONTENTS

Contents continued on following page

THE COVER—At very-low frequencies (below 100 kc), radio waves are propagated around the earth in much the same way as in a waveguide, with the earth constituting the lower wall of the guide and the ionosphere providing a sharply defined upper wall. Pictured on the cover is a representation of the waveguide mode theory of vlf propagation, showing in exaggerated scale the disposition of the electric field lines between the earth and the ionosphere for the dominant mode (order 1) of propagation. A discussion of this theory and other important aspects of vlf propagation is contained in a special group of papers selected for this issue from the recent VLF Symposium in Boulder, Colo.

Change of address (with 15 days advance notice) and letters regarding subscriptions and payments should be mailed to the Secretary of the IRE. 1 East 79 Street, New York 21, N. Y.

PROCEEDINGS OF THE IRE

Published Monthly by

The Institute of Radio Engineers, Inc.

(*Continued*)

Poles and Zeros

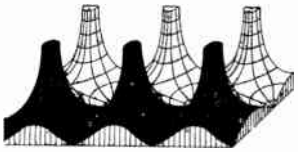

Very Low. Last January, the National Bureau of Standards, in cooperation with the Professional Group on Antennas and Propagation, was host at Boulder, Colorado to a gathering of experts in one of the oldest studies in radio science, the theory and application of very-low-frequency waves. During a three-day session, 47 papers were presented. Of these, 13 papers selected by the IRE Editorial Board and its reviewers as having general interest to radio engineers are published in this issue.

When K. A. Norton first suggested publication of these papers to your editor, some months before the Boulder symposium, we had doubts. At the time we shared the misconception that VLF waves are one of the more special of the special fields of radio. These waves at frequencies below roughly 100 kc are host to a limited range of services, they are rife with high-intensity static, and their propagation has been understood better than that of most other regions of the spectrum for better than 40 years. The Austin-Cohen formula, which predicts VLF field intensities against distance, has been giving excellent service since it was first enunciated in 1911—perhaps the only quantitative statement of the behavior of radio waves, or of anything else in the radio art, to survive in useful form from those early days. So we fell back on the standard editorial device, and asked to see the manuscripts before comitting to publish. Since this was asking to see a lot of manuscript and setting up a requirement for a lot of expert judgment, we asked the Symposium Chairman, J. R. Wait, Ken Norton and his colleagues at Boulder, the PROCEEDINGS reviewers specializing in propagation, and the reviewers of the Professional Group on Antennas and Propagation, to stand by to help in evaluating the papers.

Came January and the storm descended. The reviewing teams read 28 papers in less than a month, combining expert knowledge with sympathy for the non-expert. Jim Wait presided benignly over the situation, insisting only that the final selection be identified as IRE's choice, not his. He advised on the order of presentation and prepared the introductory comment which appears on page 739.

The result cannot be called a special issue in the strict sense, since this issue also contains almost as many pages on other subjects. But the VLF part of it comes as an eye-opener to the editor, and he suspects it will be the same to many other readers. These VLF papers may follow an old tradition but there's nothing old hat about any of them.

It turns out that the Austin-Cohen formula, derived empirically, holds best at about 25 kc. Modern propagation theory, working with boundary conditions that really bound the situation (as they do not at higher frequencies) has produced a vastly more comprehensive insight into VLF propagation and predicts its normal behavior with better accuracy over a much wider frequency range. New modes of radio propagation at *audio* frequencies have been observed and explained. Energy propagated over great distances along the earth's magnetic lines of force encounters frequency dispersion that produces ascending and descending tones. These are called whistlers; their source (whistlers' mother!) has been identified as lightning in the opposite hemisphere. The remarkable stability of VLF propagation makes possible not only super-long-range navigation on these frequencies, but also a worldwide standard of time more accurate than now provided by time signals at 2.5 mc and higher frequencies.

This is no dead art, lately elaborated for the introspection of savants. VLF has real vitality, as the following pages testify. So our thanks go to Messrs. Wait and Norton, as well as to all those who prepared and otherwise assisted in bringing together this significant group of papers. Other papers presented at the symposium are being considered for publication in the TRANSACTIONS of the PGAP, to which are referred all those whose appetite is whetted for further VLF fare.

Grass Roots. Regional Directors and Section Chairmen now have in their hands a document consigned to them by the Editorial Board, entitled "Section Survey of IRE Editorial Policies." These gentlemen have been requested (1) to bring before the membership of each Section twelve groups of questions relating to the policies and procedures now governing the PROCEEDINGS and the 28 other Institute publications and (2) to prepare a summary statement for the Board which reflects the attitudes of the Section members on the conduct of IRE editorial affairs. This survey, the first inquiry on IRE management to be referred directly to the grass roots through the personal mediation of Section officers, is a large and burdensome undertaking. The labor involved is justified only by a compelling objective: to make our publication policy directly responsive to the needs and desires of the membership at large.

To meet this objective, members at the grass roots must respond and make their attitudes and preferences known. So we ask all members to be on the alert for an announcement from their Section Chairman as to the manner in which the survey is to be conducted. Many Sections plan to devote time for discussion of these policy questions during the whole or a part of a regular meeting. If you have something to say, gripe, suggestion or good wish, show up and say it. Those who cannot attend in person are urged to write their opinions directly to their Section Chairman, basing their comments on the document in question (printed on page 884 of this issue)—D.G.F.

Scanning the Issue

VLF Symposium Papers (p. 741)—The lower end of the radio frequency spectrum, which has been neglected for many years, has suddenly become a focal point of considerable interest, due principally to the need for very long range communication and navigation systems. This interest was very much in evidence on January 23–25 of this year when the National Bureau of Standards, in conjunction with the IRE Professional Group on Antennas and Propagation, held a Symposium on the Propagation of Very-Low-Frequency Radio Waves, at which an impressive total of 47 papers were presented. Thirteen of these papers have been selected as being representative of important work in this field and of interest to the IRE membership at large. These papers constitute the first portion of this expanded issue. A fuller discussion of these papers will be found in *Poles and Zeros* (p. 737) and in an excellent introduction prepared by the Chairman of the Symposium Committee (Wait, p. 739). Suffice it to say here that the series starts with a review of our present ideas of the physical structure of the lower edge of the ionosphere where vlf waves are largely reflected, and proceeds in the next five papers to a basic theoretical discussion of the propagation of vlf waves. Six of the following papers deal in the main with the generation and various characteristics of noise caused by lightning discharges, the principal source of noise at vlf. The remaining paper considers the possibility of establishing a single vlf source as a world-wide frequency standard. Further comments on each of the papers will be found in the introduction.

Designing for Reliability (Taylor, p. 811)—In recent years there have been many papers preaching reliability in general terms. This paper distinguishes itself by describing the actual techniques of designing highly reliable circuits and systems. The discussion of specific design considerations and procedures is topped off by a detailed description of the "marginal checking" method of determining whether or not the finished design meets the given performance specifications with the desired degree of reliability. The author includes an excellent summarization of eight major types of components, listing the characteristics and applications of each that have been found to give a reliable electronic design. This material is based on eight years' experience in designing highly reliable computer systems, including the computer portion of the SAGE air defense system. The valuable lessons that have been learned and documented here form a highly significant contribution to circuit design techniques that will be of interest to many PROCEEDINGS readers.

Experience with Single-Sideband Mobile Equipment (Richardson, *et al.*, p. 823)—Single sideband has been very much in the public eye of late because it offers the possibility of substantially increasing the number of communication channels available in our now-crowded radio frequency spectrum. Among the most interested parties is the FCC, which recently asked the Joint Technical Advisory Committee to undertake an engineering study of single-sideband techniques. The JTAC, in turn, sent out a call to engineers for papers describing the latest developments in the field. These papers formed the special SSB issue of the PROCEEDINGS, published last December. One paper missed the issue because it was held up by clearance procedures. Because of its special timeliness it is now being published. It describes an experimental SSB vhf mobile radio system, such as might be used for police work, and compares its performance with comparable fm mobile equipment now in use. A feature of the system is the transmission of a weak pilot carrier along with the sideband, so as to avoid the exacting problem of generating a carrier in the receiver that is within 50 cycles of the transmitter carrier frequency. The carrier is then separated from the sideband by a phase-locked oscillator circuit similar to that used in color TV receivers. Although the pilot carrier robs the sideband of some signal power, the range of the equipment is found to be the same as for fm equipment of the same size.

Topological Analysis of Linear Nonreciprocal Networks (Mason, p. 829)—Topological methods provide the circuit designer with an important tool for analyzing the transmission properties of networks, either in place of or as a supplement to the more formal mathematical methods of analysis. By a fairly simple process of inspection and using equivalent representations of a network it is possible to arrive easily and quickly at an understanding of the network characteristics. This paper extends the topological rules of Kirchoff and Maxwell for reciprocal networks to the realm of nonreciprocal active circuits. It does so by the device of using a gyristor, a hypothetical element whose current is proportional to the sum of its two terminal voltages, and a unistor, whose current is proportional to one of its terminal voltages and independent of the others, as a means of representing any nonreciprocal network. Most important, this permits familiar Kirchoff-Maxwell expressions to be applied to nonreciprocal networks with only very minor modifications.

Theory and Experiments on Shot Noise in Semiconductor Junction Diodes and Transistors (Guggenbuehl and Strutt, p. 839)—This paper presents a general theory of shot noise in junction transistors and diodes that ties together previous work in the low-frequency region and covers new ground in the high-frequency region. The idea presented is simple and concise, leads to correct results, and makes a contribution of basic and wide-range interest to the radio engineering field. Included is a good discussion of transistor noise measurements and a presentation of noise figure formulas that will be of special interest to transistor circuit designers.

Space Charge Waves Along Magnetically Focused Electron Beams (Labus, p. 854)—This paper treats theoretically the propagation of signals along a cylindrical beam of electrons confined by a uniform magnetic field, a subject of fundamental interest and importance in the field of microwave tubes. This work is noteworthy in that it disagrees with existing theories, one of which was published here just eleven months ago. The disagreement centers on the method of calculating the charge density of the beam, leading to appreciably different results. The reviewers and editors feel that this difference in viewpoint concerns a matter of sufficient importance to warrant presenting it for the consideration of all PROCEEDINGS readers concerned.

The High Current Limit for Semiconductor Junction Devices (Fletcher, p. 862)—Present theories concerning semiconductor junction devices give us a good understanding of their operation over most of their operating range, that is, from low to quite high current densities. This paper fills in, in admirable fashion, the remaining gap from high current on up to maximum current operation, where new formulas must be derived to take into account previously neglected effects. The theory is then applied to the design of junction diodes and to a consideration of transistor emitter efficiency, accurately predicting to what extent various parameters should be varied to achieve specified results. In particular it is shown that it is possible to construct diodes with exponential characteristics over a current range of five decades and with current densities as high as 3000 amperes per cm^2, without using special alloying materials.

Introduction to the VLF Papers*

JAMES R. WAIT†, SENIOR MEMBER, IRE

PROPAGATION of radio waves at very low frequencies (from 1 to 30 kc) is characterized by the fact that the ground wave has very low attenuation and that sky waves are almost totally reflected from the ionosphere which has a height of the order of 60 to 90 km. In fact, vlf waves that have traveled considerable distances act as if they were propagated in the space between concentric reflecting spherical shells representing the earth and the lower edge of the ionosphere. The attenuation under such conditions is that caused by spreading and absorption of energy by the ground and the ionosphere. The loss in the ionosphere has diurnal, seasonal, and year-to-year variations.

The propagation at vlf was understood surprisingly well as long ago as 1911. At this time, the famous empirical formula of Austin-Cohen was proposed.[1] This formula does have some theoretical justification, although it is now known that it is only applicable for frequencies near 25 kc. Despite the fact that vlf waves propagate to great distances with small attenuation, their use has been neglected for many years. Recently, however, with the pressing need for long range navigational systems, world-wide communication systems, and tracking of atmospheric storms and hurricanes, the desirable transmission properties of vlf are again being utilized.

The symposium held recently in Boulder, Colo., was devoted to an appraisal of the basic theory and the potential applications of very low-frequency radio waves. Some 47 papers were presented in a period of three days. Most of these were preprinted and bound together into a three-volume prepublication symposium record. Of these, 13 papers were selected by the IRE Editorial Board for publication in the PROCEEDINGS in view of their general interest.

The keynote paper by Prof. A. H. Waynick is an excellent summary of the current ideas on the actual structure of the lower edge of the ionosphere where vlf waves are largely reflected. It would appear from the experimental data that the reflecting height varies consistently from 70 km during the day to 90 km at night. For an overhead sun, the maximum of electron density was placed at 80 km and had the value 600 electrons/cm^3. It would appear that the gradient of the ionosphere at the lower edge is sufficiently large to regard it as a sharp boundary for vlf reflection in many instances.

With the idealization that the lower edge of the ionosphere is abrupt, a complete solution is given for reflection of an incident plane wave in a paper by I. W. Yabroff. The effects of the losses and the earth's magnetic field on the amplitude and polarization of the ionospherically reflected wave are calculated. It is shown that some of the commonly used approximations are quite justified if attention is restricted to the field below the reflecting layer. However, the direction of the ray normals and the polarization of the transmitted wave in the ionosphere are profoundly affected by the so-called quasi-longitudinal approximation.

The conception that vlf radio waves propagate to great distances via multiple reflections between the earth and the ionosphere is expounded in the papers by J. R. Wait and K. G. Budden. Here the ionosphere is again assumed to be sharply bounded and, in view of the obliqueness of the incident rays at the ionosphere, the earth's magnetic field has a very small effect and can be neglected. The theoretical results are in good agreement with measured field-strength distance curves at a frequency of the order of 16 kc and with the observed frequency variation of the attenuation of broadband signals of atmospheric origin. The observed presence of an absorption band for frequencies of the order of 3 kc, which is not predicted by the Austin-Cohen or Watson formulas, is in complete accord with the mode theory.

The generation of vlf radiation from lightning discharges is discussed in a paper by E. L. Hill. The spectral intensity of the radiation is derived from a single parameter, the time of travel of the return stroke from ground to cloud. The calculated maximum point of the spectral curves lies at about 10 kc, and the total radiated energy is estimated to be of the order of 200,000 joules.

The radiation from lightning discharges is the main source of radio noise at vlf. The nature of atmospheric noise and the variation with location, frequency, and time are described in a paper by W. Q. Crichlow. Data are presented for the statistical variation of the noise levels from day to day and season to season in terms of amplitude-time-distribution of the effective noise power available from a lossless antenna. The principal aim of this work has been the establishment of a regular service for predicting the levels and characteristics of radio noise. The latest predictions were adopted recently by the CCIR (International Radio Consultative Committee) in Warsaw. A detailed survey of vlf noise characteristics in Ottawa and Churchill is given in a paper by C. A. McKerrow. The results compare quite favorably with the earlier predictions of the National Bureau of Standards.

* Original manuscript received by the IRE, April 11, 1957.
† National Bureau of Standards, Boulder, Colo.
[1] See L. W. Austin, *Bull. NBS*, vol. 7, p. 315; 1911.

Statistical measurements of the envelope of narrow-band atmospheric noise in the band 1 to 100 kc are given in a comprehensive paper by A. D. Watt. On the basis of available data on the characteristics of the current variations in lightning strokes, a typical spectral distribution for the dipole moment of the lightning discharge is derived. The approach here is somewhat different from that used in a previously mentioned paper by Hill. Watt shows that the peak of the radiated energy is around 4 kc and he indicates how this is modified by propagation. His calculated spectra of noise agree well with the observations at Boulder for storm centers at a range of the order of 3000 km.

The stability of transmission of 16 kc signals across the Atlantic Ocean has been studied in detail by J. A. Pierce. For a distance of 5000 km the frequency seldom changes more than 3 parts in 10^9. This is further evidence that the ionosphere is almost effectively a fixed reflector for vlf radio waves except during disturbed periods and during sunrise and sunset. The possibility is established that a single source of vlf can be made available on a world-wide basis for frequency comparison.

The waveforms of signals radiated from distant storms are described by J. Chapman and E. T. Pierce. They were able to compare the relation between the characteristics of atmospherics observed in England for sources in southeast Europe and in the southwest Atlantic Ocean. As predicted by the mode theory, the high conductivity of the sea tends to enhance the transmission in the band from 10 to 15 kc producing the smooth oscillatory type of waveform for the majority of the southwesterly sources.

A technique for analyzing naturally occurring radio signals in the audio-frequency range is described in a paper by J. K. Grierson. Its basic action is to scan the frequency-time plane in frequency at a fixed time rather than, as conventionally, in time at a fixed frequency. A short section of the signal is first stored and is then read out rapidly for analysis by a variable tuned filter. The equipment is particularly suitable for studying the gliding tones associated with the whistling type atmospheric. These "whistlers" are believed to be electromagnetic signals initiated by lightning discharges which propagate along the lines of the earth's magnetic field from one hemisphere to the other.

Acknowledgment

The holding of the symposium itself is due in a large measure to K. A. Norton, Dr. F. W. Brown, and Dr. R. J. Slutz for their enthusiastic support and valuable advice. Other members of the NBS staff who have been generous with their help in the technical program arrangements include T. N. Gautier, R. A. Helliwell, A. D. Watt, J. M. Watts, A. G. Jean, H. Cottony, Mrs. A. Murphy, and Mrs. B. E. Rees. The onerous tasks connected with local arrangements were borne mainly by R. Silberstein, Mrs. M. Halter, M. Coon, W. F. Utlaut, F. F. Fulton, Jr., R. H. Doherty, J. Kemper, J. R. Johler, and Mrs. W. Mau.

The Present State of Knowledge Concerning the Lower Ionosphere*

ARTHUR H. WAYNICK†, FELLOW, IRE

Summary—In this paper an attempt is made to summarize the current state of knowledge concerning the lower ionosphere. This includes at *D* and lower *E* region heights: electron density as functions of height and time, dissipative processes, the possible atmospheric constituents involved and their distributions, physical parameters to be considered, and solar radiations and other factors relevant in the formation of this portion of the ionosphere. Where possible, comparisons between theory and experiment are made.

Introduction

THE CHARACTERISTICS of the lower ionosphere are, of course, of fundamental importance in considering the propagation of very low-frequency radio waves to great distances. The essentially inverse statement is likewise true in that, for many years, the major exploratory tool available to the experimenter in the study of the lower ionosphere has been the use of radio waves of various frequencies in the determination of ionospheric characteristics.

The procurement of measurements, *in situ*, in the ionosphere in recent years with the aid of rocket-borne instrumentation has revolutionized the study of relevant phenomenon. By combining the results of these two methods of measurement, comparatively recently, great advances have been made in this area and this progress will doubtless continue in the immediate and near future.

In view of the rapid advances made in the last few years, this summary will be confined, in great part, to work reported upon within the last two or three years. The relevant radio data will first be outlined, followed by a summary of rocket-borne experiment results which are relevant to the lower ionosphere. Material concerned with the lower *E* and *D* regions will then be summarized.

Radio Data

The summarization of the radio data is rather arbitrarily divided into the sections outlined below.

Very Low Frequency

For many years the outstanding work of the Cambridge group on frequencies below 30 kc was the major effort in this area. This has been summarized by Bracewell, Budden, Ratcliffe, Straker, and Weekes.[1] Height variations from 70 km during the day to 85 km at night were determined and were highly reproducible at the lower frequencies from day to day and from season to season. Absorption, polarization, and other experimental factors are reported upon. Verification of many of the 16-kc measurements was reported by Hopkins and Reynolds.[2]

Low Frequency

In the frequency range 30 to 65 kc, Bracewell, Harwood, and Straker[3] have summarized a continuation of the work of the Cambridge group. Height, absorption, and polarization characteristics become more variable from day to day as the frequency of the exploring wave is increased. The average diurnal change in height is found to be about 11 km; varying from 7 to 18 km and at slightly greater heights for the higher frequency. The diurnal variation likewise becomes asymmetrical about noon at the higher frequency. The daytime variation in absorption also increases with frequency—the polarization was found to be left-hand, circular, and constant.

Helliwell, Mallinckrodt, and Kruse[4] were the first workers to report on vertical incidence long-wave pulse measurements. Their extensive results yielded a stratification in height, at night, at about 90 and 100 km on 100 kc. At 325 kc, stratification centered at 100 and 110 km was noted. These data were interpreted as an actual stratification in electron-density height profiles as a result of several studies concerning this matter.

Going to higher frequencies: Weekes and Stuart[5] outlined their important results in the frequency range 70 to 127 kc. The diurnal change in height was found to be approximately one half of that observed at 16 kc, 7–8 km, much more variable from day to day and sub-

* Original manuscript received by the IRE, January 31, 1957. The preparation of this paper was supported by the Geophysics Res. Div. of the Air Force Cambridge Res. Center under Contract AF19(604)-1304 and, in part, by the National Science Foundation under Grant G1969. Paper presented at Symposium on Propagation of Very-Low-Frequency Electromagnetic Waves, Boulder, Colo.; January 23–25, 1957.

† Ionosphere Res. Lab., The Pennsylvania State Univ., University Park, Pa.

[1] R. N. Bracewell, K. G. Budden, J. A. Ratcliffe, T. W. Straker, and K. Weekes, "The ionospheric propagation of low- and very low-frequency radio waves over distances less than 1,000 km," *Proc. IEE*, part III, vol. 98, pp. 221–236; May, 1951.

[2] H. G. Hopkins and L. G. Reynolds, "An experimental investigation of short-distance ionospheric propagation at low and very low frequencies," *Proc. IEE*, part III, vol. 101, pp. 21–34; January, 1954.

[3] R. N. Bracewell, J. Harwood, and T. W. Straker, "The ionospheric propagation of radio waves of frequency 30–65 kc/s over short distances," *Proc. IEE*, part IV, vol. 101, pp. 154–162; April, 1954.

[4] R. A. Helliwell, A. J. Mallinckrodt, and F. W. Kruse, "Fine structure of the lower ionosphere," *J. Geophys. Res.*, vol. 56, pp. 53–62; March, 1951.

[5] K. Weekes and R. D. Stuart, "The ionospheric propagation of radio waves with frequencies near 100 kc/s over short distances," *Proc. IEE*, part IV, vol. 99, pp. 1–9; November, 1952.

ject, as was the absorption, to marked solar control. Again the midday absorption increased with increasing frequency.

On the basis of available vertical incidence long-wave data, but with primary emphasis on 150-kc pulse observations, Nertney[6] deduced an empirical D-region model which would account rather closely for the experimentally observed parameters such as height, absorption, and polarization in the frequency range 16 to 150 kc. The model maximum of electron density was placed at 80 km and had the value 600 electrons/cm^3 for an overhead sun. Qualitative agreement with expected long-wave oblique incidence reflection heights was noted in comparison with experimental results available in the frequency range 20 to 200 kc.

At 300 kc and for an oblique incidence path of 1200 km, Watts[7] determined daytime midpoint heights of reflection of 65–70 km which increased to 80 km at night.

Watts and Brown[8] presented most striking vertical incidence sweep frequency records covering the range 50 to 1100 kc. An adequate summarization of their results would be too voluminous for consideration here. The frequently very complex records yielded daytime heights from apparently discrete levels in the ranges 68 to 80 km, 85–90 km, and 98–110 km; the latter appearing to be the normal E region. An echo intermediate in height between E and F was frequently noted at night. Nighttime E critical frequencies were observed but could not be subjected to an adequate study due to limitations in system gain.

Medium Frequency

Relatively weak and rapidly fading echoes in the height range 80–100 km have been observed with high-power sweep frequency equipment for several years by Dieminger.[9] They extend from the bottom frequency range of the equipment of about 1 mc to several mc and are most frequently noted in winter. A diurnal variation of about 8 km in height is noted with a minimum near noon. A weakening of the normal E region echo is found to accompany a strengthening and lowering in height of the lower echo structure.

Gardner and Pawsey[10] have reported on 2-mc pulse observations in an essentially noise-free receiving site where low-level reflection heights and reflection coefficients were determined as a function of time and season. Measurements were made on both magneto-ionic components with linear transmitted polarization. Daytime reflections were noted in the height range 70 km with a reflection coefficient of order 10^{-5}. Another reflection level near 90 km with a reflection coefficient 10^{-3} was noted during the day and night. The latter extended during the day to the regular E level of 105 km. Under certain reasonable assumptions, electron density height profiles were deduced from the slope of integrated differential absorption curves vs height for the two magneto-ionic components. For summer noon a maximum of electron density of 200/cm^3 at about 73 km was determined with an intermediate minimum of 100/cm^3 at about 100 km.

In connection with a pulsed wave interaction experiment on two frequencies near 2 mc, Fejer[11] determined electron density, N, height profiles which he states agree with the results of Gardner and Pawsey,[10] within an order of magnitude, for a similar diurnal time and season. Thus, N varied from 10^1 at 67 km to 10^4 at 90 km with a slight minimum of 8×10^2 at 78 km.

Utilizing a very unique fm technique permitting observations with reflection coefficients to 3×10^{-5} Gnanalingam and Weekes[12] observed echoes from heights near 80 km on a frequency of 1.42 mc in addition to normal E echoes at 110 km. They conclude that on the occasions when the D echo is observed and E absent, the D critical frequency is greater than the operating frequency. The distinction between total and partial reflection in D is made by comparison with simultaneous 2-mc absorption experiments. A thickness of 3 km is deduced for D region. An auxiliary experiment on six frequencies in the range 1 to 2.4 mc resulted in reflection heights of 85 km to approximately 1.4 mc with a transition to E at 110 km for frequencies slightly below and above this. These authors conclude that total reflection in D is involved for suitable frequencies. The region investigated is called sporadic D in that the height is highly variable from day to day and the low-lying echo is most frequently noted in winter.

Finally, Gregory[13] has described pulse experiments on 1.75 mc in which h'-t records were obtained during fall and winter, 1955 down to a reflection coefficient of 4×10^{-6} by the use of a very extensive transmitting-receiving antenna system. During daytime only, echoes were received in the height range 55 to 80 km; lower heights and larger reflection coefficients, ρ, being noted in winter. ρ decreased with decreasing height to the minimum of 4×10^{-6}. Persistent day and night reflections were observed with a lower boundary of about 85 km and a diurnal variation in height of ±3 km. A possible seasonal decrease of 2 km in winter was noted. In addition, a sporadic weak daytime echo below normal E at heights of 94 to 97 km was noted on occasion.

[6] R. J. Nertney, "The lower E and D region of the ionosphere as deduced from long radio wave measurements," *J. Atmos. Terr. Phys.*, vol. 3, pp. 92–107; February, 1953.

[7] J. M. Watts, "Oblique incidence propagation at 300 kc using the pulse technique," *J. Geophys. Res.*, vol. 57, pp. 487–498; December, 1952.

[8] J. M. Watts and J. N. Brown, "Some results of sweep-frequency investigation in the low frequency band," *J. Geophys. Res.*, vol. 59, pp. 71–86; March, 1954.

[9] W. Dieminger, "Short wave echoes from the lower ionosphere," *Proc. Conf. Phys. Ion.*, Phys. Soc. (London), pp. 53–57; 1955.

[10] F. F. Gardner and J. L. Pawsey, "Study of the ionospheric D-region using partial reflections," *J. Atmos. Terr. Phys.*, vol. 3, pp. 321–344; July, 1953.

[11] J. A. Fejer, "The interaction of pulsed radio-waves in the ionosphere," *J. Atmos. Terr. Phys.*, vol. 7, pp. 322–332; Dec., 1955.

[12] S. Gnanalingam and K. Weekes, "D-region echoes with a radio wave of frequency 1.4 mc/s," *Proc. Conf. Phys. Ion.*, Phys. Soc. (London), pp. 63–70; 1955.

[13] J. B. Gregory, "Ionospheric reflections from heights below the E region," *Aust. J. Phys.*, vol. 9, pp. 324–342; September, 1956.

Scatter

While in some ways rather indirect, the phenomenon of ionospheric oblique incidence scatter propagation provides evidence concerning the height of the lower ionosphere. Summaries have been published by Bailey *et al.*[14] and Bray *et al.*[15]

Bailey, Bateman, and Kirby[16] in a very extensive summary concerning this matter have reported on midpoint scattering heights deduced from both cw and pulse experiments. Daytime heights of 75–80 km and nighttime values of 85–90 km are indicated.

Relative delays between tropospheric and ionospheric scatter propagated signals have been determined by Pineo[17] to deduce daytime midpoint scatter heights between 60–75 km rising to 85–90 km at night. A possible seasonal effect is observed on the lower height.

Meteoric

In addition to providing extremely valuable information concerning the physical characteristics of the lower ionosphere the study of meteors by radio techniques has led to a study of meteoric supported oblique incidence propagation. Villard, Eshleman, Manning, and Peterson[18] have summarized the situation and conclude that the great number of ionized trails produced by meteors down to mass 10^{-5} grams at heights near 100 km may be of importance in this respect, particularly at low latitudes.

Certain normal vertical incidence radio records have shown "patchy" reflections in the height range 90–100 km and are discussed by Naismith.[19] These are attributed to a subsidiary layer in lower E region due to meteor ionization.

Experiments concerned with meteor burst propagation involving 7–10th magnitude meteors over ranges of 1000 km have been described by Villard, Peterson, Manning, and Eshleman.[20] These have been used to relate "vertical" incidence radio meteor study results to the oblique incidence case.

Weiss[21] has given histograms of meteor shower echo heights utilizing pulse and cw techniques. These maximize at about 90 km and cover the height range 80 to 100 km, dependent on the individual shower. A diurnal variation in heights is noted which is a function of season and ranges from 90 ± 5 km for the background of meteor echoes.

The theoretical basis for a persisting accumulation of meteor atoms at heights of about 100 km has been provided by Nicolet.[22] Electron production and loss characteristics are shown to be such that an electron density of approximately 10^4 should be expected to be maintained at these heights during hours of darkness, due to the above.

Rocket Data

In terms of ionospheric region formation, the important upper atmosphere phenomenon that have been, at least partly, determined by rocket-borne instrumentation are pressure, density, temperature, constituents and their height distributions, and incident solar photon flux and its penetration extending over the hard X-ray and ultraviolet portion of the spectrum. With regard to the first items the Rocket Panel Report[23] summarizes the early work. A summarization of additional work to 1954 may be found in the publication "Rocket Exploration of the Upper Atmosphere."[24]

Pressure

A summarization of gauge pressure results up to 130 km has recently been published by Newell.[25] These are believed to be valid to within 10 per cent to 75 km and by a factor of 2 or 3 above this height. In the height range of interest here values given are 0.04 mm of Hg at 70 km to 3×10^{-4} at 100 km. However, recent measures of X-ray attenuation in the 40–50Å range by Friedman and his collaborators gave values in the height range 100 to 128 km which were about $\frac{1}{3}$ less than previously considered. The revised values are now accepted.

Densities

Newell[25] has likewise summarized density measurements obtained from stagnation pressure determinations at the rocket nose and the Rayleigh formula. Values are believed accurate to within 20 per cent for lower heights and a factor of 2 or 3 to about 130 km. These range from 10^{-1} gm/m^3 at 70 km to about 10^{-3} at 100 km. The above mentioned factor of a $\frac{1}{3}$ revision as a result of X-ray measurements is also applicable here.

[14] D. K. Bailey, R. Bateman, L. V. Berkner, H. G. Booker, G. F. Montgomery, E. M. Purcell, W. W. Salisbury, and J. B. Weisner, "A new kind of radio propagation at very high frequencies observable over long distances," *Phys. Rev.*, vol. 88, pp. 141–145; April, 1952.

[15] W. J. Bray, J. A. Saxton, R. W. White, and G. W. Luscombe, "VHF propagation by ionospheric scattering and its application to long-distance communication," *Proc. IEE*, part III, vol. 102, pp. 236–260; October, 1955.

[16] D. K. Bailey, R. Bateman, and R. C. Kirby, "Radio transmission at vhf by scattering and other processes in the lower ionosphere," Proc. IRE, vol. 43, pp. 1181–1230; October, 1955.

[17] V. C. Pineo, "Oblique incidence measurements of the heights at which ionospheric scattering of vhf radio waves occurs," *J. Geophys. Res.*, vol. 61, pp. 165–169; June, 1956.

[18] O. G. Villard, V. R. Eshleman, L. A. Manning, and A. M. Peterson, "The role of meteors in extended-range vhf propagation," Proc. IRE, vol. 43, pp. 1473–1481; October, 1955.

[19] R. Naismith, "A subsidiary layer in the E region of the ionosphere," *J. Atmos. Terr. Phys.*, vol. 5, pp. 73–82; May, 1954.

[20] O. G. Villard, A. M. Peterson, L. A. Manning, and V. R. Eshleman, "Some properties of oblique radio reflections from meteor ionization trails," *J. Geophys. Res.*, vol. 61, pp. 233–247; June, 1956.

[21] A. A. Weiss, "Radio echo observations of meteors in the southern hemisphere," *Aust. J. Phys.*, vol. 8, pp. 148–166; March, 1955.

[22] M. Nicolet, "Meteor ionization and the night-time E-layer," *J. Atmos. Terr. Phys., Special Supplement on Meteor Physics*, vol. 2, pp. 99–110; 1955.

[23] Rocket Panel Report, "Pressures, densities, and temperatures in the upper atmosphere," *Phys. Rev.*, vol. 88, pp. 1027–1032; December, 1952.

[24] "Rocket exploration of the upper atmosphere," *J. Atmos. Terr. Phys., Special Suppl.*, vol. 1; 1954.

[25] H. E. Newell, "Rocket data on atmospheric pressure, temperature, density, and winds," *Ann. de Geophys.*, vol. 11, pp. 115–144; April–June, 1955.

Temperature

As pointed out by Newell,[25] temperatures are commonly derived from pressure and/or density height distribution curves utilizing the equation of state. This involves knowing, or assuming, the mean molecular mass as a function of height. Assuming mixing to be effective to about 90 km with O_2 dissociation starting at this level and the O_2 concentration decreasing linearly to about 150 km (and diffusive separation above), *i.e.*, $\overline{M}=29$ below 90 km and decreasing to an $\overline{M}=20$ at higher levels, Newell obtains: a maximum in temperature of about 270°K at 50 km decreasing to a minimum of 190°K at 75 km and increasing smoothly thereafter at greater heights to 500°K at about 150 km.

Stroud, Nordberg, and Walsh[26] indicate, from sound ranging on the explosions of grenades emitted from rockets, the following nighttime average temperature results for experiments extending over a period of 12 months: 270°K at 50 km with a lapse rate between 55–80 km of −2.5°K/km and a minimum of about 200°K at 80 km. The observed temperature variations between experiments, for a given height, was found to be rather large.

By the application of meteor impact theory Kaiser and Evans[27] deduce scale heights, H, which appear to agree with rocket results rather well. Values deduced are $H=6$ km at 85 km to 8 km at 105 km.

A synthesizing of the above, as well as other, factors has recently been published by Kallman, White, and Newell.[28] A very important conclusion for the purpose of this work is the incorporation of an unpublished deduction of R. A. Minzner to the effect that the temperature remains constant in the altitude range 75 to 91 km at the value 210°K.

Mass Spectra

Rocket-borne mass spectrometer ambient ion distributions to great altitudes were reported by Johnson and Meadows[29] but certain experimental difficulties were originally encountered. In a *nighttime* flight in July, 1955 Johnson and Heppner,[30] only *positive* ions of mass 28, attributed to N_2^+, were noted in the height range 98–120 km and over an experimental range of 5–58 AMU. No negative ions were detected. In a *daytime* flight in November, 1955, Johnson and Heppner,[31] only *negative* ions of masses 16, 22, 29, 32, and 46, attributed to O^-, unknown, unknown, O_2^- and NO_2^-, respectively, were noted in the height range 93–131 km and over an experimental range of 5–60 AMU. No positive ions were detected.

A Bennet rf mass spectrometer, Meadows and Townsend,[32] has been used to determine neutral gas composition over the height range 74–142 km during a *nighttime* flight. In addition to the normal constituents of air, mass numbers 23 (Na) between 80 and 88 km and 46 (NO_2) between 75 and 90 km, both peaking at 85 km, were detected.

Solar Radiation

While solar radiation at wavelengths less than about 3000Å can only be detected at heights above the earth's surface, it is only that portion below about 2400Å that is of importance in the present connection. A summary of the spectrographic results in the range 3000–2000Å was published by Johnson, Purcell, and Tousey.[33]

Friedman[34] has summarized the photon counter observations below 2000Å as follows: at the top of the earth's atmosphere the equivalent black body radiator is 5000°K near 2050Å. In the region 1450 to 1500Å an equivalent temperature of 4050°K. In the region 1100 to 1300Å (containing the L_α line of hydrogen) 3900°K in the surrounding continuum (0.01 erg/cm²/sec/100Å) and about 4500°K at L_α (0.1 to 0.3 erg/cm²/sec). In the soft X-ray region 10^{-3} erg/cm²/sec near 10–20Å and 10^{-2} erg/cm²/sec near 44–60Å. Of importance in this connection is the fact that the maximum rate of absorption of L_α occurs near 75 km for an overhead sun. Hard solar X radiation (<10Å) is found to be variable with solar activity, increasing greatly in intensity during disturbed solar conditions; as does L_α.

Further information concerning the solar radiation in wavelength bands 8–20Å, 44–60Å and 44–100Å for heights to 130 km have been reported by Byram, Chubb, and Friedman.[35] A total flux at the top of the earth's atmosphere over the above entire waveband of 0.1 erg/cm²/sec was determined. These data were utilized to deduce the revised estimates on air density in the height range 100–130 km previously mentioned.

Of considerable importance in this area are unpublished results of Tousey[36] (we are greatly indebted to Dr. Tousey for providing this information before publication) in which L_α at 1215.7Å was observed of value 0.4 erg/cm²/sec while, during the same flight, L_β at 1025.7Å was noted at 0.03 erg/cm²/sec.

[26] W. G. Stroud, W. Nordberg, and J. R. Walsh, "Atmospheric temperatures and winds between 30 and 80 km," *J. Geophys. Res.*, vol. 6, pp. 45–56; March, 1956.
[27] T. R. Kaiser and S. Evans, "Upper atmospheric data from meteors," *Ann. de Geophys.*, vol. 11, pp. 148–152; April–June, 1955.
[28] H. K. Kallman, W. B. White, and H. E. Newell, "Physical properties of the atmosphere from 90 to 300 kilometers," *J. Geophys. Res.*, vol. 61, pp. 513–524; September, 1956.
[29] C. Y. Johnson and E. B. Meadows, "First investigation of ambient positive-ion composition to 219 km by rocket-borne spectrometer," *J. Geophys. Res.*, vol. 60, pp. 193–203; June, 1955.
[30] C. Y. Johnson and J. P. Heppner, "Night-time measurement of positive and negative ion composition to 120 km by rocket-borne spectrometer," *J. Geophys. Res.*, vol. 60, p. 533; December, 1955.
[31] C. Y. Johnson and J. P. Heppner, "Daytime measurement of positive and negative ion composition to 131 km by rocket-borne spectrometer," *J. Geophys. Res.*, vol. 61, p. 575; September, 1956.
[32] E. B. Meadows and J. W. Townsend, "Neutral gas composition of the upper atmosphere by a rocket-borne mass spectrometer," *J. Geophys. Res.*, vol. 61, pp. 576–577; September, 1956.
[33] F. S. Johnson, J. D. Purcell, and R. Tousey, "Measurements of the vertical distribution of atmospheric ozone from rockets," *J. Geophys. Res.*, vol. 56, pp. 583–594; December, 1951.
[34] H. Friedman, "The solar spectrum below 2000 angstroms," *Ann. de Geophys.*, vol. 11(2), pp. 174–180; April–June, 1955.
[35] E. T. Byram, T. A. Chubb, and H. Friedman, "The solar *X*-ray spectrum and the density of the upper atmosphere," *J. Geophys. Res.*, vol. 61, pp. 251–263; June, 1956.
[36] R. Tousey, private communication, 1957.

It will be noted that the ranges 100–1000Å and 1500–2000Å remain essentially unexplored.

D Region

Our discussion concerning *D* region will be confined to possible atmospheric constituents involved in its formation, the solar radiations possibly contributing to its production and an outline of the available material with regards to experimental and theoretically deduced electron density-height (*N-h*) profiles. Recombination at these height levels, and other matters, will be considered towards the end of this work. For the purposes of this discussion *D* region will be *defined* to extend over the height range of approximately 60 to 90 km.

Constituents

Historically, the possible constituents involved in *D*-region formation are NO, Na, O_2 and normal air (with regard to short X rays). Bates and Seaton[37] have conclusively shown that Na cannot be of great consequence for several reasons. Within the last few years O_2 has been favored with regards to *E* region, as will be discussed later. Consequently, there remains normal air, discussed later, and NO. Material relative to air densities and constituent distribution has already been considered. There remains consideration of NO.

Mitra[38] has investigated the general problem of NO production in the height range of interest with the full understanding that many of the required parameters were unknown. The problem requires information concerning processes involving N, O, and N_2O which are as yet inadequately determined. A tentative NO distribution is deduced, assuming complete mixing, which has a maximum at 87 km. It is concluded that a maximum of electron density at about this height can be produced by L_α and of value 10^3 or 10^4 electrons/cm^3 for a feasible magnitude of the recombination coefficient.

Nicolet,[39] in a general study of the aeronomic problem of nitrogen oxides, deduces an NO distribution following the main atmosphere, *M*, with a ratio, $n(\mathrm{NO})/n(M)$, of number density less than 1 in 1000. Considering L_α as the ionizing agent (observed with the aid of rockets to 74 ± 2 km) it is concluded that, with a reasonable recombination coefficient, the peak of electron production would occur in the range 75–77 km for zenith sun. From available information it is deduced that a maximum electron density of 10^3 to 10^4/cm^3 can easily be produced under equilibrium conditions for an approximate NO number density of 10^8/cm^3.

Bates[40] summarizes the situation and concludes that NO is the only possibility that need be considered under normal conditions and indicates that, while NO has not as yet been observed via rocket experiments, theoretical studies such as those mentioned above are conclusive as regards the existence of this minor constituent at relevant heights.

D-Region Electron Density-Height Profiles—Experimental

From the experimental viewpoint, electron density-height profiles for *D*-region heights have been determined by radio techniques and with the aid of rocket-borne instrumentation. The radio results, Gardner and Pawsey,[10] Fejer,[11] and Gregory[13] have been discussed.

Seddon[41] has summarized the results of certain rocket-borne radio propagation experiments which have led to electron density profiles yielding 10^4 electrons/cm^3 at 88 km with smaller values at 85 and 90 km. Small values were also noted down to about 50 km during a daytime flight. The major limitation to date in such experiments, as far as *D* region is concerned, is that 10^4 electrons/cm^3 is the minimum density that can be measured with confidence and this appears to be on the upper borderline for expected densities.

D-Region Electron Density-Height Profiles—Theoretical

Theoretical *D*-region profiles were deduced some time ago by Pfister[42] and by Mitra[43] assuming that O_2 was the constituent involved in region formation. Bracewell[44] theoretically investigated the possibility of *D*-region formation with an unspecified minor constituent in an intense radiation field. As a result of more recent determinations of various rate coefficients, etc., these models are no longer believed to be valid.

An entirely empirical *D*-region model has been obtained on the basis of various long and short-wave radio data by Sato.[45] A modified Chapman distribution of electron density is deduced having the following characteristics: a maximum density of 2×10^4 electrons/cm^3 for summer noon at a height of about 92 km becoming 10^4 in winter. Similarly, at 90 km values of $1.8\ 10^4$ and 9×10^3 and at 75 km 6×10^2 and 3×10^2.

Further empirical *D*-region models have been determined by Nertney[6] on the basis of various long-wave experimental data and by Kobayashi[46] utilizing certain

[37] D. R. Bates and M. J. Seaton, "Theoretical considerations regarding the formation of the ionized layers," *Proc. Phys. Soc.*, vol. 63, pp. 129–140; January, 1950.

[38] A. P. Mitra, "A tentative model of the equilibrium height distribution of nitric oxide in the high atmosphere and the resulting *D*-layer," *J. Atmos. Terr. Phys.*, vol. 5, pp. 28–43; January, 1954.

[39] M. Nicolet, "The aeronomic problem of nitrogen oxides," *J. Atmos. Terr. Phys.*, vol. 7, pp. 152–169; September, 1955.

[40] D. R. Bates, "Formation of the ionized layers," *J. Atmos. Terr. Phys., Special Supplement on Solar Eclipses and the Ionosphere*, vol. 6, pp. 184–187; 1956.

[41] J. C. Seddon, "Propagation measurements in the ionosphere with the aid of rockets," *J. Atmos. Terr. Phys., Special Supplement on Rocket Exploration of the Upper Atmosphere*, vol. 1, pp. 214–222; 1954.

[42] W. Pfister, "Effect of the *D*-ionospheric layer on very low-frequency radio waves," *J. Geophys. Res.*, vol. 54, pp. 315–337; December, 1949.

[43] A. P. Mitra, "The *D*-layer of the ionosphere," *J. Geophys. Res.*, vol. 56, pp. 373–402; September, 1951.

[44] R. N. Bracewell, "Theory of formation of an ionospheric layer below *E* layer based on eclipse and solar effects at 16 kc/sec.," *J. Atmos. Terr. Phys.*, vol. 2, pp. 226–235; 1952.

[45] T. Sato, "The electron density of the *D* region," *J. Geomag. Geoelec.*, vol. 4, pp. 44–56; July, 1952.

[46] T. Kobayashi, "*D-E* layer electron model reduced from considerations of MF and HF wave absorption," *J. Rad. Res. Lab. (Japan)*, vol. 2, p. 399; 1955.

"*D-E* electron model revised from considerations referring diurnal variation of experimental results," *J. Rad. Res. Lab. (Japan)*, vol. 3, p. 279; 1956.

long-wave results as well as short-wave absorption data. Nertney's diurnal and seasonal model yields a maximum electron density of about 600 electrons/cm^3 at a height of 80 km for an overhead sun. A distinct layer is determined with the "shape" of the upper portion determined by a "scale height" of about 6 km and the lower portion of about 8–10 km. Kobayashi[46] assumes a Chapman model with an overhead sun critical frequency of 210 kc at 80 km and the electron densities for D region going to essentially zero at 60 and 90 km. Excellent agreement is indicated between medium wave and high-frequency wave oblique incidence absorption measurements, experiment and theory, with this model. In his second paper Kobayashi[46] incorporates height variations of recombination coefficient and scale height in his models.

The theoretical work in connection with physical D-region characteristics on the basis of NO by Mitra[38] and Nicolet[39] has already been discussed as well as the summarization concerning these matters by Bates.[40]

A composite, equinox noon electron density-height distribution has recently been deduced by Houston[47] (unpublished) on the basis of all available radio and rocket results. The characteristics are given in Table I. below. For completeness, the table has been extended somewhat above the heights normally associated with D region.

TABLE I

ELECTRON DENSITY-HEIGHT PROFILE—65–110 KM

Height (km)	Electron Density (cm^3)		
65	10	85	1.5×10^4
70	1.5×10^2	87	10^4
72	2×10^2	89	6×10^3
75	1.6×10^2	90	10^4
77	1.3×10^2	95	4×10^4
80	5×10^2	100	10^5
81	3.5×10^3	110	1.6×10^5
82	9×10^3		

LOWER E REGION

As for D region, our discussion concerning the lower E region will be initially confined to atmospheric constituents, solar radiations, and electron-density height profiles. In this case it will also be necessary to consider certain meteoric effects.

For the purpose of this discussion lower E region will be defined as extending over the approximate height range of 90 to about 110 km.

Constituents

As regards E region, there appears to be unanimity of opinion that the possible constituents involved are O_2 (photoionization at first ionization potential, 1027Å-L_β, 1025.7Å), normal air (soft X rays) and/or constituents resulting from meteoric effects. We shall deal with these in turn.

[47] R. E. Houston, private communication, 1957.

After many years of study by various workers the O_2-O problem has recently been solved and verified by rocket experiments. Utilizing various rocket procured data and considering the relative times of mixing, diffusion, and dissociation of O_2 and recombination of O, Nicolet and Mange[48] deduced radically new estimates of the O_2-O height distributions in the upper atmosphere. They concluded: O_2 is not dissociated below 90 km. The major portion of the dissociation takes place in the height range 90–100 km. There is a relatively large amount of O_2 above the dissociation region due to diffusive transport and mixing. O_2 follows the distribution of the main atmosphere above about 160 km.

In a further general study of O_2 dissociation, Nicolet[49] obtains further quantitative relations indicating that above about 110 km, O_2 follows a diffusive equilibrium resulting in many orders of magnitude larger O_2 number densities at F_1 and F_2 region heights in comparison to that determined assuming photoequilibrium conditions. It is further determined that mixing is the controlling factor below about 100 km due to the life time of O. Finally, an O_2-O distribution in the transition region is determined showing that this occurs between 95 and 105 km with an O maximum of about 2×10^{12} at about 105 km.

Verification of the above over the height range 110–130 km was reported by Byram, Chubb, and Friedman,[50] who determined the O_2 height distribution in this range with the use of photon counters sensitive in the range 1425–1500Å; near the maximum of the O_2 continuum and where O and N_2 effects may be neglected.

With regard to air ionized by soft X rays in the formation of E region, the rocket results on densities in the relevant height range has already been noted and the summarization of relevant X-ray intensities by Friedman[34] outlined. Similar comments apply to meteoric contributions. All of these items will be further considered in the following.

Lower E-Region Electron Density-Height Profiles—Experimental

Probably in view of the experimental difficulties involved there appears to be but little work reported in the recent literature with regard to the determination of electron density-height profiles in the lower E region by radio methods. The outstanding low frequency sweep experiments of Watts and Brown[8] already described, and the various very low, low, and medium-frequency radio experiments previously considered are the exceptions to this statement. Most of the latter, being single frequency experiments, are only suitable for the determination of a composite profile.

[48] M. Nicolet and P. Mange, "The dissociation of oxygen in the high atmosphere," *J. Geophys. Res.*, vol. 59, pp. 15–45; March, 1954.

[49] M. Nicolet, "The aeronomic problem of oxygen dissociation," *J. Atmos. Terr. Phys.*, vol. 5, pp. 132–140; July, 1954.

[50] E. T. Byram, T. A. Chubb, and H. Friedman, "Dissociation of oxygen in the upper atmosphere," *Phys. Rev.*, vol. 98, pp. 1594–1597; June, 1955.

With regard to rocket-borne measurements the situation is indeed greatly different. Thus, Seddon[51] reports a monotonic increase of electron density in the height range of interest, for a daytime flight, from approximately 0 at 90 km to about 1.6×10^4 at 105 km. Seddon, Pickar, and Jackson[52] in a later flight, deduce $N=10^4$ at 84 km increasing slowly to a slightly larger value at 92 km. From 92 to 100 km the electron density increases rapidly to about 10^5 electrons/cm^3. Jackson[53] indicates a monotonic increase from 10^4 at 92 km to 1.3×10^5 near 110 km. These plus previous flights are shown to yield lower E electron-density height gradients of from 7×10^3 to 10^4 electrons/cm^3/km for midmorning conditions. A summary NRL report has been published by Seddon[54] concerning the above work; which is based on cw techniques.

Lien, Marcou, Ulwick, Aarons, and McMorrow[55] describe rocket-borne experiments utilizing the relative time delay between pulses on two different frequencies, one of which is so high as to be essentially unaffected by the ionosphere, as the rocket proceeds into the ionosphere. The results of several midday flights covering the height range of about 90 to 130 km are given. Bifurcation is frequently noted with the lower maximum of about 5×10^4 electrons/cm^3 at approximately 95 km; the upper of value 10^5 or larger and at 110 to 120 km.[56]

Finally, Berning[57] describes results obtained using a high-frequency rocket tracking scheme. A detailed N-h profile is deduced during a flight extending to 219 km.

Lower E-Region Electron Density-Height Profiles—Theoretical

In our preceding discussion concerning D region it was concluded that, under quiet sun conditions, the solar radiation effective and the atmospheric constituent involved are now believed to be established. On this basis, the major remaining difficulty in the determination of a quiet D-region electron density-height distribution is the value of the NO density as a function of height; if current estimates regarding the recombination coefficients can be accepted.

Essentially the inverse problem exists with regard to the lower E region; in major part. While the major characteristics of the predominate constituents involved, O_2 and normal air, are known, the contributions of the competing ionizing processes remains to be clarified.

Until recently the major theoretical studies concerning E-region electron density profiles have involved extensions of the original Chapman theory to include a scale height gradient. Jones[58] extended this type of analysis by including essentially all variables, in great part from the then available rocket results, and with the assumption that the constituent involved was O_2; the ionization resulting from solar radiation in the range of 1000Å. By, in addition, utilizing various radio data an empirical O_2 height distribution is deduced which appeared to be a reasonable compromise with theory. The resulting N model approaches zero at about 86 km, for overhead sun, with a maximum varying from 95 km for zenith angle $\chi=0$ to 120 km for $\chi=90°$. The lower portion of the resulting models are very sharp compared to a Chapman and, for $\chi=45°$, yield an N gradient approaching 10^3 electrons/cm^3/km.

Continuing the above, Parkinson[59] using the above Jones[58] E model and the Mitra[38] D model deduces a nighttime lower E region model employing a nighttime recombination coefficient height and time distribution to be discussed later. By determining sunset electron density-height profiles from comparisons with theory and experiment, profiles in the height range 85 to 100 km are determined as functions of time after sunset and season. Comparison of theory and experiment, of various radio data, with the models results in good agreement. Finally, Mitra[60] in a general study of the nighttime ionization in the lower ionosphere deduces electron density-height profiles as a function of time of night on the basis of an original known sunset model from radio data. The profiles cover the range 88 to 110 km and yield the following N values at the following heights at sunset and 8 hours after sunset: 90 km—6×10^2, 4×10^2; 100—3×10^3, 1.8×10^3; 110—4×10^4, 7×10^3.

The situation with regard to formation of E region due to the ionization of air at relevant heights by soft X rays has recently become of major interest in view of rocket-borne, presumably, solar X-radiation measurements within the last few years. Rawer and Argence,[61] utilizing the then available data and estimates of O_2 distributions, exhaustively studied this problem and concluded that E region could not be accounted for by the O_2 distribution then available under the influence of

[51] J. C. Seddon, "Electron densities in the ionosphere," *J. Geophys. Res.*, vol. 59, pp. 463–466; December, 1954.

[52] J. C. Seddon, A. D. Pickar, and J. F. Jackson, "Continuous electron density measurements up to 200 km," *J. Geophys. Res.*, vol. 59, pp. 513–524; December, 1954.

[53] J. E. Jackson, "Measurements in the E-layer with the navy viking rocket," *J. Geophys. Res.*, vol. 59, pp. 377–390; September, 1954.

[54] J. C. Seddon, "Rocket Investigations of the Ionosphere by a Radio Propagation Method," Naval Res. Lab. Rep. No. 4304, 1954.

[55] J. R. Lien, R. J. Marcou, J. C. Ulwick, J. Aarons, and D. R. McMorrow, "Ionosphere research with rocket-borne instruments," *J. Atmos. Terr. Phys., Special Supplement on Rocket Exploration of the Upper Atmosphere*, vol. 1, pp. 223–239; 1954.

[56] More recent, unpublished, analysis of these data has lead to the conclusion that the previously indicated bifurcation was due to certain trajectory considerations. The actual electron density distribution is now believed to be laminations in density, as a function of height, superimposed on an average smooth height profile.

[57] W. W. Berning, "The determination of charge density in the ionosphere by radio Doppler techniques," *J. Atmos. Terr. Phys., Special Supplement on Rocket Exploration of the Upper Atmosphere*, vol. 1, pp. 261–273; 1954.

[58] R. E. Jones, "The development of an E-region model consistent with long-wave phase path measurements," *J. Atmos. Terr. Phys.*, vol. 6, pp. 1–17; January, 1955.

[59] R. W. Parkinson, "The night-time lower ionosphere as deduced from a theoretical and experimental investigation of coupling phenomena at 150 kc/s," *J. Atmos. Terr. Phys.*, vol. 7, pp. 203–234; October, 1955.

[60] A. P. Mitra, "Nighttime ionization in the lower ionosphere—part II—distribution of electrons and positive and negative ions," *J. Atmos. Terr. Phys.*, in press, 1957.

[61] K. Rawer and E. Argence, "Considérations critiques relatives à la formation de la region E de l'ionosphere," *Ann. de Geophys.*, vol. 9, pp. 1–25; January–March, 1953.

ultraviolet radiation whereas X radiation in the range 10 to 800Å, utilizing Elwert's solar model of 1952 and a $10^{6°}$K sun, could satisfactorily agree with experiment. A profile, overhead sun, having a maximum of 1.5×10^5 electrons/cm^3 at about 120 km and a "thickness" at $N=10^5$ levels of 50 km, going to approximately zero at about 85 km, was deduced. It is now known that the O_2 model used was inadequate. Even to date, no rocket measurements have been made in the 100–1000Å band so that the above pioneer work must now be considerably modified.

The recent soft X-ray rocket data reported by Friedman,[34] Byram, Chubb, and Friedman,[35] have already been summarized. The apparently first really quantitative measurements of X radiation in the height and frequency range of interest were reported by Byram, Chubb, and Friedman.[62] In spite of experimental difficulties, fluxes of 0.6 erg/cm^2/sec in the 8–18Å band and 1 erg/cm^2/sec in the 10–60Å range were determined. It is concluded that the total 1 or 2 ergs/cm^2/sec available in the solar X-ray spectrum is adequate to account for E region; although these estimates were subsequently somewhat reduced.

Watanabe, Marmo, and Pressman[63] presented an excellent summarization of the situation with regard to the competing processes in E-region formation. With the aid of detailed arguments it is shown that the several objections to the theory that E region is due to the photoionization of O_2 may satisfactorily be accounted for. In particular, it is pointed out that L_β (1025.7Å) may well be of importance in E-region production. The above matters have also been summarized by Bates.[40]

Nicolet[64] has recently considered these questions. On the basis of Tousey's measurements, previously mentioned, of L_β it is concluded that the E-region maximum of electron density is produced by an essentially monochromatic process involving L_β and O_2. The over-all electron density profile, however, will result from contributions from relevant portions of the soft X-ray spectrum acting on the various atmospheric constituents. Thus the over-all E-region shape will be more closely associated with that expected for band absorbed radiation.

The question of possible meteoric contributions to the lower E-region distribution, particularly for low over-all densities, *i.e.*, at night, has already been discussed.

In summary, it now appears that the process of E-region production is quite complex and involves both soft X-ray and ultraviolet solar radiations; the latter in the neighborhood of 1000Å. Normal air, at relevant levels, is the constituent probably ionized with major or predominate contributions from O_2 at certain levels. Under suitable conditions meteoric contributions must also be considered.

Recombination Coefficient

The recombination process is, of course, important in that it is largely the dissipative process in region formation. In view of relatively recent considerable advances the processes involved are far better understood than was the case but a few years ago. An excellent summary, including, in particular, the lower ionosphere has recently been published by Bates.[65]

Aside from eclipse results, which will not be considered here, two studies relevant to the lower ionosphere have recently been concluded. With respect to daytime recombination, Mitra and Jones[66] have deduced a recombination, α, vs height curve from a large variety of radio data and by various means. Certain sudden ionospheric disturbance experimental data are also found to lie on the resulting curve. α is found to vary from about 10^{-5} cm^3/sec at 65 km, 10^{-7} at 90 km and about 5×10^{-8} at 110 km. It is deduced that recombination through negative ions predominates below about 90 km whereas dissociative recombination predominates in the range 90 to 110 km with a transition region for the processes in the level 80 to 90 km.

Regarding nighttime recombination, Mitra[67] has concluded that both height and time variations must be considered. His study is based on an initial sunset model obtained from various radio data, although it is shown that the actual model does not appreciably affect his results. From these and other radio data, throughout the night, α is determined as a function of height for various times—leading to the following conclusions: below about 80 km, recombination processes involve negative ions and a decrease in α in time is attributed to a decrease in the negative ion to electron ratio. Above about 90 km dissociative recombination is influenced (as suggested by Nicolet[22]) by meteoric ions of low ionization potential resulting first in an initial increase in α near sunset but with a subsequent decrease as time progresses. In general, at night α is found to decrease with increasing altitude and with time (after sunset). For example, at 100 km, α at sunset is deduced to have the value of about 1.5×10^{-8} cm^3/sec reducing to 5×10^{-9} cm^3/sec six hours after sunset. Similar figures at 90 km are about 5×10^{-8} and 2×10^{-8} cm^3/sec.

Sudden Ionospheric Disturbance Effects

As far as is known at the moment, the major effects of solar flares and similar solar disturbances on the

[62] E. T. Byram, T. A. Chubb, and H. Friedman, "Solar X-rays and E-layer ionization," *J. Atmos. Terr. Phys., Special Supplement on Rocket Exploration of the Upper Atmosphere*, vol. 1, pp. 274–275; 1954.

[63] K. Watanabe, F. F. Marmo, and J. Pressman, "Formation of the lower ionosphere," *J. Geophys. Res.*, vol. 60, pp. 513–519; December, 1955.

[64] M. Nicolet, private communication, 1957.

[65] D. R. Bates, "Recombination in the ionosphere," *J. Atmos. Terr. Phys., Special Supplement on Solar Eclipses and the Ionosphere*, vol. 6, pp. 191–197; 1956.

[66] A. P. Mitra and R. E. Jones, "Recombination in the lower ionosphere," *J. Geophys. Phys.*, vol. 59, pp. 391–406; September, 1954.

[67] A. P. Mitra, "Nighttime ionization in the lower ionosphere—Part I—recombination processes," *J. Atmos. Terr. Phys.*, in press.

earth's atmosphere take place in lower E region and below. Of current great interest are the relative contributions of L_α and hard solar X radiation in the production of the enhanced ionization associated with such solar disturbances.

Friedman and Chubb[68] have prepared an excellent summary of the problem; stressing the possible contributions of intense 1–2Å X radiations which might be expected in view of observed variations in intensity below about 15Å (to about 6Å) with the aid of rockets during disturbed solar conditions.

Of interest within the immediate past are the various radio results obtained during the intense solar flare of February 23, 1956, which was observed in Tokyo starting at 0334U.T. This was most unusual in view of the radio variations observed in the dark hemisphere of the earth during the flare. Confining attention to long radio wave results; Belrose, Devenport, and Weekes[69] report a decrease in 16-kc phase height of 8 km during the event to a minimum height of 79 km for the reflection level. At oblique incidence, in the frequency range 70–300 kc, the following midday heights were depressed by 4 or 5 km and the attenuation was increased by a factor of 6 over the normal. Pierce[70] determined a depression in height of 16-kc transatlantic signals which exceeded that usually noted in going from night to day under normal conditions. Ellison and Reid[71] noted a marked diminution in the intensity of atmospherics near 24 kc and ascribe their result to the effect of cosmic ray particles on D region. Houston, Ross, and Schmerling,[72] utilizing 75-kc vertical incidence pulse observations, noted a sharp increase in absorption, a decrease in phase height of 8 km but no change in group height during the event.

It is evident that the study of the effects of solar flares and other disturbed sun phenomenon on the lower ionosphere provides a fruitful field for further research.

Movements

An excellent summary concerning horizontal movements in the ionosphere was published by Briggs and Spencer.[73] While, at least in part, a portion of the motions studied most have occurred in the lower ionosphere, relatively little experimentation has taken place utilizing long radio waves. Since the publication of this summary, the following relevant material has appeared in the literature.

Manning, Peterson, and Villard[74] utilizing meteor body Doppler observations deduced vector average drift and rms horizontal and vertical drift components in the height range 80 to 120 km. Typical horizontal average and rms values of 100 and 180 km per hour, respectively, are cited. The average vertical drift is less than 5 meters per second with the rms value between zero and 60 km per hour. Mitra and Peiffer[75] deduce a sinusoidal vertical semidiurnal velocity of drift of 1 km per hour with maximum upward motion at 21:00 in attempting to explain certain long radio wave observations at night.

In a general study of the fading of radio waves in the frequency range 16 to 2400 kc, Bowhill[76] determines quasi-periods of 7 minutes up to 70 kc while above, approximately, this frequency a 1 minute period appears and predominates at about 200 kc and above. From these data and spatial correlations, utilizing more than one receiver, structure sizes of 5 km for the slow and 1 km for the fast fading periods are deduced; leading to a model of the irregularities in the lower ionosphere which would explain the observations. Irregularity sizes deduced are 6 km near 90 km and below and approximately $\frac{1}{2}$ km near the height 100 km.

Pant[77] has determined a general model of the circulation in the upper atmosphere which will be of value in such future studies.

Conclusion

In view of the brief summarizations appearing throughout the body of this report, it is believed that the following conclusions will suffice:

1) In comparing the present material with that prepared in 1955 (Waynick[78]) it is evident that great strides have been made concerning our knowledge of the lower ionosphere within the last two or three years; 2) the determination of the electron density-height profiles in the lower E and D regions with the aid of revised rocket techniques (present methods are only capable of determining electron densities down to approximately 10^4 electrons/cm^3) would be of inestimable value in further studies; and 3) we appear to be at the threshold of the solution of many problems concerning the lower ionosphere which ionospheric physicists have sought for many years.

[68] H. Friedman and T. A. Chubb, "Solar X-ray emission and the height of the D layer during radio fade-out," *Proc. Conf. Phys. Ion.*, Phys. Soc. (London), pp. 58–62; 1955.

[69] J. S. Belrose, M. H. Devenport, and K. Weekes, "Some unusual radio observations made on 23 February 1956," *J. Atmos. Terr. Phys.*, vol. 8, pp. 281–286; March, 1956.

[70] J. A. Pierce, "VLF phase shifts associated with the disturbance of February 23, 1956," *J. Geophys. Rev.*, vol. 61, pp. 475–483; September, 1956.

[71] H. Ellison and J. H. Reid, "A long-wave anomaly associated with the arrival of cosmic-ray particles of solar origin on 23 February 1956," *J. Atmos. Terr. Phys.*, vol. 8, p. 291; March, 1956.

[72] R. E. Houston, W. J. Ross, and E. R. Schmerling, "Some effects of intense solar activity on radio propagation," *J. Atmos. Terr. Phys.*, in press.

[73] B. H. Briggs and M. Spencer, "Horizontal movements in the ionosphere," *Reps. on Prog. in Phys.*, vol. 17, pp. 245–280; 1954.

[74] L. A. Manning, A. M. Peterson, and O. G. Villard, "Ionospheric wind analysis by meteoric echo techniques," *J. Geophys. Res.*, vol. 59, pp. 47–62; March, 1954.

[75] A. P. Mitra and H. R. Peiffer, "The effect of vertical ion transport on the nighttime E-region," *J. Atmos. Terr. Phys.*, vol. 6, pp. 291–303; June, 1955.

[76] S. A. Bowhill, "The fading of radio waves of frequencies between 16 and 2,400 kc/s," *J. Atmos. Terr. Phys.*, vol. 8, pp. 129–145; January, 1956.

[77] P. S. Pant, "Circulation in the upper atmosphere," *J. Geophys. Res.*, vol. 61, pp. 459–474; September, 1956.

[78] A. H. Waynick, "The lowest ionosphere," *Proc. Conf. Phys. Ion.*, Phys. Soc. (London), pp. 1–14; 1955.

Reflection at a Sharply-Bounded Ionosphere*

IRVING W. YABROFF†

Summary—A quantitative description of the waves transmitted into and reflected from a sharply-bounded, anisotropic ionosphere with losses is given. Given curves show the effects of the earth's field and losses for a particular model of the nighttime E layer at vlf.

Introduction

OVER the past forty years, many attacks have been made on selected portions of the problem of oblique-incidence reflection from a sharply-bounded ionosphere. The isotropic case has been discussed by Stratton [1]. Booker [2] treated the wave in the anisotropic ionosphere for the lossless case and indicated a means of extension to the case of very small losses. Bremmer [3] gave an expression for the reflection coefficients, applicable to the lossless case. Budden [4] and Wait [5] calculated reflection coefficients for the case in which the Q-L approximation applied; the wave frequency is much lower than the gyro frequency and the plane of incidence is in the magnetic meridian.

It is the purpose of this paper to show how the previous work can be extended in the following respects: 1) The plane of incidence need not be in the magnetic meridian, 2) wave normal directions are calculated inside a lossy medium, and 3) no limitation is put on the wave frequency.

A numerical example is presented which illustrates for the first time (as far as is known) the behavior of the four reflection coefficients, the wave normal direction, and the rate of attenuation as the inclination of the earth's field is varied. Also shown is an example of behavior of the reflection coefficients and the wave normal direction as the angle of incidence is varied. A more complete set of numerical results will be published later.

Theory of Solution

An infinite plane electromagnetic wave propagating in free space is incident upon the plane boundary of a homogeneous, anisotropic absorptive ionosphere. Parameters used to describe the ionosphere are well known plasma, gyro, and collision frequencies defined below:

$$f_0^2 = \frac{Ne^2}{4\pi^2\epsilon_0 m} = \text{square of plasma frequency}$$

$$f_H = \frac{u_0 H_0}{2\pi m} = \text{gyro frequency}$$

$$\nu = \text{collision frequency}$$

where

N = electron density
H_0 = strength of earth's magnetic field
$-e$ = charge on an electron
m = mass of an electron
V = velocity of an electron
ϵ_0 = dielectric constant of free space $= 8.854 \cdot 10^{-12}$
u_0 = permeability of free space $= 4\pi \cdot 10^{-7}$

The coordinate system used is shown in Fig. 1.

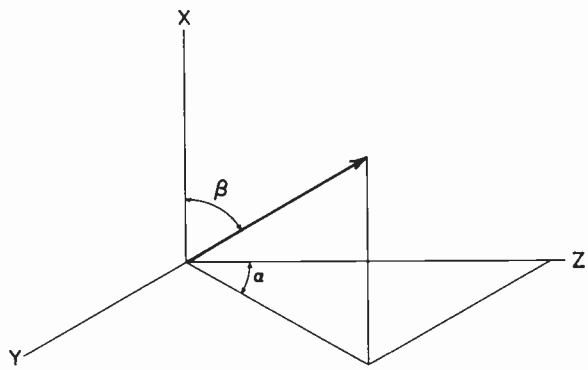

Fig. 1—Coordinate system.

The boundary is the plane $x = 0$. The ionosphere is at $x > 0$, free space at $x < 0$. Direction is described in terms of α, azimuthal angle, and β, vertical angle. The earth's magnetic field is in the $x-z$ plane at an angle β_e from the vertical. The incident wave is traveling in free space in a direction α_i, β_i. Variation of the fields of this wave is described by the real part of

$$F = F_i \exp \frac{j\omega}{c} (ct - x \cos \beta_i - y \sin \beta_i \sin \alpha_i - z \sin \beta_i \cos \alpha_i)$$

where F_i is the complex magnitude of the field at the boundary. The variation of the reflected wave is of the same form except its direction is α_i, $180° - \beta_i$.

The boundary conditions specify that the total fields tangential to the boundary must be continuous across the boundary. Thus, the field variation of the transmitted waves must be the same along the boundary as that of the incident and reflected waves. The only direction in which the variation of the field components is unspecified by the boundary conditions is the vertical. This variation must be found from the characteristics of the medium. The field variation of each of the transmitted waves can be represented as the real part of

$$F = F_t \exp j \frac{\omega}{c} (ct - Dx - y \sin \beta_i \sin \alpha_i - z \sin \beta_i \cos \alpha_i)$$

where D is a complex constant.

* Original manuscript received by the IRE, March 4, 1957. This research was supported in part by the U. S. Air Force, through the AF Cambridge Res. Center under Contract No. AF 19 (604)-785 and through the AF Office of Sci. Res. of the Air Res. and Dev. Command under Contract No. AF 18 (603)-126. Paper presented at Symposium on Propagation of Very-Low-Frequency Electromagnetic Wales, Boulder, Colo.; January 23–25, 1957.

† Stanford University, Stanford, Calif.

The physical picture of this transmitted wave is that of a set of periodically varying fields whose surfaces of constant phase are planes traveling in the direction

$$\alpha_t = \alpha_i, \qquad \beta_t = \tan^{-1}\frac{\sin\beta_i}{\mathrm{Re}\,(D)},$$

with a phase velocity

$$V_p = \frac{c}{\sqrt{(\mathrm{Re}\,D)^2 + \sin^2\beta_i}}$$

where Re (D) = real part of D.

The fields attenuate exponentially in the vertical direction at a rate, in nepers per unit distance, of

$$\frac{\omega}{c}\,\mathrm{Im}\,(D)$$

where Im (D) = imaginary part of D. Thus, there is attenuation both in the direction of phase propagation and at right angles to it (unless $\beta_i = 0$). Stratton calls this type of wave an "inhomogeneous plane wave."

Maxwell's equations and the equation of motion of an electron may be written as

$$\nabla \times E = -u_0\frac{\partial H}{\partial t}$$

$$\nabla \times H = -NeV + \epsilon_0\frac{\partial E}{\partial t}$$

$$m\frac{dV}{dt} = -eE - mvV - u_0(V \times H_0).$$

These equations are solved simultaneously to eliminate the three components of magnetic field and the resulting three equations are in matrix form,

$$\begin{pmatrix} m_{11}-a^2 & m_{12}+a_TD & m_{13}+a_LD \\ -m_{12}+a_TD & m_{22}-D^2-a_L{}^2 & m_{23}+a_La_T \\ m_{13}+a_LD & -m_{23}+a_La_T & m_{33}-D^2-a_T{}^2 \end{pmatrix}\begin{pmatrix} E_x \\ E_y \\ E_z \end{pmatrix} = 0$$

where

$$m_{11} = 1 - \frac{s^2-h_L{}^2}{s(s^2-h^2)} \qquad m_{22} = 1 - \frac{s}{s^2-h^2} \qquad s = \frac{1-j\dfrac{v}{2\pi f}}{\dfrac{f_0{}^2}{f^2}}$$

$$m_{12} = -j\frac{h_T}{s^2-h^2} \qquad m_{23} = -j\frac{h_L}{s^2-h^2} \qquad h = \frac{f_H}{f_0{}^2}$$

$$h_L = h\cos\beta_e$$

$$h_T = h\sin\beta_e$$

$$m_{13} = \frac{h_Lh_T}{s(s^2-h^2)} \qquad m_{33} = 1 - \frac{s^2-h_T{}^2}{s(s^2-h^2)} \qquad a = \sin\beta_i$$

$$a_L = \sin\beta_i\cos\alpha_i$$

$$a_T = \sin\beta_i\sin\alpha_i.$$

In order for a solution to exist (other than $E = 0$), the determinant must vanish. Setting the determinant equal to zero, we obtain

$$a_4D^4 + a_3D^3 + a_2D^2 + a_1D + a_0 = 0$$

where

$$a_4 = m_{11}$$

$$a_3 = 2a_Lm_{13}$$

$$a^2 = m_{33}a_L{}^2 + m_{22}a_T{}^2 + m_{11}(a^2 - m_{33} - m_{22}) + m_{12}{}^2 + m_{13}{}^2$$

$$a_1 = 2m_{13}(a_L{}^3 + a_La_T{}^2) - 2a_Lm_{22}m_{13}$$

$$a_0 = (m_{33} - a_T{}^2)(m_{22} - a_L{}^2)(m_{11} - a^2) + (m_{33} - a_T{}^2)m_{12}{}^2 - (m_{22} - a_L{}^2)m_{13}{}^2 + 2m_{23}m_{13}m_{12} - (a_L{}^2a_T{}^2 - m_{23}{}^2)(m_{11} - a^2).$$

The four complex roots of the quartic represent the two upgoing and the two downgoing characteristic waves which can propagate independently in the medium. For the purposes of this problem, only the values of D for the two upgoing waves are used.

It might at this point be noted that when losses are absent ($v = 0$),

$$D^2 + \sin^2\beta_i = M^2.$$

This is the square of the complex magneto-ionic refractive index according to the Appleton-Hartree formula [6]. The reason for this is that the magneto-ionic formula is derived from the assumption that all derivatives parallel to the planes of constant phase are zero. This condition is satisfied if the medium is lossless.

In addition to the calculation of D for each of the two transmitted waves, five of the six field components E_x, E_y, E_z, H_x, H_y, and H_z can be found for each of the two waves in terms of the sixth from the above set of equations. Finally, application of the continuity of the tangential E and H fields over the boundary results in four simultaneous equations, from which the magnitude and phase of the excited fields can be obtained.

As an independent check upon the above computation, the continuity of the total H field normal to the boundary can be used, since it was not used explicitly in the boundary equations. Another check which can be used is the requirement that the components of the real part of the total Poynting vector normal to the boundary must be continuous across the boundary. Both of these checks were satisfied in the numerical computations.

A Numerical Example

To illustrate the theory, numerical calculations were made for two specific models of the nighttime E layer ($f_0 = 667$ kc, $v = 1$ mc and 0, $f_H = 1.27$ mc) and a wave frequency of 10 kc. The properties of the model with losses are similar to those of a very dense lossy dielectric

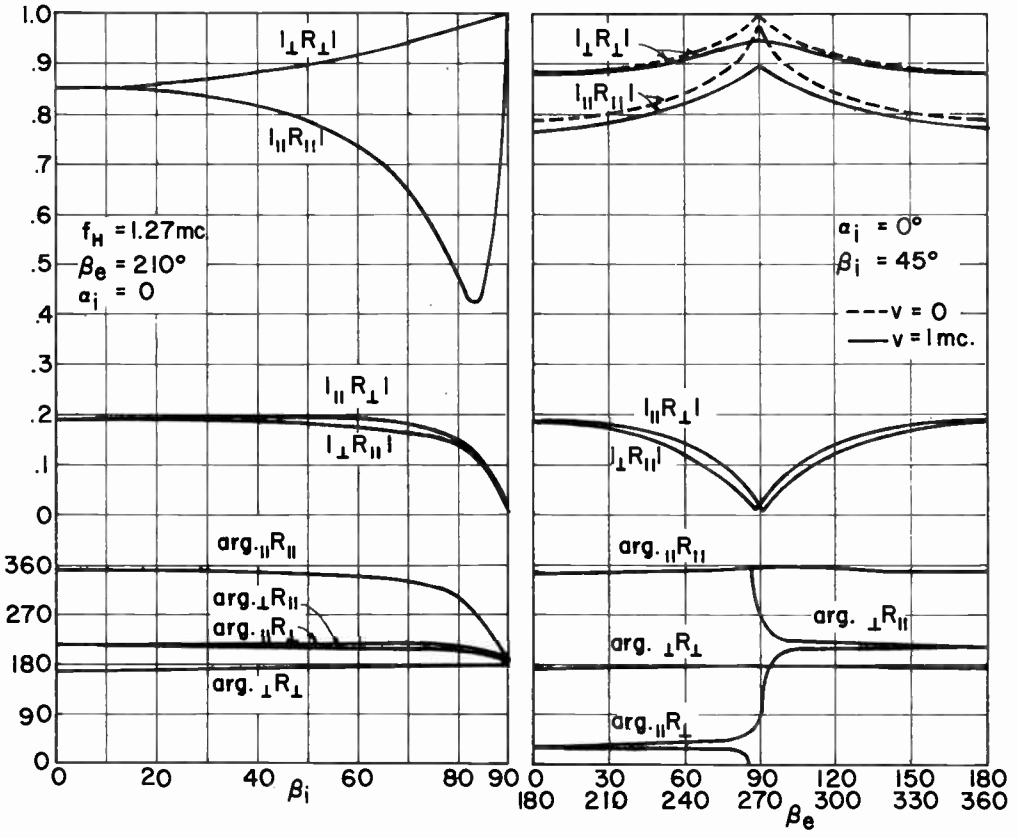

Fig. 2—Reflection coefficients vs vertical angle of incidence.

Fig. 3—Reflection coefficients vs direction of earth's field.

when the earth's field is neglected. The effect of losses and the earth's field is demonstrated through calculation of the following characteristics of the reflected and transmitted waves as functions of angle of incidence and direction of the earth's field:

1) Reflection coefficients.
2) Direction of wave normal.
3) Rate of vertical attenuation.

Reflection Coefficients

The complex ratios of the E fields of the incident and reflected waves have been calculated for two polarizations of the incident wave: parallel polarization in which the E field vector is in the vertical plane of incidence, and perpendicular polarization in which the E field vector is perpendicular to that plane. In general, there are four reflection coefficients: $_\parallel R_\parallel$, $_\perp R_\perp$, $_\parallel R_\perp$, and $_\perp R_\parallel$. The first subscript refers to the E field direction of the incident wave, while the second subscript refers in the same way to the reflected wave.

If collisions and the earth's field are neglected, the reflection coefficients have unit magnitude and $_\parallel R_\perp$ and $_\perp R_\parallel$ are zero, since the plasma frequency exceeds the wave frequency. Figs. 2 and 3 show the variation of the reflection coefficients with and without collisions when the earth's field is included. The change in Fig. 2, when collisions are added, is small and is not shown.

Fig. 3 shows that the sense of the earth's field (whether it is positive or negative) has no effect upon the reflection coefficients except to determine the sense of $_\parallel R_\perp$ and $_\perp R_\parallel$. Figs. 2 and 3 were calculated for the plane of incidence in the magnetic meridian. In any other plane of incidence (α varied through 360°), the reflection coefficients change only negligibly.

Direction of Wave Normal

In Figs. 4 and 5 the lower of the two curves in each case shown represents the characteristic wave which propagates with the least attenuation. If the azimuthal angle of incidence is not in the plane of the magnetic meridian, the vertical angle of the normal to this wave varies only negligibly.

Rate of Vertical Attenuation

In the lossless, isotropic medium, the rate of vertical attenuation is approximately 120 db/km.

If either the vertical or azimuthal angle of incidence is varied, the attenuation rate is negligibly affected.

Fig. 6 shows the attenuation rate in db/km of the two transmitted waves as the inclination of the earth's field is varied. The inclusion of the earth's field clearly reduces the attenuation of both modes, particularly near the geomagnetic poles. In the special case of zero losses ($v=0$), the attenuation of one of the modes is zero. This is usually called the extraordinary mode and accounts for the propagation of whistlers [7].

Conclusion

A general method for calculating the fields excited by a plane wave incident from any arbitrary angle upon a

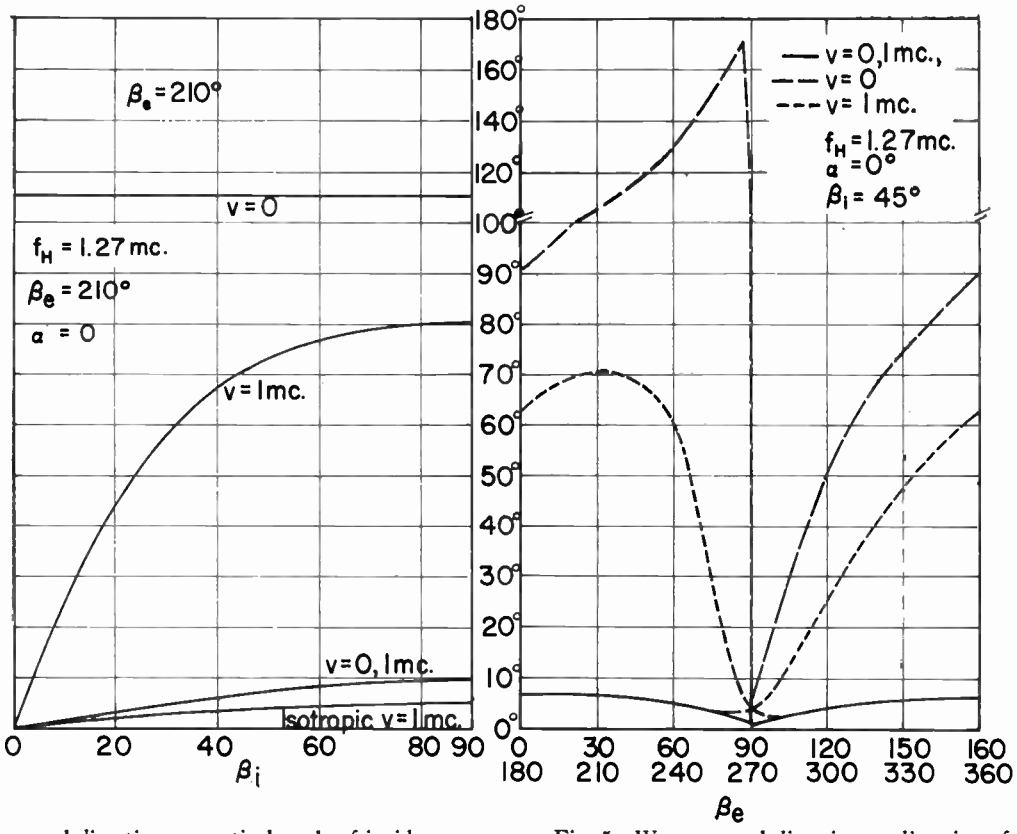

Fig. 4—Wave normal direction vs vertical angle of incidence.

Fig. 5—Wave normal direction vs direction of earth's field.

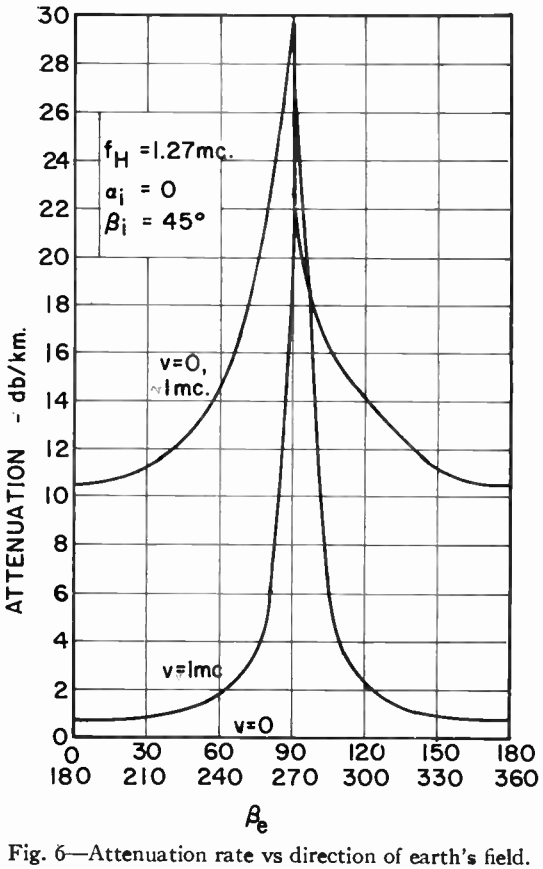

Fig. 6—Attenuation rate vs direction of earth's field.

sharply-bounded, anisotropic, absorptive ionosphere has been presented. Some numerical examples of the reflection coefficients, wave normal directions, and attenuation rates for a particular model have been presented for various angles of incidence and inclination of the earth's field.

The chief application of this method to the ionosphere is in low-frequency propagation studies. The reflection coefficients can be used either to determine a suitable model of the ionosphere from experimental results, or given a model, to predict the received signal strength and polarization. For example, the polarization of the incident wave for a given angle of incidence which will give maximum returned signal can be computed from the curves shown. The characteristics of the transmitted wave are important in the theory of whistler propagation.

Bibliography

[1] Stratton, J. A. *Electromagnetic Theory*. New York: McGraw-Hill Book Company, Inc., 1941.
[2] Booker, H. G., "Propagation of Wave Pockets Incident Obliquely Upon a Stratified Doubly-Refractory Ionosphere," *Proceedings Royal Society*, Vol. 237 (September, 1938), pp. 411–451.
[3] Bremmer, H. *Terrestrial Radio Waves*. New York and Amsterdam: Elsevier Publishing Company, 1949.
[4] Budden, K. G., "The Reflection of Very Low Frequency Waves at the Surface of a Sharply Bounded Ionosphere with Superimposed Magnetic Field," *Philosophical Magazine*, Vol. 42 (August, 1951), pp. 833–850.
[5] Wait, J. R., "Calculations of Ionospheric Reflection Coefficients at Very Low Radio Frequencies," *Journal of Geophysical Research*, Vol. 62 (March, 1957), pp. 43–56.
[6] Booker, H. G. "Some General Properties of the Formula of the Magneto-Ionic Theory," *Proceedings of the Royal Society*, Vol. 147 November, 1934), pp. 352–382.
[7] Storey, L. R. O. *Transactions of the Royal Society*, Vol. 246 (1953), pp. 113–141.

The Geometrical Optics of VLF Sky Wave Propagation*

J. R. WAIT†, SENIOR MEMBER, IRE, AND A. MURPHY†

Summary—**At distances not exceeding 1500 km, it is convenient to calculate the field strength of a vlf transmitter by geometrical optics. In such computations, it is usual to assume some equivalent height for the (ionospheric) reflecting layer with a reflection coefficient that does not vary with angle of incidence. In the present paper, the ionosphere is taken to be a homogeneous ionized medium with a sharp lower boundary. The reflection coefficient, which is a function of angle of incidence, is utilized to compute the strength of the single and multiple hop sky waves. Combining these with the numerical results of the amplitude and phase of the ground wave, the total field is obtained. The theoretical field-strength-vs-distance curves compare favorably with the experimental data of Heritage for frequencies of 16.6, 18.6, and 19.8 kc over daytime paths in the Pacific Ocean. Finally, diffraction by the earth's bulge of the first hop sky wave is considered. This effect is important at ranges greater than 1200 km or so.**

Introduction

AT FREQUENCIES of the order of 15 kc, where the wavelength is 20 km, it would seem reasonable to assume that the ionosphere is sharply bounded. In other words, the electron density can be expected to vary rapidly in a vertical distance equal to one wavelength. This approach has been employed by Bremmer[1] to calculate the strength of the received field after a number of multiple reflections between the earth and the ionosphere. By an ingenious manipulation of the geometrical-optical series, he expresses the distant field in terms of an exponential function which is identical in form to the empirical Austin-Cohen formula. A similar derivation was carried out by Rydbeck[2] who started with the Watson residue-series representation for the field. Unfortunately, Bremmer, Rydbeck, and also Schumann[3] invoked the assumption that the effective refractive index N of the ionosphere was large compared to unity. As a consequence, the magnitude of the field at a distance d varied approximately as $\exp\left[-\sqrt{\omega/2\omega_r}(d/h)\right]$ where ω_r is related to the refractive index by $N \cong [1-i\omega_r/\omega]^{1/2}$ h is the height of the ionosphere, and ω is the angular frequency. To estimate the value of ω_r, which is effectively proportional to the conductivity of the ionosphere, Bremmer compares the exponent with the corresponding factor in the Austin-Cohen formula and deduces that

$$\omega_r \times 4.6 \cong 10^7 \text{ rad/second}$$

or a conductivity of 4.1×10^{-4} mhos/meter.

It will be shown here that the above deduced value of ω_r is too large by a factor of 10^2 or more. By removing the restriction that the refractive index must be large and by computing the full geometric-optical series, good agreement can be obtained with experimental field-strength-distance curves yielding a value of ω_r in the neighborhood of 2×10^5 rad/second. Furthermore, as is shown elsewhere,[4,5] such a value of ω_r seems to be quite compatible with the waveguide-mode representation of vlf propagation to great distances.

Basic Theory

Due to the presence of the earth's magnetic field, the ionosphere is an anisotropic medium. The propagation of electromagnetic waves in such a medium is described usually by the Appleton-Hartree equations.[1] However, when the properties of medium change rapidly, the formulation becomes exceedingly complex, since coupling between the ordinary and extraordinary waves takes place. In the case of a sharp boundary, the problem becomes somewhat more tractable as indicated by Budden.[6] Employing the sharp-boundary assumption along with Booker's quasilongitudinal approximation, reflection coefficients have been calculated for a range of values of ω/ω_r and angle of incidences.[7] It was shown that for very oblique angles the reflected wave, for a vertically-polarized incident wave, is also nearly vertically polarized. On this basis, it can be concluded that, if attention is restricted to the vertical component of the distant electric field, the ionosphere is effectively isotropic. Extensive experimental evidence would appear to substantiate this hypothesis.[7]

The source is now taken to be a vertical electric dipole located on the surface of a spherical earth. On the basis

* Original manuscript received by the IRE, January 21, 1957. Paper presented at Symposium on Propagation of Very-Low-Frequency Electromagnetic Waves, Boulder, Colo.; January 23–25, 1957.

† National Bureau of Standards, Boulder, Colo.

[1] H. Bremmer, "Terrestrial Radio Waves," Elsevier Publishing Co., Amsterdam, Netherlands; 1949.

[2] O. E. H. Rydbeck, "On the propagation of radio waves," *Trans. Chalmers Univ.*, Gothenburg, Sweden, no. 34, pp. 1–168; January, 1944.

[3] W. O. Schumann, "Über die oberfelder dei der ausbreitung langer, elecktrischer wellen im system erde-lufe-ionosphare und 2 anwendungen," *Z. angew. Phys.*, vol. 6, pp. 35–43; January, 1954.

[4] J. R. Wait, "On the Mode Theory of VLF Ionospheric Propagation," paper presented at URSI meeting, Paris, France; September, 1956. NBS Rep. No. 5022, to be published.

[5] J. R. Wait and H. H. Howe, "Waveguide Mode Calculations for VLF Ionospheric Propagation Including the Influence of Ground Conductivity," paper presented at VLF Symposium, Boulder, Colo.; January, 1957.

[6] K. G. Budden, "On the propagation of a radio atmospheric," *Phil. Mag.*, vol. 43, pp. 1179–1200; November, 1952.

[7] J. R. Wait and A. Murphy, "Multiple Reflections Between the Earth and the Ionosphere in VLF Propagation," paper presented at URSI meeting, Paris, France; September, 1956. Also, *Geofisica Pura e Applicata*, vol. 35, pp. 61–72; November, 1956.

of geometrical optics, the field at a distance D in km, measured along the surface of the earth, is the sum of the ground wave and the rays reflected from the ionosphere. The ground wave is not actually a geometrical-optical term, since it is obtained from the Van der Pol-Bremmer-Norton theory[1] for propagation around the surface of a homogeneous sphere. Extensive numerical values[8] of its amplitude and phase have been previously calculated for vlf propagation and the data is employed here for the subsequent computations. The following terms of this (quasi) geometrical-optical series are considered to be pure rays which are radiated from the source, are reflected n times at the ionosphere, and are reflected $n-1$ times at the ground. The angle of incidence of the nth hop ray at the ionosphere is denoted by $\bar{\theta}_n$, and the corresponding value at the ground is θ_n. The angles are measured from the vertical. At each reflection, the amplitude of the ray must be multiplied by the appropriate reflection coefficients, $R_g(\theta_n)$ for the ground and $R_i(\bar{\theta}_n)$ for the ionosphere. Furthermore, since the earth and the ionosphere are idealized as concentric spherical surfaces, there is an over-all convergence or focusing action which tends to increase the amplitude of the received nth hop ray by a factor α_n. The convergence coefficient α_n can be derived by well-known methods.[1] The resultant vertical electric field in millivolts/meter at range D in kilometers can now be written in the following form[7]

$$E \cong \left\{ E_0 e^{-i\phi_0} + \sum_{n=1}^{\infty} E_n e^{-i2\pi f_{kc} t_n} \right\} e^{-i2\pi D/\lambda}$$

where

$$E_n \cong \frac{322\alpha_n \sin^2 \theta_n}{D + 300t_n} [R_i(\bar{\theta}_n)]^n,$$

$$\alpha_n = (1 + h/a) \left[\frac{2n \sin\left(\frac{D}{2an}\right)}{\sin \frac{D}{a}} \right]^{1/2}$$

$$\cdot \left[\frac{(1 + h/a) - \cos\left(\frac{D}{2an}\right)}{(1 + h/a)\cos\left(\frac{D}{2an}\right) - 1} \right]^{1/2} \quad \text{and}$$

$$R_i(\bar{\theta}_n) = \frac{N^2 \cos \bar{\theta}_n - (N^2 - \sin^2 \bar{\theta}_n)^{1/2}}{N^2 \cos \bar{\theta}_n + (N^2 - \sin^2 \bar{\theta}_n)^{1/2}}$$

where h and a are the height of the ionosphere and the radius of the earth, both expressed in kilometers. For convenience in applying the above formula, some of the important parameters have been calculated and listed here. The time delay t_n expressed in microseconds and denoted $t_n^{\mu s}$ is given in Table I, on the following page, for the distance or range D in kilometers and for n from 1 to 5 hops. The ionospheric heights chosen are from 60 to 100 km. In the present case, the radius of curvature of the earth is taken as 6368 km. The complement $90° - \theta_n$ of the angle of incidence of the nth hop ray at the ground is given in Table II, and the angle of incidence $\bar{\theta}_n$ of the nth hop ray at the ionosphere is given in Table III. The convergence coefficient α_n is usually quite close to unity for ranges less than 1000 km. As an example, $\alpha_n - 1$ is shown plotted in Fig. 1, p. 757, as a function of D for the first 5 hops.

$$E = \left\{ E_0 e^{-i\phi_0} + 80.5 \sum_{n=1}^{\infty} \frac{\alpha_n \sin^2 \theta_n [1 + R_g(\theta_n)]^2}{D + 300t_n} Q_n e^{-i2\pi f_{kc} t_n} \right\} e^{-i2\pi D/\lambda}$$

where λ is the wavelength in kilometers and where E_0 and ϕ_0 are the amplitude and phase of the ground wave normalized such that $E_0 = 100$ mv/m for $D = 1.605$ km (1 mile). In the above, the factor Q_n is given by

$$Q_n = [R_g(\theta_n)]^{n-1} [R_i(\theta_n)]^n$$

and t_n is the time delay expressed in milliseconds between the nth hop ray and an unattenuated direct ray along the surface of the earth between the source dipole and the observer. In other words, $D + 300t_n$ is the difference between the length of the nth hop ray and the ground ray expressed in kilometers. It should also be noted that the above formula for the transmitting and receiving antennas are assumed to be vertical electric dipoles which each have a radiation pattern $\sin \theta_n [1 + R_g(\theta_n)]$.

For propagation at frequencies below 20 kc, the ground reflection coefficient $R_g(\theta_n)$ is very close to unity for ranges less than 500 km for well-conducting ground. In the case of sea water, $R_g(\theta_n)$ is essentially unity for all ranges, and, therefore,

The data t_1, θ_1, $\bar{\theta}_1$, and α_1 are shown only for distances such that $\theta_1 < 90°$. Beyond this distance D_c, which is given approximately by $D_c \cong \sqrt{8ha}$, the earth's surface is not illuminated by the first hop sky wave in the purely geometrical-optical sense. For example, if the assumed height of reflection is 70 km, this geometrical cutoff range D_c is 1900 km. At this point, the first hop sky wave is at grazing incidence on the ground ($\theta_1 \cong 0$) and the angle of incidence $\bar{\theta}_1$ at the ionosphere is about 80°, yielding a value of the convergence coefficient of 2.5. For the moment it is assumed that D is substantially smaller than D_c. The diffraction effects which occur when D approaches D_c are discussed at a later stage in this paper.

[8] J. R. Wait and H. H. Howe, "Amplitude and Phase Curves for Ground Wave Propagation in the Band 200 c/s to 500 kc," NBS Circular 574; May, 1956.

TABLE I

$t_n^{\mu s}$ for $h=60$ km

D_{km} \ $n\rightarrow$	1	2	3	4	5
00	400.000	800.000	1200.000	1600.000	2000.000
500	54.841	189.097	393.409	649.349	941.769
1000	38.616	109.683	224.076	378.195	567.381
2000	—	77.231	137.226	219.366	323.292
3000	—	73.013	115.847	172.170	243.219
4000	—	—	110.215	154.463	208.964
5000	—	—	109.361	147.911	193.079

$t_n^{\mu s}$ for $h=70$ km

D_{km} \ $n\rightarrow$	1	2	3	4	5
00	466.667	933.333	1400.000	1866.667	2333.333
500	72.796	251.492	516.971	841.866	1206.092
1000	49.751	145.591	298.830	502.984	750.472
2000	—	99.501	180.430	291.183	430.780
3000	—	92.252	149.252	225.188	321.095
4000	—	—	139.896	199.003	272.450
5000	—	—	137.818	188.313	248.753

$t_n^{\mu s}$ for $h=80$ km

D_{km} \ $n\rightarrow$	1	2	3	4	5
00	533.333	1066.667	1600.000	2133.333	2666.667
500	93.094	320.885	651.228	1046.959	1483.535
1000	62.158	186.188	382.855	641.770	951.708
2000	56.043	124.317	229.167	372.376	552.073
3000	—	113.213	186.475	284.850	409.067
4000	—	112.087	172.473	248.633	343.768
5000	—	—	168.602	232.826	310.792

$t_n^{\mu s}$ for $h=90$ km

D_{km} \ $n\rightarrow$	1	2	3	4	5
00	600.000	1200.000	1800.000	2400.000	3000.000
500	115.656	396.570	794.430	1261.987	1770.923
1000	75.825	231.312	475.538	793.140	1168.657
2000	66.834	151.649	283.319	462.625	686.488
3000	—	135.884	227.474	351.039	506.882
4000	—	133.669	207.927	303.299	422.795
5000	—	—	201.702	281.419	379.123

$t_n^{\mu s}$ for $h=100$ km

D_{km} \ $n\rightarrow$	1	2	3	4	5
00	666.667	1333.333	2000.000	2666.667	3333.333
500	140.397	477.881	945.106	1484.918	2065.959
1000	90.735	280.795	576.264	955.763	1399.158
2000	78.267	181.470	342.761	561.590	833.319
3000	—	160.255	272.204	423.632	614.268
4000	—	156.534	246.234	362.939	509.400
5000	—	—	237.104	334.056	453.674

TABLE II

$90-\theta_n$ for $h=60$ km

D_{km} \ $n\rightarrow$	1	2	3	4	5
00	90.00	90.00	90.00	90.00	90.00
500	12.31	24.97	35.25	43.41	49.84
1000	4.56	12.31	18.96	24.97	30.39
2000	—	4.56	8.66	12.31	15.72
3000	—	1.17	4.56	7.36	9.91
4000	—	—	2.11	4.56	6.69
5000	—	—	0.34	2.64	4.56

$90-\theta_n$ for $h=70$ km

D_{km} \ $n\rightarrow$	1	2	3	4	5
00	90.00	90.00	90.00	90.00	90.00
500	14.43	28.55	39.50	47.80	54.09
1000	5.67	14.43	21.92	28.55	34.39
2000	—	5.67	10.29	14.43	18.29
3000	—	1.92	5.67	8.83	11.71
4000	—	—	2.96	5.67	8.07
5000	—	—	1.02	3.54	5.67

$90-\theta_n$ for $h=80$ km

D_{km} \ $n\rightarrow$	1	2	3	4	5
00	90.00	90.00	90.00	90.00	90.00
500	16.51	31.89	43.28	51.55	57.61
1000	6.78	16.51	24.75	31.89	38.03
2000	0.04	6.78	11.91	16.51	20.78
3000	—	2.67	6.78	10.28	13.49
4000	—	0.04	3.80	6.78	9.44
5000	—	—	1.69	4.43	6.78

$90-\theta_n$ for $h=90$ km

D_{km} \ $n\rightarrow$	1	2	3	4	5
00	90.00	90.00	90.00	90.00	90.00
500	18.54	35.00	46.63	54.75	60.55
1000	7.88	18.54	27.45	35.00	41.34
2000	0.60	7.88	13.51	18.54	23.18
3000	—	3.41	7.88	11.71	15.24
4000	—	0.60	4.63	7.88	10.79
5000	—	—	2.36	5.32	7.88

$90-\theta_n$ for $h=100$ km

D_{km} \ $n\rightarrow$	1	2	3	4	5
00	90.00	90.00	90.00	90.00	90.00
500	20.52	37.88	49.60	57.51	63.03
1000	8.97	20.52	30.02	37.88	44.33
2000	1.16	8.97	15.07	20.52	25.48
3000	—	4.15	8.97	13.13	16.95
4000	—	1.16	5.46	8.97	12.13
5000	—	—	3.03	6.20	8.97

TABLE III

θ_n for $h=60$ km

D_{km} \ $n\rightarrow$	1	2	3	4	5
00	0.00	0.00	0.00	0.00	0.00
500	75.44	63.90	54.00	46.02	39.71
1000	80.94	75.44	69.54	63.90	58.71
2000	—	80.94	78.35	75.44	72.48
3000	—	82.08	80.94	79.27	77.39
4000	—	—	81.89	80.94	79.71
5000	—	—	82.16	81.73	80.94

$\bar{\theta}_n$ for $h=70$ km

D_{km} \ $n\rightarrow$	1	2	3	4	5
00	0.00	0.00	0.00	0.00	0.00
500	73.32	60.32	49.75	41.64	35.46
1000	79.83	73.32	66.58	60.32	54.71
2000	—	79.83	76.71	73.32	69.91
3000	—	81.33	79.83	77.80	75.59
4000	—	—	81.04	79.83	78.33
5000	—	—	81.48	80.84	79.83

$\bar{\theta}_n$ for $h=80$ km

D_{km} \ $n\rightarrow$	1	2	3	4	5
00	0.00	0.00	0.00	0.00	0.00
500	71.24	56.98	45.97	37.89	31.94
1000	78.72	71.24	63.75	56.98	51.07
2000	80.97	78.72	75.09	71.24	67.42
3000	—	80.58	78.72	76.35	73.81
4000	—	80.97	80.21	78.72	76.96
5000	—	—	80.81	79.94	78.72

θ_n for $h=90$ km

D_{km} \ $n\rightarrow$	1	2	3	4	5
00	0.00	0.00	0.00	0.00	0.00
500	69.21	53.88	42.62	34.69	29.00
1000	77.62	69.21	61.05	53.88	47.76
2000	80.40	77.62	73.50	69.21	65.02
3000	—	79.84	77.62	74.91	72.06
4000	—	80.40	79.37	77.62	75.61
5000	—	—	80.14	79.06	77.62

θ_n for $h=100$ km

D_{km} \ $n\rightarrow$	1	2	3	4	5
00	0.00	0.00	0.00	0.00	0.00
500	67.23	51.00	39.65	31.93	26.52
1000	76.53	67.23	58.49	51.00	44.77
2000	79.85	76.53	71.93	67.23	62.72
3000	—	79.10	76.53	73.50	70.35
4000	—	79.85	78.54	76.53	74.27
5000	—	—	79.47	78.17	76.53

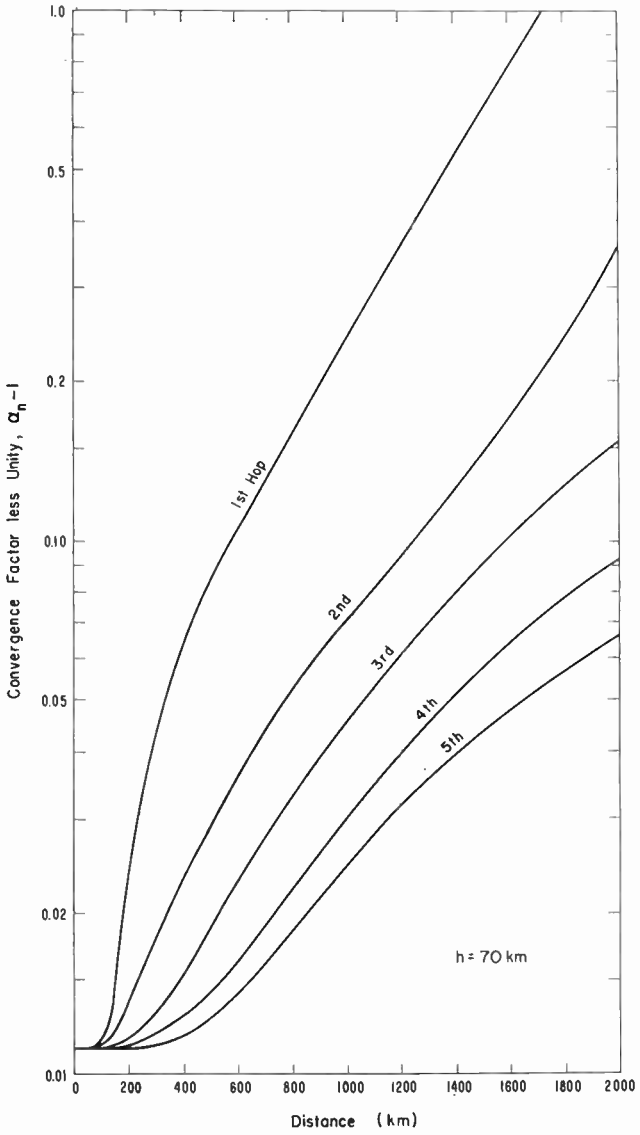

Fig. 1—The convergence coefficient as a function of distance.

Numerical Results

The amplitude $|E_1|$ of the first hop sky wave is shown plotted in Fig. 2(a) as a function of D for ω/ω_r values ranging from 0.10 to 1.75. The phase lag of $E_1(=-\arg E_1)$ is shown in Fig. 2(b) for the same range of ω/ω_r. The corresponding amplitude $|E_2|$ and phase lag of E_2 are shown in Fig. 3(a) and 3(b), respectively. Whereas these curves are valid only for an isotropic ionosphere, the extension to the anisotropic case is fairly straightforward if a more elaborate version of the factor Q_n is employed.[7] For field-strength calculation at large ranges, the isotropic representation seems to be sufficient.

Employing the preceding data for the sky-wave terms and the previously computed results[8] for the ground wave terms E_0 and ϕ_0, field strengths are calculated for frequencies of 18.6, 19.8, and 16.6 kc as a function of

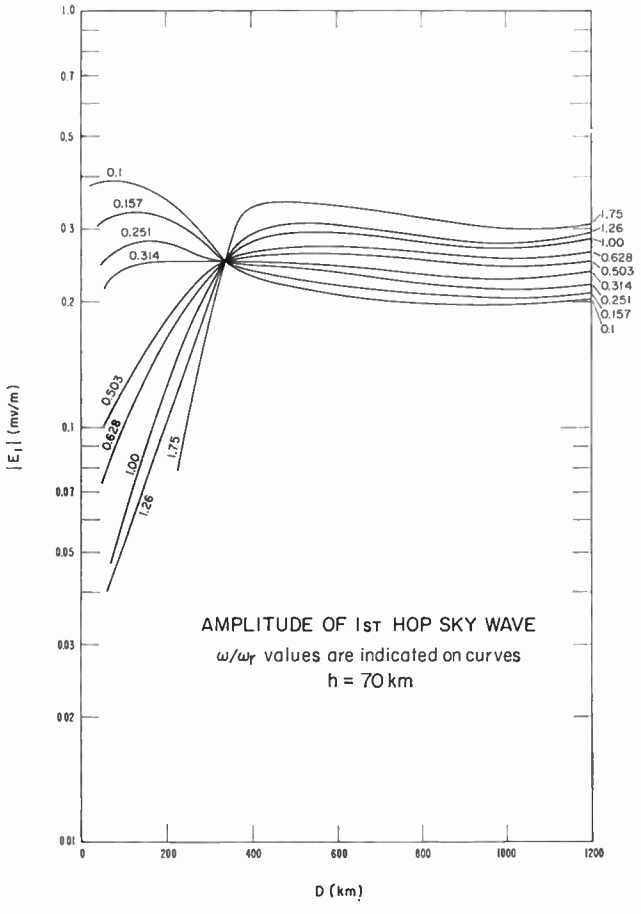

(a)

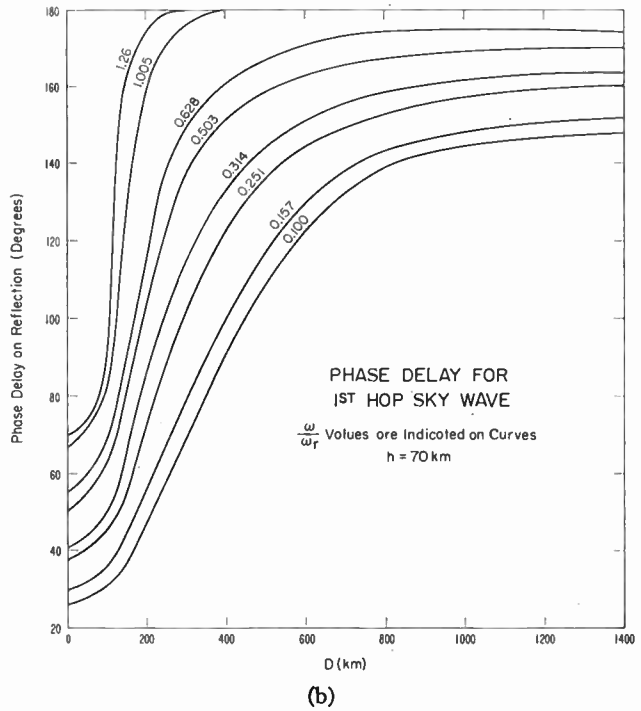

(b)

Fig. 2—The normalized amplitude and phase of the first hop sky wave as a function of distance.

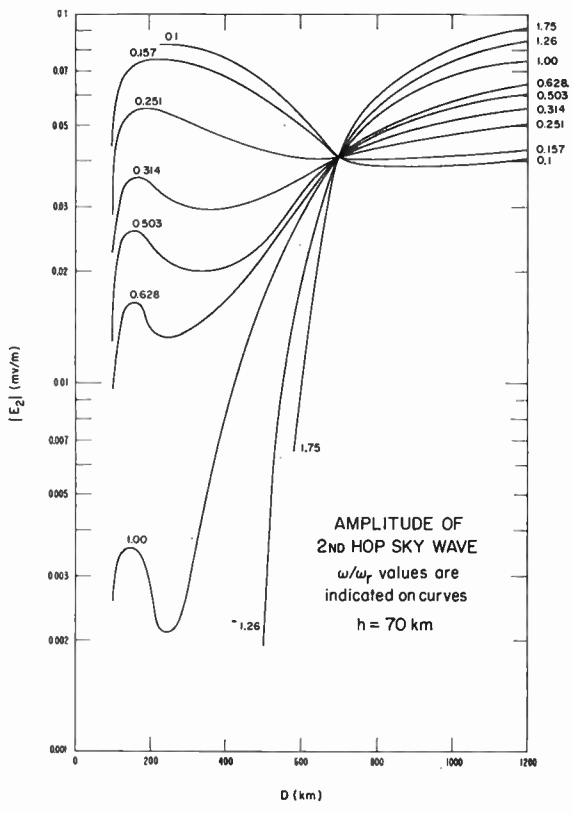

(a)

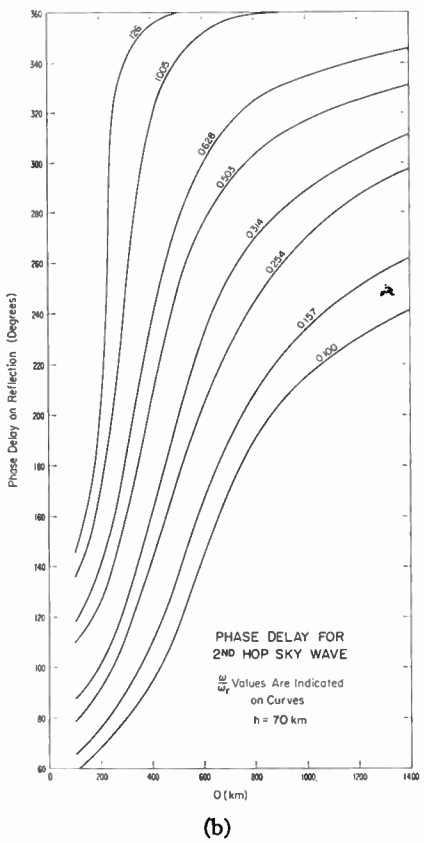

(b)

Fig. 3—The normalized amplitude and phase of the second hop sky wave as a function of distance.

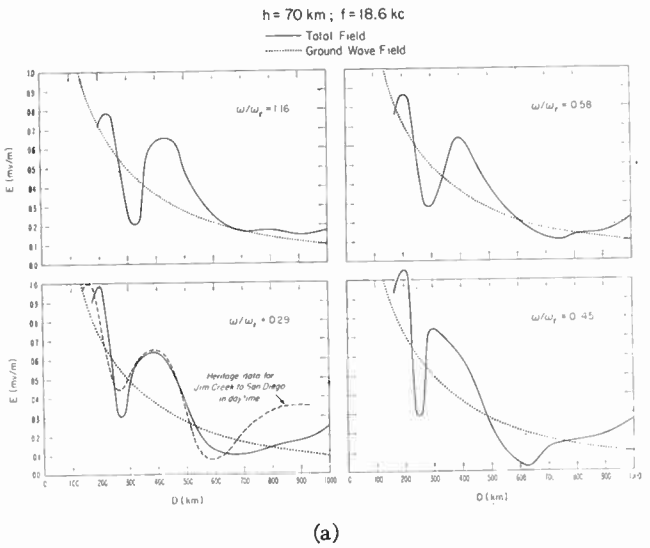

(a)

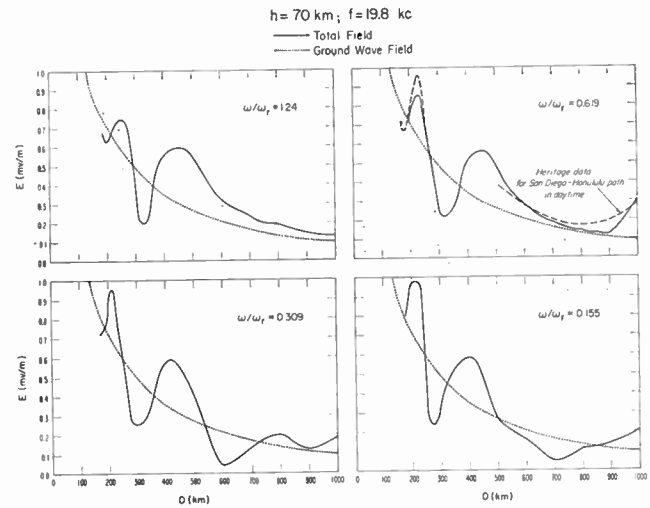

(b)

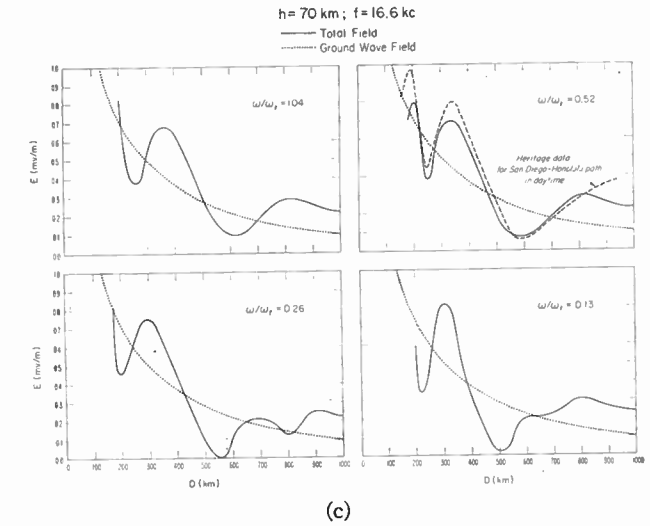

(c)

Fig. 4—Normalized field strengths plotted as a function of distance for the values of ω/ω_r indicated (Heritage's experimental results are shown with its closest theoretical counterpart).

range as shown in Fig. 4(a)–4(c). The heights are chosen to be 70 km and the ω/ω_r values indicated are chosen to correspond to ω_r values of 0.5, 1.0, 2.0, and 4.0×10^5. The ground wave by itself is indicated by a dotted curve.

Experimental data, acquired by Heritage *et al.*,[9] for paths mostly over the Pacific in daytime, are averaged and indicated by dashed curves. These would indicate that ω_r values of the order of 2.0×10^5 are compatible with experiment.

It would appear that vlf propagation over sea water or well-conducting land during daytime can be predicted quite adequately by quasi-geometrical optical methods. The computation of field strengths for nighttime conditions can proceed in the same manner: The appropriate heights are in the region from 90 to 100 km and the ω_r values are of the order of 8.0×10^5 or possibly ess.

Extension to Large Ranges

At large ranges, say beyond 1500 km, the purely geometrical description of the first hop sky wave begins to lose some of its validity. To investigate this feature, a diffraction correction can be estimated by considering the field of a downcoming plane wave in the neighborhood of the geometrical light-shadow boundary (*i.e.*, $D\cong D_c$). Although the sky wave is not actually plane, the curvature of its wave front is often negligible and, consequently, certain results in diffraction theory can be utilized. The upshot is that E_1, for a first approximation in the neighborhood of $D=D_c$, must be multiplied by a shadow factor F which is a function of the parameter $(a/\lambda)^{1/3}(D-D_c)/a$. The function F is normalized so that it approaches unity in the geometrical lit region (*i.e.*, $D\ll D_c$). The function F also occurs in the theory of flush-mounted microwave antennas and has been discussed elsewhere.[10] To illustrate its significance, the "shadow factor" $|F|$ is plotted in Fig. 5 for $f=10$ and 20 kc as a function of distance from the critical range D_c. Positive values of the ordinate correspond to the shadow region and negative values correspond to the lit region.

It is interesting to note that for vlf, the apparent increase of magnitude of the convergence coefficient α_1 as D approaches D_c is somewhat counteracted by the diffraction factor F. For example, at $D=D_c$, F is a real number near 0.7 corresponding to a 30 per cent reduction of the geometrical-optical computed field. A de-

[9] J. L. Heritage, S. Weisbrod, and J. E. Bickel, "A Study of Signal-vs-Distance Data at VLF," paper presented at VLF Symposium, Boulder, Colo.; January, 1957.

[10] J. R. Wait, "The Pattern of a Flush-Mounted Microwave Antenna," NBS Rep. No. 5028, to be published. See also "Radiation characteristics of axial slots on a conducting cylinder," *Wireless Engr.*, vol. 32, pp. 316–322; December, 1955.

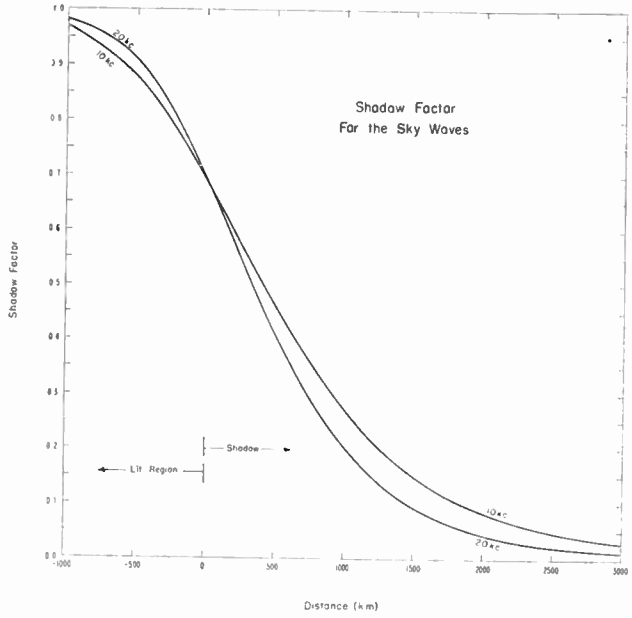

Fig. 5—The shadow factor for the diffraction of a downcoming sky wave by the "bulge" of the earth.

tailed study has been carried out by W. H. Briggs and J. R. Wait of the applications of diffraction theory to the computation of sky waves for ranges beyond their optical cutoff. Actually, the problem is somewhat more complicated than indicated above, since the downcoming wave has a curved wave front as a result of the convergence at the upper boundary. An account of this work will be reported in the near future.

The quasi-geometrical optic techniques are then seen to be very powerful if attention is restricted to ranges up to and not greatly in excess of D_c. At much larger ranges, it becomes desirable to recast the theoretical expressions for the fields into a sum of modes which becomes highly convergent for large D. This subject is treated in a companion paper.[5]

Acknowledgment

We would like to express thanks to Dr. H. H. Howe for assistance with the calculations, to A. D. Watt and A. G. Jean for helpful comments, and to Mrs. M. Halter for her assistance in preparing this paper.

The Mode Theory of VLF Ionospheric Propagation for Finite Ground Conductivity*

JAMES R. WAIT†, SENIOR MEMBER, IRE

Summary—**The space between the earth and the ionosphere is considered as a waveguide with sharply bounded walls. Employing a representation in terms of spherical wave functions of complex order, the field of a vertical dipole source is calculated for very low frequencies. It is shown that the effect of the finite conductivity of the ground is quite important for propagation to great distances. Good agreement is obtained with the experimental results of J. Heritage.**

Introduction

IN VIEW of the limitations of the commonly used optical or ray methods to calculate sky wave field intensities, it is desirable to consider an alternative and more rigorous formulation. As long ago as 1919, Watson[1] presented a formal solution for a dipole source over a spherical homogeneous earth with the ionosphere being represented by a perfectly-conducting concentric shell. More recently Bremmer[2] and Rydbeck[3] have considered the case of a spherically stratified ionosphere. In the case of vlf (very low frequencies), the upper boundary can be assumed sharp to a good approximation. This simplifies the approach somewhat and paves the way for a more definite evaluation of the mode characteristics. With this model Schumann[4] has discussed the propagation of audio frequency waves to great distances. Unfortunately, his perturbation technique for solving for the mode coefficients is not valid for frequencies above about 1000 cps and certainly cannot be employed for frequencies around 16 kc, since the ionosphere is then effectively a very poor conductor. Another approach to the problem has been made by Budden[5] who considers the earth and the ionosphere to be represented by a parallel plate waveguide with a perfectly conducting lower boundary. For some reason

* Original manuscript received by the IRE, February 6, 1957. Paper presented at Symposium on Propagation of Very-Low-Frequency Electromagnetic Waves, Boulder, Colo.; January 23–25, 1957.

† National Bureau of Standards, Boulder, Colo.

[1] G. N. Watson, "The transmission of electric waves round the earth," *Proc. Roy. Soc., London* [*A*], vol. 95, pp. 546–563; June, 1919.

[2] H. Bremmer, "Terrestrial Radio Waves," Elsevier Publishing Co., Amsterdam, Netherlands; 1949.

[3] O. E. H. Rydbeck, "On the propagation of radio waves," *Trans. Chalmers Univ.*, Gothenberg, Sweden, no. 34, pp. 1–168; January, 1944.

[4] W. O. Schuman, "Über die oberfelder bei der ausbreitung langer elektrischer wellen im system erde-luft-ionosphäre und 2 Anwendungen," *Z. angew. Phys.*, vol. 6, pp. 35–43; January, 1954.

[5] K. G. Budden, "The propagation of a radio atmospheric II," *Phil. Mag.*, vol. 43, pp. 1179–1200; November, 1952. See also F. W. Chapman and R. C. V. Macario, "Propagation of audio frequency radio waves to great distances," *Nature*, vol. 177, pp. 930–933; June, 1956, and I. A. L. Alpert, "The field of long and very long radio waves over the earth under actual conditions," *Radiotekhnika i Electronika*, vol. 1, pp. 281–292; March, 1956 (in Russian).

which is not entirely clear,[6] he introduces negative order modes which are not excited by a vertical dipole source. Furthermore, Budden[5] arrives at the conclusion that the zero order mode is dominant at all frequencies, which is not in accord with the present analysis.

It is the purpose of the present paper to reformulate the mode theory of vlf propagation under the assumption that the ionosphere and the earth are sharply bounded. The solution is expressed as a series of waveguide types modes. The characteristics of these modes are discussed in some detail.

Formulation

The earth is considered to be a homogeneous sphere of radius a, of conductivity σ_e and dielectric constant ϵ_e. The ionosphere is then represented by a spherical shell consisting of a homogeneous medium of electron density N and collision frequency g. With respect to a spherical coordinate system (r, θ, ϕ), the earth is bounded by $r=a$ and the ionosphere by $r=b$. The presence of the earth's magnetic field has been tacitly neglected. The justification for doing this is based on the numerical results obtained from quasi-geometrical-optical methods.[7] It was indicated there that for vlf propagation to great ranges, the "isotropic approximation" was very satisfactory if attention was restricted to the vertical electric field.

The origin of the field is assumed to be represented by a vertical electric dipole located $r=r_0$. If necessary, the source can be generalized to a line distribution of vertical dipoles if the need should arise. In view of the intrinsic spherical symmetry, the fields can be represented in terms of a single scalar function, ψ, as follows

$$E_r = \frac{i}{r}\eta\frac{1}{\sin\theta}\frac{\partial}{\partial\theta}\left(\sin\theta\frac{\partial\psi}{\partial\theta}\right) \tag{1a}$$

$$E_\theta = -\frac{i}{r}\eta\frac{\partial^2}{\partial\theta\partial r}(r\psi) \tag{1b}$$

$$H_\phi = -k\frac{\partial\psi}{\partial\theta} \tag{2}$$

and $E_\phi = \Pi_r = \Pi_\theta = 0$, where $\eta=(\mu/\epsilon)^{1/2}$ and $k=(\epsilon\mu)^{1/2}\omega$. In the preceding, the permeability μ is taken to be the same as free space for all of the regions ($\mu=4\pi\times10^{-7}$). The complex dielectric constant varies in the following manner:

$$\epsilon = \epsilon_e - i\frac{\sigma}{\omega} \text{ for } r < a, \tag{3a}$$

$$= \epsilon_0 \text{ for } a < r < b, \tag{3b}$$

$$= \epsilon_i = \epsilon_0\left(1 - i\frac{\omega_r}{\omega}\right) \text{ for } r > b \tag{3c}$$

where $\omega_r=\omega_0^2/g$ with $\omega_0^2=Ne^2/m\epsilon_0$. Eq. (3b) is valid for $\omega\ll g$. e and m are the charge and mass of the electron expressed in mks units. A time factor exp $(i\omega t)$ is implied. In general, a subscript e is to be affixed when reference is made to the earth and, correspondingly, a symbol i is to be used for the ionosphere.

The scalar function ψ is a solution of the wave equation appropriate for the regions. The solutions can be represented in terms of spherical wave functions as follow:

$$a_\nu h_\nu^{(1)}(k_e r)P_\nu(-\cos\theta) \text{ for } r < a$$

$$[b_\nu^{(1)}h_\nu^{(1)}(kr) + b_\nu^{(2)}h_\nu^{(2)}(kr)]P_\nu(-\cos\theta) \text{ for } b > r > a$$

$$[c_\nu^{(2)}h_\nu^{(2)}(k_i r)]P_\nu(-\cos\theta) \text{ for } r > b.$$

In the above

$$h_\nu^{(1,2)}(z) = \left(\frac{\pi}{2z}\right)^{1/2} H_{\nu+1/2}^{(1,2)}(z) \tag{4}$$

where $H_{2+1/2}^{(1,2)}(z)$ is the Hankel function of the first or second kind of order $\nu+\frac{1}{2}$ with argument z and $P_2(-\cos\theta)$ is the Legendre function.

The quantity ν is to be found from the boundary conditions which state that the tangential fields (E_θ and H_ϕ) are continuous at $r=a$, b and c. This, in turn, requires that

$$\frac{1}{k}\frac{\partial(r\psi)}{\partial r}$$

and $k\psi$ are continuous. Therefore, six equations are obtained to solve for ν. In order that nontrivial solutions are produced, the four by four determinant of the coefficients must vanish. To reduce the problem to a somewhat more palatable form, the following approximation is employed[8]

$$h_\nu^{(1,2)}(z) = \sqrt{\frac{\pi}{2z}}\,H_{\nu+1/2}^{(1,2)}(z) \cong \frac{1}{z\sqrt{\cos\alpha_z}} \cdot \exp\left[\pm iz(\cos\alpha_z - \alpha_z\sin\alpha_z) \mp i\pi/4\right] \tag{5}$$

where $\sin\alpha_z=(\nu+\frac{1}{2})/z$. This representation is known as Debye's generalization of Hankel's asymptotic series. It is valid for $z>|\nu+\frac{1}{2}|\gg1$. Therefore

$$\frac{h_\nu^{(2)}(kr)}{h_\nu^{(2)}(ka)} \cong e^{-ik(r-a)\cos\alpha} \tag{6}$$

where $\sin\alpha=(\nu+\frac{1}{2})/ka$ since $(r-a)/a\ll1$. The other spherical Hankel functions can be simplified in a similar manner. For example

$$h_\nu^{(1)}(k_e r) \propto e^{ik_e(r-a)\cos\alpha_e}$$

where $\sin\alpha_e=(\nu+\frac{1}{2})/k_e a$, and

$$h_\nu^{(1,2)}(k_i r) \propto e^{\pm ik_i(r-a)\cos\alpha_i}$$

where $\sin\alpha_i=(\nu+\frac{1}{2})/k_i a$.

[6] This is believed to be due to an error in the deformation of the integration contour.

[7] J. R. Wait and A. Murphy, "Multiple Reflections Between the Earth and the Ionosphere in VLF Propagation," paper presented at URSI meeting, Paris, France; September, 1956. Also, *Geofisica Pura e Applicata*, vol. 35, pp. 61–72; November, 1956.

[8] A. N. Sommerfeld, "Partial Differential Equations," Academic Press, New York, N. Y.; 1949.

The application of the boundary conditions then leads in a straightforward way to the following for the determination of α:

$$R_g R_i = e^{+i2kh\cos\alpha} \tag{7}$$

where $h=b-a$ and

$$R_g = \frac{k_e/\cos\alpha_e - k/\cos\alpha}{k_e/\cos\alpha_e + k/\cos\alpha} \tag{8}$$

and

$$R_i = \frac{(k_i/\cos\alpha_i) - k/\cos\alpha}{(k_i/\cos\alpha_i) + k/\cos\alpha} \tag{9}$$

The solution of the preceding transcendental equation for the determination of $\cos\alpha$, or ν, is the central task. When this is accomplished the ratios between the coefficients a_ν, b_ν, etc. are known. For example, for the air region between the earth and the ionosphere,

$$\frac{b_\nu^{(1)}}{b_\nu^{(2)}} = R_g \tag{10}$$

having inserted the proper values of $\cos\alpha$ and ν.

Determination of the Roots

It is now desirable to return to the transcendental equation, in order to obtain a more accurate determination of the characteristic values of $\cos\alpha$ which are designated as C_n for $n=0, 1, 2, \cdots$. It can be seen that (7) can now be rewritten

$$\left[\frac{(L-i)C_n - \sqrt{C_n^2L^2 - iL}}{(L-i)C_n + \sqrt{C_n^2L^2 - iL}}\right] \cdot \left[\frac{(KG-i)C_n - \sqrt{(K-1)G^2 - iG + C_n^2G^2}}{(KG-i)C_n + \sqrt{(K-1)G^2 - iG + C_n^2G^2}}\right] = e^{4\pi iHC_n}e^{-2\pi in} \tag{11}$$

where

$$C_n = (1-S_n^2)^{1/2}, \qquad L = \frac{\omega}{\omega_r}, \qquad G = \frac{\epsilon_0\omega}{\sigma},$$

$$K = \frac{\epsilon_e}{\epsilon_0}, \text{ and } H = \frac{h}{\lambda}.$$

The numerical solution of this equation has been programmed for an automatic computor and results have been obtained for a wide range of values of L, G, H, and n.[9]

For small values of L and G, the first order perturbation solution[10] can be written as follows:

$$\mathrm{Re}\,S_n \cong \left[1-\left(\frac{n\lambda}{2h}\right)^2\right]^{1/2} + \frac{\sqrt{G}+\sqrt{L}}{4\pi\sqrt{2}}\epsilon_n\left(\frac{\lambda}{h}\right)\left[1-\left(\frac{n\lambda}{2h}\right)^2\right]^{-1/2} \tag{12}$$

and

$$\mathrm{Im}\,S_n \cong -\frac{\sqrt{G}+\sqrt{L}}{4\pi\sqrt{2}}\epsilon_n\left(\frac{\lambda}{h}\right)\left[1-\left(\frac{n\lambda}{2h}\right)^2\right]^{-1/2} \tag{13}$$

where Re and Im indicate that real and imaginary parts are to be taken.[11] It can be seen from the numerical data that these formulas are only adequate for $\sqrt{L}$ and $\sqrt{G}$ less than about 0.01. However, these simple relations do provide a good check on the machine calculations, since for a specified value of the mode number, Re S_n and Im S_n should reduce to these limiting forms as L is continuously decreased.

Actually there is another rough but rather useful approximation for the determination of S_n, namely, when the value of L is of order unity and C is small. In this instance, the ionospheric reflection coefficient R_i is near -1. For example

$$R_i(C) = -\left[\frac{\sqrt{C^2L^2 - iL} - (L-i)C}{\sqrt{C^2L^2 - iL} + (L-i)C}\right] \cong -\left[1 - \frac{2(L-i)C}{\sqrt{C^2L^2 - iL}}\right]. \tag{14}$$

The ground is, however, assumed to be sufficiently well conducting that $G \ll 1$ and therefore

$$R_g(C) \cong 1 - \frac{2\sqrt{G}e^{i\pi/4}}{C}. \tag{15}$$

The solution for C can now be written

$$khC = (n-\tfrac{1}{2})\pi + \Delta(C)$$

where $\Delta(C)$ is some small number and n can take positive integral values. In accordance with the concept of perturbation, $\Delta(C)$ is replaced by $\Delta(\overline{C}_n)$ where the $\overline{C}_n$ are given by

$$kh\overline{C} = (n-\tfrac{1}{2})\pi. \tag{16}$$

To a first order

$$\Delta(\overline{C}_n) \cong \frac{e^{i\pi/4}\left(\frac{1}{\sqrt{L}} + i\sqrt{L}\right)\overline{C}_n}{\left(1 + i\frac{\overline{C}_n^2}{L}\right)^{1/2}} + \frac{e^{i3\pi/4}\sqrt{G}}{\overline{C}_n} \tag{17}$$

and consequently

$$S_n \cong \overline{S}_n - \frac{\overline{C}_n\Delta(\overline{C}_n)}{kh\overline{S}_n} \tag{18}$$

[9] The program for the machine calculation was devised by Dr. H. H. Howe and will be reported elsewhere.

[10] J. R. Wait and H. H. Howe, "The waveguide mode theory of vlf ionospheric propagation," Proc. IRE, vol. 45, p. 95; January, 1957.

[11] $\epsilon_0 = 1$
$\epsilon_n = 2$ for $n \neq 1$.

where

$$\bar{S}_n = \sqrt{1 - \bar{C}_n^2} = \left[1 - \frac{(n - 1/2)^2}{(2h/\lambda)^2}\right]^{1/2}. \quad (19)$$

A further simplification can be made when $\bar{C}_n^2/L$ is small so that

$$\left(1 + i\frac{\bar{C}_n^2}{L}\right)^{-1/2} \cong 1 - i\frac{\bar{C}_n^2}{2L} \cong 1. \quad (20)$$

With this approximation it follows that

$$\mathrm{Re}\, S_n \cong \bar{S}_n + \frac{1}{2\sqrt{2}\pi(h/\lambda)\bar{S}_n} \cdot \left[\frac{(n - 1/2)^2}{(2h/\lambda)^2}\left(\sqrt{L} - \frac{1}{\sqrt{L}}\right) + \sqrt{G}\right] \quad (21)$$

$$\mathrm{Im}\, S_n \cong \frac{-1}{2\sqrt{2}\pi(h/\lambda)\bar{S}_n} \cdot \left[\frac{(n - 1/2)^2}{(2h/\lambda)^2}\left(\sqrt{L} + \frac{1}{\sqrt{L}}\right) + \sqrt{G}\right]. \quad (22)$$

The validity of the latter two formulas depends on L being of the order of 1 and G is small (say less than 10^{-3}). For frequencies of the order of 15 kc and propagation over moderate or well conducting ground, these conditions would be met and furthermore, $\bar{C}_n^2/L$ is usually much less than unity for the first few modes.

It is not intended that these approximate formulas should be employed for detailed calculations; rather, they are introduced for the purpose of illustrating some of the important features of the modes.

Orthogonality Considerations

Before discussing the modes in any further detail, it is perhaps desirable to return to the general expression for the wave function ψ. It can be written in the form[8]

$$\psi(r, \theta) = \sum_n D_\nu z_\nu(kr) P_\nu(-\cos\theta) \quad (23)$$

where the summation is over the various modes numbered from 0 to ∞ through integral values. For the region between the earth and the ionosphere

$$z_\nu(kr) = b_\nu^{(1)} h_\nu^{(1)}(kr) + b_\nu^{(2)} h_\nu^{(2)}(kr) \quad (24)$$

$$\cong \text{const.} \times \left[e^{ik(r-a)\cos\alpha} + R_g e^{-ik(r-a)\cos\alpha}\right] \quad (25)$$

where R_g is defined by (8) and is a function of $\cos\alpha$. An alternative, but equivalent representation is

$$z_\nu(kr) \cong \text{const.} \times \left[e^{ik(b-r)\cos\alpha} + R_i e^{-ik(b-r)\cos\alpha}\right]. \quad (26)$$

The important modes are those with small attenuation, that is, where the imaginary parts of C_n or S_n are small compared to one. In such cases, $R_g \cong 1$ and $R_i \cong \pm 1$, as can be verified from the numerical results. From a physical standpoint, this must be so since incomplete reflection corresponds to high leakage from the mode.

To study the orthogonality properties of the modes, the following integral is considered

$$I = \int_{ka}^{kb} z_\nu(\rho) z_\mu(\rho) d\rho \quad (27)$$

where ν and μ are two sets of modes. Now the function $z_\nu(\rho)$ satisfies

$$\rho\frac{d^2(\rho z_\nu)}{d\rho^2} + [\rho^2 - \nu(\nu + 1)]z_\nu = 1 \quad (28)$$

and there is a similar equation for z_μ. These two equations are now multiplied by z_μ and z_ν, respectively, and integrated over the domain ka to kb, to obtain

$$I = \frac{\rho\left(z_\mu \frac{d}{d\rho}(\rho z_\nu) - z_\nu \frac{d}{d\rho}(\rho z_\mu)\right)\Big|_{ka}^{kb}}{\nu(\nu + 1) - \mu(\mu + 1)}. \quad (29)$$

For the important modes, the right-hand side of (29) is negligibly small if $\mu \neq \nu$ since the numerator vanishes at the limits ka and kb when R_g and R_i approach ± 1. For the important case for $\mu = \nu$, a normalization factor is defined by

$$N = \lim_{\mu \to \nu} \int_{ka}^{kb} z_\mu(\rho) z_\nu(\rho) d\rho = \int_{ka}^{kb} [z_\nu(\rho)]^2 d\rho \cong 2kh/\delta_n \quad (31)$$

where

$$\delta_n = \left[1 + \frac{\sin 2khC_n}{2khC_n}\right]^{-1} \cong \begin{cases} 1 & \text{for } n = 1, 2, 3 \cdots \\ \frac{1}{2} & \text{for } n = 0. \end{cases}$$

It should be remarked at this point that the modes are not strictly orthogonal since the right-hand side of (29) does not vanish identically, although it is small compared to N_ν. As the conductivity of the bounding walls approaches infinity the modes would be completely orthogonal.

Multiplying both sides of (23) by $z_\mu(kr)$ and then integrating with respect to kr from ka to kb, leads to the following formula for D_ν

$$D_\nu = \frac{1}{N_\nu P_\nu(-\cos\theta)} \int_{ka}^{kb} z_\nu(kr)\psi(r, \theta) dr. \quad (32)$$

To actually evaluate D_ν, it is desirable to let $r \to r_0$ and $\theta \to 0$, in which case

$$\psi(r, \theta) \to \psi_0(r, \theta)$$

where ψ_0 is the primary influence which is singular at $(r_0, 0)$. For a vertical electric dipole consisting of an infinitesimal element of length ds and carrying a current, I, it is well known that

$$\psi_0(r, \theta) = \frac{Ids}{4\pi r_0 k} \frac{e^{-ikR}}{R} \quad (33)$$

where $R = [r_0^2 + r^2 - 2rr_0\cos\theta]^{1/2}$.

Following the process suggested by Sommerfeld for the determination of the Green's function for the perfectly conducting sphere,[8] the integration in (32) is carried out in the immediate neighborhood of the source. It then follows that

$$D_\nu = \frac{1}{2kh}\,\frac{z_\nu(kr_0)}{\sin \nu\pi}\,\frac{Ids}{4r_0}. \tag{34}$$

In the above, $z_\nu(kr_0)\cong 2\cos\,[k(r_0-a)C_n]$ since $R_g\cong 1$. Furthermore

$$z_\nu(kr) \cong 2\cos\,[k(r-a)C_n].$$

The field, in terms of the potential function, is then given by

$$\psi(r,\theta) = \frac{Ids}{4khr_0}\sum_{n=0,1,2\cdots}^{\infty}\delta_n\cos\,(kh_0C_n)\cdot\cos\,(kh_1C_n)\,\frac{P_\nu(-\cos\theta)}{\sin\nu\pi} \tag{35}$$

where $h_0=r_0-a$ is the height of the source, $h_1=r-a$ is the height of the observer, and $\nu\cong ka\mathcal{S}_n$.

Simplified Expressions for the Field

The radial field component is of most practical interest and, therefore, attention will be confined to it. Since

$$E_r = \frac{i}{r}\,\eta\,\frac{1}{\sin\theta}\,\frac{\partial}{\partial\theta}\left(\sin\frac{\partial\psi}{\partial\theta}\right) \tag{36}$$

and

$$\frac{1}{\sin\theta}\,\frac{\partial}{\partial\theta}\left[\sin\theta\,\frac{\partial P_\nu(-\cos\theta)}{\partial\theta}\right] + \nu(\nu+1)P_\nu(-\cos\theta) = 0, \tag{37}$$

it follows that

$$E_r = \frac{Ids\,i\eta}{4khr_0r}\sum_{n=0}^{\infty}\delta_n\cos\,(kh_0C_n)\cdot\cos\,(kh_1C_n)\,\frac{\nu(\nu+1)}{\sin\nu\pi}\,P_\nu(-\cos\theta) \tag{38}$$

with $\nu\cong ka\mathcal{S}_n$. This is the final solution of the problem being valid for the air space between the earth and the ionosphere.

For purposes of computation several simplifications can be made. The asymptotic expansion for the Legendre function, given by

$$P_\nu(-\cos\theta)\cong\left(\frac{2}{\pi\nu\sin\theta}\right)^{1/2}\cdot\cos\left[\left(\nu+\frac{1}{2}\right)(\pi-\theta)-\frac{\pi}{4}\right] \tag{39}$$

is valid if $|\nu|\gg 1$ and θ not near 0 or π. Since the imaginary part of $\nu(\pi-\theta)$ is also large for $\pi-\theta$ greater than about 10° or 20°, it follows that

$$P_\nu(-\cos\theta)\cong\left(\frac{1}{2\pi\nu\sin\theta}\right)^{1/2}\cdot\exp\left[i\left(\nu+\frac{1}{2}\right)(\pi-\theta)-i\pi/4\right]. \tag{40}$$

Furthermore, the source and observer heights are usually sufficiently low that kh_0C_n and $kh_1C_n\ll 1$ and $r_0\cong r\cong a$.

The simplified form of the field can now be written

$$E_r = E_0\left[\frac{d/a}{\sin d/a}\right]^{1/2}\frac{(d/\lambda)^{1/2}}{(h/\lambda)}\cdot e^{i[2\pi d/\lambda)-(\pi/4)]}\sum_{n=0}^{\infty}\delta_n\mathcal{S}_n^{3/2}e^{-i2\pi\mathcal{S}_n(d/\lambda)} \tag{41}$$

where $d=a\theta$, the arc length between the source and the observer, λ is the free-space wavelength and $\mathcal{S}_n=(1-C_n^2)^{1/2}$. E_0 is the field of the source on a distance d on a flat perfectly-conducting earth. For $d/\lambda\gg 1$,

$$E_0 = i(\eta/\lambda)Ids(e^{-i2\pi d/\lambda})/d. \tag{42}$$

It is convenient to normalize such that $E_0=0.10$ volt/m for $d=1$ mile $=1605$ m and consequently for purposes of plotting numerical results, E_0 in (41) is replaced by 160.5/d.

The Propagation Factor, $\mathcal{S}_n$

The exponential term inside the summation of (41) determines, in the main, the propagation characteristics of the modes. It can be rewritten as follows

$$\exp\,[-i2\pi\mathcal{S}_n(d/\lambda)] = \exp\left[-\frac{2\pi d}{h}\,u_n\right]\cdot\exp\left[-\frac{i2\pi d}{\lambda}\,s_n\right]$$

where $u_n=-\mathrm{Im}\ \mathcal{S}_n(h/\lambda)$ and $s_n=\mathrm{Re}\ \mathcal{S}_n$. u_n is a dimensionless measure of the attenuation of the mode per unit distance and s_n is a dimensionless phase factor.

Employing the numerical values for Im $\mathcal{S}_n$, the attenuation factor u_n is shown plotted in Fig. 1 as a function of the ionospheric parameter $L(=\omega/\omega_r)$. The conductivity of the lower boundary is chosen such that $G=10^{-4}$ and the height of the reflecting layer, $h=4\lambda$. For example, at a frequency of 16 kc, these latter two conditions could correspond to a ground conductivity of $\sigma=0.0022$ mhos/meter and $h=70$ kilometers.

The abscissa of Fig. 1 can be regarded as a parameter which is inversely proportional to the effective conductivity of the ionospheric D layer at the height of reflection. For small values of L, the attenuation rate is directly proportional to $(\sqrt{L}+\sqrt{G})$ in conformity with (12). As L increases, the attenuation rate of the zero order mode becomes prohibitively high. The attenuation rate for the nonzero modes, on the other hand, passes through a maximum for some intermediate value of L and then falls to a broad minimum for L in the

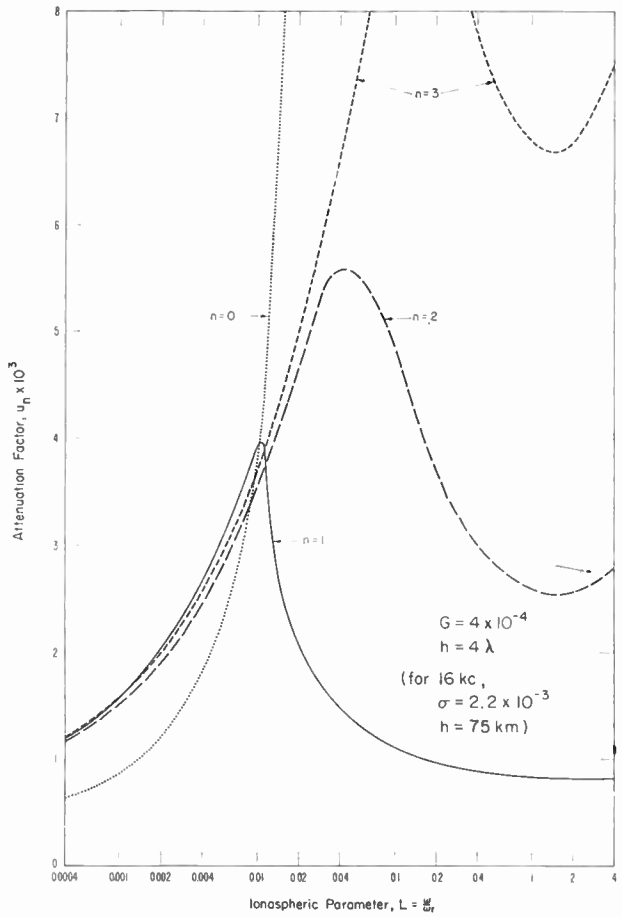

Fig. 1—The attenuation factor as a function of the reciprocal of the effective ionospheric conductivity for a fixed height.

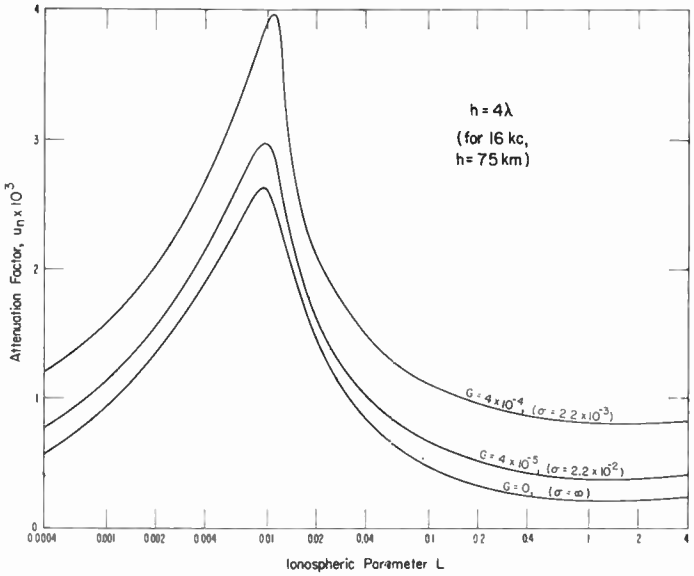

Fig. 2—The attenuation factor as a function of the reciprocal of the effective ionospheric conductivity for various ground conductivities for $n=1$.

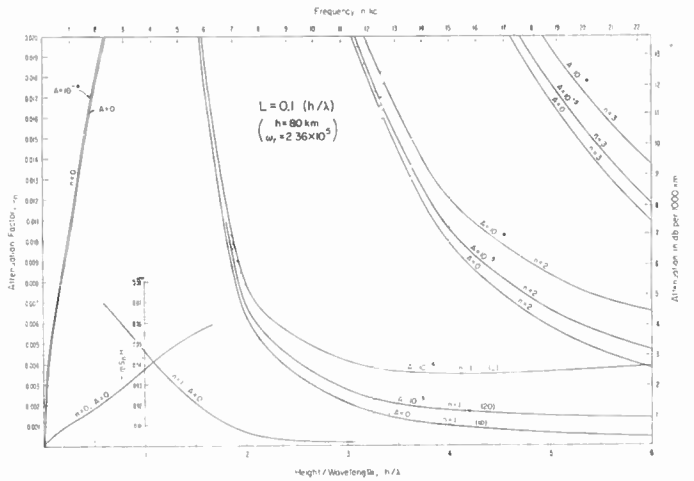

Fig. 3—The attenuation factor as a function of the height to wavelength ratio for a specified ionospheric conductivity and height and for various ground conductivities. The frequency scale in kc and the attenuation scale in db per 1000 km correspond to $h=80$ km, $\omega_r=2.36\times10^5$, and ground conductivities σ of ∞, 20, and 2 millimhos per meter.

vicinity of 1, as predicted by (22). It is seen that the first mode ($n=1$) has the lowest attenuation rate. The higher order modes (beyond $n=2$) would not be expected to be important for propagation to large distances as their attenuation rate is approximately proportional to n^2 in the region where the first mode has low attenuation.

As can be seen from the numerical results and from (22), the ground conductivity parameter G should play a significant role in the behavior of the first mode for vlf propagation. To illustrate this fact, the attenuation factor u_1 is plotted as a function of L in Fig. 2 for $G=4\times10^{-4}$, 4×10^{-5} and 0. These three values could correspond to ground conductivities in mhos/meter of 0.0022, 0.022, and ∞, respectively, when $f=16$ kc and $h=75$ km. It is very evident from Fig. 2 that the ground conductivity cannot be assumed infinite if the propagation path is over land. In the case of an over-sea path, however, it would seem to be well justified to assume a perfect lower boundary.

The behavior of the attenuation rate of the modes as a function of frequency is conveniently displayed by plotting u_n as a function of h/λ for a fixed value of ω_r and the ground conductivity σ. Such curves are plotted in Fig. 3 for $L=0.1$ (h/λ) and $A=G\lambda/h=10^{-4}$, 10^{-5}, and 0. These values could correspond, for example, to $h=80$ km and $\omega_r=2.36\times10^5$ so that in this case, a frequency scale in kilocycles and an attenuation scale in decibels per 1000 kilometers of path length may be appended to Fig. 3. The respective ground conductivities are then 2, 20, and ∞ in millimhos per meter. It can be seen, from the results in Fig. 3, that the zero-order mode is only significant at ultra low frequencies (less than 3 kc). There would seem to be very high attenuation in the region from 3 to 5 kc. Above 8 kc the first order mode is predominant although at still higher frequencies, the second and third modes are also becoming important.[12] The effect of ground conductivity is most marked for the first mode at frequencies above 8 kc.

[12] The mode numbers are here assigned by the following rule: For a fixed n, K, and H, first let h and then G vary upward from zero, then C varies continuously from the value $n/2H$. Budden, "The 'waveguide mode' theory of the propagation of very-low-frequency radio waves," this issue, p. 772, employs a different convention.

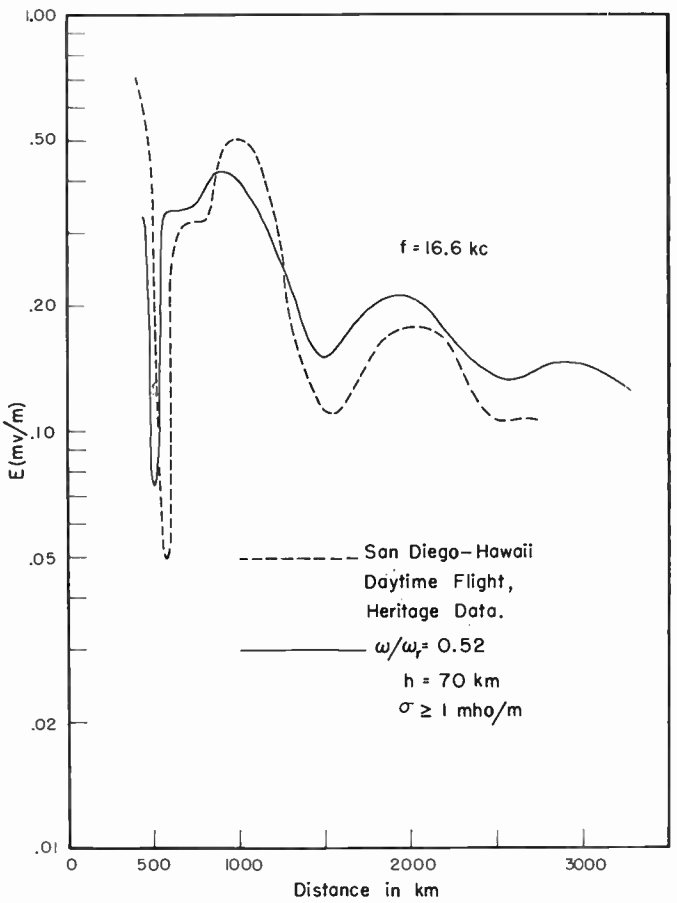

Fig. 4—An experimental field-strength-vs-distance curve for 16.6 kc over sea and the corresponding calculated curve assuming $\omega/\omega_r=0.52$ or $\omega_r=2.0\times10^5$, $h=70$ km and $\sigma\geq1$ mho/meter.

The curves in Figs. 1–3 are only selected examples from a large amount of numerical data[13] for the roots S_n. They do, however, illustrate most of the salient features of the propagational characteristics of the modes.

Field-Strength-Distance-Curves and Comparison with Experiment

It is very worthwhile to compare the theoretical results with experiment. The vertical component of the electric field of a 16.6 kc transmitter at San Diego has been recorded by Heritage, *et al.*,[14] as a function of distance. The results for a daytime flight from San Diego to Hawaii are shown by the dashed curve in Fig. 4. Assuming an ionospheric height h of 70 km and $\omega_r=2\times10^5$ (or $\omega/\omega_r=0.52$), the theoretical curve is also shown in Fig. 4. The ordinate scale is adjusted so that both curves have a ground wave field of 100 mv/m at one mile (1.605 km). The theoretical curve was calculated on the assumption that the conductivity σ of the sea was infinite (*i.e.*, $G=0$). This is justified in the present instance for σ greater than about 1.0 mho/m. The agreement between the theoretical and experimental curves is quite good. It did not seem possible to find any other set of values of ω_r and h which would produce any better agreement.

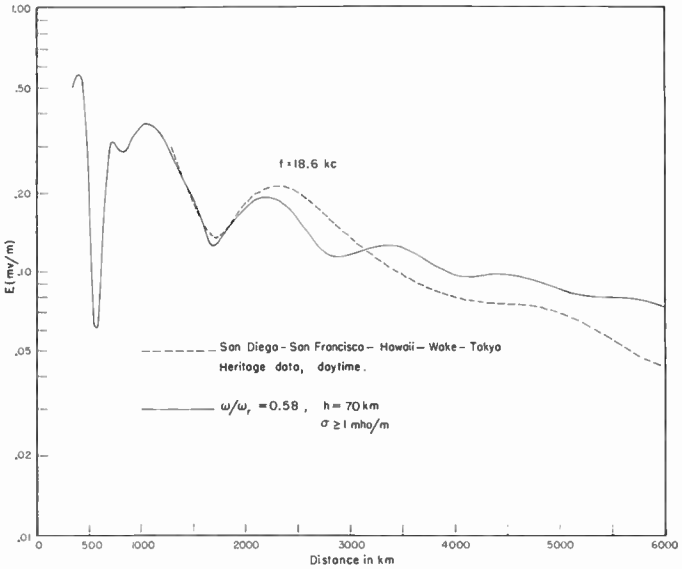

Fig. 5—An experimental field-strength-vs-distance curve for 18.6 kc over sea and the corresponding calculated curve assuming $\omega/\omega_r=0.58$ or $\omega_r=2.0\times10^5$, $h=70$ km and $\sigma\geq1$ mho/meter.

Heritage's data at 18.6 kc for a path from San Diego towards Tokyo are shown in Fig. 5. Employing the same values of ω_r and h as above, the calculated curve is also shown. The agreement here is good at the moderate ranges, but is only fair at the large ranges. The data at the large distances were, however, rather erratic; the dotted curve in Fig. 5 for $d>3000$ km is somewhat conjectural.

The experimental data for a daytime flight from the 18.6 kc transmitter at Jim Creek, Washington, over land to San Diego is shown in Fig. 6. Again choosing $\omega_r=2.0\times10^5$ and $h=70$ km, a theoretical curve is computed. In this case, however, the conductivity of the ground is taken to be 0.005 mho/m which is believed to be a reasonable average value for the path. The agreement with the experimental results is again quite good.

To illustrate the influence of the ionospheric parameter ω_r and the ground conductivity σ, a set of computed field-strength-vs-distance curves are shown in Fig. 7. The ω_r values chosen are 4.0, 2.0, and 1.0×10^5 and the σ values in millimhos/m are 2, 20, and ∞. It can be seen that as ω_r increases the ripples diminish in amplitude while the slopes are almost the same. At this frequency (18.6 kc) and for these ω_r values, the first or dominant mode is not appreciably changed as can be seen from Fig. 1 and consequently the average slopes are almost constant. On the other hand, the attenuation rate for the second order mode becomes greater as ω_r increases, which will tend to enhance the dominance of the first mode and smooth out the ripples.

[13] H. H. Howe and J. R. Wait, "Mode Calculations for VLF Ionospheric Propagation," paper no. 36 presented at VLF Symposium, Boulder, Colo.; January, 1957.

[14] J. L. Heritage, S. Weisbrod, and J. E. Bickel, "A Study of Signal-vs-Distance Data at VLF," paper presented at VLF Symposium, Boulder, Colo.; January, 1957.

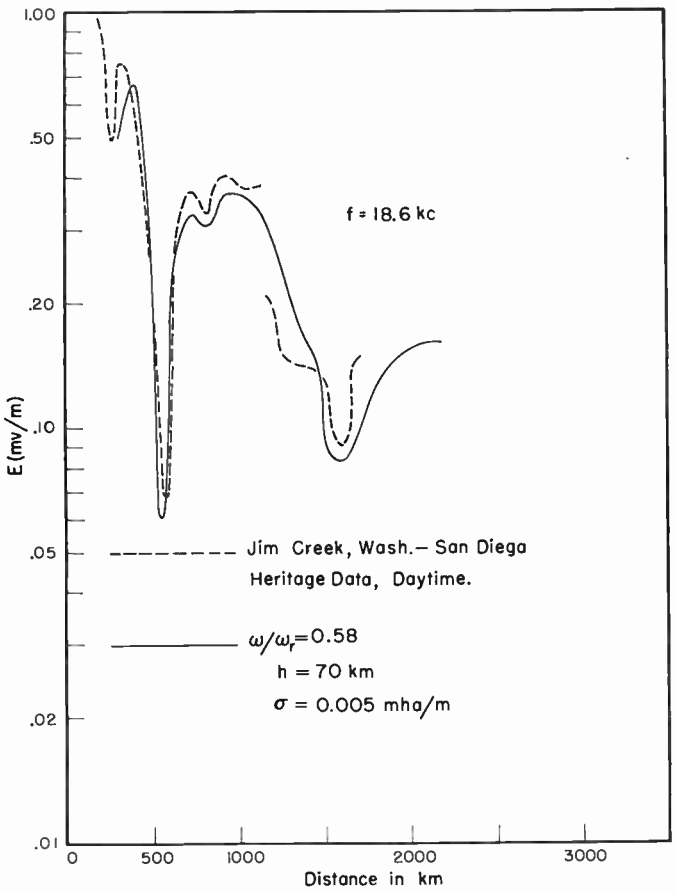

Fig. 6—An experimental-field-strength-vs-distance curve for 18.6 kc *over land* and the corresponding calculated curve assuming $\omega/\omega_r = 0.58$ or $\omega_r = 2.0 \times 10^5$, $h = 70$ km and $\sigma = 5$ millimhos/meter.

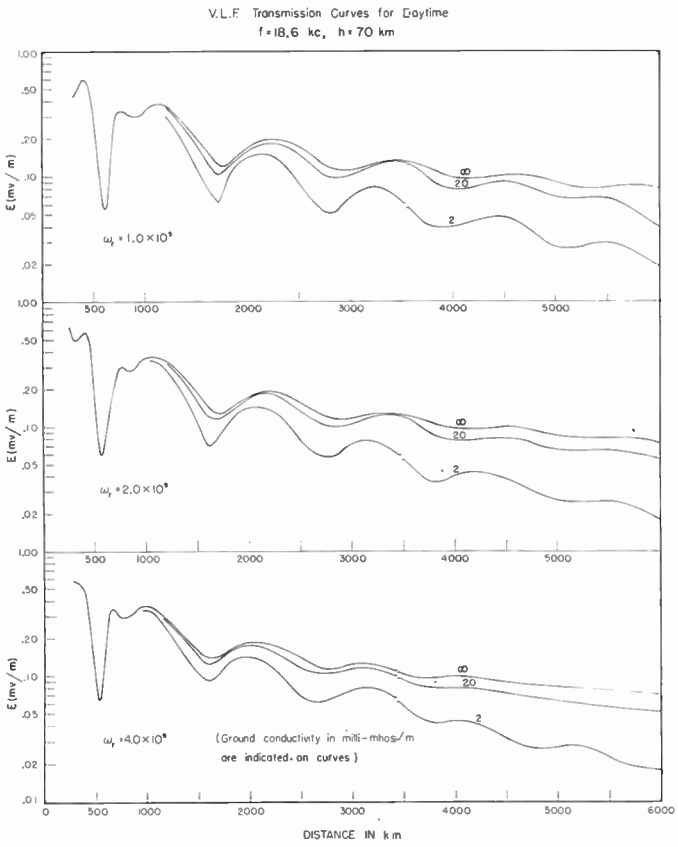

Fig. 7—Calculated field-strength-vs-distance curves for 18.6 kc for ground conductivities of 2, 20 and ∞ in millimhos/meter and ω_r values of 1.0, 2.0, and 4.0×10^5. (The height is taken to be 70 km corresponding to typical daytime conditions.)

Conclusion

The mode theory of vlf would appear to explain many of the salient features of the field-strength-vs-distance data. Furthermore, the numerical values of the parameters h and ω_r are compatible with those deduced from geometrical-optical methods[6] usable at short ranges. The sharply-bounded model of the ionosphere is limited to frequencies below about 25 kc. For higher frequencies, it appears to be necessary to adopt a stratified ionosphere. Mode calculations for this case will be reported in the near future.

Acknowledgment

The author is indebted to Dr. H. H. Howe and Mrs. A. Murphy for their assistance with the computations and to J. Heritage for giving permission to quote his experimental results. In addition, the author would like to thank K. G. Budden, E. T. Pierce, and A. G. Jean for their helpful comments.

The Attenuation vs Frequency Characteristics of VLF Radio Waves*

JAMES R. WAIT†, SENIOR MEMBER, IRE

Summary—**The theoretical dependence on frequency of the attenuation of the wave guide modes in vlf propagation is discussed in some detail. It is indicated that most of the published experimental data between 1 and 30 kc was compatible with the sharply bounded model of the ionosphere with a reflecting height of about 70 km during the day and 90 km during the night.**

IT HAS BEEN known for many years that radio waves in the very low-frequency band can propagate to great distances. Nearly always, however, there is pronounced absorption between 2 and 4 kc. On the other hand, for frequencies around 10 kc, there is very little attenuation. Apparently, in the latter case the ionosphere is behaving as a good reflector with a reflection coefficient near -1, and the ground is also a good reflector with a reflection coefficient near $+1$. For frequencies in this 10 kc region, the losses in the upper and lower bounding surfaces give rise to an attenuation coefficient of the order of 2 db per 1000 km of path length. At frequencies below the absorption band the attenuation factor is also small with a typical value of about 3 db per 1000 km of path length at about 1 kc.

It is the purpose of the present paper to present theoretical data for the attenuation coefficients of the dominant modes of propagation in a model, which idealizes the space between the ground and the ionosphere as a waveguide with concentric (sharply bounded) spherical walls. It is shown that such a model explains satisfactorily most of the observed data in the vlf range (1 kc to 30 kc).

Assuming that the source is a vertical electric dipole radiating P kilowatts, the vertical electric field in millivolts per meter at a great circle distance, d, in km from the transmitter is given by the mode sum[1]

$$E = E_0 W$$

where

$$W \cong \left[\frac{d/a}{\sin d/a}\right]^{1/2} \frac{(d/\lambda)^{1/2}}{(h/\lambda)} \left| \sum_{n=0}^{\infty} \delta_n S_n^{3/2} e^{-i2\pi S_n (d/\lambda)} \right| \qquad (1)$$

$$E_0 = \frac{300\sqrt{P}}{d}$$

and where $S_n = (1 - C_n^2)^{1/2}$ and C_n is a solution of

$$\left[\frac{(L - i)C_n - \sqrt{C_n^2 L^2 - iL}}{(L - i)C_n + \sqrt{C_n^2 L^2 - iL}}\right] \cdot \left[\frac{(KG - i)C_n - \sqrt{(K - 1)G^2 - iG + C_n^2 G^2}}{(KG - i)C_n + \sqrt{(K - 1)G^2 - iG + C_n^2 G^2}}\right] = e^{4\pi i H C_n} e^{-2\pi i n} \qquad (n \text{ is a positive integer})$$

with

$$L = \omega/\omega_r, \qquad G = \epsilon\omega/\sigma, \qquad K = \epsilon_e/\epsilon, \qquad = h/\lambda$$

and

$$\delta_n = \left[1 + \frac{\sin 4\pi H C_n}{4\pi H C_n}\right]^{-1} \sim \begin{cases} 1 & \text{for } n = 1, 2, 3 \cdots \\ 1/2 & \text{for } n = 0 \end{cases}.$$

In the above

a = radius of earth in kilometers,
λ = wavelength in km,
ω = angular frequency in radians per second,
$\omega_r = \dfrac{(\text{plasma frequency})^2}{\text{collisional frequency}}$,
ϵ = dielectric constant of free space,
ϵ_e = dielectric constant of ground,
h = separation in km between ionospheric reflecting layer and ground,
σ = conductivity of ground in mhos per meter.

The complex values of S_n ($n = 0, 1, 2, 3, \cdots$) satisfying (2) have been obtained from an automatic computer using a program devised by Dr. H. H. Howe. This aspect of the problem has been discussed elsewhere.[2]

The exponential term inside the summation of (1) determines, in the main, the propagation characteristics of the modes. It can be rewritten as follows

$$\exp\left[-i2\pi S_n (d/\lambda)\right] = \exp\left[-\frac{2\pi d}{h} u_n\right] \exp\left[-i\frac{2\pi d}{\lambda} s_n\right]$$

where $u_n = -\operatorname{Im} S_n(h/\lambda)$ and $s_n = \operatorname{Re} S_n$. u_n is a dimensionless measure of the attenuation of the mode per unit distance and s_n is a dimensionless phase factor. For the present purpose, it is convenient to discuss the attenuation in terms of the number of db per 1000 km of path length. This is denoted α_n and is related to u_n by

$$\alpha_n = \frac{8.86 \times 2\pi u_n}{h} \times 10^3.$$

* Original manuscript received by the IRE, March 3, 1957. This paper is largely based on remarks made by the author during the discussion periods of the Symposium on Propagation of Very-Low-Frequency Electromagnetic Waves, Boulder, Colo.; January 23–25, 1957.

† National Bureau of Standards, Boulder, Colo.

[1] J. R. Wait, "The mode theory of vlf ionospheric propagation for finite ground conductivity," this issue, p. 760. A similar approach had been proposed originally by K. G. Budden, "The propagation of a radio atmospheric II," *Phil. Mag.*, vol. 43, pp. 1179–1200; November, 1952.

[2] H. H. Howe and J. R. Wait, "Mode Calculations for VLF Ionospheric Propagation," paper no. 36 presented at VLF Symposium, Boulder, Colo.; January, 1957.

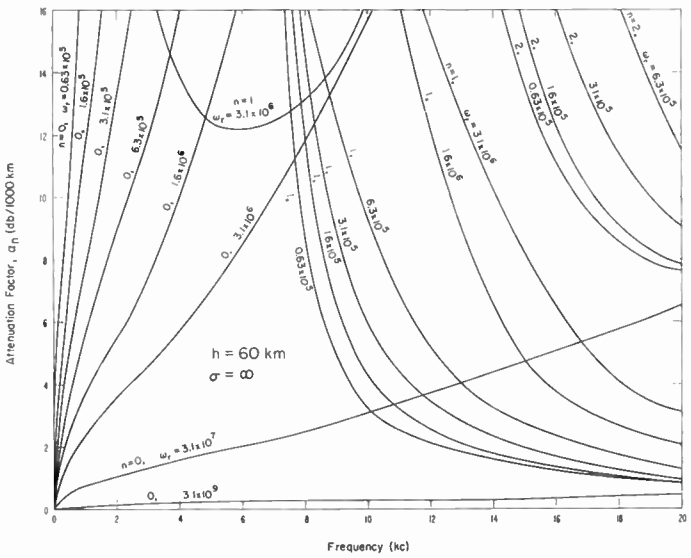

Fig. 1—The attenuation factor in decibels per 1000 km of path length as a function of the frequency in kilocycles. The mode number and the value of ω_r are indicated on each curve. The conductivity, σ, of the ground is taken to be infinite and the height of the ionospheric reflecting layer is a height, h, of 60 km.

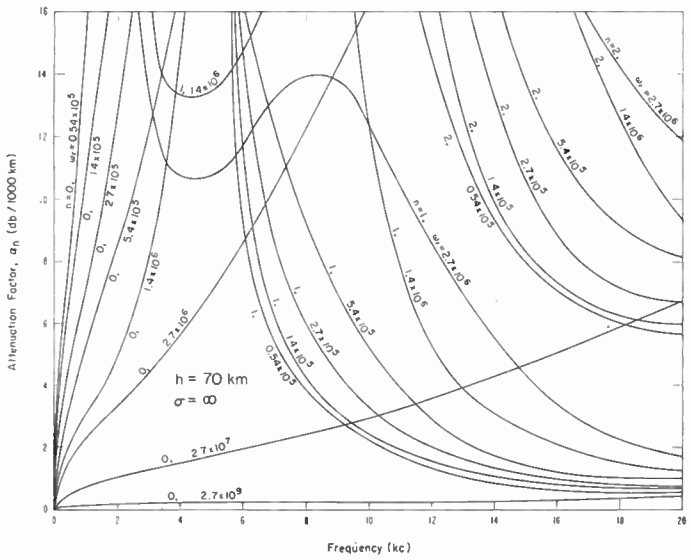

Fig. 2—Same as Fig. 1 with $h=70$ km.

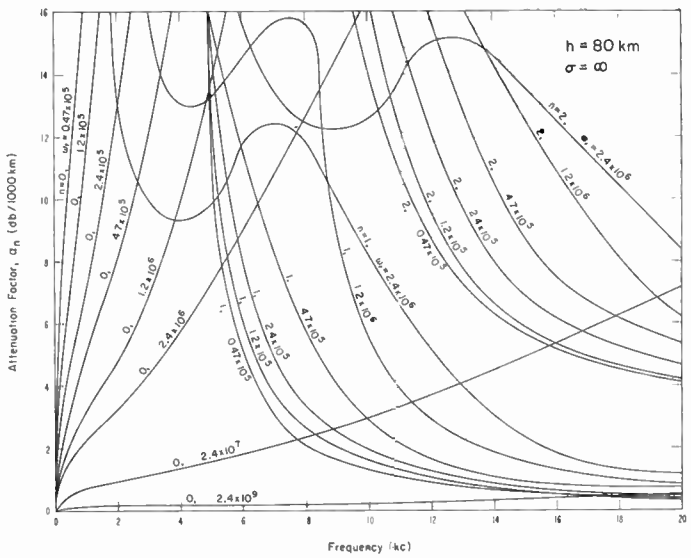

Fig. 3—Same as Fig. 1 with $h=80$ km.

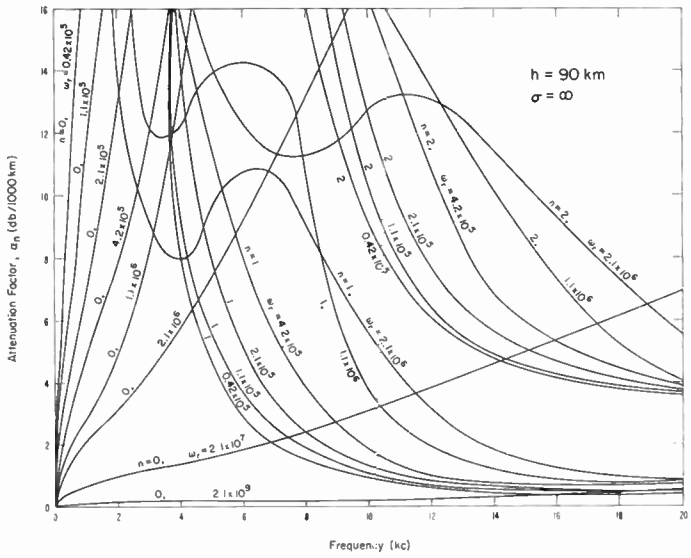

Fig. 4—Same as Fig. 1 with $h=90$ km.

The attenuation factor α_n is plotted in Figs. 1 to 4 for $\sigma=\infty$ and $h=60$, 70, 80, and 90 km, respectively. Various values of ω_r are indicated on the curves. Only the first three modes are indicated, namely, $n=0$, 1, and 2. At extremely low frequencies, of the order of 1000 cps and less, the zero order mode is dominant. In this case the attenuation is proportional to $\omega_r^{-1/2}$ or in other words it is proportional to the square root of the effective resistivity of the ionosphere at the height of reflection. In fact, if L or ω/ω_r is less than about 0.004, then

$$u_0 \cong \frac{\sqrt{L/2}}{4\pi}.$$

This simple expression is in accord with a formula derived by Schumann.[3] It would appear to predict most of the experimental results[4] for frequencies from 100 to 1000 cps, ω_r is taken to be about 10^6 and $h=70$ km in the daytime and $h=90$ km at night.

For frequencies from 6 to 16 kc or so, the attenuation rate does not vary in any simple manner with frequency.[1] At large distances (>2000 km) it appears that the first mode, labeled one, is dominant. Experimental results of Heritage[1] and Chapman and Macario[4] indicate that ω_r is about 2×10^5 and $h=70$ km for the daytime and ω_r is about 10^6 and $h=90$ km for the night.

In Fig. 5 the attenuation factor α_n is plotted for various ground conductivities taking $h=80$ km and

[3] W. O. Schumann, "Uber die oberfelder bei der ausbreitung longer wellen," *Z. angew. Phys.*, vol. 6, pp. 35–43; January, 1954.

[4] F. W. Chapman and R. C. Macario, "Propagation of audio frequency radio waves," *Nature*, vol. 177, pp. 930–933; May, 1956.

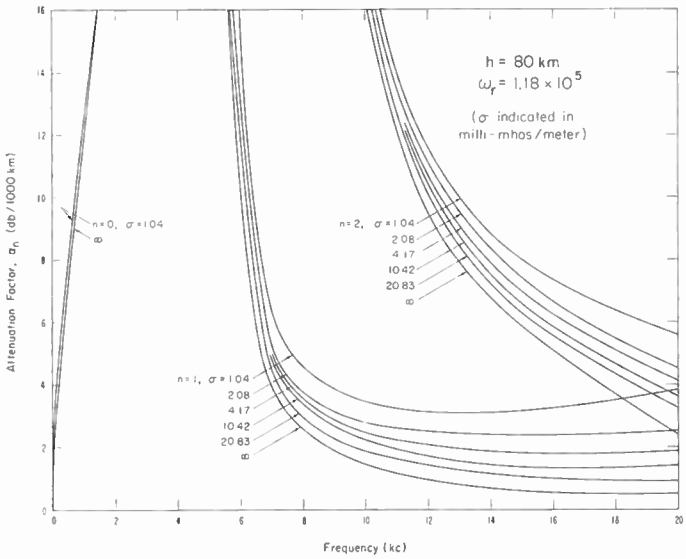

Fig. 5—The attenuation factor as a function of frequency for $h=80$ km and $\omega_r=1.18\times10^5$ and various values of ground conductivity which are indicated on the curves in millimhos/meter.

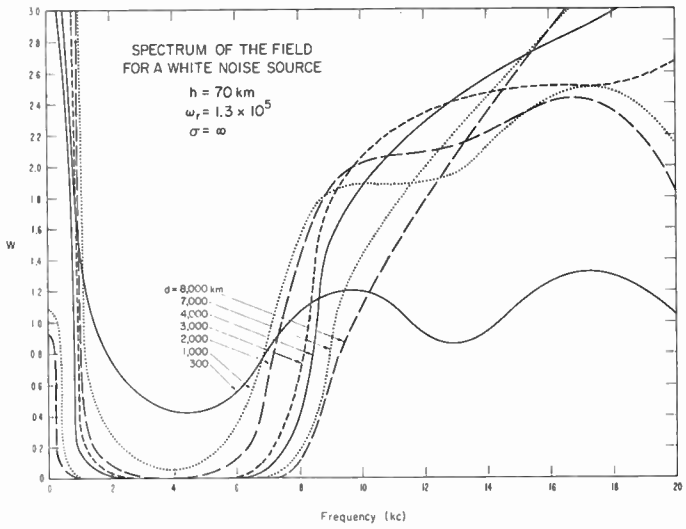

Fig. 6—The spectrum function W, at various distances, is shown plotted as a function of frequency for $h=70$ km, $\omega_r=1.3\times10^5$, and $\sigma=\infty$. W in this case corresponds to the field for a dipole source whose radiated power is constant with respect to frequency.

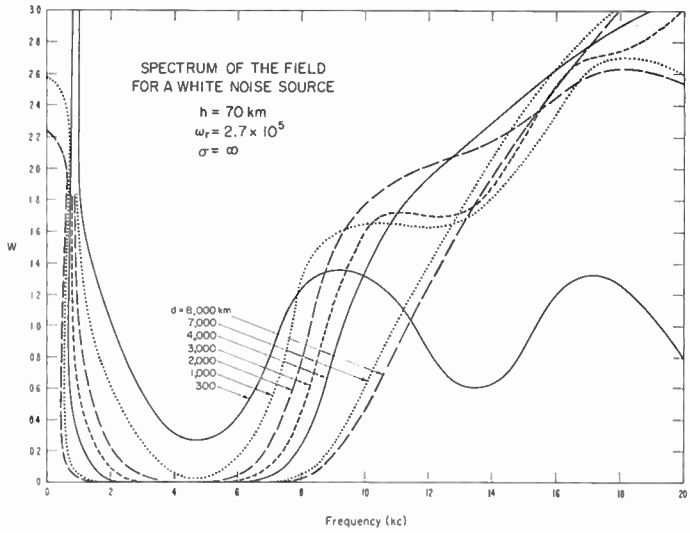

Fig. 7—Same as Fig. 6 with $\omega_r=2.7\times10^5$.

$\omega_r=1.18\times10^5$. For the extremely low frequencies, the effect of the ground losses is negligible. However, at the upper end of the vlf band the ground conductivity plays an important role. In fact, it appears that, for propagation over land with a typical conductivity of 2 millimhos per meter, the attenuation rate is just twice that for sea which has effectively an infinite conductivity. This behavior has been observed by Chapman and Pierce[5] on numerous occasions in England. They were able to compare the relation between the characteristics of atmospherics originating from sources in southeast Europe and those originating from sources in the southwest Atlantic Ocean. For example, they found that the ratio of the spectral component at 650 cps to that at 10 kc was about 50 per cent greater for the easterly sources. This result was based on averaging a large number of results for sources within 1500 km. It could be expected that the contrast would be even more striking for larger ranges.

In order to properly discuss the nature of the spectral behavior of the transmission path, it is necessary to evaluate the sum of modes for the field. In Figs. 6 and 7 the function W is plotted as a function of frequency for $\sigma=\infty$ and $h=70$ and 90 km respectively. Various distances, d, are shown on the curves, ranging from 300 to 11,500 km. The quantity W can be regarded as the spectrum of a white noise source. The spectrum E for any particular source function is obtained by employing the appropriate form for E_0, the primary field of the source. Actually, as d approaches zero, W should approach unity. An indication of this limit is evidenced in the curve for $d=300$ km which is seen to be oscillating about unity.

It is interesting to note that the higher frequencies, between 15 and 20 kc, are enhanced in the spectrum at larger ranges. Furthermore, there is a pronounced absorption band centered around 4 kc. This behavior is in accord with the observations of Chapman and Matthews[6] who measure the frequency spectra of lightning strokes as a function of range. Actually, the measured spectrum shows a peak around 10 kc. This can be explained by the fact that the spectrum of the lightning discharge has a peak around 5 kc which, when multiplied by the transfer function of the propagation path (*i.e.*, W), gives rise to a broad maximum in the resultant spectrum around 10 kc.

In Figs. 8 and 9, the spectrum function W is shown plotted as a function of frequency for $\sigma=\infty$, $d=4000$

[5] J. Chapman and E. T. Pierce, "Relations between the character of atmospherics and their place of origin," this issue, p. 804.

[6] F. W. Chapman and W. D. Matthews, "Audio frequency atmospherics," *Nature*, vol. 172, pp. 495–497; June, 1953.

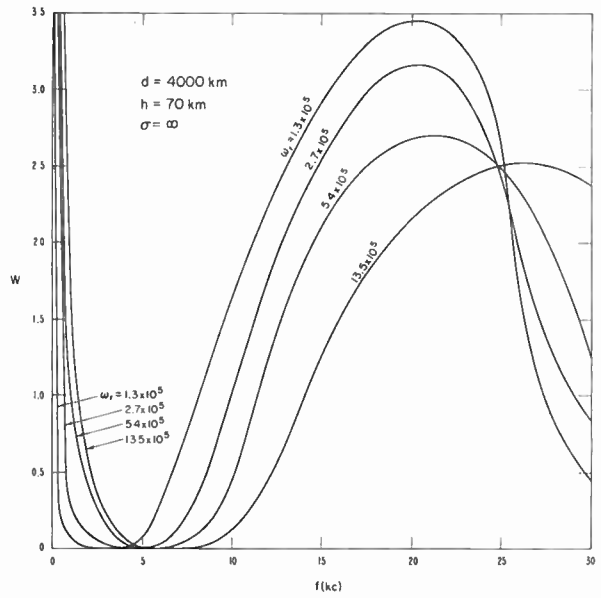

Fig. 8—The spectrum function for $d=4000$ km, $h=70$ km, $\sigma=\infty$, and various values of ω_r which are indicated on the curves.

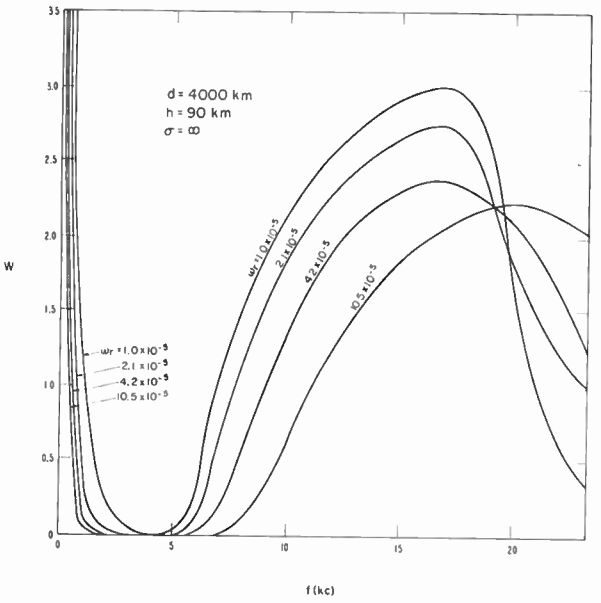

Fig. 9—Same as Fig. 8 with $h=90$ km.

km, $h=70$ km and various values of ω_r. There appears to be a broad maximum centered between 15 and 20 kc. The decrease of W for frequencies above 20 kc can be associated with the interaction of the first order and second order mode. This effect is more noticeable for the larger heights. This is compatible with Chapman and Matthews' observation that the peak in the spectrum occurs at higher frequencies in daytime, where h is around 70 km, than at nighttime, where h is around 90 km.

In Fig. 10 the spectrum function W is shown plotted for $d=4000$ km, $h=70$ km, $\omega_r=2.7\times10^5$ for various ground conductivities. Here it can be strikingly noted that the higher frequencies (above 6 kc) are enhanced relative to the lower frequencies (below 2 kc) for a path

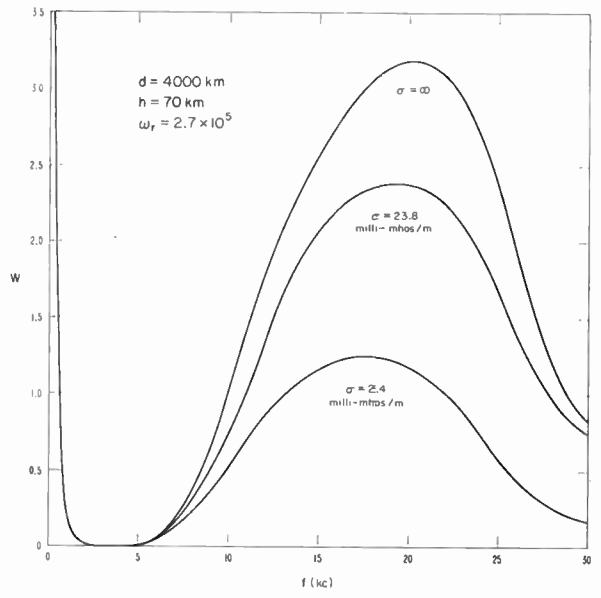

Fig. 10—The spectrum function for $d=4000$ km, $h=70$ km, $\omega_r=2.7\times10^5$, and various values of the ground conductivity which are indicated on the curves.

with a highly conducting lower boundary such as sea water. In the language of Pierce and Chapman,[5] the "oscillatory head" characteristics of frequencies around 10 kc are enhanced for a sea path relative to the "slow tail" characteristic of the frequencies below 2 kc.

It is believed that the waveguide model explains most of the salient features of the experimental data. Most of the British data can only be used for qualitative interpretation, since the current spectrum of the lightning stroke is not known. Furthermore, the distances to the strokes are not known precisely. Despite the shortcomings on the data, considerable confidence is given to the validity of the basic assumptions in the theory. It might also be mentioned that Watt[7] has recently indicated that the measured spectra of atmospheric noise at Boulder, Colo., in winter were compatible with the waveguide mode theory, if the sources could be generally located at ranges of the order of 3000 km which is not at all unreasonable.

The curves given in the present paper should be useful for interpreting future experimental results. It is particularly desirable, if the spectrum of the ground wave pulse of the source could be measured at short ranges simultaneously with the spectrum of the total field at greater ranges. It is then a simple matter to compute the primary field E_0 and hence an experimental curve for W can be obtained which is directly comparable with the calculated curves in Figs. 6 to 10.

Acknowledgment

The author would like to thank Dr. H. H. Howe and Mrs. Alyce Conda for assistance with the calculations and John Harman for preparing the illustrations.

[7] A. D. Watt and E. L. Maxwell, "Characteristics of atmospheric noise from 1 to 100 kc," this issue, p. 787.

The "Waveguide Mode" Theory of the Propagation of Very-Low-Frequency Radio Waves*

KENNETH G. BUDDEN†

Summary—**The paper relates to the theory in which the propagation of vlf radio waves is treated by regarding the space between the earth and the ionosphere as a waveguide. Its purpose is to answer some criticisms of earlier papers by Budden.[1-3] The earth is assumed to be a perfectly conducting plane, and the ionosphere is assumed to be a homogeneous medium with a sharp boundary.**

In general, there is no unique way of assigning numbers to the waveguide modes. The numbers are usually assigned by continuity with the case where the ionosphere is a perfect conductor, but this method fails for some values of the height and the conductivity.

If the product of the height and the conductivity is less than a certain critical value, the attenuation for the zero order mode has a maximum at some frequency, and thereafter decreases as the frequency increases, as was found by Budden.[1] If the critical value is exceeded, the attenuation for the zero order mode increases indefinitely with increasing frequency, as was found by Wait[4] and Liebermann.[5]

Introduction

THIS PAPER relates to the theory in which the propagation of very-low-frequency radio waves is treated by regarding the space between the earth and the ionosphere as a waveguide. The earth is assumed to be a perfectly conducting plane, and the ionosphere is assumed to be a homogeneous medium with a plane sharp boundary. It is known (see, for example, Wait[4]) that the actual propagation characteristics of the waveguide modes may be appreciably affected by finite ground conductivity and by the curvature of the earth. But the present note is more concerned with basic principles than with the actual constants of the earth and the ionosphere. Its purpose is to answer some criticisms of the papers by Budden.[1-3]

Negative Order Modes

The field at a distance from the sender is expressed as the sum of contributions from a number of modes, and Budden[1-3] included modes of negative order. Wait[4] has pointed out that there is an error in the deformation of a contour in the Budden article[2] and that negative order modes are not excited by a dipole sender, and should not be included. This appears to be correct but does not appreciably affect Budden's conclusions,[1,2] since the characteristics deduced for the modes of orders -1, -2, $\cdots$, were very close to those for modes of orders 0, 1, $\cdots$, respectively. Hence, for the particular values of ω_r and h used by Budden, inclusion of the negative order modes will not appreciably affect the form of the variation of signal with distance from the sender.

The Zero Order Mode

Wait[4] and Liebermann[5] have concluded that the attenuation of the zero order mode increases indefinitely as the frequency increases, whereas Budden[1] concluded that its attenuation has a maximum value near 2 to 5 kc and therefore decreases as the frequency increases, and that the zero order mode is dominant at all frequencies. The discrepancy between these results is explained in the following paragraphs, where it is shown that both conclusions are correct. The values of conductivity of the ionosphere assumed by Budden were lower than those assumed by Wait and Liebermann, and this accounts for the different results.

The Curve Im $(n)=0$

The field of a waveguide mode may be thought of as composed of two crossing plane waves with their normals at complex angles θ, $\pi-\theta$ to the vertical. Let $C=\cos\theta$. Then the value of C is given by

$$f(C) \equiv \frac{(L-i)C-(C^2L^2-iL)^{1/2}}{(L-i)C+(C^2L^2-iL)^{1/2}}\cdot e^{-4\pi iHC} = 1 \quad (1)$$

where $L=\omega/\omega_r$, $H=h/\lambda$, $\omega/2\pi$ is the wave frequency, λ is the wavelength in free space, h is the height of the boundary of the ionosphere, $\omega_r=4\pi\sigma/\epsilon_0$ and σ is the conductivity of the ionosphere. Eq. (1) is equivalent to the formula used by Budden[6] and by Wait.[7] The notation used here is that of Wait. An alternative expression for ω_r is $\omega_r=4\pi Ne^2/\epsilon_0 m\nu$ in unrationalized units, where N is the electron number density, ν is the collision frequency, and e, m are the charge and mass of the electron.

Eq. (1) requires that the logarithm of $f(C)$ is equal to $2\pi in$ where n is an integer. Howe and Wait[8] have computed this logarithm for various values of C, and found those values of C which made the imaginary part of n equal to zero. This gives a curve in the complex C plane whose equation is

$$|f(C)| = 1. \quad (2)$$

* Original manuscript received by the IRE, March 3, 1957. This paper is based on remarks made by the author at the Symposium on Propagation of Very-Low-Frequency Electromagnetic Waves, Boulder, Colo.; January 23–25, 1957.

† Cavendish Lab., Cambridge, England.

[1] K. G. Budden, "The propagation of a radio atmospheric," *Phil. Mag.*, vol. 42, p. 1–19; January; 1951.

[2] K. G. Budden, "The propagation of a radio atmospheric II," *Phil. Mag.*, vol. 43, pp. 1179–1200; November, 1952.

[3] K. G. Budden, "The propagation of very low frequency radio waves to great distances," *Phil. Mag.*, vol. 44, pp. 504–513; May, 1953.

[4] J. R. Wait, "The mode theory of vlf ionospheric propagation for finite ground conductivity," this issue, p. 760.

[5] L. Liebermann, "Extremely low frequency electromagnetic waves. II Propagation properties," *J. Appl. Phys.*, vol. 27, pp. 1477–1483; 1956.

[6] Budden, *op. cit.*, footnote 3, (7) and (8).

[7] Wait, *op. cit.*, with G=0.

[8] H. H. Howe and J. R. Wait, "Mode Calculations for VLF Ionospheric Propagation," paper no. 36 presented at VLF Symposium, Boulder, Colo.; January, 1957.

The values of C which correspond to possible modes must lie on this curve, and it is convenient to call these "mode points." Howe and Wait have shown that for some values of L and H the curve can have an isolated closed branch which surrounds a zero of the factor

$$R = \frac{(L - i)C - (C^2L^2 - iL)^{1/2}}{(L - i)C + (C^2L^2 - iL)^{1/2}}. \qquad (3)$$

This factor is the reflection coefficient of the ionosphere given by Fresnel's formula, for the complex angle θ, where $C = \cos\theta$. The value of θ which makes R zero is sometimes called the "complex Brewster angle." When an isolated branch of the curve surrounds this zero, arg R takes all values in the range 0 to 2π on this branch, and hence it is clear that there is one mode point on the branch. This mode may be the one that is called the zero order mode. The above process may separate it from the main sequence of the other modes, and when this happens the attenuation in this mode increases indefinitely as the frequency increases, as was found by Howe and Wait.

When an isolated branch of this kind is just about to separate off from the main curve, there must be a saddle point of $f(C)$ at some point on the curve $|f(C)| = 1$. Hence the condition is that simultaneously

$$\frac{\partial f(C)}{\partial C} = 0, \qquad |f(C)| = 1. \qquad (4)$$

This is only possible for certain values of L and H which lie on a continuous curve in the L-H plane shown in Fig. 1. For any pair of values of L and H for which the representative point in Fig. 1 lies above the curve, there is an isolated branch of the curve $|f(C)| = 1$ in the complex C plane.

Degenerate Modes

It can happen that a mode point may coincide with a saddle point of $f(C)$. The condition for this is that simultaneously

$$f(C) = 1 \qquad \frac{\partial f(C)}{\partial C} = 0. \qquad (5)$$

This fixes pairs of values of L and H, whose representative points must lie on the curve of Fig. 1. These will be called "critical points." They are shown in Fig. 1 labelled A, B, C, etc. Eq. (5) is also the condition that (1) has a double root, so that two mode points coalesce. The corresponding mode is therefore a degenerate case where two modes have identical phase velocities, attenuations, and excitation factors.

Discussion of Results

In calculating the signal received at a great distance from a very-low-frequency sender it is not necessary to know the numbers of the modes. The phase velocity, attenuation, and excitation factor for a given mode depend only upon the value of C for that mode, and not upon the integer which specifies the number of the mode. The signal can therefore be calculated provided that the values of C for the least attenuated modes are known. The numbering of the modes is merely used as a convenient way of identifying them.

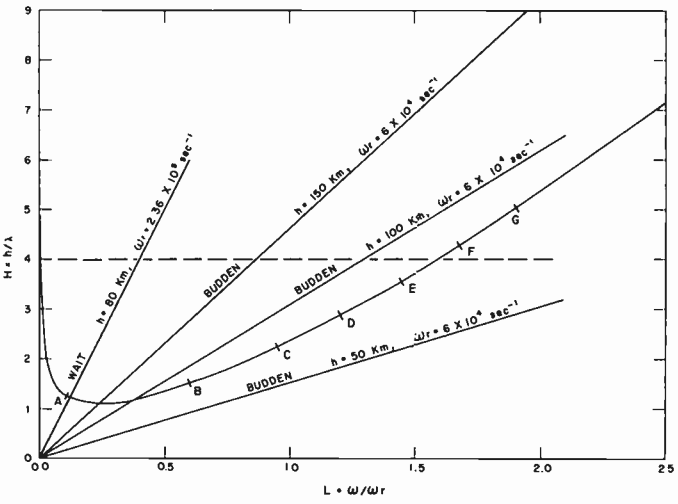

Fig. 1—The curve is the locus of points for which simultaneously $df(C)/dc = 0$ and $|f(C)| = 1$. The points A, B, C, · · · , indicate values of L and H for which two mode points coincide.

Wait[9] has given curves showing how the attenuation factor for various modes depends upon L for the fixed value $H = 4$. The line $H = 4$ is shown dotted in Fig. 1. Very low values of L correspond to a perfectly reflecting ionosphere and here there is no ambiguity about the numbering of the modes. In particular for $L = 0$, the zero order mode is unattenuated and travels with the velocity of light in free space. As L increases, the curve of Fig. 1 is crossed and the zero order mode lies on an isolated branch of the curve $|f(C)| = 1$, and its attenuation increases. When the value $L = 1.6$ is reached, the isolated branch rejoins the main curve and the mode point on it is between the mode points for the fifth and sixth modes. If the curve $|f(C)| = 1$ were examined for the values $H = 4$, $L > 1.6$ the mode point which has here been called "zero order" would appear sixth in sequence from the beginning of the curve $|f(C)| = 1$ and might equally correctly be described as "fifth order," in the sequence 0, 1, 2, 3, 4, 5, · · · . A fuller description of these phenomena is given by Howe.[10]

For an actual model of the ionosphere, the height h, and the conductivity $\epsilon_0\omega_r/4\pi$ are fixed. Hence the ratio $H/L = \omega_r h/2\pi c$ is fixed. This corresponds to a straight line through the origin in Fig. 1, and different points on this line correspond to different frequencies. Wait[11] gave curves of attenuation as a function of frequency for various modes, for the case $H/L = 10$. The corresponding line is shown in Fig. 1 and it is seen to cross the curve, so that one mode point is separated as described in the last paragraph, and its attenuation increases as the frequency increases. Now the line passes to the right

[9] Wait, *op. cit.*, Fig. 1.
[10] H. H. Howe (to be published).
[11] Wait, *op. cit.*, Fig. 3.

of the critical point A, so that the *first* order mode should be separated, and the zero order mode should remain at the beginning of the original sequence, and should be the least attenuated at higher frequencies. But the line passes very close to A where $L=0.12$, $H=1.2$. Here the values of C for the two modes of orders 0 and 1 are very close together, and in passing near the critical point the identity of these modes might be confused. It is probable that for this value of H/L Wait and Howe have interchanged the mode numbers when passing the critical point. If the line in Fig. 1 had passed to the left of A their numbering would have been that of the sequence of modes for very low values of L.

Budden[12] gave curves for $H/L=1.59$, 3.19, 4.78. The corresponding lines are shown in Fig. 1. The first does not cross the curve at all so that the zero order mode remains in the main sequence and is dominant at all frequencies. The other two lines cross the curve between the critical points A and B, so that it is the *first* order mode which appears on the isolated branch of the curve $|f(C)|=1$. Again the zero order mode remains in the main sequence and is dominant at all frequencies. A fourth curve given by Budden[13] is for $H/L=159$. The corresponding line in Fig. 1 would be very close to the line $L=0$, and would extend only up to $H=3.3$ (corresponding to the highest frequency considered, namely 20 kc). It does just cross the curve, but the conductivity is so high that attenuation is very small. In this case, however, attenuation of the zero order mode would ultimately increase indefinitely with increasing frequency.

The results given[3] were for a value of H/L close to 1.59, and this case has already been discussed.

Liebermann[5] also claimed that the attenuation of the zero order mode increases indefinitely as the frequency increases. The model of the ionosphere which he adopts for nighttime has $h=90$ km, $\omega_r=6.28\times10^5$ sec^{-1}, which gives $H/L=30$. The corresponding line in Fig. 1 would cross the curve to the left of the critical point A, so that Liebermann's conclusion is correct for this model. For the daytime Liebermann takes $h=60$ km, $\omega_r=1.26\times10^5$ sec^{-1} which gives $H/L=4$. The corresponding line in Fig. 1 would pass to the right of the critical point A so that the zero order mode is not heavily attenuated at the higher frequencies, but is the dominant mode.

The Response to a Lightning Flash

Liebermann[5] was concerned with the signal excited in the zero order mode by a lightning flash, and concluded that this mode contributes only extremely low-frequency components, because he believed that the higher frequencies are always heavily attenuated. The response would then consist only of that part of an atmospheric which is sometimes called the "slow tail." This conclusion is correct when $H/L>11.8$ (approximately), but is not correct if $H/L<11.8$. In the case discussed by Budden[1] for $H/L=1.59$ the zero order mode is dominant for higher frequencies, and the failure to realize this led Liebermann[5] to conclude that the impulse response calculated by Budden[14] was wrong. In fact it gives correctly the impulse response contributed by the higher frequencies (above about 5 kc). There would, in addition, be a slow tail response contributed by the frequencies below about 2 kc, but this would be on a time scale too long to appear in the figure.

Method of Calculation

The curve of Fig. 1 and the positions of the critical points were calculated by an approximate method. The function $R(C)$ in (3) was set equal to $R_B'(C-C_B)$ where C_B is the value of C at the complex Brewster angle, and R_B' is the value of $\partial R/\partial C$ when $C=C_B$. This is equivalent to using the first nonzero term of the Taylor expansion about the point $C=C_B$. With this approximation (4) and (5) can be solved fairly easily. Two or three points on the curve near A were also calculated more accurately and this showed that the approximate method gave an accuracy of about 5 per cent in H for a given L.

Conclusion

A detailed investigation of the theory of the waveguide modes in the space between a perfectly conducting earth and a sharply-bounded homogeneous ionosphere shows that care is needed in choosing the numbers for the modes. When the ionosphere is a perfect conductor the electric field of the wave varies sinusoidally with height, and the number of half cycles of this variation between the ground and the ionosphere is the number of the mode. If the conductivity is now imagined to decrease continuously, the characteristics of the modes change, but the same numbering system can be used, by continuity with the perfectly conducting case. This method fails, however, if certain critical values of the height, h, and the conductivity, $\epsilon_0\omega_r/4\pi$, are encountered. These are given by the critical points A, B, C, D, etc., in Fig. 1. At any one of these points the characteristics of two modes become identical, and when the critical point is passed, there is no unique way of assigning the original two numbers to the two modes.

In any given ionosphere model the behavior of the zero order mode depends on the value of $H/L=\omega_r h/2\pi c$. If $H/L<11.8$ (approximately) the attenuation of the zero order mode has a maximum at some frequency, and thereafter decreases as the frequency increases. If $H/L>11.8$ the attenuation of the zero order mode increases indefinitely with increasing frequency.

Acknowledgment

This work was done at the National Bureau of Standards, Boulder, Colo., while the author was on sabbatical leave from Cambridge University. The author is greatly indebted to the University of Colorado and to the directors and staffs of the High Altitude Observatory and NBS for providing this opportunity to work in Boulder.

[12] Budden, *op. cit.*, footnote 1, Fig. 3.
[13] Budden, *op. cit.*, footnote 1, Fig. 2.
[14] Budden, *op. cit.*, footnote 1, Fig. 5.

Very Low-Frequency Radiation from Lightning Strokes*

EDWARD L. HILL†

Summary—**A theory of the generation of low-frequency electromagnetic radiation by cloud-ground lightning strokes is presented. Only the effect of the return stroke is considered. The predicted form of the radiated pulse from the return stroke is a single cycle with a field variation which varies linearly with time. The spectral distribution of the radiated energy is found to be centered at about 11 kc, with a total width at half-maximum of 12 kc. The total energy radiated in one leader and return stroke is estimated at 220,000 joules. Some qualitative considerations on the emission of radiation at extremely low frequencies are given.**

Introduction

EXPERIMENT and theory agree in showing that the difficulty of constructing an efficient radiator of electromagnetic energy increases rapidly as the wavelength of the radiation becomes progressively greater than the linear dimensions of the region of space over which the system of currents in the radiator is allowed to oscillate. In the vlf region of the spectrum, in which the wavelength is large compared with a kilometer, one must use radiators of large physical dimensions and/or high peak power.

Natural lightning is the most effective terrestrial source of radiation in the vlf range. The emission of radiation by lightning strokes has been discussed many times in the literature from varying points of view. Usually, the discussion has been made to depend on an assumed variation of the electrical dipole moment of the cloud with time, or the discharge channel has been treated as a transmission line.[1] A physical theory of the radiation, based on the flow of electrical charge over the channel, has been developed by the writer for the case of a cloud-ground stroke. The model used is semi-empirical in that the numerical values of the physical parameters associated with the stroke have been taken directly from empirical observations of Schonland, Norinder, Pierce, *et al.*, while the radiation field has been calculated from the electromagnetic field equations.

Theory

In order to calculate the vlf radiation from a lightning stroke, one must have a knowledge of the current distribution over the whole length of the discharge channel. Such a large scale flow of charge can be expected to arise from the quasistatic charging of the channel, which is a reasonably good conductor owing to the ionization in it, in the electric field between the cloud and ground as the main leader stroke develops.

The observational evidence from slow field gradient changes associated with thunderstorms, as obtained by Pierce,[2] gives a mean value of 5 coulombs for the negative charge transferred to ground in the initial phase of the stroke. This has been interpreted as charge which is drawn from the cloud and deposited on the discharge channel during the leader stroke. After the leader has made contact with the ground, the flow of this excess charge to ground leads to the phenomenon of the return stroke.

The detailed description of this model and the calculation of the radiation field from it has been published.[3] Here it is sufficient to concentrate attention on the major physical features of the results. The growth of the leader stroke is a comparatively slow process, occupying a total time of the order of 1 m/sec. The return stroke, on the other hand, travels up the channel at a speed of the order of 3×10^7 m/sec, taking a total time of the order of 60 μsec.

While the individual steps of the leader stroke have speeds of this order, on the average they travel only about 50 meters at this rate. One can anticipate, therefore, that the bulk of the vlf radiation will arise from the return stroke, owing to its high speed and associated heavy current flow.

It becomes a relatively simple matter to calculate the radiation field given by the model, when the return stroke alone is considered. Taking a vertical discharge channel for a cloud-ground stroke with the geometrical conditions shown in Fig. 1, the magnetic field lines form horizontal circles centered on the axis of the channel, as is indicated by elementary theory. The magnitude of the radiated field varies linearly with time, being discontinuous at the beginning and end of the pulse. This last feature is not a physical reality, of course, but arises because only the return stroke has been considered.

The form of the pulse is indicated in Fig. 2. There is one main "cycle" which lasts for a time T_r, this being the time of travel of the return stroke from ground to cloud. The maximum magnitude of the radiated magnetic field is

* Original manuscript received by the IRE, February 7, 1957. Paper presented at Symposium on Propagation of Very-Low-Frequency Electromagnetic Waves, Boulder, Colo.; January, 1957.

† School of Physics, University of Minnesota, Minneapolis, Minn. Consultant to Lightning and Transients Res. Inst., Foshay Tower, Minneapolis, Minn.

[1] P. W. A. Bowe, "The waveforms of atmospherics and the propagation of very low frequency radio waves," *Phil. Mag.*, vol. 42, pp. 121–138; February, 1951.
K. G. Budden, "The propagation of a radio atmospheric II," *Phil. Mag.*, vol. 43, pp. 1179–1200; November, 1952.
J. S. Barlow, G. W. Frey, and J. B. Newman, "Very low frequency noise power from the lightning discharge," *J. Franklin Inst.*, vol. 258, pp. 187–203; September, 1954.

[2] E. T. Pierce, "Electrostatic field-changes due to lightning discharges," *Quart. J. Roy. Meteorol. Soc.*, vol. 81, pp. 211–228; April, 1955; also, "The development of lightning discharges," pp. 229–240; April, 1955.

[3] E. L. Hill, "Electromagnetic radiation from lightning strokes," *J. Franklin Inst.*, vol. 263, pp. 107–119; February, 1957.

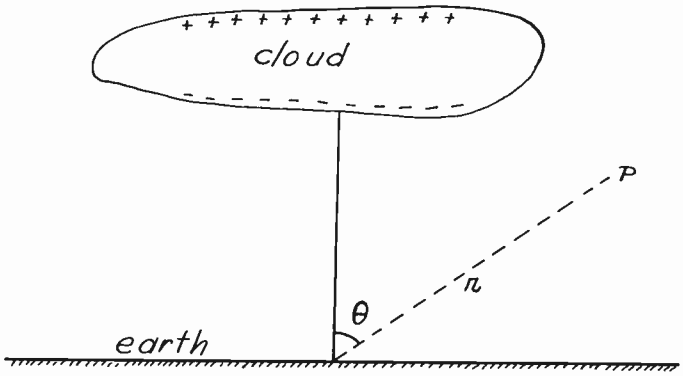

Fig. 1—Geometrical configuration for the calculation of the radiated field at the distant point P from a vertical cloud-ground lighting stroke.

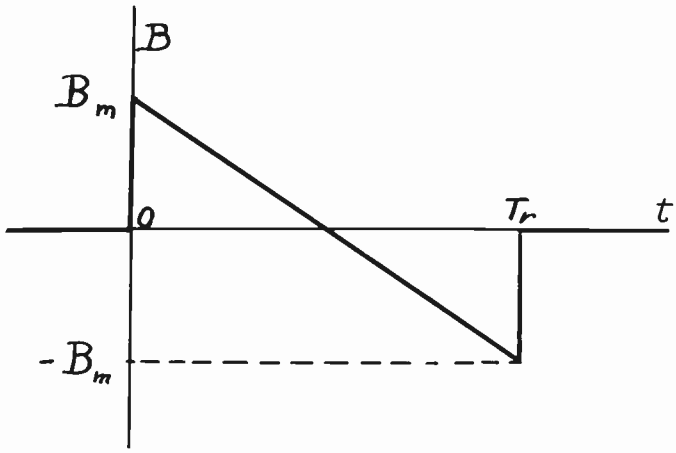

Fig. 2—Waveform of the magnetic component of the field radiated by the return stroke.

$$B_m = \frac{Q\mu_0}{\pi T_r} \cdot \frac{v_r}{c} \cdot \frac{\sin\theta}{r}, \qquad (1)$$

where Q is the total charge deposited on the channel during the leader stroke, v_r is the speed of the return stroke, c is the speed of light, and r is the distance from the stroke to the point of observation. The geometrical quantities are shown in Fig. 1.

We adopt the following numerical values from the empirical observations on actual lightning strokes as reasonable statistical averages

$$|Q| = 5 \text{ coulombs}, \quad T_r = 60\ \mu\text{sec}, \quad v_r = 3 \times 10^7 \text{ m/sec}.$$

The spectral distribution of the radiation from the return stroke can be found from a Fourier analysis of the pulse form shown in Fig. 2. The predicted spectral intensity of the total radiation emitted in all directions is given by the formula

$$R = 8 \times 10^4 F(\gamma) \text{ joules/(kc)}, \qquad (2)$$

where $\gamma = \pi T_r f$. If one takes $T_r = 60\ \mu$sec, and expresses the frequency in kc, then $\gamma = 0.19\ f_{kc}$. The function $F(\gamma)$ has the form

$$F(\gamma) = \gamma^{-4}(\sin\gamma - \gamma\cos\gamma)^2. \qquad (3)$$

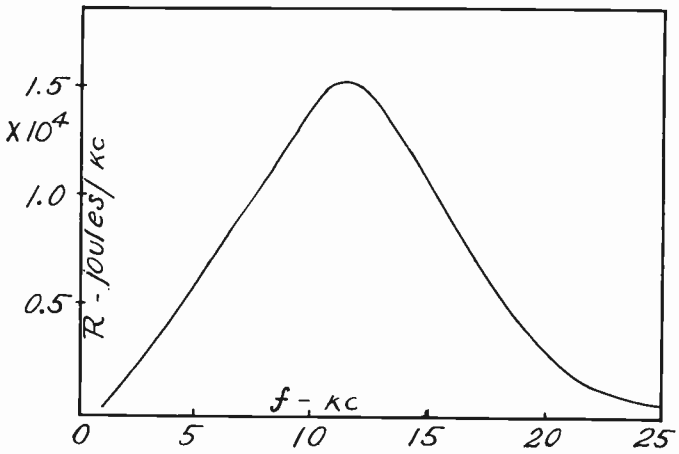

Fig. 3—Predicted form of the spectral distribution of the radiation from a cloud-ground lightning stroke.

It is of interest to note that, when the return stroke alone is considered, the form of the spectral distribution is determined by the single parameter T_r.

Fig. 3 shows the spectral distribution curve given by (2) and (3) in the vlf region. The maximum point of the curve lies at 11.2 kc, the total width at half maximum being 12 kc.

The total emitted radiation can be found by integration over the distribution and is found to be about 220,000 joules. This seems to compare favorably with the estimates made by Laby and his co-workers from their statistical measurements on atmospherics.[4] An exact comparison is not possible, since their measurements were not limited to cloud-ground strokes.

Discussion

The emitted waveforms of the transient pulses from lightning strokes are undoubtedly much more complicated than the idealized form shown in Fig. 2 for the return stroke alone. Because of the complicated branching structure of the leader stroke, the detail to be observed in the pulse will depend markedly on the sensitivity of the receiving equipment. On the other hand, it is expected that the spectral distribution predicted from the return stroke alone may be reasonably characteristic of the average properties of cloud-ground strokes. The absence of a heavy return stroke in cloud-cloud discharges makes their analysis more complicated, but they also probably emit a much smaller amount of vlf radiation on the average.

The quasistatic and induction fields associated with a ground stroke are much larger within the cloud than the radiation field. These strong localized fields act on the distributed charge distributions in the cloud and on the general ionization in the atmosphere to give rise to secondary radiation fields which are, in part, coherent with that from the main stroke itself. The energy

[4] T. H. Laby, *et al.*, "Wave form, energy and reflection by the ionosphere, of atmospherics," *Proc. Roy. Soc., London*, vol. A174, pp. 145–163; February, 1940.

which ultimately escapes as radiation may, as a consequence, be determined in significant measure by the charge and current distributions over a region of space which is appreciably larger than that which would normally be associated with the discharge channel of the main stroke. Furthermore, the relaxation of the general electric field in the cloud, incident on the development of the main stroke, may trigger other discharges within the cloud.

These considerations suggest that, particularly in the extremely low-frequency region below, say 1 kc, there may be a variety of mechanisms giving rise to extended fields which are difficult to relate causally to the main stroke.

The theory which has been given above is based on the assumption that the generation and propagation of the radiation from a lightning stroke are independent phenomena. It is somewhat problematical to what extent this division can be made consistently in the extremely low-frequency region. Many measurements have been made of the fields produced by nearby strokes.[5,6] For close strokes, the radiation field is not measured alone, but there also is a strong contribution from the quasistatic and induction fields. As a consequence, the changes in the waveforms of measured atmospherics with distance are quite complicated even when ionospheric reflection effects are not considered.[7] This situation becomes progressively more pronounced as the frequency is lowered, since the wave zone region about the source in which the local fields are important grows in size.

In response to comments by the referee, the following remarks are submitted. A more complete discussion is given by Hill.[3]

(1) MKS units are used in this paper, so that $\mu_0 = 4\pi \times 10^{-7}$ and $\epsilon_0 = 10^{-9}/36\pi$,

(2) The complete radiation formula from which (2) is derived is

$$R = \frac{8 \times 10^3}{3\pi c \epsilon_0} |Q|^2 (v_r/c)^2 F(\gamma) \quad \text{joules/(kc)}.$$

The predicted spectral distribution of the radiation depends only on the time of travel of the return stroke, T_r, while in addition, the total radiation involves only the total charge deposited on the channel during the leader stroke, $|Q|$, and the speed of the return stroke, v_r. The channel height, $h = v_r T_r$, does not appear explicitly in the formula and has been considered as a secondary variable. The maximum in the radiation intensity occurs at the frequency $f_m = 0.67/T_r$. It seems to be a general opinion among experimentalists that the measured values of f_m are not very sensitive to changes in cloud height, though they may not be strictly constant. This consideration led to the choice of $|Q|$, v_r, and T_r as the primary constants in the text. It is difficult to give a self-consistent set of numerical values for all of the parameters associated with lightning, owing to the large errors in the empirical values. It is suggested that the relative constancy of f_m may arise because the longer channel lengths give larger values of $|Q|$, which in turn may lead to increased values of v_r. The ratio $T_r = h/v_r$ may thus be more nearly constant from stroke to stroke than is either the height or the stroke speed.

ACKNOWLEDGMENT

Acknowledgment is made of research support as part of an atmospheric research program at the Lightning and Transients Research Institute under joint sponsorship of the USAF, Wright Air Development Center Communication and Navigation Laboratories, and of the Navy Department, Bureau of Aeronautics.

[5] H. Norinder and O. Dahle, "Measurements by frame aerials of current variations in lightning discharges," *Arkiv. Mat., Astron. Fysik*, Band 32A, no. 5, pp. 1–70; May, 1945.

[6] A brief review of the subject is given by B. F. J. Schonland, "Atmospheric Electricity," John Wiley and Sons, Inc., New York, N. Y., 2nd ed., ch. 4; 1953.

[7] Extensive experimental measurements have been made on these transition effects by A. W. Sullivan and his co-workers at the Univ. of Florida. The theory has been discussed by J. R. Wait, "On the waveform of a radio atmospheric at short ranges," PROC. IRE, vol. 44, p. 1052; August, 1956.

CORRECTION

Jacob Shekel, of Spencer-Kennedy Laboratories, Inc., Boston, Mass., has brought the following to the attention of Alexander J. Grossman, author of the paper, "Synthesis of Tchebycheff Parameter Symmetrical Filters," which appeared on pages 454–473 of the April, 1957, issue of PROCEEDINGS. On page 466, Fig. 8, the last term of 5) should read $+0.000061\alpha_p^2$. On page 467, Fig. 13, the last term of 1) for g_6 should be $2a_4$; and in 2), all q's should be replaced by g's. Mr. Grossman adds that the equation for T_2 in 5) should end with s_1; and the equation for the sum of the even E's in 7) should end with s_0.

Noise Investigation at VLF by the National Bureau of Standards*

WILLIAM Q. CRICHLOW†, SENIOR MEMBER, IRE

Summary—**The principal objective of the Radio Noise Section at the National Bureau of Standards is the establishment of a regular service for predicting the levels and characteristics of radio noise. The various steps necessary to establish such a service at NBS are summarized.**

The characteristics of atmospheric noise vary with location, frequency, and time, and methods of dealing with these variations are discussed.

Also discussed are new predictions of world-wide noise levels which have been prepared for the International Radio Consultative Committee (CCIR).

RADIO NOISE constitutes the basic limitation to radio reception. A determination of the weakest possible signal that will provide satisfactory service necessitates a knowledge of the noise with which it must compete.

Radio noise falls into several categories such as atmospheric, galactic, solar, precipitation, thermal, and man-made. Below about 30 mc and particularly in the vlf range, atmospheric noise is usually the most important of these types of noise, and most of our efforts in the Radio Noise Section at the National Bureau of Standards have been directed toward studies of its behavior.

Our principal objective is the establishment of a regular service for predicting the levels and characteristics of radio noise. The NBS has been responsible for publishing several previous predictions[1,2] of atmospheric radio noise levels. Our latest predictions[3] were prepared jointly with the British for the International Radio Consultative Committee (CCIR) and were adopted by the VIII Plenary Assembly of the CCIR in Warsaw, Poland in September, 1956. These new predictions are being published by the CCIR for public sale.

There are several steps in establishing a prediction service. The first step is the development of methods of measurement of radio noise. We, at the National Bureau of Standards, have developed special equipment for this purpose and have had a number of units manufactured as shown in Fig. 1. We presently have a contract for the manufacture of additional units to be used during the International Geophysical Year (IGY). This equipment operates on 8 fixed-frequency channels, covering the frequency range from 15 kc to 20 mc and provides an absolute measurement of the average noise power at the antenna. This is expressed as an effective antenna noise figure, F_a, which is defined as the noise power available from an equivalent lossless antenna in db above ktb (the thermal noise power available from the passive resistance of a circuit with bandwidth, b, and at the

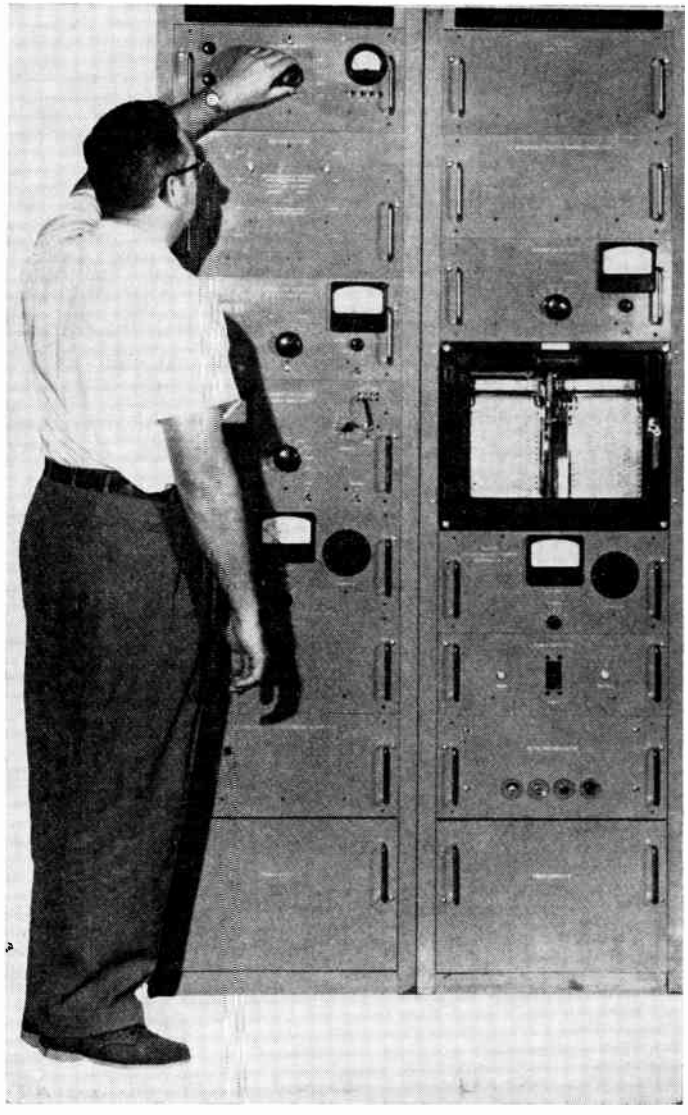

Fig. 1—Radio noise recorder developed at the National Bureau of Standards.

* Original manuscript received by IRE, February 27, 1957. Paper presented at Symposium on Propagation of Very-Low-Frequency Electromagnetic Waves, Boulder, Colo.; January 23–25, 1957.

† National Bureau of Standards, Boulder, Colo.

[1] "Ionospheric Radio Propagation," NBS Circular 462, Supt. of Doc., Washington, D. C.; 1948.

[2] W. Q. Crichlow, D. F. Smith, R. N. Morton, and W. R. Corliss, "Worldwide Radio Noise Levels Expected in the Frequency Band 10 KC to 100 MC," NBS Circular 557, Supt. of Doc., Washington, D.C.; August 25, 1955.

[3] "Revision of Radio Noise Data," International Radio Consultative Committee, VIII Plenary Assembly, Warsaw, Poland, 1956; CCIR Secretariat, Geneva.

absolute temperature, t). This method of expressing the noise is directly applicable to the "transmission loss"[4] method of measuring radio propagation.

Some of the special features of this equipment are excellent gain stability to insure accurate recordings, narrow bandwidth to minimize signal interference, low-noise figure so that low-noise levels can be recorded, and wide dynamic range so that high noise bursts will be averaged correctly. Most of the units being manufactured under the present contract will include an additional cabinet that will provide recordings of the average envelope voltage and average logarithm of the envelope voltage in addition to the average power. These three statistical moments provide information not only concerning the level of the noise but also relative to its character.

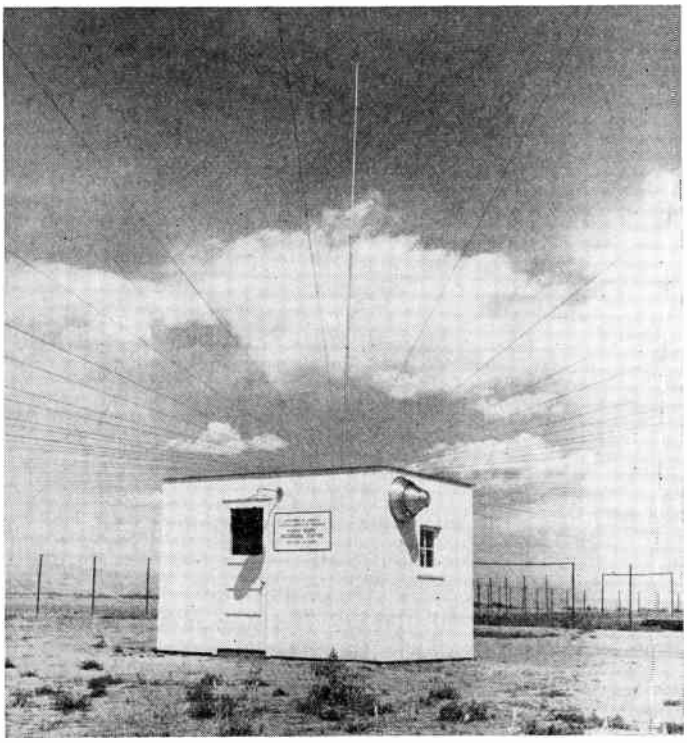

Fig. 2—Radio noise recording station near Boulder, Colo.

Our station at Gunbarrel Hill, near Boulder, Colo., is shown in Fig. 2. The antenna consists of a 21.75-foot vertical whip in the center of an elevated radial system which is attached to the metal roof of the building. This antenna system has been standardized for all of our field stations.

The second step in establishing a prediction service is the collection of data on a world-wide basis. We are installing our equipment in a network of sixteen stations to be in operation during the International Geophysical Year. The stations will be distributed over a large portion of the earth's surface as shown on the world map in Fig. 3. Five of the stations will be operated by the Central Radio Propagation Laboratory of the National Bureau of Standards, and the others will be operated by foreign governments or other agencies. The stations are coded to indicate the type of measurements to be made and the lowest recording frequency in kc is shown after the operating agency. The upper frequency will be 20 mc at all stations.

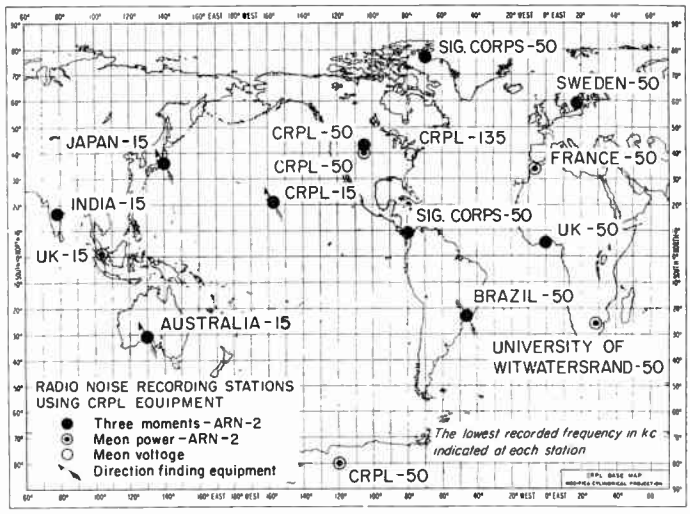

Fig. 3—Radio noise recording stations to be in operation during the International Geophysical Year.

The third step in our program is the reduction and analysis of the data. During the IGY, we will be collecting a large volume of data and will be using IBM equipment to process the data automatically for the mathematical analysis.

The fourth step is the development of methods of prediction and presentation of data. Predictions of atmospheric noise involve studies of its behavior as a function of a number of variables, the principal ones being the geographic location, the radio frequency, time of day, and season. Some of these variations are systematic and some are of a random nature and must be treated statistically. I will discuss the way in which we are dealing with these variables.

It is convenient to separate the variations with time into intervals of various lengths. Let us consider, first, the short-term variations. During periods of several minutes to about an hour, the statistical properties of atmospheric noise remain essentially constant. These have been described by several investigators[5–7] using amplitude time distributions. Fig. 4 shows a typical distribution of the short-term variations. The scales of

[4] K. A. Norton, "Transmission loss in radio propagation," PROC. IRE, vol. 41, pp. 146–152; January, 1953.

[5] A. D. Watt and E. L. Maxwell, "Measured statistical characteristics of vlf atmospheric noise," PROC. IRE, vol. 45, pp. 55–62; January, 1957.

[6] A. D. Watt and E. L. Maxwell, "Characteristics of atmospheric noise from 1 to 100 kc," this issue, p. 787.

[7] F. F. Fulton, Jr., "The effect of receiver bandwidth on amplitude distribution of vlf atmospheric noise," presented at VLF Symposium, Boulder, Colo.; January, 1957.

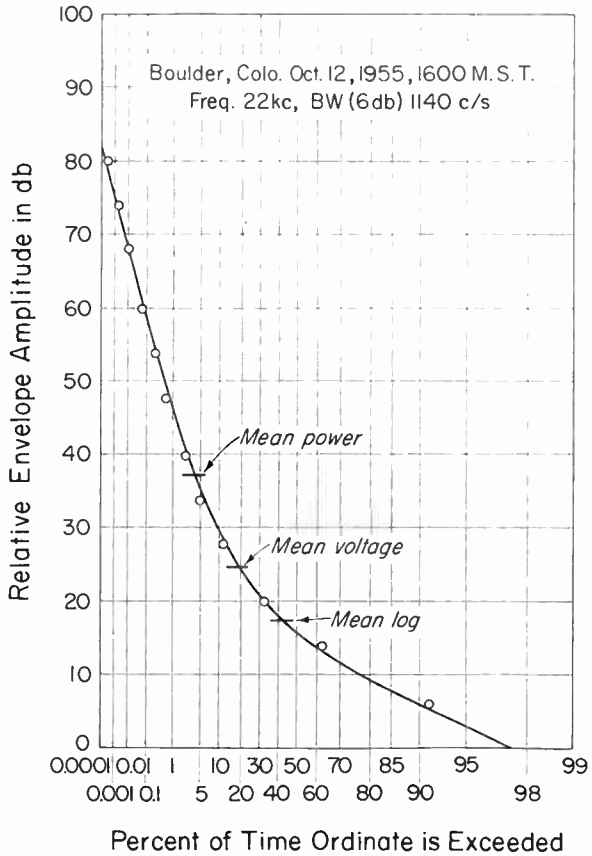

Fig. 4—Typical amplitude-time distribution of short-term variations.

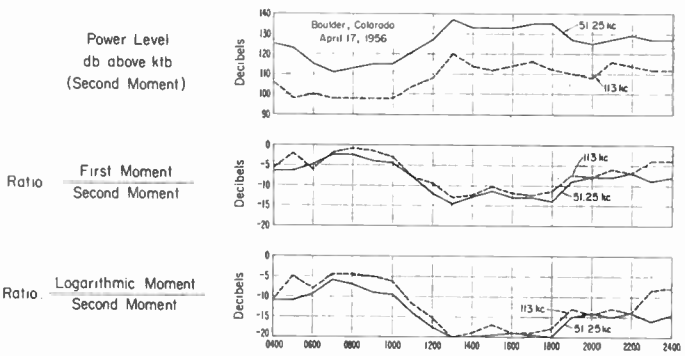

Fig. 5—Typical diurnal variations of atmospheric noise.

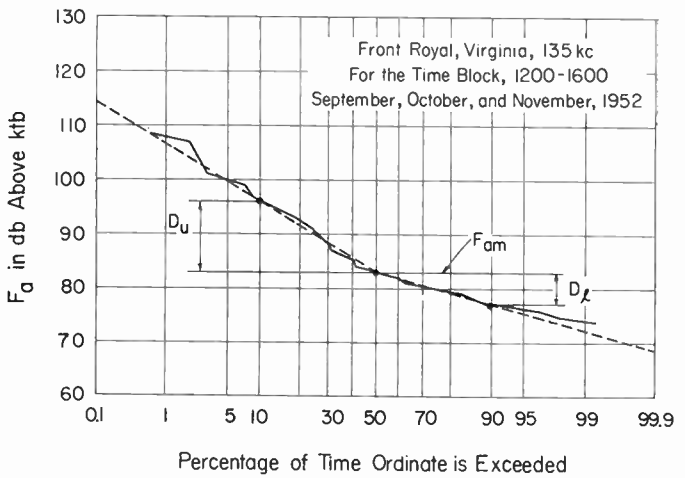

Fig. 6—Typical amplitude-time distribution of hourly noise levels.

this graph were chosen so that a Rayleigh distribution would plot as a straight line having a slope of $-\frac{1}{2}$. We see that the lower portion of this curve approaches a Rayleigh distribution, indicating overlapping pulses, but the upper portion is much steeper and results from the high amplitude bursts of short duration. Points have been indicated on the curve which correspond to measurements of the mean power, the mean voltage, and the mean logarithm of the voltage. These are the measurements made by our new equipment, and we have found that by using these measurements it is possible to approximate this complete distribution, thus providing a description of the short-term characteristics of the noise.

Fig. 5 illustrates the systematic variation of the three statistical moments of atmospheric noise as measured at Boulder, Colo. on 51.25 kc and 113 kc. The upper graph shows the variation of the power level. The level on both of these frequencies is lowest at about 8:A.M., rising to a higher level in the afternoon hours, due to the presence of local thunderstorm activity, and remaining moderately high during the nighttime hours, because of the good propagation conditions existing during this time. The center graph shows the ratio of the first moment to the second moment, or, in other words, the average voltage in db relative to the average power level, and the lower graph shows the ratio of the logarithmic moment to the second moment (the average logarithm of the envelope in db relative to the mean power value). Both of these moments, the first moment and the logarithmic moment, depart only a few db from the mean power during the morning hours when the noise level is low and in the afternoon when the mean power reaches a high level, they depart by a substantial amount, because of the increased dynamic range during the time of local thunderstorm activity. With our new equipment, continuous recordings are obtained of these three moments; thus providing continuous information on the characteristics of the atmospherics.

The statistical variation of the noise levels from day-to-day during a season at a given time of day is shown in Fig. 6 in terms of the amplitude-time distribution of the hourly values of F_a. This particular set of measurements was made at Front Royal, Va. on 135 kc during the afternoon hours. In this graph, a linear normal probability scale has been used. The curve can be represented by two straight lines, one of which goes through the median, F_{am}, and the upper decile, D_u, the other passing through the median and the lower decile, D_l. Thus, the whole curve can be described in terms of these three parameters.

Fig. 7 is a typical chart taken from our new CCIR predictions[3] and shows noise grade contours for the

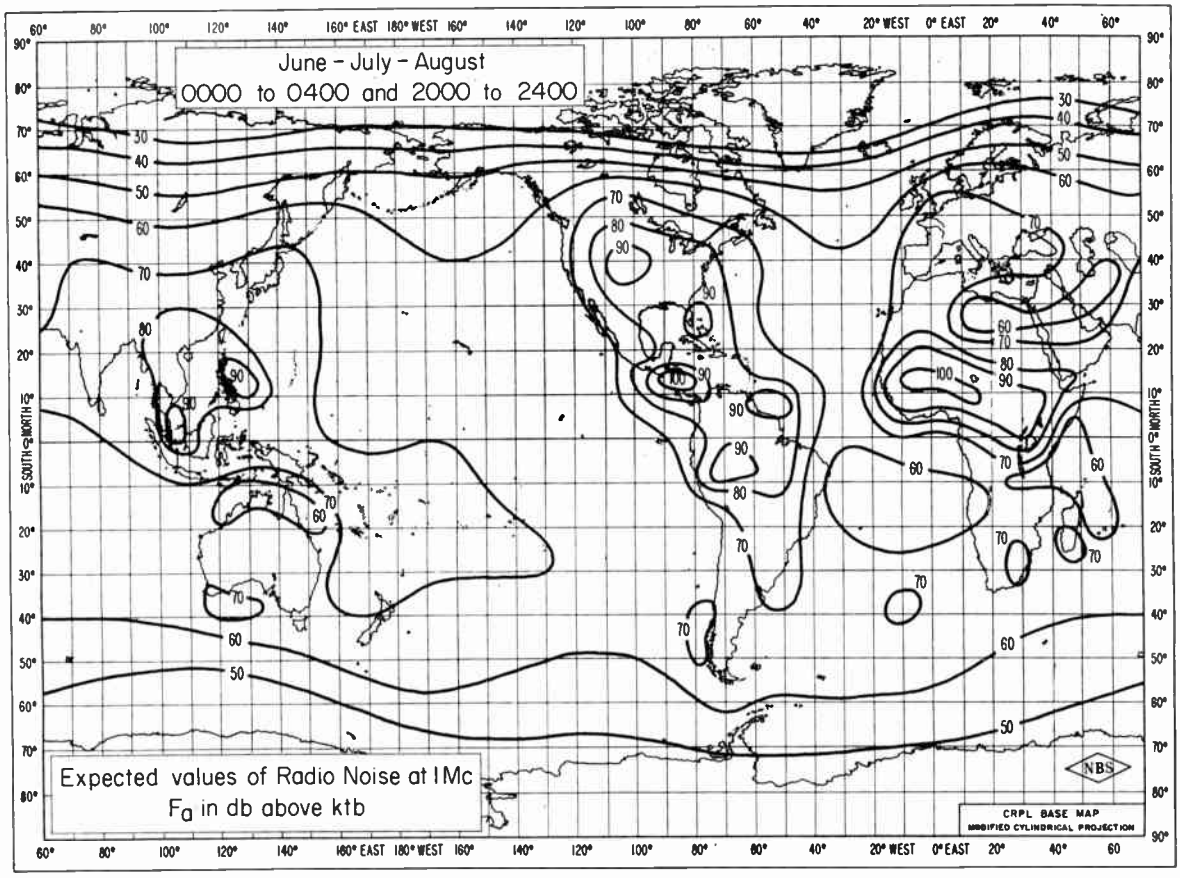

Fig. 7—Typical world distribution of noise grades.

period of time June, July, and August and for nighttime hours, local time. This chart illustrates the geographic distribution of the noise, and as the storms progress from the northern hemisphere to the southern hemisphere with seasons the noise level as received at any particular location will, therefore, show a systematic seasonal variation. Similar charts have been prepared which show the systematic variation of the noise contours with time of day, and twenty such charts cover both the diurnal and seasonal variations.

Fig. 8 is also taken from the CCIR predictions and illustrates the systematic variation of noise level with frequency. Having determined a noise grade at a particular location from a chart similar to Fig. 7, it is then possible, by use of these curves, to determine the expected noise level at any other frequency. This particular graph is for nighttime propagation conditions, and a similar set of curves has been provided to show the frequency variation during daytime propagation conditions.

Fig. 9, on the following page, shows a comparison of observations with the predictions published in NBS Circular 557[2] and with the new CCIR predictions.[3] This graph shows a distribution of the deviations of measured time block medians (median of the hourly values during a four-hour period for a season) from the predicted values and is from data obtained at Boulder, Colo., Front Royal, Va., and Tatsfield, Eng. The ob-

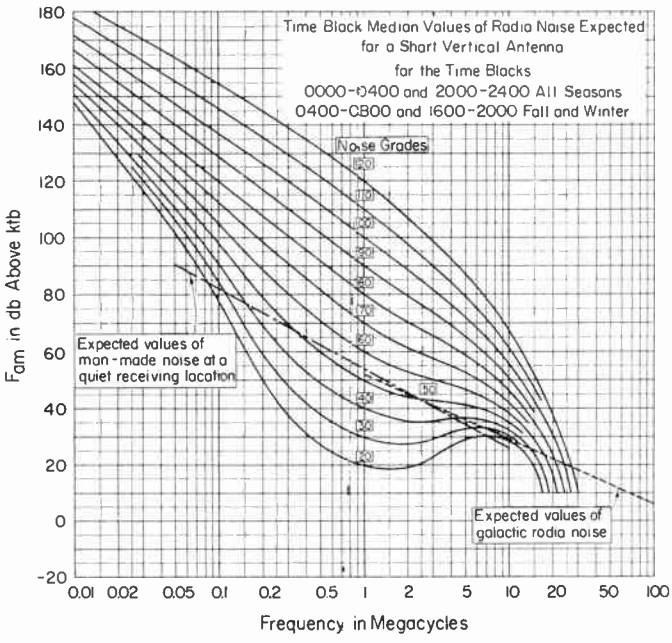

Fig. 8—Variation of noise level with frequency.

served time block median values exceeded the Circular 557 predictions by more than 2 db for 50 per cent of the time and by more than 11 db for 10 per cent of the time. The corresponding values for the CCIR predictions are −0.5 db for 50 per cent of the time and 5 db for 10 per

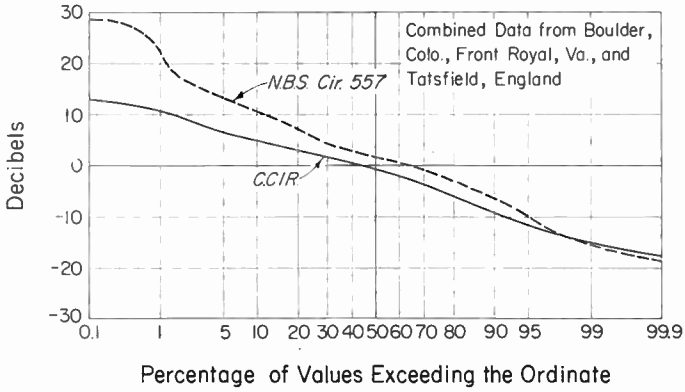

Fig. 9—Distribution of the deviations of the measured time block medians from the predicted values.

cent of the time. This distribution is not intended as an exact representation of the errors to be expected, since the observations are from only three stations; however, it is indicative that there is substantial improvement in the new predictions over the former predictions.

Even though improvements have been made in predicting average noise conditions, large uncertainties in level still exist at particular times and places. Information on the fine structure and detailed characteristics of atmospheric noise is also far from adequate. However, using data from the world-wide network of stations that is being installed during the IGY, we are confident that much further improvement can be obtained in the reliability and accuracy of future predictions.

Some Recent Measurements of Atmospheric Noise in Canada*

C. A. McKERROW†

Summary—**Some recent atmospheric noise measurements in the vlf range have been made in Canada by the Defence Research Telecommunications Establishment of the Defence Research Board. The amplitude of the mean logarithmic power (mlp) of atmospheric noise on a frequency of 10 kilocycles has been measured at Ottawa, Ontario (Latitude 45.4° N, Longitude 75.9° W), over a period of one year, beginning in October, 1955. The mlp atmospheric noise amplitude has also been measured in the sub-Arctic regions of Canada at Churchill, Manitoba (Latitude 58.8° N, Longitude 94.2° W), on a frequency of 107 kc for the period December, 1955 to August, 1956.**

A brief description of the equipment used to obtain these measurements is described. The results of the measurements are presented in the form of a graphical analysis showing the hourly median variations. These measurements are compared with previous measurements made in Canada, and with the estimated values of the National Bureau of Standards, and CCIR predictions of July, 1956.

Introduction

DURING the past year, the Defence Research Telecommunications Establishment has made some measurements of atmospheric noise in the vlf range. This paper will deal with those measurements, and it will include some historical background of previous measurements in Canada, together with a short description of the equipment, a brief analysis of the records, and a comparison of these measurements with the predictions of the National Bureau of Standards and the recent CCIR predictions of July, 1956.[1]

History

In the past, there has been very little information published on the available knowledge of atmospheric noise levels in Canada. A few measurements have been made for specified communication problems, but, in the majority of cases, these have been recorded only for a few days and, for most cases, the results have not been published. One exception is the report published by Gerson[2] under sponsorship of the American Air Force Cambridge Research Laboratories in Massachusetts. These recordings at 150 kc were made over a six month period, from January through June, 1947, for various locations in Canada.

Further related information to atmospheric noise levels in Canada can be obtained from three publications of the National Bureau of Standards.[3–5] The latest of these is NBS Circular 557.[5] This report is based mainly on NBS Circular 462, in which curves have been revised to show the expected root-mean-square median noise levels, during 4-hour time blocks, for each season of the year. The curves for the North American Continent for frequencies above 100 kc have been based on noise measurements made in southern latitudes below 40°, in conjunction with meteorological data based on

* Original manuscript received by the IRE, February 17, 1957. Paper presented at Symposium on Propagation of Very-Low-Frequency Electromagnetic Waves, Boulder, Colo.; January 23–25, 1957.

† Defence Research Board, Ottawa, Ont., Canada.

[1] CCIR Study, Group VI, "Report on Revision of Atmospheric Radio Noise Data"; July, 1956.

[2] N. C. Gerson, "Noise levels in the American sub-Arctic," PROC. IRE, vol. 38, pp. 905–916; August, 1950.

[3] "CRPL Radio Propagation Handbook," NBS Dept. of Comm.; November, 1943.

[4] "Ionospheric Radio Propagation," NBS Circular 462, Supt. of Doc., Washington, D. C.; 1948.

[5] W. Q. Crichlow, D. F. Smith, R. N. Norton, and W. R. Corliss, "Worldwide Radio Noise Levels Expected in the Frequency Band 10 KC to 100 MC," NBS Circular 557; August 25, 1955.

the distribution of thunderstorm days. For frequencies of 100 kc and lower, extrapolations of the curves have been made from measurements taken at the University of Florida.

The Defence Research Telecommunications Establishment at Ottawa have recently made two sets of measurements:

1) Mean logarithm of the instantaneous noise power (mlp) amplitude on a frequency of 10 kc at Ottawa, Ontario, for a period of one year, October, 1956.

2) MLP atmospheric noise amplitude on a frequency of 107 kc at Churchill, Manitoba, for the period December, 1955–August, 1956.

Most commercial noise measuring equipments are those of the quasi-peak type; that is, the detector charge and discharge time constants are so arranged to approximate various types of subjective interference. Therefore, the quasi-peak measurement cannot be made in terms of basic units, and it is necessary to define it by its particular time constant characteristics. This has led to numerous types of noise measuring equipments, all measuring quasi-peak, which fail to agree with one another.

It was recommended by the NBS, in a report to URSI Commission 4[6] that steps should be taken towards standardization of a mathematically significant measure of terrestrial radio noise and that a measurement of the rms noise power would seem likely to closely represent its interference value.

Equipment

A block diagram of the DRTE noise recorder is shown in Fig. 1. The antenna is a 30-foot vertical whip

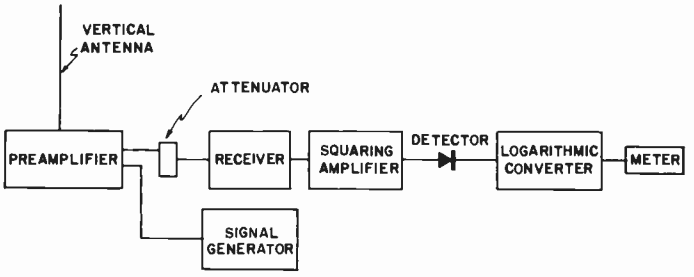

Fig. 1—DRTE atmospheric noise recorder.

with an effective antenna height of 4.5 meters. It is mounted on top of a weatherproof box which contains a broad-band preamplifier. The whole unit is mounted two feet above the ground, on a wooden platform, at the center of a radial ground screen. The ground wires are connected to ground rods at their outer end, and they are sloped upwards to the base of the preamplifier. The antenna system is situated at least 250 feet from the building containing the recorder.

The receivers are three-stage rf amplifiers. The effective bandwidths are: 10-kc receiver—970 cycles; and 107-kc receiver—4.47 kilocyles.

The output of the receiver is fed into a radio frequency squaring unit of the frequency multiplier type. This unit is similar to the type used in the National Bureau of Standards ARN 2 noise recorder. The entire receiver can accommodate approximately a 20-db range of input voltage without a change of input attenuator.

The output of the squaring unit is rectified by a silicon crystal diode detector whose output passes into a dc logarithmic converter, the output of which is integrated over a period of 10 seconds and then displayed on an Esterline Angus recorder.

The equipment is calibrated by switching the input of the preamplifier from the antenna to an artificial antenna whose electrical characteristics are the same as those of the 30-foot whip antenna. A sine wave signal from a generator, calibrated in rms volts, is injected into the artificial antenna, the results of which are marked on the recording milliameter charts as calibration points.

The hourly values are scaled from these noise charts and are appropriately corrected for antenna height and bandwidth into usable "Amplitudes of Atmospheric Noise" in units of "decibels above 1.0 microvolt per meter for a 1.0 kilocycle bandwidth." Due to the variability of the same hourly values from day to day, the statistical monthly medians for each hour are chosen to represent the daily variations. These values are plotted graphically in Fig. 2 for Ottawa, Ontario, and

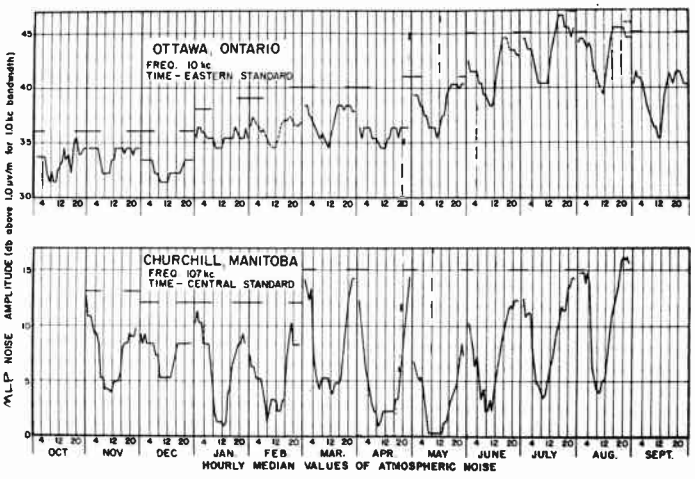

Fig. 2—MLP atmospheric noise.

Churchill, Manitoba. The solid lines above each monthly graph represent the hours of darkness in the lower ionosphere.

Analysis

From close examination of the Ottawa records, it is noticed that a very systematic change takes place. It

[6] W. Q. Crichlow, Report to URSI Commission 4 on the Question: "What are the most readily measured characteristics of terrestrial radio noise from which the interference to different types of communication systems can be determined?;" April 21, 1954.

is seen that the diurnal variation is very systematic throughout each month of the year and also that a month-to-month variation is present.

The hourly median variation from month-to-month is shown in Table I.

TABLE I

Month	Variation	Month	Variation	Month	Variation	Month	Variation
Oct.	2 db	Jan.	2 db	Apr.	2 db	July	7 db
Nov.	2 db	Feb.	3 db	May	5 db	Aug.	6 db
Dec.	2 db	Mar.	4 db	June	6 db	Sept.	6 db

As well as the daily variation, a large seasonal variation takes place. The lowest median value is 31 db in the month of December, while the highest median value is 46 db in the month of July, representing a total yearly median variation of 15 db.

Atmospheric noise is primarily caused by electromagnetic radiations due to lightning discharges. During the summer months, this noise is received from storms on the North American Continent either via ground wave, sky wave, or a combination of both. During the winter months of the northern hemisphere, most of the electrical disturbances occur in the tropical regions of South America and in the central and southern parts of the African Continent. These radiations are received mostly by sky wave propagation.

The three major factors that control the received noise level and which sometime overlap are:

1) Ionospheric absorption in the lower regions of the ionosphere due to the sun's radiations.

2) The natural tendency for thunderstorms to occur over the land mass areas, beginning in the late morning and ending in the early evening.

3) The ground wave attenuation between the received signal and the noise source.

In every month of the year you will find that heavy absorption takes place during the day, with a resulting decrease in the propagated noise. The actual time of this decrease depends on the seasonal variation of sunrise.

An increase in noise will be found also in the monthly median, either at noon or one to two hours before noon. This increase is due to the natural phenomena of thunderstorm activity increasing over the land mass area. As the sun's rays heat the earth, a flow of warm moist air rises to form vertical columns of cumulonimbus type thunder clouds. This phenomenon lasts until late afternoon and decreases about sunset. This is shown on the records as a decrease in the received noise. As the sun sets in the lower ionosphere, the absorption decreases, thus allowing the ionosphere to again become effective for the propagation of more remote storms. As can be seen from the records, the noise subsequently rises or falls depending upon the intensity of the more distant noise sources.

In Fig. 3 is shown the median value at Ottawa plotted for two specific hours of the day; 1000 hours being the quietest hour while 1800 hours is the noisiest part of the day.

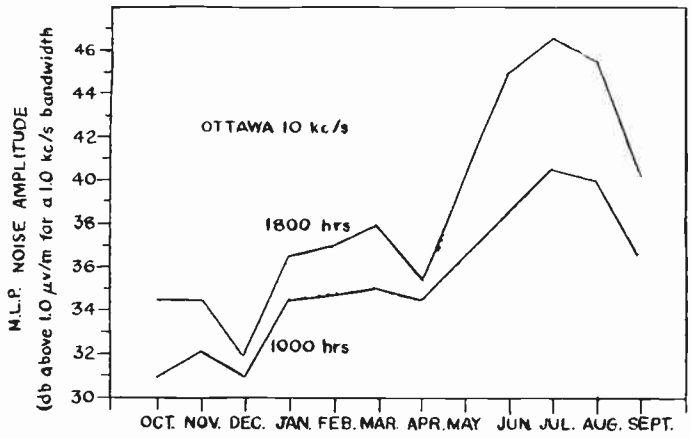

Fig. 3—Hourly median value of atmospheric noise.

The general increase from December to July is not uniform. The values of January, February, and March are 2 to 3 db higher than those for the previous three months.

This can be explained by long distance sky wave propagation from Central Africa and the African Gold Coast Region. In this three month period, between the hours of 12 noon and 3 A.M. E.S.T., the noise level in Africa is particularly high. Due to the earth's tilt, the ionospheric day-night boundary line is in such a position that, during part of the high African noise-level activity, the north Atlantic path from Africa to Canada is in complete darkness. During this time the absorption is low constituting an excellent propagation path.

Therefore, in this three month period, the noise is received from two main sources, South America and Africa, thus giving rise to a higher general noise level.

From a close examination of Churchill records, it is noticed that nearly the same systematic variation is present. There is a fairly large monthly variation as well as a diurnal variation each month of the year. It is observed that the noise does not decrease in the early morning hours during the winter months in conjunction with sunrise above Churchill, but that it begins to decrease several hours before, indicating that the ionospheric day-night boundary lies northeast by southwest. However, as the summer approaches, this line moves north and south until the early morning decrease is simultaneous with sunrise in the ionosphere above Churchill. The same general increase is noticed during the winter months at Churchill and is believed to be of the same general nature as at Ottawa.

The hourly median variations for the months are shown in Table II.

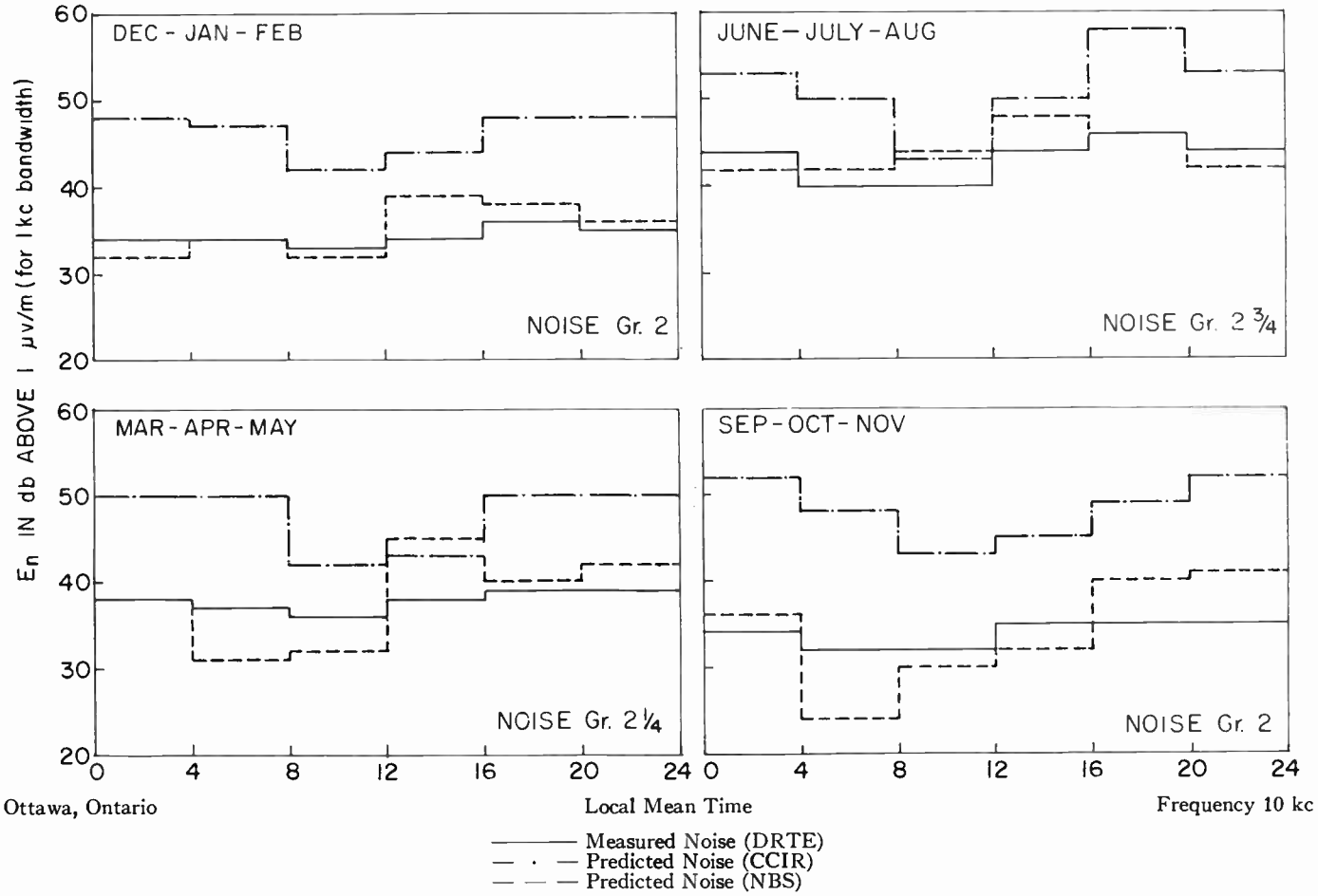

Fig. 4—Comparison of median atmospheric noise levels.

TABLE II

Month	Variation	Month	Variation	Month	Variation	Month	Variation
Nov.	8 db	Jan.	10 db	Apr.	14 db	July	11 db
Dec.	4 db	Feb.	8 db	May	9 db	Aug.	14 db
		Mar.	10 db	June	10 db		

As well as the daily variation, a large seasonal variation takes place. The lowest median value is 0.5 db in the month of May while the highest median value is 16 db in the month of August, representing a total median variation of 16.5 db.

Comparisons with Other Measurements

To compare the records taken by Gerson at 150 kc at Churchill with those obtained by DRTE is almost impossible for several reasons: Gerson's records were recorded using a quasi-peak time constant of 0.089-second charge time. The quasi-peak calibrations were made with a pulse generator. An average value was also taken over a period of 98 seconds, but for most of the time the atmospheric noise levels were below that of the receiver noise. However, the "absolute quasi-peak" recordings show a similar monthly trend to those of the DRTE records. A definite increase is seen in Gerson's records during January, February, and March.

A comparison of the recorded DRTE median noise levels during 4-hour time blocks with those predicted by the National Bureau of Standards and CCIR are shown in Fig. 4, above, and Fig. 5, on the following page. Each time block is for 4 consecutive hours within a season. The median of the hourly values within the time block is designated as the hourly time block median.

From a close observation of the Ottawa time block medians, the predicted medians are considered to be within reasonable tolerance. The predicted rms values from the NBS Circular 557 and the measured mlp values by DRTE show a very close relationship. During the autumn months, the median values from 0400 to 0800 hours did not decrease as much as had been predicted, nor did they increase as high as had been predicted during the evening hours. As to the shapes of the diurnal median variations, the new CCIR predictions which are also rms values, seem to fit the mlp observations better than those from Circular 557, and the range of values appear to be in better agreement.

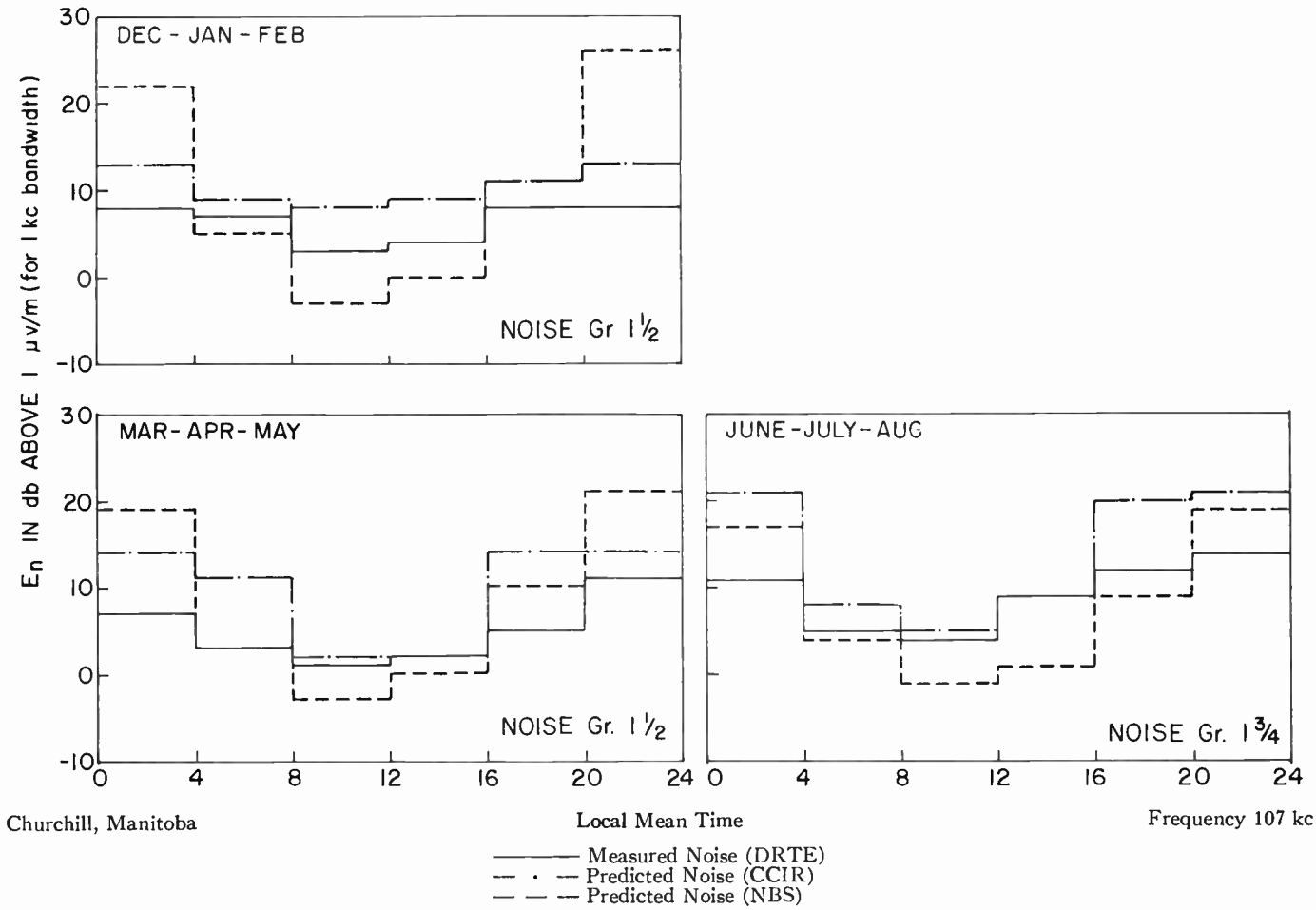

Fig. 5—Comparison of median atmospheric noise levels.

The predicted rms value by NBS and the observed mlp noise level at Churchill do not compare as favorably as those at Ottawa. In all seasons, the estimated values are too high in the evening hours and too low during the daylight hours. They are very reasonable considering the difficulties in estimating values of atmospheric noise at great distances. Again, the shapes of the new CCIR predictions fit the DRTE observations much better than the NBS predictions, and the range of values also appear to be in good agreement.

The absolute values of the CCIR predictions, for Ottawa and Churchill, are approximately 4 to 5 db higher than the observations taken by DRTE. This is to be expected, since the rms value and the mlp value are two different statistical characteristics. For normally distributed noise, the rms value is greater than the mlp value.

Conclusion

The following conclusions are drawn:

1) The Ottawa and Churchill records show a very systematic variation, both daily and seasonal.

2) During the winter months, an increase is noted both at Ottawa and Churchill.

3) The seasonal median variation on 10 kc at Ottawa is 15 db.

4) The average median level at Ottawa from September through February is approximately 33 db, while in the spring it is 35 db and in the summer months it is 42 db. All values quoted are decibels above 1.0 μv/m for a 1.0-kc bandwidth.

5) The seasonal median variation on 107 kc at Churchill is 16 db.

6) The average median levels at Churchill are: winter, 6 db; spring, 4 db; and summer, 8 db.

7) The shape of the diurnal variations compare more favorably with those of the new CCIR predictions of July, 1956 than that of the NBS Circular 557.

8) The absolute rms values of the CCIR predictions are 4 to 5 db higher than the mlp value of DRTE.

Acknowledgment

The author is pleased to express his thanks to so many of his colleagues who have been helpful in making this project possible. Special acknowledgment should be accorded to J. M. Griffin who has been responsible for a great deal of the designing, building, and maintenance of the noise equipment. I would also like to thank R. Haffer who helped scale so many of the noise charts. This program could not have been a success without the constant and invaluable criticism of W. L. Hatton.

Characteristics of Atmospheric Noise from 1 to 100 KC*

A. D. WATT†, SENIOR MEMBER, IRE, AND E. L. MAXWELL†

Summary—**The results of some preliminary statistical measurements of the envelope of narrow band atmospheric noise are presented for a range of center frequencies from 1 to 100 kc. The variation of level and dynamic range, as a function of frequency, is examined and compared with results expected on the basis of lightning discharge spectra, thunderstorm distribution, and propagation phenomena.**

Introduction

IT IS well known that the level of atmospheric noise as observed in a fixed bandwidth varies as a function of the center or observation frequency in addition to a number of other important parameters such as time, location, etc.[1] The manner in which the level varies from 1 to 100 kc is, however, not well known, and in addition very little is known about the statistical characteristics of the atmospheric noise envelope over this range.

An earlier paper[2] by the authors describes the statistical characteristics of the atmospheric noise envelope as observed at a center frequency of 22 kc including the effects of bandwidth, geographic location, antenna directivity, time, etc. It is the purpose of this paper to present some of the preliminary results obtained using similar equipment and techniques over the frequency range of 1 to 100 kc. In addition, an explanation for the results obtained based upon lightning discharge data and propagation characteristics is included. This analysis is based on first determining the radiation spectrum of a typical lightning discharge and then showing how the radiated spectrum is modified by the propagation path. These derived characteristics are then compared with observations made at Boulder, Colo.

Radiated Field of a Lightning Discharge

The exact mechanism of the lightning discharge is very complex. Schonland,[3] however, has shown that the discharge is initiated by a weakly ionized slow moving pilot streamer which in general advances from the cloud toward the ground in spurts of 30 to 200 feet with velocities in the order of 1 to 2 feet per microsecond. This pilot is followed by a highly ionized leader, Fig. 1(a), which travels at approximately 200 feet per microsecond producing a current pulse in the order of 300 amperes whose length is approximately one microsecond. The pilot again moves forward and the process repeats itself every 25 to 100 microseconds. These short pulses and the branch leaders, repeated at rates of from 10 to 40 kc radiate energy during this period known as the predischarge which has a total length in the order of

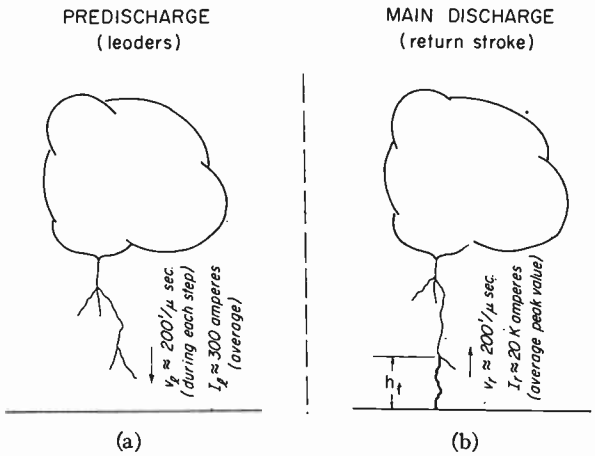

Fig. 1—Lightning discharge.

one millisecond. This length obtained by employing an average height of 5000 feet is in good agreement with observations of the electric field. Once the leader reaches the ground, the main or return stroke with average peak current values of 20 kiloamperes starts upward at a velocity in the order of 200 feet/μs. A typical recording of the electric field variations at a distance of 20 km from the source is shown (referred in amplitude only to a distance of one mile) in Fig. 2, where the relative shapes and amplitudes of the predischarge and main stroke portions are readily apparent. The current as measured at the ground has the form shown in Fig. 3(a).[4] In general the velocity decreases with increase in height as shown in Fig. 3(b). The resulting moment M, *i.e.*, the product of height and average current, is shown in Fig. 3(c). The exact formulation of M is dependent on the vertical distribution of current which probably has the form shown by the dashed curves. The moment differential dM/dt is also presented in this figure. The current and resulting moment usually has some fine structure which is caused by the increase in

* Original manuscript received by the IRE, February 4, 1957. Paper presented at Symposium on Propagation of Very-Low-Frequency Electromagnetic Waves, Boulder, Colo.; January 23–25, 1957.

† National Bureau of Standards, Boulder, Colo.

[1] W. Q. Crichlow, D. F. Smith, R. N. Morton, and W. R. Corliss, "Worldwide Radio Noise Levels Expected in the Frequency Band 10 KC to 100 MC," NBS Circular 557; August 25, 1955.

[2] A. D. Watt and E. L. Maxwell, "Measured statistical characteristics of vlf atmospheric radio noise," PROC. IRE, vol. 45, pp. 55–62; January, 1957.

[3] B. F. Schonland, "The pilot streamer in lightning and the long spark," *Proc. Roy. Soc., London*, Ser. A, vol. 220, pp. 25–28; December, 1953.

[4] G. D. McCann, "The measurement of lightning currents in direct strokes," *AIEE Trans.*, vol. 63, pp. 1157–1164; December, 1944.

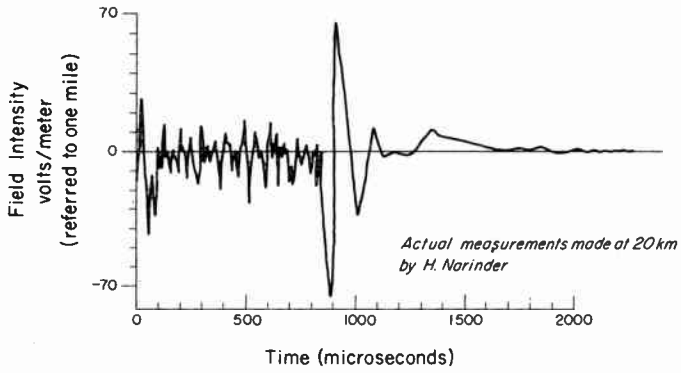

Fig. 2—Waveform of effective radiated electric field.

current when a branch point in the ionized path is reached. The removal of charge from these branches also gives rise to an effective moment which may add to or subtract from the main moment. Once this main stroke is complete, it may be followed by one or more "multiple" strokes[4] which in general follow the original ionized path and will probably have a considerably different form of leader stroke. Since over half of the cloud to ground discharges have two or more strokes,[2] this factor must be considered in determining the average relative amount of energy radiated from the predischarge and main stroke as a function of frequency.

It is well known that a changing vertical current of height, h, produces an electric field

$$E = \frac{1}{2\pi\epsilon_0}\left[\int \frac{M\,dt}{d^3} + \frac{M}{Cd^2} + \frac{dM/dt}{C^2 d}\right] \qquad (1)$$

(electrostatic) (induction) (radiation)

where:

- M is the vertical moment of the radiator, *i.e.*, instantaneous product of height times the average current (meter amperes),
- C is the velocity of light $= 3\times10^8$,
- ϵ_0 is the permittivity of free space,
- d is the distance from the source to the point of observation in meters, and
- E is the vertical field in volts/meter.

When $d > 50$ km the amplitude of the radiation term is dominant for frequencies greater than 1 kc and since we are restricting our present analysis to the effects of distant sources, we shall consider only this last term.

$$E = \frac{2dM/dt}{10^7 d}. \qquad (2)$$

With the aid of (2) it can be shown that the moment differential in Fig. 3(c) is proportional to the radiated field and if d is chosen as one mile we find the peak value of this radiated field to be 56 volts per meter. Wait[5] has

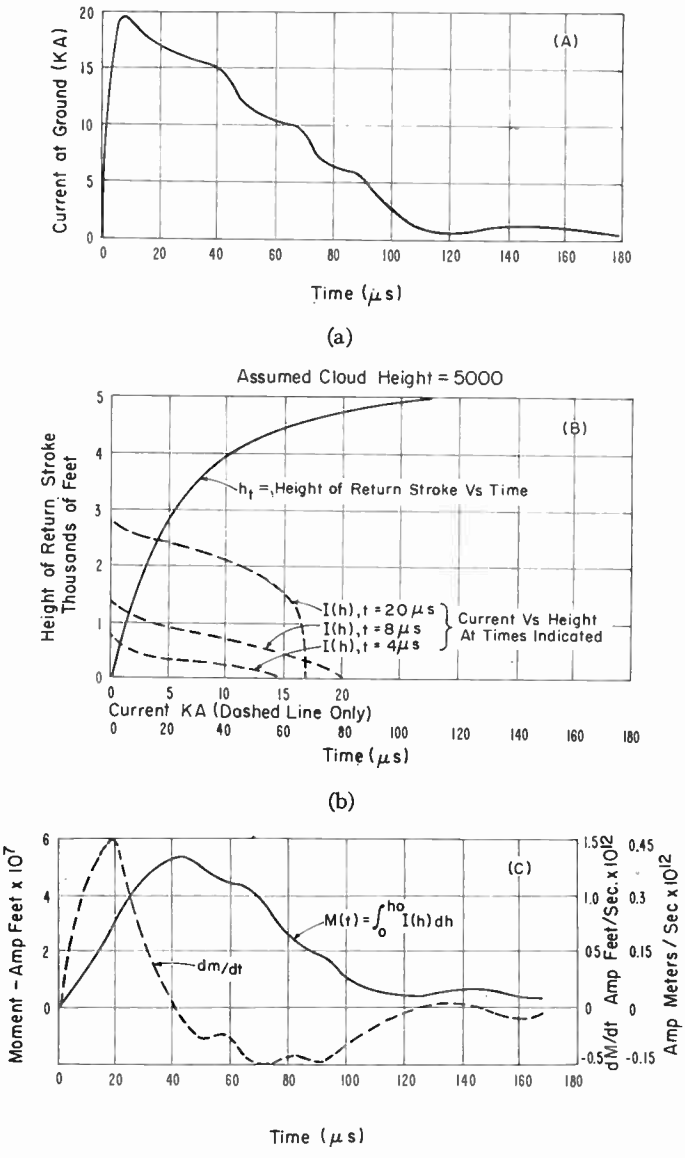

Fig. 3—Lightning discharge—main return stroke.

shown that ground-wave propagation will change the form of the observed field; however, if $d \geq 40$ km, the observed field amplitude will have essentially the same shape as the differential of the moment provided its rise time is not less than one microsecond. Norinder[6] has recorded a large number of lightning discharge fields, and it is interesting to note that their waveforms at these ranges, as was shown in Fig. 2, are similar to that shown in Fig. 3(c). When the observed levels are referred to the effective radiation field at one mile distance, the amplitudes observed are of the same order of magnitude as the 56 volts per meter obtained from

[5] J. R. Wait, "On the waveform of a radio atmospheric at short ranges," PROC. IRE, vol. 44, p. 1052; August, 1956.

[6] Harold Norinder, "The waveforms of the electric field in atmospherics recorded simultaneously by two distant stations," *Arkiv for Geofysik*, Band 2, nr 9, pp. 161–195; November, 1954.

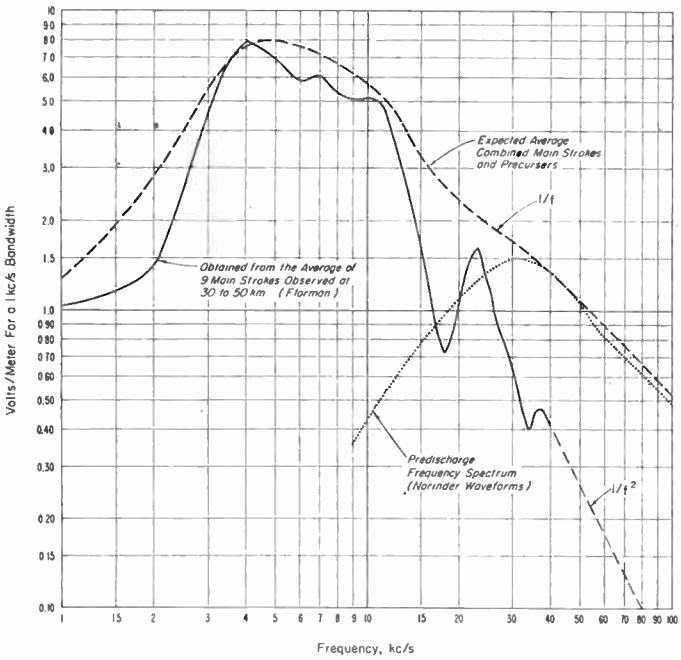

Fig. 4—Frequency spectrum of the radiation component equivalent field intensity at a distance of one mile.

Fig. 3(c) and (2). Florman[7] has recorded a large number of atmospheric waveforms which also are similar in form and amplitude. It should be mentioned, however, that in all the observed waveforms, there is a considerable variation in the details of the waveforms, particularly after the first maximum is reached, and that the effective radiated amplitudes may vary over about a 10 to 1 range. Florman, with the aid of Dr. H. H. Howe, has obtained the frequency spectrum of these recorded waveforms by automatic computer techniques. An average of 9 typical spectra, whose distances from the source were from 30 to 50 km, is shown by the solid curve of Fig. 4. The amplitudes were modified, however, assuming an inverse distance relation to obtain the effective radiated field at one mile from the source. It is obvious from Fig. 2 that a considerable amount of high-frequency energy is present in the predischarge portion which must be added to that of the main discharge if the total radiated spectrum is to be obtained. The fact that the repetition rates in the predischarge area are from 10 to 40 kc, makes the spectrum maximum in the area of 30 kc. The relative spectrum amplitude at this maximum is expected to have about the same ratio as the ratio of the time function amplitudes. Recorded fields and calculations of the maximum moment differentials indicate a ratio of predischarge to main discharge amplitudes of approximately 0.2. The predominantly triangular shape of the large areas of the main discharge indicate a $1/f^2$ decrease in spectrum components while the abrupt, at times apparently rectangular, change in the predischarge radiated field indicates substantial energy with a $1/f$ decay. On this basis, the dotted spectrum of the precursor in Fig. 4 was obtained, and the general combined spectrum is shown by the dashed curve.

It should be noted that energy from the predischarge is radiated over approximately one millisecond while the lower frequency components of the main discharge are radiated in 100 to 200 microseconds. This distinction is important in determining the effects of bandwidth and center frequency in the observed dynamic range of the atmospheric noise field.

Propagation Characteristics

Recent studies by Wait[8] have shown that the vertical electric field at great distances from the source can be represented by an expression having the form

$$E_d \cong \frac{E_0 \times 0.4 \times 10^{-(Ad/2\times10^4)}}{\sqrt{d}\cdot\sqrt{f}} \qquad (3)$$

$$1000 \leq d \leq 8000,$$

where E_d is the vertical electric field at a distance d from the source, d is this distance in kilometers, E_0 is the effective radiated field at one mile from the source usually expressed in v/m, f is the frequency in kc, and A is the attenuation factor in db/1000 km. The factor A, as obtained from the mode calculations of Wait over the range 1 to 20 kc, and from data adapted from Eckersley[9] and from Pierce[10] in the range 20 to 100 kc, is presented in Fig. 5. It should be mentioned that the values for the nighttime curves are not as well-established as those for the daytime conditions. The behavior of the reflecting layer is much less stable at night; however, it is expected that the low frequency absorption band will likely move from 4 kc down to approximately 3 kc at night, and it is also likely that the peak value of absorption will be less at night due to the fact that the ionospheric layer is higher and becomes more conductive at night.

Employing the factor A of Fig. 5 in (3), and assuming a constant E_0 (a white source of one v/m at one mile), we obtain the spectra of Figs. 6 and 7 which show the expected field at the distances indicated for a daytime sea water path and a nighttime land path. It is interesting to note the pronounced absorption band in the vicinity of 4 kc and although the exact depth is not well-established, there is experimental evidence which indi-

[7] E. F. Florman, NBS Rep. No. 3558; November 10, 1955.

[8] J. R. Wait, "On the Mode Theory of VLF Ionospheric Propagation," NBS, Rep. No. 5022; October 10, 1956. See also VLF Symposium paper no. 6; also J. R. Wait, "The mode theory of vlf ionospheric propagation for finite ground conductivity," this issue, p. 760.

[9] T. L. Eckersley, "Studies in radio transmission," *J. IEE*, vol. 27, pp. 405–459; September, 1932.

[10] J. A. Pierce, "Sky-Wave Field Intensity, I. Low- and Very Low-Radio Frequencies," Tech. Rep. No. 158, Cruft Lab., Harvard University, Cambridge, Mass.; September 1, 1952.

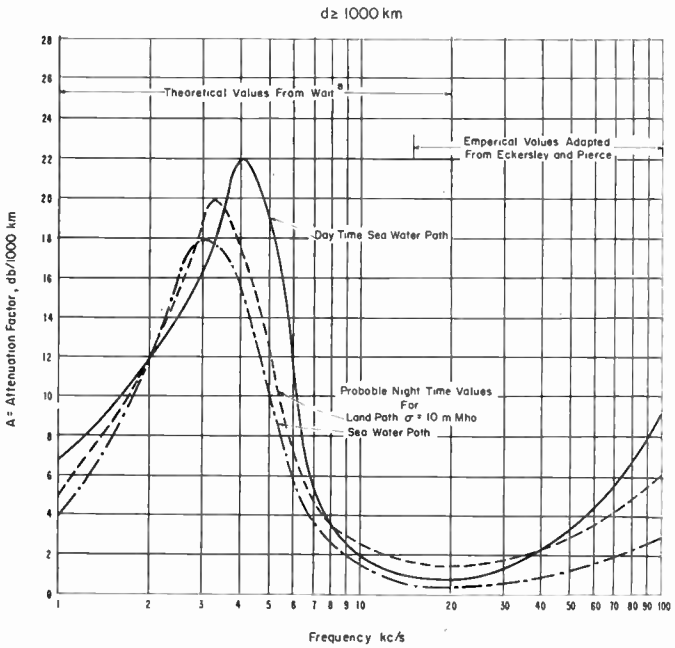

Fig. 5—Propagation formula attenuation factor A.

cates that the general order of magnitude is as shown. The sea water curves indicate a decided preference for frequencies in the order of 15 to 20 kc when long range circuits are desired, and it is interesting to note that this is the exact region where most of the existing long range vlf stations are located. The nighttime land curves have a similar shape, however, the absorption band is not as deep and what might be called the vlf pass band at 15 kc is considerably broader.

Atmospheric Noise Characteristics
Calculated Frequency Spectra

The total atmospheric noise field observed at a given location results from the sum of all the individual lightning discharge fields and any other contributing sources modified by their individual propagation paths. At any given location and time, there are a large number of distances involved; however, since the closest storm centers will in general contribute the largest percentage of energy, it is expected that the observed frequency spectrum will frequently be a function of the distance to the closest large storm center.

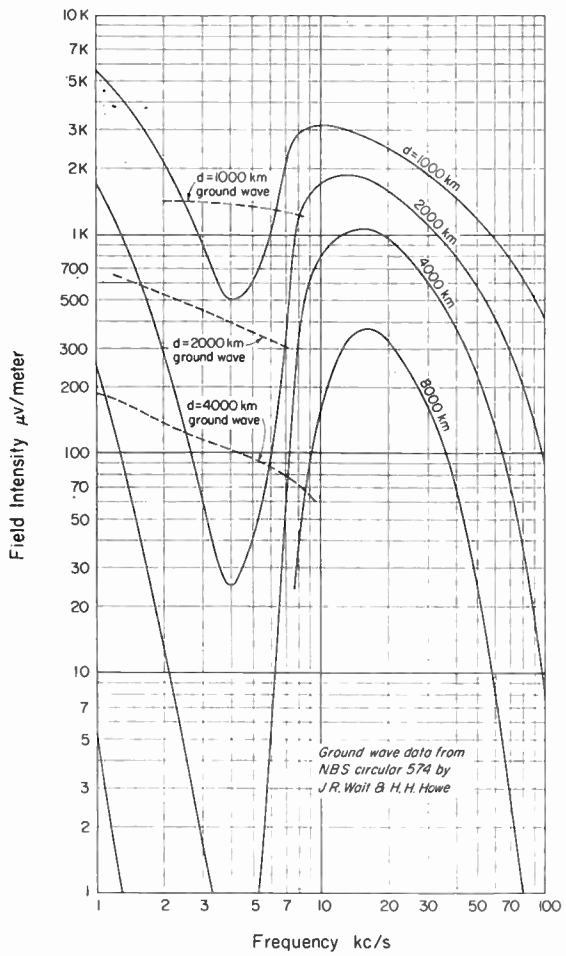

Fig. 6—Calculated frequency spectra white source—daytime sea water path radiated field = 1 volt/meter at one-mile distance from source as indicated.

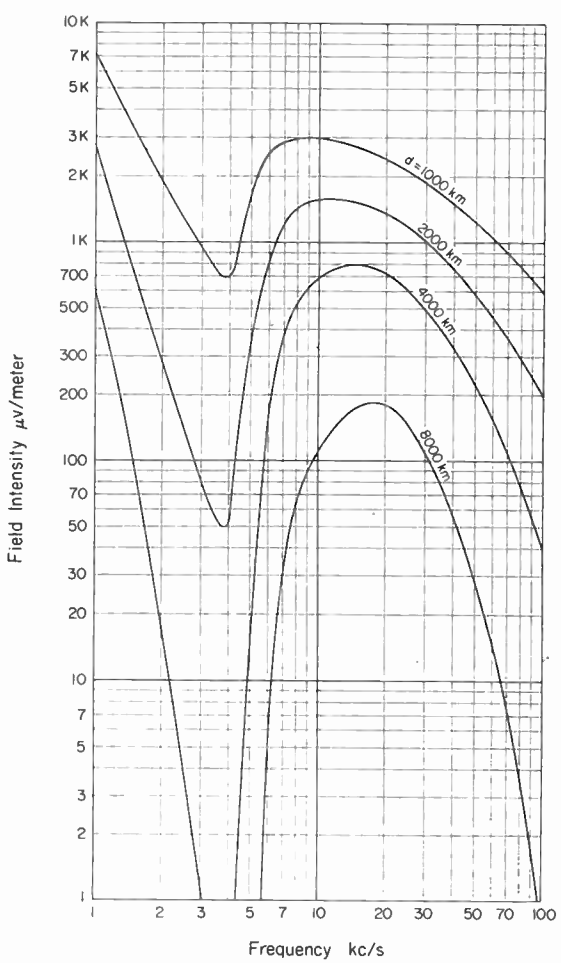

Fig. 7—Calculated frequency spectra white source nighttime land path $\sigma = 10$ mmhos radiated field = 1 volt/meter at one-mile distance from source as indicated.

Employing the combined frequency spectrum shown by the dashed line of Fig. 4 as a source, and the propagation curves of Figs. 6 and 7, we obtain the expected frequency spectrum of the atmospheric noise field with a dominant storm center at the distances indicated. These results are shown in Figs. 8 and 9.

Measured Characteristics of the Noise Field

The amplitude distribution measuring equipment described by Watt and Maxwell[2] was used as the intermediate frequency portion of a superheterodyne receiver which could be tuned from 1 to 100 kc. The same 6-inch square 15-turn loop was used as the antenna, and the amplitude distribution of the atmospheric radio noise envelope as observed in 140 cps (6 db) band centered at the frequencies indicated are shown in Figs. 10 and 11, on the next page, for typical nighttime conditions, Fig. 12 for typical daytime conditions, and Fig. 13 as a transitional period.

Values for the experimental points on the cumulative distributions are obtained by measuring the per cent of time that the noise field observed in a 140-cps band exceeds the field intensity indicated during a 100 or 200 second period. These periods are chosen to be just long enough to provide statistically constant data. Provision is made in the equipment for measuring three adjacent levels per period. This permits a complete distribution at a given frequency to be obtained in 7 to 12 minutes. Since we have chosen 10 different frequencies from 1 to 100 kc, a total time of $1\frac{1}{4}$ to 2 hours is required for the complete spectrum to be obtained.

Considerable difficulty was encountered in obtaining the daytime measurements as the local noise field frequently contaminated the 50-kc and 100-kc readings. In addition the thermal noise level of the receiver was approached during periods of low received noise field in the high percentage low field intensity regions at 4 kc and below. Any recorded field intensities where contaminated values were obtained are indicated accordingly.

In general the field intensities which are exceeded 0.1 per cent of the time can be considered as representative of the true atmospheric noise field and as a result they have been chosen to represent the variation in observed

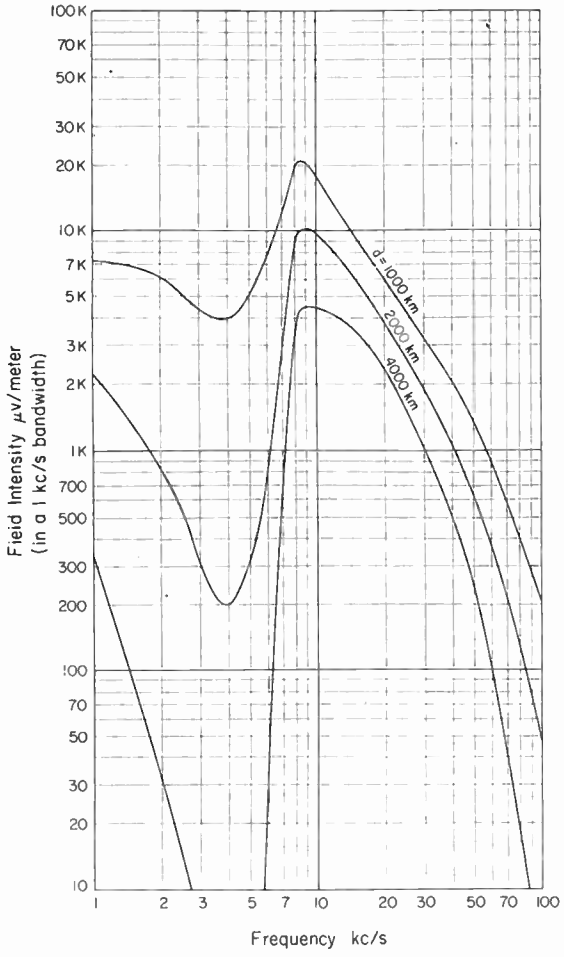

Fig. 8—Calculated frequency spectra of average lightning discharge source—daytime sea water path distance from source as indicated.

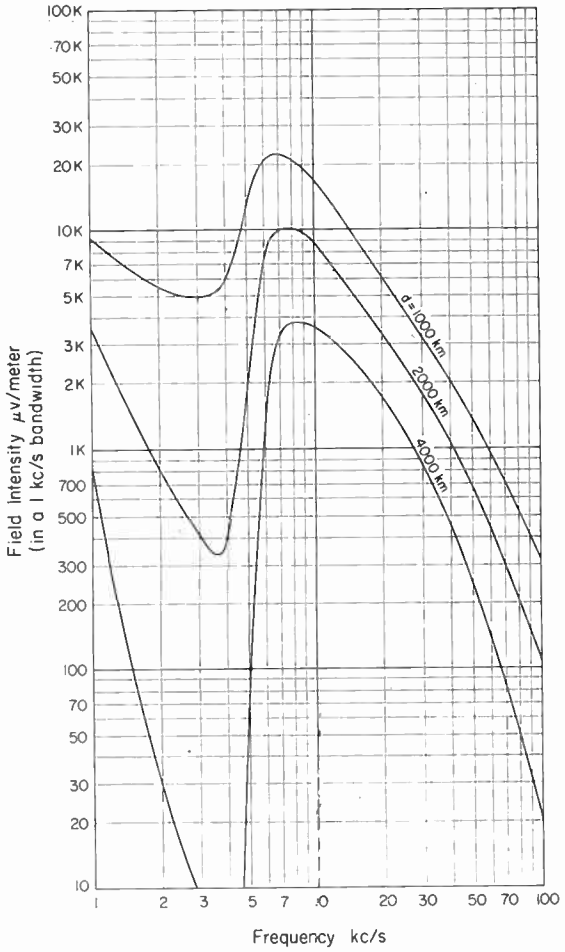

Fig. 9—Calculated frequency spectra of average lightning discharge source—nighttime land path $\sigma = 10$ mmhos distance from source as indicated.

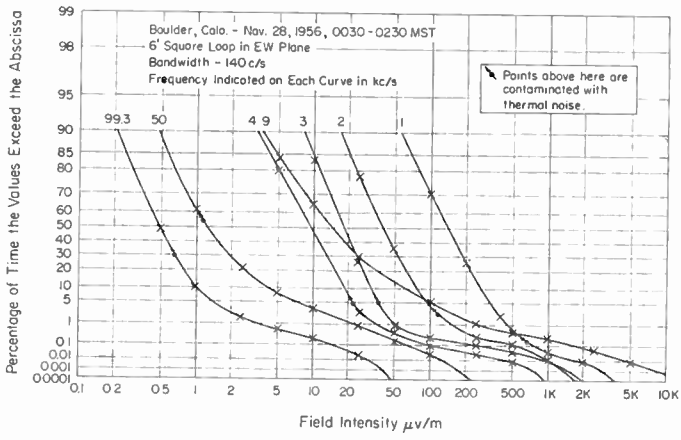

Fig. 10.

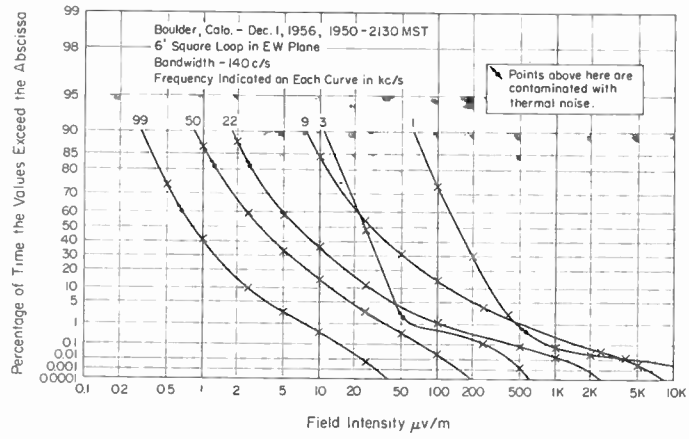

Fig. 11.

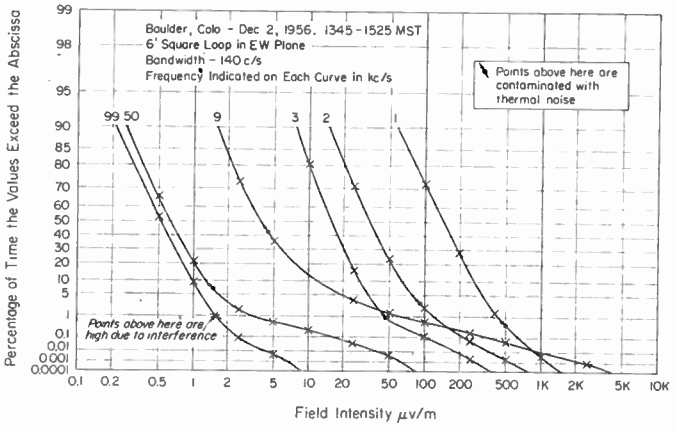

Fig. 12.

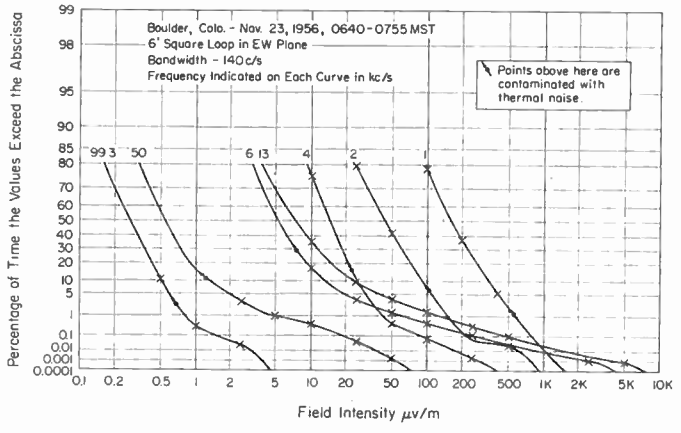

Fig. 13.

Figs. 10–13—Amplitude distribution of atmospheric noise envelope.

noise level as a function of frequency. The spectra corresponding to Figs. 10 and 11, and Figs. 12 and 13 are shown in Figs. 14 through 17 (opposite). The general shape is seen to correspond rather well with that obtained in Figs. 8 and 9. The frequency placement of the maxima and minima appears to be in good agreement with the theoretical curves, and the general amplitude level and shapes appear to indicate a distance of 2 to 4 thousand kilometers as might be expected for storms at this time of the year.

The spectra of the rms values are not shown because the rms values of the distributions would be in error due to thermal noise contamination at some of the frequencies. The actual variation of power or rms value with frequency is expected to vary in a manner similar to that shown for the 0.1 per cent values at approximately one-tenth the amplitude for these particular curves. In addition, it is expected that there will be a small systematic departure between the rms and 0.1 per cent spectra due to the change in dynamic range of the noise with frequency.

The actual atmospheric noise envelope dynamic range over a wide range of percentages cannot be obtained directly from the observed distributions because of thermal noise contamination in the low amplitude regions of the lowest frequency, less than 10 kc, distributions. In addition the low amplitude regions of the 50- and 100-kc distributions are on occasion contaminated by man-made interference. The range from 1 to 0.0001 per cent is, however, relatively free from contamination, and the resulting average dynamic range of the four sets of distributions is shown in Fig. 18 (p. 794).

The dynamic range of the noise envelope is expected to vary as a function of frequency due to two independent factors: 1) the length of time during which the energy in the particular frequency range is being radiated and 2) the effective contributions of the individual sources due to attenuation with distance. Factor one is expected to be less pronounced in a bandwidth of 140 cps than in bandwidths of 1 kc or greater because of the one millisecond average predischarge length. The fact that the effective radiation time is greater at frequencies above 20 kc should cause a decrease in observed dynamic range at center frequencies greater than 20 kc. The second factor produces an effect which is dependent upon the particular geographic distribution of thunder

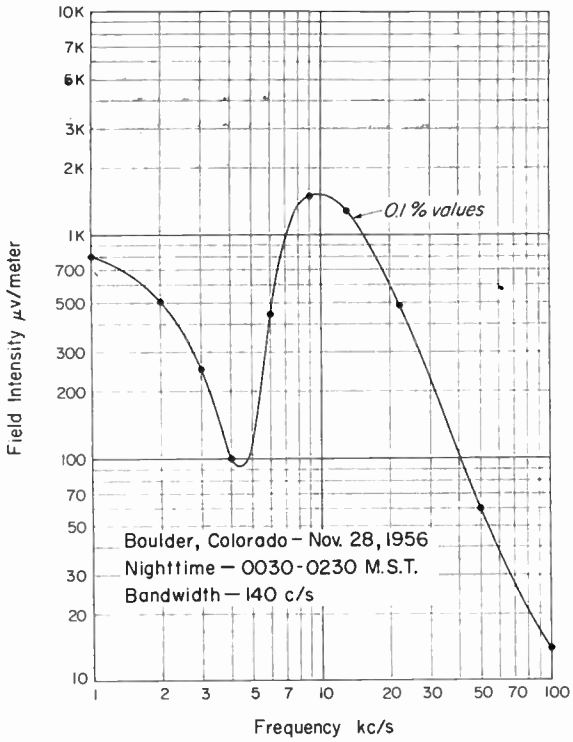

Fig. 14.

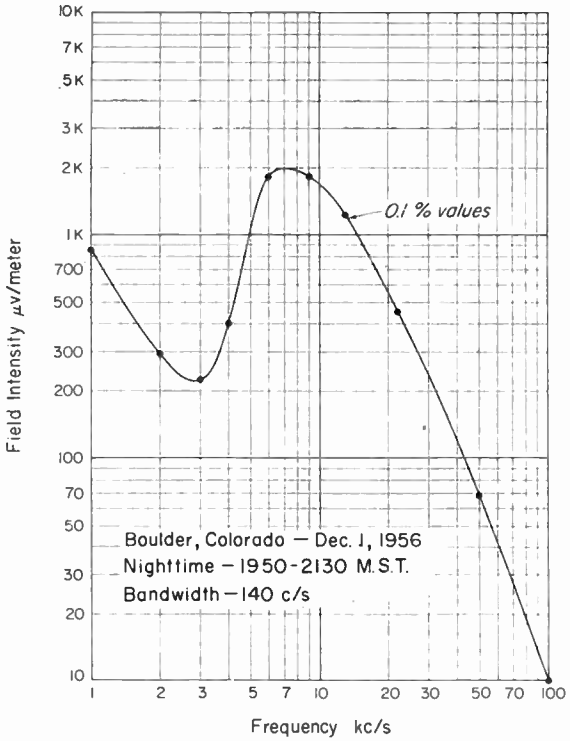

Fig. 15.

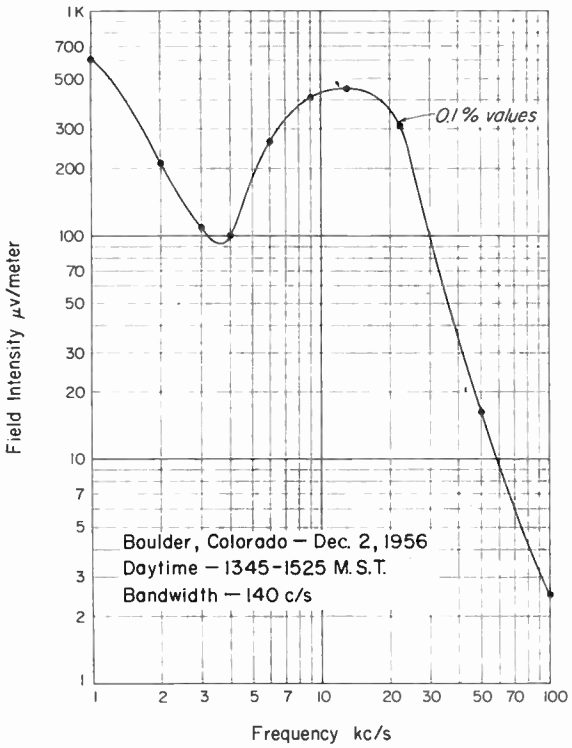

Fig. 16.

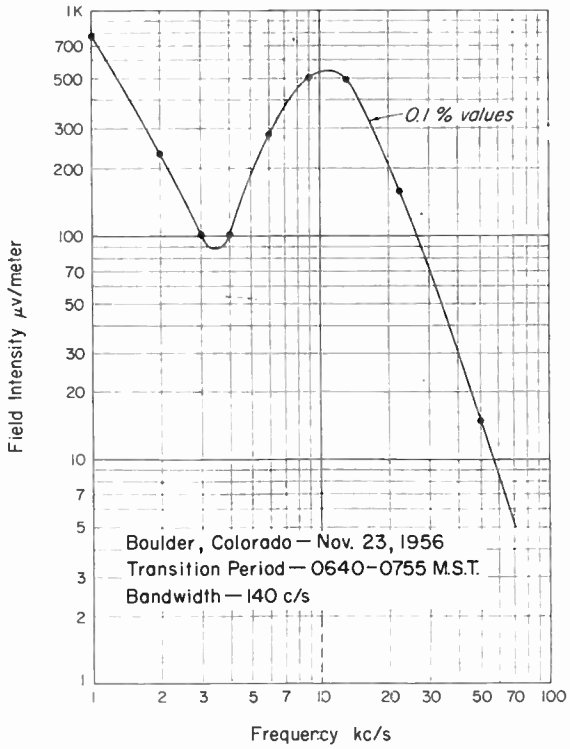

Fig. 18.

Figs. 14–17—Measured frequency spectra of atmospheric noise envelope.

storms at the time of the observation, and during periods where the minimum distance is appreciable, it is expected that a high attenuation rate will lower the dynamic range.

The observed variation in Fig. 18 agrees with these expectations; however, much more data must be obtained under a wide range of conditions before these effects can be properly evaluated.

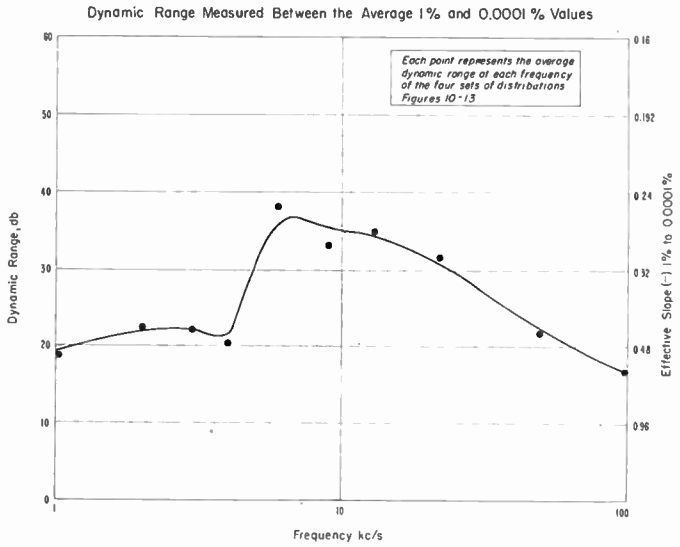

Fig. 18—Dynamic range and slope of amplitude distributions as a function of frequency.

One additional parameter which must be considered in a detailed study of atmospheric noise in this frequency range is the possibility of the whistler mode of propagation contributing to the total field and the contributions of solar excited auroral zone sources during periods of solar disturbances. Observations of the amplitude distributions and the shape of the frequency spectrum during such disturbed periods should reveal the extent of such contributions.

Acknowledgment

The authors are indebted to the following:

Dr. J. R. Wait for his assistance and many helpful suggestions; to R. M. Coon for his suggestions regarding the measurement equipment; to E. F. Florman for the use of frequency spectra calculated from his observed waveforms; and to Mrs. W. M. Mau for her assistance in performing the required computations and in preparation of the manuscript.

Intercontinental Frequency Comparison by Very Low-Frequency Radio Transmission*

JOHN A. PIERCE†, FELLOW, IRE

Summary—**Studies of signals from Rugby, England, at 16 kc and 60 kc have given evidence that a single source of standard frequency can be made available at vlf on a world-wide basis.**

At a distance of 5200 km the Doppler effects in transmission seldom exceed ±3 parts in 10^9, and a measurement can be made to 1 part in 10^9 in a few minutes. Accuracies exceeding 1 part in 10^{10} are consistently obtained by observation over several hours. Data by Allan, Crombie, and Penton, of the New Zealand Dominion Physical Laboratory, indicate that at 16 kc the diurnal Doppler effects at 18,700 km have normal maxima of the order of $1/10^8$, and that a measurement to 3 or 4 parts in 10^9 can be made in an hour or less.

These results are described and some of the effects of solar flares and magnetic disturbances are discussed.

In addition, a brief description is given of four mechanisms that have been found useful in comparing the frequency of a local oscillator with that of a vlf standard transmission.

Introduction

THIS PAPER discusses the precision with which frequency comparisons can be made at great distances by very low-frequency radio transmission.

* Original manuscript received by the IRE, February 13, 1957. The research was made possible through joint support extended to Cruft Laboratory, by the Navy Department (Office of Naval Research), the Signal Corps of the U. S. Army, and the U. S. Air Force, under ONR Contract Nonr-1866(07). Paper presented at Symposium on Propagation of Very-Low-Frequency Electromagnetic Waves, Boulder, Colo.; January 23–25, 1957.

† Cruft Lab., Harvard University, Cambridge, Mass.

For our purposes here, we may dispense with more subtle and elegant definitions and regard frequency simply as the rate of change of phase. The precision of a frequency measurement is proportional to the accuracy of phase measurement and to the time interval over which the change of phase is observed.

Even if a perfect oscillator were controlling a standard frequency transmitter, the phase at a distant receiving point would not change linearly with time, because of variations in the transmission medium. Using a less-than-perfect oscillator to measure time at the receiver, the standard frequency problem becomes one of recognizing the phase variations caused by oscillator vagaries, in as much detail as possible, in spite of changes in the transmission time. If, for example, we desire to know the relative frequency of an oscillator to a part in 10^9, but can trust the transmission medium only to a millisecond, it will take about 10^9 milliseconds, or nearly two weeks, to make the measurement. Unfortunately, there are very few oscillators in the world that can be trusted to maintain a constant frequency to such an accuracy over so long a period. If we cannot assume sufficient constancy, we may speak only of the *average* frequency of the oscillator over the measurement interval, and the average frequency may or may not be of

much interest when we cannot specify the frequency at any instant.

From these considerations, we see that intercontinental frequency comparisons to precisions of a part in 10^9 or 10^{10} must depend upon the use of either very excellent oscillators or a transmission medium having uncertainties very small compared with a millisecond. Fortunately, the latter alternative is available to us at vlf, so that high relative precision can be obtained with only moderately good oscillators.

In order to demonstrate the irregularities in transmission, it is necessary to use oscillators having much smaller irregularities. Here, fortunately, we can take advantage of the fact that a good oscillator often behaves very well indeed for a few days at a time. For studies of the variations in time of transmission, we need not be able to predict the oscillator frequency; it is enough if we can, after the fact, recognize the periods over which the consistency has been good.

Most of the data to be discussed below were obtained by observation in Cambridge, Mass. of signals radiated by the British Post Office from Rugby, England. For several years, the National Physical Laboratory has arranged for the Post Office to provide an experimental standard-frequency transmission, msf, for one hour per day at a frequency of 60 kc. Since July, 1954, they have also derived the 16-kc carrier frequency of the vlf transmitter gbr from the same excellent oscillator used to control the standard-frequency transmission.[1]

Four Methods for Measurement or Control of Oscillator Frequency

Before studying the variations observed in the phase, or time of arrival of a signal, it will be advantageous to discuss methods of observation. There is an obvious relation between the measurement of the frequency of an oscillator and the automatic control of that frequency. Both end results are represented among the following methods, and the last mechanism is particularly convenient, because it can be used in either way. The block diagrams that follow are reduced to very simple form. The notations of frequency used on them are over-simplified, and a symbol should not be taken as having exactly the same meaning in all of the diagrams.

Fig. 1 shows symbolically the photographic method used to obtain records shown in several of the figures to follow. The incoming frequency, f, is amplified and used to modulate the intensity grid of a recording oscilloscope. The local oscillator frequency, f_0, is divided down to any convenient submultiple of the incoming frequency and used to trigger a linear sweep of any convenient length. Time-of-day marks and calibration of the time-of-arrival axis may be provided in any way desired; the incoming frequency itself provides a useful scale for the latter.

[1] J. A. Pierce, H. T. Mitchell, and L. Essen, "World-wide frequency and time comparisons by means of radio transmissions," *Nature*, vol. 174, pp. 922–923; November 13, 1954.

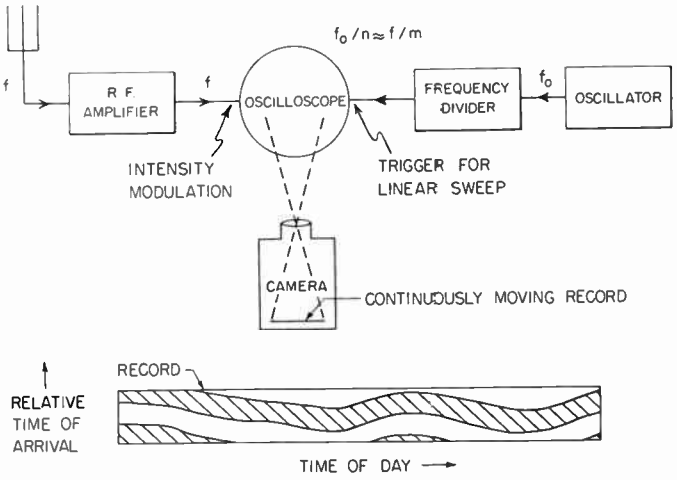

Fig. 1—A symbolic diagram of a photographic method for comparing the frequency of an incoming signal with a local oscillator.

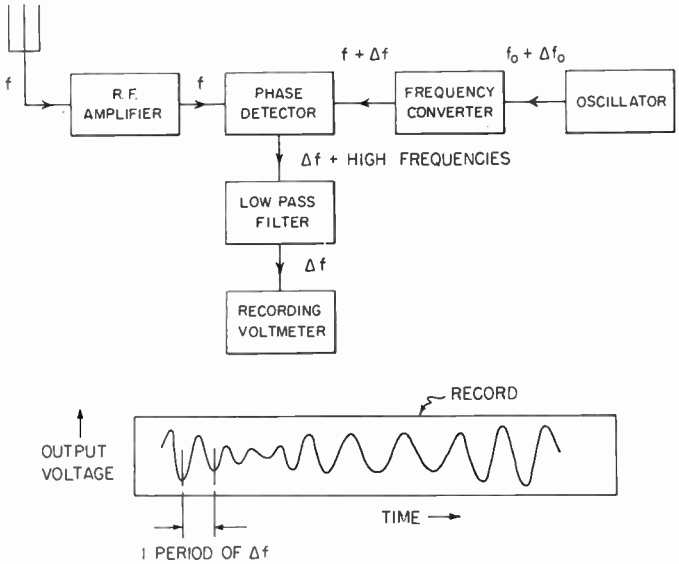

Fig. 2—A block diagram of a simple frequency comparator that can have narrow noise bandwidth.

Fig. 2 shows the simplest electronic method for comparing the incoming frequency with that of a local oscillator. This is a very powerful mechanism, first used for low-frequency radio reception, so far as I know, by W. E. Scoville of the U. S. Navy Electronics Laboratory. Here, the local oscillator frequency is converted to the nominal value of the incoming frequency, but is set off a few parts in 10^8 or less from the incoming standard, so that a beat is observed each few minutes. The method has the necessary advantage (partially obtained by photographic integration in Fig. 1) of permitting the use of very narrow bandwidths—say of 0.01 cycle or less—so that a signal can be extracted cleanly from the high ambient noise obtaining at low frequencies. The offsetting of the oscillator frequency is a disadvantage, for precise work, as one does not often have so many good oscillators that he can withdraw one from the correct frequency without misgivings. The amount of fre-

quency offset cannot be varied greatly in practice, because the amplitude of the recorded beats varies in proportion to the amplitude of the received signal. Thus, the phase of the beat can be determined accurately only at axis crossings. The period of the beats must be adjusted so that the phase can be read at appropriate intervals, usually, as mentioned above, a number of minutes. Obviously, the beat frequency should be high enough so that the sense of the frequency difference is never changed by vagaries of propagation or oscillator frequency.

Offsetting of frequency and intermittent availability of frequency data can be avoided or minimized by using two phase detectors, driven from the frequency converter at a 90° phase difference, with duplicate filters and recorders. If the gains of the two channels are accurately equal, the phase can be determined at any instant from the amplitude ratio between the two records. The sense of the frequency difference can be determined by observing which phase record is leading, and the frequency offset can be made small or zero.

An obvious derivative of the two-channel phase detector is the frequency regulator shown in Fig. 3. Here the outputs of two phase detectors operated in quadrature are used to control, respectively, the frequency of the local oscillator and the gain of the rf amplifier. The use of a separate phase detector to control the gain is, perhaps, not strictly necessary, but is a great convenience. It will be realized that the phase detector and integrator must be used if avc is to be achieved with a signal below the ambient noise level in the rf amplifier. The greatest advantage deriving from the use of both phase detectors is in recognizing proper performance. If the voltage applied to the avc circuit is steady at the normal controlled amplitude, it proves that a signal is present. If, further, the voltage applied to the reactance tube is small and substantially constant, it proves that the oscillator is under control.

We have tested a very simple version of Fig. 3, using a total of only nine tubes exclusive of power supply, with a time constant of the order of a minute. The oscillator is a simple crystal without temperature control. Using the gbr signal as a standard, the operation leaves something to be desired, as all control is lost when there is an unusually long gap in the keying sequence. However, as a demonstration of the performance that could be obtained with a continuous vlf standard frequency signal, the results are excellent.

An example of its behavior on a night of somewhat unstable transmission is shown in Fig. 4. Here, the upper half is a normal record made by the photographic method of Fig. 1. The dark band is the positive-going half cycle of the gbr carrier (at the intensity grid of the cathode-ray tube) and the breadth of the record is about 62 μs or one period at 16 kc. Below is a simultaneous record of the phase of the 16-kc signal derived from the regulator of Fig. 3, made with a separate oscilloscope

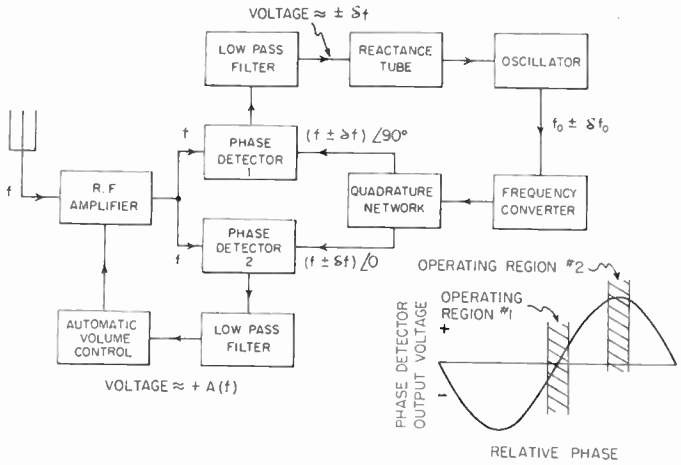

Fig. 3—A diagram of a simple regulator that locks the frequency of a local oscillator to that of an incoming signal.

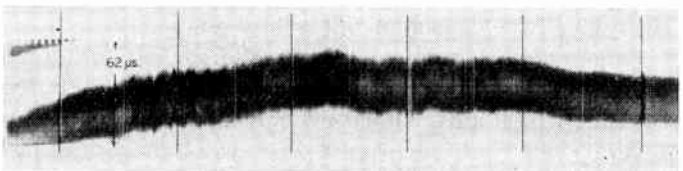

(a)

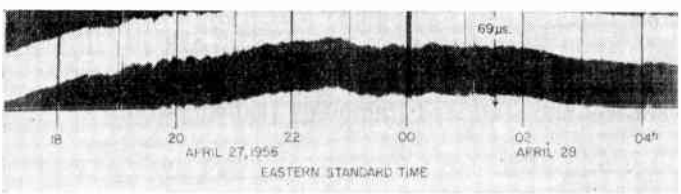

(b)

Fig. 4—(a) An example of the phase fluctuations of the gbr signal, received at Cambridge, Mass., on a night of high magnetic activity, and (b) a simultaneous record showing the behavior of the simple frequency regulator of Fig. 3.

and camera, but using the same trigger pulses. The precision of the regulator in indicated by the degree to which the two records conform. Fig. 4 shows clearly that the control of the oscillator leaves little to be desired, except for the shortness of the integration time. To extend this time, a more stable oscillator would be required. The regulator seems to be capable of staying always within a part in 10^9 with respect to the *received* frequency, or almost always within a part in 10^8 with respect to the *transmitted* frequency.

The next obvious improvement in this kind of device lies in the use of servomechanisms rather than regulators. This may be done as in Fig. 5, opposite, which also indicates the advisability of using a superheterodyne receiver; one reason is that narrower noise bandwidths can be achieved by filtering at the IF frequency. The greatest merit of the device in Fig. 5 is, however, somewhat subtle. To explain this, consider that the frequency f, represents the standard frequency as transmitted; it is modified by a Doppler effect, $d\phi_R/dt$, where the re-

ceived phase, ϕ_R, has a marked diurnal variation considerably greater than normal random fluctuations, as will be shown below. This diurnal variation may be represented by the small sketch at the top of Fig. 5. If we insert a corresponding diurnal phase shift, ϕ_S, at a frequency derived from the oscillator at the receiver, the diurnal component of the variations in transmission time can be cancelled out in the first order from the phase detector output. If this condition obtains, the phase servo does not have to track the diurnal variations so that its speed capability can be adjusted to the random fluctuations. A more important effect, however, is that the time constant of the aided tracking loop (that adjusts the oscillator frequency towards coherence with the incoming signal) can be reduced. In the absence of the diurnal variation simulation, the oscillator could be brought to coherence with the incoming signal to perhaps 1 or 2 parts in 10^{10} (assuming an almost perfect oscillator) but only with a time constant of several days, as the Doppler effects are large compared with the desired precision. In several days, unfortunately, the practical oscillator would be all too likely to change its frequency by a number of parts in 10^{10}, at least. Hence, it would be impossible to obtain a frequency coherent with the distant source to the desired degree. With the diurnal variation simulator, it appears that (at least at the distance of Cambridge from Rugby, 5200 km) the Doppler effects can be predicted and compensated to 1 or 2 parts in 10^{10}. If this be the case, the time constant of the aided tracking can be shortened to a few hours. In this condition, the equipment can retune the oscillator essentially as rapidly as its frequency vagaries occur. Obviously, the exact precision to be attained depends upon the oscillator stability.

Using an O-76-U oscillator that is likely to change frequency a number of parts in 10^{10} in a day or two, with an aided-tracking time constant of 10 hours, we have tested such a device. After three or four time constants, the servosystem brought the oscillator to a frequency in very close agreement with the transmitted frequency and maintained it there for several days with a standard deviation of 7 parts in 10^{11}. The deviations, of course, were primarily produced by fluctuations in the transmission time acting through the aided-tracking loop.

For propagational studies, we have, for the past two years, used an exactly similar device except for two factors: the absence of the diurnal variation simulator, and the absence of the aided-tracking loop. The former is obviously not wanted, and it is readily seen that the latter would only complicate the problem of keeping records of the nominal frequency of the oscillator.

A great advantage of the servomechanism device is that the over-all receiver bandwidth may be made as narrow as oscillator stability permits. The practical limit, for presently available oscillators, probably lies between 0.001 and 0.0001 cycles. The instrumentation ought to be such that the device can operate with a

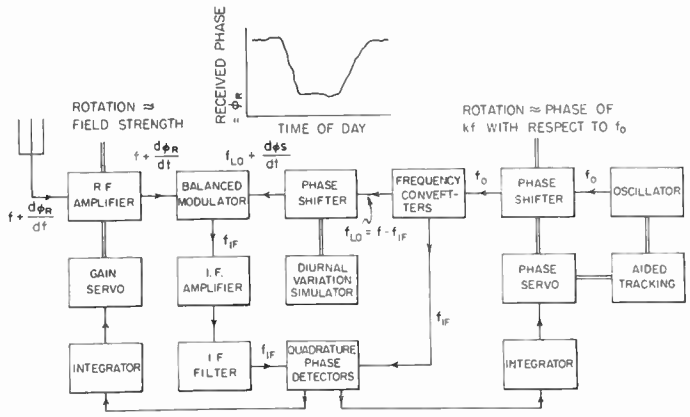

Fig. 5—A block diagram of a servo-operated device that is convenient and accurate for controlling the frequency of a local oscillator or for measuring propagational variations.

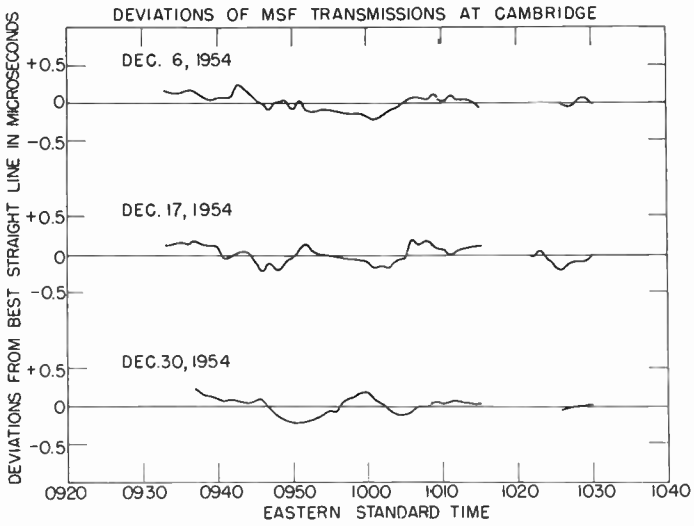

Fig. 6—Examples of the fluctuations in the time of arrival of the 60-kc standard frequency signal from msf, Rugby, received at Cambridge, Mass.

signal some 50 or 60 db below the noise in the rf amplifier bandwidth. With good IF filtering and careful phase detector design, this level is not hard to attain.

With this background, we can now turn to observations showing the uncertainty in the time of arrival of a low-frequency signal.

Precision of Frequency Measurement at 60 KC in the Daytime, at 5200 KM

The 60-kc standard frequency signal from msf is transmitted daily between 9^h30^m and 10^h30^m E.S.T., except for a gap from 10^h15^m to 10^h20^m. This signal has been recorded with a servo device similar to Fig. 5. Three examples of the phase record are shown in Fig. 6. Because it took a few minutes for the phase servo to adjust itself, the records begin a little after 9^h30^m and the five-minute gap at 10^h15^m is extended to about 10 minutes. Having assumed that any slope in the record was due to oscillator frequency discrepancy, the devia-

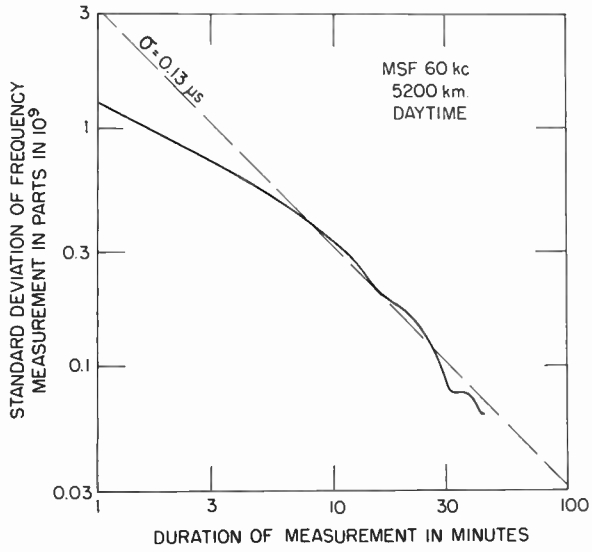

Fig. 7—The standard deviation of measurement of the frequency of the msf signal as a function of the duration of the measurement.

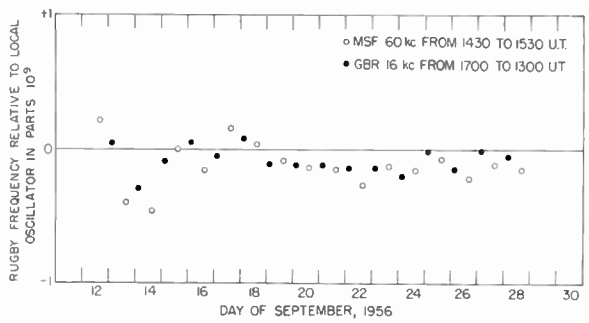

Fig. 8—An example of consistent behavior of two oscillators, on opposite sides of the Atlantic Ocean, over a period of two weeks.

tions of Fig. 6 represent random variations due to fluctuations in transmission time or noise in the receiving equipment. The important point is that the deviations seldom exceed $\frac{1}{4}$ microsecond or about 5° of phase. The standard deviation of the time of arrival has averaged about 0.1 microsecond.

A study of a number of apparently normal days' data has been carried out in the following way. The changes in deviation, derived as in Fig. 6, have been examined for all intervals of one minute, two minutes, three minutes, and so on. For intervals of less than five minutes, the slowness of the servo causes a tendency to minimize the differences in deviation. Thereafter, the magnitudes of the differences become approximately constant. From a table of all the differences between sets of points, say, ten minutes apart, a standard deviation in microseconds was computed. This standard deviation divided by the number of microseconds in the interval ($6 \cdot 10^8$ for a ten-minute interval) gave the standard deviation of the frequency measurement for that period. The results of this study are shown in Fig. 7, where it is seen that a precision of a part in 10^{10} is achieved in about thirty minutes. The irregular character of the curve of Fig. 7 is explained in part by interference from other local frequency standards and divider systems. The low values at about forty minutes are, however, apparently real. They presumably represent a tendency for phase conditions to repeat themselves at about that interval, an analog of the ordinary fading period. The dashed straight line is the relation between precision and time interval that would obtain if there were no autocorrelation in the phase-time diagram. It can easily be demonstrated that simple curvature, if concealed in the curves of Fig. 6, would yield a curve in Fig. 7 of entirely different character from that observed. We can, therefore, presume that neither acceleration in oscillator rates nor diurnal variation in the transmission time is a serious factor. The time of this transmission, by the way, is near noon at the midpoint of the path. At other times of day, diurnal variation might be important.

Occasionally, the oscillator used to provide a time standard in Cambridge seems to have very uniform characteristics for a few days at a time. On these occasions, the frequency differences between msf and the local oscillator change only slightly, or at least uniformly from day to day. An example of this consistency is given in Fig. 8, in which points derived from twenty hours of observation at 16 kc are also shown. It will be observed that the frequency of the local oscillator was in very good agreement with msf, and that the standard deviation of the frequency difference for several days in succession was of the order of 1 in 10^{10}. When it is recalled that this value must include the vagaries of the oscillators at both transmitter and receiver, it is clear that the propagational uncertainty (at least for this period) can hardly have been greater than that estimated in the derivation of Fig. 7.

Diurnal Variation of 16-KC Phase at 5200 KM

As discussed in a previous paper,[2] the simplest assumption that can be made about a crystal oscillator is that its aging rate is constant. That is, the frequency becomes higher each day at a uniform rate. If an oscillator at a receiver has an aging rate differing from that of the oscillator at a standard frequency station, the relative phase of the received signal may be made stationary at a given instant, but will not remain so. The slope of a phase-time diagram will change linearly; the phase itself will change as the square of the time, measured from the instant when the two frequencies are equal.

An example of this kind of behavior is shown in Fig. 9, where a four-day record of gbr, made by the servo method, is plotted. The high values at night and the low ones in the daytime are easily recognized. On the as-

[2] J. A. Pierce, "The diurnal carrier-phase variations of a 16-kilocycle transatlantic signal," Proc. IRE, vol. 43, pp. 584–588; May, 1955.

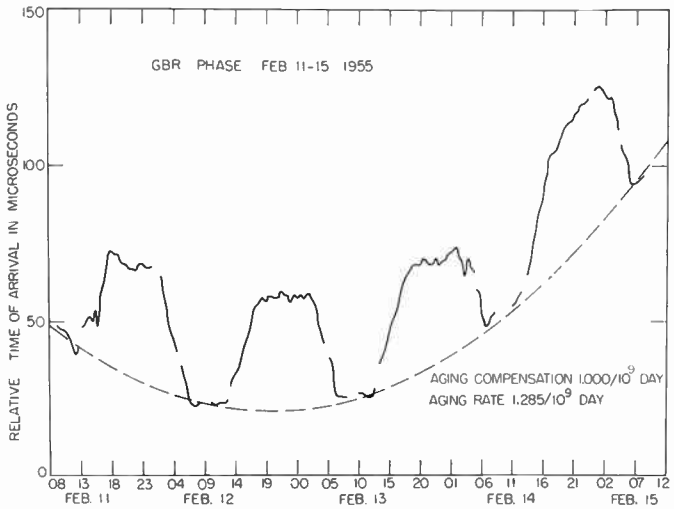

Fig. 9—A typical four-day record of the time of arrival of the 16-kc signal from gbr, showing both diurnal variation of the transmission time and curvature caused by relative oscillator aging.

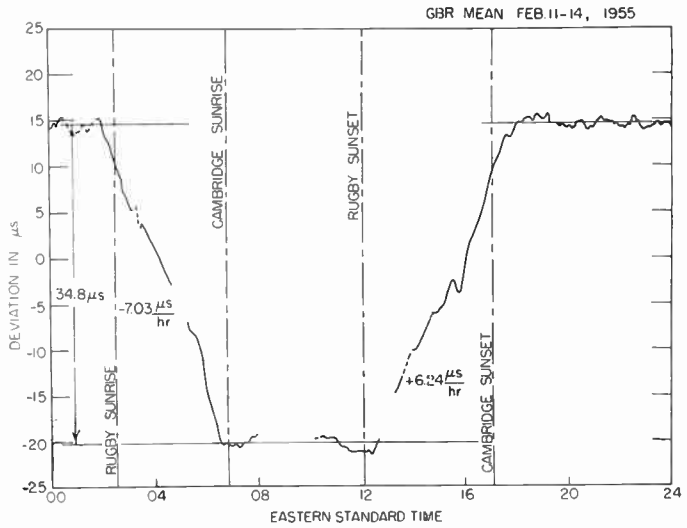

Fig. 10—The diurnal variation of the time of arrival of the gbr signal, derived from the data of Fig. 9.

sumption of a constant aging rate, a parabola, shown by the dashed line in Fig. 9, has been fitted to the daytime transmissions. This line represents the drift of phase due to oscillator characteristics. It can, as suggested above, be determined quite accurately after the fact, but it is difficult to predict. Now the departures of the observed curve from the dashed curve in Fig. 9 can be measured or computed. When averaged together, they give the diurnal curve of Fig. 10, where the deviation has been reduced to departure from the arithmetic mean.

Fig. 10 displays all the characteristic features of all of the similar records that have been made at Cambridge. Starting from the nighttime value, the transmission time decreases from about a half-hour before sunrise at Rugby to about a halfhour before sunrise at Cambridge. A substantially symmetrical effect is observed at sunset, except for a rounding-off in the final approach to the nighttime level. The depth of the trapezoidal pattern is surprisingly constant throughout the year, being about 34 ± 1 μs. The only real seasonal change is the ordinary variation in the length of the day and night; in midsummer there are only three or four hours of darkness over the whole path.

If the curves for the separate days were plotted in Fig. 10, they would seldom stray more than ± 5 μs from the mean curve. The standard deviation seems to be of the order of 2 μs.

Precision of 16-KC Frequency Measurements at 5200 KM

An analysis has been performed, like that described in deriving Fig. 7, for the 16-kc transmission, using records for a number of days. The average value and the standard deviation of the frequency measurement were derived at each hour of the day, for measurement intervals of 0.1, 0.5, 3, 24, and 72 hours. Fig. 11 shows the

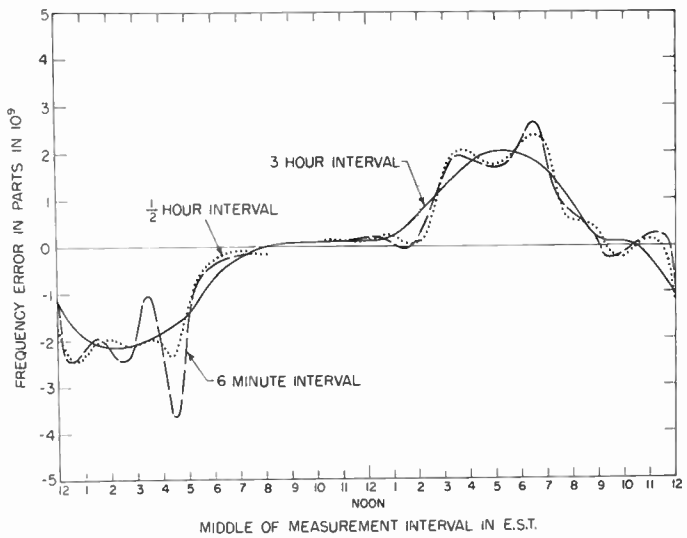

Fig. 11—Typical diurnal Doppler effects (with sign reversed) in 16-kc transmission from Rugby, England, to Cambridge, Mass.

average values, which are (in the negative sense) the Doppler effects in transmission, because the oscillator effects were removed analytically. For the six-minute interval, shown by dashes, the curve of Fig. 11 is substantially proportional to the slope of the mean diurnal phase curve (similar to Fig. 10). For the longer intervals, the curves of Fig. 11 are essentially chords of the diurnal phase curve. For measurement intervals that are multiples of 24 hours, the diurnal Doppler effect is, of course, zero. Fig. 11 shows that the sunrise and sunset periods give, at the distance of 5200 km, Doppler shifts of about 2 parts in 10^9, and that, in the daytime, the mean Doppler shift is probably less than 1 in 10^{10}. The data of Fig. 11 were taken at a season when there was not much total darkness on the path; in winter the mean nighttime Doppler shifts are also small.

Standard deviations derived in preparation of Fig. 11, and from other similar data are shown in Fig. 12. The extension of these curves to the lower right-hand corner of Fig. 12 implies that I can trust my oscillators to maintain constant characteristics to some parts in 10^{11} for several days. This may occasionally be the case, but it is not to be relied upon.

Fig. 12 shows that, at 16 kc at 5200 km, measurements can be made to 1 in 10^9 in a few minutes and to 1 in 10^{10} in about half a day. Actually, we can do a little better than this. Fig. 12 was derived using only the end point phases; constant measuring and averaging would give a precision tending to improve as the 3/2 power of time, rather than as the first power.

It will be seen by intercomparing Figs. 7 and 12 that, in the daytime, greater precision can be had in a given time at 60 kc than at 16 kc. This is presumably because a propagational vagary giving a certain phase shift changes the time of arrival less at the higher frequency. On the other hand, the 60-kc signal is probably not useful at distances much greater than that from Rugby to Cambridge, while the 16-kc signal is useful everywhere.

It is perhaps worth noting that there is no evident tendency of the curves of Fig. 12 to cross over the "ultimate" dashed line, as the curve of Fig. 7 does. This probably means that there is no typical fading period at 16 kc; or rather, that the period is so long that it is never independent of the diurnal variation.

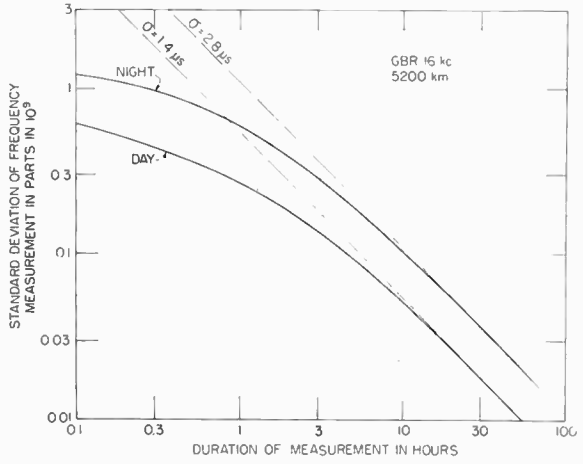

Fig. 12—The standard deviation of the 16-kc transatlantic frequency measurement as a function of the duration of the measurement.

16-KC Frequency Measurements at 18,700 KM

Allan, Crombie, and Penton, at the Dominion Physical Laboratory in New Zealand, have been observing the frequency of gbr relative to one of their oscillators.[3] They use the beat method of Fig. 2. A record taken from their report in *Nature* is shown as Fig. 13. This is an excellent example of the beat method. The variation in amplitude through a signal minimum is clearly shown. Of particular importance is the noise-free character of the sinusoidal beats, even at the great distance of 18,700 km, showing the value of narrow bandwidth—in this case about 0.01 cycle. Allan, Crombie, and Penton report that, in a normal bandwidth of 400 cycles, the gbr signal averages 20 db below the peak noise.

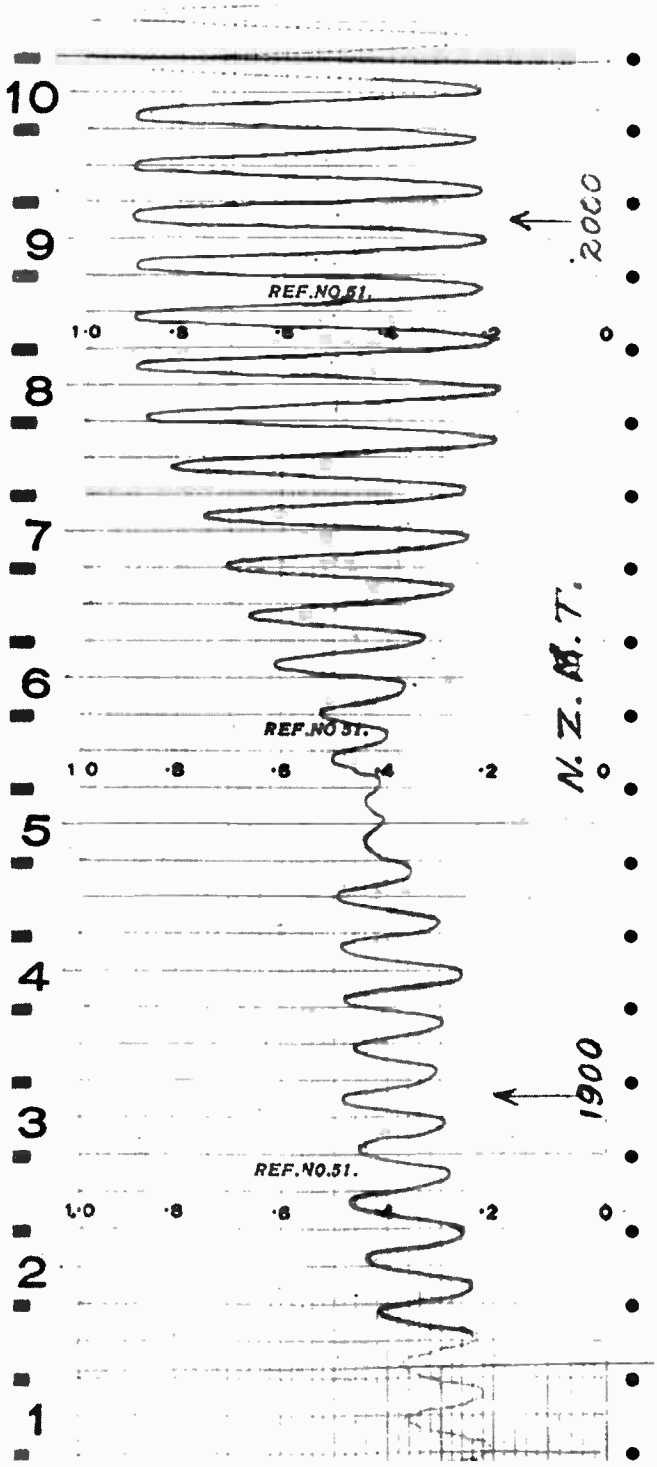

Fig. 13—A recording, reproduced from *Nature*, of beats between the gbr signal, received in New Zealand, and a local oscillator.

[3] A. H. Allan, D. D. Crombie, and W. A. Penton, "Frequency variations in New Zealand of 16 kc/s transmissions from gbr Rugby," *Nature*, vol. 177, pp. 178–179; January 28, 1956.

Fig. 14, also taken from the *Nature* article, shows a sample diurnal frequency variation. Except for periods near local sunrise and sunset, Doppler effects are not easy to measure. Allan, Crombie, and Penton claim no more precision than ± 4 parts in 10^9.

Mr. Crombie has been generous enough to send me additional examples of the New Zealand records. The diurnal frequency deviations on a dozen days between October, 1955, and March, 1956, have peaks that average about $\pm 8/10^9$, but it should be noted that on two occasions (both in October) the peak deviations exceeded $2/10^8$.

I am not able to construct a diagram (like Figs. 7 and 12) that would define the precision of measurement in New Zealand, and trust that Allan, Crombie, and Penton will presently derive one. From various tentative studies of their data, I would suggest that their figure of 4 parts in 10^9 may well represent the standard deviation for a duration of a half-hour or an hour, and that (by choosing the best time of day) a precision of $1/10^9$ might be reached in several hours. The whole question depends upon the predictability of the Doppler effects, and for the answer we must await the taking of more data.

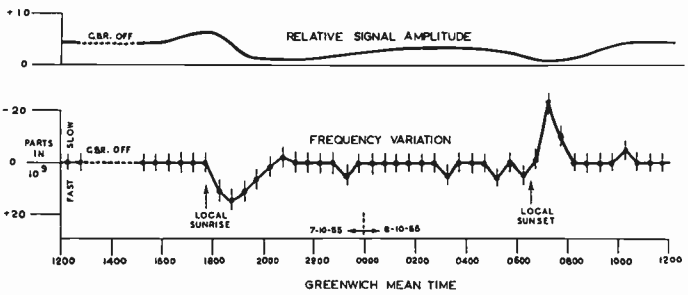

Fig. 14—A graph, reproduced from *Nature*, of the diurnal variation of the frequency of the gbr signal, received in New Zealand.

Effects of High Magnetic Activity Upon Phase

When magnetic activity is high, there is a turbulent effect upon the nighttime phase at 16 kc, and, presumably, at other low frequencies, but there is little or no effect in the daytime. An example of the nighttime behavior is given at the top in Fig. 15, where the bottom record is a corresponding example for a magnetically quiet night. These records, like those of Fig. 4, were made by the method of Fig. 1. At the bottom, the normal night is characterized by a nearly constant phase through the hours of darkness over the whole path. At the left, the end of the sunset slope can be seen, and at the right, is the beginning of the phase advance as sunlight first falls upon the eastern end of the transmission path. In the upper record the end of the sunset period and the beginning of the sunrise period can be identified approximately but, as on other nights of high magnetic activity, there is a phase uncertainty of the order of ± 5 μs. The phase discontinuities in the upper record at 0.16

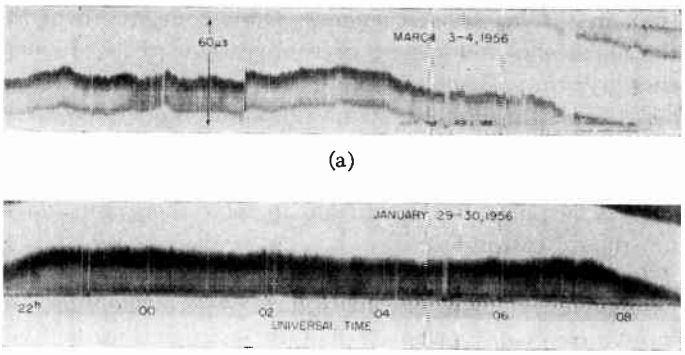

Fig. 15—(a) A gbr phase record during a night of high magnetic activity, and (b) a corresponding record on a magnetically quiet night. Note: Discontinuities in the upper record at 0.16 hours and 0.68 hours are not magnetic effects.

and 0.68 hours U.T. were caused by retuning the transmitting antenna and not by magnetic activity. Usually the deviations in frequency are not greater than ± 2 or 3 parts in 10^9, but occasionally there are frequency deviations of as much as 1 or 2 parts in 10^8 that persist for two or three minutes at a time. As an aid in judging these values, it should be mentioned that a 45° slope, in these photographic records, corresponds to a frequency difference of about $1/10^8$. It is seen that high magnetic activity greatly increases errors of measurement for intervals of a few minutes, but has little effect when the frequency measurement duration is many hours.

Effect of a Sudden Ionospheric Disturbance Upon Phase

On rare occasions, there are large Doppler effects on the received frequency. These occur during the onset of a sid that coincides, in the sunlit hemisphere of the earth, with the time of a solar flare. In an extreme case at 16 kc, the phase may advance as much as 100° in five minutes or so, then recover during the next hour. The peak Doppler effect so far observed was about 8 parts in 10^8, but this value was attained for only a minute or so.

At 60 kc, the phase shift during a sid appears to be of about the same magnitude, but the effect on frequency is not so large, because the displacement in microseconds is smaller. The peak Doppler shift so far recorded was about $15/10^9$.

On one occasion, during the great solar event of February 23, 1956, we have observed a similar effect at night.[4] The peak Doppler effect was 6 parts in 10^8. This was an event of unprecedented severity. We have seen nothing resembling it on any other occasion.

These observations, together with the smaller daytime phase fluctuations at higher frequencies noted above, suggest that the primary daytime phenomenon is a fluctuation in the phase shift at reflection, rather

[4] J. A. Pierce, "VLF phase shifts associated with the disturbance of February 23, 1956," *J. Geophys. Res.*, vol. 61, pp. 475–473; September, 1956.

than in the height of reflection. This concept fits with the surprising invariance of the average phase during the day; that is, the complete absence of the Chapman depression throughout all of the sunlit hours. We are, therefore, led to imagine an ionized layer of remarkably fixed height whose ionization gradient and conductivity vary in response to fluctuations in solar energy or in atmospheric turbulence.

It should be remarked that at night, except at 16 kc, we have only scattered bits of data. There is, so far, no indication of any great change in the variation of time of arrival at different frequencies. The corresponding model is that of a reflecting layer of constant ionic properties but of fluctuating height.

The Power Required for World-Wide Standard Frequency Service from a Single Station

Space does not permit proper development of this subject, as many studies of signal propagation and atmospheric noise level must be called upon, and, so far, the fragmentary data that are available are less than completely reliable. It is worth while, however, to examine the outline of the problem.

Little is known about possible auroral-zone effects on vlf transmission, or what may be worse, the effects of permafrost or other areas of exceptionally poor ground conductivity. In the absence of this information, it has seemed advisable to assume transmission conditions obtaining at the time of the day's greatest absorption, and also the diurnal and annual maximum noise. It is possible that the pessimistic assumption that these conditions obtain simultaneously may allow the estimation of conditions that will permit reliable frequency measurements at most locations.

The noise assumed for this study was measured in Kansas in 1953 and is shown in Fig. 16. This is the rms noise level (at the diurnal maximum in the afternoon) exceeded on only 5 per cent of the days in July and August. This is, so far as we know, approximately the greatest atmospheric noise level on the North American continent. A curve representative of noise at middle latitude at long distances from the center of the continent, and a curve of Arctic noise are also shown. The "CRPL" curve is taken from the highest contour in the latest prediction[5] of the National Bureau of Standards. In this case, only the median level is shown, but noise of this intensity is presumably encountered only in one or two small areas of the world.

Signal levels have been computed from the formula:[6]

$$\epsilon = 210\mu v/m \left(\frac{P}{\sin\theta}\right)^{1/2} e^{-0.27f^{3/4}\theta} \qquad (1)$$

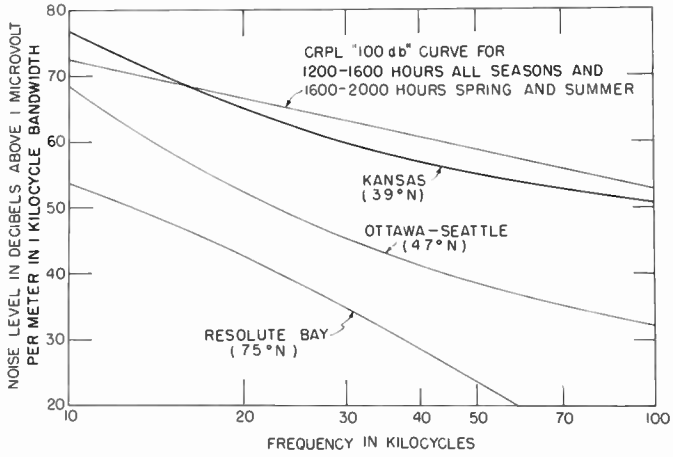

Fig. 16—Examples of the variation of atmospheric noise with frequency at various locations at the most noisy time of day.

where

- ϵ is the predicted field strength in $\mu v/m$,
- P is the radiated power in kilowatts,
- θ is the angular distance from the transmitter in radians,
- e is the base of the Naperian logarithms, and
- f is the radio frequency in kilocycles per second.

This equation has been shown to give reasonable agreement with observation at the time of minimum diurnal field strength when the sun is some 20 or 30° above the horizon.

Using this equation, field strengths were computed for various distances and frequencies and compared with the "Kansas" noise of Fig. 16. The result is shown in Fig. 17. This figure gives the signal-to-noise ratio for unit power and unit receiver noise bandwidth. At the right is a scale of radiated power required to give a signal voltage, in a receiver of 0.01-cycle noise bandwidth, that is equal to the rms noise.

Two observations may be cited in support of Fig. 17. In the summer of 1956, we successfully observed an experimental 60-kc standard-frequency transmission made by the Bureau of Standards at Boulder, Colo. The bandwidth of the receiver was somewhat more than 0.01 cycle, and, in one period, the radiated power was no more than 5 watts. At the distance of 2900 km, Fig. 17 indicates that 5 watts was required, and it is believed that the experiment would have been successful despite somewhat greater noise than actually obtained.

Also, as shown above, the frequency of gbr at 16 kc is successfully measured in New Zealand. Records of these measurements by Allan, Crombie, and Penton, during the New Zealand summer, show that there were occasional periods of two or three hours when the gbr signal fell below the noise in 0.01-cycle bandwidth. Fig. 17 shows that at 16 kc at nearly 19,000 km a radiated power of 100 kw would be required, whereas it is believed that gbr actually radiates about 30 kw.

To provide a signal useful all over the world, it is necessary to radiate the power given (on the right-hand

[5] CCIR Study Group VI, "Report on Revision of Atmospheric Radio Noise Data"; July, 1956.

[6] This formula is taken from the author's Cruft Lab. Tech. Rep. No. 158, with the constant in the exponent increased from 0.20 to 0.27. This modification is designed to yield the day's minimum signal rather than the mean daytime signal.

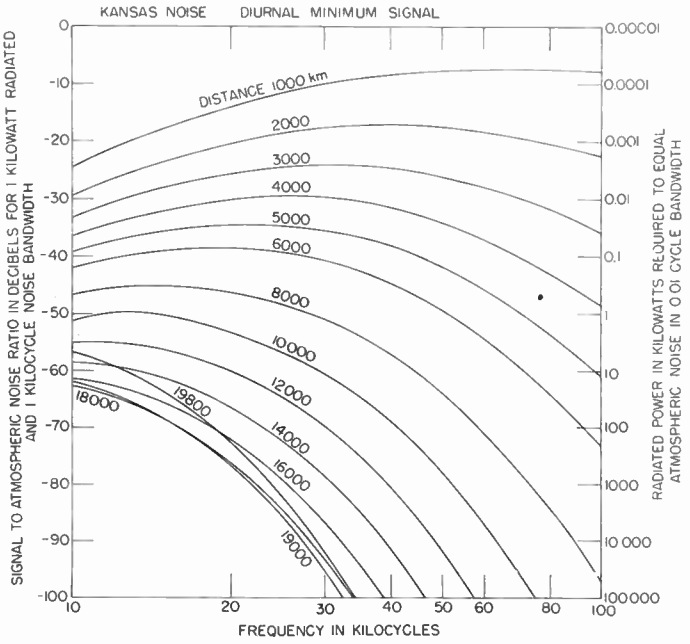

Fig. 17—Variation of signal-to-noise ratio with distance and frequency, assuming the transmission equation (1) and the Kansas noise of Fig. 16.

scale) by the envelope of all possible distances at the lower left corner of Fig. 17. Obviously, with available transmitters, this is possible only at the very lowest frequencies.

Even at these frequencies several hundred kilowatts and a very large transmitting antenna would be required. Rough estimates indicate that, assuming an effective height of 200 meters, the transmitting antenna would need to have a reactance equal to that of a capacitance of 0.05 μf. Such an antenna would have an efficiency (assuming a Q of 50 times the frequency in kilocycles in the loading coil and other loss resistances totalling 0.3 ohm) of about 7 per cent at 10 kc and 38 per cent at 20 kc.

Fig. 18 shows both the radiated power and the input power to the transmitting antenna over the limited frequency range of interest. It must be realized that the actual power level is neither critical nor accurately specified. Aside from the uncertainties mentioned above, the assumption of 0.01 cycle as a suitable bandwidth is quite arbitrary. As suggested before, the bandwidth can be made ten or a hundred times less without placing prohibitive requirements on the stability of the local oscillator.

It seems, therefore, that probably a single transmitter can provide a frequency-standardizing signal to the whole world. Such a transmitting station would certainly be expensive, but the economic factor would favor it as compared with the still-growing network of

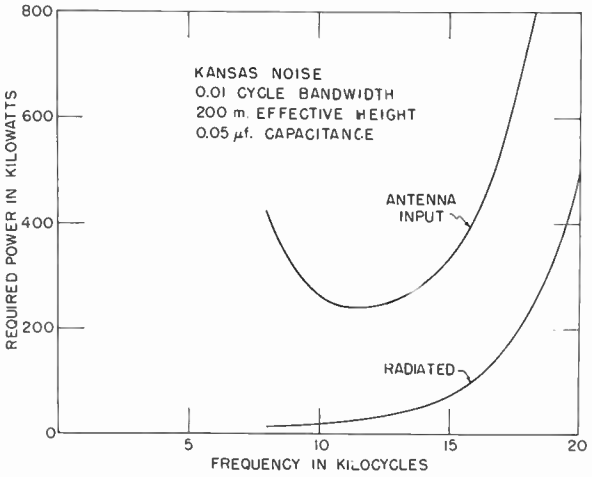

Fig. 18—An estimate of the power required to provide standard frequency service all over the world from a single vlf station.

about ten hf standard-frequency stations. Of more importance, however, is the thesis of this paper: that frequency measurements with an accuracy improved by two or three orders of magnitude can be had at very low frequencies.

Conclusion

The phase stability of vlf transmission combines with predictable diurnal variation to permit frequency comparisons of high accuracy at intercontinental distances. Except for occasional momentary deviations of several parts in 10^8 at the beginning of sudden ionospheric disturbances, a precision of a part in 10^9 is usually attainable at 5000 km in a measurement interval of a fraction of an hour. For measurements extending over several hours or from day to day, the precision exceeds a part in 10^{10}.

Even at a nearly antipodal distance, it appears that a precision of a few parts in 10^9 is attainable in an hour or so, and that errors do not exceed a part in 10^9 for measurements from day to day.

These accuracies are about two orders of magnitude better than those ordinarily credited[7] to standard frequency transmissions at high frequencies. VLF can also provide world-wide service from a single station, if it has high power.

Excellent frequency comparisons can be made using existing vlf transmitters, whenever their operating schedules permit, provided that very good oscillators are used at the receiving points. If, however, a continuously operating vlf standard were provided, the latter requirement could be relaxed, and simple receiving devices could make a common frequency continuously available to all potential users.

[7] L. Essen, "Standard frequency transmissions," *Proc. IEE*, vol. 101, pp. 249–255; July, 1954.

Relations Between the Character of Atmospherics and Their Place of Origin*

J. CHAPMAN† AND E. T. PIERCE‡

Summary—**From recent experimental work at Cambridge, Eng., it is shown that atmospherics originating from different geographical localities are systematically different in character, even when the distances of propagation are the same and there is no reason to anticipate appreciable dissimilarities in the ionospheres along the respective propagation paths. Detailed and precise information is given of how these "geographical" effects may be traced by recording and classifying types of waveforms. It is also shown that the effects are apparent for observations of atmospherics at fixed frequencies between 0.65 and 27 kc. No attempt is made to assign a reason for the geographical phenomena, but the most promising approach would seem to be by considering differences in the conductivity of the earth's surface, and in particular, those between land and sea.**

The Waveforms of Atmospherics

IT IS NOW clear that the main factors influencing the waveform of an atmospheric are the distance of the source from the observing station and the condition of the lower ionosphere; information is, however, becoming increasingly available[1-3] that even when these two factors are the same, sources in different geographical localities produce quite dissimilar types of waveform. Much of the evidence for these "geographical effects" has been presented in a rather vague and indefinite manner; the object of this note is to add precision to, and to somewhat extend, the previous conclusions.

It is first necessary to classify waveforms into types. This kind of subjective division is unfortunately dependent upon the receiver characteristics and display employed; differences are often found between classifications of two groups of workers, although results obtained by individuals within the same group are usually consistent. Here, a division is made into four types of waveform, all originating in the return stroke of the lightning flash; it is hoped that with the assistance of the brief notes and Fig. 1 the relation of this classification to others previously given may be easily recognized.

The waveform types are:

1) *Reflection*—Contains a series of five or more pulses whose spacing fits the concept of successive reflections from an ionosphere of constant height.

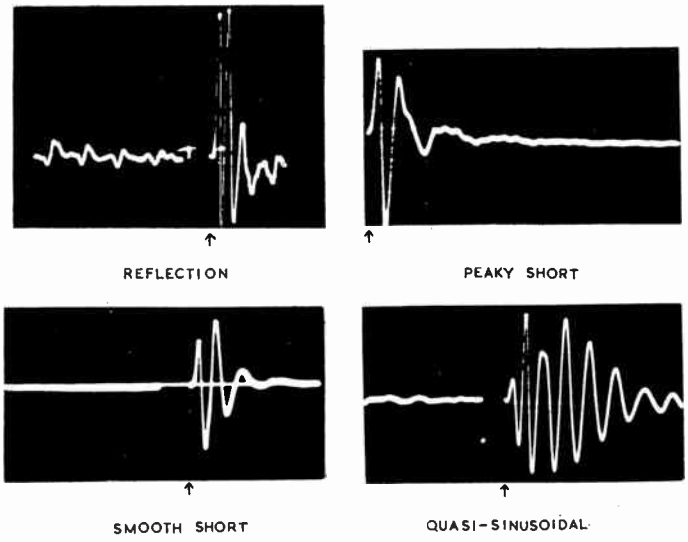

Fig. 1—These waveforms were recorded using a continuously running time-base. Triggering could therefore occur at any point on the time-base sweep and the actual starts of the waveforms are indicated by arrows. The total time of sweep is 10 milliseconds for the reflection type waveform, and 2 milliseconds for the other types.

2) *Peaky Short*—Contains five or fewer pulses which decrease rapidly in size; in view of the small number of pulses and the broad nature of some of the peaks, it is difficult to demonstrate a fit to the reflection mechanism on any stringent criterion.

3) *Smooth Short*—Contains five or less smooth oscillations of rapidly decreasing size, but which join to give a continuous variation in electric field. Does not fit the reflection concept.

4) *Quasi-sinusoidal*—Contains six or more smooth oscillations, several being of comparable amplitude. Does not fit the reflection concept.

All waveforms, recorded by standard methods[2] at Cambridge during the past few years, for which Sferics[4] estimates of the place of origin were available, were classified, as far as possible, on the above system.

Sixteen regions, defined by four zones of distance and four quadrants, centered on Cambridge, were then considered: the quadrants were North to East, East to South, etc.; the zones of distance, 0–1000 km, 1000–2000 km, 2000–3000 km, and beyond 3000 km. The results were separated into "day" and "night" categories, all waveforms received at times less than three hours removed from ground sunset or sunrise at Cambridge

* Original manuscript received by the IRE, December 11, 1956. Paper presented at Symposium on Propagation of Very-Low-Frequency Electromagnetic Waves, Boulder, Colo.; January 23–25, 1957.

† Courtald's Ltd., Coventry, Eng. Formerly with Cavendish Lab., Cambridge, Eng.

‡ Cavendish Lab., Cambridge, Eng.

[1] F. E. Lutkin, "The nature of atmospherics VI," *Proc. Roy. Soc.*, vol. 171A, pp. 285–313; June, 1939.

[2] P. G. F. Caton and E. T. Pierce, "The waveforms of atmospherics," *Phil. Mag.*, vol. 43, pp. 393–409; April, 1952.

[3] F. Horner and C. Clarke, "Some waveforms of atmospherics and their use in the location of thunderstorms," *J. Atmos. Terr. Phys.*, vol. 7, pp. 1–20; January, 1955.

[4] C. V. Ockenden, "Sferics," *Met. Mag.*, vol. 76, pp. 78–84; April, 1947.

being rejected in order to avoid possible twilight effects. Tables I and II, showing the relative percentages of the different types recorded from each region by night and by day, were then constructed; they are based on records of over a thousand individual waveforms. Some discretion was involved in the preparation of the tables; in particular, no entries are given for the regions from which few fixes were reported, and for which the percentage figures would accordingly be very misleading.

TABLE I

PERCENTAGE OCCURRENCE OF DIFFERENT WAVEFORM TYPES BY NIGHT

Distance (KM)	Direction (Quadrant)	Type of Waveform			
		Reflection	Peaky Short	Smooth Short	Quasi-sinusoidal
0–1000	N-E	82	9	—	9
	E-S	92	8	—	—
	S-W	100	—	—	—
	W-N	—	75	25	—
1000–2000	N-E	77	23	—	—
	E-S	75	20	2	3
	S-W	29	45	3	23
	W-N	100	—	—	—
2000–3000	N-E	—	—	—	—
	E-S	80	7	—	13
	S-W	1	13	15	71
	W-N	—	—	—	—
Beyond 3000	N-E	—	—	—	—
	E-S	—	—	—	—
	S-W	—	3	14	83
	W-N	—	—	—	—

TABLE II

PERCENTAGE OCCURRENCE OF DIFFERENT WAVEFORM TYPES BY DAY

Distance (KM)	Direction (Quadrant)	Type of Waveform			
		Reflection	Peaky Short	Smooth Short	Quasi-sinusoidal
0–1000	N-E	4	85	11	—
	E-S	1	71	28	—
	S-W	—	67	33	—
	W-N	—	100	—	—
1000–2000	N-E	—	39	61	—
	E-S	2	45	52	1
	S-W	—	25	67	8
	W-N	—	—	—	—
2000–3000	N-E	—	—	—	—
	E-S	—	19	81	—
	S-W	—	3	55	42
	W-N	—	—	—	—
Beyond 3000	N-E	—	—	—	—
	E-S	—	—	—	—
	S-W	—	—	65	35
	W-N	—	—	—	—

It is apparent from Table I that at night reflection waveforms are received from all distances to the South-East, but in the South-West there is a change from reflection to smooth types between 1000 and 2000 km, most of these smooth waveforms being of the quasi-sinusoidal kind. There is some evidence indicating firstly that at any instant the alteration in waveform type with distance occurs very sharply; *i.e.*, within one or two hundred kilometers, and secondly, that the transition distance varies from time to time; thus, averaging over a long period results in a transition zone rather than in a sudden changeover distance. It is therefore probably misleading to specify any single figure for the changeover distance, but nevertheless, values of 1600 km and 3000 km have been suggested by Caton and Pierce[2] and Horner and Clarke.[3] The limits 1000–2000 km, given in Table I for the transition zone, are in accord with the figure of 1600 km but not with that of 3000 km.

By day, for all directions, peaky short waveforms are the most common variety from within 1000 km, but at greater distances there is a preponderance of smooth waveforms of the smooth short kind. The effect first noted by Lutkin[1] that waveforms from the West are smoother and contain more oscillations than those from the East is confirmed by the results represented in Table II. At comparable distances, South-Westerly regions give more smooth types with a greater proportion of quasi-sinusoidal atmospherics than do the South-Eastern areas.

THE FREQUENCY CONTENT OF ATMOSPHERICS

The lack of precision involved in using subjective methods of waveform classification may be avoided by employing tuned receiver techniques as used, for example, by Bowe.[5] In order to ascertain whether the geographical effects found for waveforms are also evident in observations on fixed frequencies, Table III was constructed. This represents the averaged ratio of the responses on certain frequencies for daytime atmospherics originating within 1500 km, from sources to the East, and to the West, respectively. Table III may be considered as indicating the relative content at the different frequencies for waveforms originating, respectively, from the two directions; it is apparent that the spectrum is comparatively broad for atmospherics from the East, but narrow and peaked around 10 kc for those from the West.

TABLE III

RATIOS OF RESPONSES AT CERTAIN FIXED FREQUENCIES FOR DAYTIME ATMOSPHERICS FROM EASTERLY AND WESTERLY SOURCES

Frequencies chosen (kc)	Ratio	
	Easterly Sources within 1500 km	Westerly Sources within 1500 km
27:10	0.19	0.13
18:10	0.36	0.32
3.5 :10	0.80	0.57
0.65:10	0.78	0.55

[5] P. W. A. Bowe, "The waveforms of atmospherics and the propagation of very low frequency radio waves," *Phil. Mag.*, vol. 42, pp. 121–138; February, 1951.

Conclusion

It has been shown that relations between the character of atmospherics and their place of origin may be identified both from the study of waveforms and from records on fixed frequencies. This is, of course, not unexpected, since waveform and frequency content are of necessity interrelated, and both methods of observation reflect the modifications introduced during propagation. A paper by Chapman and Pierce[6] shows how particular types of waveform are associated with characteristic spectra; in consequence, all phenomena observed for waveforms may be expressed in terms of frequencies.

The reasons for the geographical effects are still not entirely clear. Suggested explanations include differences in propagation over land and sea paths, a dependence of propagation on orientation with respect to the earth's magnetic field, a possible distinction between lightning flashes to land and to sea, and differences between oceanic and continental thunderstorms. It is difficult to distinguish between these possible influences from observations in the British Isles, and further work in a more favorable locality is therefore highly desirable. It seems most likely, however, that the important factor is the difference in propagation over land and over sea. This interpretation is supported by experimental observations on long wave radio stations, *e.g.*, Tremellen,[7] and by the recent theoretical work of Wait.[8] It is perhaps noteworthy that the geographical phenomena are most pronounced at night when, the differences between the conductivities of the earth and the lowest ionosphere being less than by day, variations in the conductivity of the earth's surface, *e.g.*, between land and sea, may be expected to have their maximum effect.

Acknowledgment

We are grateful to Miss Shelagh M. Cussen for checking some of the data in this paper.

[6] J. Chapman and E. T. Pierce, "The waveforms, frequency spectra and propagation of atmospherics," *Proc. 1956 Paris Conf. on Wave Propagation.* Also *Onde Electrique;* May, 1957.

[7] K. W. Tremellen, "A study of ionospheric ray field intensity in the 10–30 and 500–1100 kc/s bands," *Marconi Rev.*, vol. 13, pp. 153–166; Fourth Quarter, 1950.

[8] J. R. Wait, "On the mode theory of vlf ionospheric propagation," *Proc. 1956 Paris Conf. on Wave Propagation.* Also *Geof. Pura. Applicata* (Milan)., vol. 37, June; 1957.

A Technique for the Rapid Analysis of Whistlers*

J. KENNETH GRIERSON†

Summary—**This paper discusses the design of a new type of sound spectrograph, intended for analyzing whistlers. This instrument is of the single-channel scanning type, but its basic action is to scan the frequency-time plane in frequency at a fixed time rather than, as in existing instruments, in time at a fixed frequency. The principle is as follows. First, a very short section of the signal to be analyzed (roughly equal in duration to the reciprocal of the bandwidth of the analyzing filter) is stored in the instrument electronically. The stored signal is then read out repeatedly many times faster than its original speed, and this repeated waveform is analyzed by a variable-tuned filter which sweeps once very rapidly through the expanded frequency band which the signal now occupies. The varying output from the filter, representing the variations of the amplitude of the signal with frequency at one particular time, is recorded as one line of a scan across a continuous strip display. Finally, the stored sample of signal is erased, replaced with the next sample, and the whole process repeated. An audio frequency spectrograph of this type appears to combine speed of operation with fine resolution in frequency, rendering it useful for the rapid analysis of whistlers.**

Introduction

WHISTLERS are naturally occurring radio signals of audible frequency. They may be received on a vertical wire or loop antenna, amplified by a straightforward audio-frequency amplifier, and made audible by connecting the output of the amplifier to a set of headphones or a loudspeaker; they may also be recorded on tape for subsequent analysis. Whistlers consist of gliding tones; that is, tones whose frequencies change with time; some forms of whistlers are relatively pure tones, while others (swishes) sound more like bands of noise with progressively changing mean frequency. There is interest attached to the way in which the mean frequency of the tones depends on time, and it was the need to be able to graph this dependence rapidly and automatically that initiated the present study.

This paper describes the principles involved in the design of a new type of audio-frequency spectrograph, for making a visible record of the distribution of the energy of a signal, in time and frequency. Although the technique proposed might have other uses in the audio-frequency field, it will be considered here only in application to whistlers.

Previous Use of Spectrographs in Whistler Research

The spectrograph, in various forms, has been the main research tool in the investigation of whistlers.

* Original manuscript received by the IRE, February 13, 1957. Paper presented at Symposium on Propagation of Very-Low-Frequency Electromagnetic Waves, Boulder, Colo., January 23–25, 1957.

† Defence Research Board, Ottawa, Ont., Canada.

Burton and Boardman[1] used 17 narrow-band filters, covering the range 150 to 3800 cps, which could be switched into a graphical recording system. A spectrograph used by Storey,[2] based on a design by Dudley and Gruentz,[3] incorporated two features intended to make it useful for analyzing whistlers.

Firstly, the center frequencies of the filters and the layout of the display system were so arranged that, if the frequencies of the whistlers varied with time according to Eckersley's law,[4] the variation would be recorded as a straight line.

Secondly, some attempt was made to adjust the bandwidths of the filters for maximum response according to the rates at which the frequencies of the tones were expected to be varying. The display system for this instrument consisted of a row of midget neon lamps whose brightness was recorded on photographic film.[5]

Both of these spectrographs made use of a number of filters with their input circuits connected in parallel. Alternatively, a single tuneable filter can be used through which the recorded signal is played over repeatedly, while the center frequency of the filter is either set in turn to the different values required, or else scanned continuously through the spectrum.

A scanning spectrograph of this type was developed in the Bell Telephone Laboratories[6] and subsequently applied by Potter[7] to the analysis of whistlers. Gruentz[8] has described a similar spectrograph covering a wider frequency range, a commercial version of which is now available under the trade name of Sonagraph.[9] This instrument has been used for analyzing whistlers by Helliwell *et al.*[10]

The scanning type of spectrograph, with its finer resolution in frequency, brought out some interesting detail which had not been seen with the multichannel type. Analyses of whistlers, particularly those of the "swish" variety, often show them as consisting not so much of uniform bands of noise as of large numbers of relatively discrete gliding tones following each other in close succession. Moreover, the relationship between frequency and time for a single tone departs from Eckersley's law at the high-frequency end. These features are particularly marked in whistlers observed at high magnetic latitudes, where the individual tones are well spread out and the departures set in at frequencies of a few kilocycles.

The foregoing studies show the value of an efficient audio-frequency spectrograph in the investigation of whistlers and emphasize the fact that there is no short cut to their analysis. Nothing less than a complete spectrogram can reveal all the detail which they may contain.

Review of Existing Types of Audio-Frequency Spectrograph

The multichannel type of audio-frequency spectrograph consists of a number of filters whose input circuits are connected in parallel. The operating frequencies and the pass-bands of the filters are chosen so that the incoming signal is split up into several bands of frequencies, each band then being handled by an individual filter. Each filter output actuates its own display mechanism (pen, neon tube, or trace of a crt, etc.).

If B is the bandwidth of the incoming signal and b the bandwidth of each filter, then B/b is the number of filters required for full coverage of the spectrum. It is necessary to have a large number of filters to get a high degree of frequency resolution and, consequently, a good signal-to-noise ratio.

The response of a filter to a gliding tone is maximum[4] when

$$b \approx \sqrt{\left|\frac{df}{dt}\right|}$$

where b is the bandwidth of the filter and df/dt is the time rate of change of the frequency. If df/dt is not a constant, then some compromise bandwidth must be chosen.

An average rate of change of frequency for a whistler might be 2500 cps[2], in this case a bandwidth of 50 cps would be optimum and 290 filters would be required to cover the frequency range 500 to 15,000 cps. No available apparatus has this number of filters as the practical problems involved in keeping bandwidths, center frequencies, and gains constant make the use of such a system uneconomical.

A compromise can be effected by using a few "spot frequency" filters distributed throughout the audio-frequency band, this is the principle used by the authors quoted above. This leads to the whistler disappearing at many points on the record and hence spoils "visual integration."

An alternative compromise which can be made is to widen the filter bandwidths. This leads directly to a coarser frequency resolution and a deterioration in signal-to-noise ratio.

A large number of separate channels are therefore necessary, for the satisfactory operation of a multichannel type of spectrograph to get a high-frequency resolution and a good signal-to-noise ratio. Such a system is, unfortunately, too complex to be operated economically due to the variation of the parameters of the filters and to the muliple display system.

[1] E. T. Burton and E. M. Boardman, "Audio frequency atmospherics," Proc. IRE, vol. 21, pp. 1476–1496; October, 1933.
[2] L. R. O. Storey, "An investigation of whistling atmospherics," *Phil. Trans. Roy. Soc.* (*A*), vol. 246, p. 113; July 9, 1953.
[3] H. Dudley and O. O. Gruentz, "Visible speech translators with external phosphors," *J. Acoust. Soc. Amer.*, vol. 18, p. 62; July, 1946.
[4] T. L. Eckersley, "Musical atmospherics," *Nature, London*, p. 104; January 19, 1935.
[5] N. F. Barber and F. Ursell, "Response of a resonant system to a gliding tone," *Phil. Mag.*, vol. 39, p. 345; May, 1948.
[6] R. K. Potter, "Visible patterns of sound," *Science*, vol. 102, p. 463; November, 1945.
[7] R. K. Potter, "Analysis of audio frequency atmospherics," Proc. IRE, vol. 39, p. 1067; September, 1951.
[8] O. O. Greuntz, "8000 cycle sound spectrograph," *Bell Lab. Rec.*, vol. 29, p. 256; June, 1951.
[9] Kay Electric Co., Pine Brook, N. J.
[10] R. A. Helliwell, J. H. Crary, J. H. Pope, and P. L. Smith, "The nose whistler—a new high-latitude phenomenon," *J. Geophys. Res.*, vol. 61, p. 139; March, 1956.

In the scanning type of spectrograph, a single tuned filter is used. A section of the signal is recorded and then played back several times. The played back signal is fed to the filter, whose center frequency is swept slowly through the audio-frequency band, while its gain and bandwidth are kept constant. The detected output of the filter is then a frequency analysis of the input signal.

If the bandwidth of the signal is B and the bandwidth of the filter is b, then the signal has to be played back B/b times. The analysis of the signal then takes B/b times as long as the original recording of the signal. The play back can be speeded up however. If it is speeded up by a factor n, then the bandwidth of the recorded signal becomes nB and the bandwidth of the filter must be increased to nb, to obtain the same relative resolution. The effective time of analysis in this case will be B/nb times as long as the recording time; n can be called the speedup factor and B/nb the ratio of machine time to real time. The best specifications which have been realized in commercial practice are exemplified by the Sonagraph already mentioned. The frequency coverage of the Sonagraph is 85 to 8000 cps. The recorded section of the record, which is analyzed in one operation of the Sonagraph, is 2.4 seconds and the analysis is written over 12.5 inches of paper at the output end of the machine. The analysis time is approximately 5 minutes and the filter bandwidth can be set to 45 or 300 cps. The speedup factor is 3.33. B/b is approximately 154, when b is 45 cps.

The input signal is recorded magnetically around the periphery of a drum. The drum is then rotated quickly and the recorded signal is read out by a magnetic reading head. The signal read from the drum is passed to a filter which sweeps through the audio-frequency band. A second drum, which is mounted concentrically with the first drum, rotates at the same angular speed. The second drum is used for supporting a length of facsimile paper around its curved surface. A stylus sweeps slowly across the paper in a direction parallel to the axis of the drum, while the drum rotates. The position of the stylus along the axis of the drum is linearly related to the frequency of the exploring filter.

To produce a continuous record, a section of the already independently recorded signal has to be located, rerecorded on the instrument, analyzed, and edited. The full procedure takes about 20 minutes to analyze 2.4 seconds of record. The practical ratio of machine time to real time is thus of the order of 600. Also, the machine has to be attended during the whole operation, except for the 5 minutes or so that actual analysis is taking place.

From the foregoing, it can be seen readily that no really satisfactory machine exists for the rapid analysis of routine records such as will be obtained during the International Geophysical Year, yet such records will be useless if not analyzed.

Proposal for a Rapid Scanning Audio-Frequency Spectrograph

The requirement is for a frequency analyzer which will produce a long continuous record while unattended. The frequency and time resolutions must be good and the expense must not be excessive. The requirements are best set out in the form of a tentative specification. This specification and how it might be realized form the basis of the rest of the paper.

Tentative Specification

1) The instrument must produce a frequency (ordinate) and time (abscissa) graph on paper, with Z modulation indicating power density. This graph is to be produced continuously, without editing.
2) Operation is to be unattended, except for initial setup and close-down procedures.
3) Capacity: One-hour signal time.
4) Time resolution: 20 ms (fixed).
5) Frequency resolution: 50 cps (minimum).
6) Frequency range: 500 to 15,000 cps (fixed).
7) Ratio of machine time to real time: 3.
8) Speedup factor: 100.

It has been shown that no available instrument is capable of satisfying this tentative specification. The practical problem is the quantization of the frequency time plane. Two methods of doing this, which have been discussed already, are as follows:

1) Frequency quantization by means of filters—the total frequency range is split into several bands of frequencies, both the input and the output of each filter are continuous functions of time and no storage system is necessary. This is a parallel system, since the filter inputs are in parallel.

2) Time swept quantization—a fairly long signal (2–3 seconds) is stored and rapidly read out many times. Each (identical) signal read out of the store is fed to a single filter which changes frequency slowly. This is a series system, since the successive samples are fed through the filter serially in time. The frequency-time plane is swept rapidly in the time direction and slowly in the frequency direction.

A further system of quantization also exists which may be outlined as method 3).

3) Frequency swept quantization—a short section of the input signal (20 ms) is recorded and read out rapidly many times. Each readout sample is fed to a single filter which changes frequency very rapidly. This also is a series system, but here the frequency-time plane is swept rapidly in the frequency direction and slowly in the time direction.

A comparison of the various methods follows in Fig. 1. It can be seen readily that the following factors favor the use of system 3); no editing is necessary, a continuous record is produced, and very little storage is re-

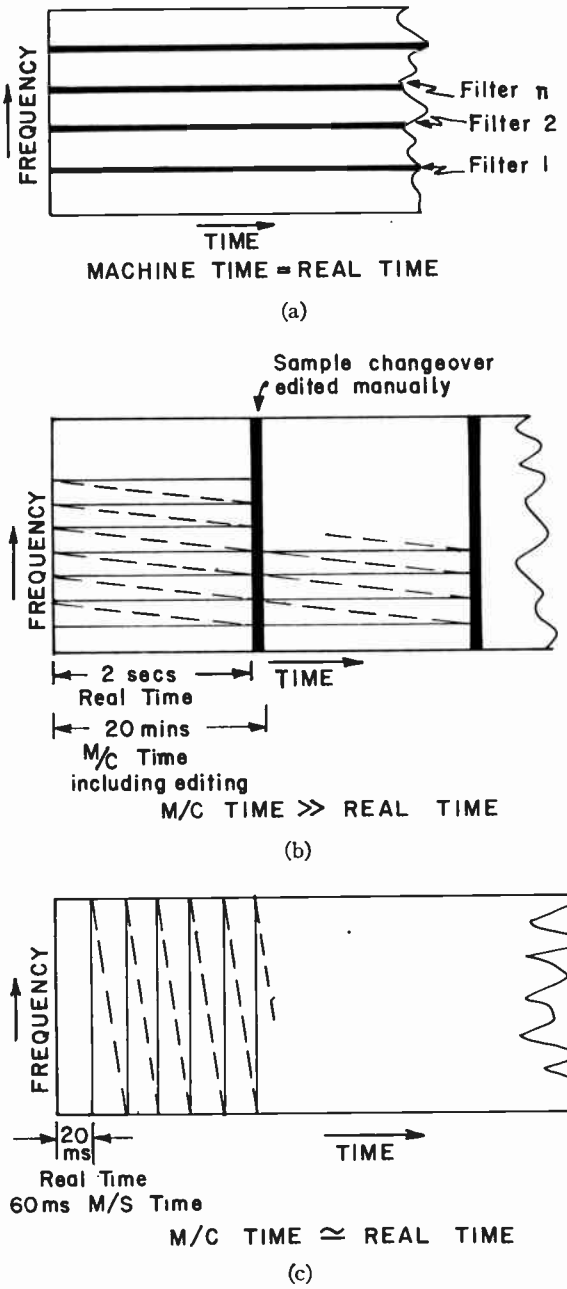

Fig. 1—(a) Parallel filter quantization—requires many filters, (b) time swept quantization—requires editing, and (c) frequency swept quantization.

quired. The disadvantage in system 3) is that an extremely high-speed readout mechanism is required, since, in order to satisfy the tentative specifications, 300 samples are to be analyzed in 60 ms.

Considering the factors above, only system 3) seems capable of producing the required results.

In a complete machine there are three main subassemblies to be considered. These subassemblies are the slow storage and fast repeated readout system, the filtering and analyzing system, and the display or written record. These subassemblies will now be considered here in detail.

Slow Storage and Fast Readout Mechanism

There are at least four basic methods which can be used for storing electrical signals, when a fast readout is required. These four methods are electrostatic, electromagnetic, magnetic, and ultrasonic storage. Electrostatic storage is the principle on which memory storage tubes, capacitor storage, and certain types of electronic storage devices work. Memory tubes are not very suitable for the above application, as information cannot be written into them and read out simultaneously. Buckbee and Luftman[11] have, however, described how two or more such tubes can be arranged to operate in sequence for purposes of bandwidth compression or expansion. The other types of capacitor device are used exclusively for the storing of digital information.

Electromagnetic storage or electroacoustic storage involves the use of delay lines which are either lumped impedances or quartz lines. The storing of information with these devices involves sampling, circulation of the sampled pulses, and the consequent need to amplify and reshape pulses frequently. They are very suitable for storing digital information in binary form, but not very suitable for the present application.

Magnetic storage devices include ferrite matrices, tape and wire recorders, and magnetic drums. Of these systems, magnetic tape recorders are ideal for the storing of analog information and, in fact, the original information in the present application is stored on magnetic tape. One method, for reading a short sample of tape record, repeatedly involves the use of a "tape scanner," which consists of a rapidly rotating drum with a number of playback heads mounted around its periphery.[12]

The present application demands that a signal of bandwidth 500 to 15,000 cps and of duration 20 ms be recorded and read out 300 times in 60 ms. The recording of the signal requires a tape speed of 15 inches per second and the playback, therefore, requires a tape speed of 1500 inches per second. The practical difficulties of handling a continuous tape at this speed are enormous; this suggests that a scanning drum approach would be a more likely way to solve the problem. An idea of the speeds involved in a scanning system can be exemplified by the following hypothetical example.

A set of recording heads consisting of 100 heads arranged in a parallel line records the input signal continuously on a 10-inch-diameter drum which is coated with a magnetic recording material. This drum rotates with such a speed that the speed of the material past the recording head is 5 inches per second. This will slow down the orignal recording speed by a factor of three. The signal is now read off this drum by a second drum, which has 100 heads mounted around its periphery.

[11] J. A. Buckbee and A. S. Luftman, "Designing storage tube equipment," *Electronics*, vol. 29, p. 126; July, 1956.
[12] M. Camrass, "Some recent developments in magnetic recording," *Acustica*, vol. 4, p. 26; January, 1954.

These heads are the readoff heads and they pass the surface of the first drum in sequence as the second drum rotates. The relative speed of the playback heads to the surface of the medium in which the signal is recorded is 1500 inches per second. If the speed of the drum is 3000 rpm, then the drum must be 10 inches in diameter (approximately). These figures suggest that the problem is at least within the realms of possibility. A diagram of the two drums appears as Fig. 2.

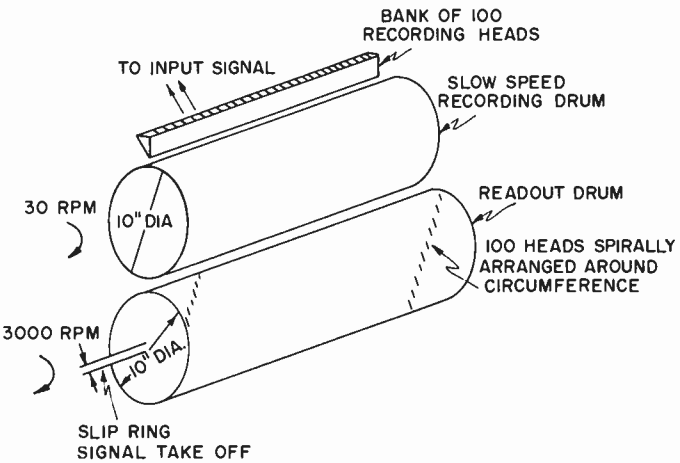

Fig. 2.

It is not suggested that the drum system is practical, but a review of its purpose is in order. Recapitulating, a signal of bandwidth 500 to 15,000 cps is recorded on magnetic tape for a period of one hour. The tape speed of this recording is 15 inches per second. The tape is now slowed down to 5 inches per second, and the signal is recorded again onto the surface of the drum continuously at the rate of 5 inches per second by a bank of 100 recording heads which are aligned in parallel. The signal is read off the drum by a set of heads which scan the drum at the rate of 1500 inches per second. 100 heads carry out this operation, each head being in contact with the recorded signal for a period of 20 ms. Therefore, in 60 ms, 20 ms of the original signal will have been scanned 300 times by the rotating head assembly. The output of the rotating head assembly, therefore, consists of 300 almost identical samples of the original signal with the time scale speeded up by a factor of 100. These samples are now fed to the filter and analyzing system. This system would be difficult to design as outlined, but it points to the practical difficulties involved.

The Filtering and Frequency Analyzing System

The input to this system consists of 300 samples which are almost identical and which occupy 60 ms of time. The bandwidth of these samples is 50 kc to 1.5 mc (the original bandwidth multiplied by the speedup factor of 100). If a filter could be designed which had a constant bandwidth of 5 kc and whose operating frequency could be swept through the band 50 kc to 1.5 mc, then the output of this filter would be the required frequency analysis. The Q of such a filter would have to change from 10 to 300 during the sweep. This is not practical.

If the samples were changed in frequency by adding 20 mc so that the input signal now became 20.05 to 21.5 mc, the Q of the filter would remain sensibly constant (varying from 4010 to 4300). The frequency conversion could be accomplished by SSB modulation.

A simpler method is to keep the filter bandwidth and operating frequency constant and then move the incoming signal relative to the filter by adding a sawtooth frequency modulated frequency to the signal. In this case, a filter at 21.5 mc with a bandwidth of 5 kc would be used. The input samples would be transcribed initially from the frequency range 50 kc to 1.5 mc up to the range 20.5 mc to 21.5 mc. This range would be swept slowly through the filter bandwidth by adding a further frequency which varied linearly from 0 to 1.45 mc every 60 ms. Thus, the effective output of the filter (after detection) would be a frequency analysis of the original signal, since the input to the analyzer is merely a linear function of the frequency distribution of the original signal.

A method of shaping the pulses,[13] known as the "gate filter technique," allows a smooth variation of the input pulse amplitude by modulating the pulses. This is used to lessen the frequency spread due to sampling. The modulated sample is fed to a very high Q tuned circuit. The amplitude of the output of the tuned circuit is measured immediately after the pulse is completed. The tuned circuit is then damped to eliminate the oscillations or ringing in the tuned circuit. The damping is then released to allow the filter to receive the next pulse.

The Display Problem

For most routine work, a qualitative display system is adequate. That is to say, that as long as frequency and time are located accurately, the energy magnitude need not be very accurate. An off-medium-high indication serves to show where the energy lies. This is due to the fact that most whistlers consist of a discrete tone, or a succession of discrete tones occurring simultaneously or sequentially. In the case of single discrete tones a crt display is adequate. If a written record is desired, facsimile equipment is available commercially which is just fast enough to write the record, though such equipment will be working somewhere near its limit.

For quantitative display, a raster can be drawn on a screen as in tv or a spot can be made to move in accordance with the magnitude of the applied voltage, and this spot can be photographed by a film moving at right

[13] J. W. F. Canning, "An Electronic Method of Frequency Analysis of a Single Pulse or of a Sample of a Continuous Waveform," R.R.E. Tech. Note. No. 212.

angles to the direction of travel of the spot. Thus, the deflection of the spot in the frequency direction will be coordinated with a displacement at right angles giving a magnitude of the energy.

Conclusion

The need exists for a high-speed frequency analyzer operating in the audio-frequency band. No suitable instrument is presently available. The paper shows that, by using a high-speed magnetic scanner, coupled to fairly standard electronic analyzing equipment, such a machine might be practical. It would be possible to produce a written record fairly easily and even a quantitative display would not be a very difficult technical problem, provided the scanner could be constructed to work efficiently. Finally, it can be stated that such an instrument would have a wide variety of applications in other fields.

Acknowledgment

The author is very much indebted to L. R. O. Storey for the statement of the problem and for continued help in the development of the ideas. The Defence Research Board (Radio Physics Laboratory) are to be thanked for permission to publish this work which forms a part or the R.P.L. Project No. 5523. Acknowledgment is made also to McGill University as the subject matter of this paper is a part of the requirements of the Graduate Faculty for the Degree of M.Sc.

Designing for Reliability*

NORMAN H. TAYLOR†, SENIOR MEMBER, IRE

Summary—**The achievement of reliability is a goal that must be pursued from the very beginning of the system design project. The first step is to consider each individual component to be used in the system and to critically analyze its capabilities and limitations. The second step in the design project is to determine the applications of these components that tend to take advantage of the best capabilities of these components and avoid their worst limitations. This report lists brief analyses of components and the resulting component applications that have been made by the staff of Lincoln Laboratory over a period of several years.**

The third and final phase of the design project is the actual electronic circuit design, based on the component analyses and applications notes derived earlier and predicated on the achievement of high reliability. The thorough design method developed by Lincoln Laboratory is described in detail. This method provides reasonable component tolerances and adequate safety margins, and incorporates marginal checking throughout the design process. A detailed example of a high-speed, vacuum-tube flip-flop is used for illustration.

Foreword

THIS PAPER highlights the work on reliability as specifically applied to digital computer technology at the M.I.T. Digital Computer Laboratory and Division 6 of Lincoln Laboratory from 1948 to 1956. The design philosophy described here has evolved through the electronic design of successively the Whirlwind I, Memory Test, AN/FSQ-7, and TX-0 computers. Subsequent operating experience with these computers has proven the philosophy and has demonstrated that the additional engineering effort required to truly "design for reliability" is well spent.

Since 1952 the International Business Machines Corporation has been associated with Lincoln Laboratory in the development of the AN/FSQ-7 computer, the heart of the SAGE System for air defense. Thus, this paper reflects the work of so many people that it represents, in fact, a joint effort of all those concerned at M.I.T. and Lincoln for the past eight years and a good many of IBM for the past four. Specific contributors are listed in the Acknowledgment.

Introduction

In approaching the problem of reliability in control systems, the concept changes considerably from the commonly accepted rules of the radio, television, and home appliance field. In the area of automatic control, the system under control is often a very costly one. It places a premium on its controlling parts; and, in military operations, human life itself is sometimes dependent on the reliability of the controlling electronics.

With such a target of reliability, the electronic designer is forced to make every design decision with reliability as his prime objective. He no longer designs a system and then, as an afterthought, "makes it reliable." He must "design for reliability" from the start, even changing the systems concept, if necessary, to insure the desired result.

* Original manuscript received by the IRE, June 22, 1956; revised manuscript received January 14, 1957. The research in this paper was supported jointly by the Army, Navy and Air Force under contract with the Mass. Inst. Tech., Cambridge, Mass.

† Lincoln Lab., M.I.T., Lexington, Mass.

Reliability is an evasive goal. It depends on three major factors each of which is dependent on the others—components, component application, and design.

Components

The choice of components certainly has a first-order effect on system reliability. Two factors in component manufacture must be considered:

Component Stability: Components drift in value with time, temperature, humidity, and altitude. Stability factors must be known and considered before design work is undertaken.

Component Reproducibility: This is a matter of production tolerances. The 1 per cent resistor is now common, but the tube with 1 per cent tolerance in plate current has never been built. Tolerances must be known to the circuit designer and taken into account before design work is started.

Component Application

The way in which a component is used—taking into consideration the problems of stability and reproducibility—is the second major factor contributing to reliability. In this area it is difficult to resort to the explicit scientific approach; the matter is one of judgment and experience and is therefore subject to controversy. The successful system is one where components are used in applications that suit their characteristics. Ideally, the natural properties of the component are exploited and its inherent weaknesses are avoided or bypassed by careful design.

Design Considerations

The design of a specific circuit can be faced after the component problems and the application or use of the components have been considered. Of the three factors in reliability, the design phase is the more difficult, because it must encompass the decisions and account for the boundary conditions imposed by the other two factors.

Components and Circuit Design

Component Applications

A good method of appraising a particular application of a component is an evaluation based on the four types of failures that are most troublesome. These are: deterioration, sudden failures, intermittents, and maladjustments.

1) *Deterioration:* Deterioration is a disease that the designer must face. Man seldom makes anything that does not deteriorate; almost everything we manufacture wears out. One must ask: "How fast is this component going to wear out in this application?" This question, while not always easy to answer, must be faced squarely.
2) *Sudden Failures:* Sudden failure needs no description. A vacuum tube losing its vacuum, a resistor opening up, a fuse blowing—these are complete, sudden failures. Now susceptible is a component to this type of failure? Now often will it happen? What are the consequences?
3) *Intermittent Failures:* These are the hard ones. It has been said, "If you really know how to get rid of the intermittents, all the other failures in the system are easy to find and easy to fix." Much of today's electronic design provides means for coping with almost all types of failures except intermittents. Against these latter, safeguards must be provided. Eventually, intermittents must be designed out of the components wherever possible.
4) *Maladjustments:* These failures are related to proper maintenance. The best possible solution is to create a design that does not require adjustments. This, of course, is not always possible, but attention must be given to which adjustments should be allowed and which procedures should be followed. If maladjustment of a system is possible, it is usually a factor contributing to poor reliability.

A good example of a component application that stands up well under the conditions described above is the memory core in a magnetic memory plane.

1) The component deteriorates slowly; in fact, present data indicate practically no change in characteristics with time.
2) Sudden failures are rare, limited to broken cores and usually occurring only in assembly.
3) Intermittents are rare; adequate insulation on the wires through the cores is all that is required.
4) No adjustments are necessary.

In addition, cores are stable with respect to temperature and humidity, and are reproducible to close tolerances.

It is obvious that the core memory itself is not useful without driving and sensing circuits. However these auxiliary circuits cannot be made as reliable as the cores themselves. (As it happens, magnetic-core storage units have run for weeks and even months with complete freedom from error. They are presently the most reliable part of high-speed computers.)

Although, as shown by this example, a core approaches the ideal as a component, 1956 techniques do not allow systems—particularly those with requirements of high-speed arithmetic units, cathode-ray-tube displays, and associated controls—to be built entirely from magnetic cores. Accordingly, the designer is faced with the choice and use of many other components that are more subject to deterioration, intermittents, sudden failures, maladjustments, instability, and limitations in

reproducibility. The following list[1] suggests an order of vulnerability, with the most vulnerable components at the head of the list: 1) vacuum tubes, 2) diodes, 3) connectors, 4) relays, 5) resistors, 6) condensers, 7) transformers, 8) inductors, and 9) cores.

A reliability program must reach back to the actual design and fabrication of the components listed above. An examination of life-test results and equipment-failure reports will yield data on the particular faults to be expected.

The individual characteristics of tubes and other components as these affect reliability are discussed in detail in the Appendix.

Circuit Design

Safety Margins: The electronic designer has been several decades behind designers in other engineering activities in providing safety margins adequate to allow for the various disturbances that may occur in a circuit during its lifetime. Designers of bridges and power stations habitually allow safety factors of 400 to 600 per cent; the systems they are designing must withstand excessive strain, and failure may result in loss of human life or expenditure of large sums. However, the electronic designer has not, until recently, been confronted with the possibility of such catastrophic consequences if his circuit should fail under stress. The increasing use of electronic controls in larger and more critical areas forces the circuit engineer to pay greater attention to incorporating safety margins in his designs.

When the circuit engineer is confronted with a design problem, he is usually asked to make a circuit perform some specific function as a portion of a system. In the computer field, such a requirement may be for a high-speed switch; the designer may be given, as performance specifications, the limits on the speed of switching, the voltage swing that such a switch should deliver, the resolution time, and perhaps some power limitation. Whether or not reliability and long life are included in these specifications, the circuit engineer must design with these goals in mind. He cannot foist unrealistic demands for tolerances and stability on the component engineer—specifying 1 per cent resistors and tubes with close tolerances on plate current and transconductance—and then glibly say, "My circuit will be as reliable as the components." It is the *circuit designer* who must know about component stability and tolerances, and who must build his design around such knowledge.

Thus the problem that really confronts the circuit designer becomes one of designing highly reliable and stable circuitry made up of components that are neither reproducible nor stable, but subject to deterioration, intermittents, maladjustment, and sudden failure.

[1] Transistors have not been included since there is not the backlog of use of the other elements in this list. On the basis of present units, they probably rank either above or below diodes.

Design Criteria: With recognition of the importance of including adequate safety margins in his design, the circuit engineer must answer certain questions regarding the component tolerances of his circuit. How much tolerance should be expected? How does the designer make provision for deviation in the components? Three criteria listed below are suggested as effective guides for the circuit designer.

1) *The circuit must meet its performance specifications with all components[2] at their worst initial tolerances, and with any component at its worst end-of-life tolerance.*

By "worst" is meant deviation of the components in whatever direction is least favorable for the circuit. Usually, several worst combinations of components must be evaluated.

The initial tolerance of a component is that to be expected when it is new; the end-of-life tolerance is wider. For example, the initial tolerance on a composition resistor might be ± 5 per cent, and end-of-life ± 15 per cent. The numbers to use for these tolerances must be the result of a component study. (See Appendix.)

In some simple circuits, it might be possible to have all components deteriorate to end-of-life at once, and still have satisfactory performance; this capability is desirable only if it requires no increase in circuit complexity. To make all circuits continue to meet their specifications when all components are at end-of-life would, in general, require the addition of more components and an increase in circuit complexity. More components result in a greater probability of intermittents; the increased complexity results in more difficult servicing. Statistically, one of a group of components will reach end-of-life while most of the others are still good; therefore, criterion 1) is suggested as being a good engineering compromise in the search for circuit longevity.

When a circuit geometry has been found that shows promise of meeting 1) above, criteria 2) and 3) must be considered and met.

2) *The circuit must be able to withstand the loss of any one of the supply voltages in itself or in any circuit connected to its input or output without component damage.*

When diode logic is used, criterion 2) will usually necessitate use of protection diodes to prevent excessive back voltages.

3) *Since all components (especially vacuum tubes) degenerate with life, circuit design should include means for detecting significant changes in component values during use of the circuit, and soon enough to insure replacement of the component before failure occurs.*

[2] "Components," as used above, include power-supply voltages, diode characteristics, tube characteristics, resistors, etc.—anything that can change to the detriment of circuit performance.

Provision of means for detecting deterioration allows near-failures of components to be discovered and eliminated during routine, scheduled maintenance periods. Costly, unscheduled down time can be minimized. Slow deterioration of tubes and other components may be observed over a period of time, and replacement can be predicted and even scheduled.

Criteria 2) and 3) make it necessary to have two different specifications of the components, one for normal use and the other for low-duty-cycle marginal checking or emergency conditions. For example, if a resistor has a normal allowed dissipation of one-half the manufacturer's rating, its marginal checking or emergency dissipation might be equal to the manufacturer's rating.

This section has touched briefly on the underlying principles of a basic design philosophy to achieve electronic reliability. The following section will describe the application of this philosophy in a method for checking circuits. Special emphasis will be given the application of this method in the design phase to ascertain if the design will meet performance specifications.

Marginal Checking

Introduction

To determine whether or not a circuit design meets the given performance specifications with the desired reliability, there is need for a method of evaluation that will:

1) Make graphically clear, in an explicit quantitative way, what tolerance a given circuit has to variations in its components.
2) Provide a method, usable in the later systems phase, of preventive maintenance that will adequately cope with the problems of component deterioration.

Such a method, called "marginal checking," was developed to a high degree of sophistication by Lincoln Laboratory; it has been extensively used in the design phases of large real-time control systems, as well as in day-by-day operation of such systems.

This section discusses the use of marginal checking in the design phase. The allowable variation of a component is determined as a function of a selected circuit parameter, usually a supply voltage. This measures the margins of circuit performance in terms of the marginal-checking parameter.

In practice, the tolerance of one of the components in the circuit is plotted against the variation in this marginal-checking parameter, as illustrated in Fig. 1. The intersection of mean-value and normal marginal-checking parameter lines near the center of the parabola indicates the operating point of the circuit—normal voltage on the circuit and normal value of the components. Using a supply voltage as the marginal-checking parameter and lowering it, a point is plotted on the contour line where the circuit fails to perform (Point 1).

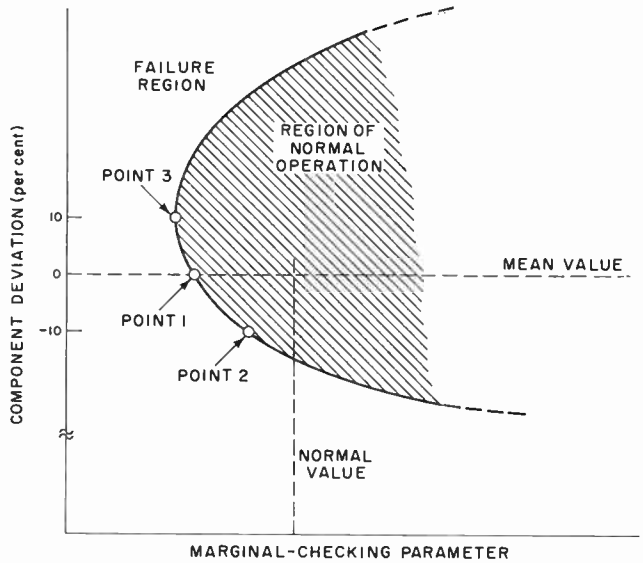

Fig. 1—Locus of failure points in a typical circuit.

This failure can be defined as the point at which the function of the circuit deviates from that prescribed in the specification. In an oscillator, for instance, the point at which the frequency shifts out of tolerance can be considered failure; in a flip-flop, the point at which some standard pulse fails to switch the position may be failure. Changing the tolerance on the component by some factor such as 10 per cent in a negative direction and again varying the marginal-checking voltage will result in a different failure point, such as Point 2 on the curve. Raising the tolerance of the component 10 per cent, another failure point, Point 3, can be plotted. Continuing this study, a contour line representing the locus of the failure point of the circuit to tolerance in componentry, as a function of some marginal-checking parameter, can be drawn enclosing an area of reliable operation. This sort of study often results in finding that the contour is not symmetrical about the operating point, and that wide safety margins occur on one side but very narrow margins occur on the other. It is interesting to note that such contours change radically with the type of circuit. In most cases, the contour would be a closed loop if the marginal-checking parameters could be varied far enough without damaging the components.

It is evident that plotting the curves and varying each of the components in even a moderately complex circuit represents a rather long and tedious study. However, remembering that the circuits under discussion may have critical applications, the designer must know how much margin a circuit has before it will fail. The acceptability of the circuit to the system can be based only on such knowledge.

Marginal Checking—Components

The application of marginal-checking procedures to components involves a variety of techniques which can be tailored for the particular problem at hand. Engineering judgment must be used to determine which

data shall be taken, and enough data must be gathered so that the effect of change in each component may be deduced.

All the component variations (or branch supply voltages where applicable) must be plotted against the marginal-checking voltage to determine that the required component tolerance is not prohibitive, and that the normal operating point is centered in the area of operation. If a component tolerance turns out to be +1 per cent and −30 per cent, clearly the design is not centered, and a different nominal value for the component is indicated. Common sense indicates that all margins will not be symmetrical. The plate-supply voltage of a cathode follower can be lowered only until grid current loads the input circuit too much, but it may be possible to raise it until arc-over occurs. The positive excursion naturally stops where the marginal-checking or emergency component ratings are exceeded.

Resistors: The effect of change of characteristics in resistors (and in tubes) may often be determined by varying the supply voltage for individual branches of the circuit, and plotting this branch supply voltage against the marginal-checking voltage to determine the area of satisfactory operation. In the case of resistive voltage dividers, a variation of the supply voltage for the divider may be converted to an equivalent change in the divider resistors.

Consider the direct-coupled amplifier in Fig. 2. The output voltage is a function of the input, $B+$, $C-$, R1, R2, and R3, so that a change of any one of these parameters will affect the output level. If the permissible excursion of $C-$ is determined experimentally (other parameters held fixed), the resulting change in the output level may be calculated. From this change in output, it is possible to calculate the equivalent change in any of the other parameters that would cause this same limiting change in output level. Using this principle, one set of data can be used to determine the required tolerance of many components.

Tubes

The Pentode: The effect of a pentode's losing emission can be simulated by reducing the screen voltage—a drop in screen voltage being equivalent to a drop in available zero-bias plate current. A rise in screen voltage will increase the cutoff voltage required, and is useful for checking the adequacy of the bias provided.

The Triode: Aging in triodes is more difficult to simulate. One method is to reduce the plate-supply voltage which, in effect, asks the tube to pass the same current at less plate voltage. Consider a simple plate-loaded triode amplifier (Fig. 3) in which the input will either be at zero bias or cutoff and the output voltage swing will be dependent on the current the tube draws at zero bias.

The load line and zero bias lines for a new and an end-of-life tube are shown in Fig. 4. The new tube would operate at Point A and the end-of-life tube at Point B.

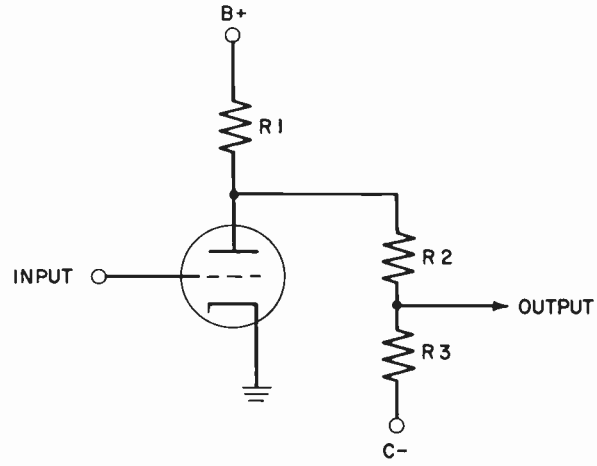

Fig. 2—Direct-coupled amplifier.

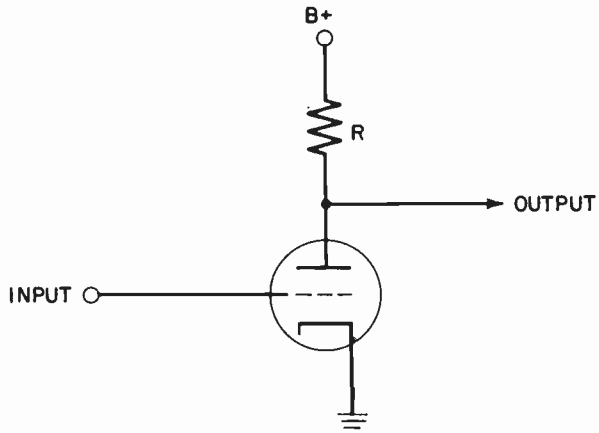

Fig. 3—Plate-loaded amplifier.

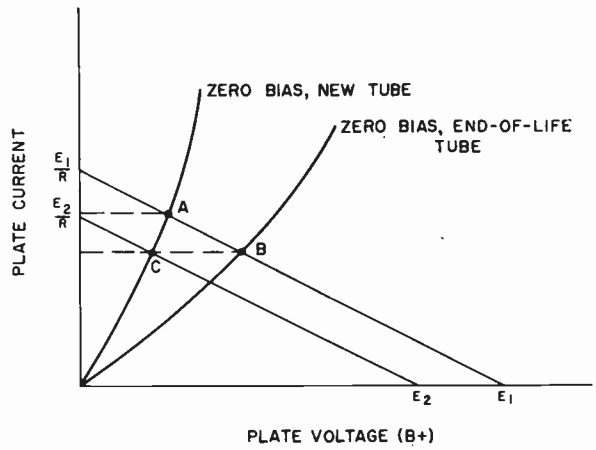

Fig. 4—Load-line chart of circuit of Fig. 3.

The output voltage swing for an end-of-life tube with $B+$ at E_1 (Point B) is the same as that for a new tube with $B+$ at E_2 (Point C), since the same plate current is switched into the load resistor for each case. In this way a circuit may be analyzed for tolerance to an end-of-life tube.

A second method of simulating aging in triodes is to substitute a different tube type whose normal charac-

teristics are close to those that would be expected from an end-of-life tube of the type to be used in the circuits. For example, a 6072 or 12AY7 has approximately the same μ as a 5965, but about one-third the zero-bias current. If a 6072 works in circuits designed for 5965's, one knows then that the circuit will tolerate an end-of-life 5965 tube.

The Semiconductor Diode: In general, diodes may deteriorate in the direction of lower back resistance or higher forward resistance. A diode with low-back resistance may be simulated by a shunt resistor across a good diode. High-forward resistance may be simulated by series resistors.

L and C Components: The variations in inductors and capacitors generally must be determined by replacing them with different values or with series-parallel combinations. Every variation that might affect the circuit should be tried.

Marginal Checking—Circuits

To illustrate the application of marginal checking to circuit design, it has seemed worthwhile to describe the techniques in terms of an example—a high-speed flip-flop designed for use in a large, high-speed digital computer.

The complete treatment of this circuit includes performance and component specifications, and an evaluation of the performance, including plots of pertinent margins of operation.

High-Speed Flip-Flop: The circuit for the high-speed flip-flop is shown in Fig. 5. Its specifications follow.

The *performance specifications* are:

1) Input: 0.08 to 0.12-μsec half-sine wave positive pulses, 20 to 40 volts amplitude, 0 to 2 mc prf, set, clear, or complement.
2) Output: Upper level, +10 to +12.5 volts; lower, level, −27 to −30.5 volts. Total transition time, less than 0.5 μsec (measured from the beginning of the pulse until the new level is reached), and a delay suitable for counting. (The same pulse is used to complement the flip-flop and to sense a gate tube connected to its output.)
3) Load that can be driven: 90 $\mu\mu$f maximum per output, with a total load of no more than 100 $\mu\mu$f.
4) Marginal checking: It must be possible to marginal-check the circuit from a remote point so that drift in the components can be detected before they cause failure of the circuit during system use.

The *component specifications* are[3]

1) Resistors: *Composition resistors* used were nominal 1 watt, derated to 0.5 watt, an initial tolerance of ±5 per cent, and an end-of-life tolerance of ±15 per cent.

[3] Components are discussed in detail in the Appendix.

Precision film resistors were 1 watt, derated to 0.5 watt, ±1 per cent initial tolerance and ±5 per cent end-of-life tolerance.

2) Capacitors: Capacitors were ceramic-dielectric, ±5 per cent initial tolerance, ±15 per cent end-of-life tolerance, and 50 per cent of manufacturer's rated value of 500 volts.
3) Pulse transformer: A small hermetically sealed canned transformer, designed to pass the standard 0.1 μsec pulses, was used.
4) Germanium diodes: A special group of diodes was specified for the system for which this flip-flop is one circuit. The diode used in this circuit is the Type W, for clamping and pulse mixing. This type is tested for pulse transmission and reverse recovery, as well as static forward and back resistance and reverse voltage breakdown. Back resistance is at least 500 K between −10 and −50 volts. Design value for back resistance is 100 K, and 50 K for the first 0.5 μsec after applying back voltage.
5) Tubes: This circuit was designed to use a low-performance twin triode that is acceptable in the terms of reliability described in the Appendix. (Twin triodes are preferable to single triodes since fewer sockets are needed.)
6) Power supplies: Centralized power supplies are used; for this system, the voltages available were +250, +150, +190, +10, −15, −30, −150, and −300. All supplies had an initial specification of ±1 per cent regulation with ±1 per cent additional allowed for voltage drops. The end-of-life figure was ±5 per cent.

Circuit Description: The circuit of the high-speed flip-flop (Fig. 5) uses cathode followers to isolate the plates from both the external load and the capacitance of the opposite grid. The plate circuits are clamped through diodes to both +10 and −30, stabilizing both the output swing and the signal transmitted to the opposite grid. This feature makes the circuit less sensitive to variations in plate currents of the triodes. The bias return of one grid divider is the marginal-checking point; this is moved above and below its nominal voltage of −150 to determine the circuit's margins.

Performance Data: Figs. 6 and 7 define the performance of the flip-flop for system timing analysis. Fig. 6 shows output and input waveforms; the time taken for the output to reach −15 is of interest since that is the level required to cut off a gate tube. Fig. 7 shows the maximum amount of capacitance and/or AND current[4] that the flip-flop can handle and still fall to the indicated voltage level within 0.5 μsec. Rise time is inherently faster than fall time.

[4] AND current is current drawn by a load connected to a positive voltage, measured when the flip-flop output is at its lower level.

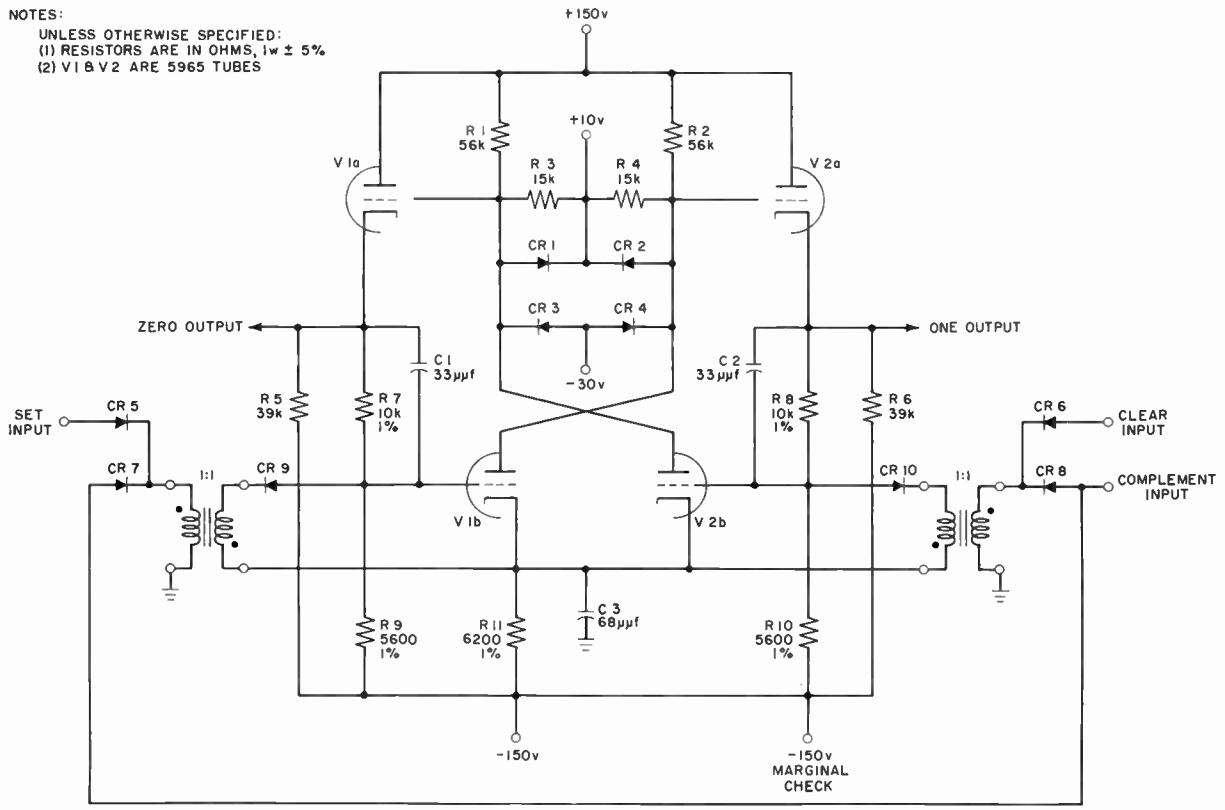

Fig. 5—High-speed flip-flop.

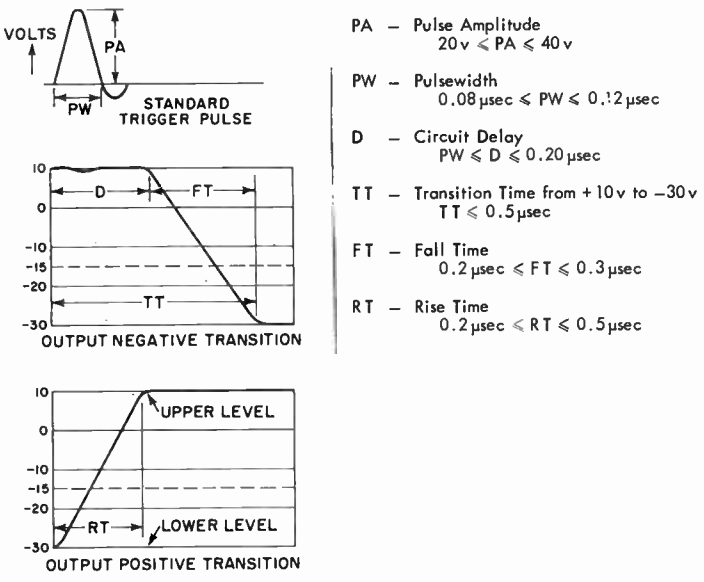

Fig. 6—Input and output waveforms.

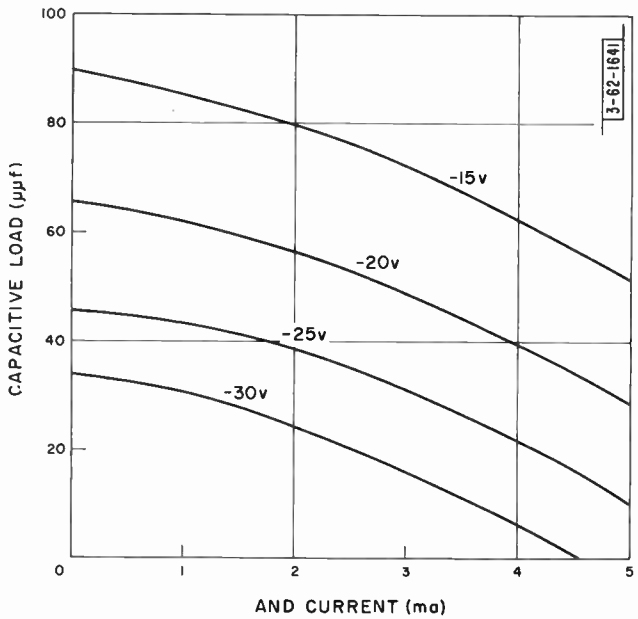

Fig. 7—Maximum load for less than 0.5 μsec fall time.

Fig. 8, next page, shows minimum complement trigger amplitude plotted against prf for various pulsewidths; Fig. 9 shows how minimum complement trigger amplitude varies with prf for different capacitive loads.

Reliability Data: Figs. 10 through 16 show reliability data, obtained by marginal checking, that indicate the component tolerances and safety margins of the circuit.

Fig. 10 shows how critical voltages in the circuit vary as the tube ages. These data were taken by reducing the filament voltage to simulate the weak tube, a very touchy method. The tube was connected to a 3-pole, 2-position switch, switched to a test position until the plate current stabilized, and then switched into the flip-flop circuit; the dc voltages were then measured.

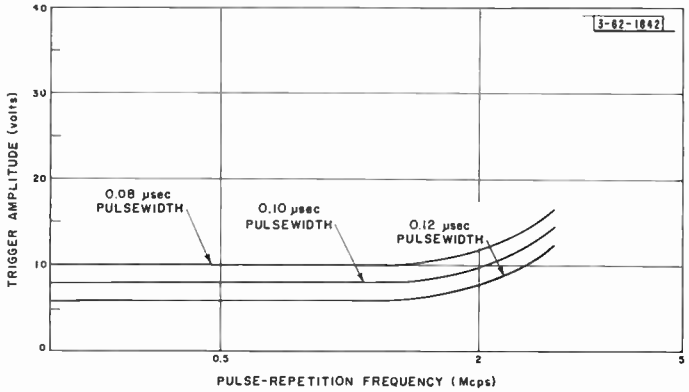

Fig. 8—Pulse-repetition-frequency response characteristics vs pulsewidth.

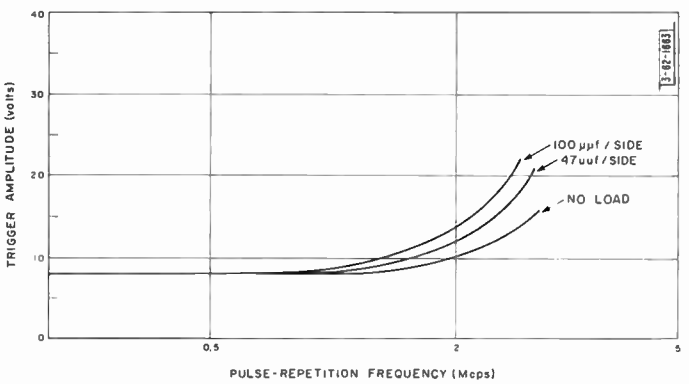

Fig. 9—Pulse-repetition-frequency response characteristics vs load.

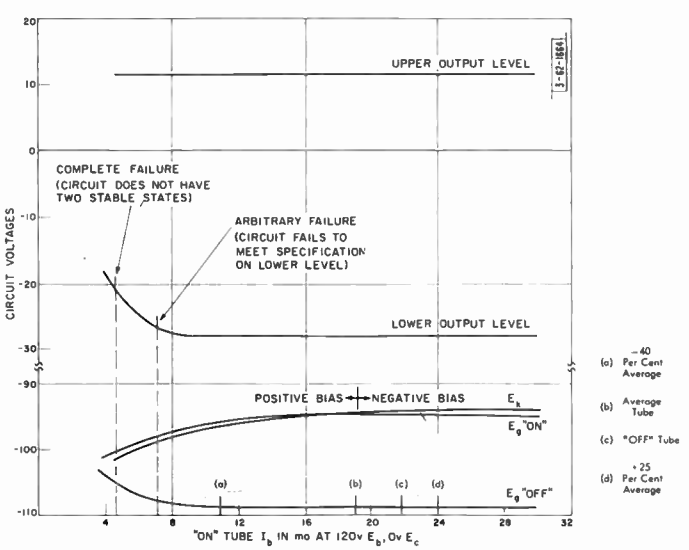

Fig. 10—Circuit voltages vs tube characteristics.

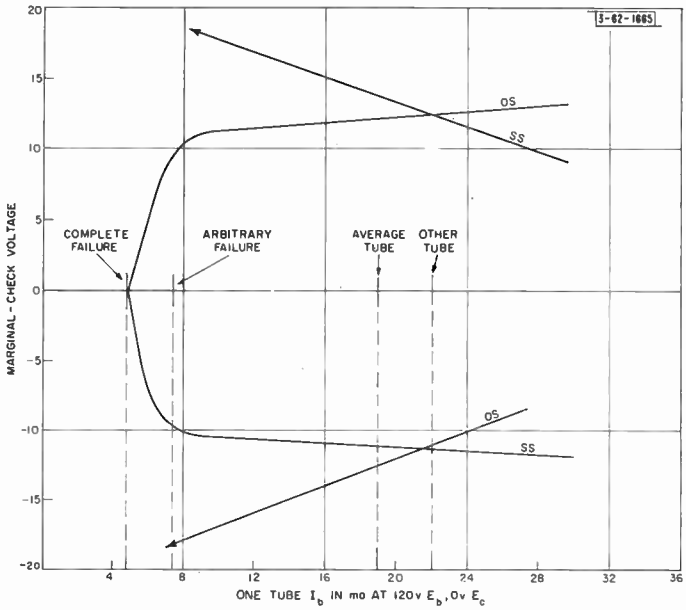

Fig. 11—Marginal-check voltages vs tube characteristics.

Notes:

1) Circuits are marginal-checked by varying one of the supply voltages to the circuit. In all these curves the marginal-check scale indicates deviation from the normal value of the marginal-check supply voltage.
2) SS denotes deviation of the marginal-check voltage on the same side of the circuit as the component being checked; OS denotes deviation of the marginal-check voltage on the other side of the circuit.

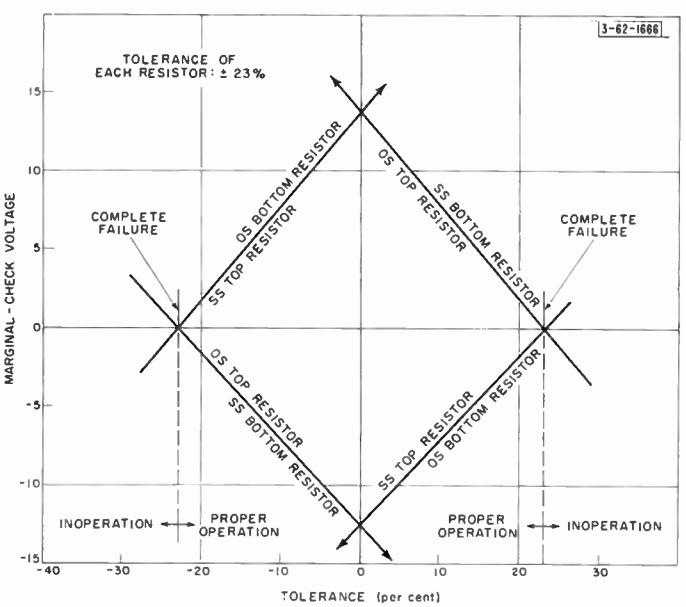

Fig. 12—Marginal-check voltages vs divider-resistor tolerance.

Fig. 11 shows the circuit margins plotted against the test plate current of one tube while the other is held fixed. The tube was "aged" by filament variations as described above.

Fig. 12 shows circuit margins plotted against the variations of the four voltage-divider resistors, R7 through R10. This linear relationship is expected, and could have been obtained analytically.

Fig. 13 shows margins plotted against tolerance of the cathode resistor, R11. A note on the curve explains how it shifts with low-current tubes, so that the apparent unbalance in tolerance is not objectionable.

Fig. 14 shows how the margins vary with the plate-load resistors, R1 and R2.

Fig. 15 shows the effect on margins of low back resistance in the −30 volt clamp diodes, CR3 and CR4.

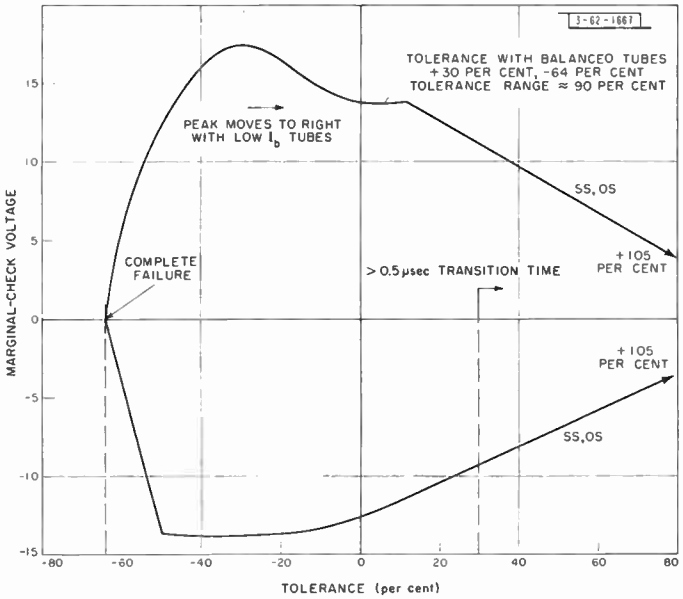

Fig. 13—Marginal-check voltages vs cathode-resistor tolerance.

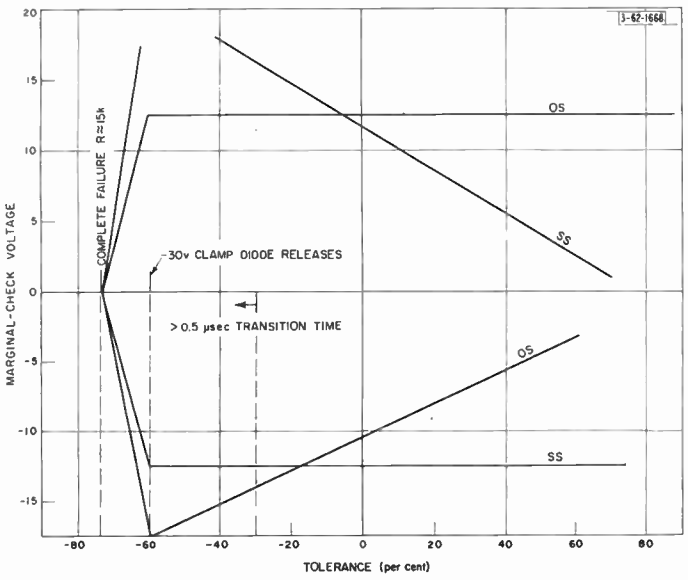

Fig. 14—Marginal-check voltages vs + 150 v plate-resistor tolerance.

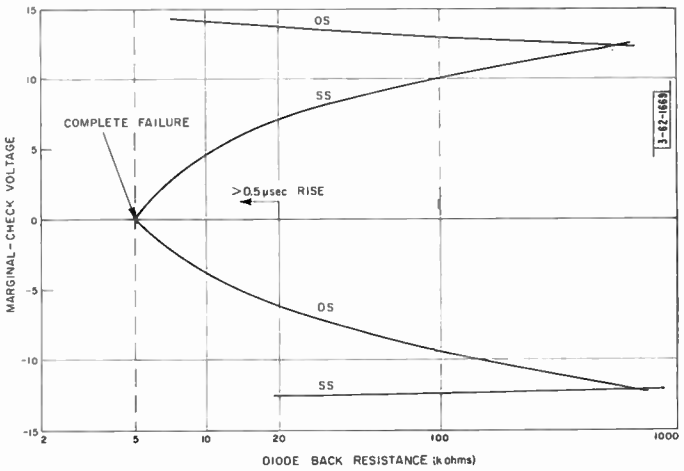

Fig. 15—Marginal-check voltage vs back resistance of −30 v clamp diode.

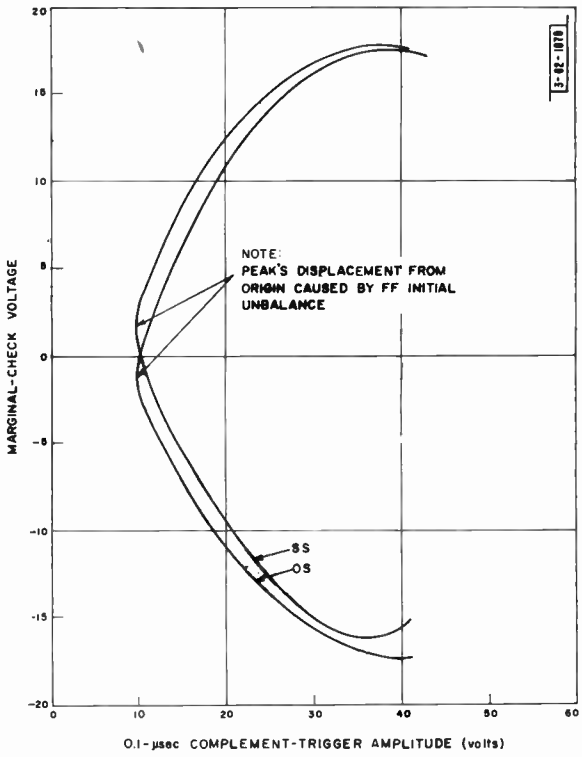

Fig. 16—Marginal-check voltage vs input-trigger amplitude.

Fig. 16 shows margins as a function of trigger amplitude. This plot is the most useful one for optimizing the final circuit, especially when the data are taken for both low and high (2-mc) prf's, maximum and minimum loads, unbalanced tubes, etc.

Other data were taken to show margins vs the back resistance of the trigger diodes (CR9 and CR10), cathode-follower plate voltage, memory capacitors (C1 and C2), cathode by-pass capacitor (C3), forward drop of input diodes (CR5 through CR8), etc.

The detailed analysis illustrated in this example gives the circuit designer quantitative figures for component tolerances and safety margins in his circuit. Using this information, the designer can extrapolate the effect of simultaneous change in several components. Only through such detailed analyses can the circuit engineer meet his design requirements for highly reliable electronic circuitry.

Digital Computer System Design

A large electronic system is made up of a number of basic circuits. In digital computers, the high-speed flip-flop is one such circuit. Each of these basic circuits must be designed with the same thoroughness with respect to its performance, component tolerances, and safety margins. Marginal-checking facilities are included in each circuit to aid in the detection of failing or deteriorating components. The basic circuits for a digital com-

puter include pulse generators, pulse amplifiers, logical gates, flip-flops, cathode followers, indicators, and blocking oscillators.

In a large digital computer system, signal levels must conform with a standard to make possible the interconnection of circuits in building block fashion. The standard signal levels for the AN/FSQ-7 computer were described in the performance specifications for the high-speed flip-flop (see Fig. 6).

Whenever possible, gate tubes and pulse amplifiers are designed to have less than unity gain with pulse inputs of less than 5 volts; greater than unity gain but less than 40 volts output for inputs between 20 and 25 volts; and for inputs of from 25 to 40 volts, to have outputs of 25 to 40 volts (see Fig. 17). This transfer characteristic creates a tendency towards standardization of pulse amplitudes, alleviating the need for special restandardizing circuits for pulses traveling through chains of gate tubes and pulse amplifiers.

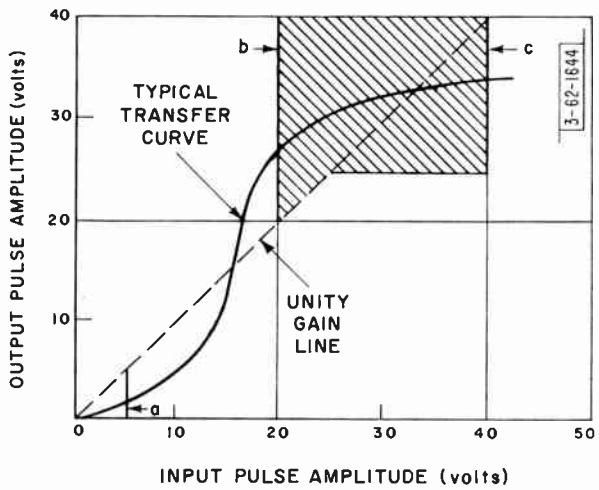

Fig. 17—Transfer characteristics. Specifications require that the transfer curve intersect vertical lines *a*, *b*, and *c*. Shading indicates normal operating region.

The use of a set of centralized dc power supplies in a large system offers many advantages over the use of several small supplies. With only one set of supplies to build, it is advantageous to devote a sizable effort to making good supplies. Greater potential reliability accrues from the use of fewer components, trouble detection equipment (such as low-voltage and over-voltage detectors), control circuitry, and emergency-supply switch gear in such supplies.

The reliability of transistor circuits is effected by basically the same principles that determine the reliability in tube circuits. Since the transistor itself is a relatively new component, it is undergoing rapid and continuous improvement. Digital computer circuit designers are now learning how to take advantage of the properties of the device in order to emphasize its strong points and to bypass its weaknesses.

Since the transistor resembles the vacuum tube in a number of respects, some of the techniques of tube-circuit design are adaptable to transistor circuits. (This parallel must not be carried too far—in no case can a transistor be "plugged" into a circuit in place of a tube and have the circuit operate equally well with component). Transistor circuits operate at an impedance level an order of magnitude below that of similar tube circuits. This reduces the problem of accidental triggering from external noise but magnifies the problem of driving several parallel stages from a single transistor stage.

Conclusion

Lincoln Laboratory has achieved impressive results in the application of the design philosophy described in this report. A typical circuit including its tube has an operating lifetime of over 100,000 hours. A routine maintenance scheme in which the marginal-checking principle is properly exploited can predict failures of over 90 per cent of the total to be expected. System operating efficiency (useful time/total time) over 95 per cent is attainable even in systems where 20,000 circuits are employed.

Appendix

Characteristics and Applications of Components

The discussion of design methods in the body of this paper has specified many components and their applications in particular circuits. Certain component characteristics and notes on applications that have led to reliable electronic design are discussed in this Appendix.

Tubes

The best tubes are assembled in air-conditioned, lint-free rooms, since the cause of many intermittent shorts has proved to be carbonized particles of lint and foreign matter within the tube envelope. Residual gases in the tube are reduced by a better than average vacuum. A tube designed for simplicity and ease of assembly will be more dependable than a complex construction. A short, rugged mount structure with a minimum of 0.005 to 0.006-inch interelectrode spacing will minimize the incidence of shorts and troubles resulting from rough handling. For mount structures longer than one inch, even wider spacings are necessary. A requirement for high transconductance is basically opposed to the requirement for high-tube reliability.

The operating temperature of the cathode must be chosen as a best compromise among several factors that affect tube life. Some of these factors are: level of emission, cathode poisoning, interface, evaporation of the coating, and sublimation of the base metal. Bulb temperature must be reduced to 80 to 100°C by forced air circulation or air-conditioning. Slots should be cut in the structural mica insulators to increase the leakage paths between the electrodes. Grid wires are plated to minimize secondary emission. Plates are designed to maximize the heat-radiating area, and are made of materials with minimum gas content. Heater voltage regulation within 2 per cent of rated value has been demonstrated to give increased tube life. DC cathode current should

be limited to 50 to 60 milliamperes per square centimeter of active cathode area. Pulse cathode current should be limited to about ten times this value, for short pulses (under one microsecond) and low duty factors (under ten per cent).

Design ratings for plate current and dissipation should be conservative and based on the results of extensive life tests. Standardization on a minimum number of tube types, and cooperation with the manufacturers' tube applications engineer to assure best use of these types, will materially reduce the incidence of interrupting tube failures.

Semiconductor Diodes

Semiconductor diodes are most often used as switching networks or as blocking or clamping devices. The principal characteristics of diodes that are of importance to the pulse circuit designer are: 1) static (dc) forward voltage drop, 2) static back current, 3) reverse voltage breakdown, 4) forward recovery, and 5) reverse recovery. The first three are relatively selfexplanatory, but forward recovery and reverse recovery are important factors that may be overlooked. When the application is at all critical with respect to forward and reverse recovery, diodes must be tested under conditions close to those expected in the circuit application.

Since diode characteristics are adversely altered by the effects of moisture and other contaminants, a sealed housing should be specified. Glass-enclosed diodes have proven more satisfactory than diodes that depend upon some waxy filling compound for moisture resistance.

The back resistance of a diode may change markedly during life. For circuits intended to give long service, the designer should use a design figure for back resistance that is considerably less than the one given in the manufacturer's specifications. A factor of five for degradation of back resistance from initial to end-of-life specifications has been used successfully.

Connectors

Connectors often give rise to intermittent contact troubles. These usually result from inadequate contact pressure, which allows oxide or other insulating films to develop on the contact surfaces. Contact spring members should be relatively long, and should be made of a nonfatiguing material. When a plug is mated with its socket, one contact surface should wipe over the mating surface for a considerable distance. Contacts should be plated with a nontarnishing metal (gold and rhodium have been satisfactory). Contact pressure from surface to mating surface should be high, while the force required to mate the connector should be moderate to avoid damage.

Relays

Relays have been major troublemakers in both military and civilian equipment for many years. The difficulties center around contact erosion, failure to make contact through oxide or foreign matter on contacts, and mechanical failure of contact springs and armature supports.

Extreme miniaturization should be avoided. A relatively large, conservatively rated coil should be used. Bifurcated (twin) contacts on each contact spring will insure that if one contact of the pair is blocked by dust or foreign matter the other one will still provide continuity. A dust cover with gasket seal should be provided. Cotton, paper, or other such organic insulations will, under the influence of dc potential and moisture, contribute to electrolytic corrosion of the windings. Nylon, cellulose acetate, and similar synthetic insulations are satisfactory. The potential of the coil should be negative with respect to the relay frame. Arc suppression networks across contacts that break current-carrying circuits should be provided. Decoupling networks or filters should be used to minimize power supply transients due to operation of relays carrying large currents.

Resistors

If intelligently selected and applied, resistors are a particularly dependable class of components. To assure long life, all standard resistors should be derated from the nominal power and voltage ratings by 50 per cent. Initial tolerances should be derated for long-life applications.

A composition carbon resistor considered by the manufacturer as a ± 5 per cent unit may vary as much as ± 20 per cent during several years' use. Composition carbon resistors are not so stable as other resistors.

Film resistors of the deposited carbon, precious metal, and electrically conductive glass film types are considerably more stable than composition resistors, but a resistor of nominally one per cent tolerance should be considered to have a 5 per cent end-of-life tolerance. Deposited carbon resistors should be hermetically sealed.

Precision wire-wound resistors are the most stable type of resistor but they are quite reactive and thus are not generally useful in fast-pulse circuitry. Wire smaller than 0.002 inch should not be used in critical equipment. The construction that employs a cast or molded plastic bobbin, with an outer housing of the same plastic, is far superior to the older ceramic bobbin, paper-wrapped, varnish-impregnated construction. Only the vitreous-enamelled (shiny coating) varieties of power wire-wound resistors are recommended.

Capacitors

If adequately specified and properly applied, capacitors need cause little trouble in electronic equipment. Capacitor failures result principally from poor construction techniques and from application of excess voltages. The manufacturer's rated voltage should be derated 50 per cent for long life applications.

Paper capacitors should be hermetically sealed in metal cans, should have at least three layers of dielectric

paper, and use a fluid impregnant such as mineral oil or one of the complex hydrocarbons (not a wax) marketed under trade names. Paper capacitors should not be used in circuits where day-to-day stability of capacitance is important.

Mica capacitors, particularly those using silver paint as the electrode material are quite stable and trouble-free. Silvered micas, though, are subject to migration of the silver across insulating boundaries under the influence of moisture and dc voltage. Ordinary molded phenolic housings are not sufficiently moisture-proof to prevent silver migration. The design tolerance should be taken as ± 10 per cent beyond the nominal purchased tolerance for nonsilvered units, and $\pm$ 5 per cent for silvered micas. Some trouble has been encountered in capacitors where the termination of the pigtail lead is only crimped in a slot in the end plate inside the body; this joint should be soldered.

Ceramic capacitors in the disk and tubular forms are quite dependable. Units over 0.001 μf use ceramic with high dielectric constant, and are quite unstable; these should be used only for bypass and decoupling applications where exact values of capacity are of no concern. In smaller values, the design tolerance should be considered to be ± 10 per cent beyond the purchased tolerance.

Electrolytic capacitors have been major trouble-makers in consumer electronic equipment. A number of reliable units are available, but the best electrolytic capacitors are "telephone quality," originally developed and produced by several suppliers for the Bell System. A 10 per cent voltage derating factor should be applied, and surge voltages seen by the capacitor should never exceed the manufacturer's rated *operating* voltage.

Transformers and Inductors

The principal troubles encountered in transformers stem from the effects of moisture which cause electrolytic corrosion and decomposition of insulation. Such troubles can be remedied by insisting upon adequate varnish impregnation of the winding, and hermetically sealing the case. Use of miniaturized transformers wound with very small wires, should be avoided. The maximum operating temperature of the windings recommended for long reliable service is 70°C. Small pulse transformers using toroidal ferrite cores have been most satisfactory for short pulse circuits. These should be hermetically sealed and operated well within the manufacturer's ratings.

RF chokes have given very little trouble in service. The vacuum-varnish impregnated coils, wound on ferrite, powdered-iron, or passive cores, have been most satisfactory.

Transistors

The transistor is a new device, dating back only to 1948 and, as such, does not have the long history of use accruing to most other electronic components. Mechanical and electrical stability of early units was poor, and this led to difficulties and poor acceptance in some quarters.

Since little life data have been accumulated on transistors, types cannot be selected on the basis of proven reliability. If transistors are to be used in large numbers, the types chosen should be those that can be manufactured with reasonable yields by present fabrication techniques. Characteristics that are important in the design of reliable transistor circuits are frequency response, power dissipation, and storage time.

During manufacturing, the transistor must be handled under extremely clean conditions and well-controlled humidity to avoid difficulties with contamination; and the transistor must be hermetically sealed to prevent leakage of water vapor into the device after fabrication.

Germanium transistors are particularly sensitive to temperature; therefore temperature limits must be rigidly observed. Silicon transistors should be used for applications where high ambient temperatures are unavoidable.

Acknowledgment

This paper is taken from the general portion of the author's Lincoln Laboratory Technical Report No. 102 of the same title. The "parent" report contains additional material of a detailed discussion (in the fourth part) of several "building block" computer circuits using transistors as well as tubes, an expanded appendix on components, and one on transistors.

In the report and in this paper particular contributions have been made by R. L. Best, W. J. Canty, K. H. Olsen, Dr. D. J. Eckl, and B. B. Paine. N. T. Jones has carried the burden of collecting and clarifying the text.

Bibliography

[1] Taylor, N. H. "Marginal Checking as an Aid to Computer Reliability," Proceedings of the IRE, Vol. 38 (December, 1950). pp. 1418–1421.
[2] ———. "Rudiments of Good Circuit Design," *Electronic Components Symposium*, Pasadena, Calif., April 30, 1953, also M.I.T. Digital Computer Laboratory Report R-224, May 19, 1953.
[3] ———. "Designing for Reliability," M.I.T. Lincoln Laboratory Technical Report No. 102, December 9, 1955 (not generally available).
[4] Forrester, J. W. "Design and Tests of Electronic Circuits for Operating Safety Margins," M.I.T. Digital Computer Laboratory Memorandum M-1828, January 27, 1953.
[5] Boyd, H. W. "Design of a Reliable Flip-Flop," *RETMA Symposium on Reliable Applications of Electronc Tubes*, Philadelphia, Pa., May 21, 1956.
[6] Hofler, J. J. "Application Techniques Leading to Reliable Circuit Performance," *RETMA Symposium on Reliable Applications of Electron Tubes*, May 21, 1956.
[7] Henney, K., *et al. Reliability Factors for Ground Electronic Equipment*, New York: McGraw-Hill Book Co., Inc., 1956.
[8] Canty, W. J. "Designing for Reliability," *Joint Military-Industry Guided Missile Reliability Symposium*, Huntsville, Ala., October 16, 1956.
[9] Daggett, N. L., and Rich, E. S. "Diagnostic Programs and Marginal Checking in the Whirlwind I Computer," 1953 IRE Convention Record, Part 7, pp. 48–54.

Experience with Single-Sideband Mobile Equipment*

R. RICHARDSON†, O. ENESS†, ASSOCIATE MEMBER, IRE, AND R. DRONSUTH†

Summary—**An experimental vhf single-sideband equipment used for performance comparison with narrow-band fm equipment is described. Problems associated with transmitter design, transmitter power, speech compression, pilot carrier recovery, sideband detection, agc response time, and ignition noise suppression are discussed. A laboratory comparison and a field comparison of the SSB equipment and the fm equipment indicates that for comparable size equipment utilizing the same final amplifier tube, an equal service range can be obtained.**

INTRODUCTION

ALTHOUGH single-sideband modulation has been used successfully in many communication systems for the past 25 years, it was only recently that the state of the art had advanced to the point where this method could be adapted to vhf mobile services. In addition, the great increase in the use of mobile services has provided impetus for the further development of this method of modulation which could greatly increase the number of communication channels now available.

The experimental SSB equipment described in this paper was designed to operate at 159.51 mc and have the same approximate physical size and comparable range as the fm equipment now in use for the mobile services.

As is well known, the main deterent to the application of SSB to the vhf frequencies has been the problem of crystal-controlled oscillator frequency stability. At present, the frequency stability of oscillators having oven-controlled crystals is approximately 2 parts per million over the temperature range $-30°C$ and $+85°C$, and since there are two high-frequency oscillators in the transmitter-receiver combination, an SSB system can be expected to have an over-all frequency stability of around 4 parts per million. In order to guarantee that communications would not be dependent upon frequency stability, the SSB equipment was designed to allow for the maximum possible frequency error between the transmitter and receiver. This represents an over-all variation of ± 638 cycles at the operating frequency of 159.51 mc. A short-term frequency instability results from the on-off action of the crystal oven thermostat. The effect of this temperature variation upon frequency stability depends on the turning point of the crystal and upon the amount of oven temperature variation. At present, this variation results in a slow cyclic frequency variation of from ± 30 to ± 150 cycles at 159.51 mc.

Investigation has shown that a locally generated carrier in an SSB receiver must be within 50 cycles of the correct frequency to give the detected voice signal the proper tonal qualities. On the basis of the expected frequency stability, reinjection of a locally generated carrier at the receiver is not feasible and a pilot carrier must be furnished by the transmitter.

Since the amount of sideband power available from the transmitter decreases rapidly as the carrier power is increased, the power of the pilot carrier must be held to minimum.

The receiver is required to separate the carrier from the sidebands and amplify the carrier prior to reinjection at the detector. With a frequency stability of 4 parts per million, the use of a narrow filter to separate the carrier from the sidebands is untenable since the sidebands can easily drift into the band-pass of the narrow filter and thereby result in a severe audio distortion. For this reason, the receiver separates the carrier from the sidebands by the use of a phase-locked oscillator circuit similar to the circuit now in common use in color TV receivers.[1–4] As will be shown later, this circuit also serves as the audio detector of the receiver, thereby resulting in a considerable simplification of the receiver. From the standpoint of the receiver, the pilot carrier must be large enough to insure that the sidebands cannot gain control of the detection circuit of the receiver. The present equipment was designed to operate with a peak sideband envelope power to carrier power ratio of 13 db.

SSB TRANSMITTER

Single-sideband transmission inherently requires a linear relationship between the input voice signal and the rf output signal of the transmitter. Nonlinearities in the transmitter can result in RF harmonic distortion, intermodulation between the carrier and the voice spectrum, and intermodulation between the voice spectrum components themselves. RF-harmonic distortion presents no appreciable problem since the rf-

* Original manuscript received by the IRE, October 1, 1956; revised manuscript received, December 20, 1956. The work presented in this paper was performed under the Signal Corps Contract DA-36-039-SC-64737, and in conjunction with R. Boykin, E. Stega, and A. Brown of the Signal Corps Engineering Laboratories.

† Motorola, Inc., Chicago, Ill.

[1] W. J. Gruen, "Theory of afc synchronization," PROC. IRE, vol. 41, pp. 1043–1048; August, 1953.

[2] G. K. Jensen and J. E. McGeogh, "An Active Filter," Naval Res. Lab. Rep. 4630, November, 1953.

[3] D. Richman, "Color-carrier reference phase synchronization accuracy of NTSC color television," Proc. IRE, vol. 42, pp. 106–133; January, 1954.

[4] D. Richman, "The dc quadricorrelator: A two-mode synchronization system," PROC. IRE, vol. 42, pp. 288–299; January, 1954.

tuned circuits are sufficiently selective to remove these components. In addition, a simple harmonic filter is used in the output of the final amplifier to insure that harmonics of the output frequency are reduced to well below the maximum allowable level. However, odd order nonlinearities will result in in-channel distortion and out-of-channel splatter. The in-channel distortion does not impose a stringent design requirement on linearity since with reasonable care its effects on intelligibility can be made very low. Splatter, on the other hand, results in interference in neighboring channels and limits the spectrum utilization that is theoretically possible with single sideband modulation.

The SSB-transmitter was designed to have the same physical size and utilize the same final amplifier tube as the fm transmitter now being supplied for the mobile services. In this way, a reasonable performance comparison between the two transmitters can be easily obtained.

There are two main ways[5] of removing the unwanted sideband; the filter method and the phase method. The filter method was selected because of its simplicity, stability, and high degree of rejection. In addition, the filter method requires no tuning adjustment as does the phase method. Referring to the block diagram of the transmitter shown in Fig. 1, a diode ring balanced

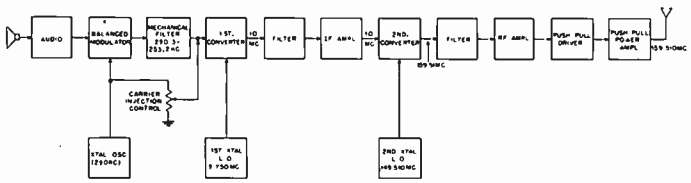

Fig. 1—Single-sideband transmitter.

modulator is used to generate the two sidebands and suppress the carrier. A mechanical filter having a bandpass from 250.3 kc to 253.2 kc is used to pass the upper sideband and provide an attenuation of at least 60 db to the lower sideband.

Because of the low starting frequency of 250 kc and the high output frequency of 159.51 mc, direct conversion to the output frequency is not practical since it would be very difficult to reduce to an acceptable level the local oscillator and the image frequency signal, which are only 250 kc and 500 kc below the output frequency. For this reason, two conversions are required.

The 10-mc filter which follows the first mixer is designed to attenuate the first local oscillator and image frequency signal 60 db below the desired sideband signal. Because the desired signal incurs a loss in passing through the filter, the filter is followed by a class A 10-mc amplifier. The signal is then converted to the output frequency of 159.51 mc, filtered, amplified, and applied to input of class AB_1 push-pull driver stage.

Push-pull operation of the driver and final amplifier results in a reduction in output capacity of approximately one-quarter the value obtained for parallel operation. Larger tank inductance can be used, resulting in a higher resonant resistance and a decrease in the rf losses in the tank circuits. The driver is operated class AB_1 to maintain good linearity and to realize a greater efficiency than possible with class A operation. Projected cutoff class B operation of the final amplifier was used because of the increased efficiency over class AB and because of a low idle current during periods of no modulation. At the operating frequency of 159.51 mc, the plate efficiency of all classes of amplifiers is considerably reduced below the theoretical value. The efficiency of class C final amplifiers, at this frequency, is from 50–60 per cent and the efficiency of the final amplifier of this transmitter is approximately 35 per cent, when delivering maximum power. The theoretical plate efficiency of class B amplifiers is given by the equation:

$$n_p = \frac{\pi}{4}\frac{E_p}{E_{bb}}$$

where E_p is the amplitude of the varying component of the plate voltage of one tube, E_{bb} is the plate voltage.

Since the plate efficiency increases with E_p and since the voice signal has a dynamic range of approximately 15 db, the plate efficiency of the final amplifier is much less than the efficiency obtained during the maximum power output condition; *i.e.*, less than 35 per cent. Reduction of the dynamic range of the voice signal by the use of peak clippers in the audio circuit can result in an increase in plate efficiency and thereby raise the average output rf power of the transmitter. The use of a peak clipper in the audio circuits has an additional advantage. As the driving power into the final is increased, the output power will reach a final limiting value dependent on the plate voltage of the final amplifier. Operation of the final amplifier into this region will result in nonlinearity and spurious signals will develop in the nearby channels. By setting the clipping level in the audio circuit to be below the level which can drive the final amplifier into plate saturation, this condition can be prevented.

Listening tests of the distortion produced by peak clipping of the voice signal indicated that clipping, which results in a peak power to average power of approximately 6 db, in the audio circuits, could be tolerated. Comparison tests were conducted of the readability of normal speech and speech clipped at various levels in the presence of white noise. The results indicate no reduction in the readability of 6-db clipped speech down to signal to noise ratios of 0 db. Below this level, the readability of normal speech was only slightly better.

[5] F. E. Terman, "Electronics and Radio Engineering," McGraw-Hill Book Co., Inc., New York, N. Y., pp. 541–543.

On the basis of the above tests, the voice signal input to the transmitter is clipped at approximately 6 db, but unfortunately this ratio increases to 10 db in passing through the 250-kc narrow filter. This effect is primarily due to the nonlinear phase shift of the low-frequency voice signal components which occurs at the edge of the band-pass of the filter.

On a linear basis, the peak power capability of the final amplifier must be such that during the peaks of the voice signal, the following equation must be satisfied.

$$P_T = [\sqrt{P_{VP}} + \sqrt{P_c}]^2 \tag{1}$$

where P_T is the required peak envelope power, P_{VP} is peak sideband envelope power, and P_c is the carrier power.

The carrier suppression ratio K is defined as the ratio of peak sideband envelope power to the carrier power;

$$K = \frac{P_{VP}}{P_c} \cdot \tag{2}$$

For a given peak envelope power P_T,

$$P_c = \frac{P_T}{(1 + K^{1/2})^2} \tag{3}$$

and

$$P_{VP} = \frac{P_T}{(1 + (1/K)^{1/2})^2} \cdot \tag{4}$$

For reasons dictated by the capabilities of the carrier restoration circuit of the receiver, the transmitter is required to have a value of $K \approx 13$ db.

Thus

$$P_c = 0.034\ P_T \tag{5}$$

and

$$P_{VP} = 0.667\ P_T. \tag{6}$$

It is difficult to ascertain the amount of splatter spectrum resulting from a specific degree of plate saturation in the final amplifier. Although the limiting value can be easily measured, it is difficult to set a value on the usable peak envelope power. If the limiting value is used in the calculations of carrier power and peak sideband envelope power of (5) and (6), the peak envelope power present during the peak of a voice signal will be less than the limiting value because of nonlinearity in the final amplifier. Operation in this manner will result in some amount of splatter. Analysis of the splatter spectrum problem is now in progress.

In order to expedite the field evaluation of the SSB equipment, the transmitter power output rating was determined on the basis given above, that is, the limiting power was measured and used as the value of P_T in (5) and (6).

The specifications of the SSB transmitter and of the fm transmitter with which it was compared in the field evaluation are given in Table I.

TABLE I

TRANSMITTER SPECIFICATIONS

	SSB Transmitter	FM Transmitter
Final amplifier tube	829B	829B
Class of operation of final amplifier	push-pull class B	push-pull class C
Final amplifier plate voltage	700 v	600 v
Measured final amplifier limiting power	169 w	
Carrier power	5.7 w	
Peak sideband envelope power	113 w	
Measured peak envelope power	135 w	
Average sideband power (voice signal)	11.3 w	
Total average output power	17 w	60 w
Final amplifier plate dissipation plate	30 w	29 w
Final amplifier efficiency (voice signal)	21.1 per cent	50.8 per cent
Total input power to transmitter	225 w	334 w
Frequency deviation		±5 kc
Operating frequency	159.51 mc	159.51 mc
Modulation control	clipped speech	instantaneous deviation control

SSB RECEIVER

The single-sideband receiver is a dual conversion receiver which utilizes the important design criteria of having a minimum of gain prior to a highly selective filter. The filter is then followed by the high-gain IF amplifier. In this way, all signals which enter the receiver are kept at a low level before the main selective circuits are encountered. This approach[6-8] which has been successfully applied to mobile radio fm receivers for the past eight years minimizes the spurious signals resulting from intermodulation of signals which are near the desired channel. In addition, desensitization of the receiver by a strong nearby signal is reduced by a significant amount.

The block diagram of the single-sideband receiver is shown in Fig. 2. The stages prior to the highly selective 4.5-kc filter are identical with present production fm receivers with the exception of the application of agc control voltage to the grid of the first IF amplifier. The selectivity of the multiple section filter which determines the receiver selectivity in the main is shown in Fig. 3. The bandwidth of 4.5 kc at the 3-db points was chosen on the basis of 3.2-kc bandwidth for the carrier and sideband with ±650 cycles for system frequency instability.

[6] D. E. Noble "Adjacent-channel operation of mobile equipment," *Electronics*, vol. 22, pp. 90–95; June, 1949.

[7] D. E. Noble, "The Sensicon Receiver Design," presented at the West Coast IRE Convention, Long Beach, Calif.; September 14, 1950.

[8] H. Magnuski, "Adjacent-channel rejection receiver," *Electronics*, vol. 24, pp. 100–104; January, 1951.

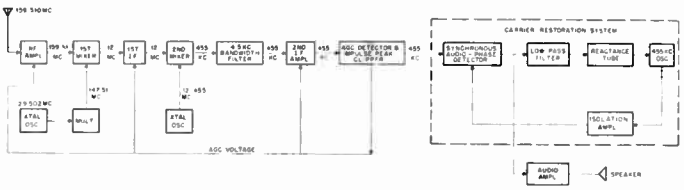

Fig. 2—Single-sideband receiver.

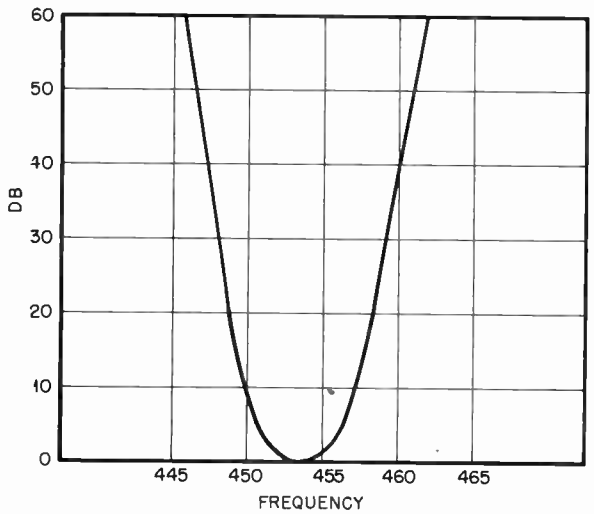

Fig. 3—Receiver second IF filter.

One of the main design problems of the SSB receiver is the separation of the carrier from the sidebands. It must be realized that the reduced carrier SSB signal cannot be directly applied to the usual AM detector circuit since the pilot carrier is of insufficient amplitude for proper recovery of the modulation information. Thus, the carrier must be separated from the sidebands, amplified to be considerably larger than the sidebands, and then mixed with the sidebands in some type of AM detector. To obtain maximum receiver sensitivity under weak signal conditions, the separated carrier must be amplitude limited to remove any amplitude variations due to noise. If this is not done, the noise variations on the carrier will be detected and will result in a reduction of the signal to noise ratio at the output of the detector. In addition, the amount of frequency modulation on the carrier due to noise variations must be kept to a low value.

The most obvious way to separate the carrier from the sideband is by the use of a narrow filter. Since the transmitter has a filter from 250.3 kc to 253.2 kc, the minimum separation between carrier and sidebands is 300 cycles. It must be realized that the sidebands cannot be allowed to enter the carrier channel of the receiver. If this occurs, the recovered audio at the detector is severely distorted. Thus, the maximum permissible width of the carrier filter is 300 cycles and the over-all system stability must be better than ± 150 cycles or 0.0001 per cent. Since this requires a stability four times better than now obtainable, this method is not feasible at the present time.

The method used in the SSB receiver to separate the carrier from the sidebands is similar to the method used in color tv receivers to phase synchronize the reference oscillator to the short bursts of reference carrier.[1–4] As shown by the portion of the receiver block diagram enclosed in dotted lines, the carrier restoration system consists of a 455-kc oscillator which is phase locked to the incoming carrier signal. In the prelocked condition, the phase detector output consists of a sinusoidal voltage at the difference frequency between the incoming signal and the 455-kc oscillator. The sinusoidal voltage is attenuated by the low-pass filter and appears at the grid of the reactance tube which then frequency modulates the oscillator at the difference frequency. If this frequency modulation is of sufficient magnitude, the output of the phase detector is no longer sinusoidal and contains a dc component which moves the average frequency of the oscillator toward the incoming signal frequency. This change in average frequency results in an increase in the dc pull-in voltage. This is a regenerative action which terminates when the oscillator is phase locked to the incoming carrier frequency. Since the amount of sinusoidal voltage present at the grid of the reactance tube is dependent upon the attenuation characteristics of the low-pass filter, the pull-in range is mainly determined by the low-pass filter. The filter also determines the time required for the oscillator to phase lock to the incoming carrier from a prelock condition. To a lesser extent, the pull-in range and pull-in time are dependent upon the frequency response of the phase detector and sensitivity of the reactance tube.

Up to this point, consideration has only been given to the effect of the carrier, but since the sidebands are also present in the phase detector, it is well to consider their effect on the system when it is locked to the carrier. To simplify the discussion, assume that the sideband components are highly attenuated by the filter. If this is the case, the sideband cannot develop a dc pull-in voltage and cannot affect the oscillator when it is locked to the carrier. If the sideband signal were to consist of a single tone signal, the output of the phase detector would be a sinusoidal voltage at the difference frequency between the carrier and the sideband signal. If the sideband is a voice modulated signal, the output of the phase detector would be the recovered voice signal. Thus the phase detector can serve as the detector of the receiver when the carrier restoration system is locked to the carrier.

Assume now that the filter characteristics are such that the sidebands, although partially attenuated, can pass through the filter and develop a dc pull-in voltage. Since the oscillator is phase locked to the carrier, any pull-in voltage developed by the sidebands will be nullified by a counteracting dc voltage developed by a change in the phase shift between the oscillator and carrier. Because the sidebands are present at the grid of the reactance tube, the oscillator will be frequency modulated by the sidebands to a small degree, and as a

result, the recovered audio is distorted to a small degree. Of course, if the dc pull-in voltage developed by the sidebands is of sufficient magnitude, the oscillator will unlock from the carrier and as a result the audio output will be unintelligible.

The attenuation characteristics of the low-pass filter must be such that the required pull-in range is obtained for signal strengths which are below the readable level and that a minimum amount of frequency modulation results from the sidebands when the system is locked to the carrier. The experimental receiver has a pull-in range of plus or minus 650 cycles for an input carrier level of approximately 0.07 microvolt. The pull-in range increases to plus or minus 1500 cycles for an input carrier strength of approximately 1 microvolt.

The system will remain locked to the carrier until a single tone sideband signal is increased to be approximately 13 db above the carrier. If the amplitude of the single tone sideband signal is increased above this level, the system may unlock from the carrier and lock to the sideband. Since a voice signal consists of a spectrum, the system can stay locked to the carrier of a voice-modulated signal having a peak sideband envelope power to carrier power ratio greater than 13 db. For a voice-modulated signal having a ratio of 13 db, the amount of frequency modulation of the oscillator by the sidebands is negligible. For the foregoing reasons, the SSB transmitter was adjusted to provide a peak sideband envelope power to average power ratio of 13 db during the equipment performance tests.

As is well known, multiple path transmission results in a considerable variation in signal strength at the input terminals of a mobile radio receiver. The reception of such a signal in a moving vehicle results in an effect which has become known as "flutter." Measurements[9,10] in the field have shown that the average variation in signal strength at 150 mc is 8 db and that the distance between signal minima when traveling straight away from the transmitter is very close to the free-space half-wavelength distance. When traveling in other directions, the distance between signal minima will be correspondingly increased. Thus, if the vehicle is traveling at 45 mph, the flutter rate can be up to 21 cycles/second.

The question arises as to whether the agc should have a fast or slow response. If a slow response agc is used, the voice signal will vary in amplitude at the flutter rate. With a fast response agc, the agc will allow the gain of the receiver to change at the flutter rate and the amplitude of the voice signal will not vary. When the signal strength is very low, such that a signal begins to drop into the noise during part of the flutter variation, a fast response will quickly raise the receiver gain and a short burst of noise at the flutter rate will be heard at the output of the receiver. If a slow response agc is used in this case, the noise will not vary at the flutter rate.

A flutter simulator was constructed in order to obtain aural observation of this problem under laboratory conditions. It was found that under strong signal conditions, that is when the minimum signal was large enough to prevent the receiver noise from coming up, the fast response agc is more desirable than the slow response agc. The slow response agc results in the addition of a warbling characteristic to the voice signal which is very annoying and distracting. Because of the noise modulation present when using a fast response agc, the slow response agc was found to be slightly better than the fast response agc under weak signal conditions. At the present, the agc response of the receiver was made sufficiently fast to minimize the warbling characteristic of the voice due to flutter.

The agc voltage of the receiver is derived from the combined carrier and sideband signal. Since the voice syllable rate and the flutter rate are in the same frequency range, there was a question as to the effect of a fast response agc upon the intelligibility of the voice signal. Listening tests in the laboratory indicated that it is very difficult to distinguish between a fast acting agc and very slow acting agc when receiving a voice signal.

As an AM receiver, the SSB receiver is basically responsive to amplitude variations at the input terminals of the receiver. Unless special techniques are employed, the amplitude disturbances at the receiver output resulting from ignition noise will be directly proportional to the size of the ignition noise at the receiver input terminal. Of course, this is true only up to the point where limiting of the disturbance occurs at the grid of an IF amplifier stage.

When the desired signal is very low in amplitude, a large ignition disturbance at the receiver input terminals can result in an audio output disturbance which is considerably larger than the desired voice signal. For this reason, the agc detector is so designed that the size of the disturbance which passes to the detector circuit cannot have an amplitude greater than the amplitude of the carrier and sideband signal at that time. Thus, the amplitude of the disturbance at the audio output of the receiver is limited to be no larger than the amplitude of the audio signal. This results in a very considerable reduction in the effect ignition noise has upon the SSB receiver.

The specifications of the SSB receiver and the fm receiver with which it is compared are shown in Table II.

TABLE II

	SSB Receiver	FM Receiver
Noise figure	10 db	10 db
Filter bandwidth at 3-db point	4.5 kc	9 kc

[9] C. F. Meyer and D. Soule, "Field Strength Study," Phoenix Res. Lab., Motorola, Inc. (Work carried out under contract with the Sig. Eng. Coles Lab. Contract DA-36-039-SC-64737, February 1956.)

[10] C. F. Meyer and D. Soule, "Path Selectivity Study," Phoenix Res. Lab., Motorola, Inc. (Work carried out under contract with the Sig. Eng. Coles Lab. Contract DA-36-039-SC-64737, May 1956.)

Equipment Performance in the Laboratory

The SSB equipment and the fm equipment were set up in the laboratory in order to obtain a range performance comparison under controlled conditions. The two equipments had the specifications shown in Table I and Table II.

As shown in Fig. 4, the equipments were arranged in such a way that a rapid change from one equipment to the other could easily be made. An observer was required to monitor one equipment and increase the attenuation to the transmitted signal until the voice was just readable in the receiver noise. The observer then switched to the other equipment and repeated the test. The general consensus of a number of observers was that the SSB signal could be attenuated an additional 1 or 2 db more than the fm signal.

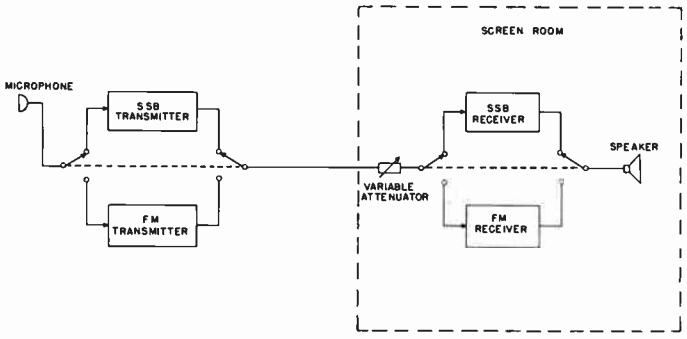

Fig. 4—Equipment arrangement for laboratory comparison of SSB and fm equipment.

To verify that the carrier restoration system supplies a carrier which is substantially free of AM and fm variations due to noise under weak signal conditions, the oscillator of the system was made inactive and a carrier of the correct frequency was furnished to the detector from an external source. A comparison of the readability of weak signals under this condition with the readability of weak signals when the carrier restoration system is in operation indicated no discernible difference between the two. Thus, the carrier furnished by the carrier restoration system under weak signal conditions is sufficiently free of noise such that no degradation in receiver sensitivity is experienced.

Equipment Performance in the Field

A field test was conducted to evaluate the performance of the SSB equipment and to make a comparison with the performance of narrow-band fm equipment. Of primary concern, during the test, was a comparison of the range obtainable from each of the two equipments. In addition, the degree to which ignition noise degraded the performance of each equipment and the susceptibility of the SSB equipment to flutter was given close attention.

The SSB receiver and the fm receiver were installed in a 1954 Ford Police Interceptor and operated from a common antenna by using a coaxial switch controlled at the dashboard of the vehicle. The SSB transmitter and the fm transmitter were set up in the laboratory and also operated from a common antenna by using a coaxial switch. The two equipments had the specifications given in Table I and Table II.

The test was conducted in the residential and industrial areas on the northwest side of the Chicago area. The performance comparison was generally made while the vehicle was in motion and under the conditions of both light and very heavy vehicular traffic.

The test was initiated immediately upon leaving the base station area. As this was a strong signal area, no ignition noise was heard on either receiver. Because of the increased amount of speech clipping in the SSB transmitter, the audio quality of the SSB reception was slightly below the audio quality of the fm reception.

As the test progressed into the medium signal strength area, a small number of ignition disturbances were heard on the SSB reception and, as yet, there were no ignition disturbances on the fm reception. No flutter was noticed on the SSB reception and communication on the two equipments was much the same.

As the signal became weaker, ignition disturbances from the vehicle and from near-by vehicles were heard on both equipments, but the SSB reception had notice ably more disturbance than the fm reception. As before, no flutter was noticed on the SSB equipment and although the fm reception was somewhat easier to read, good communication was obtained from both equipments. The audio quality of the two equipments was much the same at this point.

As the test progressed into the fringe area, the two equipments went out of range at the same point. A location where the fm reception was readable and the SSB reception was unreadable was not found. At the point of going out of range, the fm reception was, in general, not as noisy as the SSB reception. In the fringe area, noise modulation of the voice signal at the flutter rate was noticed on both types of reception.

Equivalent AM Equipment

For the purpose of comparison, it is interesting to compute the transmitter specification of an AM equipment which has an operational range comparable to the SSB equipment. Assuming the same frequency stability as for the SSB equipment, the AM receiver would require a bandwidth of 7.7 kc. On this basis, the AM receiver noise power would be 1.71 times the noise power of the SSB receiver.

Because of the correlation which exists between the two sidebands of the AM signal, the total average sideband power required of the AM transmitter would be 1.71 times the average sideband power of the single sideband signal divided by two or 9.65 w. The AM transmitter will not require the use of a narrow filter and

as a result the peak sideband envelope power to average sideband power ratio will be the same as the clipped speech ratio; *i.e.*, 6 db. For 100 per cent modulation the peak sideband envelope power and the required carrier power will each be 38.6 w and the total average power during modulation will be 48.3 w. During voice peaks, the peak envelope power of the transmitter will be 154 w. Thus, the AM transmitter requires 4.5 db more average power and 0.4 db less peak envelope power than the SSB transmitter.

ACKNOWLEDGMENT

The authors wish to thank H. Magnuski and Dr. W. L. Firestone for their assistance with the design, analysis, and experimental evaluation of this equipment. They are grateful, too, to A. Creighton and D. Reeves, of the Motorola Phoenix Research Laboratory, for their assistance in the development of the carrier restoration system in the SSB receiver.

They also wish to thank J. Cohn and L. Englebrecht for their assistance in the voice-processing studies.

Topological Analysis of Linear Nonreciprocal Networks*

SAMUEL J. MASON†, SENIOR MEMBER, IRE

Summary—**Kirchhoff and Maxwell gave us topological inspection rules for evaluating the transmission of a linear reciprocal branch network. With the addition of the unistor, a branch-like element whose current is proportional to one of its two terminal potentials and independent of the other terminal potential, or the gyristor, whose current is proportional to the sum of its two terminal potentials, we can model any linear network, in general nonreciprocal. The point is that the Kirchhoff-Maxwell methods carry over to such networks without change of form, the only modification of the transmission expression being a relatively simple sign rule for gyristor admittances or a relatively simple nullification rule for unistor admittances.**

INTRODUCTION

TOPOLOGICAL network analysis is concerned with the relationship between network transmission (the ratio of meter reading to source value for a meter and source attached to the network at two specified terminal pairs) and the structure or topology of the network. With the aid of topological methods, the transmission can be evaluated directly by inspection of the network.

In a reciprocal network the measured transfer impedance (the current-source-to-voltmeter transmission ratio) remains the same when the locations of the current source and the voltmeter are interchanged. In a nonreciprocal network the transfer impedances in opposite directions are in general unequal. The linear circuit models of vacuum-tube and transistor amplifiers are prime examples of nonreciprocal networks.

As Ku[1] emphasizes in one of his papers, Kirchhoff and Maxwell proposed topological methods for the analysis of reciprocal branch networks. Percival[2] has extended these methods to nonreciprocal networks in which the current (or voltage) of each branch is not only dependent upon the voltage (or current) of that branch but perhaps also unilaterally dependent upon the voltage (or current) of other branches in the network. The price of this extremely general characterization is a certain complexity of the resulting topological rules as compared with the Kirchhoff-Maxwell rules for reciprocal branch networks. In particular, the rules governing algebraic signs, although straightforward, are somewhat difficult, as Percival points out in his discussion.

In this paper we shall go back to the beginning and attack the problem anew, with the particular aim of keeping the topological relationships as simple as possible. In order to do this, we shall introduce nonreciprocal branch-like elements which, as it turns out, are simple enough to require only relatively minor modification of the Kirchhoff-Maxwell methods, yet general enough to permit convenient characterization of any nonreciprocal network. The team of Boisvert and Robichaud,[3] working independently in Canada, has arrived at similar ideas from the starting point of signal-flow-graph topology. Their approach, viewpoint, and interpretation are quite different, but the essential results are the same.

* Original manuscript received by the IRE, June 26, 1956; revised manuscript received, January 31, 1957. This work was supported in part by the Signal Corps, the Office of Sci. Res. (Air Res. and Dev. Command), and the Office of Naval Res.

† Dept. of Elec. Eng. and Res. Lab. of Electronics, Mass. Inst. Tech., Cambridge, Mass.

[1] Y. H. Ku, "Résumé of Maxwell's and Kirchhoff's rules for network analysis," *J. Frank. Inst.*, vol. 253, pp. 211–224; March, 1952.

[2] W. S. Percival, "The graphs of active networks," *Proc. IEE*, vol. 102, part C, pp. 270–278; September, 1955.

[3] M. Boisvert and L. P. A. Robichaud, "Direct Analysis of Electrical Networks," Rapport de Recherches No. 9, Dept. de Genie Electrique, Université Laval, Quebec, Can.; October 12, 1956.

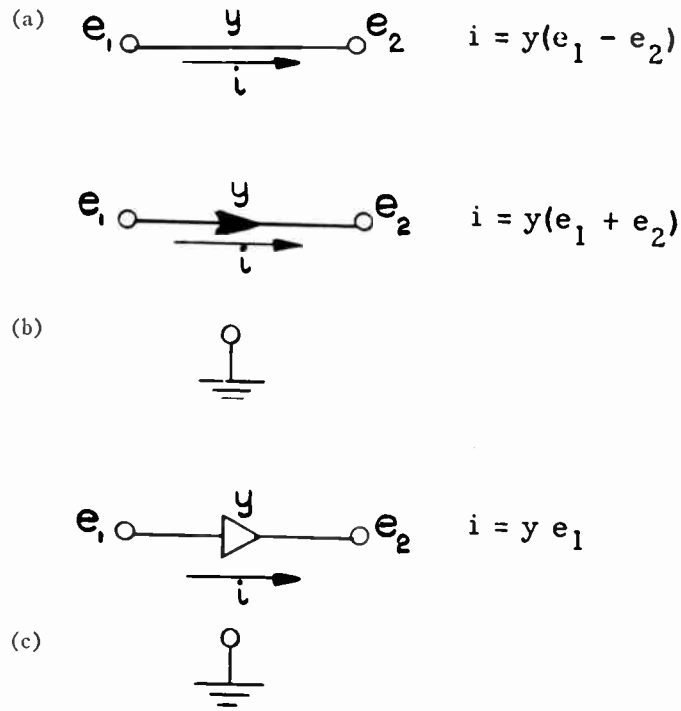

Fig. 1—Basic branch elements: (a) the reciprocal branch (resistor), (b) the antireciprocal branch (gyristor), and (c) the unilateral branch (unistor).

The purpose of this paper is to present, in compact form, a topological theory of nonreciprocal networks, to outline proofs, and to illustrate the application of such techniques to practical electronic circuit analysis problems. The proofs will be given last.

Branch Elements

The three basic branch elements are defined and compared in Fig. 1. All three are branches, in the sense that the current in each element is determined by its terminal potentials, and each element is characterized by a single complex admittance y. However, the gyristor and the unistor are not completely specified unless we also 1) indicate a branch reference direction and 2) designate the ground node from which the node voltages are to be measured. The necessity of designating a ground node means that the gyristor and unistor are, strictly speaking, three-terminal elements.

A number of elementary equivalences are presented in Fig. 2. These follow directly from the definitions of the branch elements. Fig. 3 gives the branch models of some simple multiterminal devices. The symmetric triangular triplet of three identical gyristors shown in Fig. 3(a) is the branch representation of a three-terminal device commonly called a gyrator.[4,5] The unator [Fig. 3(b)] is a cousin of the gyrator. Treated as a two-terminal-pair device, the unator has a unilateral open-circuit voltage gain equal to unity, and its input and output admittances are both equal to the unator admittance u.

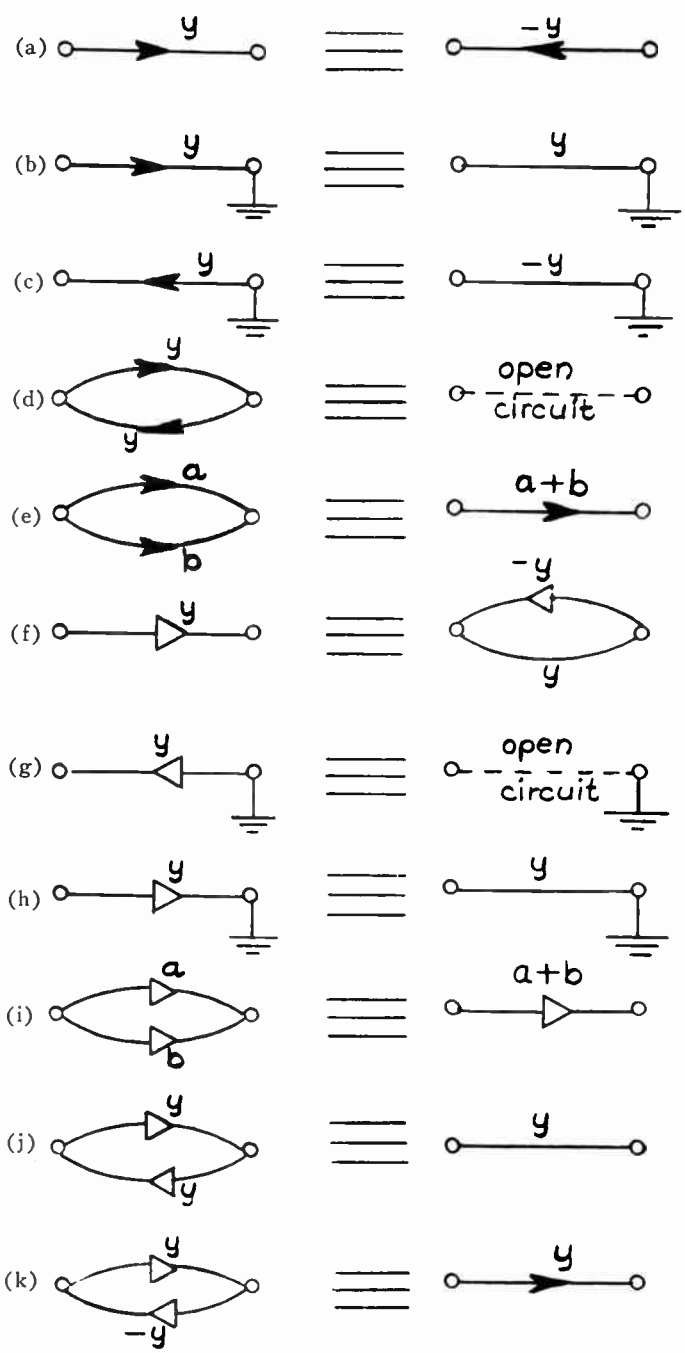

Fig. 2—Some elementary equivalences.

A controlled-source unilateral transconductance, appearing in the conventional circuit representation of a vacuum tube, has the unistor model shown in Fig. 3(c). The unistor model probably appears to be strange and unphysical at first sight, in comparison with the more familiar controlled-source representation of a transconductance. It can be argued, however (purely in the spirit of fun) that the branch model is actually closer to physical reality. A positive potential applied to the left-hand node in Fig. 3(c) causes current to flow into that node through the uppermost unistor, and the same cur-

[4] B. D. H. Tellegen, "The gyrator, a new network element," *Philips Res. Rep.*, vol. 3, pp. 81–101; April, 1948.
[5] J. Shekel, "The gyrator as a three-terminal element," PROC. IRE, vol. 41, pp. 1014–1016; August, 1953.

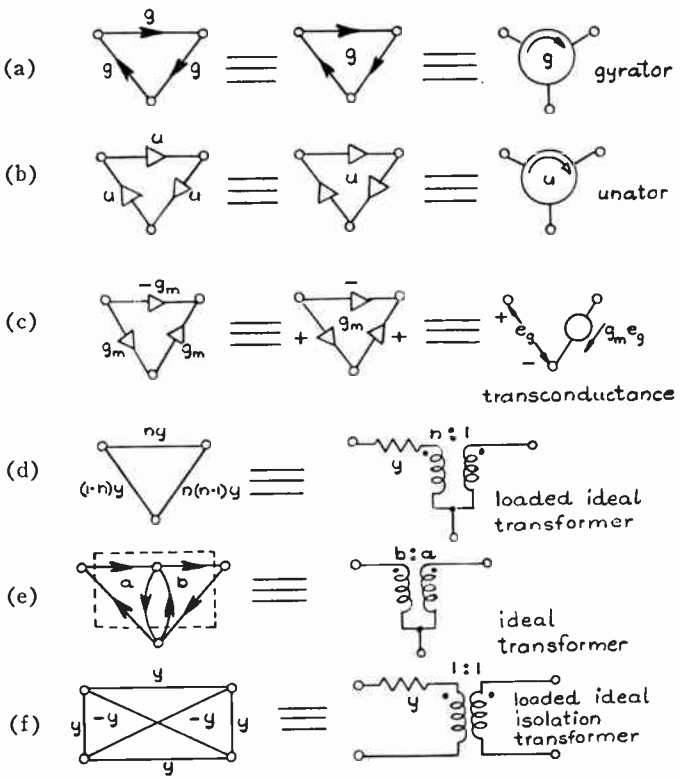

Fig. 3—Branch models of linear devices.

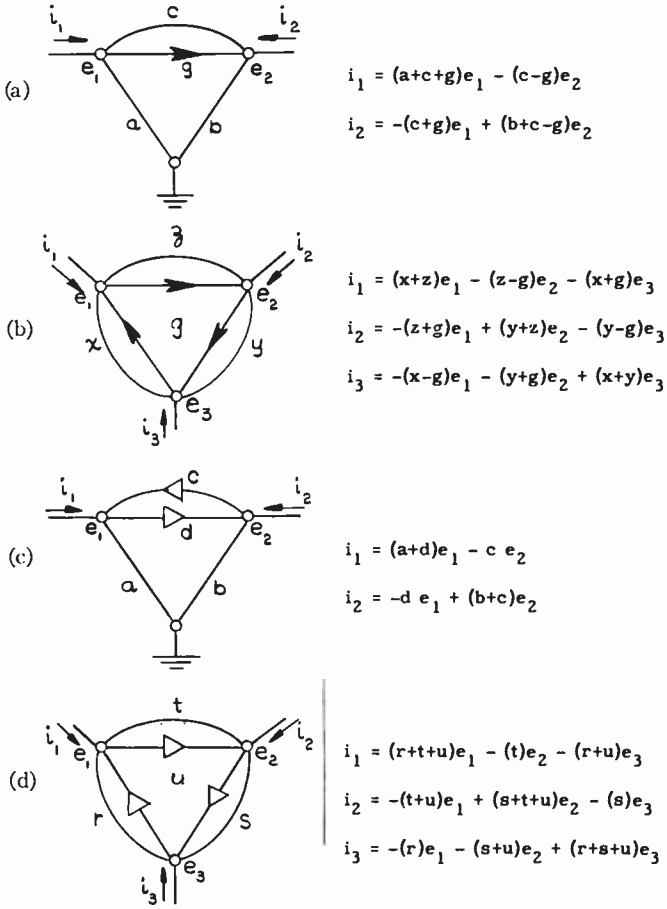

Fig. 4—Some general models of arbitrary three-terminal devices.

rent immediately leaves the node and flows downward through the left-hand unistor. This corresponds to the flow of positive current in a vacuum tube, for the (positive) current actually flows through the grid on its journey from plate to cathode.

For network models containing gyrators, unators, or transconductances, the choice of a ground node is arbitrary, since an equal change in all three of the node potentials changes the current circulating in the triangle of branches, but does not alter the flow of current from the triangle to the remainder of the network in which such a triangle may be imbedded. Such models are said to be ungrounded or "floating."

Parts (d), (e), and (f) of Fig. 3 show branch models of ideal transformers. To construct models (d) and (f), the transformer must be loaded with an auxiliary admittance element y, whereas the cascaded combination of two gyrators shown in (e) eliminates the loading at the price of an additional node. Incidentally, the cascaded combination of a gyrator and a transconductance can be used to represent either a two-terminal-pair unilateral voltage-transfer element or a two-terminal-pair unilateral current-transfer element.

Fig. 4 illustrates the manner in which an arbitrary three-terminal circuit can be represented by branches. Parts (b) and (d) of the figure are floating models in which any node may be taken as ground or datum. In model (c) a resistor and a unistor could have been used in place of the two unistors shown. A model such as (d) can also be constructed with a transconductance in place of the unator. Another possibility is a double triangle of six unistors with their values suitably constrained so as to insure a floating representation.

The point is that (complex) resistors, gyristors, and unistors are sufficient for the general process of model making. Consideration of the admittance matrix of an arbitrary nonreciprocal network shows, in fact, that a network having $n+1$ nodes can always be modeled as a connection of no more than $n(n+1)/2$ resistors plus $n(n-1)/2$ gyrators, unators, or transconductances. If the network is grounded at a specified node, the model can be constructed with $n(n+1)/2$ resistors and $n(n-1)/2$ gyristors or unistors, or with n^2 unistors alone.

In a general network model composed of resistors and gyrators, the location of gyrators is not completely arbitrary. The resistors can be thought of as strings connecting each pair of nodes. The gyrators can be visualized as triangular pieces of paper each of whose edges coincides with one of the strings. The restriction on (independent) gyrator locations is simply that the pieces of paper must not form a completely closed surface. One obvious solution is to let all of the gyrators have one node in common.

The Network Determinant

The topological analysis of branch networks proceeds from the following definitions.

tree: a connected set of branches touching all nodes in a network and not forming any loops. (In a network of n nodes a tree (a) has $n-1$ branches, (b) connects all node pairs, and (c) forms no loops. Any two of these three properties may be taken as a definition whence the third follows.) (1)

tree value: product of the branch admittances in that tree. (2)

network determinant (Δ): sum of the values of the different trees contained in the network. (3)

Fig. 5(g) shows a simple network of three branches whose admittances are a, b, and c. This network contains three different trees whose values are ab, ac, and bc, and the determinant is the sum of the tree values. The other parts of the figure show several networks and their determinants. *The determinant vanishes whenever a part or node is completely isolated from the remainder of the network*, as indicated in (c). *For a network having only one node*, either with or without an attached branch, the *determinant is identically equal to unity*, as illustrated in (e). Part (h) of Fig. 5 shows a network composed of *two connected parts having a single node in common*. For such networks *the determinant is expressible as the product of the determinants of those two parts*. This follows from the fact that a tree in each part is part of a tree in the complete network, and every tree in the complete network is a combination of such parts.

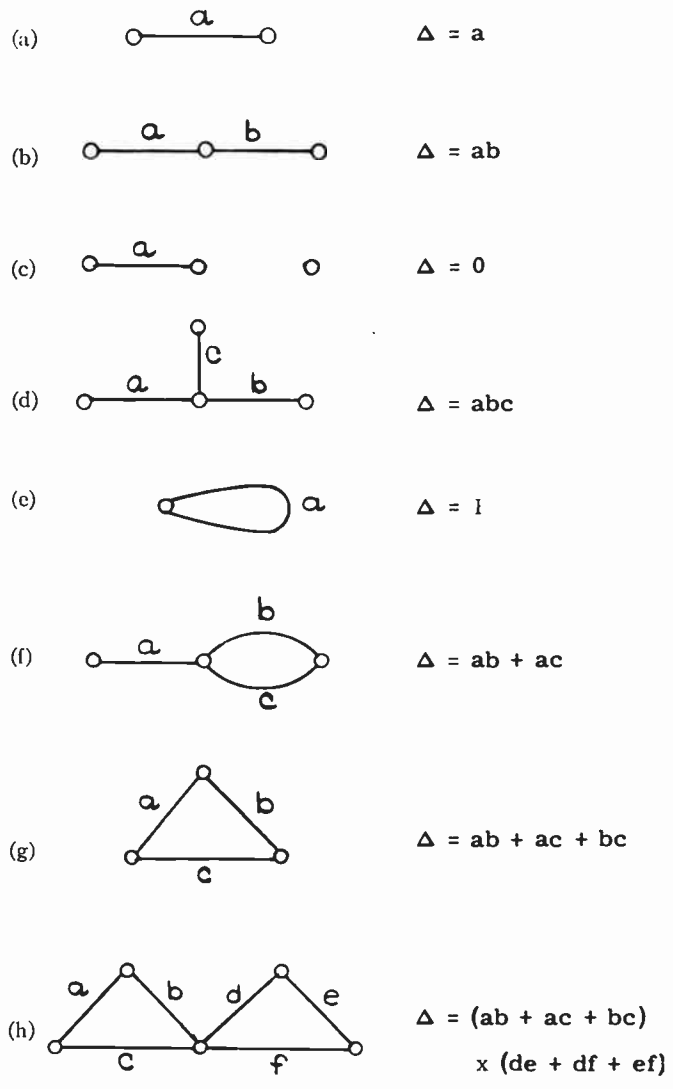

Fig. 5—Determinants of some elementary reciprocal branch networks.

Partial Factoring of Determinants

As the network becomes more complicated, the search for all possible trees becomes more tedious. The job can be done systematically by alphabetically (or numerically) ordering the branch admittances within each tree value, and then searching for trees in alphabetical sequence until the dictionary is exhausted. For all but the simplest networks it is very convenient to condense the form of a determinantal expression by grouping all the terms which contain some chosen set of branch admittances, and then writing that part of the determinant in factored form. This reduces the number of symbols in the expression, with a consequent saving of labor in the calculation of a numerical value (it is cheaper to add before multiplying). In Fig. 5(g), for example, the expanded form of Δ contains six symbols, whereas the partially factored form, $a(b+c)+bc$, has only five. In more complicated networks the saving is much greater. Fortunately, *we can write the determinant directly in a partially factored form* with the aid of the following definitions:

path: a simple string of branches terminating at two specified nodes. (A simple string does not intersect itself nor does it have dangling appendages or isolated parts.) (4)

path value (P_k): product of the branch admittances in path k. (5)

path cofactor (Δ_k): the determinant of the network remaining when all the branches in path k are short-circuited (collapsed). The cofactor is unity if the remaining network has only one node. (6)

These definitions lead to the very useful result,

$$\Delta = \sum_k P_k \Delta_k. \tag{7}$$

In accordance with accepted mathematical terminology, we shall refer to (7) as an *expansion in paths or expansion on a node pair*, even though the process actually represents, in the descriptive sense, a condensation of the determinantal expression rather than an expansion. Each cofactor Δ_k is itself a determinantal entity, and can therefore be expanded in a new set of paths. Such expansions can be continued until all remaining cofactors are unity. This means that the determinant can be evaluated entirely in terms of paths and subpaths without trees ever being considered. The amount of

actual condensation of the determinantal expression achieved by an expansion in paths will depend, of course, upon the structure of the particular network under consideration and upon the choice of node pairs for the expansion and subexpansions.

The proof of (7) follows from the fact that each tree contains one, and only one, path between two specified nodes, and that the product of a path with each of the terms of its cofactor is a tree.

Fig. 6 illustrates expansion of a determinant for two different choices of the expansion node pair. The chosen nodes are shown darkened in the figure. Observe that choice (a) accomplishes the greater amount of condensation, reducing number of symbols from 24 to 13.

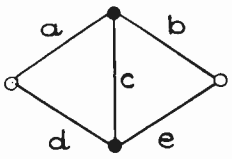

$P_1 = ad, \quad \Delta_1 = b + e$

$P_2 = c, \quad \Delta_2 = (a+d)(b+e)$

$P_3 = be, \quad \Delta_3 = a + d$

$\Delta = \Sigma P_k \Delta_k = ad(b+e) + c(a+d)(b+e) + be(a+d)$

trees: adb, ade, cab, cae, cdb, cde, bea, bed

(a)

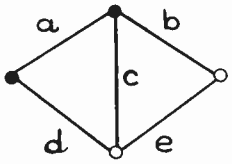

$P_1 = a, \quad \Delta_1 = (d+c)(b+e) + be$

$P_2 = cd, \quad \Delta_2 = b + e$

$P_3 = bed, \quad \Delta_3 = 1$

$\Delta = \Sigma P_k \Delta_k = a[(d+c)(b+e) + be] + cd(b+e) + bed$

(b)

Fig. 6—Expansion of a determinant on a node pair.

The Determinant of a Network Containing Gyristors or Unistors

When nonreciprocal branches are present, the rules of the game change slightly. The required modifications can be summarized as follows:

> In a network containing unistors or gyristors the ground node must be specified. A *tree value vanishes* if any *unistor points away from ground* in that tree. A *tree value is multiplied by minus one* for each *gyristor pointing away from ground* in that tree. With gyristors and unistors present, expansion of Δ in paths and cofactors is meaningful only if each path contains the ground node. Since a path is part of a tree, the special rules for tree value also apply in finding path values. (8)

Two examples are given in Fig. 7. The expansion is carried out on the two darkened nodes, and one of these is located at ground in order to insure that each path shall contain the ground node. Note that in Fig. 7(b) such paths as *bhc* disappear from the calculation, since

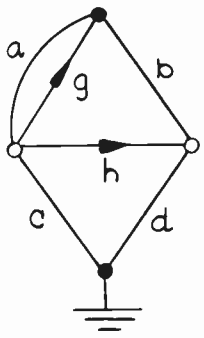

$P_1 = (a-g)c, \quad \Delta_1 = b + d - h$

$P_2 = bd, \quad \Delta_2 = a + c + g + h$

$P_3 = (a-g)\,hd, \quad \Delta_3 = 1$

$P_4 = b(-h)\,c, \quad \Delta_4 = 1$

$\Delta = c(a-g)(b+d-h) + bd(a+c+g+h) + (a-g)\,hd - bhc$

(a)

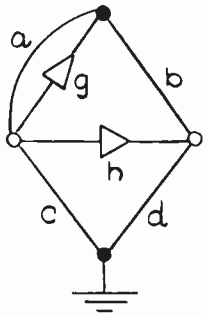

$P_1 = ac, \quad \Delta_1 = b + d$

$P_2 = bd, \quad \Delta_2 = a + c + g + h$

$P_3 = ahd, \quad \Delta_3 = 1$

$\Delta = ac(b+d) + bd(a+c+g+h) + ahd$

(b)

Fig. 7—The determinant of a network containing (a) gyristors, and (b) unistors.

a unistor points away from ground in that path. For the same reason, unistor *h* is absent from the cofactor Δ_1 of the first path *ac*.

The Determinant of a Network Containing Gyrators or Transconductances

With a gyrator present in the network, the set of all trees in the network can be divided into three classes: those containing none of the gyrator branches, those containing one, and those containing two. With the ground node designated, we can do a bit of general mental bookkeeping to find that the trees containing only one gyrator branch will occur in pairs whose values are equal but of opposite sign. Hence trees containing only one gyrator branch can be ignored when the determinant is evaluated. Moreover, the trees containing two gyrator branches will occur in triplets whose values are the same except for algebraic signs. For any fixed choice of a ground node, it can be seen that the square of the gyrator admittance enters two of the three tree values with a positive sign, and enters the third with a negative sign.

As a consequence of all this, we can expand Δ in terms of the square of the gyrator admittance to obtain

$$\Delta = (\Delta \text{ with gyrator erased}) + g^2(\Delta \text{ with gyrator collapsed}). \quad (9a)$$

In short,

$$\Delta(g) = \Delta(0) + g^2\Delta_g \quad (9b)$$

where Δ_g is the cofactor of the gyrator. If the network contains more than one gyrator, $\Delta(0)$ and Δ_g can each be expanded in terms of one of the other gyrators, and so on until all of the gyrator admittance squares have been partially factored. (Two gyrators having the same three terminals in common are, of course, equivalent to a single gyrator, and are therefore not susceptible to separate expansion.)

The network determinant defined here in terms of trees is, in fact, identical with the mathematical determinant of the node-pair voltage equations of the electric network. From the rules of the topological game, we have found that the effect of the gyrator upon Δ is independent of the choice of ground node. This checks with the physical fact that the gyrator is a floating element. For a network composed of positive real resistors, the mathematical determinant of the node-voltage equations is known to be positive. Eq. (9) shows that the addition of a real gyrator to such a network can only increase the value of the determinant and, in particular, cannot cause the determinant to become negative. This checks with the physical fact that a real gyrator is a passive lossless element.

Fig. 8(a) shows the path expansion of the determinant of a simple network containing a gyrator. In the final expression we can recognize the determinant (abc) of the network remaining when the gyrator is erased, and the determinant $(b+c)$ of the network remaining when the gyrator is collapsed. With the aid of (9) the answer could have been obtained without the choice of a ground node and subsequent expansion in paths.

Fig. 8(b) gives the path expansion for a simple network containing a floating transconductance model. The choice of ground node is arbitrary, of course, but the path expansion can be made particularly simple by locating the ground node at the grid, since only one of the three unistors then enters the calculation. It is apparent, therefore, that the determinant cannot involve the square of the transconductance g_m. Consideration of possible trees in a general network containing a transconductance shows that the determinant can be expanded as follows:

$$\Delta(g_m) = \Delta(0) + g_m \sum_k P_k^* \Delta_k^* \tag{10a}$$

P_k^* = a path between grid and plate not touching the cathode. (10b)

Δ_k^* = cofactor of P_k^* with the cathode now short-circuited to the grid or plate. (10c)

The expression for Δ in Fig. 8(b) offers an example of the general rule.

The expansion for a unator element is not so convenient or useful as the expansions for gyrators and transconductances, because the unator brings in terms involving both the first power and the square of unator admittance. Details will not be taken up here.

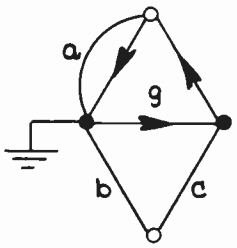

$P_1 = g(a+g), \quad \Delta_1 = b + c$

$P_2 = -g, \quad \Delta_2 = a(b+c)$

$P_3 = bc, \quad \Delta_3 = a$

$\Delta = \Sigma P_k \Delta_k = abc + g^2(b+c)$

(a)

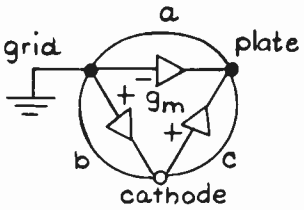

$P_1 = a, \quad \Delta_1 = b + c + g_m$

$P_2 = bc, \quad \Delta_2 = 1$

$\Delta = a(b+c) + bc + g_m(a)$

(b)

Fig. 8—The determinant of a network containing (a) a gyrator and (b) a transconductance.

The Transmission of a Branch Network

The transmission of a branch network can be measured by attaching or inserting a source branch (s) and a meter branch (m). If several sources and meters are present, only one pair need be considered at a time, since sources are superposable and meters are independent. A few more statements and rules will complete the picture and give us a topological formulation of the transmission.

transmission (T): ratio of meter reading to source value. (11)

transmission path: a path *containing the meter branch* and terminating at the two nodes where the source is attached to the network. (12)

transmission path value (P_k'): product of the branch admittances in transmission path k, with the meter branch counted as unity admittance. The associated algebraic sign is plus (or minus) if a positive source, acting through that path, tends to make the meter reading positive (or negative). (13)

transmission path cofactor (Δ_k'): determinant of the network remaining when the kth transmission path, *including the meter branch*, is collapsed. (14)

The final result, for which a proof will be indicated later, is

$$T = \frac{\sum P_k' \Delta_k'}{\Delta} = \frac{\sum P_k' \Delta_k'}{\sum P_k \Delta_k}. \tag{15}$$

For the evaluation of Δ, voltage sources and ammeters are short-circuited (collapsed) and current sources and voltmeters are open-circuited (erased). (16)

The expression for transmission T is based upon the assumption that one end of the meter is located at the ground node. Consequently, in a network containing unistors or gyristors the *transmission path value* P_k' is *zero if any unistor points away from the meter* in that path, and the transmission path value is *multiplied by minus one for each gyristor pointing away from the meter* in that path. (17)

Fig. 9 illustrates the application of the transmission formula to the calculation of impedance or admittance at a pair of terminals. In Fig. 9(a) the transmission path contains only the voltmeter. With the voltmeter short-circuited, the transmission-path cofactor is recognizable as the determinant of branches b and c in parallel. In Fig. 9(b) there are two different transmission paths which must be considered in evaluating the numerator of the transmission expression. For the denominator, short-circuiting both the meter and the source leaves a two-node network with branches b and c in parallel.

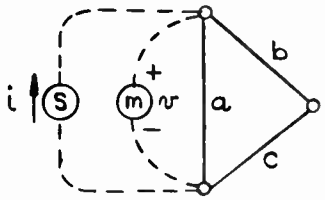

$$P_1' = 1, \quad \Delta_1' = b + c$$

$$P_1 = a, \quad \Delta_1 = b + c$$

$$P_2 = bc, \quad \Delta_2 = 1$$

$$\frac{v}{i} = \frac{\Sigma P_k' \Delta_k'}{\Sigma P_k \Delta_k} = \frac{b + c}{a(b+c) + bc} = \frac{1}{a + \frac{bc}{b + c}}$$

(a)

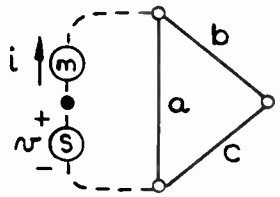

$$P_1' = a, \quad \Delta_1' = b + c$$

$$P_2' = bc, \quad \Delta_2' = 1$$

$$\Delta = b + c$$

$$\frac{i}{v} = \frac{\Sigma P_k' \Delta_k'}{\Delta} = \frac{a(b+c) + bc}{b + c} = a + \frac{bc}{b + c}$$

(b)

Fig. 9—Calculation of (a) input impedance and (b) input admittance.

Further examples are given in Fig. 10. Fig. 11, on the next page, shows the transmission of a bridge circuit 1) containing only reciprocal branches and 2) containing gyristors. Notice that transmission path P_2' in Fig. 11(a) has an associated negative sign because the source current flowing through the meter *via that path* would tend to make the meter reading negative. For the same path in Fig. 11(b), an additional minus sign enters the path value because gyristor d points away from the meter in that path.

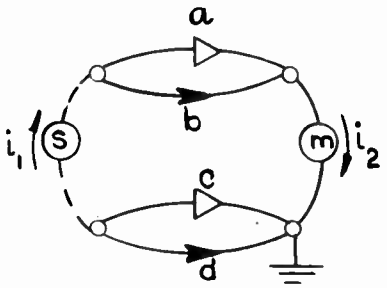

$$\frac{i_2}{i_1} = \frac{(a+b)(c+d)}{(a+b)(c+d)} = 1$$

(a)

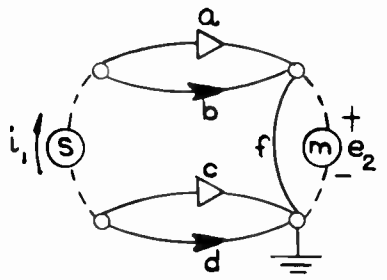

$$\frac{e_2}{i_1} = \frac{(a+b)(c+d)}{f(a+b)(c+d)} = \frac{1}{f}$$

(b)

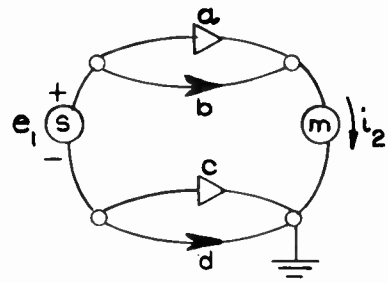

$$\frac{i_2}{e_1} = \frac{(a+b)(c+d)}{a + b + c + d}$$

(c)

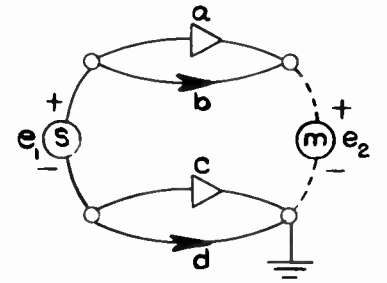

$$\frac{e_2}{e_1} = \frac{(a+b)(c+d)}{-b(c+d)} = \frac{a + b}{-b}$$

(d)

Fig. 10—Some simple network transmissions which illustrate the topological rules.

A Simple Electronic Circuit Problem

The basic cathode-follower triode circuit is shown in Fig. 12(a). Since the plate-supply potential is assumed to be fixed, the input voltage source appears between plate and grid in the linear incremental model (b). There is only one transmission path and its value is nonzero, since the grid-to-cathode unistor points toward the meter in that path. To evaluate the determinant of the network, we first short-circuit the voltage source and the ammeter, which places the two positive unistors in parallel with each other and in parallel with g_p and G_k.

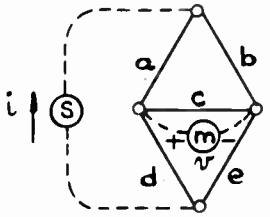

$$P_1' = ae, \quad \Delta_1' = 1$$
$$P_2' = -bd, \quad \Delta_2' = 1$$
$$P_1 = c, \quad \Delta_1 = (b+a)(d+e)$$
$$P_2 = ab, \quad \Delta_2 = d + e$$
$$P_3 = de, \quad \Delta_3 = b + a$$

$$T = \frac{v}{i} = \frac{\Sigma P_k' \Delta_k'}{\Sigma P_k \Delta_k} = \frac{ae - bd}{c(b+a)(d+e) + ab(d+e) + de(b+a)}$$

(a)

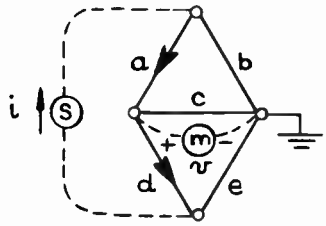

$$P_1' = ae, \quad \Delta_1' = 1$$
$$P_2' = -b(-d), \quad \Delta_2' = 1$$
$$P_1 = c, \quad \Delta_1 = (a+b)(e-d)$$
$$P_2 = -ab, \quad \Delta_2 = (e-d)$$
$$P_3 = de, \quad \Delta_3 = a + b$$

$$T = \frac{ae + bd}{c(a+b)(e-d) - ab(e-d) + de(a+b)}$$

(b)

Fig. 11—Transmissions of (a) a bridge and (b) a bridge containing gyristors.

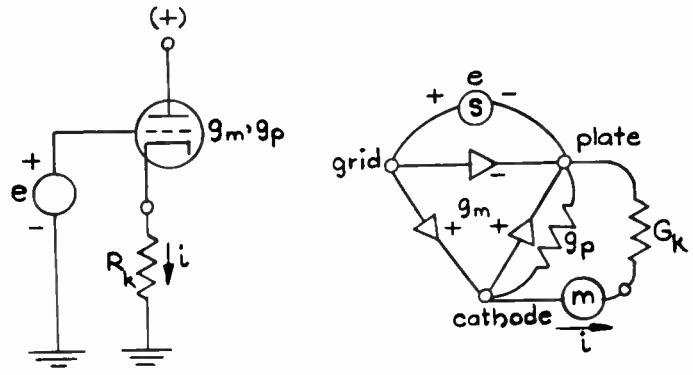

(a) (b)

$$P_1' = g_m G_k, \quad \Delta_1' = 1$$
$$\Delta = g_m + g_p + G_k$$
$$\frac{i}{e} = \frac{g_m G_k}{g_m + g_p + G_k}$$

Fig. 12—The transfer conductance of a cathode-follower.

No matter which of the two remaining nodes is chosen as ground, the determinant will be the same. Another way of arriving at the same conclusion is to notice that when the source and meter are short-circuited, the two unistors thereby placed in parallel are equivalent to a single reciprocal branch, as indicated in Fig. 2(j).

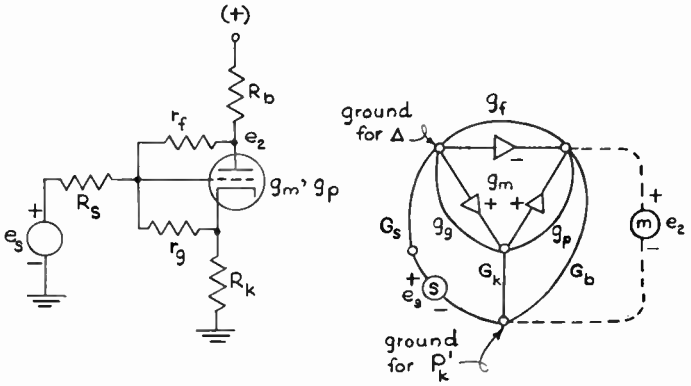

(a) (b)

$$P_1' = G_s(g_f - g_m), \quad \Delta_1 = G_k + g_g + g_p + g_m$$
$$P_2' = G_s(g_g + g_m)(g_p + g_m), \quad \Delta_2' = 1$$
$$P_1 = g_f, \quad \Delta_1 = (g_g + g_p + g_m)(G_s + G_b + G_k) + G_k(G_s + G_b)$$
$$P_2 = g_g g_p, \quad \Delta_2 = G_s + G_b + G_k$$
$$P_3 = G_s G_b, \quad \Delta_3 = g_g + g_p + g_m + G_k$$
$$P_4 = G_s G_k g_p, \quad \Delta_4 = 1$$
$$P_5 = g_g G_k G_b, \quad \Delta_5 = 1$$

$$\frac{e_2}{e_s} = \frac{\sum P_k' \Delta_k'}{\sum P_k \Delta_k} = \frac{G_s[g_f(G_k + g_g + g_p) + g_g g_p + g_m(g_f - G_k)]}{(G_s + G_b + G_k)[g_f(g_g + g_p) + g_g g_p + g_f g_m]} + G_s G_b(g_g + g_p + g_m + G_k) + G_s G_k(g_p + g_f) + G_b G_k(g_g + g_f) + G_s G_b G_k$$

Fig. 13—The voltage gain of a triode feedback amplifier.

A Triode-Amplifier Problem

A more complicated triode-amplifier circuit is shown in Fig. 13(a) and the linear incremental model in Fig. 13(b). Straightforward application of the topological rules yields the transmission expression. There is some cancellation of terms in the numerator. For example, the negative term, $G_s g_m g_g$, in $P_1'\Delta_1'$ is cancelled by an equal positive term in $P_2'\Delta_2'$. Specialized rules can be developed, enabling us to discard at the outset those terms destined for cancellation. Such rules, however, complicate the inspection process. The basic transmission-path rules used in Fig. 13 have the advantage of being simple to remember, and some cancellation of terms in the numerator is perhaps not too great a price to pay for this simplicity of method.

No cancellation of terms occurs in the denominator because in this particular example there is only one transconductance in the circuit and we can choose the grid terminal as a ground reference for the evaluation of Δ. Alternatively, the special expansion (10) can be used.

Still another approach is to expand the determinant in terms of the set of branches connecting at some particular node. The transmission denominator in Fig. 13 has been written in just such form. All trees in the network must touch the lowermost node, and therefore each tree must contain either G_s, or G_k, or G_b, or two of these, or all three. The trees containing only one of these

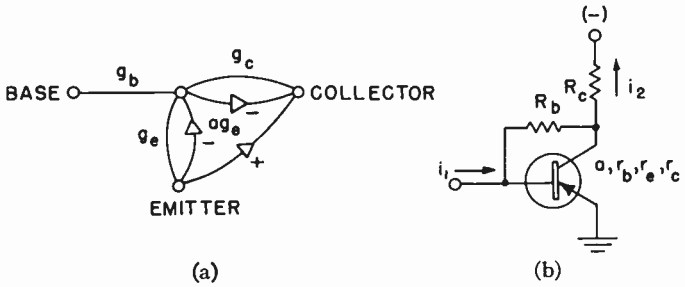

$$P_1 = P_1' = G_bG_c, \qquad \Delta_1 = \Delta_1' = g_b + g_e + (1-a)g_e$$

$$P_2 = P_2' = g_b(g_c - ag_e)G_c, \qquad \Delta_2 = \Delta_2' = 1$$

$$P_3 = g_bg_e, \qquad \Delta_3 = G_b + g_e + G_c$$

$$P_4 = G_bg_cg_e, \qquad \Delta_4 = 1$$

$$\frac{i_2}{i_1} = \frac{\sum P_k'\Delta_k'}{\sum P_k\Delta_k} = \frac{G_bG_c[g_b + g_e + (1-a)g_e] + g_bG_c(g_c - ag_e)}{G_bG_c[g_b + g_e + (1-a)g_e] + g_bG_c(g_c - ag_e)} + g_bg_e(G_b + G_c + g_e) + G_bg_cg_e$$

$$\frac{i_2}{i_1} \to \frac{[G_b - a(G_b + g_b)]G_c}{(G_b + g_b)[(1-a)G_c + g_e] + G_bg_b}, \text{ for } g_e \text{ large}$$

Fig. 14—The current gain of a transistor amplifier. (a) The unistor model of a transistor, (b) the amplifier circuit; and (c) the linear incremental circuit model.

branches can be grouped and factored as shown. The bracketed expression in the denominator of Fig. 13 is the determinant of the network remaining when any one of the three branches G_e, G_c, or G_b is short-circuited and the other two are open-circuited. Similarly, the cofactor of G_eG_b is just the determinant of the network remaining when G_e and G_b are short-circuited and G_c is open-circuited. The cofactor of $G_eG_bG_c$ is unity, since the network reduces to a single node when all three of these branches are short-circuited.

A Transistor Amplifier Problem

Fig. 14 shows a transistor amplifier (b) and its linear incremental model (c). Fig. 14(a) shows the transconductance representation of the current-transfer effect in the transistor. The transconductance is equal to ag_e, where a is the familiar current-transfer factor of the transistor and g_e is the emitter conductance. Notice that the algebraic signs of the unistor admittances are opposite to those in a vacuum-triode transconductance. The sign reversal accounts for the fact that the emitter-to-collector gain of a transistor is positive, whereas the grid-to-plate gain of a triode is negative. For the grounded-emitter connection, of course, two of the unistors disappear.

If the emitter conductance g_e is assumed to be very large, the current gain of the amplifier approaches the form shown at the bottom of Fig. 14. This limiting form can be obtained directly by formulating the paths and cofactors with the understanding that g_e is large and that all trees not containing g_e are to be ignored at the outset.

Outline of a Proof of the Topological Rule

Consider a network composed entirely of unistors. This entails no loss of generality, since both reciprocal branches and gyristors can be constructed from unistors. Attach a *voltage source* between ground and some specified node, and let e_k be the resulting voltage at node k, relative to ground. Now consider the voltage transmission ratio, as computed from (15). Let

$$u_{jk} = \text{unistor running from node } j \text{ to node } k \tag{18}$$

$$T_k = \text{transmission from source to node } k \tag{19}$$

$$N_k = \text{numerator of } T_k. \tag{20}$$

In general, the network exhibits a number of different loops. A *loop* is a simple closed path of unistors with all unistors pointing in the same direction around the closed path. The *loop value* is the product of the unistor admittances in that loop. Let

$$L_{kr} = \text{value of the } r\text{th loop containing node } k. \tag{21}$$

$$N_{kr} = \text{value of } N_k, \text{ as computed with loop } L_{kr} \text{ collapsed.} \tag{22}$$

Consideration of the transmission paths and cofactors in the numerator of the transmission expression leads to the expansions

$$\sum_r L_{kr}N_{kr} = N_k \sum_j u_{kj} \tag{23}$$

$$\sum_r L_{kr}N_{kr} = \sum_j N_ju_{jk}. \tag{24}$$

Each term of the product $L_{kr}N_{kr}$ contains exactly one unistor radiating from node k. Hence we can expand the set of products $L_{kr}N_{kr}$ in terms of either the incoming unistors u_{jk} or the outgoing unistors u_{kj} at node k.

As a consequence of (23) and (24), we have

$$N_k \sum_j u_{kj} = \sum_j N_ju_{jk}. \tag{25}$$

Now, since transmission T_j all have the same denominator, and since $T_j = e_j/e_s$, where e_s is the source voltage, we find

$$e_k \sum_j u_{kj} = \sum_j e_ju_{jk}. \tag{26}$$

Relation (26) is recognizable as the electrical node-voltage equation at node k. This result states, in effect, that *the topological rules imply the electrical node-voltage equations of the network*. Hence, the transmission computed from the topological rules must be the unique and correct transmission of the electric network.

The relationships derived above are not quite the whole story, since they obviously do not verify the form

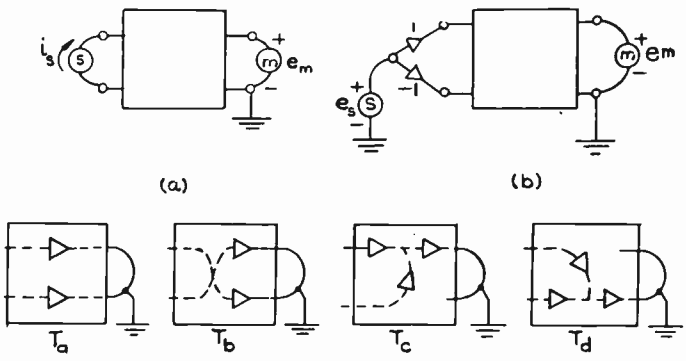

$$\frac{e_m}{e_s} = (T_a + T_c) - (T_b + T_c)$$

$$\frac{e_m}{i_s} = \frac{e_m}{e_s} = T_a - T_b$$

Fig. 15—Proof of the path rule for an ungrounded source.

of the denominator of the transmission formula (15). To verify the denominator, we need only observe that the topological formula gives unity transmission for a voltage source and a voltmeter located at the same node pair.

For the source ungrounded, the correctness of the topological transmission formula can be established with the help of Fig. 15. An ungrounded current source (a) can obviously be replaced by a grounded voltage source connected to the network through two unistors. Now consider the various ways in which a tree containing the meter branch can provide connections between each of the two input nodes and each of the two meter nodes. The four possibilities are shown in Fig. 15(c). Each of the first three configurations contains a possible transmission path from one of the input nodes to the meter, and the portion of the tree not in the transmission path represents a possible term in the transmission-path cofactor. By direct application of the grounded-source transmission formula to the network of Fig. 15(b), we find that transmissions of Type T_c cancel, leaving only T_a and T_b. It follows that the topological rules give the correct answer for an ungrounded source, provided an algebraic sign rule is included to account for the direction in which the transmission path passes through the meter.

Once the topological formula has been verified for a current source, it is a simple matter to show that the rules also accommodate voltage sources. To do this, simply attach a reciprocal branch in parallel with the current source, and then replace the combination by an equivalent voltage source in series with that branch. The topological rules are compatible with such transformations. In a similar fashion, the voltage measured across a branch and the current flowing in that branch, as computed by the topological rules, evidently satisfy Ohm's law.

Conclusion

Topological methods provide great insight into the properties of networks, and a knowledge of such methods can give much intuitive aid to the circuit designer or analyst even in those many cases when it is more convenient to formulate and solve the problem by formal matrix and determinantal methods. Topological rules are an invaluable means of checking the reasonableness of any doubtful terms in the answer or of estimating the error in an approximation, since trees and paths are easy to identify. In a practical problem involving a rather complicated network, there may be dozens or hundreds of terms in the final transmission expression. However, knowing the numerical values of the various branch admittances, we can search about in the network for those paths and trees and cofactors which will lead to numerically dominant terms. The negligible terms never need be written down at all. This is a real saving.

The topological approach offers an alternate viewpoint which complements and enhances the more familiar classical analysis methods. It is always better to know two ways of solving a problem rather than one, or seven ways rather than six, for then we can choose a particular approach or combination of approaches, or invent a new approach suggested by the others, so as to solve the problem at hand in the simplest and most satisfying manner.

Acknowledgment

Needless to say, I am greatly indebted to W. S. Percival for the background and the stimulation afforded by his classic papers. I should also like to thank R. B. Adler, G. Amster, and E. F. Bolinder, all of this Laboratory, for helpful discussions; and recent students in M.I.T. Subject 6.633 for their steadfast refusal to take things for granted.

Theory and Experiments on Shot Noise in Semiconductor Junction Diodes and Transistors*

W. GUGGENBUEHL† AND M. J. O. STRUTT†, FELLOW, IRE

Summary—**This paper presents a general theory of junction diode and transistor shot noise in the region of low-level injection currents as dependent on frequency including lf and hf regions. Equations for noise figures in the three basic transistor connections are derived; these equations are believed to be new as well as in agreement with experimental results. Experimental curves at high-level injection are presented. Coordination with previous theoretical and experimental data is shown to be satisfactory in the lf region. In the hf region, previous theoretical results, after proper adjustment, coincide with the present ones.**

I. Introduction

THIS investigation pertains to shot noise as separate from flicker noise. The term "shot noise" designates the fluctuations due to the random elementary particle character of conduction and thermal agitation, whereas "flicker noise" contains also other causes of fluctuations, due mainly to inhomogenities (traps) in the semiconductor material.[1]

At low frequencies, the experimental difference between these noise types is easy to formulate: Flicker noise intensity has approximately a 1/f spectrum; perhaps superimposed humps. Shot-noise intensity has a white spectrum (independent of frequency) at lf. At higher frequencies, shot-noise intensity becomes frequency dependent too. However, in semiconductors of purer material, flicker noise is relatively less important as compared with shot noise for frequencies above some few kilocycles.

Papers on the theory of shot noise in diodes and transistors have been published by Weisskopf,[2] Petritz,[3] Montgomery and Clark,[4] van der Ziel,[5] and Giacoletto.[6] This subject has been treated further in van der Ziel's able book on noise.[7] All these publications pertain mainly to the frequency independent lf region of shot noise. The hf region has only received scanty treatment up to this date. Van der Ziel[8] by corpuscular reasoning has established a theory of shot noise in junction diodes and transistors which pertains to lf as well as to hf regions. His solution is, however, restricted to the validity of the linear diffusion equation with volume recombination. Reference is also made to a previous paper published by the authors.[9] The theory as presented here is of a general character as regards the processes of current flow and recombination in these devices. It is limited to low current densities. Previous results of others and of the present authors are shown to be in the nature of special cases of this theory. Experiments are shown to be in good concordance with the present theory at low current densities. Deviations at high current densities are discussed.

II. Theory of Shot Noise in Semiconductor Junction Diodes at Low Current Densities

Two methods for treating noise problems are known, the thermodynamic theory (H. Nyquist) and the corpuscular theory (W. Schottky). The thermodynamic argument makes no use of special models pertaining to the random processes in electronic devices. However, the exact deviation of Nyquist's formula is valid only for thermal equilibrium; *i.e.*, the device under consideration is exchanging energy only with a surrounding closed space of the same temperature. The same amount of energy as absorbed is emitted again by the device under equilibrium conditions.

It is well known, however, that Nyquist's formula is also applied to circuits where the different parts (the impedances) are not at the same absolute temperature T.[10] Then noise power flow arises from the part of higher temperature to the parts of lower temperature. In most practical cases, the amount of energy delivered in this way from one element to the other is small compared with the total energy stored in the system. In these cases of *quasithermal equilibrium* Nyquist's formula is valid too. It may be written in the form that a device of absolute temperature T delivers a random power to a connected circuit, the optimal mean value of which is $P_a = kT\Delta f$ (k = Boltzmann's constant, Δf frequency interval under consideration, P_a available power). This thermo-

* Original manuscript received by the IRE, September 6, 1956; revised manuscript received, November 20, 1956.

† Dept. of Advanced Elec. Eng., Swiss Federal Inst. of Tech., Zurich, Switzerland.

[1] W. H. Fonger, "A determination of 1/f noise sources in semiconductor diodes and triodes," in "Transistors I." RCA Labs., Princeton, N. J., pp. 239–296; 1956.

[2] V. F. Weisskopf, "On the Theory of Noise in Conductors, Semiconductors and Crystal Rectifiers," NDRC, No. 14–133; May 15, 1943.
See also H. C. Torrey and C. A. Whitmer, "Crystal Rectifiers," McGraw-Hill Book Co., Inc., New York, N. Y.; 1948.

[3] R. L. Petritz, "On the theory of noise in *p-n* junctions and related devices," PROC. IRE, vol. 40. pp. 1440–1456; November, 1952.

[4] H. C. Montgomery and M. A. Clark, "Shot noise in junction transistors," *J. Appl. Phys.*, vol. 24, pp. 1337–1338; October, 1953.

[5] A. van der Ziel, "Note on shot and partition noise in junction transistors," *J. Appl. Phys.*, vol. 25, pp. 815–816; June, 1954.

[6] L. J. Giacoletto, "The Noise Factor of Junction Transistors," in "Transistors I," RCA Labs., Princeton, N. J., pp. 296–308; 1956.

[7] A. van der Ziel, "Noise," Prentice-Hall, Inc., New York, N. Y.; 1954.

[8] A. van der Ziel, "Theory of shot noise in junction diodes and junction transistors," PROC. IRE, vol. 43, pp. 1639–1646; November, 1955.

[9] W. Guggenbuehl and M. J. O. Strutt, "Theorie des Hochfrequenzrauschens von Transitoren bei kleinen Stromdichten," *Nachrichtentechnische Fachberichte, Beihefte der NTZ*, vol. 5, pp. 30–33; 1956.

[10] F. B. Llewellyn, "A study of noise in vacuum tubes and attached circuits," PROC. IRE, vol. 18, pp. 243–265; February, 1930; Appendix: Note 4.

dynamic result is illustrated by an equivalent noise voltage generator u_n in series with impedance Z under consideration, or by an equivalent noise current generator i_n in parallel to Z (see Fig. 1).

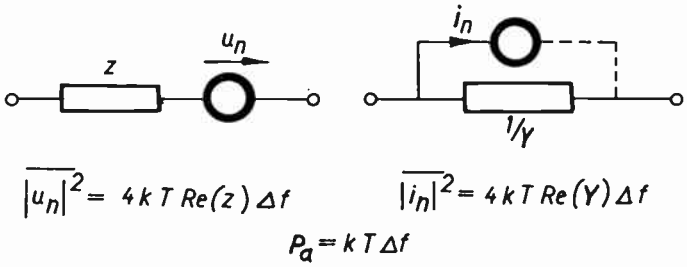

Fig. 1—Equivalent noise circuits of a two-pole of impedance Z (admittance Y) without current flowing through it.

If a device is carrying nonrandom current, thermal equilibrium does not exist and the so-called corpuscular theory of noise is mostly applied. In this theory the effects of the individual random events are integrated in the region between the terminals. This has been carried out for junction diodes and transistors in the lf region.[2,7,11,12] In the hf region, however, the calculations become cumbersome as may be seen from van der Ziel's treatment.[8]

The theory as presented here is based on a combination of thermodynamical and corpuscular arguments. It is shown, that the whole theory of noise semiconducting diodes and transistors can be formulated in a simple and concise way if some plausible assumptions concerning the noise behavior of current carrying devices are stated.

We first consider a p-n junction diode carrying the direct current I. I is assumed to be positive in the direction from p to n material. This device is not in thermal equilibrium, because a current I accompanied by a fluctuation current due to the corpuscular structure of electric charges is passing through the diode. We *assume* (*first assumption*) that a quasithermal-equilibrium condition can be restored by supplying a noise current i_{nI} to the diode terminals which exactly balances out the fluctuations accompanying the direct current I at the terminals [Fig. 2(a)]. This additional noise current is normally small compared with the dc current I and so the superposition principle of noise currents is applicable to this case. Now I can be regarded as an *exact* dc current without any accompanying random part at the terminals. No noise power exchange is connected any longer with the current I. Then the residual fluctuation power exchange will be the same as in the case of quasithermal equilibrium. It seems reasonable, to use the formula mentioned above for quasithermal equilibrium to calculate the fluctuation currents of such a diode including the supplementary noise current i_{nI}.

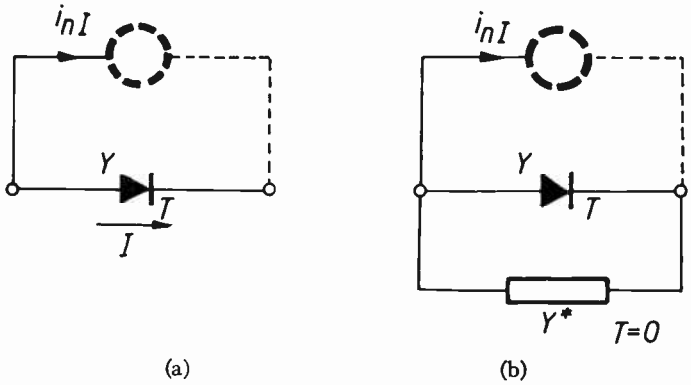

Fig. 2—(a) Semiconductor diode completed by an additional noise source i_{nI} (dotted circle) to restore quasithermal equilibrium. (b) Diode of (a) with an admittance Y^* of absolute temperature $T=0$ connected to its terminals. This entire circuit is approximately in quasi-thermal equilibrium.

A noise power is connected with this additional noise supply current i_{nI} which is necessary for restoring quasithermal equilibrium. The amount of this power P_{nI} depends on the total admittance between the diode terminals. If the diode is connected to an admittance Y^* at absolute temperature $T=0$ which is conjugate complex to the diode's admittance Y at an absolute temperature T [Fig. 2(b)] this power P_{nI} is given by

$$P_{nI} = \frac{\overline{|i_{nI}^2|}}{2\,\mathrm{Re}\,(Y)} \tag{1}$$

whereas the thermal noise power dissipated in this circuit is given by

$$P_{nth} = \frac{4kT\,\mathrm{Re}\,(Y)\Delta f}{Y + Y^*}. \tag{2}$$

Our *second assumption* concerns the direction of flow of the additional noise power P_{nI}. We assume that P_{nI} is a power source supplying power *to* the diode circuit for restoring thermal equilibrium, if the dc current I flows in the *forward* direction of the diode. On the other hand, P_{nI} is a power sink, dissipating power delivered by the diode circuit, if the dc current I is flowing in the reverse direction of the diode. This assumption is not unreasonable as the majority of the carriers constituting the direct current I have to mount against the internal potential hill of the diode, thus consuming energy, if I is a forward current. Inversely, they fall down the potential hill if I is a reverse current, thus gaining energy. But actually, there is no exact physical proof for the above assumption.

[11] W. Guggenbuehl and M. J. O. Strutt, "Experimentelle Bestätigung der Schottky'schen Rauschformeln, an neueren Halbleiterflächendioden im Bereich des weissen Rauschspektrums," *Arch. Elekt. Uebertragung*, vol. 9, pp. 103–108; 1955.

[12] W. Guggenbuehl and M. J. O. Strutt, "Experimentelle untersuchung und Trennung der Rauschursachen in Flaechentransistoren." *Arch. Elekt. Uebertragung*, vol. 9, pp. 259–269; June, 1955.

W. Guggenbuehl, "Beitraege zur Kenntnis des Halbleiterrauschens mit besonderer Beruecksichtigung von Kristalldioden und Transistoren," thesis, Swiss Federal Inst. of Tech., Zurich, Switzerland; 1955.

With these two assumptions the total short-circuit noise current i_{ntot} of the diode is given by

$$\underbrace{\overline{|i_{n\,tot}^2|} \pm \overline{|i_{nI}^2|}}_{\text{additional current noise}} = \underbrace{4kT\,\mathrm{Re}\,(Y)\Delta f}_{\text{thermal equilibrium noise}} \quad (3)$$

where the plus sign holds in the forward direction and the minus sign in the backward direction of the dc current I. Similar arguments concerning the direction of power flow hold in the well-known case of high vacuum diodes. If the high vacuum diode is operated in its current saturation region, the electrons are falling down the internal potential hill, thus being able to deliver noise power to an associated circuit. The total short-circuit noise current may be written according to our convention of the direction of additional noise power flow

$$\overline{|i_{n\,tot}^2|} = 4kT\,\mathrm{Re}\,(Y)\Delta f + 2eI\Delta f. \quad (4)$$

The expression $2eI\Delta f$ corresponds to $\overline{|i_{nI}^2|}$ of (3). Here e is the absolute value of electronic charge. Since the diode admittance Y is zero for this case the formula reduces to the well-known Schottky formula.

On the other hand, the electrons constituting the direct current I are mounting against the internal potential hill, if the diode is operated in its exponential region. The additional power source for restoring quasi-thermal equilibrium must deliver power to the diode. According to our assumption regarding the direction of power flow, this leads part to a minus sign for the current contribution to the total noise current

$$|i_{n\,tot}^2| = 4kT_c\,\mathrm{Re}\,(Y)\Delta f - 2eI\Delta f \quad (5)$$

where T_c is the cathode's absolute temperature.

Since $kT_c\mathrm{Re}(Y)=eI$ for the exponential region at lf, the above equation reduces to

$$\overline{|i_{n\,tot}^2|} = 2eI\Delta f. \quad (6)$$

This formula is well known for the exponential region of a high vacuum diode.

In order to complete the noise formula of junction diodes, the additional noise current source $\overline{|i_{nI}^2|}$ must be calculated. Since this noise current is the image of the fluctuations of the current I due to its corpuscular structure at the diode terminals, the mean square values of these two noise currents are equal. Due to the neutrality condition in the diffusion regions of the diode, the individual carriers constituting the current I are supplied to the diode terminals at the same time as a carrier is crossing the depletion layer of the junction. If the density of injected minority carriers is small compared with the majority carrier density, and if a short circuit is applied to the diode terminals, the carriers crossing the depletion layer are independent of each other. Thus, in this case, Schottky's formula for shot-noise current in a high vacuum diode may be applied and i_{nI} is given by

$$\overline{|i_{nI}^2|} = 2e|I|\Delta f. \quad (7)$$

This equation holds as long as the mean frequency f, associated with the frequency interval Δf, is small compared with the reciprocal value of the transit time through the depletion layer. This transit time is very much shorter than the lifetimes of the minority carriers, which are responsible for the ac performance of the diode. Hence, (7) may be applied to the entire frequency range of practical interest.

At high injection levels, the voltage between the diode terminals does not agree with the voltage across the depletion layer. If a short circuit is applied to the diode terminals, the voltage across the depletion layer is dependent on the number of carriers that abide in the diffusion-drift space of the diode. This voltage influences the number of carriers crossing the depletion layer. Hence, the individual crossings cannot be independent of each other. Schottky's formula (7) for current noise no longer holds in this case.

If we restrict ourselves to *low-level injection* the mean square noise current of a p-n junction diode may be written, according to (3) and (7),

$$\overline{|i_{n\,tot}^2|} = 4kT\,\mathrm{Re}\,(Y)\Delta f - 2eI\Delta f, \quad (8)$$

taking I positive in the forward and negative in the reverse directions. Thus, (8) is in agreement with our above assumption on the directions of additional noise power flow.

Some difficulties may arise regarding the noise contribution $2eI\Delta f$ of the dc current I. It is well known from lf theories of shot noise that the noise current of a diode carrying a dc current I exceeds full-shot noise. However, in these theories all individual crossings of the depletion layer associated with the creation and recombination of carriers are counted as a contribution to current noise. Since we regard only the dc current at the diode *terminals*, all events which do not affect the dc *terminal* current but are balanced out internally must not be counted in our treatment. Their contribution to noise is already included in the thermal part of (8).

A very interesting conjecture may be made regarding shot noise in semiconductor diodes at high-level injection conditions. Considering (8), the component $2eI\Delta f$ may be expected to decrease at high-level injection. Hence, in the forward direction the total noise current would *increase*. No direct experimental confirmation of this conjecture seems available at present.

III. Theory of Shot Noise in Intrinsic Junction Transistors

Eq. (8) may be applied to junction transistors, starting from an intrinsic transistor (base resistance neglected). An intrinsic transistor consists of an emitter junction diode and a collector junction diode, the dc currents of which are I_e and I_c, respectively. For the further calculation, we have to fix positive directions of

currents and voltages and our[13] adopted convention is shown in Fig. 3. Corresponding to the theory of Shockley, the currents I_e and I_c are dependent on the voltages U_e and U_c as shown in the equations of the left-hand part of Fig. 3. The coefficients I_{11}, I_{12}, I_{21}, I_{22} indicate currents which are dependent on the geometry of the intrinsic transistor and its material properties. The lower-case letters indicate ac currents and ac voltages (right-hand part of Fig. 3).

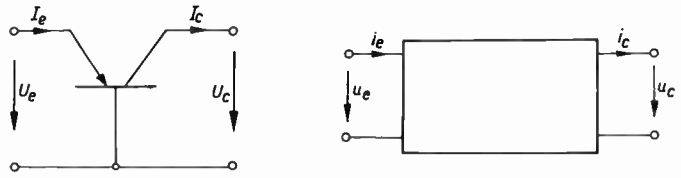

$$I_e = I_{11}\left(\exp\left(\frac{e\,U_e}{k\,T}\right)-1\right) + I_{12}\left(\exp\left(\frac{e\,U_c}{k\,T}\right)-1\right) \qquad i_e = Y_{11}\,u_e + Y_{12}\,u_c$$

$$I_c = I_{21}\left(\exp\left(\frac{e\,U_e}{k\,T}\right)-1\right) + I_{22}\left(\exp\left(\frac{e\,U_c}{k\,T}\right)-1\right) \qquad i_c = Y_{21}\,u_e + Y_{22}\,u_c$$

Fig. 3—Left: Adopted positive directions of dc currents and dc voltages of intrinsic junction transistor, including pertaining dc equations. Right: Adopted positive directions of ac currents and voltages of intrinsic transistor and pertaining ac equations.

In previous publications[14] it was established that the noise of a four-pole may be completely described by *four figures; e.g.*, by two noise sources (two mean square values) and by their complex correlation coefficient (two figures). In our case of the intrinsic transitor, the application of the results of Section II gives rise to two noise current sources, one in parallel to the emitter diode and the other to the collector diode (see Fig. 4). If the terminals of each diode are short circuited, their mutual ac influence is zero, as the current sources $Y_{12}U_c$ and $Y_{21}U_e$ of Fig. 4 become zero. Eq. (8) is then applicable to these diodes. Taking into account the positive directions of currents as adopted in Fig. 4, we obtain

$$\overline{|i_{ne}^2|} = 4kT\,\mathrm{Re}\,(Y_{11})\Delta f - 2eI_e\Delta f$$

$$\overline{|i_{nc}^2|} = 2eI_c\Delta f - 4kT\,\mathrm{Re}\,(Y_{22})\Delta f. \qquad (9)$$

Difficulties may arise with the sign of the second equation. One goes from (8) to the second part of (9) by putting $I=-I_c$ and $Y=-Y_{22}$. The second step conforms with the equivalent circuit (Fig. 4). The first step is also obvious, because I_c is taken positive in the reverse direction of the collector diode, whereas in (8) the opposite convention was adopted.

[13] M. J. O. Strutt, "Eindeutige wahl des pfeilsinnes fuer stroeme und spannungen in vierpolen mit anwendungen auf richtvierpole und gyratoren." *Archiv. für Elektrotechnik*, vol. 42, pp. 1–5; 1955.

[14] L. C. Peterson, "Signal and noise in a microwave tetrode," PROC. IRE, vol. 35, pp. 1264–1272; November, 1947.

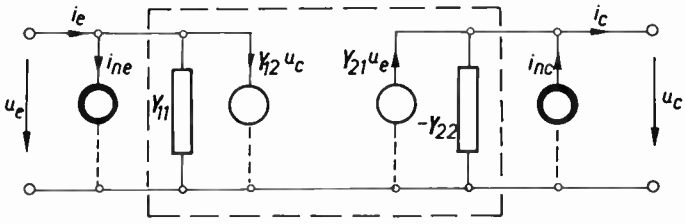

$$\overline{|i_{ne}|^2} = 4\cdot k\cdot T\cdot \mathrm{Re}\,(Y_{11})\,\Delta f - 2\cdot e\cdot I_e\,\Delta f$$

$$\overline{|i_{nc}|^2} = 2\cdot e\cdot I_c\cdot\Delta f - 4\cdot k\cdot T\cdot \mathrm{Re}\,(Y_{22})\,\Delta f$$

Fig. 4—Equivalent four-pole circuit for ac currents and voltages of intrinsic junction transistor (dashed contour). Within the contour the four-pole is noise-free. Outside the contour, two noise current sources are indicated by heavy circles.

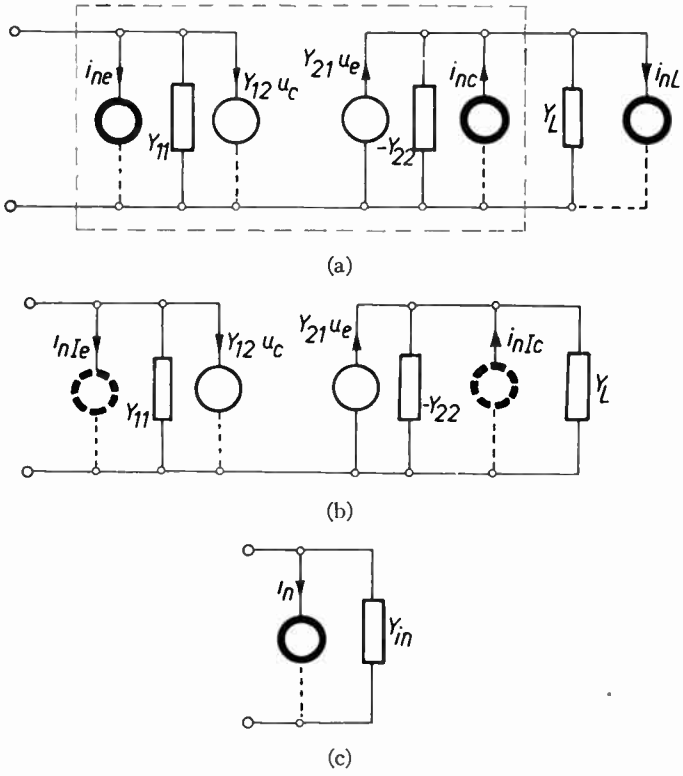

Fig. 5—Circuits for evaluation of correlation $\overline{i_{ne}{}^{*}i_{nc}}$. (a) Equivalent circuit of Fig. 4 with load admittance Y_L applied to the output terminals. The noise current source i_{nL} connected with the load Y_L is given by $\overline{|i_{nL}^2|}=4kT\,\mathrm{Re}(Y_L)\Delta f$. (b) AC equivalent circuit of an intrinsic transistor completed by two additional noise sources i_{nIe}, i_{nIc} (dotted circles) to restore quasithermal equilibrium of the four-pole. (c) Equivalent circuit for the input terminals of (a).

In order to obtain the correlation between the two noise currents i_{ne} and i_{nc}, a terminal admittance Y may be connected to the output of the four-pole. [See Fig. 5(a).] The temperature T of Y is equal to that of the four-pole. In this way a two-terminal admittance Y_{in} [see Fig. 5(c)] of temperature T is obtained (Y_{in} = input admittance of the four-pole with Y_L connected to its output).

The noise behavior of this two-terminal network may be evaluated in two ways: first, by a simple application of the equivalent noise circuit of Fig. 4 completed by a terminal admittance Y_L [Fig. 5(a)] and second, by applying similar arguments at a quasithermal equilibrium to this four-pole as was done for the junction diode in Section II [Fig. 5(b)].

If a short circuit is applied to the input terminals of the four-pole, the mean square value of the noise current i_n flowing through the short-circuit lead [Fig. 5(c)] is obtained from the equivalent circuit [Fig. 5(a)].

$$\overline{|i_n^2|} = \overline{|i_{ne}^2|} + [\overline{|i_{nc}^2|} + \overline{|i_{nL}^2|}]\left|\frac{Y_{12}}{Y_L - Y_{22}}\right|^2 + 2\,\mathrm{Re}\left(\frac{Y_{12}}{Y_L - Y_{22}}\,\overline{i_{ne}^* i_{nc}}\right) \tag{10}$$

i_{nL} indicates the short-circuit noise current of the terminal admittance Y_L. Applying (9) one obtains

$$\begin{aligned}\overline{|i_n^2|} &= 4kT\,\mathrm{Re}\,(Y_{11})\Delta f + 4kT\,\mathrm{Re}\,(Y_L - Y_{22})\Delta f\left|\frac{Y_{12}}{Y_L - Y_{22}}\right|^2 \\ &\quad - 2eI_e\Delta f + 2eI_c\Delta f\left|\frac{Y_{12}}{Y_L - Y_{22}}\right|^2 \\ &\quad + 2\,\mathrm{Re}\left[\frac{Y_{12}}{Y_L - Y_{22}}\,\overline{i_{ne}^* i_{nc}}\right]\end{aligned} \tag{11}$$

where the correlation term $\overline{i_{ne}^* i_{nc}}$ is a still unknown quantity.

For the second method of evaluation of the short-circuit noise current i_n (Fig. 5) a quasithermal equilibrium may be restored according to our assumptions of Section II. Two noise current sources are applied to the emitter and collector junctions balancing out the fluctuations of the corresponding dc currents [Fig. 5(b)]. The thermal part of the short-circuit current i_n

$$|i_{n\,\mathrm{th}}^2| = 4kT\,\mathrm{Re}\,(Y_{in})\Delta f \tag{12}$$

must be corrected by the contributions of the two additional current sources. The contribution of the additional source across the emitter junction $i_n^2 I_e - \mathrm{Index!} = 2eI_e\Delta f$ is negative according to our assumption on the direction of noise power flow in Section II. The contribution of the additional $|i_{nIc}^2| = 2eI_c\Delta f$ source across the collector is fed back to the input side by the source $Y_{12}u_e = Y_{12}i_{nIc}/(Y_L - Y_{22})$ of the equivalent circuit [Fig. 5(b)]. It must be taken positive, because I_c is counted positive in the reverse direction of the collector diode.

Thus the short-circuit noise current i_n at the input terminals of the four-pole [Fig. 5(c)] may be written as

$$\overline{|i_n^2|} = \underbrace{4kT\,\mathrm{Re}\,(Y_{in})\Delta f}_{\substack{\text{quasithermal}\\ \text{equilibrium}\\ \text{noise}}} - \underbrace{2eI_e\Delta f}_{\substack{\text{add.}\\ \text{emitter}\\ \text{source}}} + \underbrace{2eI_c\Delta f}_{\substack{\text{add.}\\ \text{collector}\\ \text{source}}}\left|\frac{Y_{12}}{Y\ \mathrm{Index} - Y_{22}}\right|^2. \tag{13}$$

Comparing (11) and (13) which represent the same result, an equation for the still unknown quantity $\overline{i_{ne}^* i_{nc}}$ is found:

$$\begin{aligned}2\,\mathrm{Re}\left[\frac{Y_{12}}{Y_L - Y_{22}}\,\overline{i_{ne}^* i_{nc}}\right] &+ 4kT\,\mathrm{Re}\,(Y_{11})\Delta f \\ &+ 4kT\,\mathrm{Re}\,(Y_L - Y_{22})\Delta f\left|\frac{Y_{12}}{Y_L - Y_{22}}\right|^2 \\ &= 4kT\,\mathrm{Re}\,(Y_{in})\Delta f.\end{aligned} \tag{14}$$

It is shown in the Appendix that this equation is satisfied by

$$\overline{i_{ne}^* i_{nc}} = 2kT(Y_{21} - Y_{12}^*)\Delta f. \tag{15}$$

This relation for the correlation term has already been noted previously by Kraus[15] for a passive linear four-pole. However, no complete derivation, as is given in the Appendix of this paper, was published by the said author. Eqs. (9) and (15) contain the complete noise theory of an intrinsic transistor.

IV. Application of the Theory to Junction Transistors. Noise Figures

In real junction transistors, several extensions of the above theory arise.

According to Shockley's theory,[16] embodied in the right-hand equations of Fig. 3, the admittances Y_{12} and Y_{22} would be practically zero under normal operating conditions (for a p-n-p transistor $U_c < 0$ and $|eU_c| \gg kT$). Experimentally, they are not zero. According to Early[17] this may be explained by the modulation of the thickness of the base layer due to the collector ac-voltage. Still, Y_{12} and Y_{22} are of a smaller order of magnitude than Y_{11} and Y_{21} and hence may be neglected in practical cases. Their contribution to noise is thus negligible.

[15] G. Kraus, "Diskussionsbeitrag zu den vortraegen ueber rauschende vierpole," *Nachrichtentechnische Fachberichte, Beihefte zur NTZ*, vol. 2, p. 40; 1955.

[16] W. Shockley, "Electrons and Holes in Semiconductors," D. Van Nostrand Co., Inc., New York, N. Y.; 1950.

[17] J. M. Early, "Effect of space-charge layer widening in junction transistors," Proc. IRE, vol. 40, pp. 1401–1406; November, 1952.

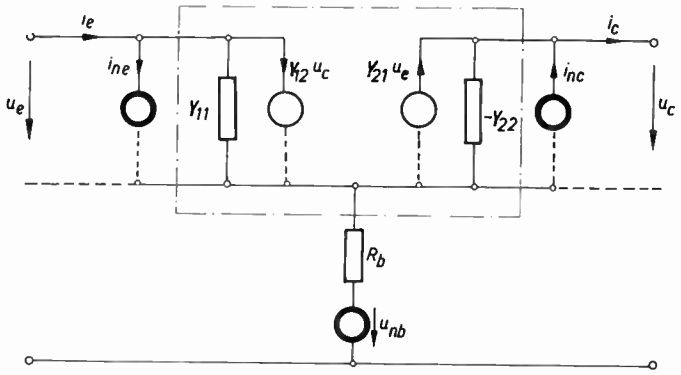

Fig. 6—Equivalent noise diagram of junction transistor, showing base resistance R_b and corresponding noise voltage source. The dashed contour indicates the intrinsic noise-free part of complete transistor.

The base layer resistance causes a contribution to transistor noise by thermal agitation. This may be accounted for by the equivalent circuit of Fig. 6. The noise voltage u_{nb} is given by

$$\overline{|u_{nb}^2|} = 4kTR_b\Delta f. \tag{16}$$

A further extension of the above theory is due to high-level injection. Webster[18] and Rittner[19] have shown that the underlying assumption of Shockley's theory[16], to the effect that the density of minority carriers in the base region is small with respect to the density of majority carriers, is already violated at currents of some ma in modern junction transistors. The reasons for the nonvalidity of (7) at high injection levels have been stated in Section II for junction diodes. Similar arguments hold for transistors. A theoretical treatment of noise at high injection levels is not given here, due to lack of detailed understanding of the ac behavior of these devices at high injection levels. The first author has recently published some theoretical considerations on this topic.[20] Experimental data as presented in Section VII show the deviation from (9) and (15) at high injection levels.

If Y_L in (13) is made infinite, the last term becomes zero. Under this condition the mean square noise current $\overline{|i_n^2|}$ must be higher, if the value of the term $2eI_e\Delta f$ becomes smaller. The latter obtains in the case of high-level injection. Hence $\overline{|i_n^2|}$ is higher at high-level injection than the value given by (13). As $\overline{|i_n^2|}$ may be shown, to be a measure for the noise figure (see Section IV), this argument would indicate, that the noise figure of a junction transistor should increase at high level injection conditions. This is exactly what our experimental values show (Section VII, Figs. 29 and 30).

[18] W. M. Webster, "On the variation of junction-transistor current-amplification factor with emitter-current," PROC. IRE, vol. 42, pp. 914–920; June, 1954.
[19] E. S. Rittner, "Extension of the theory of the junction transistor," *Phys. Rev.*, vol. 94, pp. 1161–1171; June, 1954.
[20] W. Guggenbuehl, "Theoretische ueberlegungen zur physikalischen begruendung des ersatzschaltbildes von halbleiterflaechendioden bei hohen Stromdichten," *Arch. Elekt. Uebertratung*, vol. 10, pp. 483–485; November, 1956.

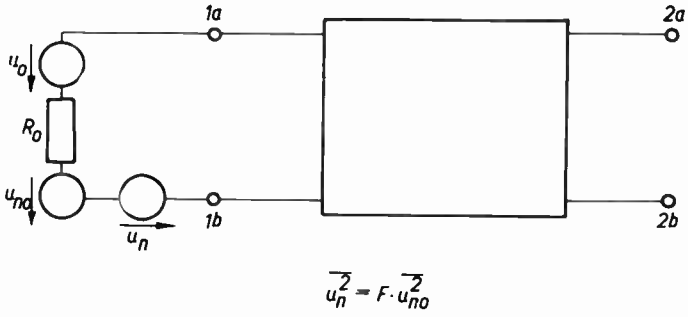

Fig. 7—Definition of noise figure of linear four-pole.

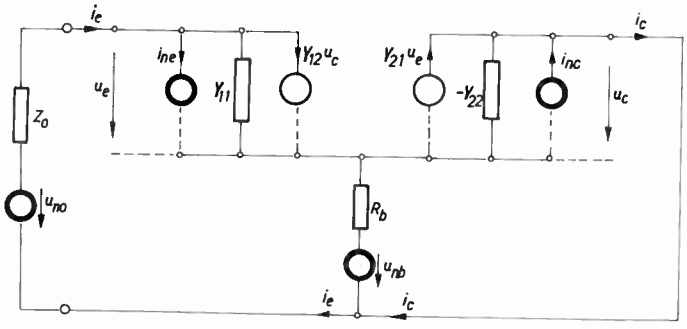

Fig. 8—Grounded base connection of junction transistor, showing two noise current sources and one noise voltage source of transistor as well as one noise voltage source corresponding to the source impedance Z_0 at the input.

In many cases, the noise figure F of junction transistors is the quantity, entering into circuit considerations. Several equivalent definitions of F are known. The one, preferable in our case, is illustrated by Fig. 7. A signal source of voltage u_0 and internal source resistance R_0 are connected to the input terminals 1a, 1b of a linear four-pole. A noise voltage u_{n0} is associated with R_0 at an absolute temperature T:

$$\overline{|u_{n0}^2|} = 4kTR_0\Delta f. \tag{17}$$

A further noise voltage u_n is connected in series with u_{n0}. This noise voltage u_n is adjusted until the total available noise power at the output terminals 2a and 2b of Fig. 7 is doubled as against the case without u_n. Then, the noise figure F is

$$F = \frac{\overline{|u_n^2|}}{\overline{|u_{n0}^2|}}. \tag{18}$$

With this definition, F may be easily calculated for the grounded base circuit (Fig. 8), the grounded emitter circuit (Fig. 9), and the grounded collector circuit (Fig. 10). Without loss of generality, in each circuit the output may be short circuited. By application of Ohm's and Kirchhoff's laws, four equations are obtained for i_e, u_e, i_c, and u_c in terms of the noise currents and voltages. From these equations, i_e, u_e, and u_c are eliminated in the cases of Fig. 8 and 9, while i_c, u_e, and u_c are eliminated in the case of Fig. 10. The resulting output current is then obtained in terms of the noise sources. Thereupon the noise voltage u_{n0} is increased until the mean

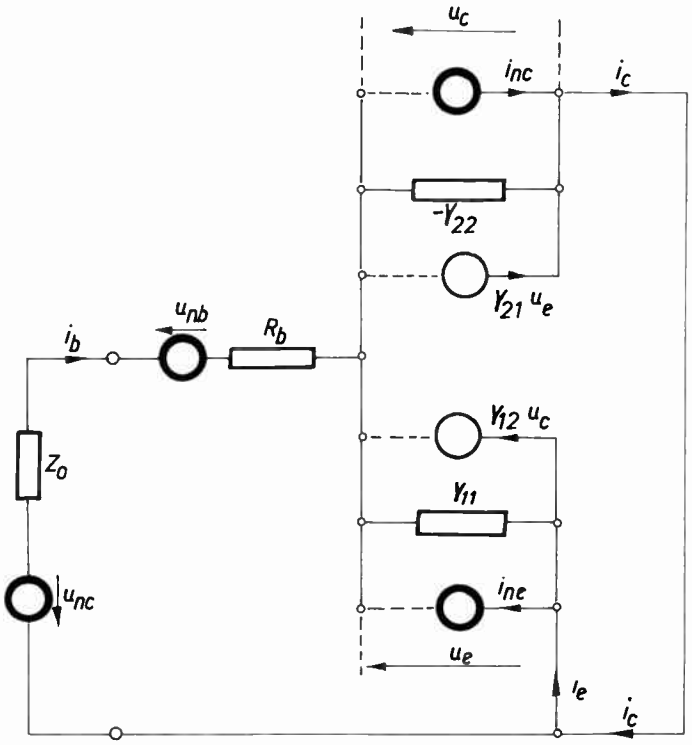

Fig. 9—Grounded emitter circuit, similar to Fig. 8.

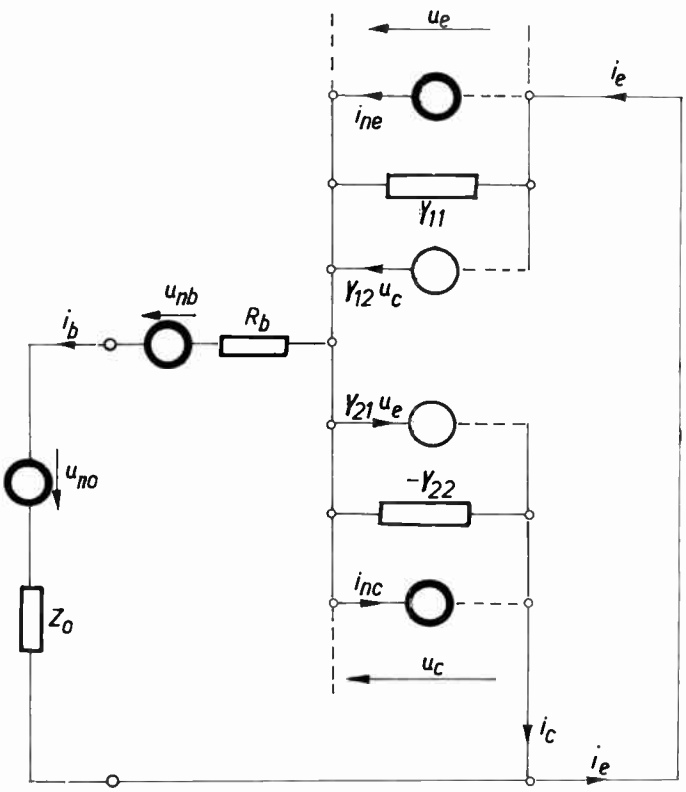

Fig. 10—Grounded collector circuit, similar to Fig. 8.

square output current is doubled. By application of (18), this yields[21] the noise figure F.

In the evaluation of F, the following assumptions are adopted, which hold good for modern junction transistors:

$$Y_{11} \gg Y_{12}, \qquad Y_{21} \gg Y_{22}, \qquad |Y_{22}R_b| \ll 1.$$

Then, the noise figures for the grounded base circuit and for the grounded emitter circuit become identical:[21]

$$F = \frac{2eI_c\left|\dfrac{R_b + \dfrac{1}{Y_{11}} + Z_0}{\alpha}\right|^2 - 2eI_e|R_b + Z_0|^2}{4kTR_0} \tag{19}$$

whereas for the grounded collector circuit we find:[21]

$$F = 1 + \frac{R_b}{R_0} + \frac{1}{4kTR_0}\left[2eI_c|Z_0 + R_b|^2 - |\alpha|^2 2eI_e\left|Z_0 + R_b - \frac{1}{Y_{21}}\right|^2 - 4kT|\alpha|^2\mathrm{Re}\left(\frac{Z_0^*}{\alpha}\right) - 4kT|\alpha|^2 R_b \cdot \mathrm{Re}\left(\frac{1}{\alpha}\right) + \frac{4kT}{|Y_{11}|^2}\cdot\mathrm{Re}\,(Y_{11})\right]. \tag{20}$$

[21] W. Guggenbuehl, B. Schneider, and M. J. O. Strutt, "Messungen ueber das hochfrequenzrauschen von transistoren," *Nachrichtentechnische Fachberichte, Beiheft zur NTZ*, vol. 5, pp. 34–36; 1956.

V. Comparison and Coordination with Previous Theoretical Results

First, we consider the lf region. With a junction diode, (8) may be transformed by application of the well-known diode equation

$$I = I_0 \exp\left(\frac{eU}{kT}\right) - I_0,$$

where I is positive in the forward direction, as is the bias voltage U. Thus,

$$\mathrm{Re}\,(Y) = \frac{dI}{dU} = \frac{eI_0}{kT}\exp\left(\frac{eU}{kT}\right) = \frac{(I + I_0)e}{kT}. \tag{21}$$

Inserting this into (8) we obtain

$$\overline{i_n^2} = 2(2Ie + 2I_0e)\Delta f - 2Ie\Delta f = 2(I + 2I_0)e\Delta f. \tag{22}$$

This equation was published previously using the corpuscular theory.[2,11] From (21) and (22) the available noise power of a junction diode is:

$$P_{AD} = \frac{1}{2}kT\Delta f\left(1 + \frac{I_0}{I + I_0}\right). \tag{23}$$

Three special cases are of practical interest:

$$I = 0, \qquad U = 0: \qquad P_{AD} = kT\Delta f; \tag{24a}$$

$$U < 0, \quad |eU| \gg kT: \qquad P_{AD} \to \frac{1}{2}kT\Delta f\frac{I_0}{I + I_0}; \tag{24b}$$

$$U > 0, \quad |eU| \gg kT: \qquad P_{AD} \to \frac{1}{2}kT\Delta f. \tag{24c}$$

Theoretical results in a later paper by Petritz[22] differ from ours by orders of magnitude in practical cases. His result, according to which P_{AD} should always be above $kT\Delta f$, is unfounded, and is contradicted by our (24) as well as by the experimental results of Section VI.

With junction transistors discussion will be limited here to intrinsic transistors, as perfect agreement exists between different authors on the contribution of the base resistance R_b. With a p-n-p transistor, normal operation conditions imply $U_c<0$ and $|eU_c|\gg kT$. In this case, $Y_{12}\ll Y_{21}$ and Y_{22} is negligible in (9). Hence, (9) and (15) reduce to

$$\begin{aligned} |i_{ne}^2| &= 4kT\,\mathrm{Re}\,(Y_{11})\Delta f - 2eI_e\Delta f; \\ |i_{nc}^2| &= 2eI_c\Delta f; \\ \overline{i_{ne}^* i_{nc}} &= 2kTY_{21}\Delta f. \end{aligned} \tag{25}$$

In the lf case,

$$\begin{aligned} Y_{11} &= \frac{e}{kT}(I_e - I_{es}); \\ Y_{21} &= \frac{e}{kT}\alpha(I_e - I_{es});\ I_e\alpha = I_c - I_{c0}. \end{aligned} \tag{25a}$$

Here I_{es} is the current I_e in the case, that *both* diodes are biased in the reverse direction: for a p-n-p transistor U_e, $U_c<0$, $|eU_e|$, $|eU_c|\gg kT$. According to the left-hand equations of Fig. 4, we have $I_{es}=-(I_{11}+I_{12})$. Of course, practically: $I_e\gg I_{es}$ and hence by (25):

$$\begin{aligned} \overline{|i_{ne}^2|} &\approx 2eI_e\Delta f; \\ \overline{|i_{nc}^2|} &\approx 2eI_c\Delta f; \\ \overline{i_{ne}^* i_{nc}} &\approx 2e\alpha I_e\Delta f. \end{aligned} \tag{26}$$

Eq. (26) is illustrated by the equivalent circuit of Fig. 11. This equivalent circuit, as well as (26), coincides with previous results of van der Ziel[8] and the authors.[12]

The equivalent circuit of Fig. 11 may be transformed to the h circuit of Fig. 12, showing the noise sources u_{nh} (voltage source) and i_{nh} (current source). We obtain

$$\begin{aligned} u_{nh} &= -\frac{i_{ne}}{Y_{11}}; \\ i_{nh} &= i_{nc} - \frac{Y_{21}}{Y_{11}}i_{ne}; \\ \overline{u_{nh}^* i_{nh}} &= \frac{Y_{21}}{|Y_{11}|^2}\overline{|i_{ne}^2|} - \frac{1}{Y_{11}^*}\overline{i_{ne}^* i_{nc}}. \end{aligned} \tag{27}$$

[22] R. L. Petritz, "On noise in p-n-junction rectifiers and transistors," *Phys. Rev.*, vol. 91, p. 231; July 7, 1956.

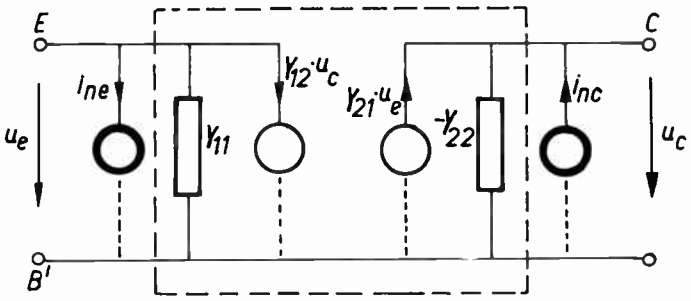

Fig. 11—Equivalent admittance circuit of intrinsic transistor (within dashed contour) with the corresponding two noise current sources (two heavy circles).

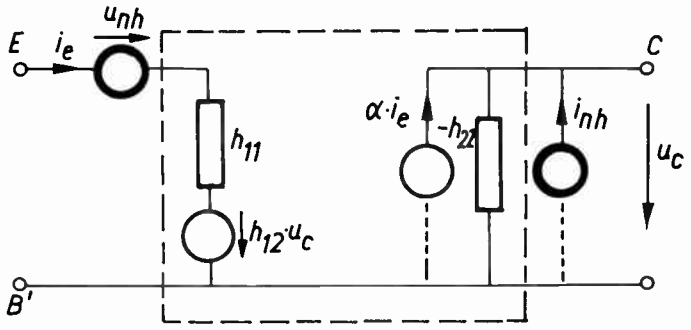

Fig. 12—Equivalent hybrid circuit of intrinsic transistor (within dashed contour) with the corresponding noise voltage source at the input (left) and noise current source at the output (right). This circuit is equivalent to Fig. 11.

Eqs. (27), (15), and (25a) yield

$$\begin{aligned} \overline{|u_{nh}^2|} &= 2kT\frac{kT}{e}\frac{I_e - 2I_{es}}{(I_e - I_{es})^2}\Delta f; \\ \overline{|i_{nh}^2|} &= 2eI_{c0}\Delta f + 2eI_e\alpha(1-\alpha)\Delta f; \\ \overline{u_{nh}^* i_{nh}} &= -\frac{kT}{e}\frac{\alpha 2I_{es}}{I_e - I_{es}}\Delta f. \end{aligned} \tag{28}$$

Here, I_{c0} is the current I_c if $I_e=0$. Normally, $I_e\gg I_{es}$. Hence,

$$\begin{aligned} |u_{nh}^2| &\approx 2kT\frac{kT}{eI_e}\Delta f; \\ |i_{nh}^2| &\approx 2eI_{c0}\Delta f + 2eI_e\alpha(1-\alpha)\Delta f; \\ \overline{u_{nh}^* i_{nh}} &\approx 0. \end{aligned} \tag{29}$$

These noise sources coincide exactly with those of Montgomery and Clark[4] and of van der Ziel.[5] They may be interpreted as due to *three* causes: 1) the emitter current I_e, 2) the collector current I_{c0}, and 3) current partition at the collector, yielding a mean square partition noise current $2eI_e\alpha(1-\alpha)\Delta f$, which is included in $\overline{|i_{nh}^2|}$ in (29).

A recent publication by Giacoletto[6] shows the equivalent noise circuit of Fig. 13. Comparing this with Fig. 11, we obtain

$$i_{ne} = i_{neb'} + i_{nce};$$
$$i_{nc} = i_{nb'c} + i_{nce}. \tag{30}$$

Hence, by (30), (25), and (25a):

$$\overline{|i_{nce}^2|} = \overline{i_{ne}^* i_{nc}} = 2e(I_e - I_{es})\alpha\Delta f;$$
$$\overline{|i_{neb'}^2|} = \overline{|i_{ne}^2|} - \overline{|i_{nce}^2|}$$
$$= 2eI_e(1-\alpha)\Delta f - 2eI_{es}(2-\alpha)\Delta f;$$
$$\overline{|i_{nb'c}^2|} = \overline{|i_{nc}^2|} - \overline{|i_{nce}^2|}$$
$$= 2eI_{c0}\Delta f + 2e\alpha I_{es}\Delta f. \tag{31}$$

In this calculation, proper attention must be paid to the sign conventions, adopted in Figs. 3, 4, 11, and 13 as well as to the sign conventions, adopted by Giacoletto.[6] If these conventions are observed, (31) is seen to coincide with Giacoletto's equations, if some further simple transformations are applied to (31).

The first author has proposed an equivalent noise circuit, obtained by analogy of a junction transistor to a high vacuum tetrode with saturated cathode current.[12] This analogy is illustrated by Fig. 14(a) and (b). In the tetrode [Fig. 14(a)], we have a cathode current I_k, a screen grid current I_{sg}, and an anode current I_a. Three noise current sources are shown in Fig. 14(a), i_{n1} corresponding to shot noise of the anode current, i_{n2} to shot noise of the screen current, and i_{np} to current partition noise. With the transistor of Fig. 14(b), three noise current sources corresponding to those of Fig. 14(a) are shown. The analogy between the tetrode and the junction transistor is perfected by the introduction of an additional noise source i_{ns} for the saturation current of the collector junction in Fig. 14(b). This equivalent circuit of Fig. 14(b) may be compared with that of Fig. 11, yielding

$$i_{ne} = i_{n1} + i_{n2};$$
$$i_{nc} = i_{n1} + i_{ns} + i_{np}. \tag{32}$$

From (32) and Fig. 14(b) we obtain

$$\overline{|i_{ne}^2|} = \overline{|i_{n1} + i_{n2}|^2} = 2eI_e\Delta f;$$
$$\overline{|i_{nc}^2|} = \overline{|i_{n1}^2|} + \overline{|i_{ns}^2|} + \overline{|i_{np}^2|}$$
$$= 2eI_e\alpha\Delta f + 2eI_{c0}\Delta f = 2eI_c\Delta f;$$
$$\overline{i_{ne}^* i_{nc}} = (i_{n1}^* + i_{n2}^*)(i_{n1} + i_{ns} + i_{np})$$
$$= \overline{|i_{n1}^2|} + \overline{i_{n1} i_{n2}^*}$$
$$= \alpha^2 2eI_e\Delta f + 2eI_e\alpha(1-\alpha)\Delta f = 2e\alpha I_e\Delta f. \tag{33}$$

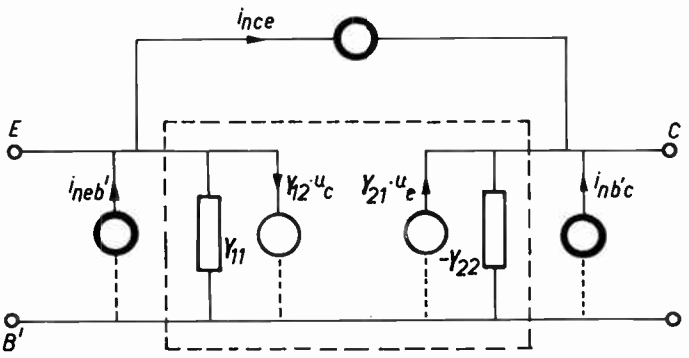

Fig. 13—Equivalent admittance circuit of intrinsic transistor (within dashed contour) with *three* noise current sources (heavy circles). This circuit is equivalent to Fig. 11.

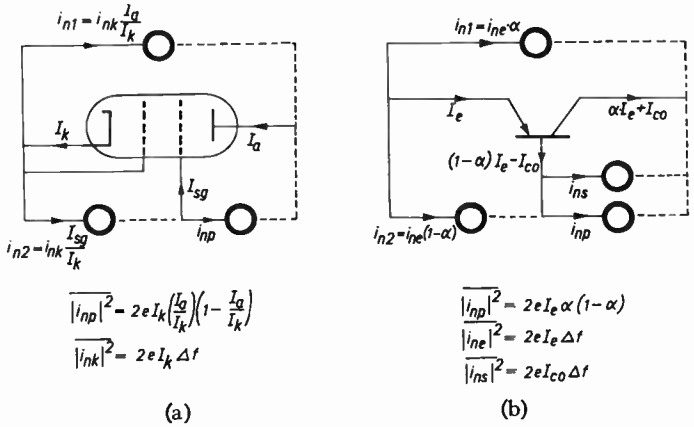

Fig. 14—Equivalent noise circuit of high vacuum tetrode (left) with saturated cathode. This is translated into an equivalent noise circuit of a junction transistor (right).

Eq. (33) coincides with (26). Thus, the equivalence of Fig. 14(a) and (b) with Fig. 11 is proved.

As regards the hf region, in a paper by van der Ziel,[8] random fluctuations due to diffusion and recombination in an element of volume are accounted for and their effects are integrated over the total diffusion space, so as to obtain the noise currents at the terminals. His diode results coincide with our (8), account being taken of the sign conventions of Figs. 3 and 4 and also of those adopted by van der Ziel.[8] With a *p-n-p* junction transistor, van der Ziel has carried out the integrations only in the case $U_c < 0$, $|eU_c| \gg kT$. The saturation currents of both junction diodes are neglected by him. The contribution of the collector saturation current I_{c0} thus does not enter into the result. The authors have found that van der Ziel's integrals [his (30) and (31)[8]] are calculable without his restrictions and these calculations have been carried out by the authors. After this, the expanded results of van der Ziel[8] coincide completely with the above (9) and (15). In the transmission-line picture of van der Ziel only the contributions of hole currents are accounted for (*p-n-p* transistor). However, his equations may be extended, so as to account for the contributions, due to the electron currents through the junctions. No alteration of his final results is caused

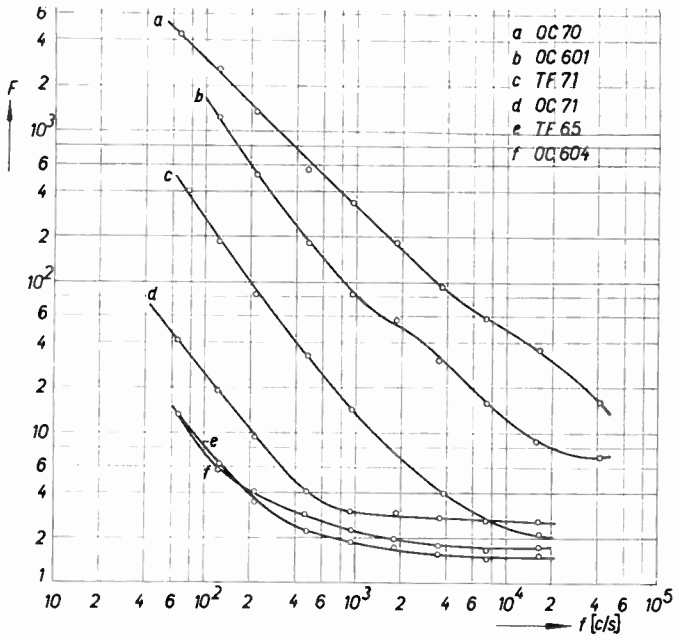

Fig. 15—Noise figure (vertical) as dependent on frequency (horizontal) for six junction transistors (European types). The types corresponding to the curves are indicated on diagram. All transistors were measured in the grounded base connection, with a source resistance of 500 ohms, at a current I_e of 0.5 ma and a voltage U_c of -2 volts (p-n-p types).

by this extension. These are, if the sign conventions of Figs. 3 and 4 are adopted,

$$\overline{|i_{ne}^2|} = 2kT\Delta f[2\,\mathrm{Re}\,(Y_{11}) - Y_{11\,0}];$$

$$\overline{|i_{nc}^2|} = 2eI_c\Delta f;$$

$$\overline{i_{ne}^* i_{nc}} = 2kTY_{21}\Delta f. \qquad (34)$$

Here $Y_{11\,0}$ is the lf value of Y_{11}. Comparing (34) with (9) and (15) shows their complete coincidence in practical cases, as $2kT\Delta f Y_{11\,0} = 2eI_e\Delta f$ if $I_e \gg I_{es}$ and Y_{22} as well as Y_{12} may be neglected in (9) and (15).

Van der Ziel's statement[8] that his theory is only valid in the case of volume recombination is discounted by the present theory of Sections II and III. This restriction does not enter into the present theory. The limitation to low-level injection, stressed in Section IV, is included in the assumptions of van der Ziel.

A further previous publication on hf noise theory of junction diodes is contained in a short note by Uhlir.[23] Uhlir's final (4) shows a typographical sign error and should read:

$$\frac{i\omega^2}{B} = 4kTG_\omega - 2qi_0.$$

In our notation $G_\omega = \mathrm{Re}(Y)$, $q = e$, $i_0 = I$, $i_\omega = i_n$, $B = \Delta f$. Thus this equation is exactly coincident with (8). Hence, Uhlir's theory must be equivalent to the present one, since no special assumptions and restrictions are involved in either.

[23] A. Uhlir, Jr., "High frequency shot noise in p-n junctions," PROC. IRE, vol. 44, pp. 557–558; April, 1956.

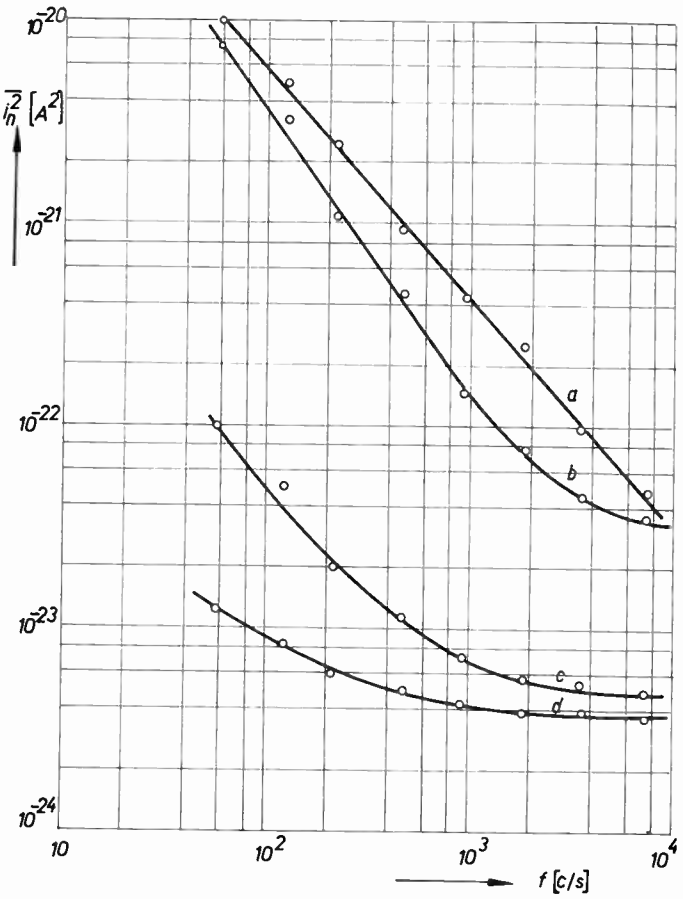

Fig. 16—Mean square noise current (vertical) at an effective bandwidth of 1 cps as dependent on frequency (horizontal) for four diodes biased in the reverse direction. Diode of curve a is point-contact type OA150 at a reverse current of 8 μa; curve b corresponds to one of the diode junctions of a transistor of type OC71 at a reverse current (increased by illumination of contact) of 60μa; curve c corresponds to same diode as curve b, but at a reverse current of 15 μa; curve d corresponds to a junction diode of type 1N92 with 12 μa reverse current.

VI. LF Experimental Data on Shot Noise in Junction Diodes and Transistors

For the sake of brevity, only a few of our experimental results are shown here. The diode, of which the noise was measured, was connected to the input grid of a low-noise tube (EF42 in grounded cathode triode connection). The diode noise was compared with that of a suitable wire-wound resistance. In the range 60 cps to 40 kc ten resonance filters were used, with effective bandwidths varying between 12 and 1500 cps. The total measuring set was arranged inside screened boxes of 1-millimeter iron plates. The first two amplifier stages were fed by batteries. A suitable thermocouple was used as indicator at the output.[11]

In the measurements, care must be taken to obtain shot noise and to exclude flicker noise. By selection from more than 100 items,[11,12] several junction transistors and diodes were found, in which shot noise was predominant above 1000 cps. By using one of the junctions of a transistor, suitable diodes were obtained. Moreover, some commercial junction diodes were also found to be

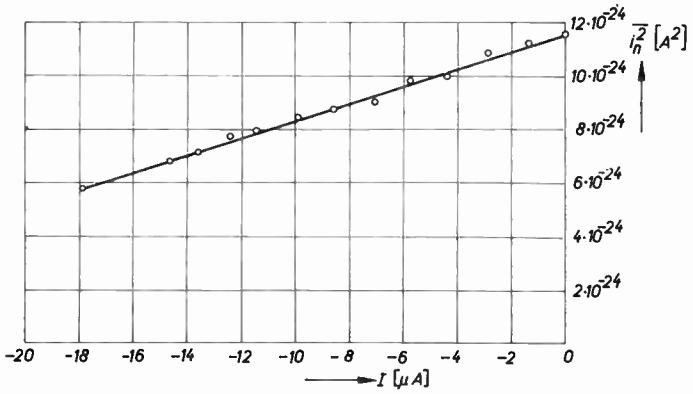

Fig. 17—Mean square noise current (vertical) at an effective bandwidth of 1 cps as dependent on reverse diode current (horizontal). Junction diode of transistor type OC71 at a frequency of 7.24 kc, the saturation reverse current being 17.7 μa (caused partly by illumination of junction). The current was altered by variation of reverse bias voltage. Curve calculated, points measured.

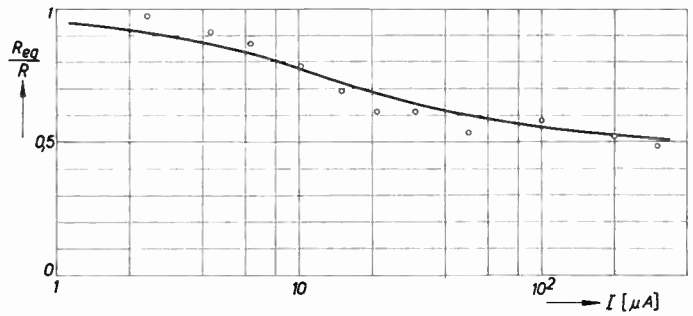

Fig. 18—Equivalent noise resistance (according to Nyquist equation) over differential resistance of diode junction (vertical) as dependent on diode forward current (horizontal) of junction diode 1N91. Curve calculated, taking account of diode resistance of 20-ohm outside junction. Points measured.

suitable. The experimental data of Figs. 15 and 16 (see preceding page), show that shot noise in curves marked *d*, *e*, and *f*, is predominant above 1000 cps. Below this frequency, flicker noise dominates. The curves of Figs. 17 and 18 show satisfactory agreement with the theory of (22) and (24). Reference is also made to measurements of Slocum and Shive.[24]

With junction transistors, the interpretation of experimental data[12] is based on the equivalent circuit of Fig. 19, which is a simple transformation of Fig. 6 as was stated in connection with (28) and (29) and Fig. 12. The four separate noise sources of Fig. 19 were checked experimentally. In order to obtain experimental data on i_{np} and i_{ns}, the source resistance R_0 of Fig. 19 was adjusted to 120 K ohms, which is large compared with R_b and with the forward resistance R_e of the emitter junction. Measuring the mean square noise current through R of Fig. 19. as dependent on I_e, the data of Fig. 20 were obtained.[12] The calculated values were obtained from (29), as $\overline{|i_{nh}^2|} = \overline{|i_{ns}^2|} + \overline{|i_{np}^2|}$. The coincidence between experimental and theoretical data is

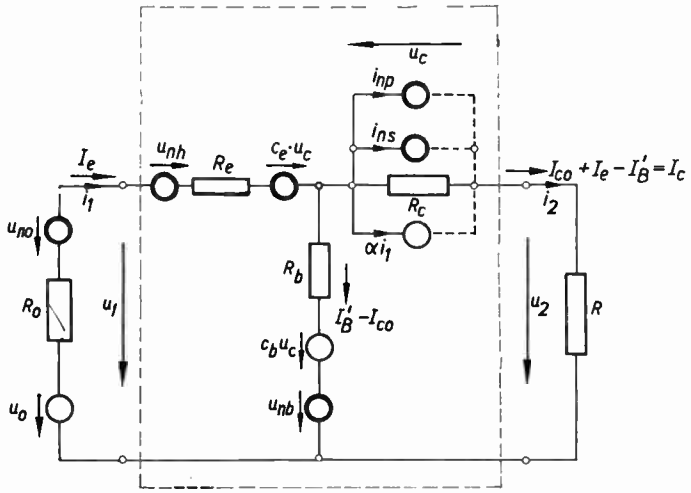

Fig. 19—Complete equivalent noise circuit of junction transistors (within dashed contour) with noise voltage sources u_{nh} and u_{nb} and noise current sources i_{np} and i_{ns}. At input is noise source u_{n0} pertaining to source resistance R_0 and at output is load resistance R.

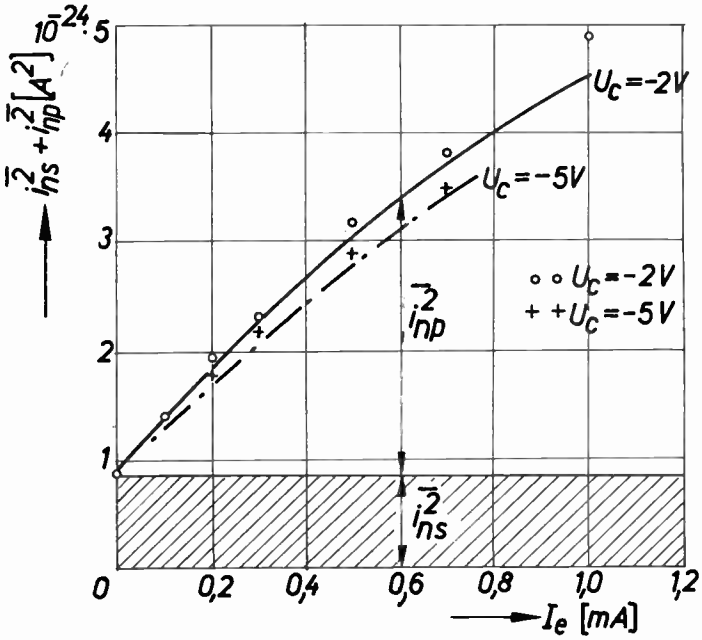

Fig. 20—Measured values of mean square noise current $\overline{i_{ns}^2} + \overline{i_{np}^2}$ (see Fig. 19) at 1-cps effective bandwidth (vertical) as dependent on emitter current I_e (horizontal) at two values of collector voltage U_c. Points measured, full curve calculated from (19). Frequency was 7.24 kc.

satisfactory. Experimental data on the emitter junction noise have already been shown in Figs. 17 and 18 to be in concordance with theory. Moreover, this noise source has been checked experimentally also with a transistor.[12] Reference is made to experimental results by Englund.[25] Hence, only the noise contribution of R_b remains to be checked. Noise figures were measured for two junction transistors of approximately equal α values but differing in R_b. The data are shown in Fig. 21. Now an additional

[24] A. Slocum and J. N. Shive, "Shot dependence of *p-n* junction phototransistor noise," *J. Appl. Phys.*, vol. 25, p. 406; March, 1954.

[25] J. W. Englund, "Noise Considerations for *p-n-p* Junction Transistors," in "Transistors I," RCA Labs., Princeton, N. J., pp. 309–321; 1956.

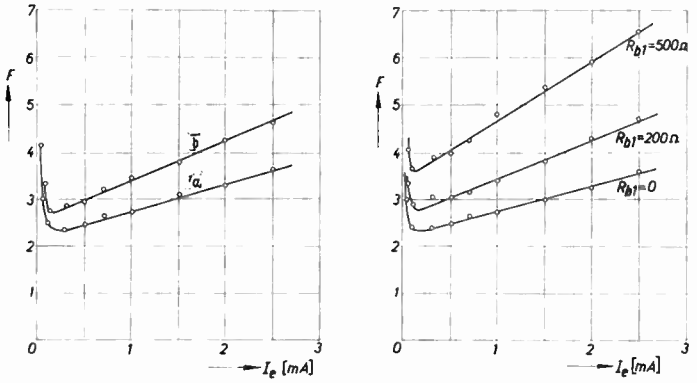

Fig. 21—Noise figures (grounded base) of junction transistors of approximately equal α values as dependent on I_e. Diagram (a) curve a: $R_b \approx 400$ ohms, $\alpha = 0.987$, curve b: $R_b \approx 600$ ohms, $\alpha = 0.988$. Diagram (b) Transistor of curve a of diagram (a), with added base resistances R_{b1} of 0.200 and 500 ohms respectively. The 200-ohm curve approximately coincides with the curve b of diagram (a). Frequency was 7.24 kc.

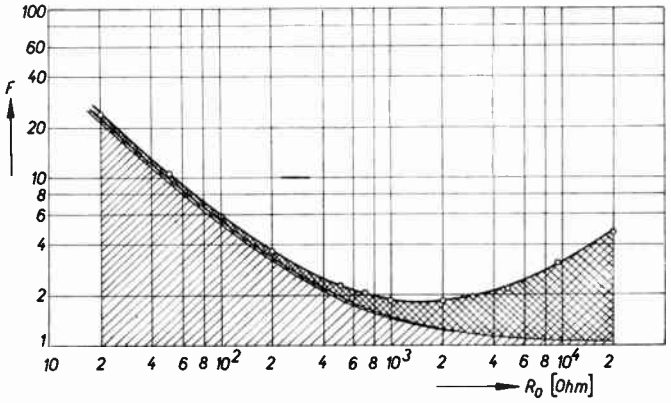

Fig. 22—Noise figures of a junction transistor at 7.24 kc as dependent on source resistance R_0 (see Fig. 19). Grounded base. Contributions to noise figure are:

from R_b.
from i_{np} and i_{ns} together (Fig. 19).
from u_{nh} (Fig. 19).

Full curve calculated, circles measured.

resistance of 200 ohms was connected in series with R_b of transistor a of Fig. 21(a). Experimental data are shown in Fig. 21(b). Obviously the 200-ohm curve of Fig. 21(b) coincides very nearly with curve b of Fig. 21(a). Thus, the noise contribution of R_b has been identified unequivocally.[12]

Experimental and calculated values of the noise figure F as dependent on source resistance R_0 and on emitter current I_e were compared (see Figs. 22 and 23). The coincidence is satisfactory. The relatively small deviations in Fig. 23 are ascribed to residual flicker noise, as this deviation is smaller at a higher frequency.[12]

The approximate equality of calculated noise figures of the grounded base, grounded emitter, and grounded collector circuits was checked experimentally.[12]

Some junction transistors with noise figures as low as 7.3 in the shot-noise lf range were found.[12]

Flicker noise in junction transistors has been investigated by different authors.[1,26]

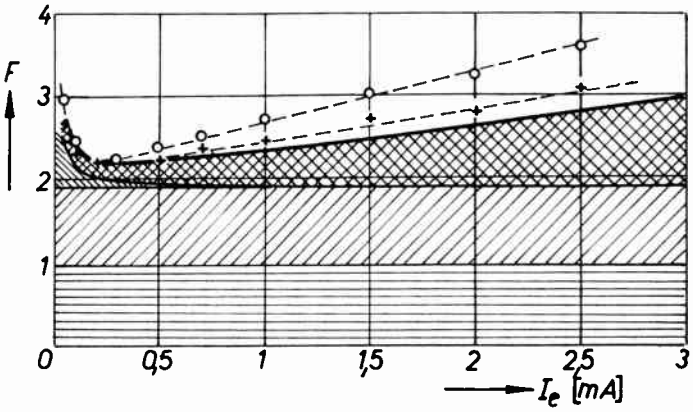

Fig. 23—Noise figures of a junction transistor at 7.24 kc (circles) and at 16.35 kc (crosses) as dependent on I_e. Contributions to F are indicated as in Fig. 22. Grounded base. Horizontally-shaded area is contribution from R_0. Full curve calculated, circles and crosses measured.

VII. HF Experimental Data on Shot Noise of Junction Transistors

A measuring set was constructed for noise measurements on junction transistors up to 10 mc. For comparisons of experimental and calculated data, an α measuring set was also constructed for this frequency range. At frequencies above 1 mc special attention was given to avoidance of spurious resonance effects.

For the sake of brevity only some of our experimental results are shown here. In Fig. 24 measured and calculated noise figures as dependent on frequency are shown for a junction transistor of (European) type OC71 in a grounded base circuit.[21] At the left, flicker

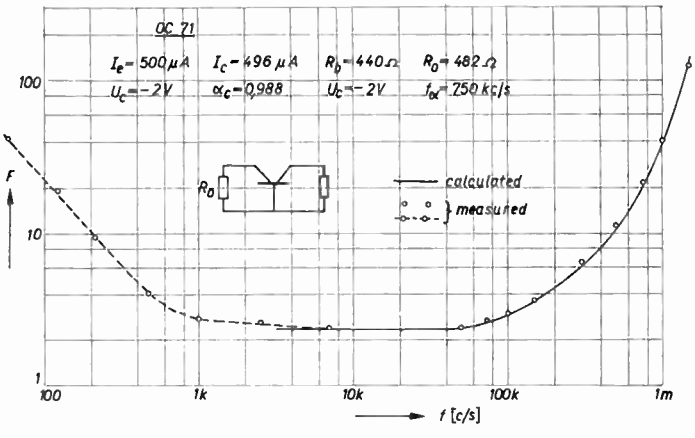

Fig. 24—Noise figure of junction transistor of European type OC71 as dependent on frequency. Data are indicated in diagram. Full curve calculated, circles measured.

[26] E. Keonjian and J. S. Schaffner, "An experimental investigation of transistor noise," Proc. IRE, vol. 40, pp. 1456–1460; November, 1952.

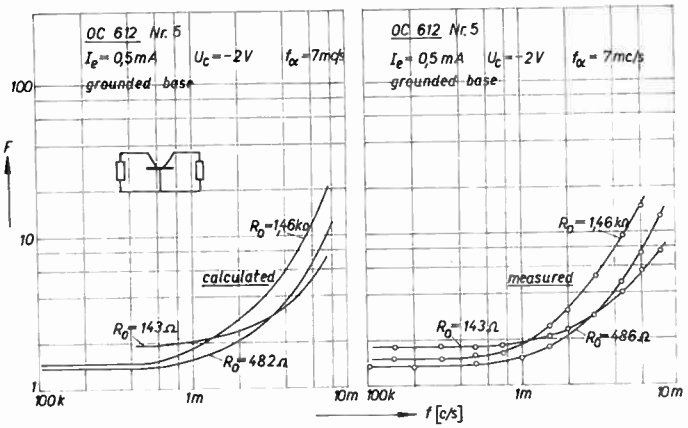

Fig. 25—Comparison of calculated and measured noise figures of hf junction transistor of European type OC612 for different source resistances, as dependent on frequency in the hf region. Data indicated in diagram.

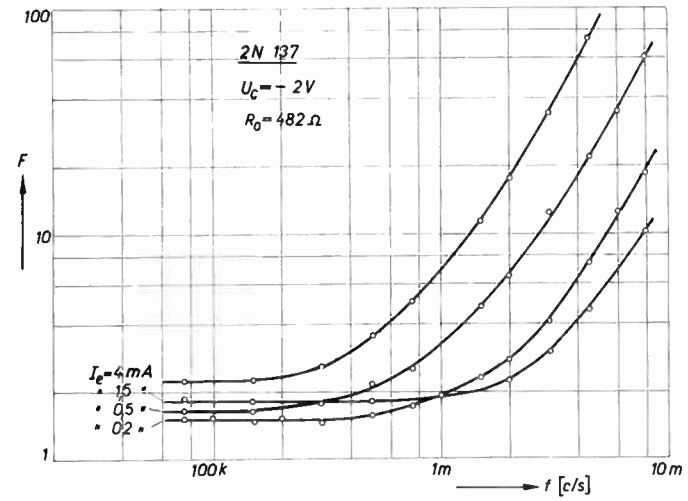

Fig. 26—Measured noise figures as dependent on frequency in the hf region of junction transistor type 2N137 at several values of I_e in the grounded base circuit. α cutoff is at 6.05 mc.

noise is present. In the center and right parts of the curve, shot noise is predominant. The coincidence of theoretical (19) and experimental values is satisfactory. This type OC71 is a lf type. Experimental and theoretical values for a hf transistor of European type OC612 for several source resistances are shown in Fig. 25. Here also, coincidence is satisfactory.[21] Experimental curves showing the effect of higher emitter currents on noise figure curves are seen in Fig. 26 for a junction transistor of type 2N137.

We now come to experimental evidence of the influence of high-level injection on noise figure. As is well known, the dependence of C_{be}' on emitter current I_e may show approximately, where high-level injection starts.[27] From the curve of Fig. 27 for a junction transistor of type OC71 it is seen, that low-level injection exists be-

[27] F. W. Herold, "New advances in the junction transistor," *Brit. J. Appl. Phys.*, vol. 5, pp. 115–126; April, 1954.

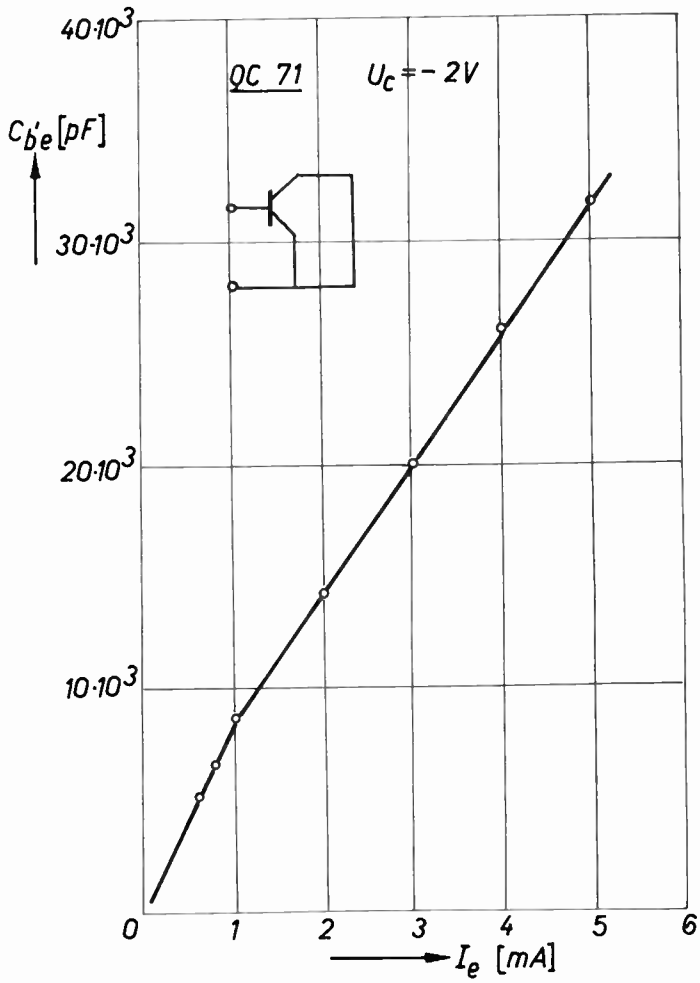

Fig. 27—Capacitance C_{be}' in grounded emitter circuit of junction transistor of European type OC71 as dependent on I_e. The variation of slope indicates boundary between low-level injection (left) and high-level injection (right).

low about 1 ma and high-level injection above 1 ma. Hence, the curve of Fig. 24 for this transistor at $I_e = 0.5$ ma lies in the low-level injection region, as does the curve of Fig. 28 for the same transistor at $I_e = 0.2$ ma. In both curves, experimental and theoretical values are in good agreement. However, the curves of Figs. 29 and 30 for the same transistor at 1.5 and 4 ma are in the high-level injection region. Coincidence between measured and calculated values of noise figures is missing.

According to the present theory (19) noise figures for the grounded base circuit and the grounded emitter circuit of the same transistor should be approximately equal. This is checked satisfactory by the experimental curves of Fig. 31 (p. 853), both measured for a source resistance of 482 ohms.

From (19) and (20) a close relation is predicted between the frequency dependence of noise figures and of α. This is checked satisfactorily by the experimental curves[21] of Fig. 32.

In the region where the noise figure increases with frequency, the experimental curves of Figs. 22 and 23

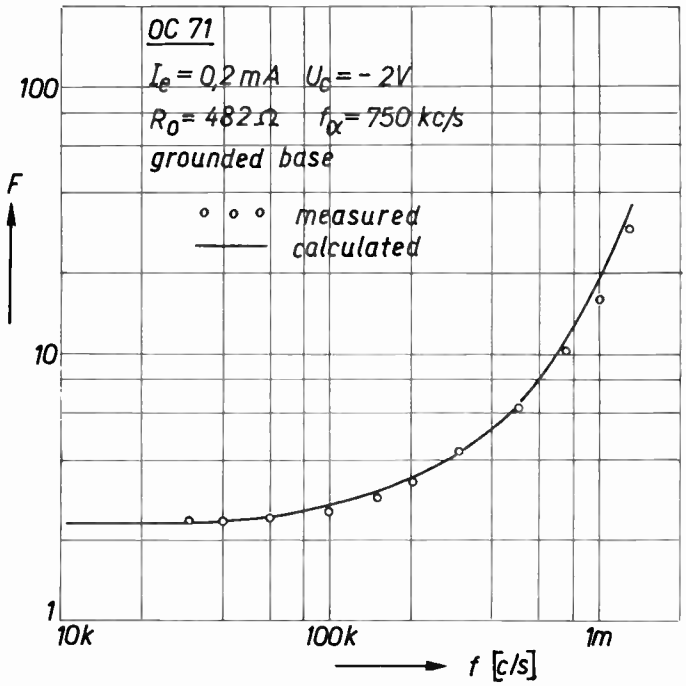

Fig. 28—Noise figures of junction transistor OC71 as dependent on frequency. Data indicated in diagram.

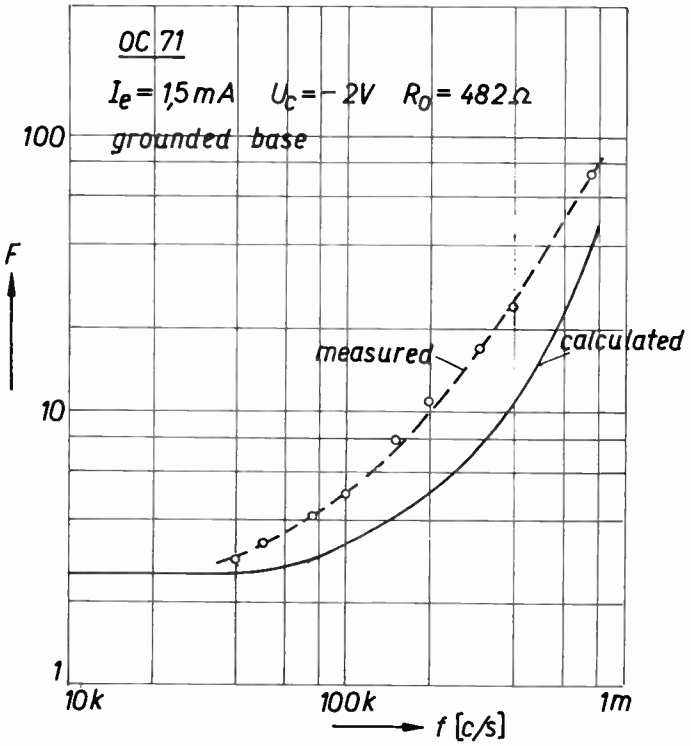

Fig. 29—Effect of high-level injection with transistor of Fig. 27 on noise figure (emitter current 1.5 ma).

showing the noise figure as dependent on source resistance and on emitter current at lf are altered, as is shown in Figs. 33 and 34 (opposite). (Reference is made to experimental curves by Bargellini and Herscher.[28] Stephenson[29] and G. H. Hanson,[30] which are in general agreement with our results.)

VIII. Conclusion

Shot noise of junction diodes and transistors at low-level injection are derived from an energy balance, taking account of thermal agitation and random corpuscular current structure. Noise figures are derived from the equations of noise current sources for the three basic transistor circuits. In the lf region, these results coincide with those of previous papers as regards noise sources, as well as noise figures. In the hf region, coincidence of the present theory with previous papers is shown to exist, if those results are properly adjusted [(van der Ziel[8]) and a typographical error corrected (Uhlir[23])]. The present noise figure equations in the hf region are believed to be new as well as of simple application.

Experimental values at low-level injection are shown to coincide satisfactorily with theory as regards noise sources as well as noise figures. Experimental results at high-level injection are presented, showing their deviation from low-level injection and from theory. Noise

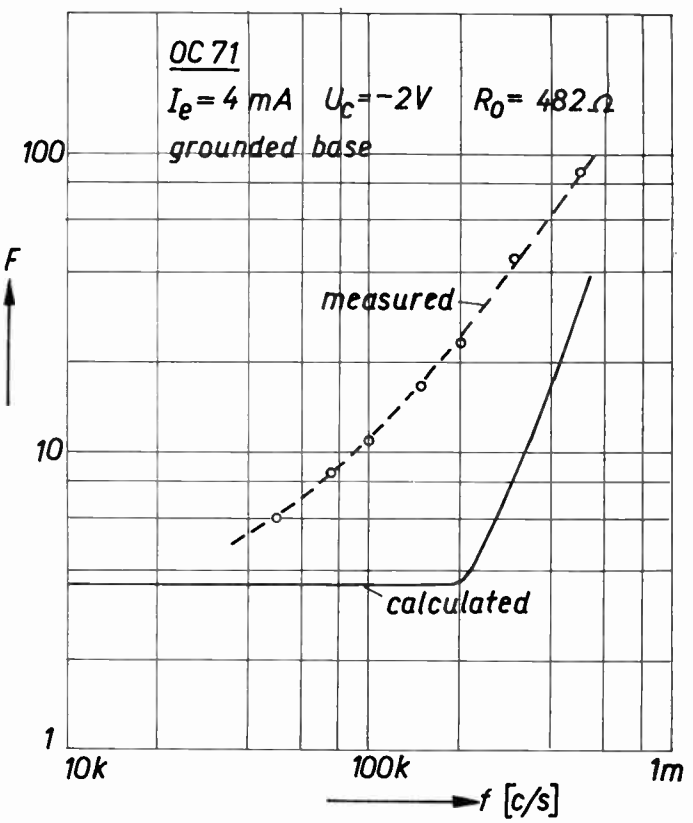

Fig. 30—Similar to Fig. 29, but at higher emitter current (4 ma).

figures at high-level injection currents (*e.g.*, above 1 ma) are shown experimentally to be well above those at low-level injection. Hence, low-level operation is recom-

[28] P. M. Bargellini and M. B. Herscher. "Investigation of noise in audio amplifiers using junction transistors," Proc. IRE, vol. 53, pp. 217–226; February, 1955.

[29] W. L. Stephenson, "Measurements of junction transistor noise in the frequency range 7-50, kc/s." *Proc. IEE*, vol. 102B, pp. 753–756; November, 1955.

[30] G. H. Hanson, "Shot noise in *p-n-p* transistors," *J. Appl. Phys.*, vol. 26, pp. 1388–1389; November, 1955.

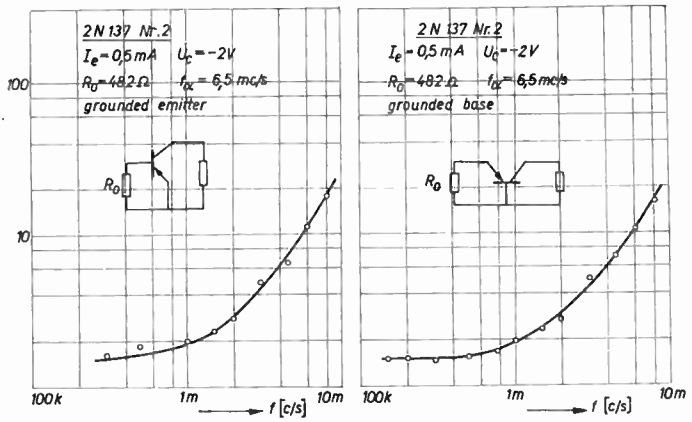

Fig. 31—Comparison of measured noise figures in grounded emitter circuit (left) and grounded base circuit (right) as dependent on frequency. Data indicated in diagram. Values at equal frequency should be equal by theory and approximately, so they are by experiment.

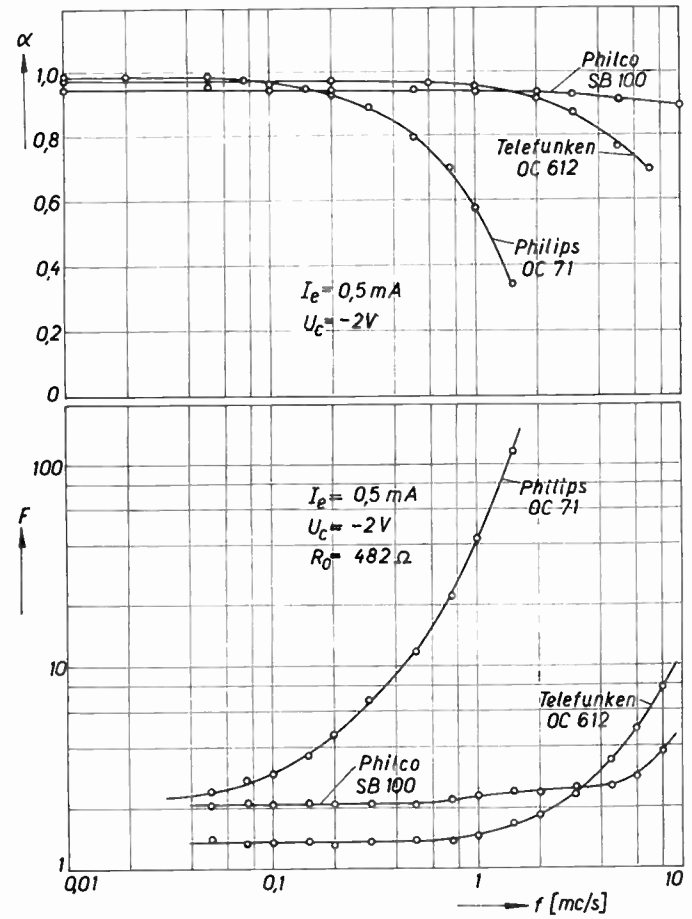

Fig. 32—Relation between measured values of noise figures and of α, both as dependent on frequency in grounded base circuit for three types of junction transistors.

mended as regards noise. As dependent on frequency, noise figures rise at frequencies where gain drops. The grounded emitter circuit has advantages, as low-noise figures occur at rather high gain, due to the matched source resistance coinciding approximately with the region of minimum noise figures as dependent on source resistance.

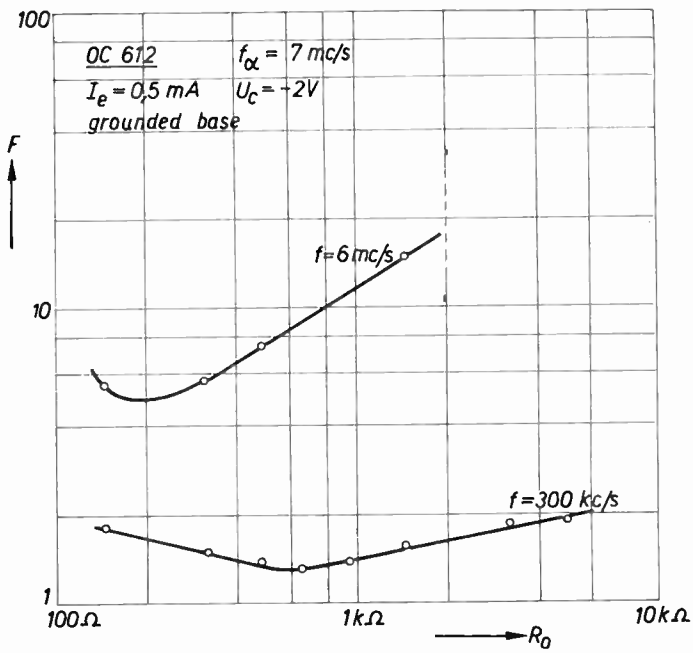

Fig. 33—Measured noise figures as dependent on source resistance R_0 at two frequencies with junction transistor OC612.

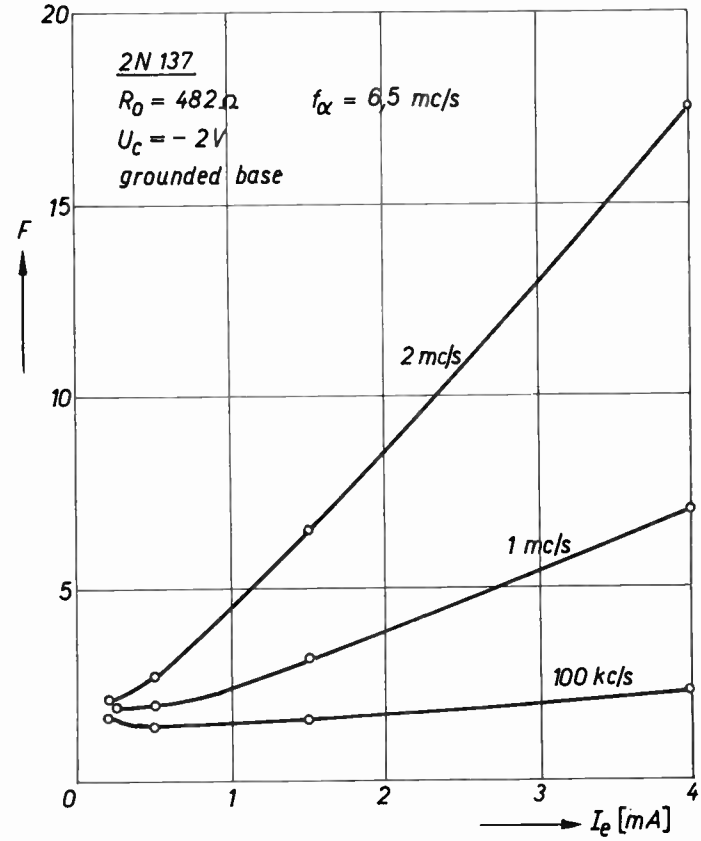

Fig. 34—Measured noise figures as dependent on I_e at three frequencies. Effects of high-level injection is to increase noise figures.

Appendix

Proof of (15) as Solution of (14)

The right-hand side of (14) may be evaluated as follows:

$$4kT\,\mathrm{Re}\,(Y_{in})\Delta f = 4kT\,\mathrm{Re}\left(Y_{11}+\frac{Y_{12}Y_{21}}{Y_L-Y_{22}}\right)\Delta f = 4kT\,\mathrm{Re}\,(Y_{11})\Delta f + 4kT\,\mathrm{Re}\left(\frac{Y_{12}Y_{21}}{Y_L-Y_{22}}\right)\Delta f$$

$$= 4kT\,\mathrm{Re}\,(Y_{11})\Delta f + 2kT\left[\left(\frac{Y_{12}Y_{21}}{Y_L-Y_{22}}\right)+\frac{Y_{12}^*Y_{21}^*}{Y_L^*-Y_{22}^*}\right]\Delta f$$

$$= 4kT\,\mathrm{Re}\,(Y_{11})\Delta f + 2kT\Delta f\left[\frac{Y_{12}Y_{21}(Y_L^*-Y_{22}^*)+Y_{12}^*Y_{21}^*(Y_L-Y_{22})}{|Y_L-Y_{22}|^2}\right]. \quad (35)$$

The final result of (35) may be extended by addition and subtraction of a further term:

$$4kT\,\mathrm{Re}\,(Y_{in})\Delta f = 4kT\,\mathrm{Re}\,(Y_{11})\Delta f + 4kT\,\mathrm{Re}\,(Y_L-Y_{22})\Delta f\frac{|Y_{12}|^2}{|Y_L-Y_{22}|^2}$$
$$+ 2kT\left[\frac{Y_{12}Y_{21}(Y_L^*-Y_{22}^*)+Y_{12}^*Y_{21}^*(Y_L-Y_{22})}{|Y_L-Y_{22}|^2}\right]\Delta f$$
$$- 2kT\left[\frac{Y_{12}Y_{12}^*(Y_L^*-Y_{22}^*)+Y_{12}Y_{12}^*(Y_L-Y_{22})}{|Y_L-Y_{22}|^2}\right]\Delta f. \quad (36)$$

Proper adjustment of the two last equations leads to

$$4kT\cdot\mathrm{Re}\,(Y_{in})\Delta f$$
$$= 4kT\,\mathrm{Re}\,(Y_{11})\Delta f + 4kT\,\mathrm{Re}\,(Y_L-Y_{22})\Delta f\left|\frac{Y_{12}}{Y_L-Y_{22}}\right|^2$$
$$+ 4kT\,\mathrm{Re}\left[\left(\frac{Y_{12}}{Y_L-Y_{22}}\right)(Y_{21}-Y_{12}^*)\right]\Delta f. \quad (37)$$

Comparing (37) with the left-hand side of (14), (15) follows easily.

ACKNOWLEDGMENT

The authors take pleasure in extending their thanks to the firms Brown Boveri and Baden and Hasler both of Berne, Switzerland, as well as to the Swiss Federal Office for the Promotion of Scientific Research at Berne for financial aid towards the execution of the above research. Their thanks are also due B. Schneider and to W. Wunderlin, both of this Institute, for their kind cooperation in obtaining these results.

Space Charge Waves Along Magnetically Focused Electron Beams*

JOHANNES LABUS†

Summary—**The propagation of perturbations along electron beams of finite diameter is determined by boundary conditions. The solutions of the problem—the phase-eigenvalues or the plasma frequency reduction factor—depend on the way the perturbations of the beam surface are taken into account. A cylindrical uncompensated beam (void of ions) confined by an arbitrary coaxial magnetic field is considered. Two different procedures are compared: one assuming a surface current, the other introducing additional but continuous ac space charges and currents over the beam cross section.**

* Original manuscript received by the IRE, November 5, 1956; revised manuscript received, February 25, 1957.
† Siemens und Halske AG., Munich, Germany.

SINCE the fundamental investigations by Hahn [1] and Ramo [2] dealing with the propagation of signals along electron beams, that problem has been of general interest. In order to simplify the theory, Hahn assumed the existence of a flowing plasma with equal positive and negative charges. In that "plasma flow," velocity and space charge density are constant over the cross section of the stream, the electron trajectories are rectilinear. The same conditions, however, can be realized within an uncompensated stream (free of ions): 1) in an infinite magnetic field ex-

tending over the cathode or at very small beam currents; 2) in a Brillouin flow confined by a finite magnetic field that is shielded from the cathode. In the latter case, the electrons have an additional angular velocity around the beam axis equal to the Larmor frequency.

The propagation of perturbations by space charge waves in a medium of drifting charges is characterized by electromagnetic waves interacting with the charges in the beam. As in optics, the typical parameters of that medium are the phase velocity or the refractive index. If the perturbation is monochromatic and of angular frequency ω, a propagation of waves is possible for certain values of the propagation constant $j\gamma=\alpha+j\beta$, in which $\beta=\omega/v_{ph}=$wave number and $\alpha=$the attenuation constant. As the values of γ are obtained from the boundary conditions (at the edge of the beam and on the surface of the surrounding medium), they can be spoken of as the eigenvalues of the problem. We may call them "phase-eigenvalues." (Likewise that designation could also be used in connection with wave guides instead of "modes." The word modes seems to be more appropriate for designating the different states of oscillations of an oscillator.) Between the phase-eigenvalues and the plasma frequency $\omega_p/2\pi$, defined for an infinitely wide flow, the relation

$$\gamma = \frac{\omega}{v_{ph}} = \frac{\omega}{v_0} - s\frac{\omega_p}{v_0} \tag{1}$$

($\omega_p^2 = e\rho_0/m\epsilon_0$, $\rho_0 = i_0/v_0$ = space charge density)

exists. The plasma frequency reduction factor s depends on the boundary conditions and therefore, it is also a characteristic parameter of the flow. For an infinitely wide flow, $s=\pm 1$; if $\omega_p/\omega<1$, there are two waves with phase velocities on either side of the drift velocity v_0 which beat together. Thus a wave "exp $j(\omega t-\omega z/v_0)$" with a phase velocity equal to v_0 is produced whose amplitudes have a standing-wave modulation of spatial period $\lambda_p=2\pi v_0/s\omega_p$. If, however, the cross section of the beam is finite, more than one pair of values of $|s|<1$ will occur, depending on the kind of flow. Then the space charge waves have higher phase-eigenvalues (modes).

Uncompensated Electron Flow

In the following, we will discuss the methods leading to the determination of the phase-eigenvalues and the reduction factors of uncompensated electron flows in coaxial magnetic fields. In the drift region of that flow, the magnetic field (B) is supposed to be constant; at the cathode it may have an abritrary value ($B_c\geqq 0$). A difference between the magnetic flux threading the cathode ($\pi b_c^2 B_c$) and the beam in the drift region ($\pi b^2 B$) causes an angular momentum and thus an angular velocity

$$\dot{\phi}_0 = \omega_L(1-K) \tag{2a}$$

wherein

$$K = b_c^2 B_c/b^2 B \tag{2b}$$

and

$$\omega_L = \frac{e}{2m}B \text{ (Larmor frequency).}$$

The value of the focusing field B in the drift region is determined by the equilibrium condition for the beam diameter

$$\omega_p = \omega_L\sqrt{2(1-K^2)} \tag{2c}$$

provided that there are no dc scallops along the beam. If $K=0$ (shielded cathode), B is the Brillouin field. In a plasma flow $K=1$. The same is also true for an uncompensated flow in which the rectilinearity of the electron trajectories is enforced by an infinite focusing field, or at dc space charges tending to zero. Apart from those idealized conditions, there always will be a difference between the magnetic flux threading the beam in the drift region and at the cathode, causing a rotation of electrons. That also will be the case, when a finite magnetic field is constant throughout drift region and cathode ($B=B_c$); due to space charges, the beam diameter will spread ($b>b_c$) and hence $K<1$.

The concept of space charge waves along a cylindrical beam, perturbed by a signal of angular frequency ω, leads to the following "Ansatz" for the time and z dependence of the ac values

$$\exp j(\omega t-\gamma z). \tag{3}$$

Assuming further that, as in a Brillouin flow, the dc velocity and space charge density are constant over the cross section of the beam for all values of K and that the field components are independent of the azimuth ϕ, the following relations are obtained from Maxwell's equation, the force equation, and continuity of charges:

$$(s^2+\sigma)\left[E_z''+\frac{1}{r}E_z'-\frac{s^2-1}{s^2+\sigma}\zeta\gamma^2E_z\right] = -\sigma\frac{\omega_L}{\omega}(1-K)\gamma\left[(rE_\phi)''+\frac{1+K}{1-K}\frac{1}{r}(rE_\phi)'+\frac{\gamma^2}{\sigma}\zeta(rE_\phi)\right] \tag{4}$$

$$E_\phi''+\left(1+\frac{2K}{1-K}\Gamma^2r^2\right)\frac{1}{r}E_\phi' - \left\{\frac{1}{r^2}\left(1-\frac{2K}{1-K}\Gamma^2r^2\right)+\gamma^2\left[\zeta-\sigma\left(\frac{2K}{1-K}\frac{\omega_p\Gamma}{\gamma^2c}\right)^2\right]\right\}E_\phi = -(1-K)\frac{\omega\omega_L r}{\zeta\gamma c^2}\cdot\left[E_z''+\left(1+\frac{2K}{1-K}\frac{\sigma}{s^2}\right)\frac{1}{r}E_z'-\zeta\gamma^2E_z\right] \tag{5}$$

wherein

$$s = \frac{\omega_q}{\omega_p} = \text{plasma frequency reduction factor}$$

$$\omega_q = \omega - \gamma v_0 = \text{plasma frequency of a finite beam } (b < \infty)$$

$$\sigma = \frac{1}{2K^2/s^2(1-K^2) - 1}; \quad \zeta = 1 - \left(\frac{\omega}{\gamma c}\right)^2 - \sigma\left(\frac{\omega_p}{\gamma c}\right)^2;$$

$$\Gamma^2 = \frac{\sigma}{\zeta s^2}(1-K)^2\left(\frac{\omega_L}{c}\right)^2. \tag{6}$$

The differential equations in (4) and (5) of the Bessel type can be reduced to one differential equation of the fourth degree for the electric field component E_z or E_ϕ, indicating that the TM and TE waves are coupled through the focusing field B. In a flow confined by an infinite magnetic field, there is $\sigma=0$ and $(1-K)\omega_L=0$. According to (2a), there will be no rotation of the electrons around the beam axis [9]. Eqs. (4) and (5) become

$$E_z'' + \frac{1}{r}E_z' + \left(\frac{1}{s^2} - 1\right)\gamma^2 E_z = 0 \tag{4a}$$

$$E_\phi'' + \frac{1}{r}E_\phi' - \left(\gamma^2 + \frac{1}{r^2}\right)E_\phi = 0 \tag{5a}$$

as in a plasma flow [2]. There is no coupling between TM and TE waves.

Brillouin Flow

The condition for stable beam radius of a Brillouin flow is $\omega_p = \sqrt{2}\omega_L$. Introducing $K=0$ in (6), $\sigma=-1$, $\zeta\approx 1$, and (4) and (5) become (Appendix)

$$(s^2-1)\left[E_z'' + \frac{1}{r}E_z' - \gamma^2 E_z\right] = \frac{\omega_L}{\omega}\gamma\left[(rE_\phi)'' + \frac{1}{r}(rE_\phi)' - \gamma^2(rE_\phi)\right] \tag{7}$$

$$E_\phi'' + \frac{1}{r}E_\phi' - \left(\frac{1}{r^2} + \gamma^2\right)E_\phi = -\frac{\omega\omega_L}{\gamma c^2}r\left[E_z'' + \frac{1}{r}E_z' - \gamma^2 E_z\right]. \tag{8}$$

With

$$u = \frac{\gamma\omega_L}{(s^2-1)\omega}(rE_\phi), \quad \text{and} \quad p^2 = \frac{(\omega_L/c)^2}{s^2-1}$$

we get

$$u'' - \frac{1-p^2r^2}{1+p^2r^2}\cdot\frac{1}{r}u' - \gamma^2 u = 0. \tag{9}$$

Disregarding the ac perturbations at the beam surface, an infinite number of solutions in the vicinity of $s=\pm 1$ is obtained from (7) and (8). An analysis, taking into account the radial displacements of the electrons at the surface, is rather cumbersome; at the actual boundary of the beam one of the coordinates is not constant, as is the case in most boundary problems. Obviously the Ansatz in (3) for the time and z dependence fails and should be replaced by a Fourier integral [4].

In order to retain the Ansatz, a surface current was assumed by Rigrod and Lewis [5] corresponding to a discontinuous magnetic field component H_ϕ. The azimuthal component E_ϕ and consequently the ac space charges were disregarded. The introduction of the discontinuity referred to seems to be rather hypothetic; it is also questionable whether the ac space charges can be disregarded, even if only the surface electrons are acted upon by the perturbing field. That field determines the initial conditions; however, farther away from that region all electrons will participate in the process of propagation.

In [6] the ac space charge and E_ϕ are taken into account. Moreover, the radial displacements of the electrons at the surface and inside the beam are replaced by additional space charges traveling along the beam, as shown in Fig. 1. Thus the total ac space charge density becomes (Appendix)

$$\rho_t = \rho + \rho_0\frac{\Delta r}{r}, \tag{10}$$

ρ and ρ_0 being ac and dc space charge densities. The additional value in ρ_t is proportional to the radial displacement Δr of the electrons inside the beam ($r<b$) and at the beam surface $r=b$. Accordingly the field components H_ϕ and H_z are added by additional terms, associated with Δi_z and Δi_ϕ. The displacement Δr depends on E_r and E_ϕ. From the boundary conditions the following relation for the phase-eigenvalues or the reduction factor is obtained:

$$\left[1 + \vartheta - \frac{\kappa}{s}(1-s^2) - \frac{J_0(\gamma b) - 1}{s^2\gamma_0 b J_1(\gamma b)}\right]\cdot\left[u'(b) + j\gamma\frac{H_0^{(1)}(\gamma b)}{H_1^{(1)}(\gamma b)}u(b)\right] = 0 \tag{11}$$

wherein

$$\vartheta = -\frac{I_0(\gamma b)}{I_1(\gamma b)}\cdot\frac{K_0(\gamma a)I_1(\gamma b) + I_0(\gamma a)K_1(\gamma b)}{K_0(\gamma a)I_0(\gamma b) - I_0(\gamma a)K_0(\gamma b)} \tag{12}$$

$$s = \frac{1}{\kappa}(1 - \gamma/\gamma_0); \qquad \kappa = \omega_p/\omega.$$

J and H are Bessel and Hankel functions; I and K are the corresponding modified functions. Equating the second bracket in (11) to zero, the solution yields an infinite number of phase-eigenvalues in the vicinity of $s=\pm 1$ [3]; those particular solutions of the problem corresponding to a rectilinear flow ($\omega_q = \pm\omega_p$) are a consequence of the Ansatz in (3). The complete solution follows from

$$1 + \vartheta - \frac{\kappa}{s}(1-s^2) - \frac{J_0(\gamma b) - 1}{s^2\gamma_0 b J_1(\gamma b)} = 0; \tag{13}$$

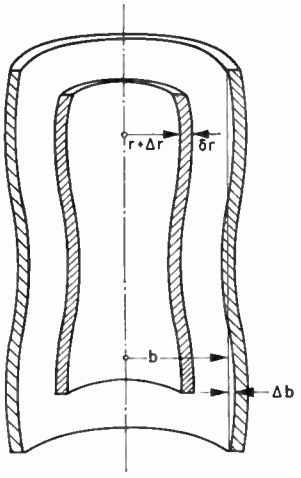

(a)

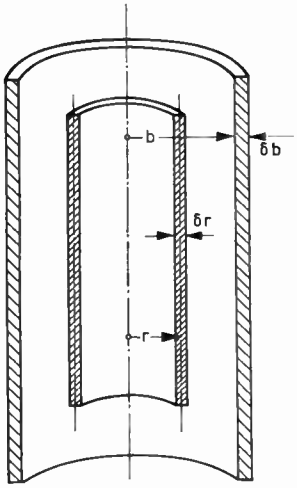

(b)

Fig. 1—(a) Electron trajectories within an electron beam; (b) rectilinear equivalent.

for small space charge parameters ($\kappa \to 0$, $\gamma \to \gamma_0$):

$$s^2 \approx K_0(\gamma_0 b)\,[I_0(\gamma_0 b) - 1]. \qquad (14)$$

While in a plasma (compensated) flow within a finite magnetic field there is an infinite number of phase eigenvalues, (14) yields two values of s, if $\kappa \to 0$. In Fig. 2 the reduction factor is plotted against $\gamma_0 b$ for $\kappa = 0$; for comparison the reduction factor of a rectilinear flow is also shown. Fig. 3 represents the fundamental pair of the reduction factor for $\kappa = 0.5$. In general, the two values of the pair are different; if κ tends to zero, they become equal.

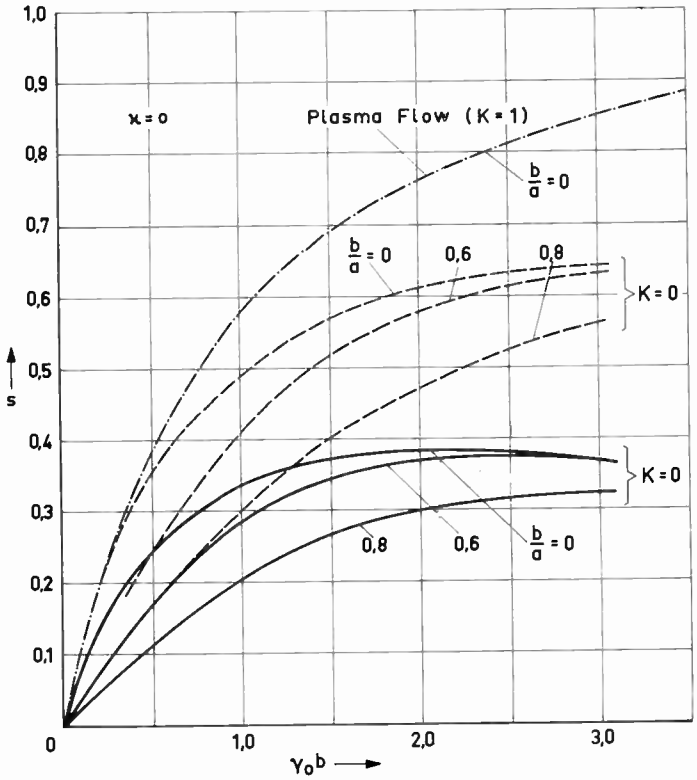

Fig. 2—Plot of the plasma frequency reduction factor s as a function of $\gamma_0 b$ (for the plasma ($K=1$)) and Brillouin (beam ($K=0$) (– – – according to Rigrod and Lewis; —— according to Labus and Pöschl)). Space charge parameter $\kappa = \omega_p/\omega = 0$; b = radius of the solid beam, a = radius of a conducting drift tube.

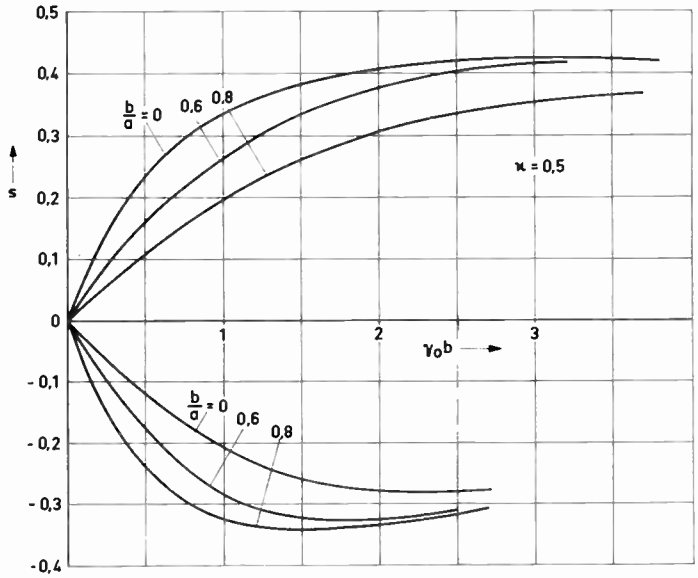

Fig. 3—Plot of the plasma frequency reduction factor for the Brillouin beam as a function of $\gamma_0 b$ and $\kappa = 0.5$.

Magnetically Confined Flow

Now we consider the general case $0 \leqq K \leqq 1$, corresponding to a magnetic field at the cathode of arbitrary value between zero and infinity. Angular velocity and the dc relation between space charge, magnetic field, and beam diameter are given in (2a) and (2c). The limiting values of K are $K=0$ (Brillouin flow) and $K=1$ (rectilinear flow). As has been pointed out, a rectilinear flow can be realized at finite space charge, if $B = B_c = \infty$. A rectilinear and a plasma flow are equivalent in that the reduction factors are the same. For a flow confined within a finite magnetic field, the reduction factor has been calculated by Brewer [7] and by Liebscher [8]. In [7] the procedure of [5] is used: the radial ac perturba-

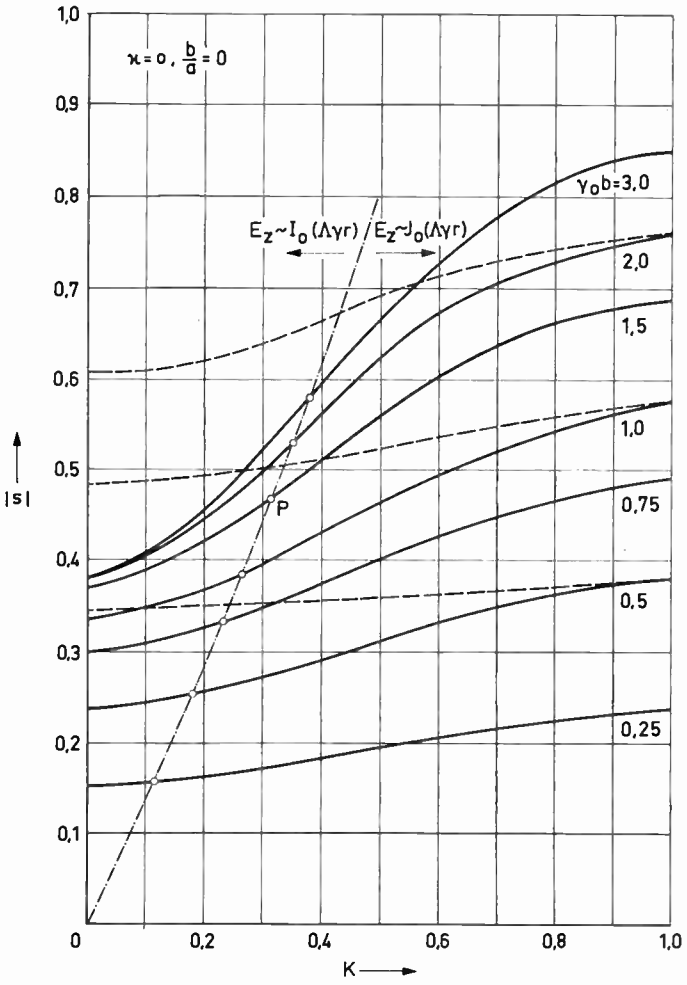

Fig. 4—Plot of the plasma frequency reduction factor as a function of the magnetic flux parameter $K=b_c^2B_c/b^2B$ (– – – according to Brewer). The index c denotes the cathode. On the left and right side of the –·–·– line the axial electric field component is given by the modified Bessel function $I_0(\Lambda\gamma r)$ and the Bessel function $J_0(\Lambda\gamma r)$ respectively.

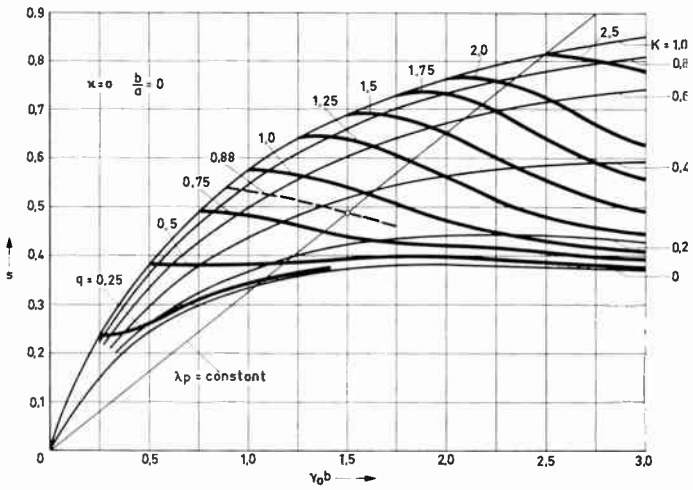

Fig. 5—Plot of the plasma frequency reduction factor s as a function of $\gamma_0 b$ with $q=\gamma_0 b_c\sqrt{B_c/B}$ and K as parameters; $\kappa=0$, $b/a=0$. Intersection points with the straight line through the origin yield s and b for a given plasma wavelength.

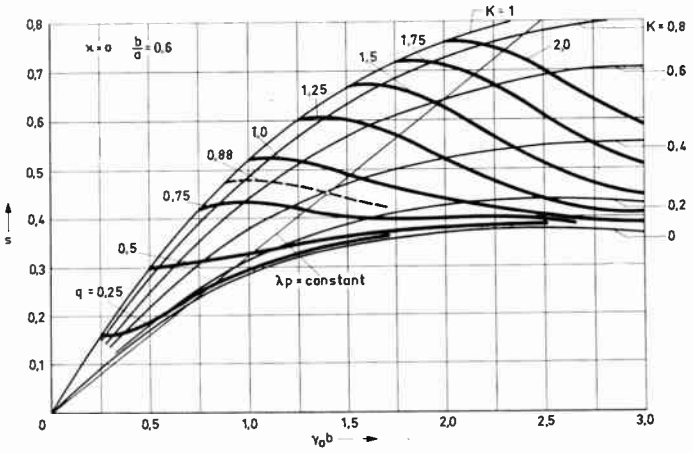

Fig. 6—Plot of the plasma frequency reduction factor s as a function of $\gamma_0 b$ with $q=\gamma_0 b_c\sqrt{B_c/B}$ and K as parameters; $\kappa=0$, $b/a=0.6$.

tions of the electrons at the beam surface are replaced by a surface current; E_ϕ and the ac space charge are disregarded. The analysis in [8] is based on the method in [6], operating with additional and continuous currents Δi_ϕ, Δi_z and fields ΔH_ϕ, ΔH_z; the differential equations of the problem are like those in (4) and (5). In [7], however, there is only one homogeneous differential equation; it is equivalent to (4), if $\zeta\approx 1$ and $E_\phi=0$ is substituted.

Figs. 4–6 are illustrative for the discussion of the results. For practical application, the parameter K, which depends on the beam radius b, proves to be inconvenient, we, therefore, introduce another parameter

$$q = \gamma_0 b_c\sqrt{B_c/B} \tag{15}$$

containing known values and being independent of b. According to (2b), $K=(q/\gamma_0 b)^2$. In order to facilitate the comparison between [7] and [8], the parameter $\Omega/\omega_p=\omega_L K/\omega_p$ in [7] has been expressed by K, through the relation $\Omega/\omega_p=K\sqrt{2(1-K^2)}$.

In Fig. 4 the reduction factor is plotted against K for $b/a=0$ and $\kappa\approx 0$. Figs. 5 and 6 represent s as a function of $\gamma_0 b$ for several values of q and K. The curves $q=$ constant start along the curve $K=1$, where $\gamma_0 b=q$; they approach the curve $K=0$ as $\gamma_0 b\to\infty$.

In Fig. 4 the results of [7] and [8] differ so much the more $K\to 0$, according to the underlying methods of analysis.

The representation of the reduction factor as a function of $\gamma_0 b$, with q as a parameter is advantageous in that the dependence on the beam radius is only in $\gamma_0 b$. The reduction factor is readily obtained from Fig. 5 or Fig. 6, if, for a given q, a certain value of b is desired. The minimum magnetic field B, necessary to obtain that beam radius, can be calculated with (2c) [9]. However, in general, the actual amount of the focusing field

is larger if dc scallops along the beam—caused by improper injection—are to be reduced. As will be noted, s varies little within larger ranges of $\gamma_0 b$, especially around $q=0.5$. Therefore small errors will occur, even if the beam radius is not known exactly.

There are problems [12] with a specified plasma wavelength. In this case, the reduction factor, as well as the beam radius, can readily be determined by means of Fig. 5 or Fig. 6. Due to

$$\lambda_p = 2\pi v_0/s\omega_p, \tag{16}$$

a linear relation between s and $\gamma_0 b$ exists

$$s = \left[3.46\ 10^5\ \frac{U_0^{5/4}}{f\lambda_p I_0^{1/2}}\right]\gamma_0 b. \tag{17}$$

(U_0 = beam voltage, f = frequency, I_0 = beam-current.) For the special values $U_0=800$v, $f=6000$ mcs, $I_0=1$ ma, $\lambda_p=24$ cm, (17) is represented by the straight lines in Figs. 5 and 6. If the cathode radius $b_c=0.04$ cm and $B_c/B=1$, then $q=0.88$. In Fig. 5 ($b/a=0$) the intersection point q of the straight line with the curve $q=0.88$ yields $s=0.485$, $b=0.0675$ cm, and $K=0.35$ in agreement with (2b).

In Fig. 6 ($b/a=0.6$) the corresponding values are $s=0.455$, $b=0.0634$ cm, and $K=0.4$.

The slope of the straight line is inversely proportional to $I_0^{\frac{1}{2}}$ (17). Therefore, at rather small beam currents or perveances the intersection points will be on curves q = constant for which K is near unity. In that case, the plasma flow will be a good approximation. However, in general, the Brillouin type of flow has to be assumed.

The Electric Field Component E_z

The first approximation for the solution of (4) is the Bessel function with the argument

$$T^2 = \frac{s^2-1}{s^2+\sigma}\cdot\gamma^2 = (\Lambda\gamma)^2. \tag{18}$$

Then

$E_z = A\cdot J_0(\Lambda\gamma r)$ if Λ^2 is positive; $s^2 > 2K^2/1-K^2$

$E_z = A\cdot I_0(|\Lambda|\gamma r)$ if Λ^2 is negative; $s^2 < 2K^2/1-K^2$

E_z = constant if $\Lambda^2=0$; $s^2=1$, or $s^2=2K^2/1-K^2$.

In Fig. 7 those configurations are plotted against r. At a specified value of K obtained from $\Lambda^2=0$, the axial field component E_z becomes constant within the beam. According to (18) that is the case, if either $s^2=1$ (corresponding to the particular solution referred to) or

$$|s| = \left(\frac{2K^2}{1-K^2}\right)^{1/2}. \tag{19}$$

In Fig. 4, (19) is represented by the dotted line. Between the ordinate $K=0$ and the intersection points P the axial field component is proportional to $I_0(\Lambda\gamma r)$;

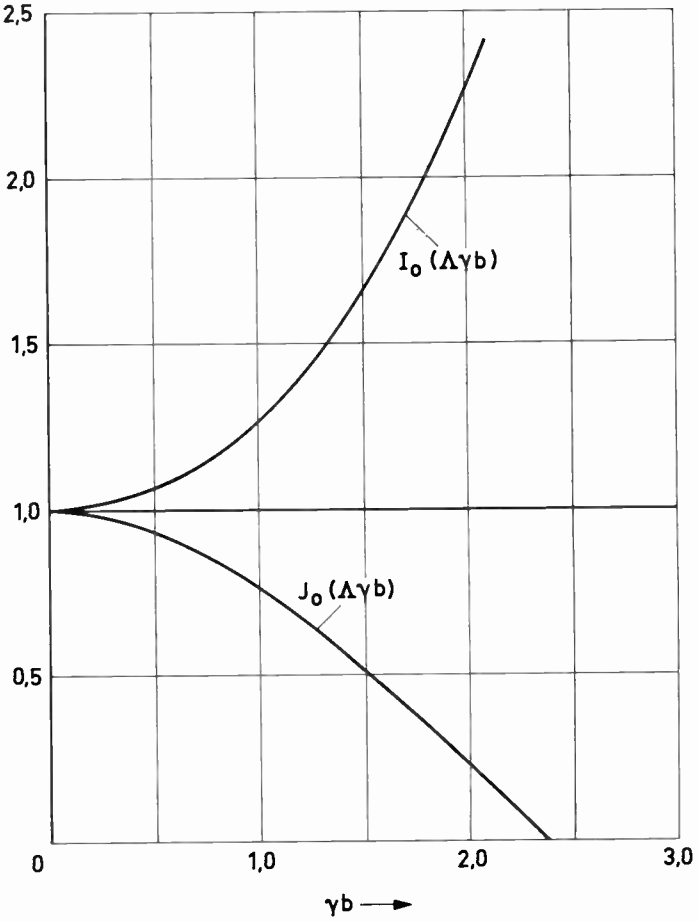

Fig. 7—Configuration of the axial electric field component E_z as a function of the radius r. $E_z \approx J_0(\Lambda\gamma r)$ for $s^2>2K^2/1-K^2$; $E_z \approx I_0(\Lambda\gamma r)$ for $s^2<2K^2/1-K^2$; E_z = constant for $s^2=2K^2/1-K^2$.

between those points and $K=1$ there is $E_z \sim J_0(\Lambda\gamma r)$ and in P there is E_z = constant.

In (4) a singularity occurs if $(s+\sigma)=0$, corresponding to a trivial solution of that differential equation if $E_\phi \equiv 0$ [7].

Experimental Test

We have shown two different procedures in the analysis of wave propagation along electron beams. They differ in their ways of considering the displacements of the beam surface. For a comparison with tests, the measurement of the plasma wavelength by means of the standing wave method seems to be appropriate. The determination of the reduction factor from (16) then depends on how accurately the beam diameter can be measured. From experimental investigations of the wave propagation along a Brillouin flow by Haus [10] and Fried [11] of M.I.T., it can be concluded that the theory based on continuous radial displacements of the electron trajectories inside the beam is the better approach, as compared with the assumption of a surface current. For a conclusive criticism, however, further experiments ought to be considered.

Appendix

The differential equations (4) and (5) are obtained by the equations of motion, the continuity of charges, and Maxwell's equations.

Writing the equation of motion

$$\frac{dv}{dt} = -\frac{e}{m}\left[E + (v \times \mu_0 H)\right] \tag{20}$$

in cylindrical coordinates and referring to (2), (3), and (6), the ac components of velocity become

$$v_r = -j\frac{e}{m}\frac{\sigma}{\omega_q}\left\{\frac{\omega_q}{\omega}E_r + j\frac{\omega_L}{\omega}\right.$$
$$\left.[(1-K)(rE_\phi)' + 2KE_\phi] + j\frac{v_0}{\omega}E_z'\right\}$$
$$v_\phi = -j\frac{e}{m}\frac{\sigma}{\omega}\left\{E_\phi + 2K\frac{\omega_L}{\omega_q}\right.$$
$$\left.\left[(1-K)\frac{\omega_L}{\omega_q}(rE_\phi)' - jE_r + \frac{v_0}{\omega_q}E_z'\right]\right\}$$
$$v_z = j\frac{e}{m\omega_q}\left\{E_z + (1-K)\frac{\omega_L}{\omega}\gamma r E_\phi\right\}. \tag{21}$$

The primes denote derivatives with respect to the radius r. The ac space charge density ρ follows from the equation of continuity:

$$\rho = \frac{m\epsilon_0}{e}\frac{\omega_p^2}{\omega_q}\left[\gamma v_z + j\frac{1}{r}(rv_r)'\right]. \tag{22}$$

With (2a), (21), (22), and $v_{\phi 0} = r\dot{\phi}_0 = r\omega_L(1-K)$ the small signal ac components of current density

$$i_r = -\rho_0 v_r$$
$$i_\phi = -(\rho_0 v_\phi + v_{\phi 0}\rho)$$
$$i_z = -(\rho_0 v_z + v_0\rho) \tag{23}$$

are calculated. The drift velocity v_0 is assumed to be independent of z and r. Introducing those expressions for the current densities into Maxwell's equations and after a rather lengthy rearrangement, the differential equations (4) and (5) for the field component E_z and E_ϕ are obtained. Moreover, the relation exists

$$E_r \approx \frac{j}{\zeta\gamma}E_z'. \tag{24}$$

In general, the inhomogeneous differential equations (4) and (5) are solved by iteration. However, the solution becomes rather simple in the case of a Brillouin flow ($K=0$). The differential equations in question, (7) and (8), can be written in the form [3]

$$L_0\left\{E_z - \frac{\gamma\omega_L}{\omega(s^2-1)}(rE_\phi)\right\} = 0 \tag{25}$$

$$L_1(E_\phi) = -\frac{\omega\omega_L}{\gamma c^2}rL_0(E_z) \tag{26}$$

wherein

$$L_0 = \frac{\partial^2}{\partial r^2} + \frac{1}{r}\frac{\partial}{\partial r} - \gamma^2;$$
$$L_1 = \frac{\partial^2}{\partial r^2} + \frac{1}{r}\frac{\partial}{\partial r} - \left(\frac{1}{r^2} + \gamma^2\right).$$

A solution of (25) which is finite at $r=0$ is

$$E_z = CJ_0(j\gamma r) + \frac{\gamma\omega_L}{\omega(s^2-1)}(rE_\phi). \tag{27}$$

(C = integration constant, J_0 = Bessel's function.)

Moreover, the field components H_ϕ and H_z are required for the boundary condition. From Maxwell's equations and (27) the latter were found to be

$$i\gamma H_\phi = -\frac{\omega\epsilon_0}{\gamma}E_z' + j\omega\epsilon_0\frac{\omega_p^2}{\omega\omega_q}(s^2-1)CJ_1(j\gamma r) \tag{28}$$

$$H_z = j\frac{(s^2-1)}{\gamma\omega_L\mu_0}\frac{1}{r}\left[E_z' + j\gamma CJ_1(j\gamma r)\right]. \tag{29}$$

The Ansatz in (3) is based on a constant beam radius. Actually, the surface electrons are subject to progressing oscillations around the undisturbed beam radius. Fig. 1(a) represents an instantaneous picture of electron trajectories at the beam surface ($r=b$) and within the beam (r), as compared with a rectilinear flow in Fig. 1(b). In [5] the displacements at the beam surface had been taken into account by a surface current producing additional terms in H_ϕ and H_z. Obviously, those radial displacements are not restricted to the beam surface, they are likewise present within the beam.

If, for reasons of the boundary conditions, we want to retain the constant beam radius, we therefore must introduce additional ac space charges $\Delta\rho$ all over the beam cross section. They are given by the condition that for a given moment, there are equal space charges within equivalent volume elements in Fig. 1(a) and (b):

$$2\pi(r+\Delta r)(\delta r)(\rho_0+\rho)dz = 2\pi r(\delta r)(\rho_0+\rho+\Delta\rho)dz.$$

Neglecting products of ac terms (small signal theory) we get

$$\Delta\rho = \rho_0\frac{\Delta r}{r}. \tag{30}$$

In (23) this value is introduced into the expressions of the ac current densities. Thus the additional current densities are found to be

$$i_z = -i_0\frac{\Delta r}{r}; \qquad i_\phi = -\rho_0 v_{\phi 0}\frac{\Delta r}{r}. \tag{31}$$

The corresponding ΔH_ϕ is obtained from Maxwell's equation

$$\frac{1}{r}\frac{\partial}{\partial r}(r\Delta H_\phi) = \Delta i_z = -i_0\frac{\Delta r}{r}. \tag{32}$$

The displacement Δr is found from (21). With $K=0$, $\sigma=-1$, and $\zeta\approx 1$, v_r becomes

$$v_r = \frac{d}{dt}(\Delta r) = \left(\frac{\partial}{dt} + v_0\frac{\partial}{\partial z}\right)\Delta r = j\omega_q \Delta r$$

$$= j\frac{e}{m\omega_q}\left[\frac{\omega_q}{\omega}E_r + j\frac{\omega_L}{\omega}(rE_\phi)' + j\frac{v_0}{\omega}E_z'\right]; \qquad (33)$$

and with respect to (24):

$$\Delta r \approx \frac{je}{m{\omega_q}^2}\left[\frac{1}{\gamma}(1+\omega_q/\omega)E_z' + \frac{\omega_L}{\omega}(rE_\phi)'\right]. \qquad (34)$$

Denoting

$$u = \frac{\gamma\omega_L}{\omega(s^2-1)}(rE_\phi) \qquad (35)$$

we get from (1), (27), (32), (34), and (35)

$$\Delta H_\phi = -\frac{i_0}{r}\int_0^r \Delta r dr = -j\frac{\epsilon_0 v_0}{\gamma r}\left\{C\frac{1+\omega_q/\omega}{s^2}\right.$$

$$\left.[J_0(j\gamma r)-1] + \left(1+\frac{\omega_q}{s^2\omega}\right)u\right\}. \qquad (36)$$

Since for $r\to 0$, $u=0(r^2)$, ΔH_ϕ vanishes near the beam axis as r. Likewise, the additional field component H_z is found to be

$$\Delta H_z = j\frac{\epsilon_0\omega_L}{\gamma}\left\{C\frac{1+\omega_q/\omega}{s^2}[J_0(j\gamma r)-1]\right.$$

$$\left. + \left(1+\frac{\omega_q}{s^2\omega}\right)u\right\}. \qquad (37)$$

Boundary Conditions

The introduction of the additional field components ΔH_z and ΔH_ϕ enables us to consider the boundary conditions along the unperturbed surface ($r=b$) of the beam. Outside the beam, the field components, whose continuity at the boundary is required, are

$$E_z = D_1 H_0^{(1)}(j\gamma r); \qquad E_\phi = D_2 H_1^{(1)}(j\gamma r);$$

$$H_\phi = \frac{\omega\epsilon_0}{\gamma}D_1 H_1^{(1)}(j\gamma r)$$

$$H_z = -\frac{\gamma}{\omega\mu_0}D_2 H_0^{(1)}(j\gamma r).$$

$H_{0,1}^{(1)}$ are Hankel's functions; $D_{1,2}$ are integration constants. Among the corresponding components inside the beam, E_z and E_ϕ are given by (27) and (35), $H_\phi+\Delta H_\phi$ and $H_z+\Delta H_z$ by (28), (29), (36), and (37). The boundary conditions referred to lead to a system of linear equations and finally to the characteristic (11) for the phase-eigenvalues and the plasma frequency reduction factor.

Bibliography

[1] Hahn, W. C. "Small Signal Theory of Velocity Modulated Electron Beams," *General Electric Review*, Vol. 42 (June, 1939), pp. 258–270.

[2] Ramo, S. "The Electronic-Wave Theory of Velocity-Modulation Tubes," Proceedings of the IRE, Vol. 27 (December, 1939), pp. 757–763.

[3] Labus, J. "Einfluss der Lorentzkraft auf die Raumladungswellen im Elektronenstrahl," *Archiv der elektrischen Übertragung*, Vol. 7 (February, 1953), pp. 88–94.

[4] Twiss, R. Q., "Propagation in Electron-Ion Streams," *Physical Review*, Vol. 88 (December, 1952), pp. 1392–1407.

[5] Rigrod, W. W., and Lewis, J. A. "Wave Propagation Along a Magneticaly Focused Cylindrical Electron Beam," *Bell System Technical Journal*, Vol. 33 (March, 1954), pp. 399–416.

[6] Labus, J., and Pöschl, K. "Raumladungswellen in ionenfreien Elektronenstrahlen," *Archiv der elektrischen Übertragung*, Vol. 9 (January, 1955), pp. 39–46.

[7] Brewer, G. R. "Some Effects of Magnetic Field Strength on Space-Charge-Wave Propagation," Proceedings of the IRE, Vol. 44 (July, 1956), pp. 896–903.

[8] Liebscher, R. "Raumladungswellen bei endlichem Magnetfeld an der Kathode einer zylindrischen Elektronenströmung," *Archiv der elektrischen Übertragung*, Vol. 11 (1957), to be published.

[9] Pierce, J. R., *Theory and Design of Electron Beams*, New York: D. van Nostrand Co., Inc., 1954.

[10] Haus, A. H., "Propagation of Signals on Electron Beams," *Quarterly Progress Report*, Massachusetts Institute of Technology (July 15, 1953), pp. 41–42.

[11] Fried, C., "Noise in Electron Beams," *Quarterly Progress Report*, Massachusetts Institute of Technology, (January, 1954), pp. 22–25.

[12] Labus, J. and Liebscher, R. "Plasma-Wavelength and the Low Noise T. W. T.," (International Congress on Microwave Tubes in Paris, 1956), *Archiv der elektrischen Übertragung*, Vol. 10 (October, 1956), pp. 421–423.

The High Current Limit for Semiconductor Junction Devices*

NEVILLE H. FLETCHER†

Summary—**At very high operating levels the density of carriers injected into the body of a semiconductor junction device is comparable with the carrier density in the emitter regions of the device. The effect of these high densities on the lifetime and mobility of carriers is considered, and new equations are derived relating the carrier densities on either side of a forward biased junction. These equations are applied to derive the forward characteristics of two diode types, and to consider the dependence of emitter efficiency on current density for alloy junction transistors.**

For a PIN diode, over a considerable current range, the forward current varies approximately as exp ($\lambda qV/kT$), where $\frac{1}{2} \leqq \lambda \leqq 1$; $\lambda = 1$ for very thin diodes, and $\lambda = \frac{1}{2}$ for thick diodes. For PIR diodes, the forward current varies as exp ($qV/2kT$). Both types show additional voltage drop at high currents. Transistor emitter efficiency decreases with increasing current, but saturates to a finite value at high currents. These predictions are in accord with experiment and suggest design considerations for optimum performance. A brief discussion is also given of the usefulness of these new results in device applications.

Introduction

THEORIES of the operation of semiconductor junction devices are conveniently classified on the basis of carrier injection level. Junction devices typically have regions of relatively high resistivity (a few ohm cm) in conjunction with regions of very low resistivity (hundredths or thousandths of an ohm cm) and these regions provide a yardstick for measuring carrier densities.

Low level theories, such as that of Shockley *et al.*,[1,2] are characterized by the fact that injected carrier densities are assumed to be very much less than the equilibrium majority carrier density in the high resistivity regions. Such theories give small signal parameters which are constants and the theory is essentially linear.

In transition theories, such as those of Webster,[3] Rittner,[4] and Misawa,[5,6] injected carrier densities are considered to be comparable with majority carrier densities in the high resistivity regions. These theories are relatively complicated and the small signal parameters are no longer constants. For very high injection levels, these theories merge with the high level theories and their form becomes simpler.

High level theories are characterized by the assumption that injected densities are very much greater than the equilibrium densities in the high resistivity regions, but still very much less than the density of carriers in the low resistivity regions. Theories in this group have been restricted to diodes, as transistors have been described by the more elaborate transition theories which include the high level case as a limit. Hall[7] has considered a two-junction diode which we can denote as PIN, while Kinman, *et al.*,[8] and Spenke[9] have treated a junction and recombination-surface diode which we shall call PIR. The interesting result of these treatments is that the diode forward current is proportional to exp ($qV/2kT$) in both cases. A conflicting theory for the PIN diode has been proposed by Kleinman,[10] who obtains an exp (qV/kT) characteristic at variance with experiment. We believe this discrepancy to be due to Kleinman's inadequate treatment of recombination in the I region. His paper does, however, include some treatment of higher level effects.

Limiting theories deal with the case of still higher injection levels, when the injected carrier density is comparable with the majority carrier density in the low resistivity regions. It is to the development of a theory of this kind that the present paper is devoted.

Phenomena at Very High Levels

Before proceeding to develop our theory, we shall examine some of the assumptions usually made and see to what extent they must be modified at the very high carrier densities which we shall encounter.

Lifetime

The recombination of excess carriers in germanium and silicon is primarily caused through the agency of trapping centers which have energy levels lying near the middle of the forbidden band. The theory of recombination through these centers has been given by Hall[11]

* Original manuscript received by the IRE, September 24, 1956; revised manuscript received February 25, 1957.

† Division of Radio Physics, Commonwealth Scientific and Industrial Research Organization, Sydney, Australia.

[1] W. Shockley, "The theory of *p-n* junctions in semiconductors and *p-n* junction transistors," *Bell Sys. Tech. J.*, vol. 28, pp. 435–489; July, 1949.

[2] W. Shockley, M. Sparks, and G. K. Teal, "The *p-n* junction transistor," *Phys. Rev.*, vol. 83, pp. 151–162; July, 1951.

[3] W. M. Webster, "On the variation of junction-transistor current-amplification factor with emitter current," PROC. IRE, vol. 42, pp. 914–920; June, 1954.

[4] E. S. Rittner, "Extension of the theory of the junction transistor," *Phys. Rev.*, vol. 94, pp. 1161–1171; June, 1954.

[5] T. Misawa, "Emitter efficiency of junction transistor," *J. Phys. Soc. Japan*, vol. 10, pp. 362–367; May, 1955.

[6] T. Misawa, "A note on the extended theory of the junction transistor," *J. Phys. Soc. Japan*, vol. 11, pp. 728–739; July, 1956.

[7] R. N. Hall, "Power rectifiers and transistors," PROC. IRE, vol. 40, pp. 1512–1518; November, 1952.

[8] T. H. Kinman, G. A. Carrick, R. G. Hibberd, and A. J. Blundell, "Germanium and silicon power rectifiers," *Proc. IEE*, vol. 103, Part A, pp. 89–111; April, 1956.

[9] E. Spenke, "Durchlass- und sperreigenschaften eines *p-i*-metallgleichrichters," *Z. Naturf.*, vol. 11a, pp. 440–456; June, 1956.

[10] D. A. Kleinman, "The forward characteristic of the PIN diode," *Bell Sys. Tech. J.*, vol. 35, pp. 685–706; May, 1956.

[11] R. N. Hall, "Electron-hole recombination in germanium," *Phys. Rev.*, vol. 87, p. 387; July, 1952.

and by Shockley and Read,[12] who find that the lifetime τ depends on the injected carrier density δp according to

$$\tau = \frac{\tau_0(1 + a\delta p)}{1 + b\delta p} \tag{1}$$

where τ_0 is the low-level lifetime and a and b are constants depending on the characteristics of the recombination centers. This relation shows that τ initially rises or falls as δp is increased, but attains a constant value at high injection levels. Experiments on germanium[13] and silicon[14] indicate that, at any rate for the samples studied, τ rises initially before attaining its high level value. The result (1) is derived on the assumption that recombination at a trap can take place instantaneously, no excited levels being involved. If an excited level is involved in the trapping process, then the recombination process takes an appreciable time, and this could conceivably limit the recombination rate and lead to an increase in τ at extremely high levels. Burton, *et al.*,[15] have shown that a concentration of 10^{12} atoms/cm^3 of nickel or 10^{13} atoms/cm^3 of copper could explain the observed lifetimes of "good" germanium crystals ($\tau \sim 10^{-4}$ sec). If this were the case, and the recombination process occupied more than 10^{-10} sec, recombination rate limiting should be appreciable at carrier densities of the order of 10^{19} pairs/cm^3. There may be additional complications, if there is more than one type of recombination center, but we shall not consider this possibility here.

Recombination by way of traps is, however, only one possible recombination mechanism. The most important remaining mechanism is photon-radiative recombination. This has been treated by van Roosbroeck and Shockley[16] who show that the recombination rate is

$$R_c = \frac{np}{n_i^2} R \tag{2}$$

where, from optical data, for germanium

$$R = 1.57 \times 10^{13} \text{ cm}^{-3} \text{ sec}^{-1} \tag{3}$$

corresponding to a lifetime of 0.75 sec, in intrinsic material. At high levels $n = p$ so that (2) shows that $\tau = 100$ μsec for $n = 4 \times 10^{17}$ cm^{-3}. Since high level lifetimes are $\sim$100 μsec in some cases,[13] this additional mechanism may reduce the lifetime for carrier densities above 10^{18} cm^{-3}.

In our discussion we shall treat high level lifetimes as constant, but recognize the possibility of variations at very high carrier densities. The effect of such variations will be negligible in most devices.

Mobility

It is well known that charged impurities reduce the mobility of holes and electrons by scattering, and this effect becomes noticeable in germanium for impurity densities greater than about 10^{16} cm^{-3}. This effect has been treated on a classical approximation by Conwell and Weisskopf[17] who derive the expression (in terms now of a diffusion coefficient)

$$D_I = 2^{7/2}\pi^{-3/2}N^{-1}\kappa^2 q^{-4} m^{-1/2}(kT)^{5/2} \cdot [\log_e (1 + 9\kappa^2 N^{-2/3} q^{-4} k^2 T^2)]^{-1} \tag{4}$$

where N is the density of singly charged impurity centers, m is the effective mass of the charge carrier, and κ is the dielectric constant of the semiconductor. The logarithmic term is an approximation taking into account the finite range of interaction with the field of each ion. A more rigorous quantum mechanical treatment by Brooks[18,19] gives a different form for this cutoff term, but agreement between the two results is reasonably good in most cases.

The result (4) has also been given in the theory of gas diffusion. In addition, Chapman and Cowling[20] discuss the case of the mutual diffusion of two groups of charged particles. This case is applicable to the interaction of holes and electrons on a classical approximation. The first approximation to the result is, for $n = p$

$$D_{12} = 3\pi^{-1/2}2^{-3/2}n^{-1}\kappa^2 q^{-4}\left(\frac{m_1 + m_2}{m_1 m_2}\right)^{1/2}(kT)^{5/2} \cdot [\log_e (1 + 16\kappa^2 n^{-2/3} q^{-4} k^2 T^2)]^{-1} \tag{5}$$

where m_1 and m_2 are the effective masses of electrons and holes, respectively. The difference in the cutoff term is not significant, as we expect a quantum correction in any case. The result (5) differs from (4) by a factor 0.294, apart from the mass term. This difference is due to the fact that Chapman's analysis, resulting in (5), includes the effects of like carrier collisions, which were neglected in the Conwell-Weisskopf result (the Lorentz approximation). Debye and Conwell[19] discuss like carrier collisions for the impurity scattering case and suggest that (4) should be multiplied by a factor of about 0.6 to allow for this effect.

[12] W. Shockley and W. T. Read, "Statistics of the recombination of holes and electrons," *Phys. Rev.*, vol. 87, pp. 835–842; September, 1952.

[13] L. D. Armstrong, C. L. Carlson, and M. Bentivegna, "PNP transistors using high-emitter-efficiency alloy materials," *RCA Rev.*, vol. 17, pp. 37–45; March, 1956.

[14] G. Bemski, "Lifetime of electrons in *p*-type silicon," *Phys. Rev.*, vol. 100, pp. 523–524; October, 1955.

[15] J. A. Burton, G. W. Hull, F. J. Morin, and J. C. Severiens, "Effect of nickel and copper impurities on the recombination of holes and electrons in germanium," *J. Phys. Chem.*, vol. 57, pp. 853–859; November, 1953.

[16] W. van Roosbroeck and W. Shockley, "Photon-radiative recombination of electrons and holes in germanium," *Phys. Rev.*, vol. 94, pp. 1558–1560; June, 1954.

[17] E. Conwell and V. F. Weisskopf, "Theory of impurity scattering in semiconductors," *Phys. Rev.*, vol. 77, pp. 388–390; February, 1950.

[18] H. Brooks, "Scattering by ionized impurities in semi-conductors," *Phys. Rev.*, vol. 83, p. 879; August, 1951.

[19] P. P. Debye and E. Conwell, "Electrical properties of N-type germanium," *Phys. Rev.*, vol. 93, pp. 693–705; February, 1954.

[20] S. Chapman and T. G. Cowling, "The Mathematical Theory of Non-Uniform Gases," Cambridge University Press, Cambridge, Eng., pp. 177–179; 1952.

In Fig. 1 we have plotted the diffusion coefficients of electrons and holes in germanium as a function of injection level. Approximate effective mass values were taken as $\frac{1}{5}$ and $\frac{1}{4}$ respectively, and the diffusion coefficient given by (5) was combined with the lattice diffusion coefficient by addition of reciprocals.

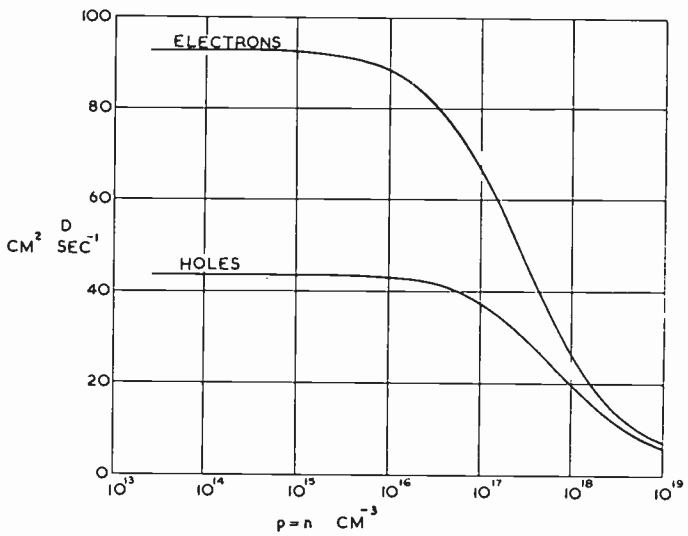

Fig. 1—Diffusion coefficients for electrons and holes in intrinsic germanium at 300°K, as functions of injected carrier density.

From this figure it is evident that hole-electron scattering is important at densities greater than 10^{17} cm^{-3}, and that at densities greater than 10^{18} cm^{-3} the electron and hole diffusion constants are essentially equal.

Of course, this whole approach represents a simple approximation, since the band structure of germanium is quite complex.[21] The assumption of an isotropic effective mass for electrons and of a single isotropic effective mass for holes is far from reality, but the effect of departures from these idealizations on the scattering process as calculated should not be large.

Degeneracy

All theories mentioned in the Introduction use Boltzmann statistics, and this is, in fact, necessary, if the results are to be obtained in simple form. This approximation leads to an error at high injection levels when the difference between Fermi and Boltzmann statistics is appreciable. This has been discussed in some detail by Shockley.[22]

From the formulas given by Herman[21] for the band structure of germanium, the effective numbers of states in the conduction and valence bands are

$$N_c \approx 1.2 \times 10^{19} \text{ cm}^{-3}$$

$$N_v \approx 3.8 \times 10^{18} \text{ cm}^{-3}.$$

[21] F. Herman, "The electronic energy band structure of silicon and germanium," PROC. IRE, vol. 43, pp. 1703–1732; December, 1956.

[22] W. Shockley, "Electrons and Holes in Semiconductors," D. Van Nostrand Co., Inc., New York, N. Y., pp. 230–249; 1950.

It is thus evident that degeneracy will first become appreciable in the valence band. From Shockley's discussion, the error in using Boltzmann statistics is less than a factor of two for predicted carrier densities less than about $4N$—a hole density of 1.5×10^{19} cm^{-3} for germanium.

In all cases, the classical result overestimates the carrier density in the band. This may have an appreciable effect at high carrier densities, but we shall use Boltzmann statistics in our discussion to follow, in order that our results may be presented in reasonably simple form.

Junction Relations

In all other theories, modulation of the conductivity of heavily doped regions has been ignored, but this is no longer valid in the high level limit. We shall now derive the correct relations between the carrier densities on either side of a PI junction. These results can be immediately extended to general PN junctions, but, since we only require the PI case, we shall restrict our discussion to this. The relations derived in this section form the basis of our treatment of the high level limit.

Boltzmann statistics show that if we have two identical sets of energy levels in thermodynamic equilibrium, but differing in energy by an amount E, then the populations of the two sets of levels will be related by

$$n_1 = n_2 e^{E/kT}. \tag{6}$$

Applying this to an abrupt PI junction, in which the equilibrium hole density in the P region is p_0 and the equilibrium hole or electron density in the I region is n_i, we find that

$$p_0 = n_i e^{q\phi/kT} = n_i e^{\theta\phi} \tag{7}$$

where ϕ is the "built in" potential difference across the junction. For brevity, we shall in future write θ for q/kT.

Now we are interested in the quasi-equilibrium or steady state case in which a current is flowing across the junction. It seems legitimate to extend the equilibrium relation (6) to cover this case, provided that the carrier density and potential gradients in the homogeneous regions are sufficiently small, for then there is no appreciable change in these quantities in one mean free path of a carrier. When this condition is not satisfied to a sufficient approximation, the relation (6) will be inaccurate, but may still be retained as a first approximation.

There is one further complication in that, when the equilibrium is disturbed in the way we are contemplating, the carrier densities tend to return to their equilibrium values with a characteristic lifetime. This will not affect our junction relations, provided the width of the junction transition region is much less than a carrier diffusion length. This will always be true for the type of junctions we shall consider. If we are to be able to treat the junction as negligibly thin, it is also necessary that the Debye length in the lightly doped regions be very much less than the minimum dimensions of these

regions. Shockley[1] discusses this at some length and shows that the Debye length in intrinsic germanium at room temperature is $\sim 7\times 10^{-5}$ cm. Since this length varies as the inverse square root of the carrier density, it is truly negligible in the cases with which we shall deal.

Suppose that these conditions are fulfilled and that we apply a voltage V to the junction in the forward direction (P region positive). Then the total junction potential is reduced from ϕ to $(\phi - V)$ and (6) gives

$$p(P) = p(I)e^{\theta(\phi-V)} \tag{8}$$

for the relation between the hole populations on either side of the junction, and

$$n(P) = n(I)e^{-\theta(\phi-V)} \tag{9}$$

for the electron populations.

In place of the relation

$$np = n_i^2, \tag{10}$$

which holds for the true equilibrium case, we now have electrical neutrality relations for the I and P regions

$$\left.\begin{aligned} p(I) &= n(I) \\ p(P) - p_0 &= n(P) - \frac{n_i^2}{p_0} \end{aligned}\right\}. \tag{11}$$

If we neglect n_i^2/p_0 in comparison with p_0, then (7)–(9) and (11) can be combined to give

$$\left.\begin{aligned} p(P) &= p_0 A \\ n(P) &= p_0(A-1) \\ p(I) &= n(I) = n_i A e^{\theta V} \end{aligned}\right\} \tag{12}$$

where

$$A = \left[1 - \frac{n_i^2}{p_0^2}e^{2\theta V}\right]^{-1} = \left[1 - e^{2\theta(V-\phi)}\right]^{-1}. \tag{13}$$

These expressions will be the basis of all that follows.

We note that the relations (12) reduce to the usual low level relations[1] for $V \ll \phi$, but as $V \to \phi$ all the carrier densities approach infinity. This actually causes no trouble, as it proves impossible to apply a voltage equal to ϕ to the junction without applying an infinite voltage to the device as a whole.

It should also be pointed out that the relations (12) are only approximate in that they employ classical statistics and are based on the assumption of quasi-equilibrium. To gain some idea of the validity of this second assumption, we observe that a mean free path in germanium or silicon at room temperature is about 10^{-5} cm.[23] Since we customarily consider regions greater than 10^{-3} cm in width, we can thus tolerate quite large carrier density variations without invalidating our assumptions.

[23] W. Shockley, "Electrons and holes in semiconductors," *op. cit.*, p. 215.

The RPINR Diode

As our first application of the theory we shall consider the case of the RPINR diode shown in Fig. 2. The two combining surfaces bounding the low resistivity regions have been introduced, both to simplify the theory and to represent a closer approach to reality, for alloy junctions, than the assumption of semi-infinite end regions. We shall define a recombining surface to be such as to maintain carrier densities at their equilibrium values at this surface, and to offer no barrier to carrier flow. In practice this could be attained by a thin semiconductor region of very low lifetime backed by metal.

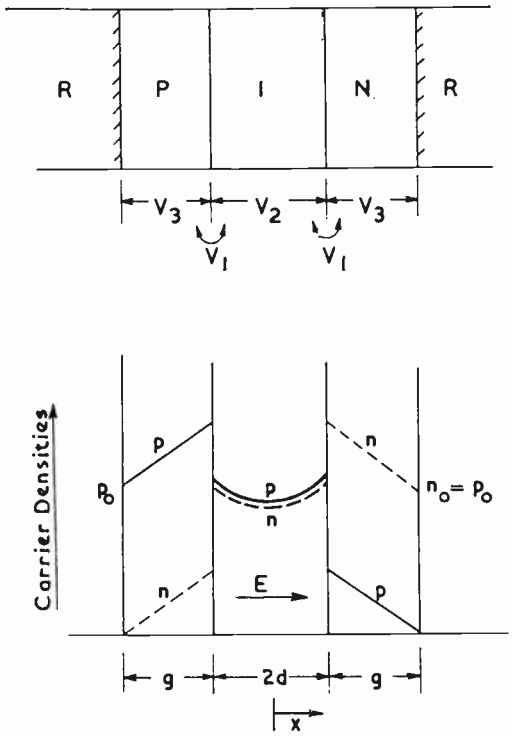

Fig. 2—The RPINR diode.

We make the simplification of neglecting volume recombination in the P and N regions, but suppose that carriers in the I region recombine with a constant high level lifetime τ. Neglect of recombination in the P and N regions makes no fundamental difference to the results. Current flow will be assumed one dimensional throughout.

With these assumptions it is possible to carry through the calculation quite generally, but the arithmetic is forbiddingly complicated. In order to elucidate the behavior of the diode, we make the simplifying assumption that electron and hole mobilities are equal and that the conductivities of the N and P regions are also equal. The first of these assumptions is not as restrictive as it first appears, since Fig. 1 shows it is reasonably true for intrinsic germanium at injection levels of 10^{17} cm^{-3} or greater, and, in any case, it will introduce only small quantitative variations from reality. We allow for impurity and carrier scattering in the N and P regions by

writing the diffusion coefficient in these regions as βD, and for hole-electron scattering in the I region by writing αD. The approximate reciprocal rule for addition of diffusion coefficients then gives

$$\left.\begin{aligned}\frac{1}{\alpha D} &= \frac{1}{D} + \frac{1}{D_{12}} \\ \frac{1}{\beta D} &= \frac{1}{D} + \frac{1}{D_{12}} + \frac{1}{D_I}\end{aligned}\right\} \tag{14}$$

where D is the diffusion coefficient due to lattice scattering, D_{12} accounts for hole-electron scattering and is given by (5), and D_I accounts for impurity scattering and is given by (4). Since holes and electrons have different scattering environments in the N and P regions, they will have slightly different β values, but we shall use a single average value in accord with our proposed approximation.

The problem is now essentially symmetric about the center of the I region, and the dimensions and carrier densities are as shown in Fig. 2. The applied voltage, V, may be conveniently divided into components as shown in the upper part of the figure. Within the I region $n = p$, so that the carrier density satisfies

$$\frac{d^2n}{dx^2} = \frac{n}{L^2} \tag{15}$$

where

$$L^2 = \alpha D\tau. \tag{16}$$

Using (12) we then find

$$n = n_i A e^{\theta V_1} \operatorname{sech} \frac{d}{L} \cosh \frac{x}{L}, \tag{17}$$

where A is defined by (13) with V_1 substituted for V. Within the I region the hole and electron current densities are given by

$$J_p = qp\alpha\mu E - q\alpha D \frac{dp}{dx} \tag{18}$$

$$J_n = qn\alpha\mu E + q\alpha D \frac{dn}{dx} \tag{19}$$

where currents are positive flowing to the right in Fig. 2. The same equations apply to the P and N regions with α replaced by β. The requirement that hole current and electron current be continuous across the junctions determines E on each side of the junctions, and with the aid of (17) the total diode current density is found to be

$$J = 2qn_i A\alpha D e^{\theta V_1} Q \tag{20}$$

where

$$Q = \frac{2A - 1}{L} \tanh \frac{d}{L} + \frac{\beta}{\alpha} \frac{n_0}{n_i} \frac{1}{g} \frac{(A - 1)}{A} e^{-\theta V_1}. \tag{21}$$

We should note that for the case of small currents ($V_1 \ll \phi$) this expression reduces exactly to Hall's expression,[7] if we put $b = 1$, as required by our assumptions, and neglect scattering.

By adding (18) and (19), E is found as a function of J in the I region, and this can be immediately integrated to give

$$V_2 = 4\theta L \left[(\tan^{-1} e^{d/L}) - \frac{\pi}{4} \right] \cosh \frac{d}{L} \cdot Q \tag{22}$$

and this is again seen to reduce to Hall's expression[7] for V_1 small.

The field in the P and N regions can be found similarly, if we observe that the carrier distribution in these regions is linear to a good approximation. Integration then yields

$$V_3 = \theta \frac{\alpha}{\beta} \frac{n_0}{n_i} g e^{-\theta V_1} \log_e [2A - 1] Q \tag{23}$$

which, for small V_1, is found to reduce to the simple ohmic voltage drop over the region concerned. The total voltage drop across the diode is

$$V = 2V_1 + V_2 + 2V_3. \tag{24}$$

We may also note in passing that if we set $d = 0$, then (20) reduces to

$$J = \frac{2qn_0\beta D}{g} (A - 1) = \frac{2qn_0\beta D}{g} [e^{\theta(2V_1 - 2\phi)} - 1] A \tag{25}$$

which is the correct result for a symmetrical RPNR diode with total built in potential 2ϕ and total applied junction voltage $2V_1$.

Diode Characteristics

The calculated forward characteristics for typical diodes with I regions of various widths are shown in Fig. 3. Values of the other parameters used are

$$g = 0.01 \text{ cm}, \quad \tau = 50\ \mu\text{sec}, \quad n_0 = p_0 = 10^{18}\ \text{cm}^{-3},$$
$$T = 300^\circ\text{K}, \quad D = 50\ \text{cm}^2/\text{sec}$$

other parameters being approximately those for germanium. It will be observed that for thick diodes the current commences as exp $(\frac{1}{2}\theta V)$ and at high levels falls off well below this value. For diodes of intermediate thickness, the characteristic is initially exp $(\frac{1}{2}\theta V)$, but rises above this value for moderate currents and over quite a large range is represented fairly well by exp $(\lambda\theta V)$ where $\frac{1}{2} \leq \lambda \leq 1$. Again the current falls off at very high levels. When $d = 0$, the characteristic is exp (θV) at all moderate levels until it finally drops off at very high levels.

Qualitatively the behavior may be expressed as follows. At low levels Hall's analysis is accurate and substantially all current flow is due to recombination in the I region. As more voltage is applied, the carrier concentration in the I region rises and the injection efficiency falls. The current flowing over both junctions varies approximately as exp (θV) and increases the slope of the curve at higher levels. At very high currents the voltage

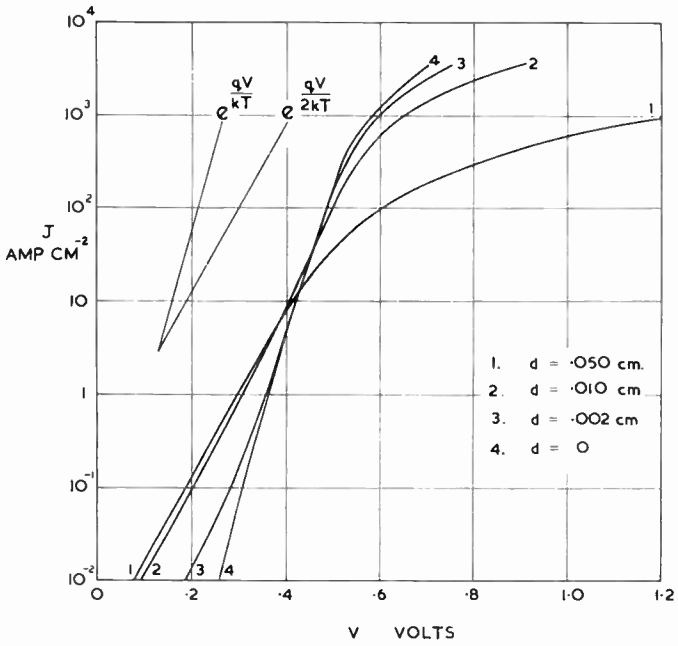

Fig 3—Theoretical RPINR diode characteristics.

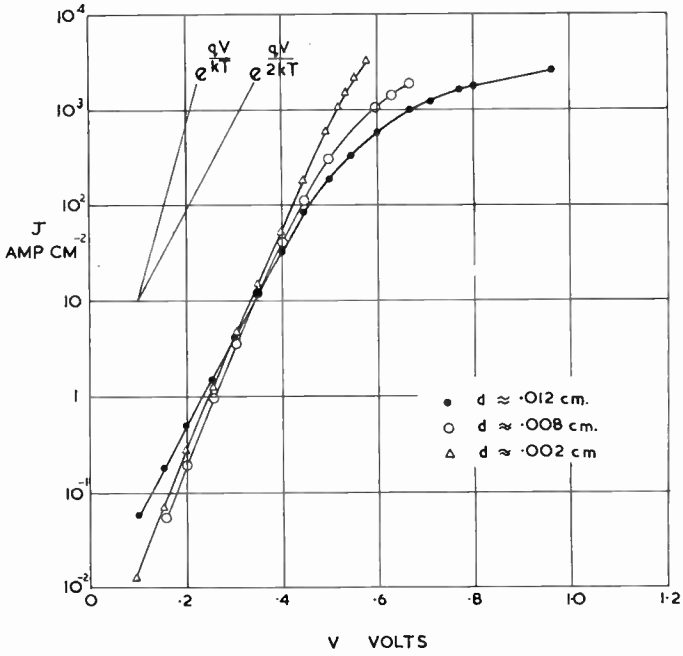

Fig. 4—Experimental characteristics for In-Ge-(SnPbSb) diodes.

drop across the I region increases greatly, voltage drops across the P and N regions become appreciable, and the curve flattens out. Hole-electron scattering magnifies this flattening by reducing the current flow for a given carrier density.

We should remark further that if the "intrinsic" region has an appreciable donor or acceptor concentration, then the low level characteristic will have the typical $[\exp(\theta V)-1]$ shape, so that there may be no $\exp(\frac{1}{2}\theta V)$ region for rather thin diodes made with nonintrinsic material. We should also point out that our analysis is not valid, even for truly intrinsic material, at currents comparable with the reverse saturation current of the device. This is not an inherent limitation of the theory, but arises because, in the interests of simplicity, we have neglected certain small terms.

Similar behavior is shown in the experimentally determined curves of Fig. 4. Diodes were made from germanium wafers of about 3 ohm cm resistivity by alloying indium to one face and a mixture of lead and tin in eutectic ratio with 5 per cent of added antimony to the other. Precautions were taken to reduce the ohmic resistance of contacts to the diode to a negligible value, and measurements were taken in a liquid bath to minimize heating effects. Since no attempt has been made to relate accurately the parameters used for the theoretical curves to those of the measured diodes, Figs. 3 and 4 should only be compared qualitatively.

Design Considerations

The results of this analysis can be applied with advantage to optimizing the design of high current diodes. Here, two things must be taken into account: the forward voltage drop at a given large current must be as small as possible, and the reverse characteristics must be adequate from both leakage and breakdown points of view.

First consider forward currents. From Fig. 3 there is clearly an optimum value of d for a general purpose diode (in this case $d \approx 0.01$ cm). For d values much larger than this, operation becomes very inefficient at high levels, while for d much smaller, operation becomes inefficient at low currents, though this is much less important and can usually be neglected.

The optimum values of g and p_0 are much more difficult to determine and depend on all the other parameters, as well as the current level at which the diode is required to work. Too large a value of g obviously makes V_3 excessive, whilst too small a value can reduce the injection efficiency of the junctions to such an extent that V_2 becomes excessive. Similarly, a low value of p_0 reduces emitter efficiency and increases V_2 and V_3, so that the curve flattens off at a relatively low current. For a very large value of p_0, the current will show little rise above $\exp(\frac{1}{2}\theta V)$, but will maintain this slope to very high current densities.

Actually, values of p_0 and g are almost completely determined by the alloying process and they cannot be varied over very large ranges without considerable inconvenience. The worth of a particular change can be determined by explicit calculation or perhaps more easily by experiment.

Now consider the reverse characteristic. Saturation and leakage currents are determined primarily by the semiconductor surface, so that changes in d have relatively little effect, provided both junctions are of good quality. The contribution of the volume to the saturation current will in any case be approximately proportional to d.

Breakdown of junctions, whether by avalanche or by Zener mechanism, is characterized by a critical field E_c, dependent in magnitude generally upon the exact impurity distribution in the junction. For the case of abrupt junctions such as we expect from the alloying process, the field distribution under reverse bias conditions is as shown in Fig. 5.

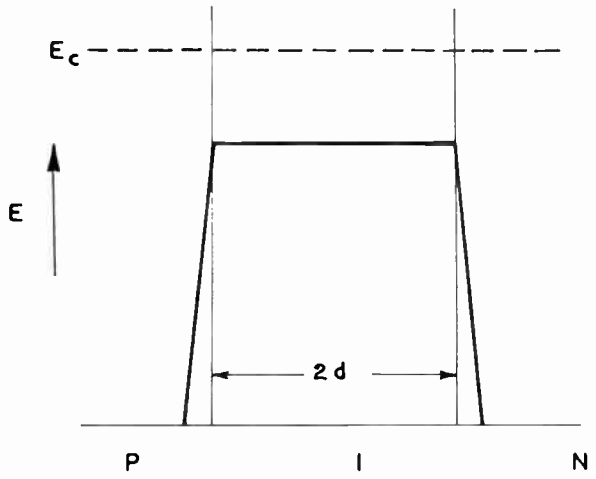

Fig. 5—Field distribution in reverse-biased PIN diode.

The voltage across the diode is given by the area under the curve, and the breakdown voltage is clearly

$$V_c = 2dE_c. \tag{26}$$

If the I region is not truly intrinsic, but lightly doped, then the top of the curve will be sloped rather than flat, and the breakdown voltage will be reduced somewhat.

For an abrupt junction on germanium, the critical field is of the order of 10^5 volts/cm[24] so that from (26) $2d \sim 10^{-5}\ V_c$. For a diode with 300-volt breakdown, we thus require $2d > 0.003$ cm and from Fig. 3 this value is small enough to give a characteristic with slope substantially θ.

The RPIR Diode

We now consider the high level theory of the RPIR diode. The analysis in this case can be carried through quite generally, though it is desirable to neglect all volume recombination if the results are to be reasonably manageable. This will have little effect on the results, provided the width of the regions considered is substantially less than a diffusion length. In the analysis whose results are presented below, we have also omitted the effects of impurity and collision scattering, since this complicates the result without affecting it very much.

The geometry of the diode is shown in Fig. 6, together with applied voltages and carrier densities.

We proceed very much as we did in the preceding section. The carrier densities in the two regions are linear to a good approximation and we can write down the equations of current flow. The requirement of continuity of hole and electron current across the junction gives the fields in the P and I regions at this point and, from the equations of current flow, the fields everywhere can be determined and integrated to give the voltage drops.

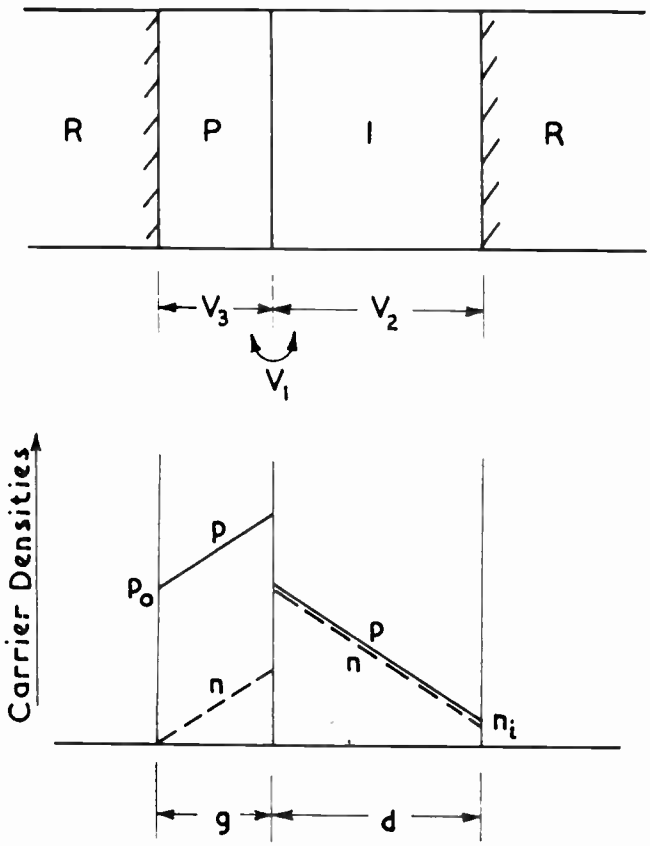

Fig. 6—The RPIR diode.

Summarizing the results we find

$$J_p = qAn_iD_pe^{\theta V_1}\left\{\frac{2A}{d} + \frac{(2A-1)}{g}\sqrt{\frac{A-1}{A}}\right\} \tag{27}$$

$$J_n = qAn_iD_ne^{\theta V_1}\left\{\frac{2(A-1)}{d} + \frac{(2A-1)}{g}\sqrt{\frac{A-1}{A}}\right\} \tag{28}$$

$$V_2 = \theta d\left\{\frac{2A-1}{d} + \frac{(2A-1)}{g}\sqrt{\frac{A-1}{A}}\right\} \cdot \{\theta V_1 + \log_e A\} \tag{29}$$

$$V_3 = \theta g\left\{\frac{2A-1}{g} + \frac{(2A-1)}{d}\sqrt{\frac{A}{A-1}}\right\} \cdot \log_e (2A-1) \tag{30}$$

$$V = V_1 + V_2 + V_3, \tag{31}$$

[24] R. D. Knott, I. D. Colson, and M. R. P. Young, "Breakdown effect in p-n alloy germanium junctions," *Proc. Phys. Soc. B (London)*, vol. 68, pp. 182–185; March, 1955.

where again A is a function of V_1. These results all reduce to the usual simple forms[8,9] for $V_1 \ll \phi$.

Diode Characteristics

In Fig. 7 we have plotted the J-V characteristic of an RPIR diode for typical parameter values, neglecting the effects of scattering. Values used were

$g = 0.01$ cm, $d = 0.02$ cm, $p_0 = 10^{18}\,\text{cm}^{-3}$, $T = 300°\,\text{K}$

other constants being appropriate to germanium.

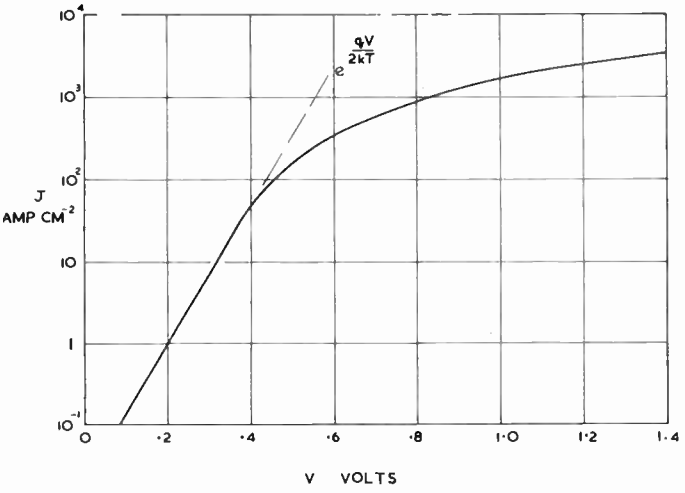

Fig. 7—Theoretical characteristic for RPIR diode (neglecting scattering).

If we had included scattering effects, region I mobilities would have been reduced about a factor of two at the top of the curve, so that the over-all current scale would be compressed by about this same factor, the curve shape being little altered.

It is seen that the curve, plotted on a logarithmic scale, is initially a straight line of slope $\frac{1}{2}\theta$, but soon falls well below this value. In this case, there is no rise above the exp $(\frac{1}{2}\theta V)$ line at any stage. The shape of this characteristic is simply explained as follows. At relatively low levels all the current is carried by holes. Half of the applied voltage appears as V_1 across the junction and half as V_2 across the I region. This gives an exp $(\frac{1}{2}\theta V)$ characteristic. At higher levels the emitter efficiency falls, and appreciable current is carried by electrons. This leads to a large increase in the voltage drop in the part of the intrinsic region near the recombination electrode, since carrier density is quite low here. V_2 thus increases and the curve flattens out.

Several diodes have been made by alloying indium to one side of a germanium wafer and pure lead or tin to the opposite side. The characteristics all have the general shape predicted above. In practice, for non-intrinsic material, the straight line portion of the curve is not very evident due to transition to the $[\exp(\theta V) - 1]$ characteristic which applies at low levels. A typical curve, in this case for a diode with a tin recombination

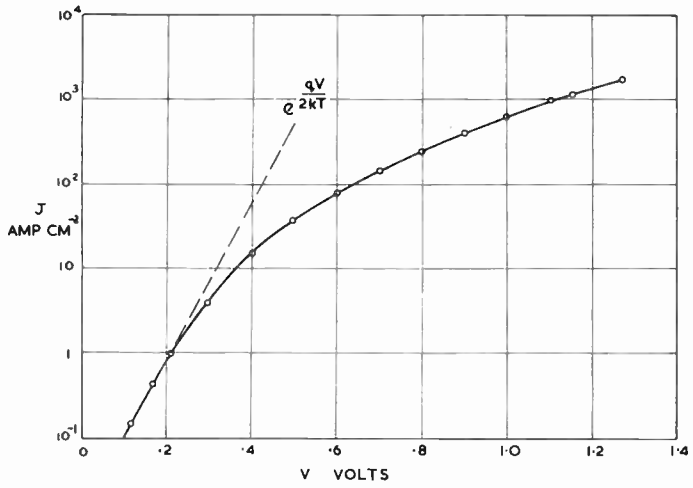

Fig. 8—Experimental curve for In-Ge-Sn diode with $d \approx 0.015$ cm.

electrode, is shown in Fig. 8. Again the parameters are different from those of the theoretical calculation and only qualitative comparison should be made.

Design Considerations

From the formulas derived above and the curves of Figs. 3, 4, 7, and 8, it is clear that the RPIR diode is somewhat inferior to the RPINR diode as a high current device. The reverse characteristic is also inferior,[9] in that a surface of high recombination velocity exists close to the reverse biased junction, and is not shielded from it by low resistivity material as in the case of the RPINR diode.

For optimum operation the intrinsic region should be as thin as allowed by breakdown considerations, and the P region doping should be as heavy as possible to maintain injection efficiency. The best attainable characteristic will not rise above the exp $(\frac{1}{2}\theta V)$ level.

Transistor Emitter Efficiency

Current flow in a junction transistor is in many ways analogous to current flow in an RPIR diode, but there is an important difference, in that the transistor is a three-terminal device and an appreciable amount of current may flow to the base contact.

Fig. 9 shows the carrier distributions in a PNP transistor under normal operation conditions. For simplicity we shall assume that the base region is intrinsic, since this assumption has no effect on the high level performance. If the collector junction is at a potential $-V_c$ with respect to the base, then the carrier density in the base at the collector junction is $n_i \exp(-\theta V_c)$, which we may neglect in comparison with injected densities. We have again assumed that a diffusion length in the emitter is long compared with its width and have assumed a recombination surface bounding the emitter region. We shall note later that an identical result is obtained if we assume a long emitter with minority carrier diffusion length g, and, of course, the two cases can be combined, if g is taken to be an appropriately weighted length.

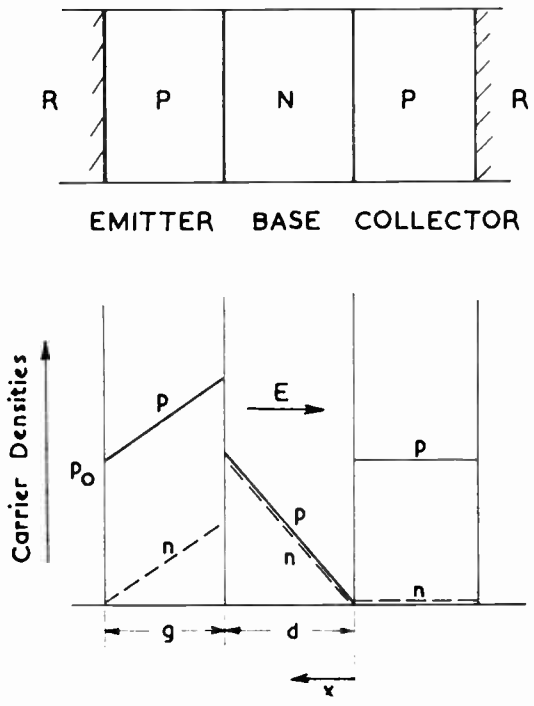

Fig. 9—RPNP transistor.

We shall treat this case quite generally, writing δD_p and ϵD_n for diffusion coefficients in the base region, and ζD_p, ηD_n for diffusion coefficients in the emitter; δ, ϵ, ζ, η are determined from scattering theory. This is not strictly accurate, since the diffusion coefficients are not constant across either base or emitter regions, but it is a sufficient approximation for our purpose. We shall take conventional currents as positive when flowing from emitter to collector and measure x as shown. Hole currents will be taken to be one dimensional, and the self-bias effect[25] of the transverse electron current will be neglected.

The electron current in the base region is not independent of x, since none of it flows through the collector junction. All of the electron current, in fact, flows transversely through the base region to the base lead. The conductivity of the various parts of the base layer depends on the injected carrier density, and if we assume this to vary approximately linearly as shown, then

$$J_n(x) = J_n(d)\frac{x^2}{d^2}. \tag{32}$$

Small departures from this assumed linearity have little effect on the final result.

Now we proceed as usual to find the fields in the base region at the emitter junction by requiring continuity of hole and electron currents across this junction. These field expressions both contain the term $dp/dx\big|_{x=d}$. To eliminate this, we observe that, from the equations of current flow, since $n=p$ in the base region,

$$J_p(d) = qE\delta\mu_p p + q\delta D_p\frac{dp}{dx} \tag{33}$$

$$\frac{x^2}{d^2}J_n(d) = qE\epsilon\mu_n p - q\epsilon D_n\frac{dp}{dx} \tag{34}$$

so that

$$\frac{dp}{dx} = \frac{1}{2qD}\left[\frac{1}{\delta}J_p(d) - \frac{1}{b\epsilon}\cdot\frac{x^2}{d^2}\cdot J_n(d)\right] \tag{35}$$

where D is D_p and $b=D_n/D_p$. Now integrating (35) from 0 to d we get, using (12) for a forward voltage V applied to the emitter junction,

$$An_ie^{\theta V} = \frac{1}{2qD}\left[\frac{d}{\delta}J_p(d) - \frac{1}{3}\frac{d}{b\epsilon}J_n(d)\right] \tag{36}$$

which may be used in conjunction with (33) and (34) for $x=d$ to eliminate the unknown gradient. The final results are

$$J_p = \frac{\dfrac{6q\delta D_p}{d}\left[\dfrac{\epsilon}{\eta}A^2n_ie^{\theta V} + \dfrac{q\delta D_p p_0}{g}(2A-1)(A-1)\right]}{3\dfrac{\epsilon}{\eta}A - \dfrac{\delta}{\zeta}(A-1)} \tag{37}$$

$$J_n = \frac{\dfrac{6q\epsilon D_n}{d}\left[\dfrac{\delta}{\zeta}A(A-1)n_ie^{\theta V} + \dfrac{3q\epsilon D_n p_0}{g}(2A-1)(A-1)\right]}{3\dfrac{\epsilon}{\eta}A - \dfrac{\delta}{\zeta}(A-1)} \tag{38}$$

where A is given by (13) and the junction voltage V appears as a variable parameter.

Since the only place the emitter length g enters the problem is in the expression for the electron density gradient in the emitter, we see that if we assume instead a long emitter with electron diffusion length L_e, then the hole and electron currents are again given by (37) and (38) with g replaced by L_e.

We observe that, for $V \ll \phi$, (37) and (38) reduce to their low level form. If we define a dc or large signal emitter efficiency by

$$\Gamma = \frac{J_p}{J_p + J_n}, \tag{39}$$

then, for $V \ll \phi$, Γ reduces to the large signal value derived from Webster's analysis.[3,26]

For large currents the expressions (37)–(39) give a different result from that obtained by Webster. This is not surprising, since Webster's treatment is inapplicable when Γ is appreciably less than unity. In fact, his treatment, invalidly extended to large currents, predicts a

[25] N. H. Fletcher, "Self-bias cutoff effect in power transistors," PROC. IRE vol. 43. p. 1669; November, 1955.

[26] N. H. Fletcher, "Note on the variation of junction transistor current amplification factor with emitter current," PROC. IRE, vol. 44, pp. 1475–1476; October, 1956. This note points out the origin of an error of a factor ½ in Webster's analysis.

limiting Γ of zero which is clearly incorrect. From the present treatment we find that for large currents

$$\Gamma \to \frac{3g + d}{6g + 4d}. \tag{40}$$

This limit is independent of whether the transistor is PNP of NPN, since, at very high levels, scattering makes electron and hole mobilities equal.

In Fig. 10 we have plotted Γ as a function of $J = J_n + J_p$ for the case of a typical PNP germanium transistor. Parameters used were

$$p_0 = 10^{18}\ \text{cm}^{-3},\ d = 5 \times 10^{-3}\ \text{cm},\ L_e(=g) = 10^{-3}\ \text{cm}$$

which are approximately the values for the transistor discussed by Webster.[3] We observe that Webster's result is a surprisingly good approximation up to current densities of 10^4 amp/cm^2 in this case. This good agreement is fortuitous since Webster neglected both J_n and all scattering effects. Agreement remains reasonably good for other values of the base width so that Webster's result is a useful approximation for "ordinary" transistors, even under conditions where his assumptions are far from valid.

We should point out that, since both surface and volume lifetime effects saturate to small values at relatively small current densities, the dc high level value of I_c/I_e is essentially just Γ.

Experimental verification of the curves shown in Fig. 10 is difficult, since the base current causes a self-bias effect[25] which considerably disturbs the injected current density distribution at high levels. However, pulse measurements at very high currents show that Γ tends to a finite value, which is approximately that predicted by the theory.

Fig. 11 shows a typical curve of J_p vs J_n (*i.e.*, collector current vs base current) found by pulse measurement of a small PNP power transistor. The straight line portion for various transistors gives values of dI_c/dI_b ranging from 0.38 to 0.44 in excellent agreement with the value near 0.4, predicted by our theory and an approximate knowledge of L_e and d for these particular transistors. The transistors used were selected because of their rather wide base width (>0.01 cm), this making the currents more easily manageable. Because of the effect referred to above, true current densities will be much higher than the nominal values shown.

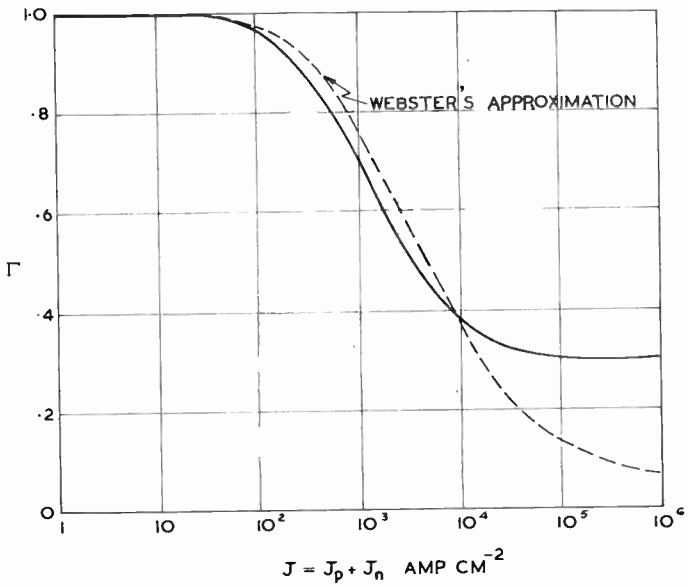

Fig. 10—Theoretical variation of dc emitter efficiency with emitter current for typical PNP transistor.

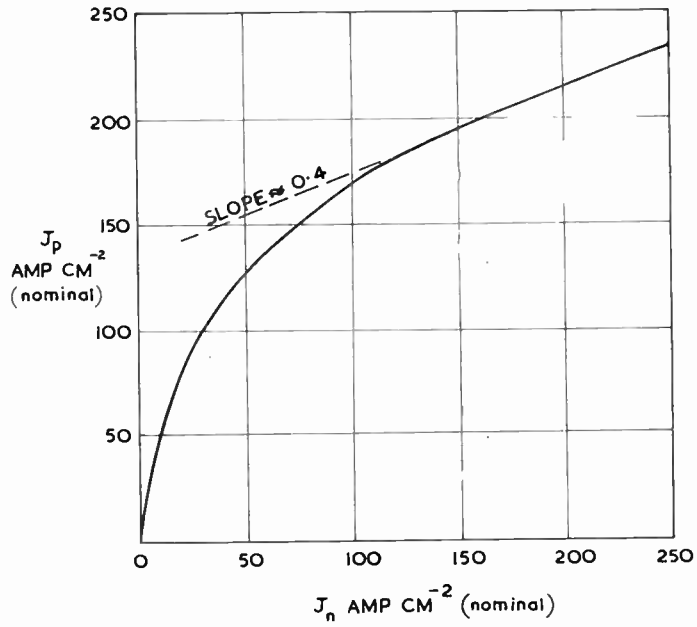

Fig. 11—Experimental relation between hole and electron current densities (derived from collector and base currents) for typical small PNP power transistor with base width ~0.01 cm.

Practical Applications

Most of our discussion so far has been concerned with device design parameters and their effect on the electrical performance of the device from the point of view of the designer. It seems appropriate to conclude with some remarks on the use of semiconductor devices at very high levels in the light of our new results.

We should first emphasize that all our results and calculations have been on the essential semiconductor structure alone and held at a fixed temperature. In practice, allowance has to be made for lead resistances and for heating effects. We have also restricted ourselves to dc considerations so that further analysis is necessary, if transient conditions are to be adequately treated.

To deal first with diodes, we have shown that, for general use, a diode with a PIN structure is usually preferable to one with a PIR structure, and that PIN diodes can be made whose forward current is fairly accurately exponential over large ranges. For example, the thinnest diode shown in Fig. 4 has an exponential characteristic over a current range of five decades, and this behavior is well supported by theory.

The usefulness of this characteristic is limited in practice by heating effects. On the other hand, for pulsed or low duty cycle circuits with time constants sufficiently long that transient effects can be neglected, the large extent of the exponential curve may be of value. With the advent of suitably designed alloyed silicon diodes it should be possible to extend the exponential characteristic several decades, because of the smaller reverse currents.

It may be worth noting in passing that most PIR diode characteristics, for example that of Fig. 8, are approximated quite well by power law curves of the form $J = A V^n$ where n lies between about 3 and 4. The fit is in some cases quite good and extends over as much as four decades of current. These may provide useful approximate power law elements in some applications.

When simple current rectification is required, diode performance is usually limited by cooling difficulties rather than by electrical limitations. For example, from Figs. 3 and 4 we can make a PIN rectifier which maintains its exponential characteristic to 1000 amps/sq cm. However, at this level the dissipation is 500 watts/sq cm for our best rectifier. This requires considerable cooling and in practice it is often convenient to spread the dissipation over a larger area which then operates at a lower current density. Typical rectifiers are not usually run at more than a few hundred amps/sq cm and often very much less if high reverse voltages are encountered.

While it is not usual to operate transistors in current ranges for which α is less than about 0.9, it is useful to know the variation of α with current at very high levels. Our analysis has shown that a naive application of Webster's formula is valid for α greater than about 0.5 for a PNP transistor, but that the ultimate α is about 0.3. Almost the same thing is true for NPN transistors on an extended current scale. The self-bias effect which we have discussed before causes further apparent variations from Webster's result for large transistors and may considerably limit the maximum current attainable. Again heating effects are very important and usually limit the allowable current before electrical restrictions become important. Alloys for improved emitter efficiency should make low α operation relatively rare in the future.

Conclusion

At very high current densities new formulas must be derived considering previously neglected effects. Of these the most important is a more accurate consideration of carrier density relationships across a junction biased in the forward direction. Formulas derived using these relations give a good description of the high current behavior of junction devices and explain the deviations from previous high level theories.

The effect of hole-electron collisions has been shown to be considerable at high carrier densities. Its effects are only secondary in determining the device characteristics, but it must be considered in any accurate calculation.

Possible further complications arising from the high carrier concentrations are departures from classical statistics (degeneracy) and the possibility of radiative recombination reducing carrier lifetime. These are found to be of minor importance at the carrier levels usually encountered in practice.

The predictions of the theory for particular devices are in good agreement with experiment and show in what manner the available parameters should be varied to achieve specific results. This is true even for practical diodes which are only approximations to the ideal diodes of the theory. In particular, we have shown both theoretically and experimentally that it is easily possible to construct diodes with exponential characteristics over as much as five decades of current and up to current densities as high as 3000 amps/sq cm, without using special alloying materials.

While in many practical applications thermal considerations forbid operation at these extreme current densities, application of the theory allows most efficient design at the current level chosen.

Acknowledgment

It is a pleasure to record my thanks to the people who have helped with this study, particularly to H. Flood, who made all the diodes used as well as the special alloying and measuring jigs, to F. Tonking, who performed the pulse measurements on transistors, and to Dr. L. W. Davies for helpful discussions.

Correspondence

Variable Delay Lines*

I have read with interest the article by Lewis and Frazier[1] about the control of delay distortion by the method of "skewed turns." This method is shown to be new over a rather complete list of references. However, it is not new over a paper which appeared in this journal only eight months ago.[2]

That paper dealt primarily with the subject of multiple tuning of tv-sweep harmonies by resonant lines. In the course of this work, we encountered in a different range of frequencies (15–150 kc) and delays (30 microseconds) the same problem as the subject paper, which deals with dispersion in the video spectrum, and as it so often happens, we hit upon the same answer.

It was, of course, known for a long time that correction of delay distortion requires a controlled amount of mutual inductance along the line.[3] We felt that the best way to accomplish this was to mould the inductive elements into thin wafers (see my Figs. 9 and 10), to assemble them back-to-back, and then to control their mutual inductance by adjusting the slant angle. Fig. 11(a) and (b), showing the effect of slant on pulse transmission, is the exact counterpart for the fine photographs given by Lewis and Frazier in their Fig. 1(a) and (b). Even the optimum value for the slant angle is of the same order: 55° in our paper[4] and >45° in theirs.[5] Possible overcompensation by this method is mentioned in both articles.

The purpose of this letter is not to discuss the futile matter of priorities, but rather to strengthen and support the thesis of the subject paper. Our experience with long delays at low frequencies is in perfect agreement with Lewis and Frazier's work at video frequencies. Hence, our concur with them, that the provision of partial overlap between essentially plane inductors is probably the best way to build constant-delay lines for wide-band applications.

When compiling their very complete list of references, this paper was probably overlooked, because it is indexed under a different subject (television sweep). The development of delay lines using the "slanting wafer" method, was not so much a goal in itself, but merely a by-product in an effort aimed at a different direction.

KURT SCHLESINGER
Motorola, Inc.
Chicago, Ill.

Author's Comment[6]

The remarks of Dr. Schlesinger in connection with the control of delay distortion in lumped networks are of interest, and we are happy to add his paper to our list of references. It had not come to our attention before our paper was completed.

Until we developed our skewed continuous winding, it had always been necessary to sectionalize the winding of a delay-line coil in order to control the mutual inductance along the line. Dr. Schlesinger's paper deals with such sectionalized windings. As was mentioned in our paper, this sectionalizing is impossible in a continuously wound distributed-constant line suitable for the variable delay application in which we were interested.

However, we should like to correct the impression that we arrived at any particular value for the optimum skew angle for a distributed-constant line. We did, of course, calculate and plot the effect of various skew angles on the effective inductance of a distributed-constant delay line coil with a particular set of geometrical dimensions. The optimum skew angle of the computed example is shown on page 199, and is 50°. The remark on page 201, to which Dr. Schlesinger apparently refers, is to the effect that the skew angle must always be greater than 45°.

We published complete equations which enable calculation of the effective inductance for any delay-line coil geometry which can be approximated by a long rectangular turn shape with any desired spacing between turns.

We have not seen the mathematical method used by Dr. Schlesinger to analyze the operation of his sectionalized pulse-forming line, but we do feel that our analysis affords considerable insight into the behavior of continuously wound delay lines.

FRANK D. LEWIS
General Radio Co.
Cambridge, Mass.

* Received by the IRE, March 14, 1957.

[1] F. D. Lewis and R. M. Frazier, "Distributed-parameter variable delay lines using skewed turns for delay equalization," PROC. IRE, vol. 45, pp. 196–204; February, 1957.

[2] K. Schlesinger, "Television sweep generation with resonant networks and lines," PROC. IRE, vol. 44, pp. 768–775; June, 1956.

[3] A. H. Turner, "Artificial lines for video distribution and delay," *RCA Rev.*, vol. 10, pp. 477–489; December, 1949.

[4] Schlesinger, *op. cit.*, p. 773.

[5] Lewis and Frazier, *op. cit.*, p. 201.

[6] Received by the IRE, March 27, 1957.

A Note on Distortion Reduction and Electrical Multiplication*

There are a number of devices (such as tubes, transistors, and carbon microphones) that utilize a resistance change $F(t)$ to provide amplification in response to an input signal.

The typical device may have the configuration shown in Fig. 1. In the usual case, voltage E is a direct current source, giving a signal transfer of

$$E_0 = \frac{ER}{R + F(t)}. \tag{1}$$

A characteristic of this function is that all possible harmonics of the function $F(t)$ are present as distortion.[1] Commonly, distortion reduction is possible only by increase in the value of R or decrease in the variable portion (signal) of $F(t)$. The purpose of this note is to call attention to an alternative method of distortion reduction that seems to have been overlooked in the literature.

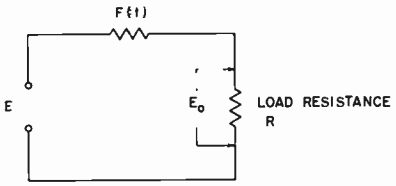

Fig. 1.

The configuration of Fig. 2 demonstrates the method.

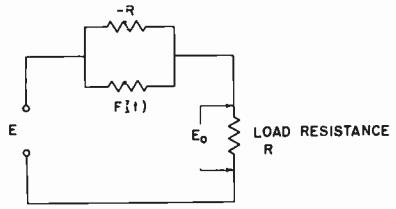

Fig. 2.

The transfer expression for E_0 developed across the load resistance is

$$E_0 = \frac{ER}{\dfrac{-RF(t)}{F(t) - R} + R} = \frac{ER}{\dfrac{-RF(t) + RF(t) - R^2}{F(t) - R}} = -E\frac{F(t) - R}{R}. \tag{2}$$

$$\text{For } F(t) = R[1 + G(t)], \tag{3}$$

$$E_0 = -EG(t). \tag{4}$$

An important corollary of (4) is that it holds the promise of modulation, mixing, and other multiplication functions with linear components. In that case, voltage E would customarily become $H(t)$ and the product

$$E_0 = -G(t)H(t) \text{ results.} \tag{5}$$

Conventional feedback manipulations show many ways to obtain the fixed value of negative resistance required. The limitations imposed by imperfections in the negative resistance have not been explored.

DAVID T. GEISER
Sprague Electric Co.
North Adams, Mass.

* Received by the IRE, February 11, 1957.

[1] See W. L. Everitt, "Communications Engineering," McGraw-Hill Book Co., Inc., 2nd ed., pp. 345–347, 349–351; 1937.

Thermal Velocity Effects in Electron Guns*

In the above paper,[1] Cutler and Hines have developed a theory which predicts the degree of spreading of an electron beam due to thermal electron velocities and gives curves of the fraction F_r of the total beam current to be found within any given radius in a beam dispersed by thermal velocities.[2,3] Danielson, *et al.*, define two special cases of F_r, F_r for $r/\sigma = r_e/\sigma = s$ which they call F_{re}; and F_r for $r/\sigma = \sigma/\sigma = 1$ which they call F_σ, both of which are functions of $r_e/\sigma = s$ only. They then show that the simultaneous solution of two second-order differential equations containing F_{re} and F_σ gives the continuous solution of r_e, the radius of the outermost nonthermal electron, and σ_1, the standard deviation, as functions of z, the axial position. In Danielson, *et al.*,[3] F_{re} and F_σ are given graphically[4] and in integral form. The purpose of this note is to point out that F_{re} may be expressed in closed form and F_σ in two simple series forms suitable for calculation.

F_r, the fraction within a radius r, is given by

$$F_r = \frac{1}{I_D}\int_0^r J(r)2\pi r dr \qquad (1)$$

$$= 2\int_0^{r/r_e} \frac{J(r)}{J_D}\frac{r}{r_e}\, d\left(\frac{r}{r_e}\right). \qquad (2)$$

Eq. (23) of Danielson, *et al.*, gives $J(r)/J_D$. If we take the upper limit of integration equal to unity in (2) then $F_r = F_{re}$, and if we take the limit as σ/r_e then $F_r = F_\sigma$

$$F_{re} = 2\int_0^1 \frac{r}{r_e} e^{-r^2/2\sigma^2} \cdot\left[\int_0^{r_e/\sigma}\frac{R}{\sigma}e^{-R^2/2\sigma^2}I_0(rR/\sigma^2)d\left(\frac{R}{\sigma}\right)\right]d(r/r_e).$$

By successive integration by parts, the bracketed integral may be reduced and we obtain.

$$F_{re} = 2e^{-s^2/2}\int_0^1 r/r_e e^{-r^2s/2r_e^2} \cdot\sum_{n=1}^{\infty}(r_e/r)^n I_n(rs^2/r_e)d(r/r_e)$$

where $s = r_e/\sigma$.

Expanding the Bessel functions in power series, bringing the integral inside the double sum, integrating term by term, and simplifying we have

$$F_{re} = e^{-s^2/2}\sum_{n=0}^{\infty}\sum_{p=0}^{\infty}\frac{(s^2/2)^{n+p}}{(n+p+1)!} - e^{-s^2}\sum_{n=0}^{\infty}\sum_{p=0}^{\infty}\sum_{m=0}^{p}\frac{(s^2/2)^{n+p+m}}{m!(n+1+p)!}$$

$$= 1 - e^{-s^2}\sum_{n=0}^{\infty}\frac{2}{s^2}\left[I_{n+1}(s^2) + I_{n+2}(s^2) + \cdots\right]$$

$$= 1 - e^{-s^2}[I_0(s^2) + I_1(s^2)].$$

* Received by the IRE, March 11, 1957.

[1] C. C. Cutler and M. E. Hines, PROC. IRE, vol. 43, pp. 307–315; March, 1955.

[2] *Ibid.*, Fig. 7.

[3] W. E. Danielson, J. L. Rosenfeld, and J. A. Saloom, "A detailed analysis of beam formation with electron guns of the Pierce type," *Bell Sys. Tech. J.*, vol. 35, pp. 375–420, March, 1956.

[4] *Ibid.*, Figs. 8 and 9.

Changing the upper limit we have:

$$F_\sigma = 1 - e^{-s^2/2}e^{-1/2}\sum_{n=0}^{\infty}(s^2/2)^n \cdot\sum_{p=0}^{\infty}\frac{s^2/2)^p}{(n+1+p)!}\sum_{m=0}^{p}\frac{1}{2^m m!}$$

$$= 1 - 2/s^2 e^{-1/2s(-1)^2}\sum_{n=1}^{\infty} n s^n e^{-s} I_n(s)$$

which converges rapidly for small s; or, using

$$e^{1/2(s^2+1)} = I_0(s) + \sum_{n=1}^{\infty}(s^n + s^{-n})I_n(s)$$

we have

$$F_\sigma = 1/s^2\left[1 - e^{-1/2(s-1)^2}\sum_{n=1}^{\infty} 2ns^{-n}e^{-s}I_n(s)\right]$$

which converges for large s.

IRVING ITZKAN
Sperry Gyroscope Co.
Great Neck, N. Y.

A Note on the Limits of Brainstorming*

Brainstorming is the application of creative thinking techniques to groups. Creative thinking techniques briefly employ gathering information, uninhibited incubation, imaginative inspiration, and detail formulation after the creative fact. A brainstorming session is one in which a group of people try to pool their imagination operating on all the facts they can summon up. They allow themselves to toy aloud with any idea, however foolish, in the hopes that it may suggest something to someone else in the group, and in the end snowball into a useful idea. These methods are becoming so pat that consultants can be hired to teach them! It is the purpose of this note to point up some of the limits and dangers involved in this seemingly fruitful concept.

The technical justification of brainstorming as well as creative thinking is Freudian because random association supposedly provides an inlet to the unconscious mind. Through group free association, not unlike group therapy in some respects, the participants expect to come up with new ideas put together from the collective jigsaw pieces of the minds engaged.

It is suggested that brainstorming can be useful only in giving birth to gadgets or their visual or verbal equivalents. Gadgets, slogans, and new twists are of course invaluable, but they are also quite superficial. At a time when the superficial is manifold and valued, it is not surprising that a systematic approach should arise for its perpetuation.

In the history of ideas not one significant contribution has come from a group of people. Great theories or points of view have always formed in the solitary mind of a single person, and new philosophies setting the tenor of an age are the province of one mind. This is not to say that schools are not formed, that mass direction has not resulted which is fruitful; but the significant departures are always one mind's departure. The great difference between present day American and European research is that the individual is valued *per se* in Europe, and allowed to putter around throughout the whole range of experience; whereas he is given a limiting task in America, one small sector of a great machine. By the sheer size of the American machine things are bound to happen, but the important things happen when the lone mind ignores the machine and ranges off on its own, a free single spirit.

Brainstorming ignores this and says that two heads are better than one. And that the important way for an individual to think creatively is to act like a group of brainstorming people! It is a point of view resulting naturally in the present American situation, but one which should be seriously questioned. The dictionary definition of brainstorm is confusion of mind, and this may not be far from the truth. The real need is to see through present desires to future hopes. A civilization changes and the change results either because of crude collective forces or of powerful individual insights which gain their strength through their truth or genuineness. It is contested that the act of brainstorming is severely limited to the formation of novel ideas or imitations and that it is a false shibboleth to set before any age.

ROBERT E. MUELLER
Caldwell-Clements Manuals Corp.
New York, N. Y.

* Received by the IRE, March 7, 1957.

Limiting Forms of FM Noise Spectra*

Recent correspondence on the subject of the rf spectrum produced by frequency modulation of a carrier by a complex modulating wave[1–4] has been followed by us with considerable interest.

The consensus of the published discussion and some as yet unpublished work on the subject[5,6] seems to be, first, that for frequency modulation by random Gaussian noise for large modulation indexes (modulation index = rms frequency deviation/bandwidth of the modulation), the rf spectrum

* Received by the IRE, February 19, 1957.

[1] R. G. Medhurst, "The power spectrum of a carrier-frequency modulated by Gaussian noise," PROC. IRE, vol. 43, pp. 752–753; June, 1955.

[2] J. L. Stewart, "Rebuttal," PROC. IRE, vol. 43, p. 754; June, 1955.

[3] R. Hamer, "RF bandwidth of frequency-division multiplex systems using frequency modulation," PROC. IRE, vol. 44, p. 1878; December, 1956.

[4] R. G. Medhurst, "Author's comment," PROC. IRE, vol. 44, p. 1878; December, 1956.

[5] D. Middleton, "Random-Frequency Modulated Waves," Johns Hopkins Univ., Rad. Lab. Rep. AF-9; February, 1955, and "The Effect of a Linear Narrow-Band Filter on a Carrier-Frequency Modulated by Normal Noise," Rep. 24; November, 1955.

[6] N. M. Blachman, "Limiting Frequency-Modulation Spectra," Tech. Mem. No. EDL-M48, Electronics Defense Lab., Sylvania, Mt. View, Calif.; June, 1955.

has a spectral shape (about the carrier frequency) proportional to the first-order probability density of the modulating noise; and second, that for low modulation indexes, there are two distinct cases as the spectrum of the modulating noise does[7] or does not[8] extend to zero frequency. Our views are in agreement with the above stated consensus. The object of this letter is to show that Dr. Stewart's limiting form,[7] the physical applicability of which has been somewhat questioned, is in fact appropriate to a considerable class of physical situations. However, the tails of the spectrum are not satisfactorily represented by the limiting form. We shall obtain a suitable expression for the spectral tails by deriving an approximating series, of which Dr. Stewart's form is the first term.

The correlation function of a sinusoidal carrier frequency-modulated by a stationary (and ergodic) Gaussian noise is, with the frequency domain representation of the modulating noise,[9]

$$R(t) = \left(\frac{A_0^2}{2}\right)\cos\omega_0 t \cdot \exp\left\{-\frac{D^2}{B}\int_0^\infty \left(\frac{1-\cos\omega t}{\omega^2}\right) w(f)\,d\omega\right\}, \quad (1a)$$

or, with the time domain representation,

$$R(t) = \left(\frac{A_0^2}{2}\right)\cos\omega_0 t \cdot \exp\left\{-D^2\int_0^{|t|}(|t|-x)r(x)\,dx\right\}. \quad (1b)$$

Here D^2 is the mean-square (angular) frequency deviation (radians^2/second^2), which is proportional to the average power of the modulating noise, and B is the equivalent rectangular bandwidth of this noise, defined by

$$B \equiv 2\pi\int_0^\infty w(f)\,df, \quad (2)$$

so that the modulation index is $\mu = D/B$, while $r(t)$ is the normalized correlation function of the modulating noise ($r(0)=1$), and $w(f)$ is the normalized spectrum of the modulating noise (max $w(f)=1$). The (peak) amplitude of the carrier is A_0, and $\omega_0 (=2\pi f_0)$ is the carrier (angular) frequency. We can drop the $(A_0^2/2)\cos\omega_0 t$ factor, keeping in mind that the spectrum which results represents the upper sideband of the complete modulated spectrum, the lower being found from inversion.

If the noise spectrum vanishes sufficiently rapidly near zero frequency that the integrals of the terms in the exponent of (1a) converge separately, then it is appropriate to separate the exponent of (1a) into two terms and expand the second exponential in a power series. If we take the cosine transform of the result and use the fact that the integral of the cosine is $\pi\delta(\omega)$, the upper sideband of the modulated wave (*i.e.*, $f>0, f=0$ being measured with f_0 as the actual zero frequency) is found to be

$$W(f) = 4\int_0^\infty R(t)\cos\omega t\,dt = \exp\left\{-\frac{D^2}{B}\int_0^\infty \frac{w(f)}{\omega^2}\,d\omega\right\} \cdot \left\{2\delta(f) + 2\pi\mu^2\frac{Bw(f)}{\omega^2} + \frac{\mu^4}{2}B^2\int_0^\infty\left[\frac{w(f-y)}{(\omega-2\pi y)^2}+\frac{w(f+y)}{(\omega+2\pi y)^2}\right]\cdot\frac{w(y)}{(2\pi y)^2}\,df + 0(\mu^6)\right\}. \quad (3)$$

This series has been previously given by Medhurst,[8] who used a band-limited white spectrum as an example, as we shall too.

If we suppose that the spectrum of the modulating noise has a lower cutoff frequency, ω_1, and is nonincreasing thereafter, then the integral in the exponent is less than (max $w=1$) and approximately equal to ω^{-2} integrated from ω_1 to ∞, giving $\exp\{-D^2/\omega_1 B\}$ for the external factor. In fact, for band-limited white noise with an upper cutoff frequency ω_2, the integral is $B/\omega_1\omega_2$ (where $B=\omega_2-\omega_1$).

Eq. (3) says that to the order μ^2, no new frequencies will be introduced by the modulation process. The μ^4 term will fill in the gap from 0 to ω_1 and from ω_2 to higher frequencies.

Specifically for band-limited white noise, we have

$$W(f) = \exp\{-D^2/\omega_1\omega_2\}\left\{2\delta(f) + 2\pi\mu^2 B\left[\frac{1}{\omega^2}\right]_{\omega_1<\omega<\omega_2} + \frac{\mu^4B^2}{2}\left(\left[\frac{\omega-2\omega_2}{\omega^2\omega_2(\omega_2-\omega)}+\frac{\omega+2\omega_1}{\omega^2\omega_1(\omega+\omega_1)}+\frac{2}{\omega^3}\log\frac{\omega_1\omega_2}{(\omega_2-\omega)(\omega+\omega_1)}\right]_{0<\omega<B} + \left[\frac{2(\omega-2\omega_1)}{\omega^2\omega_1(\omega-\omega_1)}+\frac{4}{\omega^3}\log\frac{\omega-\omega_1}{\omega_1}\right]_{2\omega_1<\omega<B+2\omega_1} + \left[\frac{2(2\omega_2-\omega)}{\omega^2\omega_2(\omega-\omega_2)}+\frac{4}{\omega^3}\log\frac{\omega_2}{\omega-\omega_2}\right]_{B+2\omega_1<\omega\leq 2B+2\omega_1}\right) + 0(\mu^6)\right\}. \quad (4)$$

which is Medhurst's result,[8] where the expressions in brackets are zero except when ω lies in the range indicated by the inequalities. It is important to note that the extension of the spectrum to frequencies higher than $2B+2\omega_1$ comes from the third and higher-order interactions [$0(\mu^6, \mu^8, \cdots$, etc.)].

The importance of the second-order terms [$0(\mu^4)$] can be seen by calculating the value of the spectrum at the upper and lower edges of the modulating noise band. One gets

$$W\left(\frac{\omega_1}{2\pi}\right) = 2\pi\mu^2\frac{B}{\omega_1^2}\left\{1+\frac{\mu^2 B}{4\pi\omega_1}\cdot\left[\frac{3}{2}-2\log 2+\cdots\right]+0(\mu^4)\right\}, \quad (5)$$

and

$$W\left(\frac{\omega_2}{2\pi}\right) = 2\pi\mu^2\frac{B}{\omega_2^2}\left\{1+\frac{\mu^2 B}{2\pi\omega_1}\cdot[1+\cdots]+0(\mu^4)\right\}, \quad (6)$$

so that, when $D^2/B\omega_1$ is equal to a few multiples of π, the high-order interactions alter the spectrum significantly. Thus, both from considerations of the rapidity of convergence of the series and of the size of the external factor, we require a lower bound on ω_1 if (3) is to be useful for calculation.

On the other hand, if the two terms in the exponent of (1a) do not converge separately, we can still obtain a useful series by rewriting (1b) as

$$R(t) = \exp\left\{-D^2|t|\int_0^\infty r(x)\,dx\right\} \cdot \exp\left\{D^2|t|\int_{|t|}^\infty r(x)\,dx + D^2\int_0^{|t|} xr(x)\,dx\right\} \quad (7)$$

and then expanding the second exponential in a power series. First let us note that

$$\int_0^\infty r(x)\,dx = \frac{\pi w(0)}{2B}, \quad (8)$$

and let $\pi w(0)\mu^2 B/2 = B'$. Then

$$R(t) = \exp\{-B'|t|\} \cdot \exp\left\{D^2\int_0^\infty G(x,t)r(x)\,dx\right\}, \quad (9)$$

where

$$G(x,t) = \begin{cases} x, & x<|t| \\ |t|, & x>|t| \end{cases}.$$

The spectrum can be evaluated from (9) in several different, but equivalent, ways. We shall follow methods which make the structure of the terms as simple as possible and, at the end, (12b), express the results in terms of the modulating power spectrum. The cosine transform of (9) can be evaluated as half the sum of two Laplace transforms of the second exponential, because the presence of the first exponential assures convergence. From the power series expansion of the second exponential, we get

$$W(f) = \frac{4B'}{\omega^2+B'^2} + 2B'[S(B'+i\omega)+S(B'-i\omega)] + B'^2[S(B'+i\omega)*S(B'+i\omega) + S(B'-i\omega)*S(B'-i\omega)]+\cdots \quad (10)$$

where the asterisk stands for convolution in the frequency domain (third and higher terms will involve multiple convolutions), and

$$S(B'+i\omega) = \frac{w(0)-w(f-iB'/2\pi)+iw_Q(f-iB'/2\pi)}{w(0)(B'+i\omega)^2}, \quad (11)$$

[7] J. L. Stewart, "The power spectrum of a carrier-frequency modulated by Gaussian noise," PROC. IRE, vol. 42, pp. 1539–1542; October, 1954.

[8] R. G. Medhurst, "RF bandwidth of frequency-division multiplex systems using frequency modulation," PROC. IRE, vol. 44, pp. 189–199; January, 1956.

[9] D. Middleton, "The distribution of energy in randomly modulated waves," *Phil. Mag.*, Ser. 7, vol. 62, p. 689; 1951.
See also Stewart, *op. cit.*, (7).

where $w_Q(f)$ is the quadrature function of the spectrum of the modulating noise, *i.e.*, four times the sine transform of the correlation function, or the Hilbert transform of the power spectrum.[10] The form of (10) is useful for showing the structure of higher order terms.

The first two terms of (10) can be rewritten as

$$W(f) = \frac{4B'}{B'^2+\omega^2} + \frac{2B'}{B'^2+\omega^2}\left\{\frac{B'^2-\omega^2}{B'^2+\omega^2}\left[1 - \frac{w(f+iB'/2\pi)+w(-f+iB'/2\pi)}{2w(0)}\right] + \frac{2B'\omega}{B'^2+\omega^2}\,\frac{w_Q(-f+iB'/2\pi)-w_Q(f+iB'/2\pi)}{2w(0)}\right\}+\cdots. \quad (12a)$$

The power spectrum has no physical reality for complex frequencies; however, from the theory of Hilbert transforms,[10] we can express (12a) entirely in terms of the ordinary power spectrum, *viz.*,

$$W(f) = \frac{4B'}{B'^2+\omega^2} + \frac{4B'^2}{(B'^2+\omega^2)}\int_{-\infty}^{\infty}\frac{(B'^2-\omega^2)[w(0)-w(y)]-2\omega(2\pi y-\omega)w(y)}{[(2\pi y-\omega)^2+B'^2]w(0)}\,dy+\cdots. \quad (12b)$$

Reducing the convolution terms to expressions involving only the modulating power spectrum gives an expression too cumbersome to be worth writing in detail.

The first term of (12) is the one previously found by Stewart,[7] starting from (1a). If the modulating noise is unlimited white noise, the correlation function, which is then $\exp(-B'|t|)$, can be explicitly evaluated from either (1a) or (1b). For any other noise spectrum, the time domain form, (1b), is much to be preferred to the frequency domain form for evaluating higher terms of approximation.

For band-limited white noise extending from 0 to ω_2, we find that (9) gives

$$W(f) = \frac{4B'}{B'^2+\omega^2}\left\{1+\frac{1}{\pi}\left[\frac{B'^2-\omega^2}{B'^2+\omega^2}\tan^{-1}\frac{2B'\omega_2}{\omega_2^2-B'^2-\omega^2} - \frac{B'\omega}{B'^2+\omega^2}\log\frac{(\omega_2-\omega)^2+B'^2}{(\omega_2+\omega)^2+B'^2}\right]+\cdots\right\}, \quad (13)$$

where the inverse tangent takes values between 0 and π.

The magnitudes of the higher-order terms in the spectrum differ as the frequency is less than or greater than the bandwidth of the modulating noise. For $\omega<\omega_2$, each term of (10) is of order μ^2 compared to the preceding term, as witness (12) and (13). The asymptotic behavior is quite different, however, in that various terms become of the same order of magnitude. In particular one can see in (11) that for frequencies high enough that $w(f)$ is nearly zero, $S \doteq -\omega^{-2}$, so that the dominant part of the second term of (10) nulls the dominant part of the first term. The dominant part of the third term of (10) is then of the same order as the subdominant parts of the first two terms. The conclusion to be drawn is that we should return to (9) (which is exact) and investigate the asymptotic behavior *ab initio*.

By a theorem of Erdélyi,[11]

$$W(f) = 4\int_0^\infty \phi(t)\cos\omega t\,dt \simeq \sum_{n=1}^{\infty}\frac{(-1)^n\phi^{(2n-1)}(0)}{\omega^{2n}}. \quad (14)$$

Now, from (9), $R(t)$ has the form

$$\phi(t) = \exp\{f(t) - |t|f'(0)\},$$

so that in evaluating terms of (14) we get

$$(f) = \sum_{n=2}^{\infty}\frac{(-1)^n}{\omega^{2n}} \cdot \sum\frac{(2n-1)!}{i!\cdots q!}f^{(i)}(0)\cdots f^{(q)}(0), \quad (15)$$

where the second sum is over all partitions of $2n-1$ not containing 1, and

$$f^{(n)}0) = B'\frac{2\omega B}{\pi w(0)}r^{(n-2)}(0), \quad (16)$$

in which the derivatives of the correlation function are right-sided ones. The leading terms are

$$W(f) \simeq \frac{4B'}{\omega^4}\cdot\frac{2\omega_2}{\pi w(0)}\left\{-r'(0)+\frac{r'''(0)}{\omega^2} + \frac{20}{\pi}\frac{B'\omega_2}{w(0)}\frac{r'(0)}{\omega^2}+0(\omega^{-4})\right\}. \quad (17)$$

Each term of the asymptotic expansion contains at least one odd derivative. Now the correlation function is an even function of time, so that all the odd derivatives vanish to the extent that the modulating noise process is mean square differentiable. In particular, for band-limited white noise, as for other noise processes which are infinitely differentiable, the tails of the modulated spectrum are exponentially small.

By comparing the asymptotic expansion of the modulating spectrum [which follows from (14) with $\phi(t)=f(t)-|t|f'(0)$] and of the modulated spectrum, we see that the leading term (though not higher order ones) is correctly given by

$$W(f) \simeq \frac{B'w(f)}{\omega^2 w(0)}. \quad (18)$$

This is in many respects the result that one would expect. From (3), the tails of the spectrum might be expected to be of order $w(f)/\omega^2$, on the grounds that the behavior of the modulated spectrum at high enough frequencies should not depend very much on whether or not the spectrum for low frequencies extends to zero, and, in fact, the rigorous analysis, which does not depend on the approximations leading to (3) or to (12), bears this out.

As an example of a modulating noise which is not infinitely differentiable, we choose white noise shaped by an RC low-pass network, giving as (normalized) correlation function $\exp[-(2/\pi)B|t|]$. The spectrum of the modulated wave is then[12]

$$W(f) = 4e^{\mu^2}\sum_{n=0}^{\infty}\frac{(6-\mu^2)^n\left(B'+\frac{2}{\pi}n\omega_B\right)}{\left\{\left(B'+\frac{2}{\pi}n\omega_B\right)^2+\omega^2\right\}n!}, \quad (19)$$

and, for $\omega \gg \omega_B$,

$$W(f) \simeq 4\frac{B'}{\omega^4}\frac{4}{\pi^2}\omega_B^2[1+0(\mu^2\cdot\omega^{-2})]. \quad (20)$$

One may then conclude that in a low-index frequency modulation problem where the modulating spectrum extends to zero frequency, the spectrum of the modulated wave will have the shape of a (high-Q) resonance curve, regardless of the shape of the modulating spectrum, at frequencies closer to the carrier than the bandwidth of the modulating spectrum. The tails of the modulated spectrum, at frequencies farther from the carrier than the bandwidth of the modulating noise, will have a form depending on the modulating spectrum (in particular, if the modulating spectrum has tails of order f^{-n}, the modulated spectrum will have tails of order f^{-n-2}).

It is, of course, important to treat the tails of the spectrum carefully since a reconcilement of (3) and (12), which on first impressions give quite different predictions for the tails, is thereby attained. At the same time we should realize that the resonance curve spectrum is a good approximation to by far the larger part of the modulated spectrum in the case where it applies.

Two examples of the size of the correction terms relative to the leading term of (12) at the frequency ω_2 are afforded by (13) and (19). Specifically, we have for band-limited white noise,

$$W(f) = W(0)\frac{\pi^2}{4}\mu^4\left\{1+\left[-\frac{1}{2} - \frac{\mu^2}{4}\left(1+\log\frac{\pi\mu^2}{4}\right)\right]+0(\mu^4)\right\}, \quad (21)$$

and, for RC noise,

$$W(f) = W(0)\frac{\pi^2}{4}\mu^4 \cdot\left\{1+\left[-\frac{1}{\pi}+\mu^2\right]+0(\mu^4)\right\}. \quad (22)$$

[10] E. C. Titchmarch, "Fourier Integrals," Oxford University Press, Oxford, Eng., ch. V, (5.3.5) and (5.3.6); 1937.

[11] A. Erdélyi, "Asymptotic approximations to fourier integrals and the principle of stationary phase," *J. Soc. Ind. App. Math.*, vol. 3, pp. 17–27, theorem 2; 1955.

[12] Middleton, *op. cit.*, p. 24, eq. (5.8), AF-9.

We see that the value of the first correction term is already an appreciable fraction of the value of the leading term and that the spectrum is quite small with respect to its value at the carrier.

In our representation, the total power in the modulated wave is unity, and the power included by the first term of (12) within the bandwidth of the modulating noise in $1-\mu^2+0(\mu^4)$. This gives some notion of when the first term alone is enough.

For instance, in a cross-talk problem in a hypothetical frequency-division multiplex system where the modulating spectra extended to zero, one would expect that the desired signal could be adequately represented by a resonance curve, but that the interfering signal, which is the tail of a spectrum from a different channel with a different center frequency, could not be.

The physical existence of the resonance curve response for the major portion of the modulated spectrum when the modulating spectrum extends to zero has been confirmed in several instances by spectra measured experimentally on magnetrons[13,14] and klystrons.[15] The condition on the modulating spectrum is satisfied in many important cases, especially in problems of oscillator stability. In this connection, let us note that one cannot treat cases in which the modulating spectrum extends to zero as though it did not. While it is certainly true that a spike of power in the modulating noise band at zero frequency can be removed by considering an equivalent shift of the carrier, a continuum extending down to zero cannot be separated into a dc spike and a band with a finite lower frequency cutoff. It is precisely the effect of the distributed components nearly, but not quite, at zero frequency, which makes the procedure leading to (12) necessary.

Perhaps the best test for deciding which of the two methods of approximation is better suited to a particular problem is that, when Medhurst's form applies [(3) *supra*], there is a prominent spike of power at the carrier frequency, while in Stewart's form [(12) *supra*], there is a smooth transition from the center of the spectrum to the tail and no spike at all. One is thus left with two alternative expressions for the low index case, one applicable if the noise band of the modulating noise extends to zero frequency, and the other applicable if the noise band has a low-frequency cutoff not too near zero. If the problem with which one is concerned is such that the low-frequency cutoff falls in the forbidden region, then we are left without any really satisfactory method of procedure, other than an explicit evaluation of $R(t)$ *in toto*, since the convergence of (3) is then too slow to be useful. A possibility might be artificially to extend the level at the low-frequency cutoff down to zero, and use the series of (12). The extra modulating power added is negligible if ω_1 has such a small value, and the alteration in the form of the spectrum will have been nearly accomplished already by the form of "fill-in" from higher-order modulation products. Actually, except for the cases where the noise band is known to extend to zero, experience indicates[4] that the low-frequency cutoff is sufficiently high that (3) is rapidly convergent in all practical cases, so that the somewhat unappealing artifice of the preceding sentence need not be used.

James A. Mullen
Raytheon Manufacturing Co.
Waltham, Mass.
David Middleton
Consultant
49 Lexington Ave.
Cambridge, Mass.

[13] D. Middleton, W. M. Gottschalk, and J. B. Wiesner, "Noise in cw magnetrons," *J. Appl. Phys.*, vol. 24, pp. 1065–1066; August, 1953.
[14] W. M. Gottschalk, "Direct detection of noise in cw magnetrons," IRE Trans., PGED-1, pp. 91–98; December, 1954.
[15] R. A. LaPlante, "Development of a low-noise X-band cw klystron power oscillator," IRE Trans., PGED-1, pp. 99–106; December, 1954.

Analysis of Systems with Dead Time by the Root-Locus Method*

In recent correspondence,[1] a simple and useful device for facilitating root-locus analysis of dynamical systems was discussed. If in a system, Fig. 1, the open-loop transfer

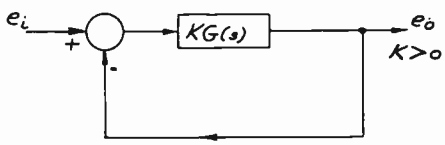

Fig. 1.

function is given as $KG(s)$, then the closed-loop characteristic equation is:

$$\frac{1}{G(s)} = -K. \tag{1}$$

If we substitute $s=x+jy$, (1) may be modified to the form:

$$f(x, y) + jg(x, y) = -K. \tag{2}$$

But since K is real, the imaginary term on the left of (2) must vanish on the loci of the roots.

Then

$$g(x, y) = 0. \tag{3}$$

Note that in consequence, $|f(x, y)| = K$, defining loop gain.

Eq. (3) is satisfied everywhere on the loci. It can be used to find real-axis breakaways, and imaginary axis crossings, ($y=0$, $x=0$, respectively). Usual care must be taken to assure that the 180° requirement ($-K$) is satisfied.

It will be shown that this technique may easily be extended to analysis of systems containing dead time. For our purposes dead time is defined[2] as having the transfer function: e^{-Ts}. If in Fig. 1, the open-loop transfer function were redefined as

$$KG(s)e^{-Ts},$$

then the characteristic equation becomes

$$\frac{1}{G(s)} = -Ke^{-Ts} \tag{4}$$

If, as before, we substitute $s=x+jy$, we have

$$f(x, y) + jg(x, y) = -Ke^{-Tx}e^{-iTy} \tag{5}$$

Multiplying both sides by e^{iTy} and gathering real and imaginary terms:

$$[f(x, y)\cos Ty - g(x, y)\sin Ty] + j[f(x, y)\sin Ty + g(x, y)\cos Ty] = -Ke^{-Tx}. \tag{6}$$

As the right side of (6) is real, the imaginary part of the left of (6) vanishes, thus defining the loci. Rearranging, the loci lie on

$$\frac{g(x, y)}{f(x, y)} = -\tan Ty. \tag{7}$$

As before, at $y=0$, we find the breakaways, and at $x=0$, the imaginary axis intercepts.

Substitution of (7) into (6) leads to a simplified expression for magnitude calculation.

$$|fe^{Tx}\sec Ty| = K. \tag{8}$$

The loci of the roots of the system with dead time may thus be calculated as modifications of the loci of the system without dead time. Stability boundaries may be easily calculated from (7) as functions of Ty.

Fred Powell
Bell Aircraft Corp.
Buffalo 5, N. Y.

* Received by the IRE, March 11, 1957.
[1] H. Lass, "A note on the root-locus method," Proc. IRE, vol. 44, p. 693; May, 1956.
[2] R. V. Churchill, "Modern Operational Mathematics in Engineering," McGraw-Hill Book Co., Inc., New York, N. Y., p. 294; 1944.

Resistance of a Partially Short-Circuited Conducting Slab*

In many experiments on the electrical properties of materials, it is necessary to apply to a specimen various "auxiliary" electrodes, in addition to the "main" current carrying electrodes. The auxiliary electrodes distort the lines of current flow and cause the resistance between the main electrodes to be lower than it would otherwise be. In this note, we calculate the amount of reduction in a fairly typical two-dimensional case. The geometry is illustrated in Fig. 1(a).

The calculation is a routine example of the method of conformal transformation. The required mapping functions are given in a number of texts.[1-3] The results may be expressed in the form:

$$\frac{R}{R_0} = \frac{KK_1'}{K'K_1} \tag{1}$$

where R and R_0 are the resistances with and without the auxiliary electrodes respectively, and K, K', K_1, and K_1' are complete elliptic integrals of the first kind, of moduli k, $\sqrt{1-k^2}$, k_1, and $\sqrt{1-k_1^2}$ respectively. The

* Received by the IRE, February 18, 1957.

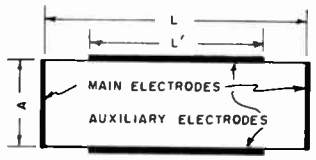

(a)

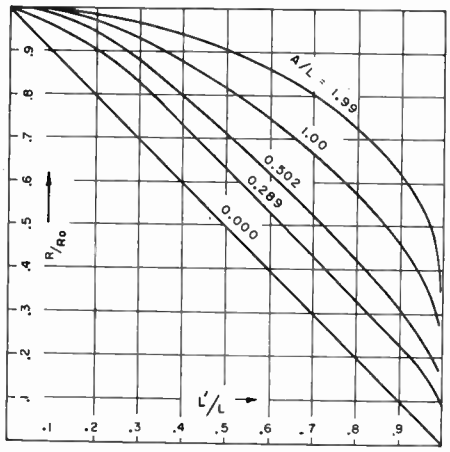

(b)

Fig. 1—(a) Electrode geometry. (The electrodes extend completely across the sample in the direction perpendicular to the plane of the figure. (b) Resistance ratio vs L'/L for several values of A/L.

moduli are given by the relations

$$K/K' = A/L \tag{2}$$

$$k_1 = dn\left(\frac{L - L'}{L} K' \middle| k'\right). \tag{3}$$

Eq. (2) determines k implicitly. Some further mathematical details are given in the Appendix.

The results are shown in Fig. 1(b), where we plot R/R_0 as function of L'/L, for several values of the width-to-length ratio of the slab as parameter.

It is seen that the effects of even small auxiliary electrodes can be quite appreciable for long thin rods.

Appendix

Since, by symmetry, the transverse bisector is an equipotential, we may start with the configuration shown in Fig. 2(a). This is mapped successively into Figs. 2(b) and 2(c). For the first mapping, the Schwartz transformation[1-3] gives

$$z = \frac{A}{2K} F(\zeta \mid k) \tag{4}$$

where $F(\zeta \mid k)$ = elliptic integral of first kind, of argument ζ and modulus k, and $K = F(1 \mid k)$.

The theory of these functions is given in many texts.[4-6]

[1] E. Durand, "Electrostatique et Magnetostatique," Masson et Cie, Paris, France, p. 348; 1953.
[2] Z. Nehari, "Conformal Mapping," McGraw-Hill Book Co., Inc., New York, N. Y., p. 280; 1952.
[3] E. Weber, "Electromagnetic Fields," John Wiley and Sons, Inc., New York, N. Y., vol. 1, p. 354; 1950.
[4] L. M. Milne-Thomson, "Jacobian Elliptic Function Tables," Dover Publications, Inc., New York, N. Y., pp. 1–39; 1950.
[5] E. T. Whittaker and G. N. Watson, "Modern Analysis," Cambridge University Press, Cambridge, England, ch. 22; 1948.
[6] H. Jeffreys and B. S. Jeffreys, "Mathematical Physics," Cambridge University Press, Cambridge, England, ch. 25; 1950.

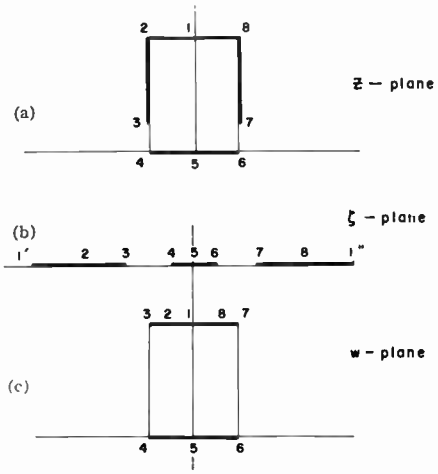

(d)

POINT	z	ζ	w
1	$iL/2$	$\pm\infty$	iB
2	$-\frac{A}{2} + i\frac{L}{2}$	$-1/k$	
3	$-\frac{A}{2} + iC$	$-1/k_1$	$-\frac{A}{2} + iB$
4	$-\frac{A}{2}$	-1	$-\frac{A}{2}$
5	0	0	0
6	$\frac{A}{2}$	1	$\frac{A}{2}$
7	$\frac{A}{2} + iC$	$1/k_1$	$\frac{A}{2} + iB$
8	$\frac{A}{2} + i\frac{L}{2}$	$1/k$	

Fig. 2—(a)–(c) Successive conformal mappings. (d) Table of values of important points in terms of the three complex variables.

The modulus k is determined by the relation[1]

$$\frac{K}{K'} = \frac{A}{L} \tag{5}$$

where

$$K' = F(1 \mid k')$$
$$k' = \sqrt{1 - k^2}.$$

The value of k_1 is determined by

$$z_8 - z_6 \equiv iC = \frac{A}{2K}\left[F\left(\frac{1}{k_1}\middle| k\right) - K\right]$$

or

$$\frac{1}{k_1} = \operatorname{sn}\left(K + \frac{2iCK}{A}\right)$$

$$k_1 = \operatorname{dn}\left(\frac{2C}{A}K \middle| k'\right) = \operatorname{dn}\left(\frac{2C}{L}K' \middle| k'\right)$$

$$= \left[1 - k'^2 \operatorname{sn}^2\left(\frac{2C}{L}K' \middle| k'\right)\right]^{1/2}. \tag{6}$$

Thus

$$\frac{C}{L} = \frac{1}{2K'} F(\alpha \mid k') \tag{7}$$

where

$$\alpha = \sqrt{\frac{1 - k_1^2}{k'^2}}. \tag{8}$$

The second transformation proceeds similarly. Instead of (5), we have

$$\frac{A}{2B} = \frac{K_1}{K_1'} \tag{9}$$

where

$$K_1 \equiv K(k_1) \equiv F(1 \mid k_1)$$
$$K_1' \equiv K(k_1') \equiv F(1 \mid \sqrt{1 - k_1^2}).$$

If the complex potential is taken as

$$\Phi = -i\frac{V}{2B} w$$

corresponding to voltage $V/2$ across the electrodes of Fig. 2(c), then the current is

$$I = \sigma(w_6 - w_4)\frac{V}{2B} = \frac{\sigma A V}{2B}$$

where

σ = conductivity of material.

The current without auxiliary electrodes would be

$$I_0 = \sigma A V / L.$$

Thus

$$\frac{R}{R_0} = \frac{I_0}{I} = \frac{A}{L}\frac{2B}{A} = \frac{K}{K'}\frac{K_1'}{K_1}. \tag{10}$$

The computations from a table of elliptic integrals[7] may be made quite simply as follows:

1) Choose a value of k' and determine (A/L) from (5).
2) Choose a suitable set of values of α, and determine corresponding values of (C/L) from (7).
3) For each α, determine k_1 from (8) to obtain K_1'/K_1.

Thanks are due to S. R. Kellner for assistance in the computations.

Daniel R. Frankl
Sylvania Electric Products, Inc.
Bayside, N. Y.

[7] E. Jahnke and F. Emde, "Tables of Functions," Dover Publications, Inc., New York, N. Y., 4th ed., p. 62; 1945.

Steady-State and Transient Analysis of Lossy Coaxial Cables*

The following results of two memoranda[1,2] which I wrote some time ago may be of interest as a supplement to the recently reported work of Wigington and Nahman.[3]

The transfer function per unit length of cable can be written as the product of two factors:

$$H(j\omega) = e^{-jK_0\omega}G(j\omega), \tag{1}$$

where the first factor contributes the constant delay which would be expected of the cable if it were lossless ($K_0 = \sqrt{\mu\epsilon}$), and the second factor, which is attributable to losses in the cable, contributes an attenuation and an excess delay (or phase shift) which are nonconstant functions of frequency.

* Received by the IRE, February 21, 1957; revised manuscript received, March 19, 1957. This work was supported by the Atomic Energy Commission under contract with Edgerton, Germeshausen, and Grier, Inc., Boston, Mass.
[1] G. L. Turin, "Frequency Characteristics of Coaxial Cables," Inter-Office Memorandum, Edgerton, Germeshausen, and Grier, Inc.; August 29, 1955.
[2] G. L. Turin, "Transient Responses of Coaxial Cables," Inter-Office Memorandum, Edgerton, Germeshausen, and Grier, Inc.; November 3, 1955.
[3] R. L. Wigington and R. S. Nahman, "Transient analysis of coaxial cables considering skin effect," Proc. IRE, vol. 45, pp. 166–174; February, 1957.

An important property of $G(j\omega)$ is that it may be considered a minimum-phase function,[4] so that its phase characteristic is completely determined by its attenuation characteristic, and *vice versa*. The formula which gives the phase shift per unit length, $B(\omega_c)$, at frequency ω_c, in terms of the attenuation characteristic is:[5]

$$B(\omega_c) = \frac{1}{\pi}\int_{-\infty}^{+\infty} \frac{dA(u)}{du} \log_e \coth \frac{|u|}{2}\, du. \quad (2)$$

Here A is the natural-logarithmic attenuation (in nepers/unit length) and u is a logarithmic frequency:

$$u = \log_e \frac{\omega}{\omega_c}. \quad (3)$$

The factor $\log_e \coth |u|/2$ in the integrand of (2) is such that it weights the values of dA/du in the immediate vicinity of $u=0(\omega=\omega_c)$ very heavily, so that the phase shift at ω_c is determined almost entirely by the attenuation in the vicinity of ω_c. This means that, practically speaking, in order to determine the phase shift at ω_c, one need know the attenuation characteristic over only a finite interval (about a decade above and below ω_c), rather than over the infinite interval $0 \leq \omega \leq \infty$ indicated by the limits on the integral.

Now, the logarithmic attenuation of a coaxial cable in the frequency range of interest (see, *e.g.*, Fig. 1 of Wigington and Nahman[3]) can be written empirically as

$$\hat{A}(\omega) = K_1\omega^{K_2}. \quad (4)$$

K_1 and K_2 can be determined from the intercept and slope, respectively, of the log-log-attenuation vs log-frequency curve for the cable. Substituting, from (3), $\omega=\omega_c e^u$ into (4), one obtains

$$A(u) = K_1\omega_c^{K_2}e^{K_2u}, \quad (5)$$

so that

$$\frac{dA(u)}{du} = K_1K_2\omega_c^{K_2}e^{K_2u}. \quad (6)$$

Thus (2) becomes

$$B(\omega_c) = \frac{K_1K_2\omega_c^{K_2}}{\pi} \int_{-\infty}^{+\infty} \cdot e^{K_2u} \log_e \coth \frac{|u|}{2}\, du. \quad (7)$$

Substituting the identity,

$$\coth \frac{|u|}{2} = \left|\frac{1+e^{-u}}{1-e^{-u}}\right|, \quad (8)$$

into (7), the integral becomes recognizable as one which has been tabulated;[6] thus

$$B(\omega) = \left(K_1 \tan\frac{\pi K_2}{2}\right)\omega^{K_2}, \quad |K_2| < 1, \quad (9)$$

where the subscript "c" has now been dropped for convenience.

Differentiation of $B(\omega)$ with respect to ω gives a delay function which indicates the amount a frequency group at frequency ω will be delayed per unit length of line in excess of the lossless delay, K_0:

$$D_e(\omega) = \frac{dB(\omega)}{d\omega} = \left(K_1K_2\tan\frac{\pi K_2}{2}\right)\omega^{K_2-1}. \quad (10)$$

Substituting (4) into (10), letting $\omega=2\pi f$ (f in cps), and remembering that there are approximately 8.686 db/neper, (10) becomes

$$\hat{D}_e(f) \cong \left(1.832\times 10^{-2}K_2\tan\frac{\pi K_2}{2}\right)\frac{A_{db}(f)}{f}, \quad (11)$$

thus giving the excess delay per unit length directly in terms of the measured attenuation per unit length in decibels.

Using (4) and (9), the lossy part of the transfer function of a line l units long can be written, for the frequency range of interest, as[7]

$$G_l(j\omega) = \left[e^{-[\hat{A}(\omega)+jB(\omega)]}\right]^l = \exp\left[-K_1l\omega^{K_2}\left(1+j\tan\frac{\pi K_2}{2}\right)\right], \quad (12)$$

or, in terms of $p=j\omega$,

$$G_l(p) = \exp\left[-\left(K_1l\sec\frac{\pi K_2}{2}\right)p^{K_2}\right]. \quad (13)$$

The inverse Laplace transform of (13), when delayed by the lossless delay K_0l, is the impulse response of the line, at least as far as waveforms whose spectra are within the considered frequency range are concerned. Thus, the impulse response of the line can be determined from a knowledge of the *measured* attenuation characteristic alone; no reference to a physical model for the line is required. Unfortunately, in order to evaluate this impulse response in terms of elementary functions, it seems necessary[8] to assume, as Wigington and Nahman have done, that $K_2=\frac{1}{2}$, and to fit K_1 to the empirical curve as well as possible. With this approximation, $G_l(p)$ becomes

$$G_l(p) = e^{-\sqrt{K_1l}\sqrt{p}}. \quad (14)$$

This is the same as the lossy part of the transfer function of (8) of Wigington and Nahman[3] when the identification $K_1 = \sqrt{2K/4R_0}$ is made.

In addition to the impulse and step responses given by Wigington and Nahman, I found much use for the response of a line l units long to an infinite ramp, $f(t)=t$, $t\geq 0$, since many waveforms [*e.g.*, the finite ramp, $F(t)$, of Wigington and Nahman[3]] can be expressed in terms of a sum of several of these, suitably scaled and delayed. This infinite-ramp response is the inverse Laplace transform of $G_l(p)/p^2$, which is tabulated,[9] for the $G_l(p)$ of (14). In the notation of Wigington and Nahman,[8] it is

$$\hat{h}(t) = (x+2\beta)\operatorname{cerf}\sqrt{\frac{\beta}{x}} - 2\alpha\sqrt{x}e^{-\beta/x}, \quad x = t - K_0l \geq 0, \quad (15)$$

where

$$\operatorname{cerf} x = \frac{2}{\sqrt{\pi}}\int_x^{+\infty} e^{-z^2}dz.$$

$\hat{h}(t)$, being in "closed" form, is perhaps slightly more useful than the finite-ramp response, $h(t)$, given by Wigington and Nahman.

George L. Turin
Hughes Aircraft Co.
Culver City, Calif.

[4] H. W. Bode, "Network Analysis and Feedback Amplifier Design," D. Van Nostrand Co., Inc., New York, N. Y., pp. 242, 299, 310; 1945.

[5] *Ibid.*, p. 313.

[6] Bateman Manuscript Project, Cal. Inst. Tech., "Tables of Integral Transforms," McGraw-Hill Book Co., Inc., New York, N. Y., vol. 1, p. 121; 1954. See transform pair 3.2(28).

[7] Dr. A. V. Balakrishnan has pointed out to me that for $0<K_2<1$ and $1<K_2<2$ the right-hand side of (12) is in the form of the characteristic function of the stable distributions of Lévy. (*Cf.*, P. Lévy, "Processus Stochastiques et Mouvement Brownien," Gauthier-Villars, Paris, pp. 176–181; 1948.) For a coaxial cable, $K_2<1$.

[8] Lévy, *op. cit.*, p. 181.

[9] Bateman Manuscript Project, *op. cit.*, p 245. See transform pair 5.6 (4).

The Autocorrelogram of a Complete Carrier Wave Received Over the Ionosphere at Oblique Incidence*

A number of autocorrelation studies[1–7] have been performed at various frequencies on the envelope of a carrier wave propagated over the ionosphere, but it appears that only one measurement of the autocorrelation function of a complete, undetected carrier has been reported.[8] Since the report describing this measurement has not been widely distributed, it is believed to be of interest to relate the nature and results of this experiment in this journal, although the data were taken several years ago and comprise only one observation.

The study was conducted on a 5-mc carrier wave generated by the WWV primary frequency standard in Beltsville, Md., and received in Cambridge, Mass., about 630 km distant. At the receiver the carrier was linearly heterodyned to a center frequency of 20 cps by a local primary frequency standard. In order to reject extraneous noise, the output of the heterodyning mixer was passed through a four-pole, maximally-flat, filter of center frequency 20 cps and bandwidth 8 cps, so that ionospheric fluctuations of up to several cycles per second could be faithfully accommodated.

A 30-minute sample of the received signal was observed, the 20-cps tone being recorded on magnetic tape. The signal appeared to have the statistics of narrow-band Gaussian noise, with the associated Rayleigh-distributed envelope. The autocorrelation function

* Received by the IRE, February 15, 1957. The research in this document was supported jointly by the U. S. Army, Navy, and Air Force under contract with Mass. Inst. Tech.

[1] R. W. E. McNicol, "Discussion on 'the fading of radio waves of medium and high frequencies,'" *Proc. IEE*, vol. 97, pt. III, p. 366; September, 1950.

[2] H. P. Hutchinson, private communication of work done in 1949.

[3] A. J. Lephakis, "Correlation Analysis of VHF Signals," Tech. Rep. No. 21, Mass. Inst. Tech., Lincoln Lab., Lexington, Mass.; May 18, 1953. (Not generally available.)

[4] K. Hirao and H. Maruyama, "Special instruments for observation and analysis of vhf fading," *J. Radio Res. Labs.* (Japan), vol. 2, pp. 207–216; April, 1955.

[5] R. B. Banerji, "The autocorrelogram of randomly fading waves," *J. Atmos. Terr. Phys.*, vol. 6, pp. 50–56; January, 1955.

[6] D. G. Brennan and M. L. Phillips, Tech. Rep. No. 93, M.I.T., Lincoln Lab., to be published. (Not generally available.)

[7] W. C. Mason, P. Duffy, and J. Skenian, M.I.T., Lincoln Lab., private communication.

[8] R. Price, "Statistical Theory Applied to Communication Through Multipath Disturbances," Tech. Rep. No. 266, M.I.T., Res. Lab. of Electronics, Cambridge, Mass., pp. 14–16; September 3, 1953.

of the sample was obtained from several days of analysis on the low-frequency correlator (LOCO) built for the Air Force Cambridge Research Center. Delay increments of 0.004 second were employed, and each point on the correlation function required three minutes of analog computation.

A half-section of the autocorrelation function thus obtained resembled the 20-cps transient that would be obtained from a filter of high Q. The zero crossings were quite uniform, implying that the power spectrum of the received carrier was nearly symmetric about 5 mc. In order to find the exact shape of the spectrum, it was required only to Fourier-transform the envelope of the autocorrelation function and then translate to 5 mc. It should be noted that, in general, the spectrum cannot be obtained from autocorrelation studies of the received envelope without some ambiguity, even assuming that the received signal is truly Gaussian.[9] A graph of the measured autocorrelation-function envelope is shown in Fig. 1, and the corresponding power spectrum, obtained by numerical computation, is presented in Fig. 2. The slightly oscillatory behavior of

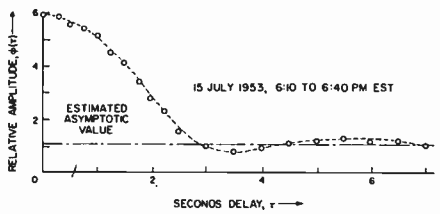

Fig. 1—Envelope of the autcorrelation function.

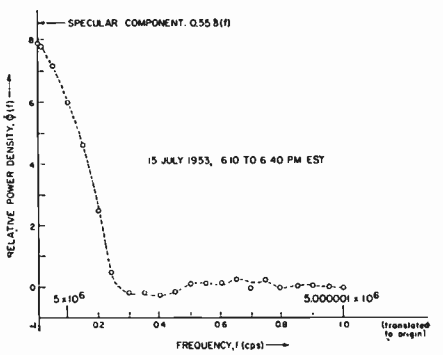

Fig. 2—Half-spectrum of WWV carrier.

the tail of the autocorrelation-function envelope is believed to be a genuine effect. Experimental inaccuracies no doubt account for the slightly negative regions in the spectrum. The explanation for the specular component is not clear; either there may have been pickup by the receiver of a 5-mc frequency that was present locally, or there actually may have been a nearly stationary mode of propagation in the ionospheric channel.

The author is indebted to Dr. Wilbur B. Davenport, Jr. for his guidance of the thesis project under which this experiment was performed, and to Dr. Jerome Elkind and Philip Fleck for their help in obtaining the autocorrelation function.

ROBERT PRICE
Lincoln Laboratory
Mass. Inst. Tech.
Lexington, Mass.

[9] H. G. Booker, J. A. Ratcliffe, and D. H. Shinn, "Diffraction from an irregular screen with application to ionospheric problems," *Phil. Trans. Roy. Soc. A*, vol. 242, pp. 579–607; September, 1950.

An Improved Operational Amplifier*

In electronic analog computers and similar applications, circuitry is needed to perform the algebraic functions and also for integration and differentiation. Some form of the circuit of Fig. 1 is usually utilized, and approximations to the required mathematical operations can be obtained. One disadvantage of this circuit is that the required open loop gain varies in inverse proportion to the allowable error. Therefore, accurate computation requires high gain amplifiers resulting in large units and instability problems. By adding an internal regenerative feedback loop to the degenerative amplifier of Fig. 1, it is possible to exactly perform the required mathematical operations without imposing a high gain requirement upon the open loop characteristics.

The circuit of Fig. 1 has the transfer function

$$G = \frac{E_{out}}{E_{in}} = -\frac{Z_2}{Z_1}\cdot\frac{1}{1+\dfrac{Z_2}{Z_1}\dfrac{1}{K+1}}.$$

If K is assumed to be large, the transfer function approximates a ratio of impedances. By proper choice of these impedances, the various mathematical operations may be performed. The error to a first approximation is

$$dG = -\frac{Z_2}{Z_1}\cdot\frac{1}{K+1}.$$

The circuit of Fig. 2 shows the internal regenerative loop.

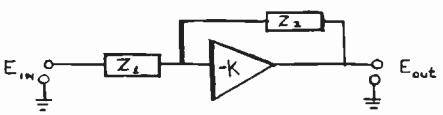

Fig. 1.

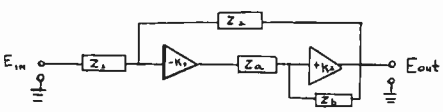

Fig. 2.

The transfer function for this circuit is

$$G_1 = \frac{K_1 Z_2 Z_b}{\left(Z_a - \dfrac{Z_b}{1+K_2}\right)(Z_1+Z_2) - Z_1 Z_b K_1}$$

if

$$Z_b = Z_a(K_2 - 1)$$

$$G_1 = \frac{-Z_2}{Z_1}.$$

* Received by the IRE, February 15, 1957.

Thus by proper adjustment of the parameters of the circuit of Fig. 2, circuits to exactly perform the required mathematical operations can be designed. If there is no objection to manually adjusting the regenerative feedback loop before each computation, an operational amplifier consisting of one duo triode plus associated parts may be used. If long-term stability of operation is required, a more complex amplifier is needed. However, for the same number of amplifier stages, the regenerative loop will always improve the computational accuracy.

RAMON NITZBERG
General Electric Co.
Defense Electronics Div.
Ithaca, N. Y.

Direct-Coupled Resonator Filters*

In the above article,[1] Mr. Cohn may find that he has overlooked two earlier notes[2,3] in his assertion that previous authors have all disregarded the frequency dependence of elements of microwave filters.

JOHN REED
Raytheon Mfg. Co.
Wayland, Mass.

Author's Comment[4]

On re-reading Mr. Reed's excellent paper,[5] I find that he has indeed considered the frequency variation of the coupling elements. There is, however, an important difference between his paper and mine, in that he restricts his attention to *quarter-wave-coupled* resonator filters, whereas I have restricted my attention to *direct-coupled* resonator filters. In my paper I was referring only to direct-coupled filters when I stated that all other published design formulas are based on frequency-independent coupling reactances. A further difference is that I have considered the total effect on the frequency response curve that is caused by the frequency variation of the coupling elements, while Mr. Reed has treated specifically the effect of this variation upon the loaded Q of a resonator in a waveguide when used either singly, or when quarter wave coupled to a second identical resonator.

It is true that I was unaware of the discussion[2] between Mr. Reed and Dr. Riblet on Dr. Riblet's earlier paper.[5] In this discussion, Dr. Riblet presents formulas that extend the work in his paper to include the frequency sensitivity of the coupling elements. Because Dr. Riblet's approach is so different from mine, a comparison would not be possible without an extensive quantitative study. Computations based upon Dr. Riblet's formulas would certainly be of great interest.

SEYMOUR B. COHN
Stanford Res. Inst.
Menlo Park, Calif.

* Received by the IRE, March 14, 1957.

[1] S. B. Cohn, PROC. IRE, vol. 45, pp. 187–186; February, 1957.

[2] H. J. Riblet and J. Reed, "Discussion on 'Synthesis of narrow-band direct-coupled filters,'" PROC. IRE, vol. 41, pp. 1058–1059; August, 1953.

[3] J. Reed, "Low Q microwave filters," PROC. IRE, vol. 38, pp. 793–796; July, 1950.

[4] Received by the IRE, March 29, 1957.

[5] H. J. Riblet, "Synthesis of narrow-band direct-coupled filters," PROC. IRE, vol. 40, pp. 1219–1223; October, 1952.

Contributors

Kenneth G. Budden was born in Portsmouth, England, on June 23, 1915. He received the B.A. degree from Cambridge University in 1936. For the next three years, he worked as a research student at the Cavendish Laboratory, Cambridge, on very low frequency radio waves, and received the M.A. and Ph.D. degrees in 1940. In 1939 he joined the Telecommunications Research Establishment of the British Ministry of Aircraft Production and worked on the design of ground radar equipment. From 1941 to 1944 he was with the British Air Commission in Washington, D. C. He was elected a Fellow of St. John's College, Cambridge in 1947 and was appointed to teach in the Department of Physics. He is presently on sabbatical leave from this position, and is working at the National Bureau of Standards Boulder Laboratories, Boulder, Colo.

K. G. BUDDEN

Dr. Budden is the author of several papers on the theory of the propagation of radio waves.

❖

John C. Chapman was born in London, England, on April 15, 1926. He was commissioned in the British Army in 1946 and served in Italy and Austria. In 1951 he received the B.A. degree with first class honors in physics from Christ's College, University of Cambridge. Subsequently, he did research on problems concerning atmospherics and the propagation of radio waves of very low-frequency; for this work he received the Ph.D. degree from the University of Cambridge in 1956.

J. C. CHAPMAN

Since 1954, Dr. Chapman has been a research physicist at Courtauld's Limited, Coventry, England, where he has been chiefly concerned with instrumentation problems.

❖

William Q. Crichlow (SM'55) was born on August 1, 1917 in Murfreesboro, Tenn. He received the B.E. degree in electrical engineering from Vanderbilt University in 1939 and was employed as transmitter engineer at Radio Station WSM, Nashville, Tenn. from 1939 to 1942.

From 1942 to 1946, he was a member of the Operational Research Staff in the Office of the Chief Signal Officer, Washington, D. C.

He joined the staff at the National Bureau of Standards, Washington, D. C., in 1946 and has conducted research studies principally in the fields of radio navigation and radio noise. He served as assistant chief of the Frequency Utilization Research Section from 1948 to 1955, and was chief of the Section from 1955 to 1956. At present, he is chief of the Radio Noise Section. During the past several years, he has been responsible for the development of a highly specialized radio-noise recorder which is being used in connection with a world-wide program of noise recording and prediction.

W. Q. CRICHLOW

❖

Richard Dronsuth was born in Chicago, Ill., on December 20, 1926. He attended the University of Illinois where in 1950 he received the B.S. degree in electrical engineering. After his graduation, he joined Motorola, Inc. in 1950. Mr. Dronsuth has had several years experience in microwave systems and field engineering. Since first joining Motorola, he has been engaged in antenna design, research on transmitter noise, and transmitter splatter and has also worked on many other vhf communications projects.

R. DRONSUTH

❖

Orville M. Eness (S'50–A'51–M'56) was born in Garner, Ia., on July 17, 1924. He attended Iowa State College, from which he received the B.S. degree in electrical engineering in 1951. After graduation, Mr. Eness accepted a position with Motorola, Inc., where he worked as a microwave systems engineer. After a year and a half of this work, he was transferred to the research department. Since that time, he has been engaged in the development of acoustic transducers, vhf receiver front ends, and also many other vhf communications projects.

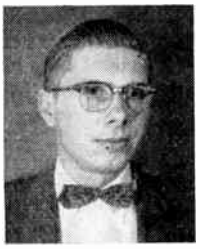

O. M. ENESS

Neville H. Fletcher was born in Armidale, Australia, on July 14, 1930. He attended the New England University College and received the B.S. degree from the University of Sydney in 1951, sharing the University medal in physics. A fellowship and Fulbright grant took him to Harvard University where he received the M.A. degree in 1953 and the Ph.D. degree in 1956 for work on the theory of impurity levels in semiconductors.

N. H. FLETCHER

While in the U. S., Dr. Fletcher was associated with Transistor Products Inc., where he was for a time assistant director of the development division. During this time he worked on power transistor design and developed special high-power types.

Since January, 1956 Dr. Fletcher has been a Research Officer with the Division of Radiophysics of the Commonwealth Scientific and Industrial Research Organization in Sydney, Australia. His work is concerned with the properties of semiconductors and semiconductor devices.

❖

J. Kenneth Grierson was born in 1922 in Yorkshire, England. After service with the RAF (1941–1946), he enrolled in mathematics and physics at Liverpool University, and graduated with the B.Sc. degree in 1949.

From 1949 to 1953, he was employed by the Dunlop Rubber Co. of Liverpool and Birmingham as a physicist. In 1953, he emigrated to Canada and has been employed by the Radio Physics Laboratory of the Defence Research Board at Ottawa since that year. His main activities lie in the design of scientific instruments, and their application to physical problems of research.

J. K. GRIERSON

His nonprofessional activities include amateur radio (VE3BLW).

Mr. Grierson is currently on educational leave at McGill University, Montreal, studying for the M.Sc. degree in communication engineering.

❖

Walter Guggenbuehl was born in Zurich, Switzerland on March 3, 1927. He received his formal education at the Swiss Federal

Institute of Technology at Zurich, where he received the degree of Electrical Engineer in 1950. From 1950 to 1956, he was first an assistant at the Electrical Department of Eidgenössische Technische Hochschule and later was a research associate at the Department of Advanced Electrical Engineering, studying problems of vacuum tubes and semiconductor devices. He received the degree of D. Techn. Sc. in 1955. His postgraduate work at the Institute was devoted to problems of transistors, crystal diodes, and associated circuits.


W. GUGGENBUEHL

In 1957 Dr. Guggenbuehl joined the Contraves AG at Zurich, where he is engaged with the transistorization of guided missiles.

❖

Edward L. Hill was born on November 3, 1904, in Hartford, Ark. He received the B.S. degree in electrical engineering in 1925 and the Ph.D. degree in physics in 1928 from the University of Minnesota, Minneapolis, Minn. In 1928 he was a National Research Fellow at Harvard University.


E. L. HILL

He became assistant professor of physics at the University of Minnesota from 1937 to 1946. He was also a research physicist at the Physical-Technical Institute in Leningrad, U.S.S.R., in 1934. During World War II, he served as a research physicist with the U. S. Navy. In 1951 he was the editor of the *Physical Review*.

Dr. Hill is a member of the American Physical Society, the American Mathematical Society, the American Acoustical Society, the American Association for the Advancement of Science, American Physics Teachers, Sigma Xi, Tau Beta Pi, and the American Association of University Professors.

❖

Johannes Labus was born on June 29, 1901 in Vienna, Austria. He received the Dr.-Ing. degree from the German Technical University in Prague, Czechoslovakia. From 1929 to 1930 he worked in the development field of the transmitter department of the General Electric Company, Schenectady, N. Y. He received the M.S. and Ph.D. degrees from Union College, Schenectady, N. Y.


J. LABUS

From 1937 to 1940 he was employed by the Czaja-Nissl Company, Vienna. During the war he was in charge of the department of electronics of the Deutsche Versuchsanstalt für Luftfahrt in Berlin. After the war, he joined the Siemens und Halske Company, Munich Germany. He is scientific collaborator in the research field of microwave electronics. Since 1932, he has been associate professor at the German Technical Universities in Prague and in Karlsruhe.

Mr. Labus is a member of Sigma Xi.

❖

For a photograph and biography of Samuel J. Mason, see pages 821–822 of the June, 1956 issue of PROCEEDINGS.

❖

For a photograph and biography of E. L. Maxwell, see page 97 of the January, 1957 issue of PROCEEDINGS.

❖

C. A. McKerrow was born at North Bay, Can., in 1919. He graduated from the North Bay Technical High School, after which he attended the Marconi Radio School in Toronto. During the early part of World War II he was employed by the Canadian Marconi Company as a marine radio operator. In 1941 he was employed by the department of transport of the Radio Monitoring Division. The period from 1945 to 1946 was spent in the eastern Arctic on the east coast of Baffin Island taking measurements of the ionosphere and other geophysical data.


C. A. MCKERROW

Mr. McKerrow joined the Radio Propagation Laboratory in 1947, which has now become the Defence Research Telecommunications Establishment, and continued research in ionospheric measurements. Later his attentions were directed to research engineering in low-frequency communications systems. For the past two years Mr. McKerrow has been engaged in the measurement of low frequency atmospheric noise in Canada.

❖

Anabeth C. Murphy was born on July 4, 1932, at Cheyenne Wells, Colo. After receiving the Bachelor of Arts degree from the University of Colorado in 1953 she joined the National Bureau of Standards, Central Radio Propagation Laboratory in Boulder, Colo., where she has been working on theoretical problems in antennas and wave propagation.


A. MURPHY

Mrs. Murphy is an associate member of the Boulder RESA branch.

Edward T. Pierce was born on May 13, 1916 in Llandudno, Wales, Great Britain. In 1937, he received the B.Sc. degree in mathematics and, in 1938, the B.Sc. degree in physics, both with first class honors from the University College of North Wales, Bangor, Wales. His research studies at the University of Cambridge, England, were interrupted by the advent of war in 1939. During the war, he held posts under the British Ministry of Supply and was particularly concerned with the development of aircraft armament.


E. T. PIERCE

In 1946, Dr. Pierce joined the faculty of the University of Cambridge being attached to the Solar Physics Observatory, where he not only pursued his main interests in atmospheric electricity, but also did work on solar observations and the airglow. He received the Ph.D. degree from the University of Cambridge in 1950.

Since 1952, he has been senior assistant in research in the Cavendish Laboratory, University of Cambridge, where he has been responsible for the prosecution of research in the Meteorological Physics Section, being concerned with problems in atmospheric electricity, cloud physics, atmospherics and radio wave propagation, etc.

Dr. Pierce is soon to take up a senior appointment with Vickers Limited, England.

❖

John A. Pierce (SM'45–F'47) was born in Spokane, Wash., on December 11, 1907. He received the B.A. degree in physics from the University of Maine. From 1934 to 1941, he was engaged in research, primarily on the physics of the ionosphere, at Cruft Laboratory at Harvard University.


J. A. PIERCE

From 1941 through 1945, he was a member of the Radiation Laboratory of the Massachusetts Institute of Technology, where he assisted in the development of the Loran system. He is now a senior research fellow at Cruft Laboratory working in the field of radio propagation.

Mr. Pierce holds the President's Certificate of Merit, the Navigation Award, and the Morris Liebmann Prize. He is a Fellow of the American Association for the Advancement of Science and the American Academy of Arts and Sciences.

❖

Roy A. Richardson was born in Chicago, Ill., on May 23, 1922. He received the degree of Bachelor of Science in electrical engineering from Illinois Institute of Technology in 1952 and has taken graduate work at Northwestern University, Evanston, Ill. Having completed his undergraduate studies

in September, 1951, he joined the communication and electronic division of Motorola, Inc., as a microwave engineer. During his employment at Motorola, Mr. Richardson has been engaged in a wide variety of research and development projects related to very high-frequency communication equipment.

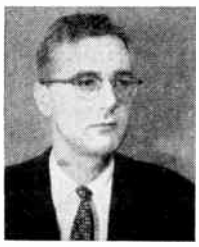

R. A. RICHARDSON

At present, he is the section leader of the communication section of the applied research department.

Mr. Richardson is a member of Tau Beta Pi and Eta Kappa Nu.

❖

Max J. O. Strutt (SM'46–F'56) was born on February 10, 1903 in Soerakarta, Java. He received his formal education at the University and Institute of Technology of Munich, from 1921–1924, and received the E.E. and D.Tech.Sc. degrees from the Institute of Technology, Delft, Holland, in 1926, and 1927, respectively. In 1927, he became the consulting research engineer of the Philips Company Ltd., at Eindhoven, Holland, and in 1948, he was appointed professor on the faculty of electricity at the Swiss Federal Institute of Technology.

M. J. O. STRUTT

In 1952, Dr. Strutt was elected director of the Institute of High Electrotechnics at the Swiss Federal Institute.

He was awarded a honorary doctorate in electrical engineering by the Institute of Technology at Karlsruhe, Western Germany, at its 125th jubilee, for his achievements in the field of technical and physical applications of the high- and ultra-high frequencies.

Dr. Strutt is a member of the Royal Institute of Engineers at the Hague, the Dutch Physical Society, the Swiss Electrotechnical Society at Zurich, the Physical Society of Zurich, and the Swiss Society of Sciences at Berne.

❖

Norman H. Taylor (SM'50) was born in Manchester, England, on November 15, 1916. He received the B.S. degree from Bates College in 1937 and the S.B. degree in electrical engineering from Massachusetts Institute of Technology in 1939. He spent the war years at the Western Electric Company. Since 1947 he has been at the Servomechanisms Laboratory, the Digital Computer Laboratory, and the Lincoln Laboratory of M.I.T., doing research and development on electronic computers. He is at present Associate Division Head of Division 6, Lincoln Laboratory.

N. H. TAYLOR

Mr. Taylor is a member of Eta Kappa Nu and Sigma Psi.

❖

James R. Wait (SM'56) was born in Ottawa, Can., in January, 1924. He attended McGill University for a brief period before enlisting in the Canadian Army in 1942. By the end of the war he was in charge of a radar maintenance group at Kingston, Ontario.

J. R. WAIT

He received the B.A.S. and M.A.S. degrees in engineering physics from the University of Toronto in 1948 and 1949 respectively. At this time he was employed as a junior research engineer at the Hydro Electric Power Commission of Ontario, where he assisted in the development of an infra-red bolometer. Returning for further graduate work to the University of Toronto, he obtained the Ph.D. degree in electromagnetic theory in 1951.

From 1949 to 1952 Dr. Wait was associated with Newmont Exploration Limited of Jerome, Ariz., where he conducted theoretical and experimental research in electrical prospecting. From 1952 to 1955 he was a section leader in the Defence Research Telecommunications Establishment in Ottawa where he was mainly concerned with theoretical problems in radiation. He has been associated briefly with McGill University during 1954 and Colorado University in 1955 where he taught graduate extension courses in electrical engineering. At present he is a consulting theoretical physicist to the Radio Propagation Engineering Division of the National Bureau of Standards in Boulder, Colo.

Dr. Wait is a member of RESA, Canadian Association of Physicists, the Society of Exploration Geophysicists, and U.S.A. Commissions III and IV of URSI.

For a photograph and biography of Arthur D. Watt, see page 97 of the January, 1957 issue of PROCEEDINGS.

❖

Arthur H. Waynick (F'57) was born in Spokane, Wash., on November 9, 1905. He attended Wayne University in Detroit, Mich., from which he received the B.Sc. degree in physics in 1935 and the M.Sc. degree in physics in 1936. During the period 1937–1939 he attended Cambridge University in England. In 1943, he received the Sc.D. degree in communications engineering from Harvard University. He also served as a Guggenheim Fellow at Cambridge during 1954–1955.

A. H. WAYNICK

Dr. Waynick is at present employed by the Pennsylvania State University as a professor, head of the electrical engineering department, and director of the Ionosphere Research Laboratory. He is a member of the United States National Committee-International Geophysical Year, Technical Panel on Ionospheric Physics. His recent experience includes service as past chairman of the IRE Professional Group on Antennas and Propagation, past chairman of the U. S. National Committee of URSI, and the head of the U. S. delegation to the general assembly of URSI at The Hague, Netherlands in 1954.

Dr. Waynick is a member of the Institute of Electrical Engineers, the American Geophysical Union, the American Society of Engineering Education and Sigma Xi.

❖

Irving W. Yabroff was born in Oakland, Calif., on January 26, 1928. After serving with the Army Air Force from 1945 to 1946, he obtained the B.A. degree in psychology from Stanford University, Stanford, Calif., in 1950. In 1953, he received the M.S. in electrical engineering and will receive the Ph.D. from Stanford this year.

I. W. YABROFF

He has held a research assistantship in the Radio Propagation Laboratory at Stanford University for the past two years. Presently he is working at the Stanford Research Institute in Menlo Park, Calif. on both propagation studies and weapons systems analysis.

Section Survey of IRE Editorial Policies

Reprinted below is the text of a survey recently sent to all IRE Sections, as discusssed in *Poles and Zeros* (p. 737 of this issue).—*The Editor.*

Background Data on IRE Publications

Proceedings of the IRE

Sent monthly to all members, including Students; overall distribution currently about 65,000 copies. Contains technical papers of outstanding merit and/or widespread interest; review and tutorial papers; IRE Standards; departments comprising news of IRE activities, commentary, reviews and abstracts of the technical literature, book reviews and correspondence. Special issues on technical subjects of general interest are published at intervals; present policy is to publish not more than four nor less than two special issues per year. Papers are published on an average of five months after receipt of original manuscript from authors.

IRE Directory

Published annually in October. Sent to all members except students. Contains alphabetical and geographical listings of all members except students, classified listings of products, and an alphabetical list of commercial organizations.

IRE Professional Group Transactions

Published individually by 24 Professional Groups and sent to the respective PG members and Affiliates; available to others on a subscription basis. Overall distribution about 250,000 copies annually. Individual PG Transactions have circulations ranging from 1,500 to 7,000 per issue. Publication varies with the Group, from one to six issues per year. Each Transactions contains technical papers of special interest to the Group, news and commentary on Group activities.

IRE Student Quarterly

Published in February, May, September and December and sent to all Student Members without extra charge. Available to others on a subscription basis ($3.00 per year to members). Current distribution is about 11,000 copies per issue, with extra distribution to potential student members in September. Contains technical and semi-technical articles aimed at student level; news of IRE and Student Branch activities; humor; articles on career guidance and related subjects of interest to students.

IRE National Convention Record

Published annually as soon after the National Convention as possible (published in July in 1956). Contains papers presented at National Convention; abstracts are published if full text is not supplied by authors. Contents published as received from authors without additional review or editing. Published in nine or ten sections. Overall distribution about 60,000 copies. Individual sections sent without extra charge to Professional Group members and Affiliates; available to others on subscription basis.

IRE WESCON Convention Record

To be published annually, beginning with 1957 WESCON Convention. Anticipated total distribution about 65,000 copies.

Questions on Editorial Policy
IRE Section Survey

1. Proceedings—Specialized papers vs. general articles. The majority of the papers published in the Proceedings are highly technical, many of them fully intelligible only to specialists. These papers are published primarily to serve the immediate interests of creative workers in a particular field, to permit them to base their extensions of the art on expertly evaluated contributions of others. Secondarily, they are published for reference interest of a larger group, to permit later "catching up" with the developments which underlie important new fields. It is recognized that few members will find more than two or three of these specialized papers of immediate interest in any single issue. The Editorial Board feels that this policy of publishing some papers for experts is sound, but that each issue should also contain papers of general nature, reviewing subjects of current technical interest on a broad basis, particularly for the benefit of workers outside the particular field covered.

Questions: Do Section members agree with this policy? Do they feel that it is being carried out effectively? If not, what change in emphasis as between general and specialized papers is recommended?

2. Proceedings—Interpretation of highly specialized material. To assist the non-specialist to appreciate the importance of technical papers, the department "Scanning the Issue" is prepared each month by the Managing Editor.

Questions: Do Section members wish this service to be expanded or modified? If so, in what way?

3. Proceedings—Review and tutorial papers. The present objective of the editors is to publish at least one paper per issue which reviews a technical field or development (Review Paper) or teaches the application of theory or techniques (Tutorial Paper). These may use technical terms and symbols appropriate to the subject, but are written with the non-specialist in mind. Recent examples are "Molecular Amplification and Generation

of Microwaves" (Wittke, March, 1957), "Controlled Fusion Research—An Application of the Physics of High Temperature Plasmas" (Post, February, 1957) and "Survey of Mechanical Filters and Their Applications" (Hathaway and Babcock, January, 1957).

Questions: Do these papers hit the mark in subject matter? In treatment? Should they be published more frequently? Less frequently? NOTE: Each Section Chairman is particularly urged to submit at least two suggested subjects for Review or Tutorial Papers which reflect the current interests of their Section members.

4. PROCEEDINGS—Use of mathematics and special symbols. Mathematical demonstrations and derivations are often essential to the presentation of technical advances, and are especially valuable to permit the specialist to evaluate for himself the validity and rigor of the conclusions reached in a paper. Mathematical treatment is, however, often used in a paper which would be quite clear and readily evaluated without it.

Questions: Should the editors and reviewers make a particular point of urging authors to rely on mathematical treatment only where it is essential? Should a strong effort be made to confine involved mathematics to an appendix to the paper?

5. PROCEEDINGS—Regular departments. The following departments are published monthly:

Scanning the Issue
Poles and Zeros
Correspondence
Contributors
IRE News and Radio Notes
Technical Committee Notes
Book Reviews
Abstracts and References

Questions: Which of these departments are read regularly by the Section members? Which are valued for reference? Should any of the departments be expanded? Any added? Any reduced or eliminated?

6. PROCEEDINGS—Mechanical aspects.

Questions: Do the Section members have suggestions concerning typography, makeup of pages, or arrangement of papers, departments and advertisements? In what condition are copies of the PROCEEDINGS received after shipment through the mails?

7. Directory—Professional Group Listing. General Comment. It has been suggested that the *Directroy* would provide an important additional service if membership in Professional Groups were added to the alphabetical listing of members. Certain of the Professional Groups publish membership lists in TRANSACTIONS but these are not available to all IRE members.

Questions: Does a majority of the Section membership favor such PG membership listings in the *Directory?* Are there any other suggestions concerning content and arrangement of the *Directory?* Is there a strong preference concerning the date of issue (currently issued in October)? Is the *Directory* kept at hand and consistently referred to?

8. Student Quarterly—General comment.

Questions: (For students, student branch officers and college representatives within the Section): What comment have readers of the *Quarterly* to offer concerning subject matter of articles, technical level, arrangement of issues, non-technical features, cartoons, frequency of publication? Is the *Quarterly* effective as a recruiting aid for the Student Branches?

Questions: (For non-student Section members): What percentage of non-student members regularly see and read the *Quarterly?* What is the opinion of those that read it in respect to its value for the older members of the IRE? Is the practice of occasional reprinting of *Quarterly* articles in the PROCEEDINGS generally approved?

9. Convention Record—General comment. The time required to secure typed manuscript from all authors of Convention papers, plus make-up and printing, as presently organized, makes necessary a delay in publishing the Convention Record of about four months from the close of the Convention. The papers are published without editing or review, as received from the authors.

Questions: Are these arrangements considered satisfactory? Is the make-up and arrangement of the nine volumes (by Professional Groups) satisfactory?

10. PG TRANSACTIONS—General comment. Note: It is suggested that questions on the TRANSACTIONS be referred to the respective PG Chapter Officers, where Chapters exist within a Section.

Questions: Most of the questions relating to the PROCEEDINGS (Item 1 through 6 above) apply in some measure to policies governing the TRANSACTIONS, and comments in each of these categories are solicited. In addition, comments regarding the relative technical level and degree of specialization as between TRANSACTIONS and PROCEEDINGS are desired. Should TRANSACTIONS carry book reviews? What frequency of publication (annually, biennially, quarterly, bimonthly) is deemed advisable for specific PG fields? If Affiliates are associated with PG chapters, do their comments differ from those of IRE members?

11. All Publications—Specific preferences. Section Officers are requested to report the preference of the members surveyed in respect to specific papers (identified where possible by title and author), departments, and classes of subject matter in all IRE publications. By examining such specific reactions from all the Sections, a pattern not foreseen in the questions posed above may be discerned. One possible approach is to refer to the two most recent issues of the PROCEEDINGS, read the table of contents and ask for a show of hands of those who found the particular items of special interest.

12. Suggestions at Large. Aspects of IRE publications policy not recognized as of interest and concern to Section members may have been omitted in the above outline. Any and all suggestions from the "grass roots" are welcome and will receive serious study by the Editorial Board.

IRE News and Radio Notes

Calendar of Coming Events and Author's Deadlines*

RETMA Symposium on Applied Reliability, Hotel Syracuse, Syracuse, N. Y., June 10–11

PGMIL Nat'l Meeting, Sheraton-Park Hotel, Washington, D. C., June 17–19

ACM Nat'l Meeting, Univ. of Houston, Houston, Tex., June 19–21

Brit. IRE Convention, Univ. of Cambridge, Eng., June 27–July 1

International Symposium on Physical Problems of Color Television, Paris, France, July 2–6 (DL*: May 1)

WESCON, Fairmont Hotel and Cow Palace, San Francisco, Calif., Aug. 20–23 (DL*: May 1)

URSI General Assembly, Boulder, Colo., Aug. 22–Sept. 5

Special Technical Conference on Magnetic Amplifiers, Penn Sheraton Hotel, Pittsburgh, Pa., Sept. 4–6 (DL*: June 11, D. Feldman, Bell Tel. Labs., Whippany, N. J.)

Industrial Electronics Symposium, Morrison Hotel, Chicago, Ill., Sept. 24–25

Nat'l Electronics Conference, Hotel Sherman, Chicago, Ill., Oct. 7–9 (DL*: June 1, V. H. Disney, Armour Res. Found., Chicago, Ill.)

IRE Canadian Convention, Exhibition Park, Toronto, Can., Oct. 16–18

East Coast Aero. & Nav. Conf., Lord Baltimore Hotel & 7th Reg. Armory, Balt., Md., Oct. 28–30

PGED Meeting, Shoreham Hotel, Wash., D. C., Oct. 31–Nov. 1 (DL*: Aug. 1, W. M. Webster, RCA, Somerville, N. J.)

PGNS Annual Meeting, Henry Hudson Hotel, New York City, Oct. 31–Nov. 1 (DL*: June 30, W. A. Higinbotham, Brookhaven Nat'l Labs., Upton, N. Y.)

Annual Symp. on Aero Commun., Hotel Utica, Utica, N. Y., Nov. 4–6

Radio Fall Meeting, King Edward Hotel, Toronto, Can., Nov. 11–13

PGI Conference, Atlanta-Biltmore Hotel, Atlanta, Ga., Nov. 11–13 (DL*: July 15, R. L. Whittle, Fed. Telecommun. Labs., 1389 Peachtree St., N.E., Atlanta 9, Ga.)

Mid-America Electronics Convention, Kan. City Mun. Audit., Kan. City, Mo., Nov. 13–14

PGVC Nat'l., Conf., Hotel Statler, Washington, D. C., Dec. 4–5. (DL*: July 1, G. E. Woodside, 1145 19th St., N.W., Wash., D. C.)

* DL = Deadline for submitting abstracts.

British IRE Holds Convention

The British Institution of Radio Engineers will hold its convention at the University of Cambridge from June 27 to July 1. The convention theme will be "Electronics in Automation" and thirty papers covering office machinery and information processing machine tool control, chemical and other processes, simulators, automation in the electronics industry, and automatic measurement and inspection will be presented during six sessions.

Guests attending the entire convention will be accommodated in King's College. Further details may be obtained from the British Institution of Radio Engineers, 9 Bedford Square, London, W. C. 1, England.

Engineering Education Note

It may be of interest to IRE members at large that the Board of Directors has approached the Engineers Council for Professional Development with the proposal that the IRE become a constituent member of that body.

Guided Missile Symposium Is Announced for Nov. 5–7

The annual Joint Military-Industry Guided Missile Reliability Symposium, sponsored this year by the Office of the Assistant Secretary of Defense for Engineering and the Chief of the Bureau of Aeronautics, Navy Department, will be held at the Naval Air Missile Test Center, Point Mugu, California. Participants will meet in technical sessions on November 5 and 6. November 7 will be reserved for visits to the Center's technical and operational areas.

Organizations desiring to send delegates to the symposium should select delegates by August 15 since attendance will be limited. Persons desiring to attend must have a secret security clearance.

Individuals and organizations wishing to present papers should submit abstracts of approximately 250 words no later than June 15, 1957. It is desired that contributions bear a security classification not higher than confidential and that abstracts be unclassified, if possible. Papers are invited on the following subjects: component problems, mathematical treatment, plant techniques, and testing techniques. Authors of papers selected for review will be notified by July 1 and will be expected to submit completed papers by July 15 for final selection. Security classification and clearances for all papers to be presented should be obtained directly by the authors from their contracting officer or authorized representative, keeping in mind that foreign scientists may attend the symposium. It is planned to have papers preprinted and distributed to advance registrants to permit review of papers by those desiring to engage in discussions.

All communications concerning meetings should be addressed to: Commander, NAMTC, Reliability Symposium, Code CEN-1, U. S. Naval Air Missile Test Center, Point Mugu, Calif.

IRE Facsimile Test Chart Available From Retma

A test chart has been in the course of preparation for the last few years under the direction of the Technical Committee on Facsimile of the IRE and arrangements have been made for its sale through RETMA. This chart contains a wide variety of patterns expressly designed for the testing of facsimile equipment and systems. Because of these characteristics it may also be useful in other arts. A reduced reproduction of the chart is shown below.

IRE FACSIMILE TEST CHART

It is a high quality glossy photographic print made under carefully controlled conditions to assure uniformity between different prints. The overall size is $9\frac{1}{4}\times12\frac{1}{4}$ inches with the test patterns limited to $8\frac{1}{2}\times11$ inches to allow for trimming.

Patterns are provided for checking single and multiple line definition, readability of different type faces, skew, index of cooperation, transient characteristics, jitter and grouping.

It contains a 15 step density tablet from paper white to about 1.7 with the densities calibrated. The maximum tolerance is ±0.05 density unit up to 0.32 density and ±0.11 density unit up to 1.00 density.

Eight of the sections will give different types of modulation patterns for synchronous oscilloscope display when scanned with a 2.75π inch scanning line.

Instructions are furnished with the chart which identify and describe each pattern on the chart and indicate its use.

The IRE Facsimile Test Chart is available from the Radio-Electronics-Television Manufacturers' Association, Engineering Department, 11 West 42 Street, New York 36, N. Y., at the following prices:

Quantity	Copy of Instructions w/each Chart	Copy of Instructions w/each 10 Charts
1	$1.50	
10	10.50	$10.00
50	40.00	37.50
100	65.00	60.00

AVAILABLE BACK COPIES OF IRE TRANSACTIONS

The following issues of TRANSACTIONS are available from the Institute of Radio Engineers, Inc., 1 East 79th Street, New York 21, New York, at the prices listed below:

Sponsoring Group	Publications	Group Members	IRE Members	Non-Members*
Aeronautical and Navigational Electronics	PGAE-5: October 1952 (6 pages)	$0.30	$0.45	$0.90
	PGAE-6: December 1952 (10 pages)	0.30	0.35	0.90
	PGAE-8: June 1953 (23 pages)	0.65	0.95	1.95
	PGAE-9: September 1953 (27 pages)	0.70	1.05	2.10
	Vol. ANE-1, No. 2, June 1954 (22 pages)	0.95	1.40	2.85
	Vol. ANE-1, No. 3, September 1954 (27 pages)	1.00	1.50	3.00
	Vol. ANE-1, No. 4, December 1954 (27 pages)	1.00	1.50	3.00
	Vol. ANE-2, No. 1, March 1955 (41 pages)	1.40	2.10	4.20
	Vol. ANE-2, No. 2, June 1955 (49 pages)	1.55	2.30	4.65
	Vol. ANE-2, No. 3, September 1955 (27 pages)	0.95	1.45	2.85
	Vol. ANE-2, No. 4, December 1955 (47 pages)	1.40	2.10	4.20
	Vol. ANE-3, No. 1, March 1956 (42 pages)	1.30	1.95	3.90
	Vol. ANE-3, No. 2, June 1956 (54 pages)	1.40	2.10	4.20
	Vol. ANE-3, No. 3, September 1956 (89 pages)	1.05	1.55	3.15
	Vol. ANE-4, No. 1, March 1957 (44 pages)	1.50	2.25	4.50
Antennas and Propagation	Vol. AP-1, No. 1, July 1953 (30 pages)	1.20	1.80	3.60
	Vol. AP-1, No. 2, October 1953 (31 pages)	1.20	1.80	3.60
	Vol. AP-2, No. 1, January 1954 (39 pages)	1.35	2.00	4.05
	Vol. AP-2, No. 2, April 1954 (41 pages)	2.00	3.00	6.00
	Vol. AP-2, No. 3, July 1954 (36 pages)	1.50	2.25	4.50
	Vol. AP-3, No. 4, October 1954 (36 pages)	1.50	2.25	4.50
	Vol. AP-3, No. 1, January 1955 (43 pages)	1.60	2.40	4.80
	Vol. AP-3, No. 2, April 1955 (47 pages)	1.60	2.40	4.80
	Vol. AP-4, No. 1, January 1956 (100 pages)	2.65	3.95	7.95
	Vol. AP-4, No. 4, October 1956 (96 pages)	2.10	3.15	6.30
	Vol. AP-5, No. 1, January 1957 (172 pages)	3.20	4.80	9.60
	Vol. AP-5, No. 2, April 1957 (72 pages)	1.75	2.60	5.25
Audio	PGA-7: May 1952 (47 pages)	0.90	1.35	2.70
	PGA-10: November–December 1952 (27 pages)	0.70	1.05	2.10
	Vol. AU-1, No. 8, November–December 1953 (27 pages)	0.90	1.35	2.70
	Vol. AU-2, No. 1, January–February 1954 (38 pages)	1.20	1.80	3.60
	Vol. AU-2, No. 2, March–April 1954 (31 pages)	0.95	1.40	2.85
	Vol. AU-2, No. 3, May–June 1954 (27 pages)	0.95	1.40	2.85
	Vol. AU-2, No. 4, July–August 1954 (27 pages)	0.95	1.40	2.85
	Vol. AU-2, No. 5, September–October 1954 (22 pages)	0.95	1.40	2.85
	Vol. AU-2, No. 6, November–December 1954 (24 pages)	0.80	1.20	2.40
	Vol. AU-3, No. 1, January–February 1955 (20 pages)	0.60	0.90	1.80
	Vol. AU-3, No. 3, May–June 1955 (30 pages)	0.85	1.25	2.55
	Vol. AU-3, No. 5, September–October 1955 (33 pages)	0.90	1.35	2.70
	Vol. AU-3, No. 6, November–December 1955 (36 pages)	0.95	1.40	2.85
	Vol. AU-4, No. 1, January–February 1956 (27 pages)	0.75	1.10	2.25
	Vol. AU-4, No. 2, March–April 1956 (17 pages)	0.55	0.80	1.65
	Vol. AU-4, No. 3, May–June 1956 (34 pages)	0.80	1.20	2.40
	Vol. AU-4, No. 4, July–August 1956 (23 pages)	0.60	0.90	1.80
	Vol. AU-4, No. 5, September–October 1956 (31 pages)	0.60	0.90	1.80
	Vol. AU-4, No. 5, November–December 1956 (36 pages)	0.80	1.20	2.40
	Vol. AU-5, No. 1, January–February 1957 (16 pages)	0.45	0.65	1.35
Automatic Control	PGAC-1: May 1956 (97 pages)	1.95	2.90	5.85
	PGAC-2: February 1957 (108 pages)	1.95	2.90	5.85
Broadcast Transmission Systems	PGBTS-2: December 1955 (54 pages)	1.20	1.80	3.60
	PGBTS-4: March 1956 (21 pages)	0.75	1.10	2.25
	PGBTS-5: September 1956 (51 pages)	1.05	1.55	3.15
	PGBTS-6: October 1956 (32 pages)	0.80	1.20	2.40
	PGBTS-7: February 1957 (62 pages)	1.15	1.75	3.45
Broadcast and Television Receivers	PGBTR-1: July 1952 (12 pages)	0.50	0.75	1.50
	PGBTR-5: January 1954 (96 pages)	1.80	2.70	5.40
	PGBTR-7: July 1954 (58 pages)	1.15	1.70	3.45
	PGBTR-8: October 1954 (20 pages)	0.90	1.35	2.70
	Vol. BTR-1, No. 1, January 1955 (68 pages)	1.25	1.85	3.75

* Colleges, universities, subscription agencies and all libraries may purchase at IRE member rate.

(Continued on page 888)

HIGHEST NAVAL CIVILIAN AWARD GIVEN TO JAMES H. TREXLER

J. H. Trexler (S'41–A'44), electronic scientist at the U. S. Naval Research Laboratory, has recently been given the Distinguished Civilian Service Award, the Navy's highest civilian award. The award, presented by the Assistant Secretary of the Navy for Air Garrison Norton, was granted to Mr. Trexler for "exceptionally outstanding service . . . in the field of basic research in countermeasures."

J. H. TREXLER

A native of Missoula, Montana, Mr. Trexler joined NRL in May, 1942 as a radio engineer. Prior to that, he attended the Engineering School at Southern Methodist University from 1936 to 1941. While there he gained much experience in the field of direction finders by building numerous directional receiving systems to study the characteristics of meteor spherics. He was also employed with Sutton, Steele & Steele in Dallas, Texas from 1939 to 1941 and as control room engineer with Radio Station WRR from 1940 to 1942.

Mr. Trexler's chief technical work has been in long-range vhf direction finding, cosmic ray noise, meteor spheric, and HF direction finding. To further his studies and research work in this field, he has visited radio communication stations in this country as well as abroad. He is also a member of the Scientific Research Society of America.

In October, 1945 he was given the Meritorious Civilian Service Award for "exceptional skill and outstanding accomplishment in developing radio frequency filters to eliminate radar interference in radio direction finders." The Meritorious Civilian Service Award is the second highest award a civilian employee can receive.

H. BEVERAGE WINS LAMME MEDAL FOR ENGINEERING ACHIEVEMENTS

The American Institute of Electrical Engineers has awarded the Lamme Gold Medal to H. H. Beverage (A'15–M'26–F'28).

H. BEVERAGE

He is vice-president of RCA Communications, Inc., and director of the radio research laboratory, RCA Laboratories. The presentation will be at the summer meeting of the AIEE in Montreal, Canada, June 24, 1957.

Dr. Beverage was cited "for his pioneering and outstanding engineering achievements in the conception and application of principles basic to progress in national and world-wide radio communications."

He holds more than forty patents in radio communications. He is co-inventor of the wave antenna and the diversity system for high frequency reception.

Summer Statistical Seminar Begins at Dedham July 29

A two-week summer statistical seminar will be held at the Endicott House in Dedham, Massachusetts, beginning July 29, 1957. The first week will be devoted to the general topic of time series with emphasis on turbulence, aeronautics, ship motion, and communication, under the chairmanship of Leo Tick of New York University.

The program for the second week will include business applications, reliability, and data reduction topics, as part of the general discussion of the impact of computers on statistical problems. Max Woodbury is chairman of this program.

Further information can be obtained from M. E. Terry, Bell Tel. Labs., Murray Hill, N. J., or the secretary, Geoffrey Beall, Gillette Safety Razor Co., Boston, Mass.

Radio Club of America, Inc. Re-Elects its Slate of Officers

The Radio Club of America, Inc., re-elected F. A. Gunther president of the organization for 1957. Serving with him again are W. A. Knoop, Jr., vice-president; O. J. Morelock, Corresponding Secretary; J. J. Stantley, Treasurer; and J. H. Bose, Recording Secretary.

Directors for the coming year include: E. V. Amy, R. R. Batcher, G. E. Burghard, H. W. Houck, F. A. Klingenschmitt, R. H. McMann, Jr., J. B. Minter, Harry Sadenwater, F. H. Shepard, Jr., and A. F. Toth.

The Radio Club of America, the oldest group of its kind in this country, includes outstanding men in the field of radio engineering and invention both in this country and abroad.

E. W. Henry Wins Fellowship to Continue Graduate Study

The National Academy of Sciences-National Research Council has announced the awarding of a predoctoral fellowship to E. W. Henry (S'54–M'56), presently with the United States Air Force at Dayton, Ohio.

This fellowship, sponsored by the IRE Professional Group on Electronic Computers, is administered by the NAS-NRC. It is awarded to outstanding young scientists for graduate training in electronic computers.

Mr. Henry was born in Wichita Falls, Texas in 1932. He received his B.S.E.E. degree *magna cum laude* from the University of Notre Dame in 1954 and his M.S.E.E. in 1955 from the same university. He majored in electrical engineering with a minor in electronics. Since graduation he has been on active duty in the Air Force as a lieutenant, assigned to the Communication and Navigation Laboratory, Wright Air Development Center, Dayton, Ohio. His tour of duty ends in June, 1957.

He plans to pursue his fellowship in the Department of Electrical Engineering at Stanford University, California, beginning in September, 1957. His present program of study toward his doctorate involves advanced training and research in servomechanism electronics and will include electronic computer theory and advanced network theory to facilitate servo system solutions.

AVAILABLE BACK COPIES OF IRE TRANSACTIONS—(Continued)

Sponsoring Group	Publications	Group Members	IRE Members	Non-Members*
	Vol. BTR-1, No. 2, April 1955 (40 pages)	$0.95	$1.45	$2.85
	Vol. BTR-1, No. 3, July 1955 (51 pages)	0.95	1.45	2.85
	Vol. BTR-1, No. 4, October 1955 (19 pages)	0.95	1.40	2.85
	Vol. BTR-2, No. 1, April 1956 (30 pages)	1.10	1.65	3.30
	Vol. BTR-2, No. 2, July 1956 (21 pages)	0.85	1.25	2.55
	Vol. BTR-2,jNo. 3, October 1956 (32 pages)	1.05	1.55	3.15
Circuit Theory	Vol. CT-1, No. 4, December 1954 (42 pages)	1.00	1.50	3.00
	Vol. CT-2, No. 4, December 1955 (88 pages)	1.85	2.75	5.55
	Vol. CT-3, No. 2, June 1956 (74 pages)	1.60	2.40	4.80
	Vol. CT-3, No. 4, December 1956 (104 pages)	1.90	2.85	5.70
	Vol. CT-4, No. 1, March 1957 (28 pages)	0.65	0.95	1.95
Communications Systems	Vol. CS-2, No. 1, January 1954 (83 pages)	1.65	2.50	4.95
	Vol. CS-2, No. 2, July 1954 (132 pages)	2.25	3.25	6.75
	Vol. CS-2, No. 3, November 1954 (181 pages)	3.00	4.50	9.00
	Vol. CS-4, No. 2, May 1956 (182 pages)	2.90	4.35	8.70
	Vol. CS-4, No. 3, October 1956 (59 pages)	1.05	1.55	3.15
	Vol. CS-5, No. 1, March 1957 (129 pages)	2.30	3.45	6.90
Component Parts	PGCP-1: March 1954 (46 pages)	1.20	1.80	3.60
	PGCP-3: April 1955 (44 pages)	1.00	1.50	3.00
	Vol. CP-3, No. 1, March 1956 (35 pages)	1.70	2.55	5.10
	Vol. CP-3, No. 2, September 1956 (44 pages)	1.75	2.60	5.25
	Vol. CP-3, No. 3, December 1956 (52 pages)	1.90	2.85	5.70
	Vol. CP-4, No. 1, March 1957 (36 pages)	1.35	2.00	4.05
Electronic Computers	Vol. EC-4, No. 4, December 1955 (40 pages)	0.90	1.35	2.70
	Vol. EC-5, No. 2, June 1956 (46 pages)	0.90	1.35	2.70
	Vol. EC-5, No. 3, September 1956 (72 pages)	1.05	1.55	3.15
	Vol. EC-5, No. 4, December 1956 (96 pages)	1.50	2.25	4.50
	Vol. EC-6, No. 1, March 1957 (72 pages)	1.15	1.70	3.45
Electron Devices	Vol. ED-1, No. 2, April 1954 (75 pages)	1.40	2.10	4.20
	Vol. ED-1, No. 3, August 1954 (77 pages)	1.40	2.10	4.20
	Vol. ED-1, No. 4, December 1954 (280 pages)	3.20	4.80	9.60
	Vol. ED-2, No. 2, April 1955 (53 pages)	2.10	3.15	6.30
	Vol. ED-2, No. 3, July 1955 (27 pages)	1.10	1.65	3.30
	Vol. ED-2, No. 4, October 1955 (42 pages)	1.50	2.25	4.50
	Vol. ED-3, No. 1, January 1956 (74 pages)	2.10	3.15	6.30
	Vol. ED-3, No. 2, April 1956 (40 pages)	1.10	1.65	3.30
	Vol. ED-3, No. 3, July 1956 (45 pages)	1.35	2.00	4.05
	Vol. ED-3, No. 4, October 1956 (48 pages)	1.45	2.15	4.35
	Vol. ED-4, No. 1, January 1957 (112 pages)	2.60	3.90	7.80
Engineering Management	PGEM-1: February 1954 (55 pages)	1.15	1.70	3.45
	Vol. EM-3, No. 1, January 1956 (29 pages)	0.95	1.40	2.85
	Vol. EM-3, No. 2, April 1956 (15 pages)	0.55	0.80	1.65
	Vol. EM-3, No. 3, July 1956 (37 pages)	0.90	1.35	2.70
	Vol. EM-4, No. 1, March 1957 (44 pages)	1.00	1.50	3.00
Industrial Electronics	PGIE-1: August 1953 (40 pages)	1.00	1.50	3.00
	PGIE-2: March 1955 (81 pages)	1.90	2.85	5.70
	PGIE-3: March 1956 (110 pages)	1.70	2.55	5.10
Information Theory	PGIT-3: March 1954 (159 pages)	2.60	3.90	7.80
	PGIT-4: September 1954 (234 pages)	3.35	5.00	10.00
	Vol. IT-1, No. 2, September 1955 (50 pages)	1.90	2.85	5.70
	Vol. IT-1, No. 3, December 1955 (44 pages)	1.55	2.30	4.65
	Vol. IT-2, No. 2, June 1956 (51 pages)	1.65	2.45	4.95
	Vol. IT-2, No. 3, September 1956 (224 pages)	3.00	4.50	9 00
	Vol. IT-2, No. 4, December 1956 (64 pages)	1.85	2.75	5.55
Instrumentation	PGI-3: April 1954 (55 pages)	1.05	1.55	3.15
	PGI-4: October 1955 (182 pages)	2.70	4.05	8.10
	Vol. 1–6, No. 1, March 1957 (72 pages)	1.50	2.25	4.50
Medical Electronics	PGME-2: October 1955 (39 pages)	0.85	1.25	2.55
	PGME-4: February 1956 (51 pages)	1.95	2.90	5.85
	PGME-6: October 1956 (72 pages)	1.25	1.85	3.75
	PGME-7: December 1956 (49 pages)	1.00	1.50	3.00
Microwave Theory and Techniques	Vol. MTT-2, No. 3, September 1954 (54 pages)	1.10	1.65	3.30
	Vol. MTT-3, No. 1, January 1955 (47 pages)	1.50	2.25	4.50
	Vol. MTT-3, No. 4, July 1955 (54 pages)	1.60	2.40	4.80
	Vol. MTT-3, No. 5, October 1955 (59 pages)	1.70	2.55	5.10
	Vol. MTT-4, No. 1, January 1956 (63 pages)	1.65	2.45	4.95
	Vol. MT-4, No. 2, April 1956 (69 pages)	1.70	2.55	5.10

*** Colleges, universities, subscription agencies and all libraries may purchase at IRE member rate.**

(Continued on page 889)

AVAILABLE BACK COPIES OF IRE TRANSACTIONS—(Continued)

Sponsoring Group	Publications	Group Members	IRE Members	Non-Members*
	Vol. MTT-4, No. 3, July 1956 (54 pages)	$1.25	$1.85	$3.75
	Vol. MTT-4, No. 4, October 1956 (84 pages)	1.85	2.75	5.55
	Vol. MTT-5, No. 1, January 1957 (80 pages)	1.75	2.60	5.25
Military Electronics	Vol. MIL-1, No. 1, March 1957 (32 pages)	0.90	1.35	2.70
Nuclear Science	Vol. NS-1, No. 1, September 1954 (42 pages)	0.70	1.00	2.00
	Vol. NS-2, No. 1, June 1955 (15 pages)	0.55	0.85	1.65
	Vol. NS-3, No. 1, February 1956 (40 pages)	0.90	1.35	2.70
	Vol. NS-3, No. 2, March 1956 (31 pages)	1.40	2.10	4.20
	Vol. NS-3, No. 3, June 1956 (24 pages)	1.00	1.50	3.00
	Vol. NS-3, No. 4, November 1956 (144 pages)	4.50	6.75	13.50
	Vol. NS-4, No. 1, March 1957 (52 pages)	1.80	2.70	5.50
Production Techniques	PGPT-2: April 1957 (148 pages)	2.85	4.25	8.55
Reliability and Quality Control	PGQC-2: March 1953 (51 pages)	1.30	1.95	3.90
	PGQC-3: February 1954 (39 pages)	1.15	1.70	3.45
	PGQC-4: December 1954 (56 pages)	1.20	1.80	3.60
	PGRQC-5: April 1955 (56 pages)	1.15	1.75	3.45
	PGRQC-6: February 1956 (66 pages)	1.50	2.25	4.50
	PGRQC-7: April 1956 (52 pages)	1.10	1.65	3.30
	PGRQC-8: September 1956 (58 pages)	1.10	1.65	3.30
Telemetry and Remote Control	PGRTRC-1: August 1954 (16 pages)	0.85	1.25	2.55
	PGRTRC-2: November 1954 (24 pages)	0.95	1.40	2.85
	Vol. TRC-1, No. 1, February 1955 (24 pages)	0.95	1.40	2.85
	Vol. TRC-1, No. 2, May 1955 (24 pages)	0.95	1.40	2.85
	Vol. TRC-1, No. 3, August 1955 (12 pages)	0.70	1.05	2.10
	Vol. TRC-2, No. 1, March 1956 (22 pages)	1.00	1.50	3.00
Ultrasonics Engineering	PGUE-1: June 1954 (62 pages)	1.55	2.30	4.65
Vehicular Communications	PGVC-5: June 1955 (78 pages)	1.50	2.25	4.50
	PGVC-6: July 1956 (62 pages)	1.55	2.30	4.65

* Colleges, universities, subscription agencies and all libraries may purchase at IRE member rate.

Project to Study Teacher Shortage in Engrg. Schools

A $10,000 grant from the National Science Foundation will support the first phase of a comprehensive study of how American engineering colleges may attract and keep top-flight engineering teachers.

The American Society for Engineering Education, sponsor of the project, says the Science Foundation grant will be used for preliminary work on a study "to determine and describe in detail the character and magnitude of the manpower and related financial needs of engineering colleges" and for organizing a full-scale attack on the problem.

When these needs are better understood, the society's project will go on to identify and specify the problems to be solved in meeting these needs, to determine and describe the special opportunities, satisfactions, and problems of engineering teaching, and to formulate the conditions which engineering colleges must fulfill to attract and develop good teachers for their faculties.

The ASEE project, titled officially "The Development of Engineering Faculties," is under the direction of an executive committee of which Dean H. L. Hazen of the Graduate School at the Massachusetts Institute of Technology is chairman. W. H. Miernyk of Northeastern University is Executive Director. The facilities of Northeastern's Bureau of Business and Economic Research, of which Dr. Miernyk is Director, will be used.

Other members of the project's executive committee are J. C. Boyce, Vice-President of Illinois Institute of Technology; Dean G. B. Carson of the College of Engineering, Ohio State University; M. D. Hooven of the Public Service Gas and Electric Co., Newark, N. J., President of ECPD; and W. C. White, Vice-President of Northeastern University. The American Society for Engineering Education has the support of the Engineers Council for Professional Development, Engineers Joint Council, and the National Committee for the Development of Scientists and Engineers. The committee will make a progress report of its work at the ASEE Annual Meeting at Cornell University.

IRE Mid-America Convention Set for Kansas City, Mo.

The IRE Mid-America Electronics Convention will be held in Kansas City, Mo., November 13–14, in the Kansas City Municipal Auditorium. Papers should be submitted for presentation on the general subjects of simulation council, medical electronics, engineering management, airborne electronics, analysis, new products, automation, instrumentation, human engineering, semiconductors, and electronics in the field of nucleonics.

Information on papers presented to S. R. Tyler, 2804 W. 74 St., Prairie Village 13, Kan. for submission should contain a title, an abstract of between 100 and 200 words, and require about 20 to 25 minutes for presentation.

Following is the list of personnel concerned with the Convention: General Chairman, W. H. Ashley, Jr.; Vice-Chairman and Treasurer, Allan Shontz; Publicity, Paul Constant; Advertising and Exhibits, T. V. Anderson; Program, S. R. Tyler; Publications, J. L. Kennedy; Hospitality, F. K. Hyer; Registration, I. H. Rubaii; and Facilities, Leo Schlesselmann.

At the luncheon for speakers and committee members during the 1957 IRE-SIAM Operations Research Symposium were: (left to right, front row) Harry Stein, Harry Vantine, Rudy Drenick, and Herbert Gurk. (Left to right, back row) John Mayberry, A. Schroeder, Martin Shubik, Sidney Kaplan, E. A. Fasko, J. G. Brainerd Murlun Corrington, G. Kaskey, A. Mullins, Hayden Ringer, and R. E. Johnson The symposium was held at the University of Pennsylvania, Philadelphia, Pa.

CURRENT IRE STANDARDS

(Continued)

48 IRE 22.S1 Standards on Television: Methods of Testing Television Receivers, 1948. Adopted by ASA. (ASA C16.13-1949)	$1.00
53 IRE 22.S1 Standards on Television: Definitions of Color Terms, Part I, 1953	$0.50
55 IRE 22.S1 Standards on Television: Definitions of Color Terms, 1955	$0.60
50 IRE 23.S1 Standards on Television: Methods of Measurement of Television Signal Levels, Resolution, and Timing of Video Switching Systems, 1950	$0.70
54 IRE 23.S1 Standards on Television: Methods of Measurement of Aspect Ratio and Geometric Distortion, 1954. Adopted by ASA. (ASA C16.23-1954)	$0.60
55 IRE 23.S1 Standards on Television: Definitions of Television Signal Measurement Terms, 1953	$1.00
50 IRE 23.S2 Standards on Television: Methods of Measurement of Time of Rise, Pulse Width, and Pulse Timing of Video Pulses in Television, 1950	$0.75
50 IRE 23.S3 Standards on Television: Methods of Measurement of Electronically Regulated Power Supplies, 1950	$0.75
45 IRE 24.S1 Standards on Radio Wave Propagation: Definitions of Terms Relating to Guided Waves, 1945	$0.20
50 IRE 24.S1 Standards on Wave Propagation: Definitions of Terms, 1950	$0.60
55 IRE 26.S1 Standards on Graphical and Letter Symbols for Feedback Control Systems, 1955	$0.25
55 IRE 26.S2 Standards on Terminology for Feedback Control Systems, 1955	$0.50
56 IRE 27.S1 Standards on Methods of Measurement of the Conducted Interference Output of Broadcast and Television Receivers in the Range of 300 KC to 25 MC, 1956	$0.50
56 IRE 28.S1 Standards on Letter Symbols for Semiconductor Devices, 1956	$0.50
56 IRE 28.S2 Standards on Solid-State Devices: Methods of Testing Transistors, 1956	$0.80

PROFESSIONAL GROUP NEWS

The Third Annual Technical Conference of the IRE Professional Group on **Electron Devices** will be held on October 31 and November 1 at the Shoreham Hotel, Washington, D. C., it has been announced by A. K. Wing, Jr., Federal Telecommunications Laboratories, chairman of the general committee for the conference.

Abstracts of technical papers proposed for the conference should be submitted by August 1 to the program chairman, W. M. Webster, RCA Semiconductor Division, Somerville, N. J. The subject matter of the proposed papers should concern developmental techniques and devices, such as electron tubes and transistors.

The Professional Group on **Instrumentation** and the Atlanta Section, IRE, will sponsor the Third IRE Instrumentation Conference and Exhibit at the Atlanta-Biltmore Hotel, November 11–13, 1957.

"Data Handling" will again be the theme of the technical program. Authors are invited to submit papers in the field of instrumentation for data handling. Suggested topics include analogue-digital conversion, use aspects of computers, editing equipment, information theory aspects, and input-output equipment. Information concerning proposed papers, including an abstract of approximately 200 words should be sent to R. L. Whittle, Program Chairman, Federal Telecommunications Laboratories, 1389 Peachtree St., N. E., Atlanta 9, Ga., before July 15, 1957. Papers accepted for presentation at this conference will be published in the PGI TRANSACTIONS.

The fourth Annual Meeting of the IRE Professional Group on **Nuclear Science** will be held in New York City on October 31 and November 1, 1957. Headquarters will be established at the Henry Hudson Hotel. The Atomic Industrial Forum and the American Nuclear Society will hold meetings earlier the same week. Arrangements will be made for admission to meetings of the other societies and participants may attend the Atomic Exposition in the Coliseum.

All members interested in contributing papers in the field of nuclear engineering with particular emphasis on realtor instrumentation and controls are invited to submit titles and abstracts on or before June 30 to: W. A. Higinbotham, Brookhaven National Laboratories, Upton, N. Y.

OBITUARIES

R. D. Duncan, Jr. (A'13–M'25–SM'43–L'55) died recently. He had been a consulting engineer with the Radio Corporation of America at Camden, N. J.

Previously he had served with the U. S. Department of Commerce, the Radio Section of the Bureau of Standards and the U. S. Army Signal Corps in various capacities. He did early work on portable radio development.

He obtained his bachelor's degree in electrical engineering from Washington University, St. Louis, Mo., in 1914, and authored several technical papers for publication.

Mr. Duncan, an IRE Life Member, was one of those who attended the first meeting of the IRE in 1912. He was a member of the IRE Papers Committee in 1933 and the Papers Review Committee in 1946–1951.

Marion E. King (SM'52) died February 26. He had been with the Bureau of Ordnance, Navy Department, at Washington, D. C. as division engineer in their quality control division.

A graduate of North Carolina State College in 1923, he received a bachelor's degree in electrical engineering. He had been associated with Western Electric Co., Victor Talking Machine Co., Bell Tel. Labs., Philco Corp. and the Signal Corps, before coming to the Bureau of Ordnance where he had been employed for eleven years prior to his death.

He had been on the administrative committee of the IRE Professional Group on Reliability & Quality Control. He was finance chairman of last January's Third National Symposium on Reliability & Quality Control in Electronics.

—CALL FOR PAPERS— 1958 NUCLEAR CONGRESS

The 1958 Nuclear Congress will be held in Chicago at the International Amphitheater, March 17–21, 1958. The IRE is among the sponsoring organizations, with particular cognizance in the field of instrumentation. In particular, we hope to be able to contribute papers in the following areas: high-temperature instrumentation, monitoring and health instrumentation, instrumentation systems, non-nuclear (process) instrumentation for reactors, and safety, startup and control instrumentation for reactors. More general papers are also suitable. It will often emerge that techniques remote from nuclear science have nevertheless been used successfully in nuclear applications. We would like to see these form part of a distinctive IRE contribution to the congress.

The deadline for the submission of abstracts is July 1, 1957. Please submit your papers to: D. I. Cooper, IRE Representative, Program Committee, 1958 Nuclear Congress, Room 2900, 330 W. 42 St., New York 36, N. Y. Manuscripts will be due October 1, 1957.

George W. Pierce (M'13–F'15) (L) died recently. He had been Rumford Professor of Physics, Emeritus, and Gordon McKay Professor of Communication Engineering, Emeritus, of Harvard University.

G. W. PIERCE

Dr. Pierce had received his education from the University of Texas and Harvard University. His professional experience was entirely with Harvard, where he served as Chairman of the Division of Physical Sciences from 1927 to 1940 until his retirement.

Among his most important inventions were the crystal oscillator and the magnetostriction oscillator invented during the twenties. He also authored three books, and numerous technical articles.

He was a member of the American Academy of Arts and Sciences, National Academy of Sciences, American Institute of Electrical Engineers, American Physical Society, Acoustical Society of America, Sigma Xi, and the IRE, the latter of which he was president in 1918 and 1919. In 1929 he was awarded the IRE Medal of Honor, and in 1943 the Franklin Institute bestowed upon him the Franklin Medal.

TECHNICAL COMMITTEE NOTES

The **Audio Techniques** Committee met at IRE Headquarters on April 19 with Vice-Chairman D. S. Dewire presiding for the major part of the meeting. The entire meet-

ing was devoted to the discussion of the Proposed Standard on Audio Techniques: Definitions of Terms.

Chairman K. R. McConnell presided at a meeting of the **Facsimile** Committee held on March 15 at the Times Building. The chairman announced that RETMA had received final prints of the IRE Facsimile Test Chart and would start filling orders shortly. The major portion of the meeting was devoted to the discussion of the Proposed Standards on Facsimile: Methods of Measurement.

The **Measurements and Instrumentation** Committee met at IRE Headquarters on March 19 with Chairman P. S. Christaldi presiding.

W. D. George, Chairman of Subcommittee 25.1 on Basic Standards and Calibration Methods, reported that definitions have been prepared and are in draft form presently. These cover such terms as voltage, frequency, attenuation, etc. Work on these will be continued and they will be circulated to the Measurements and Instrumentation Committee as soon as possible.

M. J. Ackerman, Chairman of Subcommittee 25.10 on Oscillography reported that his subcommittee has completed a list of Definitions of Terms for Oscillography. This list consists of approximately 85 terms, which were submitted to the main committee for review. Mr. Ackerman said that his subcommittee is now proceeding on methods of measurement relating to amplifier, sweep, brightness, etc. They anticipate that about forty methods of measurement will accommodate needs; it is planned to complete this work in 1958.

Chairman G. A. Morton presided at a meeting of the **Nuclear Techniques** Committee held at the National Bureau of Standards in Washington, D. C. on March 28. The committee discussed the program and personnel for the Sixth Scintillation Counter Symposium which was tentatively scheduled for January 27–28, 1958 at Washington, D. C. The committee also discussed the Scintillation Counter Definitions, which are presently under consideration in committee.

The **Piezoelectric Crystals** Committee held a meeting at IRE Headquarters on March 18 with Chairman Hans Jaffe presiding. The committee discussed the need for standardization of magnetostriction definitions, and it was decided to form a subcommittee to cover this subject. The committee discussed and reviewed a Proposed Standard on Ferroelectric Crystals: Definitions.

The committee discussed, amended and unanimously approved a Proposed Standard on Piezoelectric Crystals: Determination of the Elastic, Piezoelectric and Dielectric Constant.

Dr. Jaffe reviewed briefly the status and history of the Proposed Standards on Piezoelectric Ceramics. The goal of this work is to prepare a simple standard for those concerned with testing of piezoelectric ceramics. It is planned to have a draft of a complete report ready for the next meeting of the Piezoelectric Crystals Committee.

H. Goldberg, Chairman, presided at a meeting of the **Radio Transmitters** Committee held at IRE Headquarters on March 20. The major portion of the meeting was devoted to discussion of the proposed revision of the 1948 Standards on Transmitters: Definitions of Terms.

The **Standards** Committee held a luncheon meeting at the Belmont Plaza Hotel in New York on March 19 with Chairman M. W. Baldwin presiding.

Ernst Weber, IRE Standards Coordinator, gave a brief outline of IRE's activity with regard to the following international organizations: The International Electrotechnical Commission, The International Radio Consultative Committee, The International Scientific Radio Union, and the International Radio Conference.

Mr. Baldwin, Chairman of the Standards Committee, gave an outline of the Standards Committee achievements during the past committee year.

Chairman J. L. Jones presided at a meeting of the **Video Techniques** Committee held at IRE Headquarters on March 22. The major portion of the meeting was devoted to discussion of revisions for the IRE Standards on Television: Methods of Measurement of Television Signal Levels, Resolution, and Timing of Video Switching Systems, 1950.

Books

Television Engineering Handbook, ed. by D. G. Fink

Published (1957) by McGraw-Hill Book Co., Inc., 330 W. 42 St., N. Y. 36, N. Y. 1496 pages +27 index pages +xiv pages. 1159 figures. 9¼×6¼. $18.00.

This book represents a prodigious amount of work on the part of the experts who helped to compile it. The editor is to be sincerely complimented for undertaking a work of such magnitude and for the care with which he has chosen the outstanding specialists charged with writing the individual chapters.

It contains within its covers an enormous amount of information which has hitherto been available only in many different textbooks and in numerous articles in technical magazines. On top of that, it contains a substantial amount of new information which, as far as this reviewer is aware, has not heretofore been published anywhere.

As an example of such new information, attention should be called specifically to Chapter 10, "Composite Video Signals, Waveforms, and Spectra." This chapter contains numerous painstakingly computed and plotted graphs of the frequency content of different forms of television signals, monochrome as well as color, and the information in these graphs should be of great interest and most informative to anyone interested in the detailed nature of television signals, especially in view of the excellent reproductions used in portraying them.

Another place where much new material is incorporated is in Chapters 15 and 16 on "Television Receivers," circuit functions and circuit design. These two chapters together cover over 300 pages and give a lot of detailed circuit information which has not been available heretofore, at least not in any easily accessible form. Altogether, the book is a most valuable addition to the literature on the technical aspect of television and, as such, it should be a part of the library of any engineer working in this general field.

And now for some of the criticisms which any self-respecting reviewer feels it his duty to include in a review. The book is called a handbook and, as such, the information should be arranged so that any specific subject or detail can be referred to in one particular place without the necessity of looking all through the book for cross references. There is a certain lack of correlation between the information supplied by the many different authors in the different chapters, with the result that this is not always possible.

For instance, Chapter 1 on "Numbers, Equations, and Definitions" discusses in one paragraph the CIE system of color specification and gives a fair amount of detail regarding the specification. It does not, however, say what CIE is, or where and how the specification originated. Later on, in Chapter 4, "Color Vision and Colorimetry," there is a little more information about the CIE system and what the CIE stands for, but that's not obvious to the person who starts by looking up information in Chapter 1, since no cross reference is given. Similarly in the worthwhile and already mentioned Chapter 10 on composite video signals, there are numerous references to the NTSC and to the FCC color signals, and there are references to such signals as the "Sunflower Girl" and the "Tulip Garden." To those of us who have been in the field for a long time and have taken part in the committee work and the many deliberations that went into establishing the present color television system, the references are self-evident. But the book is supposed to be a handbook, and it is hoped one which will be of service to younger engineers, both in its present edition and in future revised editions. To those younger engineers some of the references made are not self-evident and must be somewhat confusing. It would have been helpful if a separate chapter had been included giving a brief history of how we arrived at the present standards of television, what NTSC and

FCC stand for, and what part they played in the establishment of these standards. To be sure, this is all covered very well and very thoroughly in other books, but one primary purpose of a handbook, such as this is supposed to be, is to avoid chasing information in six other books not so readily available as this is hoped to be.

Another omission struck this reviewer as rather odd. In the very comprehensive chapter on television receivers there is, of course, very detailed discussion of the circuits around a color television receiver using a shadow mask type of tube. Since this is by far the most common type of tube used, this is as it should be. There is also a fairly complete discussion of the specific circuits used with the Philco "apple" color tube. In view of the fact that this tube is quite new and not yet commercially available, this is very gratifying and will be appreciated by a larger number of people working in the field. There is, however, no discussion at all of the circuitry used with the Lawrence tube or chromatron tube, in spite of the fact that receivers with these types of tube have been available, even though not in large quantities. This is an unfortunate omission and it is hoped that it will be rectified in any future edition of the book.

Finally, one more criticism. Some of the chapters have very excellent bibliographies and lists of references, which is highly to be commended. As an outstanding example of this, one might mention Chapter 5 on "Cathode-Ray Devices," which has a total of 106 references, although in this particular chapter no distinction is made between true references as referred to in the text and bibliographical references included for general information. On the other hand, in Chapter 15, "Television Receivers—Circuit Functions and Block Diagrams," there is not a single reference, in spite of the fact that the fundamental problems discussed in this chapter are obviously not meant to be original.

In conclusion, this reviewer would like to emphasize that the criticisms made above are definitely intended to be constructive. The book will serve a definite need in the field of technical literature on television and it is only hoped that the criticisms may assist the editors and the authors in making the second edition even more of a true handbook on the subject.

A. G. Jensen
Bell Tel. Labs.
Murray Hill, N. J.

An Introduction to Junction Transistor Theory by R. D. Middlebrook

Published (1957) by John Wiley & Sons, Inc., 440 Fourth Ave., N. Y. 16, N. Y. 287 pages+4 pages of appendix+4 index pages+xxiv pages. Illus. 9½×6¼. $8.50.

The author succeeded in filling a gap in the transistor literature by creating a book for electronic engineers who are interested in the physical aspects of transistor operation. It forms a bridge between the physics of semiconductors and the circuit properties of junction transistors.

This book provides a continuous development of basic junction transistor theory, starting with a thorough qualitative analysis of the most important fundamental physical principles and ending with the derivation of a new high frequency equivalent circuit. The standard knowledge of mathematics, physics, and electronics of an electronics engineer is sufficient for understanding this book.

The main chapters of the book deal with: qualitative development of junction transistor theory; qualitative and quantitative semiconductor physics; current flow in semiconductors; boundary values for forward biased *p-n* junctions (energy diagram, carrier distribution, etc.); *p-n* junctions under applied d-c potential; *pnp* transistors (internal capacitance and feedback effects); small-signal a-c equivalent circuits (complete and simplified configuration for circuit applications).

The qualitative explanations are very clear and easy to read. The quantitative analysis is straightforward and the mathematical formulas are carefully derived and discussed. Repetitions on purpose are helpful in learning the rather complicated principles of transistor action. Many figures clarify the physical meaning of mathematical derivations. A new high-frequency equivalent circuit, derived from the physics of the transistor and proven experimentally up to about twice the cutoff frequency, is a major contribution.

Only the classical references are mentioned in each chapter. It is felt that more experimental results should have been given to provide a comparison with the calculations. The very important topics of high injection and surface effects are treated rather briefly. Also, the drift transistor is not mentioned, but the modest title of the book "An Introduction to . . . " tells the reader that this book does not intend to be a sort of a "handbook on transistor theory." A discussion of many of the formulas with respect to silicon devices (not just germanium ones) would have been desirable.

This book is well written and the transistor theory discussed in a surprisingly clear, logical, and concrete manner. The electronics engineer and the student who is not satisfied with transistor knowledge from the "black box" point of view will gain a thorough understanding of basic transistor problems (the "hows" and "whys") by studying the pages of this book.

Peter Kaufmann
Raytheon Manufacturing Co
Newton, Mass

Radio Astronomy by J. L. Pawsey and R. N. Bracewell

Published (1955) by Oxford University Press, 114 Fifth Ave., New York 11, N. Y. 354 pages+1 page of appendix+5 index pages+vi pages. 150 figures and 23 plates. 9½×6¼. $8.80.

Astronomy may be divided into three epochs: the pre-telescopic before Galileo, the telescopic from Galileo to the present, and the radio-electronic epoch which we are now entering. Through the application of antennas and receivers to astronomical observations, radio is opening a new window on the universe while electronic techniques and methods are widening the scope of purely optical observations.

This astronomical research at radio wavelengths has created a new science, radio astronomy. To date but few books devoted to this subject have been written. One of the most recent and most comprehensive is *Radio Astronomy* by J. L. Pawsey and R. N. Bracewell. At the time the book was written both were members of the Radio Physics Laboratory of the Commonwealth Scientific and Industrial Research Organization (CSIRO) in Sydney, Australia. Although Pawsey continues with the CSIRO, where he directs the radio astronomy work, Bracewell has recently joined the staff of Stanford University, California. For many years the CSIRO has been one of the most active and productive research centers in radio astronomy so it is not surprising that much of the text material is derived from the extensive publications of the Sydney organization.

The book covers the broad aspects of radio astronomy from antenna and receiver theory to pure astrophysics with a good balance and blending of subject matter. The book is both descriptive and analytical and is at a level suitable as a textbook on radio astronomy, The extensive bibliography also makes it valuable as a reference book to workers in the field. Some of the specific topics treated are antennas, receivers, thermal noise, radio waves in ionized gases, solar physics, galactic structure, discrete radio sources, cosmic radio background, lunar radio emission, extraterrestrial radio echos, radio detection of meteors and the effect of the earth's atmosphere on extraterrestrial radio waves. The wide range of topics covered and the numerous excellent illustrations and tables make the book valuable to both the casual and active worker in radio astronomy.

J. D. Krause
Ohio State University
Columbus, Ohio

Niederfrequenz- und Mittelfrequenz-Messtechnik für das Nachrichtengebiet by A. Wirk and H. G. Thilo

Published (1956) by S. Hirzel Verlag, Stuttgart N., Germany. 230 pages+4 index pages+viii pages. Illus. 9½×6¼. DM 28.00.

This monograph on "Measurements in Communication Engineering at Low and Intermediate Frequencies" is written by two members of the Siemens & Halske Laboratories in Berlin and Munich, Germany. It contains a detailed description and discussion of measuring equipment and techniques for the audio-frequency range up to a few megacycles. Special emphasis is put on testing of telephone circuits, components, and transmission lines. The first chapter gives definitions and general remarks on comparison methods, null methods, and deflection-type measurements, calibrations, shielding, and stray fields. The next chapter describes rc-generators for frequencies up to 1 mc, and an interesting beat-frequency generator employing a ring-modulator with four copper-oxide rectifiers. These rectifiers and the attendant circuitry were brought to a high degree of perfection at the Siemens & Halske Laboratories and were used extensively for voltage and current measurements in the audio-frequency range (Chapter 3). Null indicators for bridge measurements, test receivers, and vacuum tube voltmeters are discussed in Chapter 4. Subsequent chapters deal with the measurement of frequency, frequency spectra, nonlinear distortion, and noise in transmission systems. Considerable

space is devoted to bridge measurements of resistance, capacitance, inductance, mutual inductance, impedance, and small loss tangents. Difficulties due to stray capacitances and asymmetries with respect to ground are pointed out and effective shielding and compensating methods are given. Particular emphasis is put on techniques for precise determination of small loss tangents. An unusual bridge employing a tapped choke for measuring capacitances merits special mentioning. The remainder of the book is devoted to techniques and instrumentation for testing transmission systems and covers measurement of characteristic impedance, insertion loss, frequency response, crosstalk, and nonlinear distortions.

Throughout the book, which is well written and profusely illustrated, pictures and descriptions of production-engineered equipment supplement the general discussion of methods and techniques. As mentioned in the preface, the book is essentially restricted to a description of development work done at the Siemens & Halske Laboratories. Most of the references pertain to this work and are dated before 1945. Non-German publications are mentioned only twice. This tends to decrease the value of the book as reference material, since the reader cannot but wonder how all the other contributions to this field compare with those mentioned in the book. Nevertheless, there is much useful information for those who work in audio engineering, low-frequency communications, and carrier systems up to one or two megacycles. The precise techniques and the superb instrumentation described may also be of considerable help to the solution of measurement problems in material research and component development.

H. VON AULOCK
Bell Tel. Labs.
Whippany, N. J.

Abstracts of IRE Transactions

The following issues of "Transactions" have recently been published, and are now available from the Institute of Radio Engineers, Inc., 1 East 79th Street, New York 21, N. Y. at the following prices. The contents of each issue and, where available, abstracts of technical papers are given below.

Sponsoring Group	Publication	Group Members	IRE Members	Non-Members*
Antennas & Propagation	Vol. AP-5, No. 2	$1.75	$2.60	$5.25
Audio	Vol. AU-5, No. 1	.45	.65	1.35
Communications Systems	Vol. CS-5, No. 1	2.30	3.45	6.90
Electron Devices	Vol. ED-4, No. 1	2.60	3.90	7.80
Instrumentation	Vol. I-6, No. 1	1.50	2.25	4.50
Nuclear Science	Vol. NS-4, No. 1	1.80	2.70	5.40

*** Public libraries and colleges may purchase copies at IRE Member rates.**

Antennas & Propagation

VOL. AP-5, NO. 2, APRIL, 1957

News and Views (p. 173)

Contributions—Some Electromagnetic Transmission and Reflection Properties of a Strip Grating—R. I. Primich (p. 176)

Some theoretical and experimental results for the reflection and transmission of an uniform plane electromagnetic wave, normally incident on an ideal strip grating, are presented. The theory is based on the variational method, and the measurements were made at normal incidence in a parallel plate region operating in the 8- to 10-cms wavelength range. A few results for oblique incidence are also included; the experiments in this case were carried out at 1.24-cm wavelength in a parallel plate spectrometer. There was reasonable agreement between theory and experiment throughout.

The Dependence of Microwave Radio Signal Spectra on Ocean Roughness and Wave Spectra—C. I. Beard and I. Katz (p. 183)

This paper is an extension of previous work on reflection of microwaves from an ocean surface. The present analysis, dealing with spectra, is based on data obtained in a one-way X-band propagation experiment performed across the Golden Gate, San Francisco. Two paths of 9000 and 15,000 feet were used. To describe the ocean surface, wave gages were mounted on a piling driven into the Golden Gate channel.

Radio-signal spectra are found to be broader than the ocean-wave spectra and the spectral breadth a function of ocean roughness. The important result of this analysis is the establishment of a linear relationship between ocean roughness and the spectral breadth of the radio signals. Ocean roughness is measured by the product of the standard deviation of the wave height and the grazing angle divided by the radio-wave length. Radio spectral breadths are determined by the frequencies at which each spectrum drops to the 0.9-, 0.8-, 0.7-, 0.5-, 7.25-, and 0.1-power points. The breadths are then expressed as ratios of these frequencies to the frequency of the peak in the simultaneous ocean-wave spectrum.

The analysis now enables one to predict the approximate shape of the spectrum of the radio signal received in a one-way transmission path given only a knowledge of the geometry, radio-wave length, ocean-wave height, and the peak frequency in the ocean spectrum.

Step Discontinuities in Waveguides—W. E. Williams (p. 191)

The method developed by Wiener and Hopf for solving a certain class of integral equations is applied to the problem of a discontinuity in cross section of a rectangular waveguide. We consider the problem of two waveguides of infinite width and different heights joined together with a short step when the only non-vanishing component of the magnetic field is that parallel to the edges of the step. It is assumed that the fundamental mode is incident in the larger channel traveling towards the step. For values of the channel height such that only the fundamental mode is propagated without attenuation (this problem has been treated in the "Waveguide Handbook"), our results are in very good agreement with the results given there. The present analysis is extended to cover the case where the larger channel is capable of supporting the mode above the fundamental without attenuation. Some numerical values are given for the ratio between the reflected and incident energies for various values of the channel and step heights.

The Transient Behavior of the Electromagnetic Ground Wave on a Spherical Earth—J. R. Wait (p. 198)

Some calculations are presented to show the nature of the transient ground wave radiated from an electric dipole which is situated over a spherical earth. The moment of the dipole is considered to vary with time in a linear manner. It is shown that the departure of the leading edge of the radiation field from a step function form is a consequence of diffraction and loss in the finitely conducting ground.

An Experimental Investigation of the Diffraction of Electromagnetic Waves by a Dominating Ridge—J. H. Crysdale, J. W. B. Day, W. S. Cook, M. E. Psutka, and P. E. Robillard (p. 203)

The diffraction of electromagnetic waves by a dominating tree-covered ridge north of

Ottawa has been the subject of an experimental investigation. The measurements were made at 173, 493, and 1785 mc using both horizontally and vertically polarized radiation. The measurement period extended from late in the winter until early in the summer of 1955. The bulk of the experimental data consists of the results of height-gain and azimuth-gain measurements. Estimates of diffraction loss have been deduced from these results for the component of the radiation which was not reflected by the terrain between the ridge and the terminals of the experimental circuits. These deduced experimental diffraction losses exceed the predictions of Fresnel-Kirchhoff knife-edge diffraction theory, the discrepancies increasing with increasing frequency. There was no evidence of either a pronounced polarization dependence or a pronounced seasonal dependence.

A Helical Line Scanner for Beam Steering a Linear Array—Louis Stark (p. 211)

A new type of antenna beam scanner which uses the phasing principle for beam steering a linear array is described. The scanner consists of a bank of helical line trombone phase shifters which provide a variable delay circuit for each element of the linear array. The circuits are ganged mechanically by connecting the slides of the trombone phase shifters to a lever arm drive. Short helix sections concentric with the main lines are used to couple the slide of each trombone phase shifter to the main helical lines.

Measurements of phase characteristics, insertion loss, and vswr of the trombone phase shifters have been carried out. Isolation between phase shifting circuits has also been measured. Radiation studies were conducted using a ten-element scanner in conjunction with a vertical slot array antenna having ten bays. Patterns showing beam scanning out to 52° from broadside are included.

A Simple Solution to the Problem of the Cylindrical Antenna—J. G. Chaney (p. 217)

It is recognized that the variational solution of the cylindrical antenna does not minimize $|Z_{in}-Z_0|$, as implied by Storer; but yields a minimax of the impedance function. Furthermore, the variational solution may be interpreted as simply placing two currents in parallel upon the antenna, following which, the solution for the magnitudes of the currents and for the driving point impedance may be found by elementary circuit analysis. Consequently, a first-order solution by the generalized circuit is found by postulating a linearly-attenuated traveling wave to be superimposed upon the sinusoidal standing wave. The results show excellent correlation with other theoretical and measured results for both the driving point impedance and the current distribution along the antenna.

Investigations with a Model Surface Wave Transmission Line—G. Goubau and C. E. Sharp (p. 222)

This paper summarizes the results of experimental studies conducted with a scale model of a surface wave transmission line (swt line) for long-distance transmission. The purpose of the experiments was to determine the effect of supports, bends, and sags on the transmission loss of such a line. Also, the coupling between parallel identical lines has been measured and compared with the theory.

Formulas and other information are given which may be applied to the design of a swt line for long-distance transmission.

Antenna-to-Medium Coupling Loss—Harold Staras (p. 228)

This paper presents an improved estimate of one of the more important systems parameters on a scatter circuit, namely, the antenna-to-medium coupling loss. The work presented in this paper differs from the earlier work of Booker and de Bettencourt in that it permits evaluating the coupling loss even when nonconical, nonidentical antennas are used at either end of the scatter circuit, and it also permits taking the anisotropy of atmospheric turbulence into account. An important conclusion is reached that the coupling loss is not shared equally by the two antennas (*i.e.*, transmitting and receiving) even if they are identical. This is a phenomenon which should be fully appreciated by engineers designing a scatter circuit or when measuring the coupling loss experimentally.

Precipitation Particle Impact Noise in Aircraft Antennas—R. L. Tanner (p. 232)

It has been found that precipitation static noise is produced in antennas under plastic surfaces, even though these surfaces are covered by conductive films. In this paper, the noise is shown to be due to a noise-producing mechanism associated with the acquisition of charge by individual precipitation particles upon impact in the antenna field region. The existence of such a mechanism is demonstrated theoretically and substantiated by experiment. Production of such noise in antennas is analogous to production of shot noise in vacuum tubes. Calculated results indicate that in practical antennas this process is capable of generating noise voltages sufficient to disable lf and mf equipment such as the adf radio compass.

Communications—The Exact Solution of the Field Intensities from a Linear Radiating Source—R. N. Ghose (p. 237)

Experimental Measurement of the Absorption of Millimeter Radio Waves Over Extended Ranges—C. W. Tolbert and A. W. Straiton (p. 239)

Contributors (p. 242)

Audio

Vol. AU-5, No. 1, January–February, 1957

PGA News (p. 1)

High-Speed Duplication of Magnetic Tape Recordings—J. M. Leslie, Jr. (p. 5)

The high-speed duplication of previously recorded magnetic tapes has made the tape radio network practical. For example, each of the two major radio networks in Mexico duplicates over 19,000 seven-inch reels of taped programs per month for their several hundred affiliated stations. Since the tapes are erasable and wire program circuits are seldom used, these networks operate very economically, and the quality of their recorded programs is unimpaired by losses in transmission.

Likewise, the adoption of automatic programming systems for radio broadcasting will create a demand for syndicated magnetic tape programs and tape libraries.

High-speed magnetic tape duplicators are also utilized for the mass production of tape recordings for entertainment, education, churches, libraries for the blind, reviews of professional publications, and sales information for large field sales organizations.

The Ampex Model S-3200 tape duplicator with ten slaves will produce up to ten copies at one time of 15, $7\frac{1}{2}$, or $3\frac{3}{4}$ ips master recordings at 60 ips. The copies can be recorded to be reproduced either at the speed of the master or at half speed; *i.e.*, $3\frac{3}{4}$ ips copies from a $7\frac{1}{2}$ ips master. The duplicates may be either half-track, double-track, full-track, or two-track stereophonic.

Comparisons are made of the degradation of the signal-to-noise ratio, frequency response, and distortion with respect to the number of generations of the duplicates. With optimum adjustment of the equipment, it is very difficult to identify the fourth generation copy from the master recording.

Compensation Networks for Ceramic Phonograph Reproducers—B. B. Bauer (p. 8)

This paper examines the theory and practice of compensation networks for ceramic phonoreproducers. It shows that even though the RIAA Recording Characteristic is defined in terms of velocity, an amplitude-responsive reproducer may be used to match this characteristic in an ideal manner.

Evaluation of High-Powered Outdoor Sound Systems—R. W. Benson (p. 11)

Outdoor installations of high-powered sound systems have been made for the purpose of communicating over large areas from systems located on tall buildings and on airplanes. In order to evaluate the performance of these systems it is necessary to use actual speech materials rather than perform simple physical measurements. Airborne systems are affected greatly by the Doppler shift in frequency which cannot be accounted for in a physical evaluation of a system and reflections from buildings introduces echoes for which it is impossible to calculate the effect upon intelligibility. Speech materials have been used to determine both the intensity levels as a function of distance and angle, as well as the intelligibility of the system for various power levels. The results of these studies lead directly to the design of more efficient communication systems. The application of the results of two studies is shown for the design of optimum systems.

Contributors (p. 16)

Communications Systems

Vol. CS-5, No. 1, March, 1957

(*Papers Presented at the Second Annual Symposium on Aeronautical Communications, October 8–9, 1956, Utica, N. Y.*)

Aeronautical Communications—J. W. Worthington, Jr. (p. 3)

USAF Aeronautical Communications: A Link in the Servo Control Loop—Col. F. W. Donkin (p. 4)

This paper stresses the importance of understanding Air Force operational concepts as a basis for sound systems engineering of the communications-electronics support elements. It discusses some of these concepts with respect to operations of the Military Air Transport Service and the Strategic Air Command. It shows a need for an aeronautical communications servo control loop.

A Method for Studying Air Force Air-Ground Data Transmission Requirements—J. E. Barmack (p. 8)

This paper describes a research approach to the development of requirements for airborne communication systems. It is not proposed as an operational method to be used by the various commands. The procedure involves the pulling together in a rigorous and systematic way, the best judgments of people with considerable and diverse operational experience. Frailties of judgment are minimized by:

1) working with small units, *i.e.*, with judgments about the operating characteristics of messages to be transmitted between sender and receiver in a particular phase of a sortie of a specific type of weapon system used for a particular mission by each of the major commands.
2) defining terms and making these definitions always available.
3) developing a rationale for future operations in which assumptions about the future are specified and made known to all respondents.
4) identifying discrepancies and challenging judgments.
5) obtaining command concurrence on the basic data.

The product was nine reports, eight classified and one unclassified. Only the unclassified findings can be referred to here.

A New Look at Communications in the Field Army—H. P. Hutchinson (p. 11)

This paper outlines the characteristics applicable to voice, written message and visual modes of communications together with a philosophy of attack in the problem. The paper places major emphasis on the determination of systems requirements from the viewpoint of the user's needs rather than the technique used. An example is given of a proposed radio net organization in the infantry division.

The Four Systems Tests—Maj. Walter White, Jr. (p. 15)

This paper highlights the efforts of the Army Signal Corps and particularly those of the Army Electronic Proving Ground (AEPG), Fort Huachuca, Arizona, in the fields of air navigation and traffic control, battle area surveillance, electronic warfare, and grid or area communications. These systems will provide the working tool to improve command control as the technology of warfare changes because of scientific advances in atomic and other fields.

The Contributions of Aeronautical Communications to Public Safety Systems—W. C. Collins (p. 23)

The Atomichron: An Atomic Frequency Standard—R. T. Daly and J. H. Holloway (p. 25)

A One-Kilowatt High Level Modulated UHF Amplifier With Low Distortion—C. R. Ellis, K. H. Owen, and G. R. Weatherup (p. 28)

UHF Communication System Interference Reduction Through the Use of Selective Filters—M. W. Caquelin (p. 35)

Modern trends in uhf communication systems indicate an ever increasing use of greater numbers of channels, higher transmitter powers and decreased antenna spacing. This all adds up to an ever increasing number of systems interference problems. In most instances, a system can be rendered "interference free" by adding sufficient selectivity between the receiver or transmitter and its antenna. This added selectivity can be acquired by the use of a new low-loss tunable filter employing two high-Q, aperture coupled, resonant cavities in tandem. The physical construction of these equipments, as well as operating characteristics, will be discussed in this paper.

A 600 Kilowatt High Frequency Amplifier—J. O. Weldon (p. 40)

A description is given of the electrical circuits and mechanical construction of a power amplifier designed primarily for use in single sideband suppressed carrier operation having a peak envelope power output of 600,000 watts. The amplifier is also designed to handle an off-on keyed CW signal or frequency shift keyed signal at a continuous power output of 300,000 watts. Some of its features are continuous range motor tuning of all circuit elements over the frequency range from 4 to 30 megacycles, an unique method of opening the amplifier by motor elevation of the plate section and a sliding drawer grid section for tube removal and a fault amplifier, a type of protective system using a hydrogen thyratron to short-circuit the high voltage rectifier in case of internal arcing in the power amplifier tube.

The power amplifier uses a single tube. The gain in linear operation with resistance loading on the grid circuit is approximately 40.

This amplifier was originally developed under a Signal Corps development contract.

Conservation of Communications Bandwidth for Traffic Control—J. L. Ryerson (p. 53)

This paper analyzes the quantity of information present in a group of aircraft moving at known average velocities within a definite geographical sector. Computations of time required between determination of the position of each aircraft is computed on the basis of the residuals of an infinite time series representation of aircraft position. The positional information quantities and the time intervals required between samples are utilized to compute the time rate of flow of information, and this, in turn, used to compute the bandwidth of physical data transmission equipment required to get this information at a central point.

A dead reckoning device is added in each aircraft so that it may ascertain its position for longer sampling intervals. The velocity information utilized by the dead reckoning system is assumed to be transmitted to the ground where it is stored for tracking, which is a process of dead reckoning on the ground. The bandwidth of the system is then recomputed and it is shown that the use of relatively inexpensive dead reckoning equipment capable of measuring velocities to within 10 per cent of the actual value is capable of further reducing the system bandwidth by a factor of 10.

Curves are shown illustrating bandwidth requirements near 3 kc for 200 aircraft in a 256 mile radius without the use of inexpensive dead reckoning. By the use of dead reckoning either 200 aircraft may be handled at 300 cps or 2000 aircraft at 3 kc.

Results of UHF Mutual Environment Test Program at Rome Air Development Center—Joseph Berliner and John Augustine (p. 60)

This report is a summary of uhf mutual interference tests performed at the Rome Air Development Center, Rome, New York.

Initial tests were performed in the Laboratory and at the Verona Test Site of RADC by RADC engineers to obtain interference characteristics and operational parameters of the uhf communications equipment. The results of these tests, which are presented in Phase A, were submitted to Bell Telephone Laboratory engineers at Whippany, N. J. for use in their study program to obtain a uhf frequency allocation plan for SAGE.

The field test program which followed was established to check the compatibility of the BTL uhf frequency families which resulted from the aforementioned study. Specifically, a determination was made of the interfering effects which occur when combinations of single channel uhf transmitters and receivers are operated simultaneously in close frequency and physical association. This work was performed at the Verona Test Site of RADC by Collins Radio Company under Contract AF 30(602)-1402 under the direction and with the assistance of engineers from the Interference Analysis and Control Branch (RCSGA) of the Rome Air Development Center. Complete detailed information on test procedures and test results is contained in the contractor's final reports listed in the bibliography at the end of the report.

Air Force Communication Problem and the Future Air Force Operational Communication System—C. K. Chappuis (p. 82)

Air Force communications has expanded from the most elementary requirements in World War I to an enormous military worldwide industry. It exceeds the requirements and capabilities of commercial systems without standardization, engineering, installation and maintenance capabilities required for the job. A new system concept is proposed to reduce types of equipments, increase efficiency and reduce engineering, installation, operation, maintenance and supply problems.

An Integrated High Frequency Single Sideband System—M. I. Jacob (p. 87)

Some Factors Affecting Intelligibility in Single Sideband Communications—N. H. Young (p. 96)

Synchronous Communications—J. P. Costas (p. 99)

It can be shown that present usage of amplitude modulation does not permit the inherent capabilities of the modulation process to be realized. In order to achieve the ultimate performance of which AM is capable synchronous or coherent detection techniques must be used at the receiver and carrier suppression must be employed at the transmitter.

When a performance comparison is made between a synchronous AM system and a single-sideband system it is shown that many of the advantages normally attributed to single-sideband no longer exist. SSB has no power advantage over the synchronous AM (DSB) system and SSB is shown to be more susceptible to jamming. The performance of the two systems with regard to multipath or selective fading conditions is also discussed. The DSB system shows a decided advantage over SSB with regard to system complexity, especially at the transmitter. The bandwidth saving of SSB over DSB is considered and it is shown that factors other than signal bandwidth must be considered. The number of *usable* channels is not necessarily doubled by the use of SSB and in many practical situations *no increase* in the number of usable channels results from the use of SSB.

The transmitting and receiving equipment which has been developed under Air Force sponsorship is discussed. The receiving system design involves a local oscillator phase-control system which derives carrier phase information from the sidebands alone and does not require the use of a pilot carrier or synchronizing tone. The avoidance of superheterodyne techniques in this receiver is explained and the versatility of such a receiving system with regard to the reception of many different types of signals is pointed out.

System test results to date are presented and discussed.

The Possibility of Extending Air-Ground UHF Voice Communications to Distances Far Beyond the Radio Horizon—T. F. Rogers, L. A. Ames, and E. J. Martin (p. 106)

Certain of the results of a detailed research investigation of 220 mcps tropospheric "scatter" field strengths at long distances and high altitudes carried out here at the Air Force Cambridge Research Center are reviewed in some detail. On the basis of the airborne data obtained to date, supplemented by fading statistics obtained here and elsewhere, reasonable initial estimates can be made of the uhf radio wave path loss expected to obtain for various percentages of the time out to distances of several hundreds of miles and up to altitudes of several tens of thousands of feet. It is concluded, upon the basis of these path loss estimates, and initial airborne voice reception tests, that the scatter mode of propagation will permit the extension of reliable good quality air-ground uhf voice communication to distances far beyond the radio horizon.

Some Considerations Concerning Nuclear Radiations for Application to Aeronautical Navigational Aids—M. J. Cohen and H. C. Gibson, Jr. (p. 122)

A brief introduction to nuclear radiation physics and particularly gamma radiation is followed by a discussion of methods of measuring emitter to detector distance. Consideration is given to statistical accuracy of range measurements as well as to an example of a possible aircraft landing system.

Electron Devices

VOL. ED-4, NO. 1, JANUARY, 1957

The Tetrode Power Transistor—J. T. Maupin (p. 1)

Power transistor circuits are characterized by the fact that the collector current must swing over a wide range of values during any complete cycle of operation. One disadvantage of present-day alloyed junction power transistors is that the current gain decreases with increasing collector current. This causes distortion in linear applications and makes temperature stabilization in switching circuits more difficult. Power transistors having emitter areas large enough to handle currents in the

amperes range can be made as tetrodes by use of an annular ring geometry. Experimental results show that the gain characteristics can be altered by applying a bias voltage or a portion of the signal voltage transversely across the base. The gain characteristic can be made flatter for improved fidelity in audio applications, or even reversed to give increasing gain with collector current for certain switching applications.

Practical circuitry utilizing the improved gain characteristics of power tetrodes has been developed, and the annular geometry permits the fabrication of tetrodes using conventional alloying techniques.

The Effect of Collector Capacity on the Transient Response of Junction Transistors—J. W. Easley (p. 6)

The effect of collector depletion layer capacity on the transient response of junction transistors to a current input is calculated for the case of a resistive load. Expressions are given for the small-signal rise-time of the common-base, emitter, and collector configurations and for the large-signal turn-on and decay times of the common-emitter and collector configurations. The analysis shows that the transient durations under most conditions of operation are approximately $(1+\omega_\alpha R_L C_c)$ times those which would be predicted for the short-circuit output approximation reported by Moll. Experimental results are reported which exhibit an excellent agreement with the analysis over a wide range of $\omega_\alpha R_L C_c$.

An empirical examination has been made of the dependence of large-signal switching time on the range of operation point excursion. A satisfactory approximate representation of this dependence is provided by a first-order correction factor, which takes into account the functional dependence of ω_α and C_c on collector voltage.

A Theory of Voltage Breakdown of Cylindrical *P-N* Junctions, with Applications—H. L. Armstrong (p. 15)

In certain *p-n* junctions, such as those made by the alloy method, edges on the junction surface will, by field concentration, lead to lower inverse breakdown voltages than would otherwise be obtained. These edges are approximated by pieces of circular cylinders, and a formula for the voltage breakdown of a circular cylindrical junction obtained. The results agree qualitatively with those found for certain alloy-type diodes.

Base-Width Modulation and the High-Frequency Equivalent Circuit of Junction Transistors—Jakob Zawels (p. 17)

The effect of base-width modulation on the exact small-signal, high-frequency equivalent circuit of *p-n-p* (and *n-p-n*) junction transistors is examined. It is found that (except for the effect on the base spreading resistance) base-width modulation only helps to determine the magnitude of one element. Failure to recognize this fact has resulted in the past in the "discovery" of "new" elements and the creation of a multiplicity of equivalent circuits. Through the use of an engineering approach, the most important of these circuits are related to the exact circuit, and hence their degree of approximation becomes apparent. The effect of a high injection level of minority carriers is also mentioned.

Finally, the equivalent circuit of *p-n-i-p* (and *n-p-i-n*) transistors is discussed.

Thermionic Current in a Parallel-Plane Diode—L. J. Giacoletto (p. 22)

An approximate formula is developed for the current of a parallel-plane diode including the effects of initial velocities of emission. For an oxide-coated cathode ($T=1000°K$) the approximate result is:

$$J \quad 2.33 \quad 10^{-6}\frac{V^{3/2}}{x^2} \cdot \left[1 \quad \frac{11.4(J_s x^2)^{1/4}}{V^{3/4}} \quad \frac{3.22(J_s x^2)^{1/8}}{V^{3/2}}\right]$$

where, J, J_s, and x are in suitable units such that jx^2 and $j_s x^2$ are in amperes and V in volts. A comparison is made between this result, Child's 3/2 power solution, and the Epstein-Fry-Langmuir solution. The result given above being an explicit solution of the current is particularly advantageous over prior approximate solutions.

The Gain and Bandwidth Characteristics of Backward-Wave Amplifiers—M. R. Currie and D. C. Forster (p. 24)

The problem of designing backward-wave amplifiers to yield specified pass band characteristics is discussed. Detailed universal curves of gain and bandwidth for both single-circuit and cascade amplifiers are presented. Simple charts are developed which facilitate the design procedure. Experimental results are correlated with the theory and indicate its usefulness. The skirt-selectivity of cascade amplifiers is discussed. A specific design example is given to demonstrate the design method and to indicate the range of bandwidths obtainable from helix-type amplifiers.

Small-Signal Wave Effects in the Double-Base Diode—J. J. Suran (p. 34)

Frequency and transient response equations for the current-transfer ratios of the double-base diode are calculated from theory and checked experimentally. To obtain these results, the device is operated as a small signal amplifier in the negative-resistance region and the frequency response characteristics thus obtained are used to predict the device behavior. The effects of carrier recombination and electric field upon the response characteristics are evaluated and experimental results are presented.

Stability of Cylindrical Electron Beam in Nonsinusoidal Periodic Magnetic-Focusing Fields—D. C. Buck (p. 44)

The Theory of Mendel, Quate, and Yocum is extended to include experimental and analytical examination of magnetic fields whose axial variation is periodic, but not sinusoidal. Magnetic fields of this type are encountered in many typical periodic focusing structures. Minimum-ripple flow is achieved by setting the rms value of the magnetic field equal to the Brillouin value of the field.

The fraction of a beam current traversing a long hollow drift tube has been measured as a function of the amount of departure of the magnetic field variation from a sinusoidal one.

Space-Charge Effects in Klystrons—W. E. Waters, Jr. (p. 49)

The effects due to the dc field of the space charge in a reflex klystron have been calculated on a digital computer. It is found that the electronic efficiency may be reduced by a factor as large as 10 under space charge conditions which may exist in a typical low-voltage tube. Small signal theories which include the effects of the dc space charge are presented for the reflex klystron and two-gap klystron amplifiers and oscillators. The small signal theory is used primarily to aid in the interpretation of the computer calculations. The theory predicts that the efficiency of the two-gap oscillator may be reduced by a factor no greater than 3.7, but that the power gain of the two-cavity amplifier may be increased by as much as 13.7. It is also found that the inclusion of space charge effects will in general require different applied dc voltages for operation at the center of the various electronic modes, as compared with the infinitesimal-space-charge conditions.

Upon comparing the theoretical calculations with actual reflex klystron data, it has been found that the theory adequately explains the behavior of the power output, efficiency, and electronic bandwidth as the beam current is varied, for conditions of moderate or small space charge. For conditions of large space charge the theoretical model does not represent the conditions in an actual tube with sufficient accuracy; it is pointed out how the theory may be improved and how the present work may be useful as a starting point for further calculations.

High-Speed Gating Circuit Using the E80T Beam Deflection Tube—L. Sperling and R. W. Tackett (p. 59)

This paper describes a high-speed gate circuit for an information sampling system employing the E80T beam deflection tube. The time required to open this gate fully is less than 7 millimicroseconds.

This gate is superior to conventional multigrid gates in that the circuits are less complex, more reliable and have only minimal signal feed-through. Furthermore, a preliminary stage of pulse stretching is available without additional circuit elements.

Low-Voltage Color Tube Gun Assembly with Periodic Focusing—P. H. Gleichauf and H. Hsu (p. 63)

One type of color tube, often referred to as the post acceleration color tube, requires a gun of unique design. The gun operates at relatively low voltages of 5000 to 7000 volts as compared with 20,000 to 30,000 volts in other types of color tubes. The tricolor gun assembly described consists of three individual guns arranged in a plane. This limits the inside diameter of the electrodes to 0.358 inch as compared with half an inch or more in conventional guns. The individual guns are either triodes or tetrodes with periodic focusing. In spite of the above mentioned restrictions the spot size is about 0.038 inch at 300 microamperes screen current per gun and 7000 volts anode voltage. The depth of focus is very satisfactory because of small beam diameter.

Traveling-Wave Tube Gain Fluctuations with Frequency—S. A. Cohen (p. 70)

Periodic traveling-wave tube gain fluctuations with frequency are described in terms of fundamental tube parameters and readily measurable quantities using the simplified one-wave theory of Pierce. An analysis of the feedback existing in a traveling-wave amplifier due to mismatches in the discontinuity regions is presented. Thus, the form, periodicity, and magnitude of these fluctuations and their dependence upon the beam voltage are quantitatively determined. The microwave structure is analyzed from a network point of view and the circuit parameters are defined with mismatches in the lumped center attenuator and at the ends of the slow-wave transmission line. The gain fluctuations are related to the cold circuit parameters and standing wave measurements. Pertinent experimental data, indicating the correlation of gain fluctuations to vswr variations, are included, in addition to an elementary discussion of the distortion effects possible due to such periodic gain variations in a traveling-wave tube.

Development of a Medium Power L-Band Traveling-Wave Amplifier—L. W. Holmboe and M. Ettenberg (p. 78)

The development and performance of a high gain medium power traveling-wave amplifier are described. Powers up to 7 watts at 15 per cent efficiency have been achieved. The small signal gain approaches 50 db in the middle of the band, and exceeds 35 db over a 2 to 1 range of frequencies.

The tube itself consists of a glass-supported helix with a metal shell at one end housing the cathode structure, and a copper collector at the other end. The input and ouput couplings are made by means of coupled helices which are mounted in a brass tube or matching structure which is external to the vacuum envelope. The matching structure is supported in the focusing solenoid.

Potential-Minimum Noise in the Microwave Diode—A. E. Siegman and D. A. Watkins (p. 82)

An analysis of the potential-minimum region in the microwave diode is presented which predicts the amount of noise convection current at the potential minimum under conditions present in guns of low-noise traveling-wave tubes and klystrons. Contrary to previous work by one of the authors, this analysis partially includes the effects of finite transit angle between the cathode and potential minimum. The results indicate that under certain conditions of space-charge limitation, the noise convection current may be larger than full shot noise, whereas under other conditions reduction by as much as a factor of four may be obtained. When the results of this work are applied to the noise-figure theory of traveling-wave tubes and klystrons, it is found that their minimum obtainable noise figure may be in the vicinity of 4 db rather than the previously predicted 6 db with reasonable cathode current densities. For very large current densities or low operating frequencies, the present theory indicates that there is no theoretical limit to the minimum noise figure of such devices, in agreement with the previous work.

Electron Bunching and Energy Exchange in a Traveling-Wave Tube—S. E. Webber (p. 87)

A physical picture of electron-wave interaction, electron bunching, and energy exchange in the traveling-wave tube is obtained by a study of the problem of electrons moving in a traveling electromagnetic wave of constant amplitude. This very simple analysis results in an easily understood qualitative description of the details of the interaction mechanism at large signal within an operating traveling-wave tube.

Linear Beam Tube Theory—C. C. Wang (p. 92)

This paper presents the basic theories underlying the principles of operation of linear beam tubes. These theories are more general than the previous ones because they can be applied equally well to all types of tubes using linear electron beams. The tube types will differ only in the rf circuits that are being used. Emphasis of the theories is placed on the fundamental equations involved rather than the analytic solutions of these equations. The concept of electromagnetic and hydrodynamic power flow is emphasized in the treatments. The purpose is to leave the details of the solution to the electronic computer that is now being adapted to this type of problem. To this end, the equations are only developed in such a way as to facilitate programming in the computer.

To illustrate the use of the theory, the special cases of the traveling-wave tube in which a waveguide mode is continuously interacting with the beam, and the klystron tube in which the interaction takes place in a limited space, will be developed in more detail. To further avoid mathematical complexities, electron motion, limited to the longitudinal direction, will be emphasized, and only the small-signal case will be treated. However, sufficient fundamental ideas will be presented so that the extension to the cases involving transverse electron motions and the large signal operation can be easily accomplished.

Instrumentation

Vol. I-6, No. 1, March, 1957

Abstracts of Papers in This Issue (*WESCON Papers*)

Adjustable Pulse Width High-Voltage Pulsed Power Supply—Victor Wouk (p. 3)

A new type of high-voltage pulser, employing series and shunt switching tubes is described. The circuit overcomes limitations of previous types of high-voltage pulsers regarding adjustable pulse shapes and, particularly, widths.

A specific application to a 10-kv pulser is described, with pulse repetition rates from 10 cps to 10 kc, rise and decay times of 2 microseconds, and adjustable duty cycles from 0.001 to 0.99.

Transistorized Logarithmic Time and Amplitude Quantizer—E. Gott and J. H. Park, Jr. (p. 7)

It is often desirable when converting an analog time or amplitude to digital form to have a uniform relative error. In this paper relative error is taken to mean the maximum possible error in a measurement divided by the value of the measurement. The arithmetic mean of the endpoints of the measured interval is used as the value of the measurement. Uniform relative error is accomplished with geometric spacing of the intervals.

A transistor circuit has been built which receives analog information and yields a train of pulses geometrically spaced with the number of pulses proportional to the logarithm of the magnitude of the input. The geometric series pulses are produced by comparing a fast rising linear sweep with a slower reference sweep and producing an output pulse and discharging the fast sweep when the sweeps coincide. Circuits employing point contact and junction transistors are used and experimental results agree closely to the theory. An application of such a quantizer is the analysis of pulse modulation.

A Practical Application of Phase Measuring Techniques to Precision Angle and Distance Measurements—W. J. Thompson (p. 12)

A method is discussed for the application of phase measuring techniques to the accurate determination of the spatial coordinates of a remote, active target. Separate systems are developed for the determination of slant range and direction cosines of the target with respect to the systems' coordinate center. Techniques are described for applying the basic principles to practical electronic equipments. The results of tests of the equipment in the field are used to compare predicted accuracies with those practically obtained.

An integrated system is presented along with methods of combining the equipments for situations of multiple dimensions and for situations of multiple targets.

A Multipressure Measuring System—M. B. Bain (p. 18)

An economical multipressure measuring system to replace mercury multimanometers has been developed for use in supersonic wind tunnels. The main components include an accurate strain-gage type of pressure transducer, multitap pressure selector valves, and a high-speed encoder with paper-tape recording. The system will record pressures in reduced or coefficient form, obviating the need for subsequent computations, and thus speeding up the data reduction. In addition it will increase the wind-tunnel operating pace by requiring less time for the pressure lines from the model to the manometer to be stabilized. Accuracy is comparable to that attained by the present manometer system.

An Improved Design for Audio-Type Exponential Attenuators—Jack Bacon (p. 23)

This paper is concerned with minimizing the positional error occurring in continuously variable exponential audio attenuators as a result of a linear approximation existing between taps. It is shown that there is an optimum value of load resistance for which the error is minimized. Curves for the design of such attenuators are given.

Electronic Instrumentation of a Device to Automatically Count and Size Particles in a Gas—E. S. Gordon, D. C. Maxwell, Jr., and N. E. Alexander (p. 27)

This paper describes the electronic instrumentation of a device called an aerosoloscope for automatic counting and sizing of aerosol particles.

Particles from 1 to 64 microns in diameter and counting rates up to 100 particles per second are handled by the instrument. The aerosol is diluted and drawn across a high-intensity light beam; a multiplier phototube receives a portion of the light energy scattered by each particle. The resulting electrical pulses are amplified and classified by size into 12 groups by a unique pulse height discriminator. Glow-transfer tubes and registers are used to count the pulses within the various groups. Dynamic range problems and system noise are briefly discussed.

An Experimental Method for Obtaining the Transfer Function of a Rate Gyro—M. Bendet and F. P. Hercules (p. 35)

A gyroscopic element is defined, and the fundamental principle of the gyroscopic phenomenon is considered from an elementary point of view. The Law of the Gyroscope is established.

The three fundamental properties of the gyroscope are developed from the statement of the law, and it is shown that a gyroscope can be employed as a means for obtaining a reference line in inertial space (the free gyro), as a means for measuring angular velocities with respect to inertial space (the rate gyro), and as an inegrator with respect to time in inertial space (the integrating gyro).

Gyroscopic instruments are briefly considered, and a method for experimental study of a rate gyro is presented.

An Improved Subcarrier Discriminator—E. D. Heberling (p. 43)

A refinement of the pulse-averaging type discriminator is described. The new discriminator was designed to provide improved stability.

Complete Linear Characterization of Transistors from Low Through Very High Frequencies—H. G. Follingstad (p. 49)

A theory of insertion measurement is presented which permits accurate and complete linear characterization of transistors from low through very high frequencies. Using available measuring facilities the method has been verified experimentally up to 100 mc.

A Novel Apparatus for the Measurement of Phase Angle—A. E. Mostafa and M. H. Shaltout (p. 63)

The present work deals with a new type of phase-measuring apparatus which is suitable for both radio and audio frequency. The main principle of the apparatus is that a system composed of two oscillators in a synchronized state with a given signal v_1 and connected in tandem can act as a good radio frequency limiter as well as a constant output radio frequency phase shifter. The signal v_1 used for synchronization is one of two signals, v_1 and v_2, between which the phase angle is required. The output of the second synchronized oscillator, being independent of the amplitude of v_1, is adjusted to be in phase with it. If the second voltage v_2 together with the output voltage of the second oscillator is applied to a detector circuit, the required phase angle can be directly measured by the amount of capacity detune required to bring v_2 and the output of the oscillator in phase. The inphase condition can be indicated by the detector circuit. An apparatus based on this principle has been constructed. A theoretical analysis is given and an experimental investigation is carried out; the results obtained agree well with the theoretical predictions.

Nuclear Science

Vol. NS-4, No. 1, March, 1957

Ionization Chamber Survey Instrument—W. A. Higinbotham and B. Pollock (p. 1)

A wide range survey instrument is described.

Ranges are 20 mr/hour to 20 r/hour full scale. The thin plastic ionization chamber is easily replaced if contaminated. A three-tube, negative feedback circuit with low battery drain is used. The input resistor selector switch is a new design with high insulation. It is nonmicrophonic and does not cause transients when changing ranges.

Regulation of the Individual Dynode Voltages for Photomultiplier Tubes—O. R. Harris and B. d'E. Flagge (p. 3)

An individual dynode voltage regulating system has been devised which can be mounted on the phototube socket in much the same manner as, and with no more difficulty than, the common bleeder resistance voltage divider.

Two types of these regulators have been investigated; the first using silicon diodes, and the second using NE-2 neon tubes.

The statistical spread of beta-ray counts was reduced from (±) six standard deviations to nearly the normal spread of (±) three standard deviations. The photometric sensitivity range of linearity was increased by an order of magnitude.

Nuclear Reactor Start-Up Simulation—J. P. Franz and N. F. Simcic (p. 11)

This paper describes the problem of simulating nuclear reactor start-up with an electronic analog computer. The reactor kinetic equations are discussed and the range that their solution must cover is defined. Source range simulation and alternate methods of simulating the intermediate range are presented. The use of reactor period signal in the intermediate range is described. In the power range, which includes a representation of the heating and temperature effects, the inherent advantages of a pressurized water reactor are outlined. The portion of the start-up simulation which applies to nuclear reactors in general is summarized. The areas of modification necessary for the simulation of other than pressurized water reactors is outlined.

Frequency Response Measurements of Power Reactor Characteristics—H. Estrada, Jr. (p. 15)

The problem of measuring fundamental characteristics of an inherently stable power-producing reactor is described. It is noted that, in the power range of operation of such a plant, reactivity is a function not only of control rod position, but also of power itself. The mechanism of the latter effect involves the various inherent coefficients of reactivity. The result is that conventional, low-power methods can be used neither to obtain rod calibrations, nor to determine temperature coefficient in the very range of operation where these characteristics assume importance.

It is shown that a number of parameters including those mentioned above may be measured by effecting small sinusoidal perturbations in control rod position over a range of frequencies. The resultant frequency responses are analyzed by the familiar transfer function-block diagram method.

Certain inherent advantages of the method are cited including:

1) Ability to separate effects which predominate in different frequency regions.
2) Improved reproducibility of power range measurements. Disturbances induced by steam plant changes, inherently nonreproducible, are avoided.
3) Good accuracy of data. The measurement replies primarily on good differential accuracy, easier to obtain from operational instrumentation than good absolute accuracy.
4) Ability to check data reproducibility by obtaining several cycles of data at each frequency.

A brief description is included of the manner by which the technique is used to determine the following nuclear properties:

1) perturbing rod calibration,
2) temperature coefficient of reactivity,
3) neutron generation lifetime,
4) fractional production of delayed neutrons, and
5) mean delayed neutron decay constant.

It is also noted that certain thermal and hydraulic characteristics of the plant can be determined using the method:

1) Effective over-all heat transfer coefficient of the core.
2) Over-all heat transfer coefficient of the primary plant to secondary plant heat exchanger.
3) Primary coolant flow loop transport time.

Further, it is pointed out that the reactor plant frequency responses constitute a quantitative check on the accuracy of the differential equations used in the construction of plant simulators (analog computers), devices which are used extensively in the transient analysis of power reactors.

A Self-Checking Radiation Monitor—K. C. Speh and W. E. Landauer (p. 19)

A self-checking system of circuits is expected to provide a new high in operational reliability for the set of radiation monitors described. Developed under sponsorship of the Bureau of Ships, these monitors can readily be adapted for application in any nuclear installation where radiation monitoring must be performed. Three basic channels are provided to measure accurately the gamma radiation in the range from 1 to 1000 mr/hr, the thermal neutron flux from 20 to 20,000 thermal neutrons/cm^2 sec, and the air-particle concentration from 10^{-9} to 10^{-6} μC/cm^3 or from 10^{-8} to 10^{-5} μC/cm^3.

Checking of each channel is performed by periodically (and automatically) placing a small radioactive source next to the detecting element in each channel. This results in a signal near the maximum range of each channel. During such checks, the alarm-indicating circuit is disconnected and the channel output applied to a comparator circuit; there will result a "circuit fault" indication if any part of the signal-handling or the checking circuits has failed. The philosophy and the limitations of the checking scheme are discussed.

The calibration of the air-particle channel is in terms of a specific isotope. Calibrations for other isotopes can be prepared. Shielding is applied to the detecting element in the air-particle channel in order to minimize counts due to the ambient gamma background. The gamma detector has shielding to equalize its response to radiation at energies between 80 kev and 2 mev.

The Relative Stability of Boiling and Pressurized Light Water Moderated Reactors—John Macphee (p. 25)

This paper compares the stability of a given heterogeneous core when operated with a pressurized or subcooled water cooling system in which the power is removed by boiling. In order to provide a basis for comparison the following assumptions are made: 1) reactor power is the same in both cases, 2) the core geometry is the same in both cases, 3) in the case of subcooled operation, coolant flow rate and core inlet temperature are held constant, and 4) in the case of boiling operation reactor pressure is constant. Assumptions 3) and 4) imply that the load equals power generated at all times. The core geometry and the values of the various system parameters are taken from published literature wherever possible. It is shown that the results of this analysis are readily predictable from physical reasoning.

Designing Heterogeneous Reactors for Stability—D. Little and M. A. Schultz (p. 30)

A study of the nonlinear kinetics of heterogeneous reactors can lead to basic design criteria which are useful in designing stability into a given reactor. The design of most reactors is usually based upon other physical parameters such as reactivities, heat transfer surfaces, metallurgical conditions, and operating lifetimes. The question of reactor stability is often deferred on the design schedule until these other parameters have so closely bounded the design that only incidental changes are possible. It is fortunate that many reactors are naturally stable over wide ranges of design conditions.

Nonlinear kinetics have been examined in two ways in the past. The first method is to modify the basic reactor kinetic equations to include the effects of temperature, pressure, or poisoning. Solutions of these equations generally can be obtained with some approximation being needed. The second method consists of obtaining the transfer function of a simple reactor and modifying the characteristics of this reactor by feedback networks. The first method has been used successfully by Weinberg and Ergen for homogeneous reactors and by Lipkin and others for heterogeneous reactors. The second method is an engineering one which is capable of giving considerable information over a wide range of variables and will be used in this paper with suitable approximation to examine the stability of heterogeneous reactors.

Electronics at the French Atomic Energy Commission—M. M. Surdin (p. 34)

This paper gives a description of the organization and functioning of the Electronic Division of the Atomic Energy Commission of France. The Division is organized into four sections, Physical Electronics, General Electronics, Industrial Electronics, and Radioactive Isotopes Measurement. The sections are subdivided into groups. There are approximately 200 persons in the Division. Descriptions are given in this paper of typical development projects and method of operation. Some examples of interesting instruments are given together with a brief description of their operation.

Design and Use of the Reactivity Computer—G. S. Stubbs (p. 40)

The basic, underlying variable of reactor control is the reactivity. We may regard the reactivity as a measure of the deviation from equilibrium of the neutron balance in a reactor. Or more precisely, we may define the reactivity as the average excess number of neutrons produced per fission that cause further fission, "excess" being the number over and above the one-neutron-per-fission that is required to maintain a self-sustaining fission reaction.

Reactor control may be described as the process of changing the neutron environment within a reactor so as to produce momentary excursions in the reactivity from its equilibrium value of zero. The measurement of these excursions in reactivity is the subject of this paper.

Two electrical analog computer designs are described which compute the reactivity from electrical signals which are provided by conventional reactor instrumentation systems. One computer utilizes a neutron flux input signal; the other employs a log-rate (of neutron flux) input signal. Applications of these computers in control system analysis and reactor instrumentation are discussed.

Radioactive Tracer Study of Sewage Field in Santa Monica Bay—R. L. Ely, Jr. (p. 49)

In an unique experiment just completed in Santa Monica Bay, Calif., radioactive isotopes were successfully used to trace dispersion of sewage effluent in ocean waters. The results help to establish proper design procedures to insure against beach pollution in a current expansion of the Los Angeles sewage system.

To effect the experiment twenty curies of scandium-46 were mixed with sewage effluent and discharged into the sea. Scientists aboard a laboratory ship then took radioactive measurements over a wide area to determine dilution rate and direction of diffusion.

Report of the Secretary—1956

To the Board of Directors
The Institute of Radio Engineers, Inc.

Gentlemen:

The Annual Report for 1956, the 45th anniversary of the founding of the IRE, is herewith submitted.

Growth in all departments continues. The total membership went up 17.1% and it should be noted that a 15.6% increase in foreign members indicates expanding activity internationally. A significant statistic concerns the Student grade which had its largest net growth in seven years, the number going up 41.6%. The total membership of all grades at the close of the year was 55,494. (See Fig. 1 and Table I.)

The popularity of the Professional Group system has now brought the total paid membership of the Groups to 53,015. Another index of Group activities expansion is the large increase in the number of Transactions pages, which went up 44% during the year.

IRE affairs can be seen as continuing in a sound and satisfactory condition.

Respectfully submitted,

Haraden Pratt

Haraden Pratt
Secretary

February 6, 1957

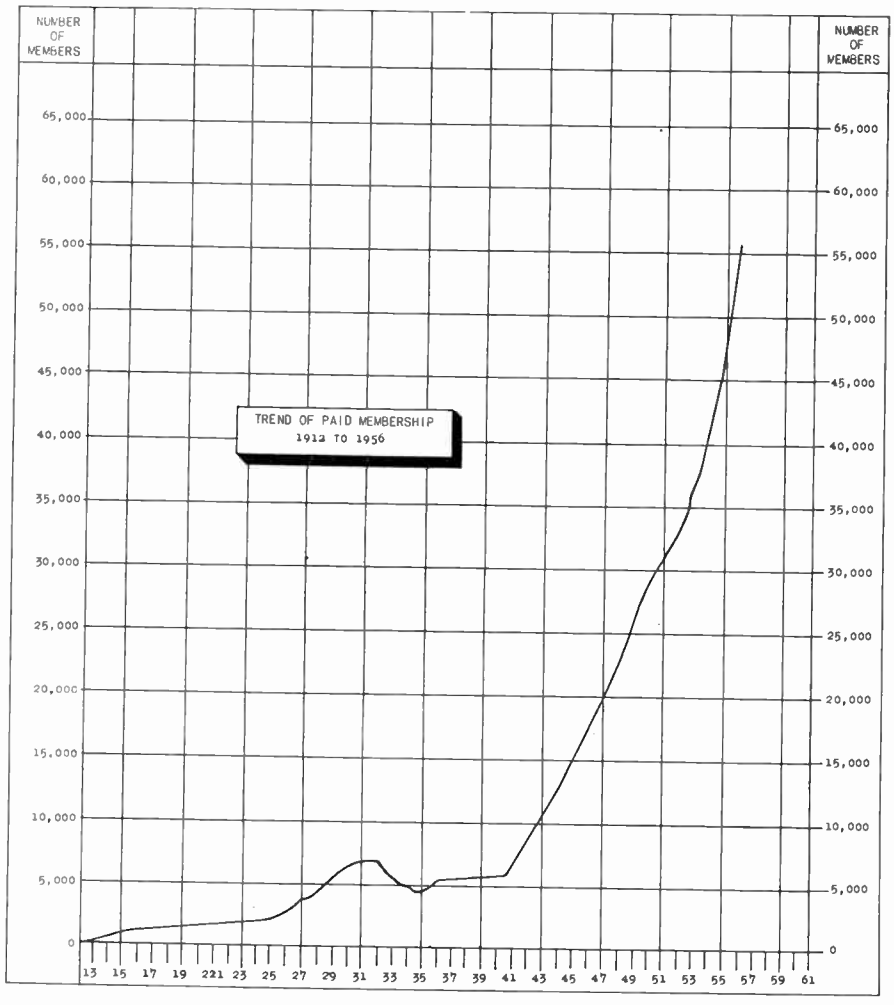

Fig. 1.

TABLE I

Total Membership Distribution by Grades, 1954–1956

Grade	As of Dec. 31, 1956		As of Dec. 31, 1955		As of Dec. 31, 1954	
	Number	% of Total	Number	% of Total	Number	% of Total
Fellow	635	1.1	565	1.2	489	1.2
Senior Member	6,486	11.6	5,643	11.9	4,780	11.4
Member	19,110	34.6	13,360	28.2	6,107	14.6
Associate	18,879‡	34.0	20,492†	43.2	24,846*	59.5
Student	10,384	18.7	7,328	15.5	5,556	13.3
Totals	55,494		47,388		41,778	

* Includes 803 Voting Associates. † Includes 396 Voting Associates. ‡ Includes 388 Voting Associates.

It is with deep regret that this office records the death of following members of the IRE during the year 1956.

Fellows

Beltz, Willis Henry (SM'53, F'56)
d'Humy, Fernand E. (A'41, SM'45, F'49)
Ehret, Cornelius D. (F'16, L'51)
McDonald, Arthur Stephen (M'23, F'41)
Pickard, Greenleaf W. (M'12, F'15)(L'47)
Pierce, George W. (M'13, F'15) (L'48)
Reoch, Alexander Ernest (M'14, F'16) (L'49)

Senior Members

Bagnall, Vernon B. (A'30, M'40, SM'43)
Bruns, Elmer E. (A'28, SM'45)
Carlton, Milton B. (SM'54)
Davis, William C. (SM'49)
Dixon, George P. (SM'46)
Duncan, R. D., Jr. (A'13, M'25, SM'43) (L'55)
Filgate, John T. (A'29, M'36, SM'43)
Franks, Christopher J., III (M'35, SM'43)
Giroud, Pierre (SM'55)
Hanscom, William Wallace (A'12, M'14, SM'43) (L'47)
Hershman, Joseph B. (A'28, SM'45)
Hollenberg, Arthur V. (M'50, SM'50)
Lett, Robert Pritchard (A'44, M'45, SM'51)
Malsch, Johannes R. (M'54, SM'54)
McMillan, Fred O. (M'41, SM'43)
Meyer, Raymond B. (SM'48)
Nelson, James Richard (A'27, M'29, SM'43)
Okolicsanyi, Ferenc (SM'54)
Reiskind, H. I. (SM'52)
Robertson, Norman C. (A'30, M'39, SM'43)
Salton, Lynn V. (M'23, SM'46)
Wankel, Ferdinand A. (SM'48)

Members

Adams, Atlas O. (M'52)
Allen, Wilfrid G. D. (M'54)
Bailey, Bruce (A'46, M'55)
Bales, Nicolas M. (M'50)
Carlisle, Charles H. (M'46)
Carty, Maurice F. (S'54, M'55)
Fenton, Norman L. (S'48, A'50, M'54)
Foster, Arnot P. (A'41, M'45)
Fuller, John S. (M'55)
Hannigan, Walter T. (M'53)
Hayes, George W. (A'13, M'55) (L'49)
Hazlehurst, Edward (A'38, VA'39, M'55)
Helt, Scott (A'47, M'48)
Hills, Elmer G. (A'41, M'55)
Hintz, Robert T. (A'30, VA'39, M'55)
Hollander, Albert G. II (S'46, A'50, M'44)
Hurwitz, Arthur M. (S'51, A'52, M'54)
Jacobsen, Per Kjeldberg (M'55)
Korb, Anton W. (M'47)
Lasby, Ray O. (S'49, A'50, M'55)
Laube, Otto T. (A'39, M'55)
Laurie, Bill A. (M'46)

TABLE II

SUMMARY OF INCOME AND EXPENSE, 1956

Income		
Advertising	$1,143,942.50	
Member Dues and Convention	1,061,128.02	
Subscriptions	125,112.72	
Sales Items: Binders, Emblems, etc.	92,397.82	
Investment Income	26,942.55	
Miscellaneous Income	1,714.06	
TOTAL INCOME		$2,451,237.67
Expense		
Proceedings Editorial Pages	377,197.56	
Advertising Pages	636,698.64	
Directory	194,979.63	
Section and Student Branch Rebates	109,507.15	
Professional Group Expense	142,759.85	
Sales Items	66,073.44	
General Operations	449,986.29	
Convention Cost	330,479.09	
TOTAL EXPENSE		2,307,681.65
Reserve for Future Operations—Gross		$ 143,556.02
Depreciation		19,787.40
Reserve for Future Operations—Net		$ 123,768.62

TABLE III

BALANCE SHEET—DECEMBER 31, 1956

Assets		
Cash and Accounts Receivable	$ 459,113.46	
Inventory	26,387.65	
TOTAL CURRENT ASSETS		$ 485,501.11
Investments at Cost	1,182,109.69	
Buildings and Land at Cost	912,316.70	
Furniture and Fixtures at Cost	205,388.46	
Other Assets	50,507.21	
TOTAL		2,350,322.06
TOTAL ASSETS		$2,835,823.17
Liabilities and Surplus		
Accounts Payable		$ 101,515.74
Deferred Liabilities	$ 718,861.25	
Professional Group Funds on Deposit	135,222.62	854,083.87
TOTAL LIABILITIES		955,599.61
Reserve for Depreciation		81,110.35
Surplus Donated	595,286.61	
Surplus	1,203,826.60	
TOTAL SURPLUS		1,799,113.21
TOTAL LIABILITIES AND SURPLUS		$2,835,823.17

Liebmann, Gerhard (A'40, M'56)
Michon, Alfred Edgar (A'37, M'45)
Nowick, Chester A. (M'53)
Plusc, Igor (M'45)
Rand, Donald M. (S'54, M'56)
Reed, DeWitt M. (M'46)
Robinson, Bruce Ross (M'53)
Shanklin, John P. (M'47)
Shields, Russell A., Jr. (S'46, A'49, M'55)
Silent, Harold C. (A'19, M'55)
Sorg, Harold E. (M'48)
Sutton, Robert A. (M'48)
Tedder, Paul M. (A'46, M'55)
Trimmer, Fred H. (M'54)
Tringham, William S. L. (A'38, M'55)
Weeman, Roy La Vergne (M'56)
Weiss, Walter A. (A'41, M'55)

Voting Associates

Bainbridge-Bell, L. H. (A'26, VA'39)
Gatkin, Thomas E. (J'37, A'39, VA'39)
Thornley, Howard W. (A'38, VA'39)

Associates

Abramson, Arthur S. (S'53, A'54)
Alig, Robert J. (A'52)
Almy, John Wehn (A'54)
Boulay, Henry E. (S'49, A'51)
Cole, John C., Jr. (S'52, A'53)
Elliott, Ralph W. (A'54)
Faiella, Albert L. (A'55)
Fryburg, Charles H. (A'50)
Fryer, Leonard (A'38)
Gentry, William E. (A'50)
Ghirlando, Felix L. (A'38)
Gorden, Henry Colin (A'53)
Gottesman, Noel Henry (A'53)
Hinton, Robert Donald (A'55)
Hobgood, Marion P. (S'49, A'51)
Hommel, Ralph E. (A'54)
Kropf, Robert G. (A'51)
McHugh, Joseph Edwin, III (S'51, A'52)
Norcross, James B. (S'44, A'49)
Noyes, Robert A. (A'53)
Riggins, H. C. (A'52)
Short, Kenneth R. (S'53, A'54)
Sulpizio, Thomas John (A'51)
Titherington, Richard H., Jr. (A'55)
Van Landingham, Francis H. (S'52, A'54)
Walker, Paul M. (A'50)
Zilles, Frank J. (A'50)

Students

Collins, Frank J. (S'54)
Strumer, Jay K. (S'55)
Tufts, Frank C. (S'55)

Fiscal

A condensed summary of income and expenses for 1956 is shown in Table II, and a balance sheet in Table III.

Editorial Department

IRE publication activities continued their healthy growth during 1956, due largely to the substantially increased output of the TRANSACTIONS of the Professional Groups. The total IRE publication output for the year reached a new high of 97 issues totaling 12,908 pages, a 16% increase over the previous year.

PROCEEDINGS OF THE IRE

Two new monthly features were added to the PROCEEDINGS in 1956: an editorial page, called "Poles and Zeros," where matters of general interest to the membership are discussed by the Editor; and "Scanning the Issue," in which the papers in the issue are briefly reviewed by the Managing Editor. In addition, the program of publishing invited review and tutorial papers on important topics reached full stride during the year, with eight such papers appearing in the ten regular issues.

The year was highlighted by the appearance of two special jumbo issues: the October Ferrites issue and the December Single Sideband issue. The latter was published with the collaboration of the Joint Technical Advisory Committee in connection with studies they are making for the Federal Communications Commission.

The number of PROCEEDINGS pages published during 1956 is shown in Table IV and Fig. 2. The number of papers, 164, was about the same as the previous year's total of 170. A record high of ten IRE Standards also appeared.

The backlog and publication time of papers, which were greatly reduced two years ago, remained at a satisfactorily low point. The backlog of extra material awaiting publication amounted to about one-half to one issue, and the speed with which papers were published averaged five to six months.

TABLE IV

VOLUME OF PROCEEDINGS PAGES

	1956	1955	1954	1953
Editorial	1996	2060	1884	1860
Advertising	2800	2372	2072	2146
TOTAL	4796	4432	3956	4006

The volume of material reviewed for PROCEEDINGS was approximately the same as in the previous year. A total of 273 papers comprising 2106 pages was considered. The percentage of papers accepted dropped from 40% in 1955 to 32% in 1956, while the percentage referred to the TRANSACTIONS for publication consideration rose from 29% to 40%. The proportion rejected dropped slightly from 31% to 27%. These figures reflect the continuing shift of the more specialized papers from the PROCEEDINGS into the TRANSACTIONS.

TRANSACTIONS

The year 1956 saw the TRANSACTIONS output of the Professional Groups continue

to increase greatly, as shown in Fig. 2, The Editorial Department published 69 issues of TRANSACTIONS totaling 5044 pages for 23 Groups during 1956, representing a 44% increase over the 1955 totals of 56 issues totaling 3504 pages for 21 Groups. Thirteen of the Groups employ letterpress printing and the remainder, offset reproductions. A summary of TRANSACTIONS material published is given in Table V.

TABLE V

VOLUME OF TRANSACTIONS PAGES

	1956	1955	1954	1953
Groups Publishing	23	21	18	15
No. of Issues	69	56	51	32
No. of Pages	5044	3504	3714	1798

IRE NATIONAL CONVENTION RECORD

The practice of publishing a IRE NATIONAL CONVENTION RECORD containing papers presented at the IRE National Convention, begun in 1953, was continued. The 1956 IRE NATIONAL CONVENTION RECORD, containing 261 papers and 17 abstracts totaling 1696 pages, was issued in nine parts. Approximately 40,000 paid members of Professional Groups received free of charge a copy of that Part pertaining to the field of interest of his Group.

IRE STUDENT QUARTERLY

The IRE STUDENT QUARTERLY, begun in 1954 was issued 4 times in 1956 and totalled 226 pages. The publication is sent free to all IRE Student Members as part of a program of increased services to students.

IRE DIRECTORY

The 1956–1957 IRE DIRECTORY was published in September, containing 1004 pages including covers, of which 417 were membership listings and information, and 587 were advertisements and listings of manufacturers and products.

CONFERENCE PUBLICATIONS

The *Proceedings of the 1955 Eastern Joint Computer Conference*, sponsored jointly by the IRE, AIEE and Association for Computing Machinery, was published by the Editorial Department in June, 1956. The issue contained 104 pages.

Technical Activities

Technical Committees

During 1956 the 26 Technical Committees and their 108 subcommittees held 244 meetings, of which 232 were held at IRE Headquarters and 12 elsewhere.

The six Standards listed herewith, having been approved by the Standards Committee and the IRE Board of Directors, were published in the PROCEEDINGS OF THE IRE in 1956, and reprints are now available.

56 IRE 9.S1 June—
Standards on Facsimile: Definitions of Terms, 1956
56 IRE 28.S1 July—
Letter Symbol Standards for Semiconductor Devices, 1956
56 IRE 27.S1 August—
Standards on Methods of Measurement of the Conducted Interference Output of Broadcast and Television Receivers in the Range of 300 KC to 25 MC, 1956
56 IRE 7.S3 August—
Standards on Electron Devices: TR and ATR Tube Definitions, 1956
56 IRE 8.S1 September—
Standards on Electronic Computers: Definitions of Terms, 1956
56 IRE 28.S1 November—
Standards on Solid State Devices: Methods of Testing Transistors, 1956

The following two Standards were approved by the Standards Committee in 1956 and will be published in the PROCEEDINGS OF THE IRE early in 1957:

57 IRE 7.S4
Standards on Electron Tubes: Physical Electronics Definitions

57 IRE 14.S1
Standards on Piezoelectric Crystals: The Piezoelectric Vibrator: Definitions and Methods of Measurement

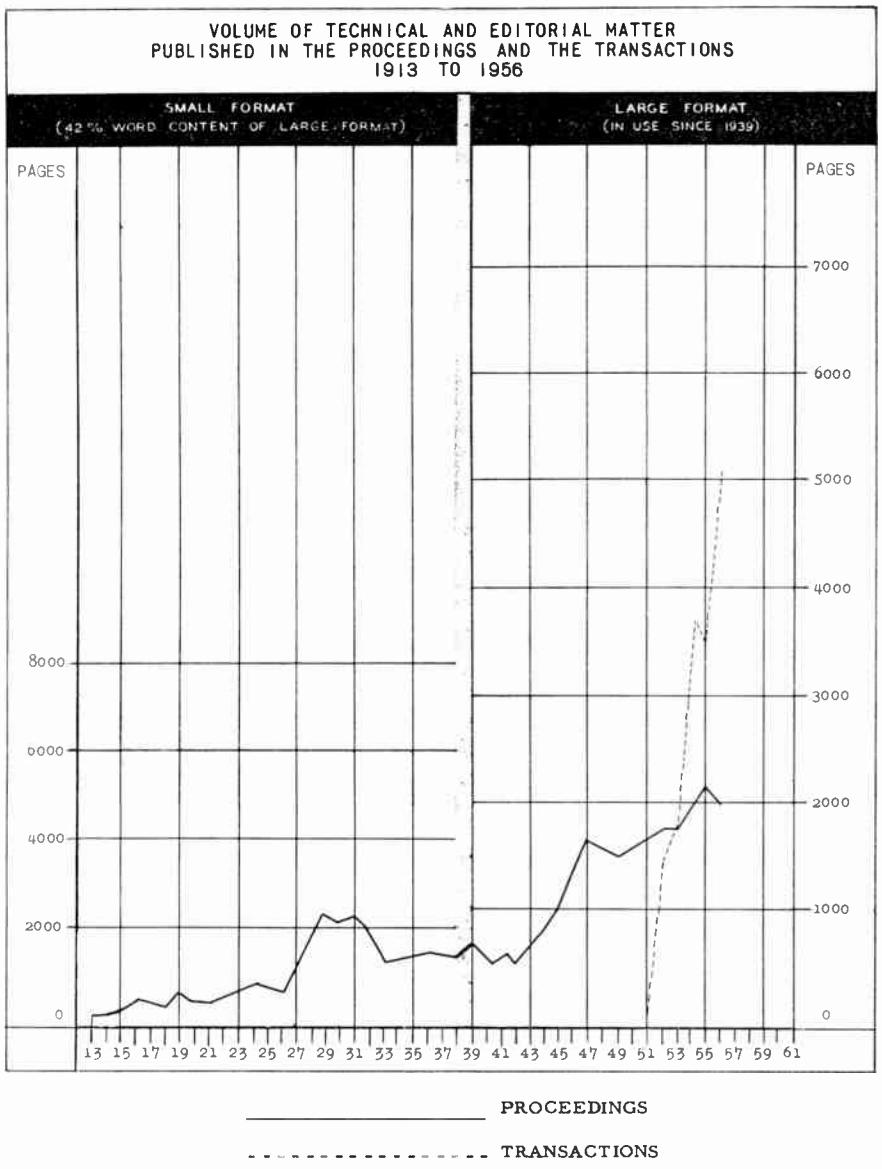

Fig. 2.

IRE is directly represented on 30 Committees of the American Standards Association and sponsors two of them: the ASA Sectional Committee on Radio and Electronic Equipment, C16, and the ASA Sectional Committee on Sound Recording, Z57. One IRE Standard received approval of the American Standards Association as an American Standard in 1956, and is now available to International Standards Organizations.

IRE actively participated in International Standardization in 1956 and was represented at the Munich meeting of the International Electrotechnical Commission in June, 1956.

Appointed IRE Delegates on Other Bodies

The IRE appointed delegates to a number of other bodies for a one-year period—May 1, 1956 to April 30, 1957 (as listed on page 911 of this issue).

The Annual Spring Meeting of the International Scientific Radio Union (URSI) was held on April 30–May 2, 1956 at the Nation-

al Bureau of Standards in Washington, D. C. It was co-sponsored by the following IRE Professional Groups: Antennas and Propagation, Circuit Theory, Instrumentation and Microwave Theory and Techniques. The URSI Fall Meeting was held on October 11–12, 1956 at the University of California, Berkeley. The URSI Spring Meeting for 1957 has been scheduled for May 22–25 at the Hotel Willard, Washington, D. C. The 12th General Assembly of URSI will be held August 22 to September 5, 1957 in Boulder, Colorado.

Numerous responses to the questions under study by the various CCIR Study Groups have been received in IRE during 1956. A list of all material received from these organizations was distributed quarterly to the Chairmen of all Technical Committees, Professional Groups and Definitions and Measurement Subcommittees. During 1956 the Executive Committee of the U. S. Preparatory Committee of CCIR held 6 meetings and the 14 Study Groups held approximately 56 meetings.

The Joint Technical Advisory Committee

The Joint Technical Advisory Committee and its Subcommittees held a total of 11 meetings in addition to the annual dinner.

Volume XIII, the cumulative annual report of the JTAC Proceedings was published in 1956. This included Section I—official correspondence between the Federal Communications Commission and the Joint Technical Advisory Committee (IRE—RETMA). Also included were other items of correspondence pertinent to the actions of the JTAC. Section II of the report contained approved Minutes of Meetings of the Joint Technical Advisory Committee for the period 1 July 1955 to 30 June 1956.

A new subcommittee was formed by JTAC. The Subcommittee on Study of Single Sideband Transmission (56.1) was formed on January 26, 1956 for the purpose of reviewing and summarizing in form suitable for integrated publication, all available information relating to single sideband transmission and to analyze the technical factors that relate to the most favorable integration of this form of single sideband transmission. IRE was commended by the Federal Communications Commission for its outstanding contribution to the literature on single sideband theory and practice in the December, 1956 issue of the PROCEEDINGS OF THE IRE.

The JTAC Subcommittee on Study of Spurious Radio Emissions (52.2) presented a report on "Principles Affecting the Probability of Serious Interference" which will be included in the Annual Volume of the Proceedings of JTAC. A study in the operation of the Cooperative Interference Committees was completed by Subcommittee 52.2.

The JTAC Subcommittee on Radio Frequency Interference from Arc Welders (54.2) submitted a response to FCC concerning the Notice of Proposed Rule Making FCC 56-459, 31405 in Docket No. 11467. JTAC offered assistance to the JIC group on further investigation of reduced duty cycle operation.

The International Electrotechnical Commission (IEC)

The International Electrotechnical Commission held its meeting in Munich June 26–July 6, 1956. Fifteen countries were represented: Belgium, Czechoslovakia, Denmark, Finland, France, German Federal Republic, Italy, Japan, Netherlands, Norway, Sweden, Switzerland, United Kingdom, United States of America and Yugoslavia.

IRE members were active in IEC Technical Committee 12 on Radio Communication, and Technical Subcommittee 12-1 on Measurements.

A list of all documents and material received in the Technical Department from the IEC was distributed to the Chairmen of all Professional Groups, Technical Committees and Subcommittees.

Professional Group System

General. There are currently 24 Professional Groups operating actively within the IRE. A new Professional Group on Education is in the process of formation and it is expected that it will be approved before the 1957 IRE National Convention.

Approximately 50% of all IRE members have taken advantage of the Professional Group System which now has a total paid membership of 53,015. Included are 3,619 Student members of the IRE who have joined the Groups at the special Student member rate of $1.00 annually.

Financial and editorial assistance were among the many services rendered by Headquarters to the Groups during 1956. In addition, the Office of the Technical Secretary provided administrative services for Group operations, the planning of meetings, advance publicity and the recording and mailing for all activities, including 847 mailings to Group members.

Symposia. The procurement of papers and actual management of national symposia are entirely in the hands of the Professional Groups. Each of the Groups sponsored one or more technical meetings in the past year in addition to Technical Sessions at the IRE National Convention, the WESCON, The National Electronics Conference and other joint meetings, for a total of 44 meetings of national import in 1956.

Publications. 23 Groups are currently publishing IRE TRANSACTIONS covering their specific fields of interest and to date 236 issues (15,564 pages) have appeared. The 24th Group will begin to publish its TRANSACTIONS early in 1957. During the past year 23 Groups published 69 TRANSACTIONS containing 5,044 pages.

Nine of the Groups are currently on a regularly stated publication schedule, and thirteen are now printing by letterpress.

In addition to IRE TRANSACTIONS, several Groups are issuing proceedings of meetings jointly sponsored with other societies, such as the Eastern and Western Joint Computer Conferences, the Electronic Components Conference, *et al.*

Professional Group Chapters. 185 Professional Group Chapters have been organized by Group members in 44 IRE Sections. Chapter growth is continuing at a healthy rate. The Chapters are meeting regularly and sponsoring meetings in the fields of interest of their associated Groups in the various Sections. The newest Group, the Professional Group on Military Electronics, formed on September 7, 1955, already has 10 official Chapters.

Section Activities

We are glad to welcome ten new Sections into the IRE during the past year. They are as follows: Alamogordo-Holloman, Florida West Coast, Fort Huachuca, Fort Worth, Regina, Rio de Janeiro (Brazil), South Bend-Mishawaka, Southern Alberta, Tucson, and Wichita.

The total number of Sections is now 90.

The Tucson, Wichita and Fort Huachuca Subsections became full Sections in the year 1956. The Des Moines-Ames Section was dissolved by the Board of Directors on November 14, 1956.

The Subsections of Sections now total 26, the following being formed in 1956: Gainesville (Central Florida), Hampton Roads (North Carolina-Virginia), Las Cruces-White Sands Proving Ground (El Paso), Memphis (Huntsville), New Hampshire (Boston), Panama City (Northwest Florida), San Fernando Valley (Los Angeles), Shreveport (Dallas), and Western North Carolina (North Carolina-Virginia).

A growing major activity of many Sections and the larger Subsections in recent years is the publication of a local monthly bulletin to fulfill the need for announcing to the Section member the increasing activities of the Section, including (1) Section meetings (2) Professional Group Chapter meetings and (3) information on the local and national level of interest.

Thirty-three Sections and Subsections now issue these monthly publications.

Student Branches

The number of Student Branches formed during 1956 was 5, all of which operate as IRE-AIEE Branches. The total number of Student Branches is now 135, 107 of which operate as joint IRE-AIEE Branches.

Following is a list of the Student Branches formed during the year: Univ. of Alabama, Laval Univ., Univ. of Santa Clara, South Dakota State College, and Vanderbilt Univ.

IRE COMMITTEES—1957

EXECUTIVE

J. T. Henderson, *Chairman*
W. R. G. Baker, *Vice-Chairman*
Haraden Pratt, *Secretary*

D. G. Fink
A. V. Loughren
J. D. Ryder
Ernst Weber

ADMISSIONS

J. L. Sheldon, *Chairman*

H. S. Bennett
T. M. Bloomer
L. A. Byam, Jr.
E. T. Dickey
A. D. Emurian
L. O. Goldstone
J. A. Hansen
A. V. Loughren, *ex officio*
F. S. Mabry
H. G. Miller
W. L. Rehm
N. B. Ritchey
L. M. Rodgers
G. M. Rose, Jr.

APPOINTMENTS

J. D. Ryder, *Chairman*

J. T. Henderson
E. W. Herold
A. V. Loughren
K. V. Newton
D. E. Noble
J. R. Whinnery
C. F. Wolcott

AWARDS

L. R. Fink, *Chairman*

Robert Adler
F. J. Bingley
Cledo Brunetti
H. Busignies
R. M. Fano
E. B. Ferrell
D. E. Foster
A. V. Haeff
C. J. Hirsch
D. R. Hull
J. F. Jordan
J. E. Keto
C. N. Kimball
Urner Liddel
K. A. Norton
J. C. R. Punchard
George Sinclair
A. W. Straiton
Irven Travis
W. L. Webb
H. W. Wells
E. M. Williams
H. A. Zahl

AWARDS COORDINATION

A. V. Loughren, *Chairman*

F. B. Llewellyn
Ernst Weber

CONSTITUTION AND LAWS

A. W. Graf, *Chairman*

S. L. Bailey
I. S. Coggeshall
R. A. Heising
W. R. Hewlett

EDITORIAL BOARD

D. G. Fink, *Chairman*
E. W. Herold, *Vice-Chairman*
E. K. Gannett, *Managing Editor*

Ferdinand Hamburger, Jr.
T. A. Hunter
A. V. Loughren
W. Norris Tuttle

EDITORIAL REVIEWERS

W. R. Abbott
M. A. Acheson
R. B. Adler
Robert Adler
H. A. Affel
H. A. Affel, Jr.
W. J. Albersheim
B. H. Alexander
A. E. Anderson
J. A. Aseltine
W. S. Bachman
H. G. Baerwald
E. M. Baldwin
J. T. Bangert
W. L. Barrow
J. M. Barstow
B. L. Basore
B. B. Bauer
W. R. Beam
L. L. Beranek
P. P. Beroza
F. J. Bingley
H. S. Black
J. T. Bolljahn
H. G. Booker
J. L. Bower
W. E. Bradley
J. G. Brainerd
D. R. Brown
J. H. Bryant
Werner Bucholz
Kenneth Bullington
J. H. Burnett
R. P. Burr
C. R. Burrows
W. E. Caldes
H. J. Carlin
T. J. Carroll
J. A. Chambers
H. A. Chinn
Marvin Chodorow
J. W. Christensen
L. J. Chu
J. K. Clapp
E. L. Clarke
L. E. Closson
J. D. Cobine
R. E. Colander
J. W. Coltman
P. W. Crapuchettes
M. G. Crosby
C. C. Cutler
Sidney Darlington
B. J. Dasher
W. B. Davenport, Jr.
A. R. D'Heedene
A. C. Dickieson
Milton Dishal
Wellesley Dodds
Melvin Doelz
R. B. Dome
H. D. Doolittle
J. O. Edson
W. A. Edson
D. W. Epstein
Jess Epstein
W. L. Everitt
R. M. Fano
L. M. Field
J. W. Forrester
W. H. Forster
G. A. Fowler
R. W. Frank
G. L. Fredendall
H. B. Frost
E. G. Fubini
I. A. Getting
L. J. Giacoletto
E. N. Gilbert
Bernard Gold
W. M. Goodall
A. W. Graf
J. V. N. Granger
V. H. Grinich
A. J. Grossman
R. A. Gudmundsen
E. A. Guillemin
A. V. Haeff
N. I. Hall
W. W. Harman
D. B. Harris
A. E. Harrison
L. B. Headrick
P. J. Herbst
J. K. Hilliard
C. J. Hirsch
Gunnar Hok
J. L. Hollis
W. H. Huggins
J. F. Hull
R. G. E. Hutter
D. D. Israel
E. T. Jaynes
A. G. Jepsen
R. L. Jepsen
Harwick Johnson
E. C. Jordan
Robert Kahal
Martin Katzin
W. H. Kautz
R. D. Kell
C. R. Knight
W. E. Kock
Rudolph Kompfner
J. B. H. Kuper
A. E. Laemmel
H. B. Law
R. R. Law
Vincent Learned
M. T. Lebenbaum
W. R. Lepage
F. D. Lewis
W. D. Lewis
J. G. Linvill
F. B. Llewellyn
S. P. Lloyd
A. W. Lo
J. R. MacDonald
Nathan Marchand
Nathan Marcuvitz
F. L. Marx
W. P. Mason
G. L. Matthaei
W. J. Mayo-Wells
E. D. McArthur
D. O. McCoy
Knox McIlwain
Brockway McMillan
R. E. Meagher
T. H. Meisling
Pierre Mertz
H. R. Mimno
S. E. Miller
A. R. Moore
Norman Moore
G. E. Mueller
E. J. Nalos
H. Q. North
K. A. Norton
W. B. Nottingham
B. M. Oliver
H. F. Olson
G. D. O'Neill
P. F. Ordung
C. H. Page
R. M. Page
R. C. Palmer
C. H. Papas
M. C. Pease, III
R. W. Peter
H. O. Peterson
W. H. Pickering
J. A. Pierce
W. J. Poch
A. J. Pote
R. L. Pritchard
C. F. Quate
W. H. Radford
J. R. Ragazzini
J. A. Rajchman
H. J. Riblet
D. H. Ring
Stanley Rogers
T. A. Rogers
H. E. Roys
V. H. Rumsey
J. D. Ryder
R. M. Ryder
Vincent Salmon
A. L. Samuel
H. A. Samulon
O. H. Schade
S. W. Seeley
Samuel Seely
O. G. Selfridge
Samuel Sensiper
R. F. Shea
R. E. Shelby
Donald Shuster
W. M. Siebert
D. B. Sinclair
George Sinclair
David Slepian
R. W. Slinkman
C. E. Smith
O. J. M. Smith
L. D. Smullin
R. A. Soderman
A. H. Sommer
R. C. Spencer
J. R. Steen
Leo Storch
A. W. Straiton
D. E. Sunstein
Charles Susskind
G. C. Sziklai
G. K. Teal
J. C. Tellier
E. R. Thomas
H. P. Thomas
H. E. Tompkins
J. G. Truxal
D. F. Tuttle, Jr.
L. C. Van Atta
K. S. Van Dyke
E. K. Van Tassel
S. N. Van Voorhis
O. G. Villard, Jr.
R. L. Wallace, Jr.
L. G. Walters
C. C. Wang
D. A. Watkins
D. K. Weaver, Jr.
S. E. Webber
W. M. Webster
P. K. Weimer
Louis Weinberg
J. R. Weiner
H. G. Weiss
J. O. Weldon
J. M. West
G. W. Wheeler
H. A. Wheeler
J. R. Whinnery
W. D. White
J. B. Wiesner
Irving Wolff
G. O. Young
L. A. Zadeh

EDUCATION

Samuel Seely, *Chairman*

V. A. Babits
A. B. Bereskin
E. M. Boone
C. C. Britton
J. N. Dyer
I. O. Ebert
W. A. Edson
C. L. Foster
Ferdinand Hamburger, Jr.
A. E. Harrison
H. E. Hartig
E. W. Herold
G. B. Hoadley
T. A. Hunter
S. B. Ingram
T. F. Jones
Jerome Kurshan
H. A. Moencl
A. D. Moore
P. H. Nelson
R. E. Nolte
J. M. Pettit
J. L. Potter
G. A. Richardson
J. D. Ryder
George Sinclair
H. H. Stewart
A. W. Straiton
O. I. Thompson
W. N. Tuttle
David Vitrogan
D. L. Waidelich
J. R. Whinnery
D. G. Wilson
A. L. Winn
M. E. Zaret

FINANCE

W. R. G. Baker, *Chairman*

J. T. Henderson
A. V. Loughren
Haraden Pratt
J. D. Ryder

HISTORY

Haraden Pratt, *Chairman*

Melville Eastham
Lloyd Espenschied
Keith Henney
H. W. Houck
L. E. Whittemore

Nominations

J. D. Ryder, *Chairman*

S. L. Bailey, J. W. McRae, J. T. Henderson, K. V. Newton, E. W. Herold, H. W. Wells, A. V. Loughren, J. R. Whinnery

Policy Advisory

C. F. Wolcott, *Chairman*

J. F. Byrne, E. W. Herold, J. N. Dyer, A. B. Oxley, A. W. Graf, F. A. Polkinghorn, Samuel Seely

Professional Groups

W. R. G. Baker, *Chairman*
A. W. Graf, *Vice-Chairman (Central Div.)*
M. E. Kennedy, *Vice-Chairman (Western Div.)*
Ernst Weber, *Vice-Chairman (Eastern Div.)*

Victor Azgapetian, W. J. Morlock, M. S. Corrington, J. D. Noe, J. E. Eiselein, C. H. Page, R. M. Emberson, A. C. Peterson, Jr., D. G. Fink, Leon Podolsky, R. A. Heising, W. M. Rust, Jr., J. T. Henderson, J. D. Ryder, T. A. Hunter, J. S. Saby, A. V. Loughren, L. C. Van Atta, C. J. Marshall, Lewis Winner

Chairmen of Professional Groups, *ex officio.*

Tellers

G. P. McCouch, *Chairman*

Tore Anderson, Charles Gorss, P. G. Hansel, G. F. Maedel, Raymond J. Keogh, David Sillman, Ned A. Spencer

Special Committees

Armed Forces Liaison Committee

G. W. Bailey, *Chairman*

IRE-IEE International Liaison Committee

F. S. Barton, F. B. Llewellyn, Ralph Bown, C. G. Mayer, R. H. Davies, R. L. Smith-Rose, Willis Jackson, J. A. Stratton

Professional Recognition

G. B. Hoadley, *Chairman*

C. C. Chambers, W. E. Donovan, H. F. Dart, C. M. Edwards

Technical Committees

20. Standards Committee

M. W. Baldwin, Jr., *Chairman*
C. H. Page, *Vice-Chairman*
R. F. Shea, *Vice-Chairman*
L. G. Cumming, *Vice-Chairman*

J. Avins, D. R. Brown, W. R. Bennett, T. J. Carroll, J. G. Brainerd, P. S. Carter, A. G. Clavier, W. A. Lynch, G. A. Deschamps, A. A. Macdonald, S. Doba, Jr., Wayne Mason, J. E. Eiselein, D. E. Maxwell, D. Frezzolini, H. R. Mimno, E. A. Gerber, G. A. Morton, A. B. Glenn, J. H. Mulligan, Jr., H. Goldberg, W. Palmer, V. M. Graham, R. L. Pritchard, R. A. Hackbusch, P. A. Redhead, H. C. Hardy, R. Serrell, D. E. Harnett, H. R. Terhune, A. G. Jensen, W. E. Tolles, I. M. Kerney, J. E. Ward, J. G. Kreer, Jr., E. Weber, W. T. Wintringham

20.5 Definitions Coordinating

C. H. Page, *Chairman*

P. S. Carter, J. G. Kreer, Jr., E. A. Laport

20.8 Basic Terms

J. G. Brainerd, *Chairman*

M. W. Baldwin, Jr., C. H. Page

20.11 Coordination of Comments on International Standard Proposals

L. G. Cumming, *Chairman*

20.12 Ad Hoc Committee on Envelope Delay

P. S. Christaldi, *Chairman*

W. L. Behrend (alt.), N. J. Oman, S. Doba, Jr., J. R. Popkin-Clurman, A. D. Fowler, G. L. Fredendall, W. T. Wintringham

2. Antennas and Waveguides

G. A. Deschamps, *Chairman*
A. A. Oliner, *Vice-Chairman*
K. S. Packard, *Secretary*

P. S. Carter, D. C. Ports, H. A. Finke, W. Sichak, W. C. Jakes, Jr., G. Sinclair, Henry Jasik, P. H. Smith, P. A. Loth, K. Tomiyasu, R. L. Mattingly, W. E. Waller, M. S. Wheeler

2.4 Waveguide and Waveguide Component Measurements

A. A. Oliner, *Chairman*

P. A. Loth, K. Packard, W. E. Waller

2.5 Methods of Antenna Measurement

R. L. Mattingly, *Chairman*

W. C. Jakes, Jr., D. J. LeVine, W. Sichak

3. Audio Techniques

Iden Kerney, *Chairman*
D. S. Dewire, *Vice-Chairman*

A. A. Alexander, A. H. Lind, C. A. Cady, R. C. Moody, R. H. Edmondson, F. W. Roberts, A. P. Evans, L. D. Runkle, F. K. Harvey, F. H. Slaymaker, F. L. Hopper, R. E. Yaeger

3.1 Audio Definitions

D. S. Dewire, *Chairman*

W. E. Darnell, A. A. McGee, W. F. Dunklee, L. D. Runkle, C. W. Frank, R. E. Yaeger

3.3 Methods of Measurement of Distortion

R. C. Moody, *Chairman*

L. H. Bowman, J. J. Noble, F. Coker, E. Schreiber, J. French, R. Scoville, L. D. Grignon, K. Singer, F. Ireland, A. E. Tilley, E. King, P. Vlahos, P. Whister

3.4 Methods of Measurement of Noise

F. K. Harvey, *Chairman*

C. A. Cady, B. M. Oliver, J. P. Smith

4. Circuits

W. A. Lynch, *Chairman*
J. T. Bangert, *Vice-Chairman*

W. R. Bennett, H. L. Krauss, J. G. Brainerd, S. J. Mason, A. R. D'Heedene, C. H. Page, T. R. Finch, E. H. Perkins, R. M. Foster, E. J. Robb, W. H. Huggins, J. J. Suran, R. Kahal, W. N. Tuttle, L. Weinberg

4.2 Linear Lumped-Constant Passive Circuits

L. Weinberg, *Chairman*

J. A. Aseltine, G. L. Matthaei, R. Kahal, J. G. Truxal

4.3 Circuit Topology

R. M. Foster, *Chairman*

R. L. Dietzold, E. A. Guillemin, S. Goldman, J. Riordan

4.4 Linear Varying-Parameter and Nonlinear Circuits

W. R. Bennett, *Chairman*

J. G. Kreer, Jr., C. H. Page, J. R. Weiner

4.7 Linear Active Circuits Including Networks with Feedback Servomechanism

E. H. Perkins, *Chairman*

E. J. Angelo, Jr., J. M. Manley, W. A. Lynch, C. F. Rehberg

48. Circuit Components

A. R. D'Heedene, *Chairman*

4.9 Fundamental Quantities

H. L. Krauss, *Chairman*

P. F. Ordung, J. D. Ryder

4.10 Solid State Circuits

J. J. Suran, *Chairman*

R. H. Baker, A. W. Lo, E. Gonzalez, R. D. Middlebrook, R. A. Henle, D. O. Pederson, F. P. Keiper, Jr., A. K. Rapp, J. G. Linvill, G. H. Royer, R. R. Webster

4.11 Signal Theory

W. H. Huggins, *Chairman*

6. Electroacoustics

H. C. Hardy, *Chairman*
H. S. Knowles, *Vice-Chairman*

B. B. Bauer
M. Copel
W. D. Goodale, Jr.
C. J. LeBel
H. F. Olson
V. Salmon
F. M. Wiener
A. M. Wiggins
P. B. Williams

7. Electron Tubes

P. A. Redhead, *Chairman*
G. A. Espersen, *Vice-Chairman*

J. R. Adams
E. M. Boone
A. W. Coolidge
P. A. Fleming
K. Garoff
T. J. Henry
E. O. Johnson
W. J. Kleen
P. M. Lapostolle
R. M. Matheson
L. S. Nergaard
G. D. O'Neill
A. T. Potjer
H. J. Reich
A. C. Rockwood
H. Rothe
W. G. Shepherd
E. S. Stengel
R. G. Stoudenheimer
B. H. Vine
R. R. Warnecke
S. E. Webber

7.1 Tubes in Which Transit-Time Is not Essential

T. J. Henry, *Chairman*

T. A. Elder
W. T. Millis
R. E. Spitzer
A. K. Wing
A. H. Young

7.2 Cathode-Ray and Storage Tubes

J. R. Adams, *Chairman*

R. Dressler
H. J. Evans
J. T. Jans
L. T. Jansen
R. Koppelon
J. C. Nonnekens
G. W. Pratt
D. Van Ormer

7.2.2 Storage Tubes

A. S. Luftman, *Chairman*
J. A. Buckbee, *Secretary*

A. Bramley
A. E. Beckers
Joseph Burns
G. Chafaris
C. L. Corderman
M. Crost
D. Davis
Frances Darne
M. D. Harsh
B. Kazan
H. Hook
J. A. McCarthy
W. E. Mutter
D. L. Schaefer
H. M. Smith
W. O. Unruh

7.3 Gas Tubes

A. W. Coolidge, *Chairman*

J. H. Burnett
E. J. Handley
R. A. Herring
D. E. Marshall
G. G. Riska
W. W. Watrous
A. D. White
H. H. Wittenberg

7.3.1 Methods of Test for TR and ATR Tubes

L. W. Roberts, *Chairman*
A. Marchetti, *Secretary*

N. Cooper
H. Heins
F. Klawsnik
I. Reingold
R. Scudder
E. Vardon
R. Walker

7.4 Camera Tubes, Phototubes, and Storage Tubes in Which Photo-Emission is Essential

R. G. Stoudenheimer, *Chairman*

M. Adelman
H. H. Brauer
S. F. Essig
G. W. Iler
F. W. Schenkel
A. H. Sommer

7.5 High-Vacuum Microwave Tubes

E. M. Boone, *Chairman*

J. H. Bryant
R. L. Cohoon
H. W. Cole
G. A. Espersen
M. S. Glass
P. M. Lally
R. A. LaPlante
A. W. McEwan
R. R. Moats
H. L. McDowell
M. Nowogrodzki
S. E. Webber

7.5.1 Non-Operating Characteristics of Microwave Tubes

M. Nowogrodski, *Chairman*
R. L. Cohoon, *Secretary*

M. S. Glass
R. C. Hergenrother
E. D. Reed
F. E. Vacarro

7.5.2 Operating Measurements of Microwave Oscillator Tubes

R. R. Moats, *Chairman*
R. A. LaPlante, *Secretary*

T. P. Curtis
G. I. Klein
J. T. Sadler
M. Siegman
W. W. Teich

Consultants

A. E. Harrisan
J. F. Hull
T. Moreno
J. S. Needle
E. C. Okress
W. G. Shepherd

7.5.3 Operating Measurements of Microwave Amplifier Tubes

P. M. Lally, *Chairman*
H. L. McDowell, *Secretary*

J. Berlin
H. W. Cole
H. J. Hersh
R. C. Knechtli
A. W. McEwan
S. E. Webber
G. Weibel

7.6 Physical Electronics

R. M. Matheson, *Chairman*

R. W. Atkinson
J. G. Buck
L. Cronin
H. B. Frost
P. N. Hamblenton
J. M. Lafferty
J. E. White

7.6.2 Noise

H. A. Haus, *Chairman*

W. B. Davenport
W. H. Fonger
W. A. Harris
S. W. Harrison
E. K. Stodola
T. E. Tapley

7.8 Camera Tubes

B. H. Vine, *Chairman*

B. R. Linden
M. Rome
D. H. Schaeffer
C. E. Thayer

8. Electronic Computers

D. R. Brown, *Chairman*
R. D. Elbourn, *Vice-Chairman*

S. N. Alexander
W. T. Clary
M. K. Haynes
L. C. Hobbs
J. R. Johnson
M. Middelton, Jr.
C. D. Morrill
G. W. Patterson
J. A. Rajchman
R. Serrell
Q. W. Simkins
R. L. Snyder, Jr.
W. H. Ware
C. R. Wayne
J. R. Weiner
C. F. West
Way Dong Woo

8.3 Static Storage Elements

M. K. Haynes, *Chairman*

H. R. Brownell
T. G. Chen
J. D. Lawrence
W. Olander
J. Rajchman
E. A. Sands
R. Stuart-Williams
D. H. Toth
C. B. Wakeman

Consultants

R. R. Blessing
R. O. Endres
C. C. Horstmann
M. F. Littmann
N. B. Saunders

8.3.1 Methods of Measurement of Bobbin Cores

C. B. Wakeman, *Chairman*

L. R. Adams
N. Cushman
B. Falk
A. Fitzgerald
E. A. Gaugler
M. Geroulo
J. R. Jaquet
R. Kodis
H. A. Lewis
C. Lufcy
R. W. Olmsted
W. Schaal
W. Sielbach
C. Williams

8.4 Definitions (Eastern Division)

R. D. Elbourn, *Chairman*

J. R. Johnson
R. P. Mayer
G. W. Patterson

8.5 Definitions (Western Division)

W. H. Ware, *Chairman*

L. C. Hobbs
H. T. Larson
W. E. Smith
W. S. Speer
R. Thorensen

8.6 Magnetic Recording for Computing Purposes

S. N. Alexander, *Chairman*

8.8 Analog Computers—Definitions and Symbols

C. D. Morrill, *Chairman*

8.9 Digital Computer Logical and Block Diagram Symbols

G. W. Patterson, *Chairman*
J. S. Murphy, *Vice-Chairman*

C. F. Lee
M. P. Marcus
R. P. Mayer
R. J. Nelson
A. J. Neumann
J. J. O'Farrell
G. E. Poorte

9. Facsimile

D. Frezzolini, *Chairman*
P. Mertz, *Vice-Chairman*

H. F. Burkhard
A. G. Cooley
D. K. DeNeuf
J. Hackenberg
J. R. Hancock
J. V. Hogan
B. H. Klyce
L. R. Lankes
R. N. Lesnick
K. R. McConnell
G. G. Murphy
M. P. Rehm
H. C. Ressler
R. B. Shanck

26. Feedback Control Systems

J. E. Ward, *Chairman*
E. A. Sabin, *Vice-Chairman*

M. R. Aaron
G. S. Axelby
V. B. Haas, Jr.
R. J. Kochenburger
D. P. Lindorff
W. K. Linvill
D. L. Lippitt
J. C. Lozier
T. Kemp Maples
W. M. Pease
P. Travers
R. B. Wilcox
S. B. Williams
F. R. Zatlin

26.1 Terminology for Feedback Control Systems

F. Zweig, *Chairman*

G. R. Arthur — J. S. Mayo
C. F. Rehberg

26.2 Methods of Measurement and Test of Feedback Control Systems

V. Azgapetian, *Chairman*

R. Gordon — M. Matthews
A. F. Stuart

10. Industrial Electronics

J. E. Eiselein, *Chairman*
E. Mittelmann, *Vice-Chairman*

R. E. Anderson — E. W. Leaver
W. H. Brearley, Jr. — H. R. Meahl
G. P. Bosomworth — J. H. Mennie
R. I. Brown — W. D. Novak
Cledo Brunetti — H. W. Parker
J. M. Cage — S. I. Rambo
E. W. Chapin — E. A. Roberts
R. D. Chipp — R. J. Roman
D. Cottle — W. Richter
C. W. Frick — C. E. Smith
R. A. Gerhold — C. F. Spitzer
H. C. Gillespie — L. W. Thomas
A. A. Hauser, Jr. — W. R. Thurston
G. W. Jacob — M. P. Vore
E. A. Keller — J. Weinberger
T. P. Kinn — V. Wouk
S. L. Yarbrough

10.1 Definitions

R. J. Roman, *Chairman*

W. H. Brearley, Jr. — C. W. Frick
D. W. Cottle — W. Hausz
J. E. Eiselein — E. Mittelmann
C. F. Spitzer

10.3 Industrial Electronics Instrumentation and Control

E. Mittelmann, *Chairman*
W. H. Brearley, Jr., *Vice-Chairman*

C. F. Bagwell — E. A. Keller
S. F. Bartles — D. Krett
R. I. Brown — C. W. Miller
H. Chestnut — J. Niles
D. Esperson — W. D. Novak
E. A. Goggio — C. F. Spitzer
C. E. Jones — L. W. Thomas
N. P. Kalmus — W. A. Wildhack

11. Information Theory and Modulation Systems

J. G. Kreer, Jr., *Chairman*
P. Elias, *Vice-Chairman*

P. L. Bargellini — S. Goldman
N. M. Blachman — H. W. Kohler
W. R. Bennett — E. R. Kretzmer
T. P. Cheatham, Jr. — N. Marchand
L. A. DeRosa — L. Meacham
M. J. E. Golay — J. F. Peters
D. Pollack

11.1 Modulation Systems

D. Pollack, *Chairman*

11.2 East Coast Information Theory

P. Elias, *Chairman*

R. M. Fano

11.3 West Coast Information Theory

N. M. Blachman, *Chairman*

J. H. Tillotson

25. Measurements and Instrumentation

J. H. Mulligan, Jr., *Chairman*
C. D. Owens, *Vice-Chairman*

M. J. Ackerman — G. B. Hoadley
P. S. Christaldi — G. A. Morton
J. L. Dalke — M. C. Selby
G. L. Fredendall — R. M. Showers

25.1 Basis Standards and Calibration Methods

M. C. Selby, *Chairman*

S. L. Bailey — G. L. Davies
F. J. Gaffney

25.2 Dielectric Measurements

J. L. Dalke, *Chairman*

C. A. Bieling — F. A. Muller

25.3 Magnetic Measurements

C. D. Owens, *Chairman*

W. E. Cairnes — R. C. Powell
D. I. Gordon — J. H. Rowen
P. H. Haas — E. J. Smith

25.4 Audio-Frequency Measurements

R. Grim — R. A. Long

25.5 Video Frequency Measurements

J. F. Fisher — H. A. Samulon
C. O. Marsh — W. R. Thurston

25.6 High Frequency Measurements

G. B. Hoadley, *Chairman*

R. A. Braden — E. W. Houghton
I. G. Easton — D. Keim
F. J. Gaffney — B. M. Oliver
B. Parzen

25.8 Interference Measurements

R. M. Showers, *Chairman*

H. E. Dinger — F. M. Greene
C. W. Frick — A. W. Sullivan

25.9 Measurement of Radio Activity

G. A. Morton, *Chairman*

25.10 Oscillography

M. J. Ackerman, *Chairman*

F. J. Bloom — G. R. Mezger (alternate)
W. G. Fockler — M. S. Rose
C. F. Fredericks — A. L. Stillwell
H. M. Joseph — H. Vollum

29. Medical Electronics

W. E. Tolles, *Chairman*

A. M. Grass — L. H. Montgomery, Jr.
J. P. Hervey — H. M. Rozendaal
T. F. Hueter

16. Mobile Communication Systems

A. A. Macdonald, *Chairman*
W. A. Shipman, *Vice-Chairman*

N. Caplan — N. H. Shepherd
D. B. Harris — D. Talley
N. Monk — T. W. Tuttle
J. C. O'Brien — A. Whitney

12. Navigation Aids

W. Palmer, *Chairman*
H. I. Metz, *Vice-Chairman*

A. M. Casabona — H. R. Mimno
D. G. C. Luck — A. G. Richardson
L. M. Sherer

12.2 Standard DF Measurements

E. D. Blodgett, *Chairman*
J. Kaplan, *Vice-Chairman*
R. Silberstein, *Secretary*

A. D. Bailey — W. M. Richardson
H. I. Butler — J. A. Solga
J. J. Kelleher — J. O. Spriggs
F. M. Kratokvil — C. A. Strom, Jr.
A. A. Kunze — S. R. Thrift
J. T. Lawrence — J. H. Trexler
H. R. Mimno — H. W. von Dohlen

12.3 Measurement Standards for Navigation Systems

F. Moskowitz, *Chairman*
S. B. Fishbein, *Secretary*

P. Adams — G. Litchford
R. Alexander — J. T. MacLemore
S. Anderson — G. E. Merer
R. Battle — J. S. Pritchard
S. D. Gurian — P. Ricketts
P. Hansel — Abe Tatz
V. Weihe

13. Nuclear Techniques

G. A. Morton, *Chairman*

R. L. Butenhoff — R. W. Johnston
D. L. Collins — T. R. Kohler
D. C. Cook — W. W. Managan
Louis Costrell — M. A. Schultz

14. Piezoelectric Crystals

E. A. Gerber, *Chairman*
I. E. Fair, *Vice-Chairman*

J. R. Anderson — Hans Jaffe
J. H. Armstrong — E. D. Kennedy
H. G. Baerwald — T. M. Lambert
R. Bechmann — W. P. Mason
W. G. Cady — W. J. Merz
W. A. Edson — C. F. Pulvari
W. D. George — P. L. Smith
R. L. Harvey — R. A. Sykes
E. J. Huibregtse — K. S. VanDyke

14.1 Ferroelectric Memory Material and Devices

J. R. Anderson, *Chairman*

J. H. Armstrong — E. D. Kennedy
E. J. Huibregtse — Walter Merz
C. Pulvari

14.2 Piezoelectric Measurements

R. Bechmann, *Chairman*

I. E. Fair — W. D. George
C. R. Mingins

14.4 Definitions for Magnetostriction

S. L. Ehrlich, *Chairman*

H. G. Baerwald — P. L. Smith
R. L. Harvey — R. S. Woollett

14.5 Piezoelectric Ceramics

H. Jaffe, *Chairman*

D. Berlincourt — T. Lambert
T. Kinsley — D. Schwartz

27. Radio Frequency Interference

A. B. Glenn, *Chairman*

C. C. Chambers — E. C. Freeland
J. F. Chappell — W. F. Goetter
E. W. Chapin — J. A. Hansen
K. A. Chittick — S. D. Hathaway
L. E. Coffey — J. B. Minter
M. S. Corrington — W. E. Pakala
H. E. Dinger — D. W. Pugsley
N. Flinn — W. A. Shipman
R. M. Showers

27.1 Basic Measurements

M. S. Corrington, *Chairman*

E. W. Chapin — E. O. Johnson
F. M. Greene — V. Mancino
W. S. Skidmore

27.2 Definitions

C. W. Frick — R. M. Showers

27.3 Radio and TV Receivers

R. J. Farber, *Chairman*

A. Augustine — C. G. Seright
E. W. Chapin — P. Simpson
M. S. Corrington — W. S. Skidmore
E. C. Freeland — M. Soja
R. O. Gray — R. C. Straub
E. O. Johnson — D. H. Thomas
W. R. Koch — F. R. Wellner
W. G. Peterson — A. E. Wolfram
R. S. Yoder

27.4 Radio Transmitters

W. F. Goetter, *Chairman*

H. S. Walker — V. Mancino

27.5 Industrial Electronics

27.7 Mobile Communications Equipment

W. Shipman, *Chairman*

W. C. Baylis — J. R. Neubauer
J. F. Chappell — N. Sheppard
A. MacDonald — B. Short
R. C. Stinson

27.12 Navigational and Communication Equipment

17. Radio Receivers

D. E. Harnett, *Chairman*
W. O. Swinyard, *Vice-Chairman*

J. Avins — I. J. Melman
K. A. Chittick — G. Mountjoy
L. E. Closson — J. N. Phillips
A. S. Goldsmith — L. Riebman
D. J. Healey III — J. D. Reid
J. J. Hopkins — L. M. Rodgers
K. W. Jarvis — S. W. Seeley
J. K. Johnson — F. B. Uphoff
W. R. Koch — R. S. Yoder

17.8 Television Receivers

W. O. Swinyard, *Chairman*

W. R. Alexander — W. R. Koch
J. Avins — C. O. Marsh
J. Bell — I. J. Melman
C. E. Dean — B. S. Parmet
E. Floyd — E. Pufahl
E. C. Freeland — G. F. Rogers
W. J. Gruen — S. P. Ronzheimer

17.10 Automatic Frequency and Phase Control

F. B. Uphoff, *Chairman*

R. Davies — W. R. Koch
K. Farr — R. N. Rhodes
W. J. Gruen — D. Richman
L. Riebman

15. Radio Transmitters

H. Goldberg, *Chairman*
A. E. Kerwien, *Vice-Chairman*

J. H. Battison — L. A. Looney
M. R. Briggs — J. F. McDonald
A. Brown — S. M. Morrison
H. R. Butler — J. Ruston
T. Clark — G. W. Sellers
W. R. Donsbach — B. Sheffield
L. K. Findley — J. B. Singel
H. E. Goldstine — B. D. Smith
F. B. Gunter — M. G. Staton
R. N. Harmon — V. E. Trouant
J. B. Heffelfinger — I. R. Weir
P. J. Herbst — V. Ziemelis

15.1 FM Transmitters

J. Ruston, *Chairman*

J. Bose — N. Marchand
J. R. Boykin — P. Osborne
H. P. Thomas

15.2 Radio-Telegraph Transmitters up to 50 MC

B. Sheffield, *Chairman*

J. L. Finch — F. D. Webster
J. F. McDonald — I. R. Weir

15.3 Double Sideband AM Transmitters

J. B. Heffelfinger, *Chairman*

W. T. Bishop, Jr. — D. H. Hax
E. J. Martin, Jr.

15.4 Pulse-Modulated Transmitters

B. D. Smith, *Chairman*

R. Bateman — H. Goldberg
L. V. Blake — G. F. Montgomery
L. L. Bonham — W. K. Roberts

15.5 Single Sideband Radio Communication Transmitters

J. B. Singel, *Chairman*

W. B. Bruene — L. Kahn
J. P. Costas — A. E. Kerwien
H. E. Goldstine — E. A. Laport

15.6 Television Broadcast Transmitters

R. N. Harmon, *Chairman*

E. Bradburd — L. A. Looney
W. F. Goetter — J. Ruston
F. E. Talmage

19. Recording and Reproducing

D. E. Maxwell, *Chairman*
R. C. Moyer, *Vice-Chairman*

M. Camras — A. W. Friend
W. R. Chynoweth — C. J. LeBel
F. A. Comerci — W. E. Stewart
E. W. D'Arcy — L. Thompson
T. G. Veal

19.1 Magnetic Recording

R. C. Moyer, *Chairman*

J. S. Boyers — K. I. Lichti
M. Camras — C. B. Pear
F. A. Comerci — E. Schmidt
E. W. D'Arcy — W. T. Selsted
W. H. Ericson — T. L. Vinson
O. Kornei — R. A. VonBehren

19.2 Mechanical Recording

L. Thompson, *Chairman*

W. S. Bachman — R. C. Moyer
S. M. Fairchild — F. W. Roberts
A. R. Morgan — A. S. R. Tobey

19.3 Optical Recording

T. G. Veal, *Chairman*

P. Fish — E. Miller
J. A. Maurer — C. Townsend

19.5 Flutter

F. A. Comerci, *Chairman*

S. M. Fairchild — U. Furst
C. J. LeBel

28. Solid State Devices

R. L. Pritchard, *Chairman*
W. M. Webster, *Vice-Chairman*
V. P. Mathis, *Secretary*

J. B. Angell — L. T. MacGill
S. J. Angello — W. J. Mayo-Wells
Abraham Coblenz — C. W. Mueller
L. Davis, Jr. — W. J. Pietenpol
J. M. Early — R. H. Rediker
J. J. Ebers — J. R. Roeder
H. Epstein — C. A. Rosen
H. Goldberg — B. J. Rothlein
J. R. Hyneman — R. M. Ryder
J. P. Jordan — J. Saby
N. R. Kornfield — B. R. Shepard
A. W. Lampe — S. Sherr
J. R. Macdonald — C. F. Spitzer

28.4 Semiconductor Devices

S. J. Angello, *Chairman* (AIEE)
J. M. Early, *Chairman* (IRE)

J. B. Angell — L. T. MacGill
R. L. Bright — H. T. Mooers
E. N. Clarke — C. W. Mueller
A. Coblenz — R. L. Pritchard
S. K. Ghandi — B. J. Rothlein
J. D. Johnson — H. N. Sachar
C. H. Knowles — A. C. Scheckler
R. M. LeLacheur — A. P. Stern
B. R. Lester — R. L. Trent

28.4.2 Methods of Test for Transistors for Linear CW Transmission Service

A. Coblenz, *Chairman*

Definitions and Letter Symbols of Semiconductors

B. J. Rothlein, *Chairman*

28.4.4 Methods of Test for Semiconductor Devices for Large-Signal Applications

R. L. Trent, *Chairman*

A. W. Berger
C. Huang
R. M. LeLacheur
R. L. Wooley

28.4.5 Methods of Test for Bulk Semiconductors

E. N. Clarke, *Chairman*

D. C. Cronemeyer
I. Drukaroff
J. R. Haynes
A. Kestenbaum
M. F. Lamorte
B. J. Rothlein
K. W. Uhler

28.4.7 Transistor Internal Parameters

R. L. Pritchard, *Chairman*

R. B. Adler
J. B. Angell
J. M. Early
W. M. Webster

28.4.9 Semiconductor Diode Definitions

C. H. Knowles, *Chairman*

L. D. Armstrong
D. C. Dickson
F. F. Finnegan
J. D. Johnson
R. P. Lyon
B. Seddon
D. R. Smith
K. D. Smith
E. L. Steele
J. R. Thurell

28.5 Dielectric Devices

H. Epstein, *Co-Chairman* (AIEE)
C. A. Rosen, *Co-Chairman* (IRE)

J. H. Armstrong
W. D. Bolton
J. Bramley
R. B. Delano, Jr.
H. Diamond
D. P. Faulk
R. Gerson
R. B. Gray
F. P. Hall
S. R. Hoh
H. F. Ivey
B. Jaffee
N. R. Kornfield
E. E. Loebner
E. F. Mayer
A. Myerhoff
H. I. Oshry
C. F. Pulvari
N. Rudnick
E. A. Sack
E. Schwenzfeger
F. A. Schwertz
G. Shaw
B. R. Shepard
C. F. Spitzer
L. E. Walkup

28.5.1 Nonlinear Capacitor Definitions

E. A. Sack, *Chairman*

28.5.2 Dielectric Electro-Optic Definitions

E. E. Loebner, *Chairman*

28.5.3 Definitions, Formation and Utilization of Electrostatic Images

F. A. Schwertz, *Chairman*

28.6 Magnetic Devices

R. W. Rochelle, *Chairman* (IRE)
D. G. Scorgie, *Chairman* (AIEE)

A. Applebaum
D. R. Brown
T. H. Crowley
R. L. Harvey
M. L. Kales
C. A. Maynard
T. R. McGuire
J. A. Osborn
J. A. Rajchman
J. B. Russell
H. F. Storm
V. C. Wilson
G. F. Pittman
M. Sirvetz
C. L. Hogan
H. W. Katz

21. Symbols

H. R. Terhune, *Chairman*
R. T. Haviland, *Vice-Chairman*

H. W. Becker
E. W. Borden
D. C. Bowen
M. C. Cisler
W. A. Ford
I. L. Marin
C. D. Mitchell
E. W. Olcott
M. B. Reed
C. F. Rehberg
R. V. Rice
M. P. Robinson
M. S. Smith
R. M. Stern
H. P. Westman

21.3 Functional Representation of Control, Computing and Switching Equipment

E. W. Olcott, *Chairman*

T. G. Cober
H. F. Herbig
E. W. Jervis
H. P. Kraatz
W. G. McClintock
F. T. Meyer
J. S. Osborne
T. J. Reilly
A. C. Reynolds, Jr.

21.5 New Proposals and Special Assignments

M. P. Robinson, *Chairman*

21.7 Letter Symbols

C. F. Rehberg, *Chairman*

M. C. Cisler
G. A. Deschamps
A. C. Gilmore, Jr.
R. M. Stern

22. Television Systems

W. T. Wintringham, *Chairman*
W. F. Bailey, *Vice-Chairman*

M. W. Baldwin, Jr.
J. E. Brown
K. A. Chittick
C. G. Fick
D. G. Fink
P. C. Goldmark
R. N. Harmon
J. E. Hayes
A. G. Jensen
I. J. Kaar
R. D. Kell
D. C. Livingston
H. T. Lyman
L. Mautner
J. Minter
A. F. Murray
D. W. Pugsley
D. B. Smith
A. J. Talamini

22.2 Television Picture Element

D. C. Livingston, *Chairman*

J. B. Chatten
A. V. Bedford
P. W. Howells
P. Mertz

23. Video Techniques

S. Doba, Jr., *Chairman*
G. L. Fredendall, *Vice-Chairman*

S. W. Athey
A. J. Baracket
J. M. Barstow
J. H. Battison
E. E. Benham
K. B. Benson
E. M. Coan
L. B. Davis
V. J. Duke
J. R. Hefele
J. L. Jones
R. T. Petruzzelli
W. J. Poch

23.1 Definitions

G. L. Fredendall, *Chairman*

I. C. Abrahams
R. F. Cotellessa
S. Deutsch
W. C. Espenlaub

23.3 Video Systems and Components: Methods of Measurement

J. R. Hefele, *Chairman*

I. C. Abrahams
G. M. Glassford
A. Lind
N. E. Sprecher
E. Stein
W. B. Whalley

23.4 Video Signal Transmission: Methods of Measurement

J. M. Barstow, *Chairman*

K. B. Benson (Alternate for W. B. Whalley)
R. D. Chipp (Alternate for H. Mate)
M. H. Diehl
E. E. Gloystein
H. P. Kelly
H. Mate
R. M. Morris
J. R. Popkin-Clurman
E. B. Pores
E. H. Schreiber
L. Staschover
J. W. Wentworth
W. B. Whalley

24. Wave Propagation

T. J. Carroll, *Chairman*

H. H. Beverage
H. G. Booker
K. Bullington
C. R. Burrows
A. G. Clavier
A. B. Crawford
J. T. deBettencourt
J. H. Dellinger
F. H. Dickson
H. Fine
I. H. Gerks
W. D. Hershberger
M. Katsin
M. Kline
M. G. Morgan
H. O. Peterson
M. L. Phillips
J. A. Pierce
J. C. W. Scott
J. C. Simon
R. J. Slutz
R. L. Smith-Rose
J. B. Smyth
A. W. Straiton
O. G. Villard, Jr.
J. P. Voge
J. R. Wait
A. T. Waterman
A. H. Waynick

IRE REPRESENTATIVES IN COLLEGES

Adelphi College: I. Feerst
*Agricultural and Mechanical College of Texas: H. C. Dillingham
*Akron, Univ. of: P. C. Smith
*Alabama Polytechnic Institute: H. E. O'Kelley
Alabama, Univ. of: P. H. Nelson
Alaska, Univ. of: R. P. Merritt
*Alberta, Univ. of: J. W. Porteous
Arizona State College: C. H. Merritt
*Arizona, Univ. of: H. E. Stewart
*Arkansas, Univ. of: W. W. Cannon
Augustana College: V. R. Nelson
Brigham Young University: D. Bartholomew
*British Columbia, Univ. of: A. D. Moore
*Polytech. Inst. of Bklyn. (Day Div.): M. V. Joyce
*Polytech. Inst. of Bklyn. (Eve. Div.): G. J. Kent
Brooklyn College: E. H. Green
*Brown University: C. M. Angulo
*Bucknell University: G. A. Irland
Universidad de Buenos Aires: A. DiMarco
Buffalo, Univ. of: W. Greatbatch
*Calif. Institute of Technology: H. C. Martel
*Calif. State Polytech. College: H. Hendriks
*Calif. University of: H. J. Scott
California, Univ. of at L.A.: W. L. Flock
Capitol Radio Eng. Inst.: L. M. Upchurch, Jr.
*Carnegie Inst. of Tech: J. B. Woodford, Jr.
*Case Inst. of Tech: J. R. Martin
Catholic University of America: G. E. McDuffie, Jr.
Central Technical Institute: J. E. Lovan
*Cincinnati, Univ. of: A. B. Bereskin
*Clarkson College of Tech: W. J. Strong
*Clemson College: L. C. Adams
*Colorado Agri. and Mech. College: C. C. Britton
*Colorado, Univ. of: C. T. Johnk
*Columbia University: P. Mauzey
*Connecticut, Univ. of: H. W. Lucal
*Cooper Union School of Eng.: J. B. Sherman
*Cornell University: T. McLean
Dartmouth College: M. G. Morgan
*Dayton, Univ. of: L. H. Rose
*Delaware, Univ. of: L. P. Bolgiano, Jr.
*Denver, Univ. of: E. F. Vance
*Detroit, Univ. of: G. M. Chute
DeVry Technical Inst.: W. B. McClelland
*Drexel Inst. of Tech.: R. T. Zern
Duke University: H. A. Owen, Jr.
*Fenn College: K. S. Sherman
*Florida, Univ. of: M. H. Latour
*George Washington Univ.: G. Abraham
*Georgia Inst. of Tech.: B. J. Dasher
Gonzaga University: H. J. Webb
Harvard University: C. L. Hogan
Hofstra College: B. Zeines
Houston, Univ. of: W. L. Anderson
Howard University: W. K. Sherman
*Illinois Inst. of Tech.: G. T. Flesher
*Illinois, Univ. of: P. F. Schwarzlose
Institute Technologico De Aeronautica: Chen To Tai
*Iowa State College: G. A. Richardson
*Iowa, State Univ. of: J. E. Fankhauser
*John Carroll Univ.: Appointment later
*Johns Hopkins University: W. H. Huggins
*Kansas State College: K. W. Reister
*Kansas, Univ. of: D. Rummer
*Kentucky, Univ. of: N. B. Allison
*Lafayette College: F. W. Smith
Lamar State College of Tech.: F. M. Crum
LaSalle College: D. T. Best
*Laval University: J. E. Dumas
*Lehigh University: L. G. McCracken
Louisiana Polytechnic Inst.: D. L. Johnson
*Louisiana State Univ.: L. V. McLean
*Louisville, Univ. of: S. T. Fife
Lowell Technological Institute: C. A. Stevens
Loyola University: J. H. Battocletti
McGill University: F. S. Howes
*Maine, Univ. of: C. Blake
*Manhattan College: C. J. Nisteruk
Manitoba, Univ. of: H. Haakonsen
*Marquette Univ.: E. W. Kane
*Maryland, Univ. of: H. W. Price
*Mass. Inst. of Tech.: J. F. Reintjes
*Mass., Univ. of: J. W. Langford
*Miami, Univ. of: F. B. Lucas
*Michigan College of Mining and Tech.: R. J. Jones
*Michigan State University: I. O. Ebert
*Michigan, Univ. of: J. E. Rowe
Milwaukee School of Eng'g: T. I. Lyon
*Minnesota, Univ. of: L. T. Anderson
*Mississippi State College: H. H. McCown
*Missouri School of Mines and Metallurgy: R. E. Nolte
*Missouri, Univ. of: J. C. Hogan
Mohawk Valley Tech. Inst.: W. R. Pulhamus
*Montana State College: R. C. Seibel
Multnomah College: A. B. Tyle
*Nebraska, Univ. of: C. W. Rook
*Nevada, Univ. of: W. L. Garrott
*Newark College of Eng.: D. W. Dickey
*New Hampshire, Univ. of: F. A. Blanchard
*New Mexico College of A. and M. Arts: H. A. Brown
*New Mexico, Univ. of: R. K. Moore
*New York, College of the City of: H. Wolf
*New York Univ. (Day and Eve. Div.): L. J. Hollander
*North Carolina State College: E. G. Manning
*North Dakota Agri. College: E. M. Anderson
*North Dakota, Univ. of: C. Thomforde
*Northeastern University: R. S. Rochefort
*Northwestern University: C. W. McMullen
*Norwich Univ.: R. F. Marsh
*Notre Dame, Univ. of: C. Hoffman
Oberlin College: C. E. Howe
*Ohio State Univ.: C. E. Warren
*Ohio University: D. B. Green
*Oklahoma A and M College: H. T. Fristoe
Oklahoma Inst. of Tech.: H. T. Fristoe
*Oklahoma, Univ. of: C. E. Harp
*Oregon State College: A. L. Albert
Ottawa, Univ. of: L. A. Beauchesne
Pacific Union College: I. R. Neilsen
*Pennsylvania State University: H. J. Nearhoof
*Pennsylvania, Univ. of: R. Berkowitz
*Pittsburgh, Univ. of: J. Brinda, Jr.
*Pratt Institute: D. Vitrogan
*Princeton University: J. B. Thomas
Puerto Rico, Universidad de: B. Dueno
*Purdue University: W. H. Hayt, Jr.
Queen's University: H. H. Stewart
RCA Institutes, Inc.: P. J. Clinton
*Rensselaer Polytechnic Institute: H. D. Harris
*Rhode Island, Univ. of: M. J. Prince
*Rice Institute: C. R. Wischmeyer
*Rose Polytechnic Institute: P. D. Smith
Royal Tech. University of Denmark: G. Bruun
*Rutgers University: C. V. Longo
Ryerson Institute of Technology: Appointment later
*Saint Louis University: G. E. Dreifke
*San Diego State College: C. R. Moe
*San Jose State College: H. Engwicht
*Santa Clara, Univ. of: H. P. Nettesheim
Saskatchewan, Univ. of: A. M. Michalenko
*Seattle University: F. P. Wood
*South Carolina University: R. G. Fellers
South Dakota State College of Agriculture and Mechanic Arts: J. N. Cheadle
*South Dakota School of Mines & Technology: D. R. Macken
*Southern Calif., Univ. of: G. W. Reynolds
*Southern Methodist University: P. Harton
Southern Technical Institute: R. C. Carter
Southwestern Louisiana Institute: G. B. Bliss
*Stanford University: J. Linvill
*Stevens Institute of Technology: E. Peskin
*Swarthmore College: C. Barus
*Syracuse University: R. E. Gildersleeve
Tennessee A. & I. State University: F. W. Bright
*Tennessee, University of: J. R. Eckel, Jr.
*Texas College of Arts and Industries: J. R. Guinn
*Texas Technological College: C. Houston
*Texas, University of: W. H. Hartwig
Texas Western College: T. G. Barnes
*Toledo, University of: D. J. Ewing
*Toronto, University of: G. Sinclair
*Tufts University: A. L. Pike
*Tulane University: J. A. Cronvich
*Union College: R. B. Russ
*U. S. Naval Postgrad. School: G. R. Giet
*Utah State Agricultural College: W. L. Jones
*Utah, University of:
*Utah, University of: D. K. Gehmlich
Valparaiso Technical Institute: E. E. Bullis
Valparaiso University: W. Shewan
*Vanderbilt University: P. E. Dicker
*Vermont, University of: P. R. Low
*Villanova University: J. A. Klekotka
*Virginia Polytechnic Inst.: R. R. Wright
*Virginia, University of: W. P. Walker
*Washington, State College of: R. D. Harbour
*Washington University: H. A. Crosby
*Washington, University of: F. D. Robbins
Washington & Lee University: R. E. Alley
*Wayne University: D. V. Stocker
Wentworth Institute: T. A. Verrechhia
Wesleyan University: K. S. Van Dyke
Western Ontario, Univ. of: E. H. Tull
*West Virginia University: C. B. Seibert
*Wisconsin, Univ. of: G. Koehler
Wichita, Univ. of: A. T. Murphy
*Worcester Poly. Inst.: H. H. Newell
*Wyoming, Univ. of: E. M. Lonsdale
*Yale University: J. G. Skalnik

* Colleges with IRE Student Branches.

IRE REPRESENTATIVES ON OTHER BODIES

ASA Conference of Executives of Organization Members: G. W. Bailey, L. G. Cumming, alternate

ASA Standards Council: E. Weber, A. G. Jensen, alternate, L. G. Cumming, alternate

ASA Electrical Standards Board: M. W. Baldwin, L. G. Cumming, E. Weber, A. G. Jensen, alternate

ASA Acoustical Standards Board: E. Weber, L. G. Cumming, alternate

ASA Graphic Standards Board: H. R. Terhune, R. T. Haviland, alternate

ASA Nuclear Standards Board: G. A. Morton, W. E. Shoupp, alternate, L. G. Cumming, alternate

ASA Sectional Committee (C16) on Radio: (Sponsored by IRE) E. Weber, Chairman, D. E. Harnett, M. W. Baldwin, Jr., L. G. Cumming, Secretary

ASA Sectional Committee (C39) on Electrical Measuring Instruments: J. H. Mulligan, C. D. Owens, alternate

ASA Sectional Committee (C42) on Definitions of Electrical Terms: M. W. Baldwin, Jr., J. G. Brainerd, A. G. Jensen, J. G. Kreer, Jr.

ASA Subcommittee (C42.1) on General Terms: J. G. Brainerd

ASA Subcommittee (C42.6) on Electrical Instruments: R. F. Shea

ASA Subcommittee (C42.13) on Communications: J. C. Schelleng

ASA Subcommittee (C42.14) on Electron Tubes: P. A. Redhead

ASA Sectional Committee (C60) on Standardization on Electron Tubes: R. L. Pritchard, P. A. Redhead

ASA Sectional Committee (C61) on Electric and Magnetic Magnitudes and Units: S. A. Schelkunoff, J. W. Horton, E. S. Purington

ASA Sectional Committee (C63) on Radio-Electrical Coordination: A. B. Glenn, R. M. Showers

ASA Sectional Committee (C67) on Standardization of Voltages—Preferred Voltages—100 Volts and Under: No IRE Voting Representative: Liaison: J. R. Steen

ASA Sectional Committee (C83) on Components for Electronic Equipment: P. K. McElroy

ASA Sectional Committee (C85) on Terminology for Automatic Controls: J. E. Ward, E. A. Sabin

ASA Sectional Committee (Y1) on Abbreviations: H. R. Terhune, R. T. Haviland, alternate

ASA Sectional Committee (Y10) on Letter Symbols: H. R. Terhune, R. T. Haviland, alternate

ASA Subcommittee (Y10.9) on Letter Symbols for Radio: C. F. Rehberg

ASA Subcommittee (Y10.14) on Nomenclature for Feedback Control Systems: J. E. Ward, W. A. Lynch, E. A. Sabin

ASA Sectional Committee (Y14) on Standards for Drawing and Drafting Room Practices: Austin Bailey, K. E. Anspach, alternate

ASA Sectional Committee (Y15) on Preferred Practice for the Preparation of Graphs, Charts and other Technical Illustrations: C. R. Muller, M. P. Robinson, alternate

ASA Sectional Committee (Y32) on Graphical Symbols and Designations: Austin Bailey, A. G. Clavier, A. F. Pomeroy, alternate

ASA Sectional Committee (Z17) on Preferred Numbers: H. R. Terhune

ASA Sectional Committee (Z57) on Sound Recording: (Sponsored by IRE) H. E. Roys, Chairman, F. A. Comerci, Representative, A. W. Friend, alternate, L. G. Cumming, Secretary

ASA Sectional Committee (Z58) on Standardization of Optics: T. Gentry Veal, E. Dudley Goodale, alternate

American Association for Advancement of Science: J. G. Brainerd

*International Radio Consultative Committee of U. S. Delegation: A. G. Jensen, Ernst Weber, L. G. Cumming, alternate

*U. S. National Committee of the International Scientific Radio Union (URSI) Executive Committee: S. L. Bailey, Ernst Weber, alternate

*Joint IRE-RETMA-SMPTE-NARTB Committee for Inter-Society Coordination (Television) (JCIC): W. J. Poch, M. W. Baldwin, L. G. Cumming, alternate

National Bureau of Standards Technical Advisory Committee: H. G. Booker, Chairman, W. L. Everitt, S. L. Bailey, H. W. Wells, J. B. Wiesner, A. H. Waynick

National Research Council—Div. of Eng. and Indus. Research: F. B. Llewellyn

*U. S. National Committee of the International Electrotechnical Commission: M. W. Baldwin, Ernst Weber, L. G. Cumming, A. G. Jensen, alternate

National Electronics Conference: J. J. Gershon

* Submitted for approval of the Executive Committee.

compared, and good agreement is obtained if radiation from the feed is taken into account.

621.396.677.71 1339
Analysis of a Terminated-Waveguide Slot Antenna by an Equivalent-Circuit Method—L. B. Felsen. (IRE TRANS., vol. AP-4, pp. 16–26; January, 1956.) For abstract, see PROC. IRE, vol. 44, p. 715; May, 1956.

621.396.677.75 1340
Ferrite-Rod Antennas Operate in X-Band—F. Reggia, F. G. Spencer, R. D. Hatcher, and J. E. Tompkins. (*Electronics*, vol. 30, pp. 159–161; January 1, 1957.) The ferrite in a typical antenna forms a dielectric rod radiator coupled to a waveguide, and may have a 20:1 gain for a beamwidth of 28 degrees and vswr of 1.2. Arrays can be made by spacing the rods along the waveguide or by magnetic coupling from resonant cavities. By using the Faraday effect, mode switching, array scanning, and beam lobing are possible.

AUTOMATIC COMPUTERS

681.142 1341
Definitions of Terms for Program-Controlled Electronic Computers—(*Nachrichtentech. Z.*, vol. 9, pp. 434–436; September, 1956.) About 40 proposed terms are listed with their definition and English equivalent.

681.142 1342
The Design and Applications of a General-Purpose Analogue Computer—R. J. A. Paul and E. L. Thomas. (*J. Brit. IRE*, vol. 17, pp. 49–73; January, 1957.) The design and construction are considered in detail with particular emphasis on amplifier gain, bandwidth, and phase shift. A computer whose design is based on this analysis and has some novel features is described. Its use on a variety of problems illustrates its wide range of application. See also 2299 of 1956 (Paul).

681.142 1343
Use of Analogue Computers for Solving Boundary Problems, Algebraic, Transcendental and Integral Equations—I. M. Vitenberg and E. A. Gluzberg. (*Avtomatika i Telemekhanika*, vol. 17, pp. 590–600; July, 1956.)

681.142 1344
Radioactive-Fall-Out Computer—(*Electronic Ind. and Tele-Tech.*, vol. 15, pp. 57, 136; September, 1956.) Electronic analog techniques are used in a new computer to make rapid predictions of fall-out based on wind velocities and particle sizes.

681.142:621.374.3 1345
V.H.F. Pulse Techniques and Logical Circuitry—Rosenheim and Anderson. (See 1374.)

CIRCUITS AND CIRCUIT ELEMENTS

621.3:539.169 1346
Effects of Radiation on Electronic Components—R. D. Shelton. (*Electronic Ind. and Tele-Tech.*, vol. 15, pp. 57, 126; September, 1956.) Methods of testing for damage resulting from exposure to nuclear radiation are discussed and effects on various classes of components are described. Gamma radiation is mainly harmful to the insulation of resistors and capacitors; transistors and all devices depending on an ordered crystal lattice are very susceptible to neutron bombardment.

621.3.048:621.315.616.9 1347
Problems in Casting Electronic Components—H. G. Manfield. (*Elec. Mfg.*, vol. 56, pp. 142–144; October, 1955.) Precautions to be taken in applying casting resins to resistors, capacitors, rectifiers, iron-core components, and instrument wires are noted.

621.316.5.064.43 1348
The Erosion of Electrical Contacts by the Normal Arc—W. B. Ittner, III and H. B. Ulsh. (*Proc. IEE*, Part B, vol. 104, pp. 63–68; January, 1957.) "Within the experimental errors the material transfer from the cathode was found to be directly proportional to the total charge passed in the arc—a relationship first proposed by R. Holm [*Electrical Contacts*, 1946]. It is shown that, for most practical purposes, the cathode "normal arc" transfer can be calculated with a reasonable accuracy according to the formula given by Llewellyn Jones [3436 of 1946].

621.318.4.011.1 1349
The Short-Circuited Turn—T. Roddam. (*Wireless World*, vol. 63, pp. 114–117; March, 1957.) The equivalent circuit is examined mathematically and the practical implications of the analysis in commonly met situations are considered.

621.318.4.011.32 1350
Mutual Inductance of Two Coaxial Circular Cylindrical Coils with a Layer of Contiguous Turns of Fine Wire—R. Cazenave. (*Ann. Télécommun.*, vol. 11, pp. 174–179; September, 1956.) Calculations are made for the two particular cases in which the coils are: *a*) axially coextensive, and *b*) axially adjacent.

621.318.5 1351
Mathematical Theory of the Synthesis of Contact (1, *k*)—Poles—G. N. Povarov. (*C.R. Acad. Sci. U.R.S.S.*, vol. 111, pp. 102–104; November 1, 1955. In Russian.)

621.319.4.012 1352
The Effective Power [dissipation] of a Lossy Capacitor Loaded by a Train of Rectangular Pulses—H. Eisenlohr. (*Frequenz*, vol. 10, pp. 292–293; September, 1956.) Formulas are derived based on an equivalent series circuit of loss-free capacitor and resistance; they are applicable to different types of dielectric loss.

621.372:621-526 1353
A Less-than-Minimum-Phase-Shift Network—R. F. Destebelle, C. J. Savant, and C. J. Savant, Jr. (*Electronic Ind. and Tele-Tech*, vol. 15, pp. 60–61, 106; September, 1956.) The minimum phase shift attainable in a linear network for a given attenuation can be reduced by introducing nonlinear circuits, thus preventing instability. A servosystem is described in which instability in a high-*Q* tuned amplifier is prevented by use of a phase-sensitive demodulator.

621.372.2 1354
Distributed-Parameter Variable Delay Lines using Skewed Turns for Delay Equalization—F. D. Lewis and R. M. Frazier. (PROC. IRE, vol. 45, pp. 196–204; February, 1957.) An analysis of the method of equalization is given, and the performance of experimental variable delay lines is discussed.

621.372.4:621.376.32:621.314.7 1355
Equivalent Reactances using Junction-Type Semiconductor Triodes—L. N. Kaptsov and K. S. Rzhevkin. (*Radiotekhnika i Elektronika*, vol. 1, pp. 670–679; May, 1956.) Transistor analogs of reactance-tube circuits are discussed.

621.372.412+[534.131:548.0 1356
Simple Modes of Vibration of Crystals—Mindlin. (See 1298.)

621.372.413 1357
Change of Characteristic Frequencies of Electromagnetic Resonators—Yu. N. Dnestrovski. (*C.R. Acad. Sci. U.R.S.S.*, vol. 111, pp. 94–97; November 1, 1956. In Russian.) The perturbation of the resonance frequencies of cavities by small changes in the shape of the cavity or by the insertion of small ideally conducting bodies is calculated by a method of successive approximations. The general perturbation formula obtained is in agreement, in the case of a conducting sphere, with the formula obtained by Maier and Slater (2265 of 1952). The general method can also be used in calculating the changes in the characteristic values due to changes of ϵ and μ inside the cavity.

621.372.413 1358
Cavity with Linear Tuning, for Metre and Decimetre Wavelengths—C. Brot and A. Soulard. (*C.R. Acad. Sci., Paris*, vol. 243, pp. 1848–1850; December 5, 1956.) A coaxial cavity is described in which the inner conductor comprises the combination of a fixed tube and an axial plunger. Displacement of the plunger within the tube varies the lumped capacitance without varying the distributed inductance. To avoid disturbing the edge effects, the plunger carries with it a teflon plug with a metal base, which is under spring pressure from the opposite side.

621.372.413:537.533:530.145 1359
Quantum Effects in the Interaction between Electrons and High-Frequency Fields: Vacuum Fluctuation Phenomena—I. R. Senitzky. (*Phys. Rev.*, vol. 104, pp. 1486–1491; December 1, 1956.) Previous calculations (369 and 3186 of 1955) gave a divergent result for the dispersion, due to the quantum properties of the field, in the velocity of an electron passing through a cavity. By a transformation the divergence has been eliminated and the mean velocity increment and the dispersion obtained.

621,372.5:621.376.3:621.3.018.78 1360
Frequency-Modulation Distortion in Linear Networks—Brown. (See 1581.)

621.372.543.2:[621.372.2+621.372.8 1361
Direct-Coupled-Resonator Filters—S. B. Cohn. (PROC. IRE, vol. 45, pp. 187–196; February, 1957.) Specific design formulas are given for lumped-constant elements, waveguide, and strip or other TEM transmission line, and for pass band response functions of the maximally flat or Tchebycheff types. Practical results compared with theoretical responses show that the formulas are accurate for large bandwidths.

621.372.55:621.397.24 1362
New Equalizers for Local TV Circuits—H. M. Thomson. (*Bell. Lab. Rec.*, vol. 34, pp. 346–349; September, 1956.) Equalizer units for the A2A system, which are required to equalize over the frequency range from about 100 cps to 4.5 mc for cable lengths from a fraction of a mile upwards, include eight fixed equalizers in a bridged-T network together with three compound equalizers having adjustable frequency characteristics and an all-pass phase-equalizing section.

621.372.56.029.6:621.372.8 1363
A Secondary Microwave Attenuator—H. A. Prime. (*J. Sci. Instr.*, vol. 33, pp. 448–449; November, 1956.) The arrangement described comprises a flexible resistive vane which is "bowed" into the middle of the waveguide by means of a micrometer screw; the screw is shielded by the vane so that it does not cause reflections.

621.372.632 1364
High-Frequency Power Rating. Application of Theory to a Mixer Stage with Known Nonlinear Characteristic—H. Fark. (*Frequenz*, vol. 10, pp. 294–296; September, 1956.) Equations

with relevant curves and tables are given for diode mixer circuits.

621.372.632 1365
Frequency Conversion by means of a Nonlinear Admittance—C. F. Edwards. (*Bell Sys. Tech. J.*, vol. 35, pp. 1403–1416; November, 1956.) Mathematical analysis is presented for a heterodyne conversion transducer which uses a nonlinear capacitor and a nonlinear resistor in parallel. Curves are given showing the change in admittance and gain with change in the characteristics of the nonlinear element. The conditions under which a conjugate match is possible are specified and conclusions indicate that a nonlinear capacitor alone is the preferred element for modulators, and a nonlinear resistor alone is best for converters.

621.372.632:621.373.423 1366
The Serrodyne Frequency Translator—R. C. Cumming. (PROC. IRE, vol. 45, pp. 175–186; February, 1957.) A linear sawtooth waveform causes transit-time modulation of an S-band traveling-wave tube to produce up to 57-mc frequency translation. The loss for a translation of 30 mc is 1 db for 20 db rejection of unwanted frequencies. The effect of certain practical factors in limiting the performance are discussed and a general spectrum analysis is given, applicable to problems where arbitrary modulating waveforms are used.

621.373.4/.5 1367
The Theory of Oscillators—W. Herzog and E. Frisch. (*Nachrichtentech. Z.*, vol. 9, pp. 310–341, July; pp. 420–423, September; pp. 449–455, October, 1956.) Analysis of oscillation conditions in a circuit comprising a pentode tube and a three-terminal network is applied to derive general design principles for a tube or transistor oscillator insensitive to load changes, and the stability and efficiency of a tuned oscillator are discussed.

621.373.421.13 1368
How to Design Colpitts Crystal Oscillators—H. E. Gruen. (*Electronics*, vol. 30, pp. 146–150; January 1, 1957.) Design data are presented as performance graphs for typical circuits.

621.373.43 1369
Second-Order Nonlinear Systems. Applications to Electronics—L. Sideriades. (*C.R. Acad. Sci., Paris*, vol. 243, pp. 1850–1852; December 5, 1956.) Analysis relevant to the operation of nonsinusoidal oscillators is presented.

621.373.44 1370
A Versatile Rectangular Pulse Generator—G. O. Crowther, L. H. Light, and C. F. Hill. (*Electronic Eng.*, vol. 29, pp. 8–12; January, 1957.) Description of an instrument for generating positive or negative pulses of up to 100 v and of 1 μs–12 ms duration, with repetition frequency 1 cps–150 kc. A variable-delay triggering facility is provided.

621.372.52:621.314.7 1371
Analysis of a Nearly Harmonic Oscillator with Semi-conductor Triode at Frequencies Above α Cut-Off—K. S. Rzhevkin, L. A. Logunov, and L. N. Kaptsov. (*Radiotekhnika i Elektronika*, vol. 1, pp. 647–653; May, 1956.) Analysis is presented for a grounded-base transistor oscillator. Experimental results indicate that the upper frequency limit is about six times the α-cut-off frequency, this being somewhat lower than the calculated limit. The calculated and measured frequency/emitter-current and frequency/collector-voltage characteristics with a point-contact transistor and a junction transistor are presented graphically.

621.373.52:621.314.7 1372
Analysis of Processes in the Blocking Oscillator with Semiconductor Triode—K. Ya. Senatorov and G. N. Berestovski. (*Radiotekhnika i Elektronika*, vol. 1, pp. 654–669; May, 1956.)

621.374.3:621.317.755 1373
Transistors Generate Geometric Scale—E. Gott and J. H. Park, Jr. (*Electronics*, vol. 30, pp. 180–183; January 1, 1957.) Fast and slow sawtooth voltages are generated and compared in a discriminator. When equal, the fast generator recycles to produce a chain of pulses spaced in geometric progression.

621.374.3:681.142 1374
V.H.F. Pulse Techniques and Logical Circuitry—D. E. Rosenheim and A. G. Anderson. (PROC. IRE, vol. 45, pp. 212–219; February, 1957.) Selection of components and design of circuits for using 10-mμs pulses in an experimental digital computer with a pulse repetition frequency of 50 mc.

621.374.4:621.385.029.6 1375
Frequency Division using a Reflex Klystron—E. N. Bazarov and M. E. Zhabotinski. (*Radiotekhnika i Electronika*, vol. 1, pp. 680–681; May, 1956.) Theory and a brief note on the practical realization are given.

621.375.1:512.3 1376
Application of the Method of Orthogonal Polynomials in Solving some Problems in the Analysis and Synthesis of Multistage Amplifiers—S. V. Samsonenko. (*Radiotekhnika i Elektronika*, vol. 1, pp. 623–626; May, 1956.) The relations between output signal, input signal, and system parameters are analyzed.

621.372.2:621.372.542.2 1377
Stagger-Tuned Low-Pass Amplifier with High Cut-Off Frequency—G. Mahler. (*Frequenz*, vol. 10, pp. 296–303, September; pp. 319–328, October, 1956.) The optimum value of the product of bandwidth and amplification obtainable for a given frequency characteristic is calculated. It can be achieved by using two-terminal sections in cascade-connected non-identical stages of Tchebycheff type. The design of a 40-mc 50-db low-pass amplifier is given as an example; in theory its amplification over the pass band does not change by more than ±2 per cent. The use of quadripole sections in amplifiers with nonidentical stages is also investigated.

621.375.2.024:621.314.58:621.314.63 1378
Silicon Diode Chopper Stabilizes D.C. Amplifier—L. Fleming. (*Electronics*, vol. 30, pp. 178–179; January 1, 1957.) "Stability of 100 microvolts per hour is possible with high-back-resistance silicon diodes in contrast with 2 millivolts an hour using direct-coupled thermionic amplifiers. Input impedance is one hundred times greater than with germanium crystals. Practical biological amplifier also uses phase detector that cuts rectified dc requirement."

621.375.2.121:621.397.5 1379
Wide-Band Amplifier Design—J. Kason. (*Electronic Eng.*, vol. 29, pp. 39–41; January, 1957.) A discussion of practical design procedure for a band-I amplifier with 30-mc bandwidth.

621.375.2.122 1380
Heater Voltage Compensation for D.C. Amplifiers—J. B. Earnshaw. (*Electronic Eng.*, vol. 29, pp. 31–35; January, 1957.) The concept of a fictitious voltage source to represent heater voltage fluctuations is examined and a detailed analysis of three compensation circuits together with experimental results is given.

621.375.4 1381
The Neutralization of Selective Transistor Amplifiers—G. Meyer-Brötz. (*Arch. elekt. Übertragung*, vol. 10, pp. 391–397; September, 1956.) Various neutralizing circuits are discussed and the influence of frequency and operating conditions on their performance is investigated.

621.375.4:621.314.7 1382
The Stabilization of the D.C. Operating Point of Junction Transistors—(See 1611.)

621.375.4:621.316.825 1383
Thermistors Compensate Transistor Amplifiers—A. J. Wheeler. (*Electronics*, vol. 30, pp. 169–171; January 1, 1957.) Temperature compensation of class-B push-pull transistor amplifiers is necessary to minimize distortion and prevent runaway. Typical compensating circuits using thermistors are described and equations for calculating component values and restrictions on use of two types of thermistor material are given. Design technique gives an approximation to the desired linear decrease in bias with increase in ambient temperature.

621.376.22:621.385.5 1384
A Simple Square-Law Circuit with High Frequency Response—H. N. Coates. (*Electronic Eng.*, vol. 29, pp. 41–42; January, 1957.) "By applying a signal to both control and suppressor grids of a pentode tube, it is possible to balance out changes in the tube anode current proportional to the signal fundamental and to generate a component proportional to its square, which is available without additional filtering and consequent restriction of bandwidth."

GENERAL PHYSICS

530.12 1385
Variation of Integrals and the Field Equations in the Unitary Field Theory—H. A. Buchdahl. (*Phys. Rev.*, vol. 104, pp. 1142–1145; November 15, 1956.)

530.145 1386
Exact Quantum Dynamical Solutions for Oscillator-Like Systems—M. Kolsrud. (*Phys. Rev.*, vol. 104, pp. 1186–1188; November 15, 1956.)

534.01:621.373 1387
Subharmonic and Superharmonic Oscillations of a Bilinear Vibrating System—C. P. Atkinson and L. O. Heflinger. (*J. Frank. Inst.*, vol. 262, pp. 185–190; September, 1956.) Response curves of a bilinear vibrating system obtained with an electronic analog system are presented. The existence of superharmonic and subharmonic components is shown, and their relation to the natural frequency range of the free vibrations is discussed. Numerical values of the circuit parameters of the analog system are given in an appendix.

535.23:535.36 1388
Radiative Transfer with Distributed Sources—R. G. Giovanelli and J. T. Jefferies. (*Proc. Phys. Soc., London*, vol. 69, pp. 1077–1084; November, 1956. Expressions are derived for the total intensity of the diffuse radiation in composite media.

536.758 1389
Calculation of Entropy for some Special Probability Distributions—M. M. Bakhmet'ev. (*Radiotekhnika i Elektronika*, vol. 1, pp. 613–622; May, 1956.) Probability distributions which can be approximately expressed by geometrical progressions are discussed.

537.2 1390
Generalization of Coulomb's Fundamental Law—B. Konorski. (*Arch. Elektrotech.*, vol. 42,

pp. 381–397; September 20, 1956.) Comprehensive analysis is presented for electrostatic systems comprising two spheres.

537.523:621.314.6 1391

Studies of Rectification in a Gas (Nitrogen) Discharge between Coaxial Cylindrical Electrodes: Part 1—Theory of Rectifications in A.C. Silent Discharges. Part 2—Rectification in Semiozonizers—V. L. Talekar. (*J. Electronics*, vol. 2, pp. 205–238; November, 1956.) An equation is developed connecting the rectification and the applied potential in discharge tubes of GM-counter type. An expression is derived for the limiting frequency below which the theory should be valid. An experimental investigation at 50 and 500 cps is reported to determine the effects of pressure, interelectrode distance, etc. on rectification in semiozonizers or Maze-type counters. Results are in agreement with theory.

537.525.3 1392

Investigation of Photoelectrically Effective U.V. Radiation from a Corona Discharge in H_2 and O_2—W. Bemerl and H. Fetz. (*Z. angew. Phys.*, vol. 8, pp. 424–429; September, 1956.)

537.533 1393

Diffraction and Interference Fringes in Electron Optics: Fresnel Diffraction, Young's Apertures and Fresnel's Biprism—J. Faget and C. Fert; L. de Broglie. (*C.R. Acad. Sci., Paris*, vol. 243, pp. 2028–2029; December 17, 1956.) Experiments were made using circular or linear sources and a magnetic lens interposed in the path of the beam between the diffracting object and the screen; results are reproduced photographically. The appended note by de Broglie emphasizes the importance of the work, which shows that the wave associated with the electron constitutes a long coherent wavetrain.

537.533:535.215 1394

Examination of Metals Subjected to Mechanical Constraint using the Photoemission Microscope—R. Goutte, C. Guillaud, and R. Arnal. (*C.R. Acad. Sci., Paris*, vol. 243, pp. 2026–2028; December 17, 1956.) An investigation was made of the photoemission from Au, Ag, and Pd strips with and without applied tension. The surfaces were illuminated obliquely by ultraviolet radiation and a magnification of about 30 was obtained on the luminescent screen. The emission is estimated to increase by about 10 per cent up to rupture point.

537.533:537.56 1395

Effective Cross-Sections of Neutral Hydrogen, Helium and Argon Atoms for Electron Collisions—H. W. Drawin. (*Z. Phys.*, vol. 146, pp. 295–313; September 21, 1956.)

537.533:621.38.032.21 1396

Material [presented] at the All-Union Conference on Cathode Electronics (Kiev, 25th–29th November 1955)—(*Bull. Acad. Sci. U.R.S.S., sér. phys.*, vol. 20, pp. 975–1076; September, 1956. In Russian.) Digests of ten papers and full texts of the following are presented (see also 80 of 1957):

Some Results and Problems in the Field of Cathode Electronics—N. D. Morgulis (pp. 977–992).

Secondary-Electron Emission (Position and Prospects)—L. N. Dobretsov. (pp. 994–1007).

Secondary-Electron Emission from Dielectrics and Metals—A. R. Shulman (pp. 1008–1022).

Some Anomalies of the Secondary-Electron Emission Characteristics of Magnesium Alloys—V. N. Lepeshinskaya (pp. 1025–1028).

Secondary-Electron Emission of Nickel-Based Alloys—B. S. Kul'varskaya (pp. 1029–1037).

Influence of Electron Bombardment on Photoelectron Emission of Complex Photocathodes—L. N. Bykhovskaya. (pp. 1052–1064).

Influence of Adsorbed Films of Barium Atoms and Barium Oxide Polar Molecules on the Electron Work Function of Tungsten, Gold and Germanium—V. M. Gavrilyuk. (pp. 1071–1075).

537.533.74 1397

Analytical Representation of Hartree Potentials and Electron Scattering—W. J. Byatt. (*Phys. Rev.*, vol. 104, pp. 1298–1300; December 1, 1956.) Gives analytical fits to the Hartree curves for 19 neutral atoms.

537.533.8:535.215 1398

The Correlation between Secondary Emission and Photoelectric Emission in Low-Pressure Discharges—W. Kluge and A. Schulz. (*Z. Phys.*, vol. 146, pp. 314–319; September 21, 1956.) Experiments on cathodes with caesium oxide or caesium antimonide coatings are reported; the results indicate that the same emission centers are responsible for secondary electrons and photoelectrons.

537.56:538.6:523.752 1399

Simulation of Solar Prominence in the Laboratory—Bostick. (See 1419.)

537.562:538.6 1400

Controlled Fusion Research—an Application of the Physics of High-Temperature Plasmas—R. F. Post. (PROC. IRE, vol. 45, pp. 134–160; February, 1957. *Rev. Mod. Phys.*, vol. 28, pp. 338–362; July, 1956.) A review of the implications and the physical conditions required for the generation of power from controlled fusion reactions. It is suggested that the fusion fuel may exist in the form of a plasma confined by, say, a magnetic field and the electrodynamic properties of such a system are investigated.

538.114 1401

Ferromagnetic Sphere in a Strong Field—B. M. Fradkin. (*Zh. Tekh. Fiz.*, vol. 26, pp. 1048–1059; May, 1956.) Magnetic induction in the sphere, remagnetization of a previously magnetized sphere, and the magnetic moment of the sphere are investigated, taking account of the demagnetizing effect of the surface. The hysteresis loops are approximated by rectangles.

538.3 1402

New Approach to the Quantum Theory of the Electron—H. C. Corben. (*Phys. Rev.*, vol. 104, pp. 1179–1185; November 15, 1956.) A theoretical treatment of quantized fields avoiding expansion in plane waves, relates free-electron theory to Maxwell's equations, the Dirac neutrino equation, and motion in an em field.

538.561:537.534.8 1403

Emission of Electromagnetic Radiation by the Impact of Positive Ions of Hydrogen on Metal Surfaces—R. M. Chaudhri, M. Y. Khan, and A. L. Taseer. (*Phys. Rev.*, vol. 104, pp. 1492–1493; December 1, 1956.) One photon is emitted from a nickel surface for about 10^8 incident protons of energy 300–3000 ev. The wavelength of the radiation lies between 3300 and 4000 amp.

538.561:539.185:539.154.3 1404

Cherenkov Radiation of Neutral Particles with a Magnetic Moment—N. L. Balazs. (*Phys. Rev.*, vol. 104, pp. 1220–1222; December 1, 1956.) The Cherenkov radiation caused by magnetic and electric dipoles is calculated. In the visible spectrum the energy loss per unit path per unit frequency range for a neutron is 10^{-15} that for an electron.

538.566 1405

Exterior Electromagnetic Boundary-Value Problems for Spheres and Cones—L. L. Bailin and S. Silver. (IRE TRANS., vol. AP-4, pp. 5–16; January, 1956.) For abstract, see PROC. IRE, vol. 44, p. 715; May, 1956.

538.566 1406

Fields in Imperfect Electromagnetic Anechoic Chambers—R. F. Kolar. (*RCA Rev.*, vol. 17, pp. 393–409; September, 1956.) A method is presented for predicting the performance of anechoic chambers from transmission-line measurements on small samples of the absorbent material used for the walls. The calculated results are supported by measurements made in front of a wall 12 feet square.

538.566:535.43]+534.26 1407

High-Frequency Scattering—T. T. Wu. (*Phys. Rev.*, vol. 104, pp. 1201–1212; December 1, 1956.) Scattering by a circular cylinder and by a sphere is treated by considering the creeping waves on the universal covering space. This enables the total scattering cross section of the obstacle to be found; but the method can be extended to give additional results, such as the current distribution on the obstacle.

538.566:535.43 1408

Approximation Method for Short Wavelength or High-Energy Scattering—L. I. Schiff. (*Phys. Rev.*, vol. 104, pp. 1481–1485; December 1, 1956.) "The approximation method developed in a recent paper [*ibid.*, vol. 103, pp. 443–453; July 15, 1956] is extended to the scattering theory of Maxwell's equations and of the Schrödinger equation with spin-orbit interaction."

538.566:535.43 1409

Back-Scattering for Arbitrary Angles of Incidence of a Plane Electromagnetic Wave on a Perfectly Conducting Spheroid with Small Eccentricity—Y. Mushiake. (*J. Appl. Phys.*, vol. 27, pp. 1549–1556; December, 1956.) The scattering of a plane em wave by a perfectly conducting spheroid with small eccentricity is treated by expanding the scattered field in a series of spherical vector wave functions. An expression for the first-order solution of the back scattered field is obtained for arbitrary angles of incidence of a plane wave. The numerical values of echo areas computed from the first-order expression are shown for various cases and rough experimental results are discussed.

538.612 1410

A Theory of Magnetic Double Refraction—A. D. Buckingham and J. A. Pople. (*Proc. Phys. Soc., London*, vol. 69, pp. 1133–1138; November 1, 1956.) A theory of the birefringence produced in a substance perpendicular to a strong magnetic field.

538.63 1411

Theory of Galvanomagnetic Phenomena in Metals—I. M. Lifshits, M. Ya. Azbel', and M. I. Kaganov. (*Zh. Eksp. Teor. Fiz.*, vol. 31, pp. 63–79; July, 1956.) A theory for metals in strong magnetic fields is presented; no special assumptions regarding the law of conduction, electron dispersion, or the form of the collision integral are made.

GEOPHYSICAL AND EXTRATERRESTRIAL PHENOMENA

523.16:621.396.677 1412

Two-Dimensional Aerial Smoothing in Radio Astronomy—R. N. Bracewell. (*Aust. J. Phys.*, vol. 9, pp. 297–314; September, 1956.) Theory developed previously for the one-dimensional case [1638 of 1955 (Bracewell and Roberts)] is generalized. The basic processes of interpolating and filtering data are discussed.

Details of technique for the restoration of smoothed data are presented. The flux density of a source is shown to be given exactly by summing one in four of the isolated values observed at the "peculiar intervals" associated with the Fourier components of the spatial temperature distribution.

523.165 1413

Effects of a Ring Current on Cosmic Radiation. Impact Zones—E. C. Ray. (*Phys. Rev.*, vol. 104, pp. 1459–1462; December 1, 1956.) An investigation of the effects of a ring current on the "0900" (geomagnetic local time) impact zone of flare-associated increases in cosmic-ray intensity has been carried out for 55 trajectories. For particles of rigidities 2, 6, and 10 kmv traveling vertically towards the earth, the longitude of impact may be shifted by ring currents by up to half an hour.

523.165:523.75 1414

Time Variations of Cosmic-Ray Intensity—R. R. Brown. (*J. Geophys. Res.*, vol. 61, pp. 639–646; December, 1956.) "The time variations of cosmic-ray intensity associated with a large solar flare and a period of strong solar activity are reported. A possible interpretation of these semiregular time variations in terms of matter emanating from the sun is considered."

523.5:621.396.11 1415

Phase Changes and Resonance Effects in Radio Echoes from Meteor Trails—J. S. Greenhow and E. L. Neufeld. (*Proc. Phys. Soc., London*, vol. 69, pp. 1069–1076, plate; November 1, 1956.) A discussion of the resonance effects which occur when the ionization column has diffused to such a diameter that the dielectric constant at the center reaches -1.4. The measurements are in good agreement with the phase changes predicted by the theory of scattering of radio waves from meteor trails.

523.5:621.396.11:551.510.535 1416

Long-Range Meteoric Echoes via F-Layer Reflections—J. T. deBettencourt and W. A. Whitcraft, Jr. (IRE TRANS., vol. AP-4, pp. 72–76; January, 1956.) For abstract, see PROC. IRE, vol. 44, p. 716; May, 1956.

523.5:621.396.11.029.62:551.510.535 1417

A Theory of Long-Duration Meteor-Echoes Based on Atmospheric Turbulence with Experimental Confirmation—H. G. Booker and R. Cohen. (*J. Geophys. Res.*, vol. 61, pp. 707–733; December, 1956.) The theory assumes that a meteor trail is rendered rough by the action of small eddies in the atmosphere. If loss of electrons from the trail is neglected, the field strength of a long-duration meteor echo in its decay phase should be inversely proportional to the cube of time subsequent to formation of the trail. This is verified experimentally in the early part of the decay. Measurements of the frequency dependence of the echo are related to the results of vhf ionospheric scatter transmission. An important part of the phenomenon of radio echoes from meteor trails has itself to be interpreted in terms of incoherent scattering, due to atmospheric turbulence.

523.72.029.6:523.75 1418

On the Association of Solar Radio Emission and Solar Prominences—J. P. Wild and H. Zirin. (*Aust. J. Phys.*, vol. 9, pp. 315–323; September, 1956.) Cinematograms of prominences made during the years 1949–1955 have been compared with records of solar radiation at 167 mc. No close correlation was found between limb events and variations of rf radiation, but some eruptions were found to be associated with simultaneous radio bursts. Three such cases are discussed in detail. A study of the limb passages of large sunspots indicated that spot groups showing looped prominences and downward streaming from the corona tended to produce radio noise storms. This result is ascribed to the fact that the seat of such storms must lie in the corona and in the presence of strong ordered magnetic fields.

523.752:537.56:538.6 1419

Simulation of Solar Prominence in the Laboratory—W. H. Bostick. (*Phys. Rev.*, vol. 104, pp. 1191–1193; November 15, 1956.) Two plasma sources having an electric potential difference were located at the poles of a horseshoe magnet at a pressure $\sim 30\mu$ Hg. A plasma glow is formed at each source with streamers following the magnetic field between sources. The streamers resemble the curved solar prominences between two sunspots of opposite magnetic characteristics as in Alfven's theory (*Cosmical Electrodynamics*, p. 88, 1950), but with current flowing along the prominence. The theory of streamer formation is mentioned briefly.

550.383 1420

Measurements at Sea of the Vertical Gradient of the Main Geomagnetic Field during the *Galathea* Expedition—J. Esbersen. P. Andreasen, J. Egedal, and J. Olsen. (*J. Geophys. Res.*, vol. 61, pp. 593–624; December, 1956.) Three relative self-recording magnetometers were lowered to depths of 500 to 5000 m to test the fundamental theory of Blackett for the main geomagnetic field. Trial results were against the theory—in accordance with gradient measurements in mines.

550.384 1421

The Lunar-Diurnal Magnetic Variation and its Relation to the Solar-Diurnal Variation—J. Egedal. (*J. Geophys. Res.*, vol. 61, pp. 748–749; December, 1956.) An abnormally large lunar-diurnal variation of the vertical magnetic component was found to exist at Amberley, New Zealand, during the night hours.

550.385 1422

On the Geomagnetic Storm Effect—E. N. Parker. (*J. Geophys., Res.*, vol. 61, pp. 625–637; December, 1956.) The high electrical conductivity of the region around the earth invalidates customary models for producing storm fields with impressed current systems. The main phase of a storm implies upward displacement of magnetic lines of force. Two models are developed quantitatively, based on heating of the upper atmosphere and on gravitational capture of interplanetary hydrogen.

550.385 1423

Notes on the Morphology of SC [sudden commencements]—T. Oguti. (*Rep. Ionosphere Res. Japan*, vol. 10, pp. 81–90; June, 1956.)

550.385:551.510.535 1424

Studies on P.S.C. [polar sudden commencements]—Y. Kato and T. Watanabe. (*Rep. Ionosphere Res. Japan*, vol. 10, pp. 69–79; June, 1956. Discussion pp. 79–80.) "Facts obtained from observation of psc suggest that its origin is outside the ionosphere. Particularly, the daily behavior of the horizontal perturbing vector of psc can be explained by the shielding effect of the nonuniform ionosphere."

550.389 1425

A Method of Interpolating Magnetic Data under Conditions of Mutual Consistency—A. J. Zmuda and J. F. McClay. (*J. Geophys. Res.*, vol. 61, pp. 667–672; December, 1956.) Rigorous relations connecting surface variations of different elements are introduced into interpolation formulas needed with discrete data, so that resulting charts are mutually consistent.

551.510.53:551.593 1426

Distribution in the Upper Atmosphere of Sodium Atoms Excited by Sunlight—T. M. Donahue, R. Resnick, and V. R. Stull. (*Phys. Rev.*, vol. 104, pp. 873–879; November 15, 1956.) Theoretical calculations of the density of sodium atoms in the $^2P_{3/2}$ state at 70–100 km, taking into account the effect of resonance absorption on direct and earth-reflected radiation.

551.510.53:551.593 1427

A Calculation of the Sodium Dayglow Intensity—T. M. Donahue. (*J. Geophys. Res.*, vol. 61, pp. 663–666; December, 1956.) Calculation of the resonance scattering from a sodium layer between 70 and 100 km is based on the density of sodium excited by the sun.

551.510.53:551.593 1428

On the Remarks of D. R. Bates and B. L. Moiseiwitsch (1956) regarding the O_3 and [excited] O_1 Hypotheses of the Excitation of the OH Airglow—V. I. Krassovsky. (*J. Atmos. Terr. Phys.*, vol. 10, pp. 49–51; January, 1957.) Comment on paper noted in 3042 of 1956.

551.510.535 1429

A Dynamo Theory of the Ionosphere—M. Hirono and T. Kitamura. (*J. Geomag. Geoelect.*, vol. 8, pp. 9–23; March, 1956.) The differential equations of the dynamo theory are solved by numerical integration, taking account of the daily variation of the anisotropic conductivity. It is shown that the observed magnitude of the winds in the E region is consistent with the requirements of the dynamo theory and that at night some part of the electrons in the lower F region will descend into the E region in middle latitudes.

551.510.535 1430

Observation at Akita of Ionospheric Drift—Y. Ogata. (*Rep. Ionosphere Res. Japan*, vol. 10, pp. 91–92; June, 1956.)

551.510.535 1431

Ionosphere Electron-Density Measurements with the Navy Aerobee-HI Rocket—J. E. Jackson, J. A. Kane, and J. C. Seddon. (*J. Geophys. Res.*, vol. 61, pp. 749–751; December, 1956.) A description of electron-density measurements made on June 29, 1956, from the E region up to the lower F_2 region, above White Sands, New Mexico.

551.510.535 1432

Studies of the E Layer of the Ionosphere: Part 1—Some Relevant Theoretical Relationships—E. V. Appleton and A. J. Lyon. (*J. Atmos. Terr. Phys.*, vol. 10, pp. 1–11; January, 1957.) The Chapman continuity equation refers to electron density at constant height, whereas measurements refer to the peak of a layer and require some modification of the equation (see *The Physics of the Ionosphere*, p. 20, 1955). The theory is now extended to include changes in Chapman's basic assumptions. The following have been investigated: *a*) vertical gradients in the scale height of the ionized gas and the effective recombination coefficient, *b*) loss of electrons by attachment, and *c*) the introduction of a vertical transport term.

551.510.535 1433

Ionospheric Reflections from Heights Below the E Region—J. B. Gregory. (*Aust. J. Phys.*, vol. 9, pp. 324–342; September, 1956.) Observations were made during the period February–July, 1955, using high-sensitivity pulse equipment operating at 1.75 mc and capable of detecting low ionospheric regions with voltage reflection coefficients exceeding 4×10^{-6}. Daytime reflections were received from several levels between 95 and 53 km, and continuous reflections from a region with a lower boundary at about 85 km. The frequency of occurrence and the strength of these lower-level reflections

increase markedly during winter. Correlation between decrease in strength of E-region reflections and increase in strength of lower-level reflections is demonstrated from records of high absorption conditions during winter days.

551.510.535 1434

Cusp-Type Anomalies in Variable-Frequency Ionospheric Records—G. H. Munro and L. H. Heisler. (*Aust. J. Phys.*, vol. 9, pp. 343–358; September, 1956.) "Anomalous cusps which frequently appear at the high-frequency end of ionosonde records of the F_2 region are explained as the result of modification of the ion distribution during the passage of typical traveling disturbances. They indicate the presence, not of vertical stratification, but of horizontal gradients of ionization causing oblique reflection. It is suggested that other anomalous cusps are of similar origin. Anomalies on records of the F_1 region are also shown to be caused by traveling disturbances."

551.510.535 1435

Divergence of Radio Rays in the Ionosphere—G. H. Munro and L. H. Heisler. (*Aust. J. Phys.*, vol. 9, pp. 359–372; September, 1956.) Traveling disturbances in the ionosphere are investigated by examining the differences between the traces for the ordinary and extraordinary rays on $h'f$ and $h't$ records. Results of numerous observations confirm the theoretical prediction of the divergence of the two rays in the F region at Sydney, Australia, indicating an actual separation of the order of 30 km near the maximum of ionization. They also indicate that a traveling disturbance always has an apparent vertical component of progression, assumed to result from a forward tilt in the front of the disturbance.

551.510.535:523.51 1436

Meteorite Impacts to Altitude of 103 Kilometres—O. E. Berg and L. H. Meredith. (*J. Geophys. Res.*, vol. 61, pp. 751–754; December, 1956.) A new type of meteorite-impact detector is described. Above 85 km one impact per cm^2 per 57 seconds was recorded.

551.510.535:523.78 1437

Drift Measurement of the E Layer during the Solar Eclipse 30 June 1954—L. Harang and K. Pederson. (*J. Atmos. Terr. Phys.*, vol. 10, pp. 44–45; January, 1957.) An apparent change in direction was due to the changeover from normal E to E_s reflections at the maximum phase of the eclipse.

551.510.535:538.566 1438

The Scattering of Electromagnetic Waves by Plasma Oscillations—Hokkyo. (See 1565.)

551.510.535:550.385 1439

Disturbances in the F_2 Region of the Ionosphere associated with Geomagnetic Storms—T. Sato. (*Rep. Ionosphere Res. Japan*, vol. 10, pp. 35–48; June, 1956.) The extent to which these variations in the F_2 region can be accounted for as resulting from vertical drift of electrons is examined in relation to geomagnetic observations at Watheroo.

551.510.535:550.385 1440

Daily Variations of the Electrical Conductivity of the Upper Atmosphere as deduced from the Daily Variations of Geomagnetism: Part 2—Non-equatorial Regions—H. Maeda. (*Rep. Ionosphere Res. Japan*, vol. 10, pp. 49–68; June, 1956.) Results of previous studies are interpreted from the point of view of the anisotropy of ionospheric conductivity. A formula for the world distribution of ionospheric conductivity is proposed. Part 1: 1719 of 1956.

551.510.535:621.396.11 1441

Turbulence in the Ionosphere with Applications to Meteor Trails, Radio-Star Scintillation, Auroral Radar Echoes, and Other Phenomena—H. G. Booker. (*J. Geophys. Res.*, vol. 61, pp. 673–705; December, 1956.) Irregularities in electron density responsible for incoherent scattering of radio waves in the ionosphere are discussed, assuming isotropic turbulence in the neutral molecules, with allowance for the effect of the earth's magnetic field on associated irregularities in the density of the charged particles. The atmospheric model used is based on rocket observations. Tentative formulas deduced for large and small eddies, depend on a quantity w, which is the rate of supply of turbulence energy to the large eddies and also the rate of removal of turbulence energy from the small eddies, measured per unit mass of atmosphere. Resulting values of w are higher in the ionosphere than the troposphere, but are shown to be possible and reasonable. Among other applications considered is the possibility of radio communication via incoherent scattering in the F region. Forty three references.

551.510.535:621.396.11 1442

The Absorption of Short Radio Waves in the Ionosphere—J. D. Whitehead. (*J. Atmos. Terr. Phys.*, vol. 10, pp. 12–19; January, 1957.) Measured reflection coefficients (ρ) in England for frequencies (f) in the range 2–4 mc can be represented by $-\log \rho = C + B/(f+f_L)^2$. C varies with solar zenith angle, but B does not, whereas B depends on solar activity, while C does not. B is very variable and controls the abnormally high winter absorption. Since C is not zero, appreciable absorption must occur outside the nondeviating region.

551.510.535:621.396.11 1443

The Nondeviative Absorption of High-Frequency Radio Waves in Auroral Latitudes—S. Chapman and C. G. Little. (*J. Atmos. Terr. Phys.*, vol. 10, pp. 20–31; January, 1957.) This is higher and more variable than absorption at lower latitudes. It is also much less patchy than auroral forms would indicate if auroral particles were directly responsible for it. It is suggested that slow-speed auroral particles cause direct ionization down to about 80–90 km and that they may also generate X rays which penetrate down to 80 or even 40 km, to cause ionization and nondeviative absorption at high latitudes. The mechanism is investigated and tentative tables of data are given.

551.510.535:621.396.11 1444

Some Measurements of Ionospheric Absorption at Delhi—S. N. Mitra and S. C. Mazumdar. (*J. Atmos. Terr. Phys.*, vol. 10, pp. 32–43; January, 1957.) "The results of some measurements of ionospheric absorption taken at Delhi during June, 1954 to December, 1955 are described. The measurements were carried out on 5 and 2.5 mc. A brief description of the experimental setup is included in the paper. The analysis of data shows that the diurnal variation of absorption gives $|\log \rho| \propto |(\cos \psi) f^{0.62}$. The value of αN has been indicated from the observed value of the "relaxation time." The absorption at night has been observed to be considerable at our latitude. It has been postulated from the low value of the exponent in the diurnal variation factor, the magnitude of the relaxation time, and from direct measurements of absorption on E_s and F echoes, that the main absorption is probably taking place in the D region."

551.510.535:621.396.11 1445

Simultaneous Signal-Strength Measurements on Continuous and Pulsed Radio-Wave Transmissions Reflected from the Ionosphere—Rao and Ramana. (See 1568.)

551.510.535:621.396.11:523.75 1446

Ionospheric Absorption Observed on the 23rd February 1956 at Kjeller and Tromsö—F. Lied. (*J. Atmos. Terr. Phys.*, vol. 10, p. 48; January, 1957.) Absorption was abnormally high during daylight.

551.510.535"1956":621.396.11 1447

Ionosphere Review, 1956—T. W. Bennington. (*Wireless World*, vol. 63, pp. 145–146; March, 1957.) The rapid increase in solar activity during 1956 is related to corresponding changes in ionospheric critical frequencies and radio communications.

551.594.21 1448

Initial Electrification Processes in Thunderstorms—R. Gunn. (*J. Met.*, vol. 13, pp. 21–29; February, 1956.) An analysis of thunderstorm electrification processes in clouds entirely above freezing temperature leads to a quantitatively correct explanation of the principal observed features of the earliest phases of electrification.

551.594.5 1449

The Aurora in Middle and Low Latitudes—S. Chapman. (*Nature, London*, vol. 179, pp. 7–11; January 5, 1957.) A brief review of reports on the occurrence of the aurora in the lower latitudes with a note on the I.G.Y. program of observations.

551.594.5 1450

On the Energy Distribution of Secondary Auroral Electrons—D. R. Bates, M. R. C. McDowell, and A. Omholt. (*J. Atmos. Terr. Phys.*, vol. 10, pp. 51–53; January, 1957.) The result of calculations on the impact of protons on neon.

551.594.6 1451

The Recording of the Mean Level of Atmospherics at Kilometre and Myriametre Wavelengths—F. Carbenay. (*C.R. Acad. Sci., Paris*, vol. 243, pp. 1904–1906; December 5, 1956.) Records obtained at Bagneux on a wavelength of 11 km are reproduced. Comparison of records of mean level and of successive peaks, obtained with receivers of different bandwidths, indicates that the atmospherics have the properties of short pulses, defining the operating threshold of the receiver.

551.594.6:621.396.11.029.4 1452

Low-Frequency Electromagnetic Radiation 10–900 Cycles per Second—J. Aarons. (*J. Geophys. Res.*, vol. 61, pp. 647–661; December, 1956.) The spectrum of atmospherics received on a site remote from man-made interference was analyzed with a narrow-band (2–6 cps) amplifier. Diurnal patterns show a maximum around local midnight, with a peak in the band between 40 and 200 cps. Radiation at the gyrofrequency of the sodium ion may have given an increase in narrow-band energy near 33 cps, observed for several hours. A hypothesis for the origin of the "dawn chorus" is presented.

551.594.6:621.396.11.029.4 1453

Extremely-Low-Frequency Electromagnetic Waves: Part 1—Reception from Lightning; Part 2—Propagation Properties—L. Liebermann. (*J. Appl. Phys.*, vol. 27, pp. 1473–1483; December, 1956.) The received fields, at frequencies below 500 cps and distances of several thousand kilometres were observed by recording waveforms of atmospherics. Two main types of waveform were found. Diurnal variations in propagation were small. Waveforms of atmospherics were examined in terms of waveguide theory. Only one of the two main types considered could be explained by using a simple model for the earth-ionosphere waveguide. The conductivity of the ionosphere and variations in absorption were deduced.

LOCATION AND AIDS TO NAVIGATION

621.396.932 1454

The Analysis of Radio Bearings in the Presence of Rotating Fields—H. Gabler, G. Gresky, and M. Wächtler. (*Arch. elekt. Übertragung*, vol. 10, pp. 383–391; September, 1956.) The influence of out-of-phase reflections on the indication of a cro direction finder is similar to the effects of in-phase reflections causing the main bearing error. Experiments on board the research ship "Gauss" confirm the theoretical results.

621.396.932 1455

A New Ship's Direction-Finder with Visual Indication: Telegon III—A. Troost. (*Telefunken Ztg*, vol. 29, pp. 109–116; June, 1956. English summary, pp. 134–135.) The system described uses a new type of "magic eye" indicator, which shows two luminous lines of equal length for the minimum-signal setting of the goniometer. Aural balance indication is also available. For description of the original Telegon, see 139 of 1952 (Runge, et. al.).

621.396.96 1456

Radar Back-Scattering Cross-Sections for Nonspherical Targets—P. N. Mathur and E. A. Mueller. (IRE TRANS., vol. AP-4, pp. 51–53; January, 1956.) For abstract, see PROC. IRE, vol. 44, p. 715; May, 1956.

621.396.96 1457

Radar Terrain Return at Near-Vertical Incidence—R. K. Moore and C. S. Williams, Jr. (PROC. IRE, vol. 45, pp. 228–238; February, 1957.) A mathematical analysis of the backscatter of radiation pulses from the ground, with particular reference to the deformation of the pulses. Results are applicable to radio altimeters.

621.396.96.029.6:551.578 1458

The Effect of "Hydrometeors" on Centimetre Waves—B. Abild. (*Elektronische Rundschau*, vol. 10, pp. 249–252; September, 1956.) The term "hydrometeors" is used to indicate regions of precipitation in the atmosphere. Reflection and attenuation effects occurring at these regions are discussed with reference to their dependence on wavelength. For observations on clouds, the optimum operating wavelength for radar equipment is around 5 mm. Technical data are tabulated for British and U.S. commercially available 3-cm-λ weather radar equipment, and an outline is given of investigations in Germany.

MATERIALS AND SUBSIDIARY TECHNIQUES

535.215:546.23:537.533.9 1459

Volume Generated Currents and Secondary Effects in Amorphous Selenium Films—W. E. Spear. (*Proc. Phys. Soc., London*, vol. 69, pp. 1139–1147; November 1, 1956.) The films, between 3 and 9μ thick, were subjected to electron bombardment, and the resulting current was studied in relation to the average depth of penetration of the bombarding beam.

535.215:546.482.21 1460

Photoelectron Emission from CdS—Yu. A. Shuba. (*Zh. Tekh. Fiz.*, vol. 26, pp. 1129–1135; May, 1956.) The object of this experimental investigation was to obtain data on the energy structure and the mechanism of the interaction between light and electrons in CdS. The results give support to the concept of the exciton mechanism of the interaction and indicate that the photoelectric constants of the material may vary during photoelectron emission.

535.215:547.9 1461

Photo- and Semi-conduction of Aromatic Hydrocarbon Crystals—L. E. Lyons and G. C. Morris. (*Proc. Phys. Soc., London*, vol. 69, pp. 1162–1164; November 1, 1956.) A discussion of the spectral dependence of the photocurrent in a series of compounds not previously known to be photoconductors.

535.37 1462

The Luminescence of Inorganic Crystalline Substances—(*J. Phys. Radium*, vol. 17, pp. 609–832; August/September, 1956.) This issue is devoted to papers presented and discussed at an international conference in Paris, France, in May, 1956. Short abstracts in English are given. Recent experimental work on the effects of chemical composition and external influences is analyzed to illustrate or modify various theories regarding the mechanism of luminescence. The following papers are included:

The Luminescence of Electronically Active Solids—H. W. Leverenz (pp. 612–615).

The Photoluminescence of Calcium Metaantimoniate Activated with Bismuth—R. Bernard and J. Janin (pp. 616–619).

Some Observations on Energy Transfer in Halophosphates—J. L. Ouweltjes (pp. 641–644).

The Intensification Effect due to Metals of the Iron Group and the Height of the Fermi Level in Luminescent Sulphides—N. Arpiarian (pp. 674–678).

The Luminescence Efficiency of Crystal Phosphors—V. V. Antonov-Romanovsky (pp. 694–698).

Theoretical and Experimental Investigations of some Properties of Electron Traps and Luminescent Centres in Sulphides—D. Curie (pp. 699–704).

Infrared Emission from Germanium—P. Aigrain and C. Benoit à la Guillaume (pp. 709–711).

The Effect of the Field and Temperature on the Brightness Waveforms in Electroluminescence—J. Mattler (pp. 725–730).

The Spectral Distribution of the Electroenhancement Effect in CdS-ZnS Mixtures Activated by Manganese and Silver—G. Destriau (pp. 734–736).

The Intensification and Quenching of Luminescence in Manganese-Activated Zinc Sulphides by Alternating Electric Fields—H. Gobrecht and H. E. Gumlich (pp. 754–757).

The Mechanism of Electroluminescence—R. Goffaux (pp. 763–768).

Electroluminescent Capacitors in Oscillatory Circuits—A. Luyckx, M. Weiler, and A. J. Stokkink (pp. 769–772).

Electrical and Optical Properties of some Semiconductors: Zinc Oxide, Zinc Sulphide, Selenium—R. Freymann, Y. Balcou, M. L. Blanchard, H. Corneteau, M. Freymann, B. Hagène, M. Hagène, M. LePage, J. Meinnel, and R. Rohmer (pp. 806–812).

535.37 1463

Solid-State Luminescence Theory and Oscillator Strengths in KCl:Tl—R. S. Knox and D. L. Dexter. (*Phys. Rev.*, vol. 104, pp. 1245–1252; December 1, 1956.) Comparison of experimental and theoretical results indicates defects in the existing quantitative theory.

535.37 1464

Cathodoluminescence Spectra of Alkali Halides—B. D. Saksena and L. M. Pant. (*Z. Phys.*, vol. 146, pp. 205–216; September 14, 1956. In English.)

535.37:546.472.21 1465

Luminescence in ZnS:Cu,Cl Single Crystals—T. B. Tomlinson. (*J. Electronics*, vol. 2, pp. 293–300; November, 1956.) The impurity responsible for the green and blue bands in "spectrographically pure" single crystals of ZnS is proved to be Cu, in the presence of Cl.

535.37:546.472.21 1466

Flashes of Luminescence in Zinc-Sulphide Phosphors and the Two-Stage Excitation Mechanism—N. A. Tolstoi. (*C.R. Acad. Sci. U.R.S.S.*, vol. 111, pp. 582–584; November 21, 1956. In Russian.)

535.376 1467

Electroluminescence—D. W. G. Ballentyne. (*Wireless World*, vol. 63, pp. 128–132; March, 1957.) Sustained emission of light can be obtained from an unexcited phosphor by suspending it in the dielectric of a capacitor to which an alternating field is applied. Recent progress is described and possible applications to illumination, television, and storage of binary-code numerical data are discussed briefly. For full paper, see *Marconi Rev.*, vol. 19, pp. 160–175; 4th Quarter, 1956.

537.226/.228.1:546.431.824–31 1468

The Effect of the Polarization Conditions on the Piezoelectric Properties of Barium Titanate—S. V. Bogdanov, B. M. Vul, and R. Ya. Razbash. (*Zh. Tekh. Fiz.*, vol. 26, pp. 958–962; May, 1956.) Polycrystalline $BaTiO_3$ elements must be polarized in a strong dc field. With specimens of appreciable thickness (15–25 mm), fields of the order of 30–50 kv/cm have to be used, with the attendant inconvenience and possible damage to the specimen. Lower polarizing voltages can be used if the temperature at which polarization is carried out is raised; the dielectric strength is not affected (Vul, *et al.*, *Zh. Eksp. Teor. Fiz.*, vol. 20, pp. 465–470; May, 1950). This has been confirmed experimentally; but even at temperatures approaching the Curie point, the polarizing voltage should not be below 5 kv/cm.

537.226/.227 1469

Dynamic Theory of the Ion Lattices of Ferroelectric Crystals in Static Conditions—V. Kh. Kozlovski. (*Zh. Tekh. Fiz.*, vol. 26, pp. 963–976; May, 1956.)

537.226/.227 1470

Thiourea, a New Ferroelectric—A. L. Solomon. (*Phys. Rev.*, vol. 104, p. 1191; November 15, 1956.) Crystals are orthorhombic at room temperature. With electrodes on (010) faces, a pronounced dielectric anomaly is found at $-104.8°C$. The coercive field is less than 1000 v/cm at 60 cps and $-110°C$.

537.226/.227:546.431.824–31 1471

Discontinuous Field-Induced Transitions in Barium Titanate Above the Curie Point—M. E. Drougard. (*J. Appl. Phys.*, vol. 27, pp. 1559–1560; December, 1956.)

537.226/.227:546.431.824-31 1472

Dielectric Losses and Electrical Conductivity of Barium Titanate Ceramics Cooled Below the Phase Transition at 120°C—J. Meisinger. (*Z. angew. Phys.*, vol. 8, pp. 422–424; September, 1956.) Measurements were made on specimens of pure $BaTiO_3$ and on specimens including CrO_3 or WO_3 cooled rapidly from 500°C to room temperature. Losses were observed to be high immediately after the cooling process, but decreased exponentially with time, the decrease being more rapid with higher storage temperatures up to 80°C.

537.226 1473

Conference on the Electrical and Physicochemical Properties of Solid Dielectrics [Tomsk, September 1955]—S. S. Gutin. (*Uspekhi Fiz. Nauk*, vol. 59, pp. 755–763; August, 1956.) Report on over thirty papers presented at the conference.

537.311.31:621.396.822 1474

Noise in Metallic Conductors—H. Bittel and K. Scheidhauer. (*Z. angew. Phys.*, vol. 8,

pp. 938–948; September, 1956.) Measurements have been made at temperatures from 63° to 90°K. The long-wave limit of spectral response and the bulk electrical properties are both consistent with an ionization energy of 0.16 ev for the In centres. An apparent variation of quantum efficiency in the range 5–8 μ is noted. The results suggest an effective recombination coefficient of about 10^{-6} cm^3 at 90°K, rising steeply on cooling; this demands a much more active recombination mechanism than is provided by existing theories.

537.311.33:546.281.26 1494
Observation at Low Temperature of the Debye Dipolar Absorption of SiC: Levels Near 0 01 to 0.03 eV—M. Freymann, R. Goffaux, M. Hagène, and J. LeBot. (*C.R. Acad. Sci., Paris*, vol. 243, pp. 2048–2050; December 17, 1956.)

537.311.33:546.289 1495
The Measurement of Drift Mobility in Germanium at High Electric Fields—A. F. Gibson and J. W. Granville. (*J. Electronics*, vol. 2, pp. 259–266; November, 1956.) The emitter and collector contacts of a conventional drift-mobility specimen are replaced by a light-spot and a section of waveguide respectively. The increase in microwave absorption due to the injected carriers is used as a measure of their density. The technique may be used advantageously at high electric field strengths and when the minority-carrier lifetime is small. An experimental value of 5.8×10^{-6} cm sec^{-1} is determined for the saturated drift velocity of electrons in Ge.

537.311.33:546.289:535.215 1496
The Stationary Distribution of Excess Charge Carriers in Germanium during its Partial Illumination—S. V. Bogdanov. (*Zh. Tekh. Fiz.*, vol. 26, pp. 917–926; May, 1956.) Unidimensional analysis is presented for a thin homogeneous specimen of Ge partly illuminated. Surface recombination is neglected. The distribution of excess carriers in the illuminated and nonilluminated regions is determined; it obeys an exponential law. The associated space charge and internal field are also determined. A potential difference is set up between the illuminated and nonilluminated parts which increases with illumination, diffusion length, and specific resistance.

537.311.33:546.3-1-289-28 1497
Conduction Band Structure of Germanium-Silicon Alloys—M. Glicksman and S. M. Christian. (*Phys. Rev.*, vol. 104, pp. 1278–1279; December 1, 1956.) Galvanomagnetic measurements at room temperature show that in alloys with Si content greater than 23 per cent the electronic conduction takes place in energy minima which are spheroids oriented along the [100] axes in the reduced zone.

537.311.33:546.431–31:621.385.032.216 1498
Electrical Conductivity of Barium Oxide Single Crystals as a Function of Temperature and Excess Barium Density—R. T. Dolloff. (*J. Appl. Phys.*, vol. 27, pp. 1418–1426; December, 1956.)

537.311.33:546.561–31 1499
Linear and Quadratic Zeeman Effects and the Diamagnetism of the Exciton in a Cuprous Oxide Crystal—E. F. Gross and B. P. Zakharchenya. (*C.R. Acad. Sci. U.R.S.S.*, vol. 111, pp. 564–567; November 21, 1956. In Russian.)

537.311.33:546.873.221 1500
Electrical Properties of Bismuth Chalcogenides: Part 1—Electrical Properties of Bismuth Sulphide Bi_2S_3—P. P. Konorov. (*Zh. Tekh. Fiz.*, vol. 26, pp. 1126–1128; May, 1956.) The electrical conductivity and thermo-emf of polycrystalline compressed specimens was investigated over the range from room temperature to 600°K. The main conclusion reached is that the material is a typical semiconductor with an energy gap of 1 ev.

537.311.33:547:535.215 1501
Electrical Conductivity and Photoconductivity of Phthalocyanines—A. T. Vartanyan and I. A. Karpovich. (*C.R. Acad. Sci. U.R.S.S.*, vol. 111, pp. 561–563; November 21, 1956. In Russian.) Metal-free phthalocyanine (ph) and Cu-, Zn-, and Mg-phthalocyanine complexes were investigated. The specific conductivities of ph, ph-Cu, and ph-Zn, prepared by sublimation in vacuum and subsequent heat treatment at 200 degrees, are of the order of $10^{-12}-10^{-13}\Omega^{-1}.cm^{-1}$ at room temperature and increase with temperature according to the formula $\sigma=\sigma_0\exp(-\epsilon/2kT)$, where $\epsilon\approx1.7$–1.8ev. The conductivity of ph-Mg is about 10^5 times higher, due to oxygen impurity; $\epsilon\approx1.2$ev. Over the range 0 degrees–150 degrees the temperature dependence of the photocurrent is given by $i_{ph}=a\exp(-\epsilon_{ph}/2kT)$, where ϵ_{ph} lies between 0.5 and 0.65 ev. At temperatures below 0 degrees the law deviates from the exponential type. Optical activation energies lie between 1.53 and 1.61 ev, thermal activation energies being about 0.2ev higher.

537.311.33:621.314.7 1502
Grain-Boundary Transistors—H. F. Mataré. (*Elektronische Rundschau*, vol. 10, pp. 209–211, August; pp. 253–255; September, 1956.) Semiconductor crystal-lattice defects and the resulting grain boundaries are investigated (see also 3086 and 3764 of 1956). The artificial production of these conditions and their application in transistors are outlined. The electrical properties of the lattice defects were examined by means of special micromanipulating equipment described.

537.312.62 1503
Surface Energies in Superconductors—H. W. Lewis. (*Phys. Rev.*, vol. 104, pp. 942–947; November 15, 1956.) "A variational method is applied to calculate the surface energy at the normal/superconducting interface in a superconductor. Both the Casimir-Gorter theory, as formulated by Bardeen [*ibid.*, vol. 94, pp. 554–563; May 1, 1954], and the phenomenological energy-gap model are used. A comparison is made with the available experimental data."

537.312.62:534.23–8 1504
Ultrasonic Attenuation at Low Temperatures for Metals in the Normal and Superconducting States—W. P. Mason and H. E. Bömmel. (*J. Acoust. Soc. Amer.*, vol. 28, pp. 930–943; September, 1956.)

537.32:549.212 1505
Anisotropic Thermoelectric Effects in Graphite—A. R. Ubbelohde and J. Orr. (*Nature, London*, vol. 179, pp. 193–194; January 26, 1957.)

538.22 1506
Magnetic Structures of the Polymorphic Forms of Manganous Sulphide—L. Corliss, N. Elliott, and J. Hastings. (*Phys. Rev.*, vol. 104, pp. 924–928; November 15, 1956.) Measurements of neutron diffraction patterns and magnetic susceptibility of all three polymorphic forms. Possible lattice ordering schemes are discussed.

538.22:538.653.1 1507
Magnetic Susceptibility of NiO and CuO Single Crystals—J. R. Singer. (*Phys. Rev.*, vol. 104, pp. 929–932; November 15, 1956.) Measurements of changeover from isotropic to anisotropic susceptibility with mechanical stress during annealing.

538.221 1508
"Lozenge" and "Tadpole" Domain Structures on Silicon-Iron Crystals—L. F. Bates and P. F. Davis. (*Proc. Phys. Soc., London*, vol. 69, pp. 1109–1111, plates; November 1, 1956.)

538.221 1509
Investigation of Palladium-Nickel-Copper Ternary Alloys—J. Cohen. (*C.R. Acad. Sci., Paris*, vol. 243, pp. 1845–1847; December 5, 1956.)

538.221 1510
Influence of the Curie Point on the Oxidation of Magnetite Fe_3O_4, Iron, Nickel, and some Iron Alloys—L. Seigneurin and H. Forestier. (*C.R. Acad. Sci., Paris*, vol. 243, pp. 2052–2054; December 17, 1956.)

538.221:538.632 1511
Theory of Hall Effect in Ferromagnetics—N. S. Akulov and A. V. Cheremushkina. (*Zh. Eksp. Teor. Fiz.*, vol. 31, pp. 152–153; July, 1956.) Brief note on the theory presented by Karplus and Luttinger (698 of 1955). The discrepancy noted between the theoretical and experimental relations of the Hall constant and resistivity is attributed to the existence of a Hall effect of a second kind.

538.221:539.16 1512
Influence of Pile Irradiation on the Magnetic Properties of Zinc Ferrite—H. Forestier, G. Eischen, and G. Guiot-Guillain. (*C.R. Acad. Sci., Paris*, vol. 243, pp. 1842–1845; December 5, 1956.) Thermomagnetic analysis indicates the existence of a Curie-point effect in $ZnO.Fe_2O_3$ exposed to neutron bombardment. The effect disappears if the period of heat treatment is sufficiently prolonged.

538.221:539.23 1513
Resonance and Reversal Phenomena in Ferromagnetic Films—R. L. Conger and F. C. Essig. (*Phys. Rev.*, vol. 104, pp. 915–923; November 15, 1956.) Experimental results demonstrate the proportionality between magnetization reversal time and magnetic-resonance-absorption line width.

538.221:621.318.134 1514
The Permeability of Copper Ferrite in Rapidly Varying Fields: Effects in the Curie Region—K. Stierstadt. (*Z. Phys.*, vol. 146, pp. 169–186; September 14, 1956.) The temperature variation of the reversible permeability of various specimens of Cu ferrite was investigated at frequencies between 15 and 60 mc, using a resonance arrangement. The fine structure of the μ/T curves indicates that the magnetization process just below the Curie point is different from that at lower temperatures. The crystallographic transition of $Fe.CuFe.O_4$ at about 360°C and the reversible and irreversible formation of $Fe_2.CuFe_3.O_8$ are discussed in detail.

538.222 1515
The Magnetic Properties of Mg_2Sn—L. L. Korenblit and A. P. Kolesnikov. (*Zh. Tekh.Fiz.*, vol. 26, pp. 941–944; May, 1956.) An experimental investigation was carried out which showed that the paramagnetism of an impurity Mg_2Sn is most probably associated with the paramagnetism of the free electron gas in the Mg_2Sn crystal.

539.232 1516
Type of Ion Migration in a Metal/Metal-Oxide System—O. Flint and J. H. O. Varley. (*Nature, London*, vol. 179, pp. 145–146; January 19, 1957.) A technique is outlined for determining the nature of ion migration in a

small electric field at room temperature. Experiments were carried out on two Zr electrodes covered with thin oxide layers and separated by a sintered compact of zirconia.

539.234 1517
Electron-Diffraction Study of the Formation of Aluminium-Antimony Alloys as Thin Films—P. Michel. (*C. R. Acad. Sci., Paris*, vol. 243, pp. 2063–2065; December 17, 1956.) Films formed by the simultaneous or successive evaporation of Al and Sb were studied.

621.3.013.782:538.221 1518
Magnetic Shielding with Multiple Cylindrical Shells—W. G. Wadey. (*Rev. Sci. Instr.*, vol. 27, pp. 910–916; November, 1956.) Formulas are given for computing the shielding ratio for any number of concentric shells of contemporary high-permeability materials. Both static and alternating fields are considered; in the static case end-effect data are also given.

621.316.825 1519
Thermistors for High Temperatures—P. T. Oreshkin. (*Bull Acad. Sci. U.R.S.S., tech. Sci.*, no. 8, pp. 128–130; August, 1956. In Russian.) The electrical properties of oxides of Al, Mg, Zn and mixtures of Al and Mg oxides were investigated at temperatures of up to 1570 degrees. Results are presented graphically for Al_2O_3.

621.318.13:621.372.56.029.6 1520
Manufacture of Reduced Iron Powder for the Microwave Attenuator—A. Nishioka. (*Rep. elect. Commun. Lab., Japan*, vol. 4, pp. 16–19; August, 1956.) A grain size of less than 5μ was achieved by a method based on the reduction of ferric oxalate. The process is described and the prevention of oxidation is outlined. In another article (*ibid.*, pp. 33–36) the author discusses methods for the assessment of particle size distribution in such powders.

621.318.13:621.372.56.029.64 1521
Microwave Dissipative Material—M. Y. El-Ibiary. (*Electronic Radio Engr.*, vol. 34, pp. 103–107; March, 1957.) The material is made by loading a cold-setting resin with carbonyl-iron powder. The properties are controllable and reproducible. Measurements at 3 cm are compared with theory, but only qualitative agreement is found.

621.318.134:[537.226+538.22].029.6 1522
Ferrites with Low Losses at U.H.F.—R. G. Mirimanov, L. G. Lomize, and N. V. Ryumshina. (*Radiotekhnika i Elektronika*, vol. 1, pp. 681–682; May, 1956.) A brief note on ferrites containing some, or all, of the following: Fe_2O_3, MgO, MnC_2, and calcium titanate. The loss tangent, tan δ, is about 10^{-3} in the 3-cm-λ band, μ varies between about 0.4 and 0.9 for the different ferrites and ϵ between 6.9 and 38.

621.357.53:621.384.613 1523
On Internally Metallizing a Betatron Toroid by Vacuum Deposition—K. R. Allen, F. Ashworth, and G. Siddall. (*J. Sci. Instr.*, vol. 33, pp. 445–446; November, 1956.) The practical details given are generally relevant to the production of coatings on the internal surface of apparatus.

621.357.7 1524
Materials used in Radio and Electronic Engineering: Part 5—The Electrodeposition of Metals—(*J. Brit. IRE*, vol. 17, pp. 35–47; January, 1957.) A survey covering the uses of electroplated coatings, their principal features, treatment after plating, and the testing of the deposit. A summary of British Standards Institution and Ministry of Supply specifications is given.

MATHEMATICS

512.99 1525
Minimization of Boolean Functions—E. J. McCluskey, Jr. (*Bell Sys. Tech. J.*, vol. 35, pp. 1417–1444; November, 1956.)

512.99 1526
Detection of Group Invariance or Total Symmetry of a Boolean Function—E. J. McCluskey, Jr. (*Bell Sys. Tech. J.*, vol. 35, pp. 1445–1453; November, 1956.)

517.512.2 1527
A Simplified Procedure for Finding Fourier Coefficients—J. F. Gibbons. (PROC. IRE, vol. 45, p. 243; February, 1957.)

MEASUREMENTS AND TEST GEAR

621.317.18:621.373.421.1 1528
Grid-Dip Oscillator—H. B. Dent. (*Wireless World*, vol. 63, pp. 121–123; March, 1957.) A cr tuning indicator replaces the grid-current indicator. The instrument can be used up to 120 mc.

621.317.3:621.387.001.4 1529
Method of Tracing the Dynamic Control Characteristic of a Thyratron—Dehors and Mazières. (See 1621.)

621.317.328:621.396.81.029.62 1530
Measurement of Height-Gain at Metre Wavelengths—Saxton, Kreielsheimer, and Luscombe. (See 1578.)

621.317.335+621.317.411].029.6:621.318.134 1531
Measurement of the Parameters of Ferrites at U.H.F—V. V. Nikol'ski. (*Radiotekhnika i Elektronika*, vol. 1, pp. 447–468; April, and pp. 638–646; May, 1956. Correction, *ibid.*, vol. 1, p. 888; June, 1956.) Theory is presented of the experimental determination of the permeability tensor and the permittivity of ferrites by cavity-resonator methods. Spherical, cylindrical, and disk specimens in cylindrical or quadrangular-prism resonators are considered. Experimental results obtained by different methods are compared.

621.317.34:621.317.729:621.372.2 1532
An Investigation into some Fundamental Properties of Strip Transmission Lines with the Aid of an Electrolytic Tank—B. G. King and J. M. C. Dukes. (*Proc. IEE*, Part B, vol. 104, p. 72; January, 1957.) Comment on 2283 of 1956 and author's reply.

621.317.343:621.317.729:621.372.2 1533
Measurement of the Characteristic Impedance of Uniform Lines by means of the Electrolyte Tank—H. O. Koch. (*Frequenz*, vol. 10, pp. 277–283; September, 1956.) The method described avoids the use of high frequencies. Details of the apparatus and test results are given, and potential sources of error are discussed.

621.317.35 1534
A Method for the Continuous Recording of Harmonics—H. Nottebohm. (*Elektronische Rundschau*, vol. 10, p. 256; September, 1956.) The method of distortion-factor measurement described achieves a high degree of resolution over a continuous frequency spectrum. By means of a pulse-controlled electronic switch, a stepped curve is produced which is a frequency-transposed approximation to the signal waveform; this is analysed in the normal way.

621.317.382.029.64:537.533 1535
Microwave Power Measurements employing Electron-Beam Techniques—H. A. Thomas. (PROC. IRE, vol. 45, pp. 205–211; February, 1957.) An electron beam is accelerated transversely across an evacuated section of waveguide supporting a TE_{10} mode. The transit time is adjusted to give maximum interaction of the field with the electrons. The energy gained by the latter is measured in terms of a dc stopping potential which in turn can be related to the field. The power flow is then calculated from the Poynting vector. Some preliminary measurements with a 20-w cw source are described.

621.317.4 1536
Comparison of Methods of Magnetic Field Measurement—V. Andresciani. (*Piccole Note Ist. super. Poste e Telecomunicazioni*, vol. 5, pp. 629–643; September/October, 1956.) The accuracy of measurements made by means of bismuth spirals and by ballistic fluxmeter is compared with that obtainable by the nuclear-resonance meter [3480 of 1956 (Andresciani and Sette)], and the relative advantages of the methods are assessed. The error due to rapid probe withdrawal in the ballistic method is calculated.

621.317.431 1537
Simple 60-c/s Hysteresis Loop Tracer for Magnetic Materials of High or Low Permeability—D. H. Howling. (*Rev. Sci. Instr.*, vol. 27, pp. 952–956; November, 1956.) Designed for use with long specimens such as wires or tape.

621.317.44:538.632:537.311.33 1538
The Self-Field Error in the Measurement of the Tangential Field Strength in Iron by means of the Hall Effect—F. Kuhrt and W. Hartel. (*Arch. Elektrotech.*, vol. 42, pp. 398–409; September 20, 1956.) The error due to the magnetic field associated with the current through the semiconductor plate is evaluated, and its dependence on the geometrical and physical properties of the plate is discussed for three different arrangements. Field strengths of the order of a millioersted can be measured.

621.317.7:537.54:621.396.822.029.6 1539
The Noise of Gas-Discharge Tubes and its Application to Microwave Noise Measurements—E. Suchel. (*Elektronische Rundschau*, vol. 10, pp. 242–246; September, 1956.) A neon-filled noise diode suitable for insertion into waveguides, and a test circuit for noise-figure measurements in the 3-cm-λ region are described.

621.317.72 1540
An Electrostatic Null Detector—J. Hart and A. G. Mungall. (*J. Sci. Instr.*, vol. 33, pp. 411–412; November, 1956.) A simple arrangement for use in a high-resistance bridge circuit comprises a movable plate suspended between two fixed plates. The sensitivity is better than 0.5 v, and the device has been used for potential measurements from 0 to 1000 v; its capacitance is about 3 pF.

621.317.729 1541
Electrolytic Tank, Design and Applications—P. A. Kennedy and G. Kent. (*Rev. Sci. Instr.*, vol. 27, pp. 916–927; November, 1956.) Survey of theory and design, with description of the Harvard tank and discussion of experimental errors.

621.317.733:538.569.4.029.6 1542
Accurate Method for Measurement of Microwave Attenuation—J. A. Fulford and J. H. Blackwell. (*Rev. Sci. Instr.*, vol. 27, pp. 956–958; November, 1956.) The change in microwave power fed to a thermistor is compared with an equal amount of lf (1-kc) power supplied to the same thermistor through a precision attenuator. The comparison is effected by restoring the balance of a bridge containing two thermistors in an arrangement which compensates against drift in the microwave power output.

621.317.737:621.385.029.6 1543
An X-Band Magnetron Q-Measuring Apparatus—J. R. M. Vaughan and J. R. G. Twistleton. (*Proc. IEE*, Part B, vol. 104, p. 6; January, 1957.) Comment on 2493 of 1956 and author's reply.

621.317.755:621.314.7.001.4 1544
Characteristic Tracer for Power Transistors—S. Kramer and R. Wheeler. (*Electronic Ind. and Tele-Tech*, vol. 15, pp. 58–59, 88; September, 1956.) CRO equipment capable of dealing with peak power levels up to 1 kw is described.

621.317.755:621.374.3 1545
Transistors Generate Geometric Scale—Gott and Park (See 1373.)

621.317.761 1546
Heterodyne Frequency Meter for Pulsed and Continuous Frequency Measurements—H. P. Hirschl. (*Aust. J. Appl. Sci.*, vol. 7, pp. 205–214; September, 1956.) A meter for the range 2–100 mc is described. It is accurate to within 100 cps per mc for pulses of duration $>50\ \mu s$; the shielding is such that the instrument can be used close to a transmitter.

621.317.761 1547
An Electronic Device for the Absolute and Relative Measurement of Frequencies between 10 and 200000 c/s—A. Drigo and M. Pizzo. (*Ricerca Sci.*, vol. 26, pp. 2739–2746; September, 1956.) The equipment described consists of an electronic scaler counting the half-waves of the same sign in an electrical oscillation. It is gated photoelectrically by a pendulum, and an accuracy within 0.1 per cent is claimed.

621.317.784:621.314.63 1548
A Crystal-Diode Wattmeter—G. Zinsli. (*Bull. schweiz. elektrotech. Ver.*, vol. 47, pp. 893–901; September 29, 1956.) The instrument described is built up from a number of resistors and Ge diodes; it operates on the principle of multiplying together two voltages by rectification and double difference formation. The frequency range is 0–100 kc.

OTHER APPLICATIONS OF RADIO AND ELECTRONICS

534.2–8 1549
Pulsed F.M. tests Ultrasonic Propagation—R. R. Unterberger. (*Electronics*, vol. 30, pp. 143–145; January 1, 1957.) A sonar system for seismic research, using a frequency-sweep sine-wave generator and a wide-band (165–240 kc) receiver, which may be gated to accept any part of the variable-frequency cycle.

535.341–1:621.317.733 1550
Simple Aid to Infrared Intensity Measurements—C. B. Arends and D. F. Eggers, Jr. (*Rev. Sci. Instr.*, vol. 27, pp. 939–940; November, 1956.) An electromechanical device for accurate determination of absorption intensity directly from spectral curves.

536.531 1551
The Zero Stability of the Symmetrical Hot-Wire Bridge—R. Schneider. (*Arch. tech. Messen*, no. 248, pp. 199–202; September, 1956.) The influence of manufacturing tolerances, current fluctuations, and ambient temperature on stability is investigated.

539.16.08 1552
The Measurement of Radioactivity—D. Taylor. (*Proc. IEE*, Part B, vol. 104, pp. 7–14; January, 1957.) Chairman's address, Measurement and Control Section. An instrument is described for the continuous monitoring of α-active material in solution with γ- and β-active matter also present. The ultimate sensitivity of radioactive assay, and measurements relating to human body radioactivity, radiation dosage, and nuclear reactors are also considered.

621–52:681.142 1553
Ship Stabilization: Automatic Controls, Computed and in Practice—J. Bell. (*Proc. IEE*, Part B, vol. 104, pp. 20–26; January, 1957.) Predictions by step-by-step and analog methods are given, the functioning of the analog computer being described, and examples of results presented. Some practical results from sea experience and a brief account of a stabilizing demonstration on a model are included.

621.316.728:[621.314.63+621.314.7 1554
Power Regulation by Semiconductors—F. H. Chase. (*Elec. Eng., New York*, vol. 75, pp. 818–822; September, 1956.) Applications of semiconductor diodes and transistors in power regulators are described.

621.384.6 1555
Problems in the Radio Engineering and Electronics of Powerful Cyclic Accelerators of Heavy Charged Particles—A. L. Mints. (*Radiotekhnika i Electronika*, vol. 1, pp. 543–559; May, 1956.) A survey, with particular reference to the phasotron (synchrocyclotron) and the synchrophasotron (proton synchrotron) of the U.S.S.R. Academy of Sciences. The former accelerates protons to energies up to 700 mev, the latter to 10 kmev. The projected 50-kmev synchrophasotron is also mentioned.

621.384.622 1556
Achromatic Beam Translation Systems for Linear Accelerators—K. L. Brown. (*Rev. Sci. Instr.*, vol. 27, pp. 959–963; November, 1956.) Magnetic deflection systems which dispose of secondary particles and give translation without energy dispersion.

621.385.833 1557
Distribution of Electron Density over an Electron-Optical Image—I. G. Stoyanova. (*Zh. Tekh. Fiz.*, vol. 26, pp. 990–995; May, 1956.) Report of an experimental investigation to determine the effect of the atomic weight of the substance under observation, the amount of the substance, and the accelerating voltage on the distribution of electron density over electron-microscope images.

621.385.833 1558
The Experimental Determination of Focal Lengths and Principal Planes of Asymmetric Unipotential Electron Lenses—C. W. F. Everitt and K. J. Hanssen. (*Optik, Stuttgart*, vol. 13, pp. 385–398; September, 1956.) Whereas four shadow images are generally necessary for the determination of asymmetric lenses, it is shown that three images will suffice for the special case of unipotential lenses. A description of a simple test method is illustrated by experimental results.

621.385.833 1559
Geometrical Aberrations in Strong-Focusing [electron] Lenses—M. Y. Bernard and J. Hue. (*C.R. Acad. Sci., Paris*, vol. 243, pp. 1852–1854; December 5, 1956.) Third-order equations of the electron trajectories in es and magnetic lenses are derived and discussed.

621.385.833 1560
Calculation of the Induction and its Derivatives along the Axis of a Magnetic Electron Lens [with the form of a figure] of Revolution—M. Laudet. (*C.R. Acad. Sci., Paris*, vol. 243, pp. 1855–1857; December 5, 1956.)

621.387.4 1561
The Spreading of the Discharge in Self-Quenching Counter Tubes: Part 1—E. Huster and E. Ziegler. (*Z. Phys.*, vol. 146, pp. 281–294; September 21, 1956.) Experimental evidence indicates that the discharge is spread along the tube by photons.

621.387.4 1562
Standard Deviation of Dead-Time Correction in Counters—L. L. Campbell. (*Canad. J. Phys.*, vol. 34, pp. 929–937; September, 1956.) A formula is derived for the standard deviation of the corrected count for random events.

621.397.6:535.623 1563
High-Resolution Flying-Spot Scanner for Graphic Arts Colour Applications—L. Shapiro and H. E. Haynes. (*RCA Rev.*, vol. 17, pp. 313–329; September, 1956.) Description of slow-speed scanning and reproducing systems serving respectively as input and output devices for an electronic computer providing color correction in the production of half-tone plates for color printing. A 10-inch kinescope simultaneously scans three precisely registered color separation plates. Four images representing the required printing-ink colors are recorded photographically in sequence from a second kinescope.

621.56:537.311.33:537.322.1:536.581 1564
Thermoelectric Micro-refrigerators—K. E. Iordanishvili and L. S. Stil'bans. (*Zh. Tekh. Fiz.*, vol. 26, pp. 945–957; May, 1956.) Semiconductor thermoelements have been developed in which the Peltier effect is used for lowering temperature by more than 60 degrees in the region of room temperature. Refrigerators using these elements have been constructed; for small volumes (under 1 litre) this type of refrigerator is an improvement on both the absorption and the compression types. Theory is discussed and results are given of an experimental investigation into the following: *a*) three-stage refrigeration by means of a thermo-battery; *b*) combined refrigeration (first stage—compression machine, second and third stages—thermoelectric refrigerators); *c*) thermostatic control of small volumes for use in radio equipment, etc.

PROPAGATION OF WAVES

538.566:551.510.535 1565
The Scattering of Electromagnetic Waves by Plasma Oscillations—N. Hokkyo. (*J. Geomag. Geoelec.*, vol. 8, pp. 1–8; March, 1956.) The theory of plasma oscillations is applied to the problem of the scattering of waves of frequency about 1 kmc in the ionosphere E layer. It is assumed that regions exist in which the electrons oscillate coherently; these regions are effective in scattering waves of frequencies about $\omega_p(c/v)$, where ω_p is the plasma frequency, c the velocity of light, and v the mean velocity of thermal agitation. The influence of the size of the oscillating region is studied.

621.396.11 1566
Approximate Formula for the Distance of the [radio] Horizon in the Presence of Superrefraction—V. A. Fok. (*Radiotekhnika i Elektronika*, vol. 1, pp. 560–574; May, 1956.) The formula derived applies to an atmospheric duct near the earth's surface, in which the refractive index varies parabolically with height.

621.396.11:551.510.535 1567
The Present State of Research in the Field of Ionospheric Scatter Propagation—J. Grosskopf. (*Nachrichtentech. Z.*, vol. 9, pp. 393–403; September, 1956.) Report based on papers published in PROC. IRE, vol. 43; October, 1955 (see 234 of 1956). See also 554 of 1956.

621.396.11:551.510.535 1568
Simultaneous Signal-Strength Measurements on Continuous and Pulsed Radio-Wave Transmissions Reflected from the Ionosphere—B. R. Rao and K. V. V. Ramana. (*Curr. Sci.*,

temperature dependence and the manufacturing spread of transistor dc parameters are investigated with reference to experiments on Ge and Si types and production samples. Circuits using resistance networks for stabilizing dc operation of transistors are described; satisfactory results were achieved. The ac performance of stabilizing circuits, and the use of temperature-sensitive elements are also discussed.

621.314.7.001.4:621.317.755 1612
Characteristic Tracer for Power Transistors—Kramer and Wheeler. (See 1544.)

621.383:546.682.86 1613
An Infrared Photocell based on the Photoelectromagnetic Effect in Indium Antimonide—C. Hilsum and I. M. Ross. (*Nature, London*, vol. 179, p. 146; January 19, 1957.) The schematic arrangement and the spectral sensitivity curve of a typical cell are given.

621.383.001.4 1614
Tracer Experiments in Photocells—W. E. Turk. (*J. Electronics*, vol. 2, pp. 267–269; November, 1956.) A method is developed for observing the distribution of Cs in vacuum photocells by a radioactive tracer technique.

621.385.029.6 1615
The Performance of Space-Charge Diodes at Ultra-high Frequencies considering a Maxwellian Velocity Distribution—H. Paucksch. (*Nachrichtentech. Z.*, vol. 9, pp. 410–414; September, 1956.) An integral equation for the small-signal displacement current in a plane parallel diode is given which can be solved by numerical methods. Values of admittance and slope in a practical example are at variance with Müller's solution (*Hochfrequenztech. u. Elektroakust.*, vol. 41, pp. 156–167; May, 1933. 1933 Abstracts, p. 443.)

621.385.029.6 1616
Notes on the Multi-reflection Klystron—B. Meltzer. (*Electronic Radio Engr.*, vol. 34, pp. 109–112; March, 1957.) 100 per cent efficiency is possible in principle if transit times are correct. The mode of operation, the electrode system required, and the effect of incorrect transit times are discussed.

621.385.029.6:621.317.737 1617
An X-Band Magnetron *Q*-Measuring Apparatus—J. R. M. Vaughan and J. R. G. Twistleton. (*Proc. IEE*, Part B, vol. 104, p. 6; January, 1957.) Comment of 2493 of 1956 and author's reply.

621.385.032.216:537.311.33:546.431–31 1618
Electrical Conductivity of Barium Oxide Single Crystals as a Function of Temperature and Excess Barium Density—R. T. Dolloff. (*J. Appl. Phys.*, vol. 27, pp. 1418–1426; December, 1956.)

621.387:621.316.722.1:621.396.822 1619
Gas-Filled Voltage Stabilizers—K. B. Reed and J. F. Dix. (*Electronic Radio Engr.*, vol. 34, p. 113; March, 1957.) Note of noise measurements in the frequency range 20 cps–10 mc confirming remarks of Benson (972 of 1957).

621.387:621.318.57 1620
Operation of a Cold-Cathode Gas Triode in a High-Impedance Self-Biasing Circuit—M. Silver. (PROC. IRE, vol. 45, pp. 239–242; February, 1957.) Explanation of spurious triggering and suggested cures.

621.387.001.4:621.317.3 1621
Method of Tracing the Dynamic Control Characteristic of a Thyratron—R. Dehors and C. Maizières. (*Rev. Gén. Élec.*, vol. 65, pp. 505–508; September, 1956.) A method is described which enables the characteristic, free from parasitic signals, to be traced rapidly on the screen of a cro.

MISCELLANEOUS

621.3.002 1622
The Electronic Age—R. C. G. Williams. (*Proc. IEE*, Part B, vol. 104, pp. 15–19; January, 1957.) Chairman's address, Radio and Telecommunication Section. The broad field of production, design, and technical administration in the radio and electronics industry is considered. Mention is made of the impact of new materials and techniques on a number of applications in radio, television, automation, and atomic energy.